DEVELOPMENT AND APPLICATION OF CHEMICAL TOOLS FOR THE STUDY OF S-ADENOSYL-L-METHIONINE-DEPENDENT METHYLTRANSFERASES

A Dissertation

Presented to the Faculty of the Weill Cornell Graduate School

of Medical Sciences

In Partial Fulfillment of the Requirements for the Degree of

Doctor of Philosophy

By

Ian R. Bothwell

May 2015

DEVELOPMENT AND APPLICATION OF CHEMICAL TOOLS FOR THE STUDY OF S-ADENOSYL-L-METHIONINE-DEPENDENT METHYLTRANSFERASES

Ian R. Bothwell, Ph.D.

Cornell University, 2015

Methyltransferases represent a class of enzyme responsible for the modification of biomolecules through the transfer of individual methyl units. The cofactor, S-adenosyl-L-methionine (SAM), serves as the methyl source for the vast majority of these enzyme-catalyzed reactions. These transformations have broad implications for many biological processes, ranging from the biosynthesis of essential cellular metabolites and pharmaceutically relevant natural products to the regulation of gene expression and protein function through the modification of nucleic acids and polypeptides. In addition, the malfunction of methyltransferase activity has been strongly implicated in a number of disease states including developmental disorders and carcinogenesis. As such, there has been significant effort in recent years to better understand these enzymes, their substrates, and the biological effects associated with their activity. Despite increased interest, the study of these processes has proven difficult using traditional biochemical or genetic techniques. In light of this, the research described herein has been aimed at the development of novel chemical tools and approaches for the study of these enzymes, with an emphasis on protein methyltransferases (PMTs). This research can be broadly categorized into two main focuses: (i) the implementation of Bioorthogonal Profiling of Protein Methylation (BPPM), in which substrates of specific PMTs are determined

through the use of engineered enzymes, SAM analogues and bioorthogonal chemistry; and (ii) the development of a selenium-based SAM analogues, one of which has shown broad compatibility toward a wide variety of wild-type enzymes including: protein, nucleic acid and small-molecule methyltransferases. With these tools in hand, novel substrates for the G9a and GLP1 protein lysine methyltransferases have been identified, and a versatile selenium-based SAM mimic has demonstrated potential as a useful tool for the enzymatic functionalization of proteins and small molecules.

BIOGRAPHICAL SKETCH

Ian Bothwell was born and raised in a small town in northeast Texas to Debora and Roger Bothwell. In 2003, he began his undergraduate studies at Southwestern University in Georgetown, Texas, where his interests in synthetic organic chemistry and molecular biology solidified. Following graduation, Ian began a research fellowship at the National Institutes of Health, performing microarray analysis related to fundamental embryonic developmental processes. With a foundation in chemistry, molecular biology and modern genetic approaches Ian then began to pursue his doctoral degree through the Tri-Institutional Ph.D. Program in Chemical Biology in New York City. Over the course of his graduate career, Ian worked to establish chemical tools and approaches for the study of protein methyltransferases under the mentorship of Dr. Minkui Luo at Memorial Sloan-Kettering Cancer Center.

TABLE OF CONTENTS

LIST OF FIGURES AND TABLES

LIST OF PUBLICATIONS

- **Bothwell, I. R**. and Luo, M. (2014). Chemical Reporters for the Study of Post-translational Modifications Catalyzed by Native Enzymes. *Molecules* (invited review). *Manuscript in preparation.*

- **Bothwell, I. R.** and Luo, M. (2014). Large-scale, Protection-free Synthesis of Se-Adenosyl-L-selenomethionine Analogues and Their Application as Cofactor Surrogates of Methyltransferases. *Org. Lett.* 16 (11), 3056-59.

- Islam, K.; Chen, Y.; Wu, H., **Bothwell, I. R.**; Blum, G.; Zeng, H.; Dong, A.; Zheng, W.; Min, J.; Deng, H. and Luo, M. (2013). Defining Efficient Enzyme-Cofactor Pairs for Bioorthogonal Profiling of Protein Methylation. *PNAS.* 110 (42), 16778-83.

- Winter, J. M.; Chiou, G.; **Bothwell, I.R.**; Xu, W.; Garg, N. K.; Luo, M. and Tang Y. (2013). Expanding the Structural Diversity of Polyketides by Exploring the Cofactor Tolerance of an Inline Methyltransferase Domain. *Org. Lett.* 15 (14), 3774–77.

- Blum, G.; **Bothwell, I. R.**; Islam, K. and Luo, M. (2013). Profiling Protein Methylation with Cofactor Analogue Containing Terminal Alkyne Functionality. *Curr. Protocols Chem. Biol.* 5 (1), 67-88.

- **Bothwell, I.R.**; Islam, K.; Chen, Y.; Zheng, W.; Blum, G.; Deng, H. and Luo, M. (2012). Se-Adenosyl-L-selenomethionine Cofactor Analogue as a Reporter of Protein Methylation. *J. Am. Chem. Soc.* 134 (36), 14905-12.

- Islam, K.; **Bothwell, I.**; Chen, Y.; Sengelaub, C.; Wang, R.; Deng, H. and Luo, M. (2012). Bioorthogonal Profiling of Protein Methylation using Azido Derivative of S-adenosyl-L-methionine. *J. Am. Chem. Soc.* 134 (13), 5909-15.

CHAPTER 1: INTRODUCTION

1.1 METHYLTRANSFERASES: VERSATILE ENZYMES WITH DIVERSE SUBSTRATES

Methyltransferases are enzymes characterized by their ability to transfer one or more single-carbon methyl groups onto their substrates. Although genetically and structurally diverse, the overwhelming majority of these enzymes utilize S-adenosyl-L-methionine (SAM) as a cofactor and methyl source[1] for the modification of essentially every type of biomolecule, including: natural products, lipids, carbohydrates, nucleic acids, and proteins. [1-4] The first SAM-dependent methyltransferase identified was nicotinamide N^1-methyltransferase (originally dubbed nicotinamide methylkinase due to the reconstituted enzyme system's reliance on ATP and methionine), which was identified in 1951 by G. L. Cantoni and is responsible for the generation of N^1-methynicotinamide.[5] Since then, SAM-dependent enzymes responsible for the methylation of the vast array of additional substrates have been characterized.[6] In the wake of these discoveries, a broader understanding of the biological functions influenced by these enzymes is currently being pursued.

Over the past decade, one of the most intensely examined topics of research related to methyltransferase activity has been epigenetic regulation of gene expression. In eukaryotes, DNA is normally found bound to octomeric histone protein (histones H2A, H2B, H3, and H4) complexes, which wind the genomic material into compact structures known as nucleosomes (the basic unit of chromatin). The theory of epigenetic regulation stipulates that, through the modification of DNA, histones, and other factors, eukaryotic

gene expression can be tightly controlled and regulated through the modulation of chromatin structure.[7] Along with other modifications (phosphorylation, acetylation, ubiquitylation, etc.), methylation is thought to play an essential role in this process, particularly through the methylation of genomic DNA and the histone proteins that bind and sequester it.[8, 9] In the context of this theory, methylation marks, deposited by protein or nucleic acid methyltransferases ('writers'), serve as binding motifs for specific methyl-recognizing proteins ('readers').[7] These reader proteins may then interact with a variety of other effectors, such as chromatin remodelers, DNA repair proteins, or transcription factors, in order to elicit a response. In recent years, however, several of these writer enzymes have been found to methylate non-histone targets as well.[10] Research focused on the discovery and study of these non-histone targets is the primary topic of this dissertation, and a more detailed discussion of these enzymes and their substrates is provided in section 1.3.

Another area of research related to these enzymes is in the field of natural product methyltransferases (NPMTs). These enzymes represent the most diverse class of methyltransferases across species and are involved in the biosynthesis of a vast array of metabolites and pharmaceutically relevant compounds, where the addition of a methyl group is often essential for altering the pharmacological properties of the natural product.[6] Classic examples may include such enzymes as phenylethanolamine N-methyltransferase or histamine N-methyltransferase, which are responsible for the methylation of norepinephrine and histamine, respectively. However, there are hundreds of natural products that rely upon the activity of NPMTs for their biosynthesis. Indeed, NPMT activity can be found across essentially every class of natural product, with

biosynthetic activities ranging from essential metabolites, alkaloids, terpenoids and polyketides, up to nonribosomal peptides (NRPs) and ribosomally synthesized and posttranslationally modified peptides (RiPPs).[6, 11-13]

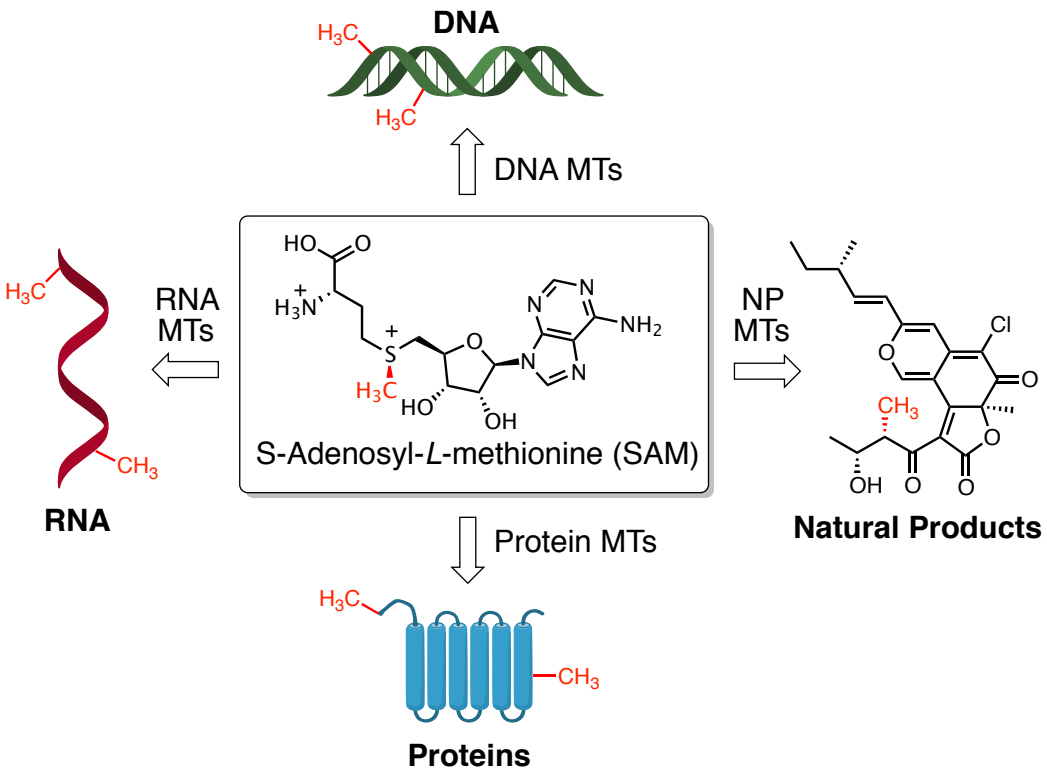

Figure 1.1: Representation of the scope of biological transmethylation reactions catalyzed by SAM-dependent methyltransferases. The sulfonium-methyl group (in red) of SAM is chemically reactive and transferable to a wide variety of proteins, nucleic acids, and small-molecules.

1.2 S-ADENOSYL-L-METHIONINE: CHEMISTRY AND FUNCTION

S-Adenosyl-L-methionine (Figure 1.1) was first described by G. L. Cantoni in 1953 as the chemically active source of transferable methyl groups in the biosynthesis of N^1-methynicotinamide.[5, 14] This discovery was brought about by the earlier observations that methionine was serving as a methyl source and that ATP was required for its activation, which together helped to inform its structural identity.[15] The biosynthesis of this molecule is carried out by S-adenosylmethionine synthetase (SAMs; a.k.a.

Methionine adenosyltransferase, MAT; or methionine activating enzyme, MAE), which transfers the sulfur group of methionine to the C-5' position of ATP, yielding SAM and generating phosphate/diphosphate as byproducts.[16] SAM synthetase is ubiquitously found across all of domains of life, with the exception of some parasitic species that take up SAM produced by their hosts.[17, 18]

In terms of chemical reactivity, SAM's ability to function as a methyl source stems from the presence of its high-energy sulfonium group, which imparts sufficient electrophilic character to the adjacent methyl group in order to make it susceptible to nucleophilic attack by suitable nucleophiles.[14] Enzymatic transfer of the sulfonium-methyl group to oxygen, nitrogen, and sulfur nucleophiles is traditionally thought to occur through an S_N2-like mechanism, proceeding through a trigonal planar transition state.[19] In recent years, however, a number of SAM-dependent methyltransferases have been described that utilize radical-based mechanisms to carry out their transformations. These enzymes make use of [4Fe-4S] clusters and the relatively low bond cleavage energies between the sulfonium-carbon bonds of SAM to generate a 5'-deoxyadenosyl radical. This key intermediate can in turn abstract a proton from the target substrate, activating it for subsequent modification.[20] Due to the high reactivity of their intermediates, radical-SAM methyltransferases are capable of methylating carbons that might not otherwise be nucleophilic. This can be exemplified by the activity of enzymes such as RlmN or Cfr, which are capable of methylating C-2 and C-8, respectively, of adenosine in bacterial 23S ribosomal RNA.[20]

In addition to SAM's function in transmethylation reactions, it is also involved in several other biochemical pathways. The first major pathway is polyamine biosynthesis,

which is thought to play a key role in cell survival and DNA repair.[21] In this pathway, the α-aminobutyrate moiety of SAM is first decarboxylated through the activity of adenosylmethionine decarboxylase, forming adenosylmethioninamine.[22] Subsequent enzymatic transfer of the propylamine group to putrescine or spermidine yields spermidine or spermine, respectively. Another major pathway dependent on the chemical reactivity of SAM is the biosynthesis of ethylene, a crucial signaling molecule in plants. Also referred to as the Yang cycle (after its discoverer), ethylene biosynthesis relies upon the activity of 1-aminocyclopropane-1-carboxylate (ACC) synthase to convert the α-aminobutyrate group of SAM to ACC. Carbon dioxide and hydrogen cyanide are then eliminated from this intermediate through the activity of ACC oxidase to yield ethylene.[23]

Due to its intrinsic reactivity, however, SAM is also subject to spontaneous degradation via several routes (Figure 1.2). The first and most prominent route occurs through intramolecular lactonization of the α-aminobutyrate moiety of SAM, yielding 5'-methylthioadenosine and homoserine lactone.[24] This pathway is highly pH dependent, demonstrating a roughly 10-fold rate enhancement corresponding to the relative pK_a's of SAM's amino acid moiety.[25] In the second route, the chiral sulfonium center of (S,S)-SAM (the biochemically active epimer of SAM) is capable of racemization to afford the (R, S) epimer of SAM, which is incompatible towards enzymatic transmethylation reactions.[26] Lastly, SAM is capable of depurination via base-promoted deprotonation of C-5' in ribose, yielding 5'-ribosylmethionine and adenine.[27] The relatively high acidity of the C-5' protons, which have an apparent pK_a of ~11.5, is thought to result from the presence of the sulfonium group directly adjacent.[25, 28]

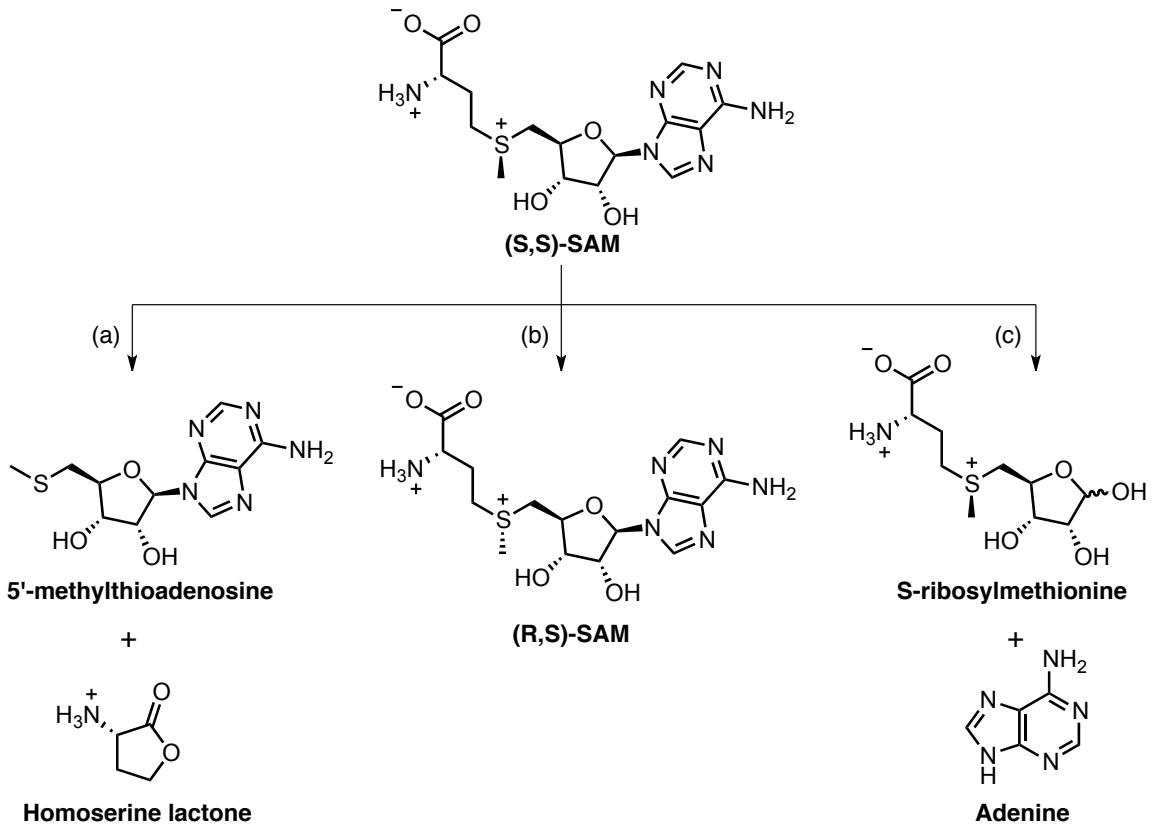

Figure 1.2: Inherent degradation pathways associated with SAM reactivity. Route (a) involves intramolecular lactonization of the carboxylate with the γ-carbon of SAM's α-aminobutyrate moiety. Route (b) takes place through racemization of the sulfonium group. Route (c) is the result of a concerted reaction dependent on deprotonation of C-5'.

SAM Analogues

With an appreciation for the biochemistry of SAM in mind, several groups (including ours) have explored the use of SAM analogues as potential tools for the study of SAM-dependent methyltransferases.[29-35] Development of these analogues has focused on substitution of the transferable methyl group with a variety of different functionalized R-groups in order to explore their enzyme compatibility. Generally, these analogues can be categorized into four major structural groups (based on substitution at the carbon β to the sulfonium group): β-sp^3, β-sp^2, β-sp^1, and β-carbonyl (Figure 1.3).

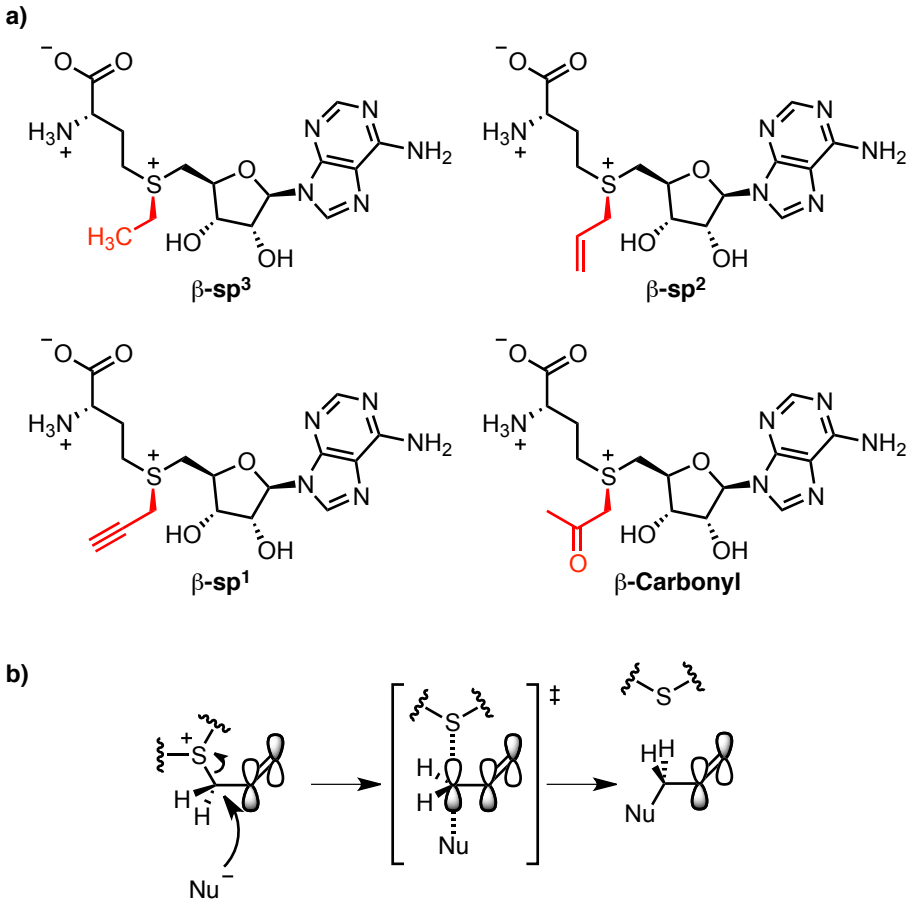

Figure 1.3: **Representation of the various classes of SAM analogues.** (a) The four general classes of SAM analogues studied to date. As a general trend, β-sp^3- and β-sp^1-hybridized analogues are unreactive or unstable, respectively. Both β-sp^2- and β-carbonyl-hybridized analogues have been reported to be active as enzyme cofactors. (b) The rationale behind the observed β-sp^2- and β-carbonyl-analogue activity involves transition state stabilization during alkyl transfer.

Initial studies by Dalhoff and colleagues were the first to examine the cofactor reactivity of a subset of these SAM analogues towards several wild-type DNA methyltransferases.[29] Findings from this initial report established that SAM analogues containing β-sp^3-hybridized substituents are typically inactive towards wild-type methyltransferases; whereas β-sp^2 and β-sp^1 hybridized analogues remain active, assuming their R-groups do not contain too much steric bulk and are stable (see chapter 3). The proposed rationale behind this observation stems back to the mechanism associated with transmethylation. In the case of β-sp^2 and β-sp^1 hybridized analogues, it

was originally thought that conjugation of the *p* orbital formed during the transition state to the adjacent π system in these analogues facilitates the S_N2 transfer reaction.[29] This notion has held true through future studies as well, with β-sp^3 analogues demonstrating no activity towards other classes of methyltransferase.[32] Together with observations by our group and others, these findings have helped to inform the design and synthesis of additional SAM analogues containing chemical handles compatible with bioorthogonal chemistry (see section 1.5).

1.3 PROTEIN METHYLTRANSFERASES

Despite the recent groundswell of interest in determining the roles that they play in epigenetic processes, many protein methyltransferases (PMTs) do not appear to be limited to histone modification. In fact, several of these putative histone methyltransferases have thus far demonstrated no activity towards recombinant histones, histone peptides, or nucleosomes. As such, it has become increasingly appreciated that these enzymes may have a much broader variety of substrates beyond histones. Coupled with the recent identification of numerous demethylating enzymes, protein methylation is now implicated as key signaling modification akin to phosphorylation or ubiquitylation.[10, 36] Numerous reports have surfaced in recent years describing non-histone targets for methyltransferases previously characterized as 'histone methyltransferases'. For example, the GLP1, G9a, SET8 and several other methyltransferases have all been shown to methylate the tumor suppressor p53 protein in order to modulate its function.[37-39] Furthermore, a handful of other proteins modified by lysine or arginine 'histone' methyltransferases have been identified, including: ERα, NF-κB, DNMT1, STAT3,

FOXO1, and p300, to name a few.[36] This information has gradually lead to a reclassification of these eukaryotic "histone methyltransferases" as general "protein methyltransferases", in order to more accurately describe their function.

This shift should come as no surprise, however, as a number of dedicated non-histone protein methyltransferases have been studied for decades and are known to play important roles in basic biological phenomena. For example, bacterial chemotaxis is regulated, in part, through the modification of glutamate residues in methyl-accepting chemotaxis proteins (MCPs) by the CheR protein glutamylmethyltransferase.[40] MCPs are integral membrane proteins that act as receptors for chemoattractants or chemorepellants in order to transmit chemical information from the surrounding environment to the flagellar machinery. It is now known that posttranslational modification of these receptors may dramatically alter sensitivity towards their ligands and thus dictate whether a cell remains motile or is stationary. In addition, the methylation of the C-terminal carboxylate group in the Ras GTPase, which is an important driver for some cancers, is thought to be crucial for its localization and activity.[41] This modification is carried out by isoprenylcysteine carboxyl methyltransferase following prenylation and proteolysis of the C-terminal CAAX motif of Ras, and is thought to aid in the localization of Ras to target membranes by masking the negative charge of the carboxylate. Lastly, protein methylation has more recently been implicated in host immune response evasion by some enteropathogenic bacteria. Following invasion of a host cell, some enteropathogenic *E. coli* strains are capable of secreting numerous effector proteins via type III secretion systems. One such effector, NleE, was recently shown to disrupt NF-κB signaling, which is important for the upregulation of pro-inflammatory cytokines, through SAM-dependent

cysteine methylation of the human TAB2 and TAB3 adaptor proteins.[42] Specifically, NleE targets and inactivates key zinc-coordinating cysteine residues required for the structural integrity of N-terminal Npl4 zinc finger domains in TAB2/3, which are critical for downstream signaling and activation of NF-κB. Together, these examples serve to illustrate the scope of functions that can be influenced by the activity of PMTs.

As a primary focus of the research outlined herein, my work has been in the pursuit of developing novel tools and techniques for the study of methyltransferases, with a partial emphasis on protein lysine methyltransferases as a model system. As such, a detailed description of the structure and function of these enzymes will be provided in the following subsection.

Protein Lysine Methyltransferases (PKMTs)

The human genome is thought to encode for roughly 50 methyltransferases capable of methylating the ε-amino group of lysine.[43] Interestingly, most of the PKMTs in humans contain a conserved catalytic domain known as the SET (suppressor of variegation 3-9, enhancer of zeste and trithorax) domain, with the exception being the DOT1L protein. Generally speaking, the SET domain contains two distinct binding sites: (i) a cofactor-binding site for SAM, and (ii) a peptide-binding groove for enzyme substrates. In most cases, these pockets are found on opposite faces of the SET domain, separated by a hydrophobic channel lined with tyrosine and phenylalanine residues.[44] In terms of catalytic mechanism, it is thought that the target lysine residue is positioned inside this hydrophobic channel during recognition of the target polypeptide, where it comes into close proximity with the methyl group of SAM. Subsequent deprotonation of

the ε-amino group by an adjacent conserved tyrosine then activates the target lysine for transmethylation.[45] Furthermore, because these enzymes contain two distinct binding pockets for cofactor and peptide, many are capable of transferring multiple methyl groups to the target lysine in a processive manner. As a result, many PKMTs are further classified by the number of methyl groups they typically transfer to a specific residue (i.e. mono-, di-, or tri-methyltransferases).

Although the specific substrates of all human PKMTs have not yet been fully determined, many have been shown to methylate lysine residues on histones, including histone H3 K4, K9, K27, K36, and K79, as well as histone H4 K20.[8, 45] For example, the G9a, GLP1, SUV39H1, SUV39H2, SETDB1, and SETDB2 enzymes are all capable of di/tri-methylating K9 of histone H3. Furthermore, both G9a and GLP1 have also been shown to methylate H3K27. In contrast, the SET8 and SET7/9 enzymes have been classified as histone mono-methyltransferases and are capable of methylating H4K20 and H3K4, respectively.[8] While not clear in all cases, the methylation of H3K4, H3K36 and H3K79 have typically been associated with transcriptional activation, whereas H3K9, H3K27, and H4K20 methylation are associated with repression.

Although the detailed physiological mechanisms are not yet known, the activity of some PKMTs have been strongly implicated in human disease. In addition to the examples listed in the sections above, dysregulation or deletion of several PKMTs has been associated with a number of pathogenic states, particularly cancer development and progression. EZH2 (enhancer of zeste homologue 2; a H3K27 PKMT), for example, is thought to act primarily as a transcriptional repressor and is overexpressed in several cancers including lymphoma, breast, and prostate cancer.[46, 47] In contrast, retinoblastoma

protein-interacting zinc finger 1 (RIZ1; a H3K9 PKMT), which is involved in cell-cycle arrest and apoptosis, and has been shown to be down-regulated or deleted in breast, liver, cervical and colon cancers.[48]

Several developmental disorders have also been tightly associated with PKMT function. One such disorder, Kleefstra syndrome (a.k.a. 9q34 deletion syndrome), has been directly attributed to the deletion of the GLP1 H3K9 methyltransferase from the end of chromosome 9.[49] Although rare, the physical and neurological symptoms of this disorder are quite severe, and are characterized by heart, genital and renal defects, as well as seizures, facial hypoplasia, and severe mental retardation. Indeed, knockout of GLP1 in transgenic mouse models resulted in embryonic lethality due to severe growth defects.[50] Furthermore, postnatal knockdown of GLP1 in the forebrain neurons of mice, although not lethal, resulted in a significant impairment of cognitive and adaptive abilities.[51] With these examples in mind, it is clear that PMT dysfunction is likely related to a wide variety of human disease states. Thus, much recent research has been aimed at the development of new ways to study the targets and functions of PMTs.

1.4 CONVENTIONAL APPROACHES TO STUDY METHYLTRANSFERASE ACTIVITY

Given its importance in fundamental biological processes and implication in human disease, numerous tools and approaches have previously been applied or developed in order to study methyltransferases.[52] Many of these technologies retain inherent limitations, however, due to complex protein interactions required for methyltransferase activity and the chemically subtle nature of the methyl mark. These

approaches will be discussed in the following subsections, along with descriptions of their advantages and drawbacks.

Enzyme-Coupled Assays

One approach used to examine methyltransferase activity has been to monitor the formation of the transmethylation reaction byproduct, S-adenosyl-L-homocysteine (SAH). This can be achieved through enzyme-coupled detection assays in several ways: (i) enzymatic conversion of SAH to L-homocysteine, which can then be reacted with a fluorogenic dye, and (ii) luminescent assays relying on the activity of luciferin/luciferase.

In the first format, enzymatic reactions containing a methyltransferase, known substrates, and SAM or SAM analogues are allowed to progress. Following completion of the reaction, the resultant product mix will contain methylated peptide and SAH. SAH may then be hydrolyzed to L-homocysteine and adenosine through the activity of SAH hydrolase (SAHH). The resultant free thiol of L-homocysteine is then covalently coupled to a Michael-accepting coumarinic dye (CPM), which results in a quantifiable fluorescent signal at specific excitation and emission wavelengths.[53, 54] For the second assay, although the initial experimental setup is similar to that of the first, SAH is instead converted into adenosine triphosphate (ATP) through the activity of several enzymes. Adenine is first liberated from SAH through the activity of 5'-methylthioadenosine/SAH nucleosidase (MTAN). Then, through the activity of adenine phosphoribosyl transferase (APRT), the liberated adenine is converted to adenosine monophosphate (AMP) prior to transformation into ATP by a third enzyme, pyruvate orthophosphate dikinase (PPDK). Subsequent reaction between ATP and luciferin/luciferase yields a chemiluminescent

signal. It should be noted that this assay is extremely sensitive, with a detection limit of 0.3 pmol for SAH.[55] Together, these approaches have several advantageous qualities, including rapid high-throughput formatting and versatility between different enzymes, cofactor analogues, and substrates. However, some limitations do exist, such as a general incompatibility with thiol-based reducing agents (due to reactivity towards the CPM dye), high background signals, and a potential for false positives.

Antibody-Based Approaches

Antibodies developed against specific methylated antigens provide a powerful and convenient way to detect the presence of modified residues within proteins or peptides. Indeed, many antibodies for methyl-lysine and methyl-arginine residues are commercially available and can be easily applied for western blot analysis, enzyme-linked immunosorbent assays (ELISA), or chromatin immunoprecipitation (ChIP) experiments.[56, 57] To date, numerous studies have relied upon these antibodies to detect methylation patterns both *in vitro* and *in vivo*. Despite their widespread use and high sensitivity, however, several concerns arise in some circumstances. These include issues such as antibody specificity and sequence dependence; where an antibody developed against a specific epitope may cross react with an irrelevant structural feature, or not interact at all with a peptide of slightly different amino acid sequence, leading to false positives and negatives. Another common concern relates to the processivity of many lysine or arginine methyltransferases, in which a specific antibody may not be able to differentiate between mono-, di-, or tri- methylated residues. Lastly, the problem of enzyme redundancy is a common issue, especially when examining methylation *in vivo*.

In living systems, there are often multiple PMTs capable of methylating the same residue.[56] For example, G9a, GLP1, SUV39H1/2, and SETDB1/2 are all capable of di/tri-methylating histone H3K9.[8] Even when combined with genetic approaches, such as knockdown or knockout of specific methyltransferases, attempting to correlate a change in observable methylation patterns can be challenging.

Isotopic Labeling

The use of isotopically labeled SAM as a means to monitor enzyme activity has been a mainstay for much of the biochemical research on PMTs. Use of radioactive ^{3}H-SAM in particular has been a versatile means of measuring enzyme kinetics and is often used for screening potential PMT inhibitors *in vitro*.[52, 58, 59] Non-radioactive deuterated SAM (CD_3-SAM) has also proven to be a powerful tool for the study of PMT activity, especially when combined with mass spectrometry-based detection, as is the case in SILAC (stable isotope labeling with amino acids in cell culture) experiments.[60] Although a powerful tool for *in vitro* study and top-down proteomic analysis of methylated proteins, some drawbacks do exist. First, kinetic measurements using ^{3}H-SAM are often very labor intensive and require the handling of hazardous radioactive materials. Second, radiometric and proteomic studies via SILAC approaches are sometimes unable to clearly attribute observable methylation marks to the activity of specific enzymes.

Array-Based Technologies

To date, several attempts have been made towards the development of peptide- or protein-based arrays for the determination of PMT substrates. These arrays have utilized

a variety of different detection methods, including fluorescently labeled antibodies, recombinant methyl-binding protein domains, and autoradiography. In 2008, Rathert and colleagues reported the synthesis of peptide arrays containing methylated peptides from known substrates of the G9a PKMT. Using recombinant GST-HP1β (a methyl-lysine binding chromodomain-containing 'reader' protein) coupled to αGST antibodies, the authors were able to demonstrate array-based detection of many previously reported substrates of G9a.[61] In 2011, Levy and colleagues expanded upon this approach using ProtoArray® technology (Invitrogen), which contain 9,500 purified recombinant human proteins arrayed on nitrocellulose slides. These slides were treated with a recombinant human PKMT, SETD6, in order to methylate potential substrates. Detection of substrates was performed using two methods: (i) autoradiographic detection from ^{3}H-SAM used during the enzymatic reaction, and (ii) antibody-based detection using fluorescently labeled pan-methyl-lysine antibodies. Following *in vitro* validation, the authors were able to detect six previously unreported substrates for the SETD6 enzyme.[62]

Although this array-based approach has been able to identify novel PMT substrates, major drawbacks still persist. First, many of the proteins spotted on commercially available arrays do not contain full-length protein sequences; meaning potential methylation sites could be easily overlooked. Second, these approaches still often utilized antibody-based detection methods, which are limited according to the issues discussed in the previous subsection. Lastly, transmethylation reactions on protein arrays generally use highly purified recombinant PMTs. This is potentially problematic, as it is currently known that many PMTs act as members of larger multimeric protein

complexes[63] and, in some cases, the presence of other protein factors is essential for proper enzyme activity and specificity.

In summary, current methods for studying PMTs are often limited by similar complicating factors, namely: (i) redundant PMT activity *in vivo*, (ii) difficulty dissecting the processive methylation activities of some PMTs, and (iii) a reliance on multimeric complex formation for relevant PMT activity and specificity. With these factors in mind, research in the Luo laboratory has been focused on the development of alternative, chemistry-based methodologies as a means of determining or functionalizing the substrates of specific methyltransferases. With this technology in hand, the ultimate goal of our research is to gain a better understanding of the biological processes associated with PMT activity.

1.5 RESEARCH OBJECTIVES

With an appreciation for the physiological roles of methyltransferases in fundamental biological processes and the limitations of current methodologies available for their study, the research presented herein is directed towards two primary objectives. The first has involved the development of a technique for the unambiguous determination of enzyme-specific methyltransferase substrates, termed Bioorthogonal Profiling of Protein Methylation (BPPM). This approach combines cofactor analogue development, enzyme engineering, and bioorthogonal chemistry in order to covalently modify specific enzyme targets for subsequent enrichment and analysis.[64] The second objective has focused on expanding the non-natural cofactor repertoire for methyltransferases through

the use of selenium-based SAM analogues, which were hypothesized to exhibit superior chemical properties in comparison to some sulfur-based SAM analogues. Included in this objective was the development of a SAM cofactor mimic for direct application towards the study of wild-type methyltransferases.[34]

(i) Development and Application of BPPM Technology

Inspired by the "Bump and Hole" strategy popularized by the Shokat laboratory[65], our group has envisioned a chemical-biology approach (BPPM) for the identification of novel PMT substrates. BPPM relies upon crystallographic data and activity-based screening methods in order to rationally engineer a specific methyltransferase to be able to utilize non-natural SAM analogues. Ideally, these analogues should contain a chemical handle compatible with bioorthogonal chemistries, such as Cu(I)-catalyzed azide-alkyne cycloaddition (CuAAC) reactions, and not be compatible with wild-type methyltransferases. After reintroduction of an engineered enzyme back into the cellular milieu and supplying it with a compatible SAM analogue, enzymatically labeled substrates can then be conjugated to fluorescent or affinity-based chemical probes and identified by fluorescence imaging or MS-MS analysis prior to target validation using conventional biochemical approaches, such as those described in section 1.4.

As a model system for the development of this technology, our initial research focused on the G9a and GLP1 PKMTs. As discussed in chapter 2, we have successfully engineered both enzymes to allow them to utilize a number of cofactor analogues. Furthermore, proteomic analysis of G9a- and GLP1-labeled substrates in HEK293T cell lysates has successfully confirmed a number of novel substrates for these enzymes.[64]

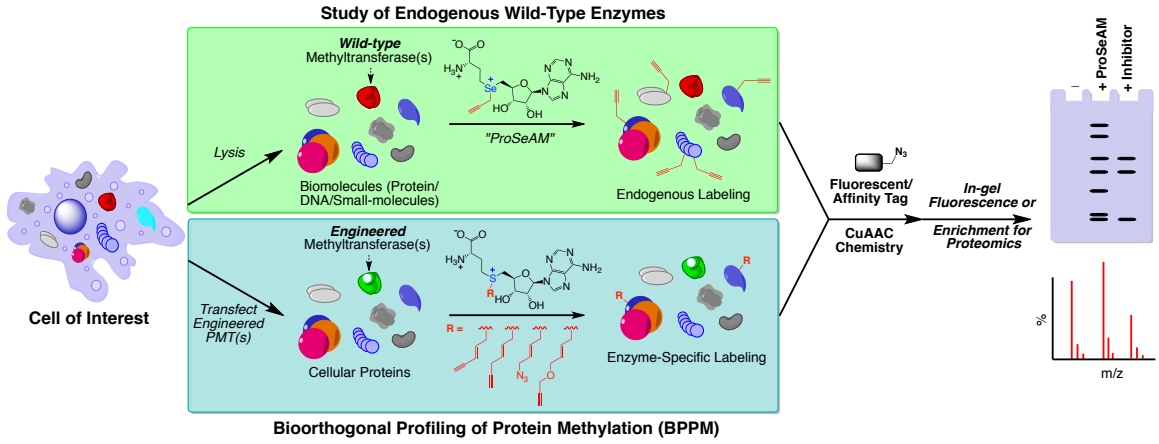

Figure 1.4: General diagram of chemical-biology-based approaches to the study of biological transmethylation reactions. Bottom panel, the bioorthogonal approach (BPPM) to identify PMT substrates involving protein engineering and bulky SAM analogues. Top panel, the selenium-based SAM analogue, ProSeAM, demonstrates potential as a chemical reporter for wild-type enzymes and is complimentary to BPPM.

(ii) Selenium-Based SAM Analogue Development

A cornerstone of our research focuses on the development of SAM analogues in order to examine their compatibility towards wild-type or engineered methyltransferases. Unfortunately, many of the initial sulfur-based SAM analogues reported in the literature required the presence of an sp^2-hybridized carbon β to the sulfonium-center in order to be enzymatically active.[29, 32] Furthermore, many β-sp^1-hybridized SAM analogues have demonstrated significant instability at physiologically relevant pH ranges.[34, 35] These features have, in essence, restricted structural variants of SAM analogues to those containing β-sp^2 or β-carbonyl-hybridized carbons. In an effort to expand the number of cofactor analogues available to the scientific community, we proposed substituting the reactive sulfonium-center with a selenonium moiety as a means of overcoming these limitations. Because the chemistry of the selenonium group is similar to that of a sulfonium, we predicted that we might be able to: (a) increase the reactivity of β-sp^3-

hybridzed carbons, thus making them compatible with engineered methyltransferases, and (b) circumvent the instability inherent in β-sp^1-hybridized cofactors. As a result of this objective, we have been able to successfully develop a selenium-based SAM cofactor mimic, ProSeAM,[34] which has demonstrated compatibility with a wide variety of protein and natural product methyltransferases.[12]

1.6 REFERENCES

1. Cantoni, G. L., Biological methylation: selected aspects. *Annual review of biochemistry* **1975,** *44*, 435-51.
2. Schubert, H. L.; Blumenthal, R. M.; Cheng, X., Many paths to methyltransfer: a chronicle of convergence. *Trends Biochem Sci* **2003,** *28*, 329-35.
3. Law, J. H., Biosynthesis of Cyclopropane Rings. *Acc. Chem. Res.* **1971,** *4*, 199-203.
4. Siedlecki, P.; Zielenkiewicz, P., Mammalian DNA methyltransferases. *Acta Biochim Pol* **2006,** *53*, 245-56.
5. Cantoni, G. L., Methylation of nicotinamide with soluble enzyme system from rat liver. *J Biol Chem* **1951,** *189*, 203-16.
6. Liscombe, D. K.; Louie, G. V.; Noel, J. P., Architectures, mechanisms and molecular evolution of natural product methyltransferases. *Natural product reports* **2012,** *29*, 1238-50.
7. Strahl, B. D.; Allis, C. D., The language of covalent histone modifications. *Nature* **2000,** *403*, 41-5.
8. Kouzarides, T., Chromatin modifications and their function. *Cell* **2007,** *128*, 693-705.
9. Bernstein, B. E.; Meissner, A.; Lander, E. S., The mammalian epigenome. *Cell* **2007,** *128*, 669-81.
10. Huang, J.; Berger, S. L., The emerging field of dynamic lysine methylation of non-histone proteins. *Curr. Opin. Genetics Dev.* **2008,** *18*, 152-158.
11. Zhang, Q.; van der Donk, W. A., Catalytic promiscuity of a bacterial alpha-N-methyltransferase. *FEBS letters* **2012,** *586*, 3391-7.
12. Winter, J. M.; Chiou, G.; Bothwell, I. R.; Xu, W.; Garg, N. K.; Luo, M.; Tang, Y., Expanding the structural diversity of polyketides by exploring the cofactor tolerance of an inline methyltransferase domain. *Organic letters* **2013,** *15*, 3774-7.
13. Ansari, M. Z.; Sharma, J.; Gokhale, R. S.; Mohanty, D., In silico analysis of methyltransferase domains involved in biosynthesis of secondary metabolites. *BMC bioinformatics* **2008,** *9*, 454.

14. Cantoni, G. L., S-Adenosylmethionine; a new intermediate formed enzymatically from L-methionine and adenosinetriphosphate. *J Biol Chem* **1953,** *204*, 403-416.
15. Borsook, H. a. J. W. D., On the Role of the Oxidation in the Methylation of Guanidoacetic Acid. *J. Biol. Chem.* **1947,** *171*, 363-375.
16. Cantoni, G. L.; Durell, J., Activation of methionine for transmethylation. II. The methionine-activating enzyme; studies on the mechanism of the reaction. *J Biol Chem* **1957,** *225*, 1033-48.
17. Stephens, R. S.; Kalman, S.; Lammel, C.; Fan, J.; Marathe, R.; Aravind, L.; Mitchell, W.; Olinger, L.; Tatusov, R. L.; Zhao, Q.; Koonin, E. V.; Davis, R. W., Genome sequence of an obligate intracellular pathogen of humans: Chlamydia trachomatis. *Science* **1998,** *282*, 754-9.
18. Tucker, A. M.; Winkler, H. H.; Driskell, L. O.; Wood, D. O., S-adenosylmethionine transport in Rickettsia prowazekii. *J Bacteriol* **2003,** *185*, 3031-5.
19. Ho, D. K.; Wu, J. C.; Santi, D. V.; Floss, H. G., Stereochemical studies of the C-methylation of deoxycytidine catalyzed by HhaI methylase and the N-methylation of deoxyadenosine catalyzed by EcoRI methylase. *Archives of biochemistry and biophysics* **1991,** *284*, 264-9.
20. Grove, T. L.; Benner, J. S.; Radle, M. I.; Ahlum, J. H.; Landgraf, B. J.; Krebs, C.; Booker, S. J., A radically different mechanism for S-adenosylmethionine-dependent methyltransferases. *Science* **2011,** *332*, 604-7.
21. Tabor, C. W.; Tabor, H., Polyamines. *Annual review of biochemistry* **1984,** *53*, 749-90.
22. Pegg, A. E.; Xiong, H.; Feith, D. J.; Shantz, L. M., S-adenosylmethionine decarboxylase: structure, function and regulation by polyamines. *Biochemical Society transactions* **1998,** *26*, 580-6.
23. Lin, Z.; Zhong, S.; Grierson, D., Recent advances in ethylene research. *Journal of experimental botany* **2009,** *60*, 3311-36.
24. Parks, L. W.; Schlenk, F., Formation of alpha-amino-gamma-butyrolactone from S-adenosylmethionine. *Archives of biochemistry and biophysics* **1958,** *75*, 291-2.
25. Iwig, D. F.; Booker, S. J., Insight into the polar reactivity of the onium chalcogen analogues of S-adenosyl-L-methionine. *Biochemistry* **2004,** *43*, 13496-509.
26. Wu, S. E.; Huskey, W. P.; Borchardt, R. T.; Schowen, R. L., Chiral instability at sulfur of S-adenosylmethionine. *Biochemistry* **1983,** *22*, 2828-32.
27. Parks, L. W.; Schlenk, F., The stability and hydrolysis of S-adenosylmethionine; isolation of S-ribosylmethionine. *J Biol Chem* **1958,** *230*, 295-305.
28. Borchardt, R. T., Mechanism of alkaline hydrolysis of S-adenosyl-L-methionine and related sulfonium nucleosides. *J Am Chem Soc* **1979,** *101*, 458-463.
29. Dalhoff, C.; Lukinavicius, G.; Klimasauskas, S.; Weinhold, E., Direct transfer of extended groups from synthetic cofactors by DNA methyltransferases. *Nat. Chem. Biol.* **2006,** *2*, 31-32.

30. Lee, B. W.; Sun, H. G.; Zang, T.; Kim, B. J.; Alfaro, J. F.; Zhou, Z. S., Enzyme-catalyzed transfer of a ketone group from an S-adenosylmethionine analogue: a tool for the functional analysis of methyltransferases. *J Am Chem Soc* **2010,** *132*, 3642-3.
31. Peters, W.; Willnow, S.; Duisken, M.; Kleine, H.; Macherey, T.; Duncan, K. E.; Litchfield, D. W.; Luscher, B.; Weinhold, E., Enzymatic site-specific functionalization of protein methyltransferase substrates with alkynes for click labeling. *Angew Chem Int Ed Engl* **2010,** *49*, 5170-3.
32. Islam, K.; Zheng, W.; Yu, H.; Deng, H.; Luo, M., Expanding cofactor repertoire of protein lysine methyltransferase for substrate labeling. *Acs Chem Biol* **2011,** *6*, 679-84.
33. Islam, K.; Bothwell, I.; Chen, Y.; Sengelaub, C.; Wang, R.; Deng, H.; Luo, M., Bioorthogonal profiling of protein methylation using azido derivative of S-adenosyl-L-methionine. *J Am Chem Soc* **2012,** *134*, 5909-15.
34. Bothwell, I. R.; Islam, K.; Chen, Y.; Zheng, W.; Blum, G.; Deng, H.; Luo, M., Se-adenosyl-L-selenomethionine cofactor analogue as a reporter of protein methylation. *J Am Chem Soc* **2012,** *134*, 14905-12.
35. Willnow, S.; Martin, M.; Luscher, B.; Weinhold, E., A Selenium-Based Click AdoMet Analogue for Versatile Substrate Labeling with Wild-Type Protein Methyltransferases. *Chembiochem* **2012**.
36. Zhang, X.; Wen, H.; Shi, X., Lysine methylation: beyond histones. *Acta biochimica et biophysica Sinica* **2012,** *44*, 14-27.
37. Huang, J.; Dorsey, J.; Chuikov, S.; Perez-Burgos, L.; Zhang, X.; Jenuwein, T.; Reinberg, D.; Berger, S. L., G9a and Glp methylate lysine 373 in the tumor suppressor p53. *J Biol Chem* **2010,** *285*, 9636-41.
38. Shi, X. B.; Kachirskaia, L.; Yamaguchi, H.; West, L. E.; Wen, H.; Wang, E. W.; Dutta, S.; Appella, E.; Gozani, O., Modulation of p53 function by SET8-mediated methylation at lysine 382. *Mol. Cell* **2007,** *27*, 636-646.
39. Chuikov, S.; Kurash, J. K.; Wilson, J. R.; Xiao, B.; Justin, N.; Ivanov, G. S.; McKinney, K.; Tempst, P.; Prives, C.; Gamblin, S. J.; Barlev, N. A.; Reinberg, D., Regulation of p53 activity through lysine methylation. *Nature* **2004,** *432*, 353-360.
40. Van Der Werf P, K. D. J., Identification of a gamma-glutamyl methyl ester in bacterial membrane protein involved in chemotaxis. *J Biol Chem* **1977,** *252*, 2793-5.
41. Chiu, V. K.; Silletti, J.; Dinsell, V.; Wiener, H.; Loukeris, K.; Ou, G.; Philips, M. R.; Pillinger, M. H., Carboxyl methylation of Ras regulates membrane targeting and effector engagement. *J Biol Chem* **2004,** *279*, 7346-52.
42. Zhang, L.; Ding, X. J.; Cui, J.; Xu, H.; Chen, J.; Gong, Y. N.; Hu, L. Y.; Zhou, Y.; Ge, J. N.; Lu, Q. H.; Liu, L. P.; Chen, S.; Shao, F., Cysteine methylation disrupts ubiquitin-chain sensing in NF-kappa B activation. *Nature* **2012,** *481*, 204-+.
43. Schapira, M., Structural Chemistry of Human SET Domain Protein Methyltransferases. *Current chemical genomics* **2011,** *5*, 85-94.
44. Qian, C.; Zhou, M. M., SET domain protein lysine methyltransferases: Structure, specificity and catalysis. *Cell. Mol. Life Sci.* **2006,** *63*, 2755-2763.

45. Dillon, S. C.; Zhang, X.; Trievel, R. C.; Cheng, X., The SET-domain protein superfamily: protein lysine methyltransferases. *Genome biology* **2005,** *6*, 227.
46. Valk-Lingbeek, M. E.; Bruggeman, S. W.; van Lohuizen, M., Stem cells and cancer; the polycomb connection. *Cell* **2004,** *118*, 409-18.
47. Collett, K.; Eide, G. E.; Arnes, J.; Stefansson, I. M.; Eide, J.; Braaten, A.; Aas, T.; Otte, A. P.; Akslen, L. A., Expression of enhancer of zeste homologue 2 is significantly associated with increased tumor cell proliferation and is a marker of aggressive breast cancer. *Clin. Cancer Res.* **2006,** *12*, 1168-1174.
48. He, L.; Yu, J. X.; Liu, L.; Buyse, I. M.; Wang, M. S.; Yang, Q. C.; Nakagawara, A.; Brodeur, G. M.; Shi, Y. E.; Huang, S., RIZ1, but not the alternative RIZ2 product of the same gene, is underexpressed in breast cancer, and forced RIZ1 expression causes G2-M cell cycle arrest and/or apoptosis. *Cancer research* **1998,** *58*, 4238-44.
49. Stewart, D. R.; Kleefstra, T., The chromosome 9q subtelomere deletion syndrome. *American journal of medical genetics. Part C, Seminars in medical genetics* **2007,** *145C*, 383-92.
50. Tachibana, M.; Sugimoto, K.; Nozaki, M.; Ueda, J.; Ohta, T.; Ohki, M.; Fukuda, M.; Takeda, N.; Niida, H.; Kato, H.; Shinkai, Y., G9a histone methyltransferase plays a dominant role in euchromatic histone H3 lysine 9 methylation and is essential for early embryogenesis. *Genes Dev* **2002,** *16*, 1779-91.
51. Schaefer, A.; Sampath, S. C.; Intrator, A.; Min, A.; Gertler, T. S.; Surmeier, D. J.; Tarakhovsky, A.; Greengard, P., Control of cognition and adaptive behavior by the GLP/G9a epigenetic suppressor complex. *Neuron* **2009,** *64*, 678-91.
52. Luo, M., Current chemical biology approaches to interrogate protein methyltransferases. *Acs Chem Biol* **2012,** *7*, 443-63.
53. Wang, R.; Ibanez, G.; Islam, K.; Zheng, W.; Blum, G.; Sengelaub, C.; Luo, M., Formulating a fluorogenic assay to evaluate S-adenosyl-L-methionine analogues as protein methyltransferase cofactors. *Mol Biosyst* **2011,** *7*, 2970-81.
54. Collazo, E.; Couture, J. F.; Bulfer, S.; Trievel, R. C., A coupled fluorescent assay for histone methyltransferases. *Anal. Biochem.* **2005,** *342*, 86-92.
55. Ibáñez, G.; McBean, J. L.; Astudillo, Y. M.; Luo, M., An Enzyme-coupled Ultrasensitive Luminescence Assay for Protein Methyltransferases. *Anal. Biochem.* **2010,** *PMID: 20227379*, in press.
56. Quinn, A. M.; Simeonov, A., Methods for Activity Analysis of the Proteins that Regulate Histone Methylation. *Current chemical genomics* **2011,** *5*, 95-105.
57. Egelhofer, T. A.; Minoda, A.; Klugman, S.; Lee, K.; Kolasinska-Zwierz, P.; Alekseyenko, A. A.; Cheung, M. S.; Day, D. S.; Gadel, S.; Gorchakov, A. A.; Gu, T.; Kharchenko, P. V.; Kuan, S.; Latorre, I.; Linder-Basso, D.; Luu, Y.; Ngo, Q.; Perry, M.; Rechtsteiner, A.; Riddle, N. C.; Schwartz, Y. B.; Shanower, G. A.; Vielle, A.; Ahringer, J.; Elgin, S. C.; Kuroda, M. I.; Pirrotta, V.; Ren, B.; Strome, S.; Park, P. J.; Karpen, G. H.; Hawkins, R. D.; Lieb, J. D., An assessment of histone-modification antibody quality. *Nature structural & molecular biology* **2011,** *18*, 91-3.

58. Dhayalan, A.; Dimitrova, E.; Rathert, P.; Jeltsch, A., A continuous protein methyltransferase (G9a) assay for enzyme activity measurement and inhibitor screening. *J. Biomol. Screen.* **2009,** *14*, 1129-1133.
59. Lakowski, T. M.; Zurita-Lopez, C.; Clarke, S. G.; Frankel, A., Approaches to measuring the activities of protein arginine N-methyltransferases. *Anal. Biochem.* **2010,** *397*, 1-11.
60. Ong, S. E.; Mittler, G.; Mann, M., Identifying and quantifying in vivo methylation sites by heavy methyl SILAC. *Nat Methods* **2004,** *1*, 119-26.
61. Rathert, P.; Dhayalan, A.; Murakami, M.; Zhang, X.; Tamas, R.; Jurkowska, R.; Komatsu, Y.; Shinkai, Y.; Cheng, X. D.; Jeltsch, A., Protein lysine methyltransferase G9a acts on non-histone targets. *Nat. Chem. Biol.* **2008,** *4*, 344-346.
62. Levy, D.; Liu, C. L.; Yang, Z.; Newman, A. M.; Alizadeh, A. A.; Utz, P. J.; Gozani, O., A proteomic approach for the identification of novel lysine methyltransferase substrates. *Epigenetics Chromatin* **2011,** *4*, 19.
63. Fritsch, L.; Robin, P.; Mathieu, J. R.; Souidi, M.; Hinaux, H.; Rougeulle, C.; Harel-Bellan, A.; Ameyar-Zazoua, M.; Ait-Si-Ali, S., A subset of the histone H3 lysine 9 methyltransferases Suv39h1, G9a, GLP, and SETDB1 participate in a multimeric complex. *Mol Cell* **2010,** *37*, 46-56.
64. Islam, K.; Chen, Y.; Wu, H.; Bothwell, I. R.; Blum, G. J.; Zeng, H.; Dong, A.; Zheng, W.; Min, J.; Deng, H.; Luo, M., Defining efficient enzyme-cofactor pairs for bioorthogonal profiling of protein methylation. *Proc Natl Acad Sci U S A* **2013,** *110*, 16778-83.
65. Bishop, A. C.; Ubersax, J. A.; Petsch, D. T.; Matheos, D. P.; Gray, N. S.; Blethrow, J.; Shimizu, E.; Tsien, J. Z.; Schultz, P. G.; Rose, M. D.; Wood, J. L.; Morgan, D. O.; Shokat, K. M., A chemical switch for inhibitor-sensitive alleles of any protein kinase. *Nature* **2000,** *407*, 395-401.

CHAPTER 2: ENGINEERING THE G9a AND GLP1 PROTEIN LYSINE METHYLTRANSFERASES FOR BPPM

2.1 INTRODUCTION

PKMTs utilize the SAM cofactor as a methyl donor to modify the ε-amino group of target lysine residues in a variety of different protein substrates. Methylation of these residues may occur processively, resulting in mono-, di-, or tri-methyl lysine, each of which may be associated with different biological outcomes through interaction with specific methyl-lysine binding proteins.[1, 2] Furthermore, the activities of several of the ~50 PKMTs in humans have been implicated in numerous biochemical processes and human diseases such as modulation of protein function, epigenetic regulation of gene transcription, carcinogenesis, and developmental disorders.[2-5] Despite their importance in human health, a detailed understanding of the full substrate profiles of these enzymes has remained elusive, in part, due to limitations in current biochemical and genetic methodologies (section 1.4). To address this problem, our group has envisioned a strategy for determining the substrates of specified methyltransferases, termed bioorthogonal profiling of protein methylation (BPPM). In order to demonstrate the utility of this strategy, it was first applied to the G9a and GLP1 PKMTs as model system. Much of the work presented in this chapter was performed in close collaboration with a former member of the Luo lab, Dr. Kabirul Islam, and has been previously published.[6, 7]

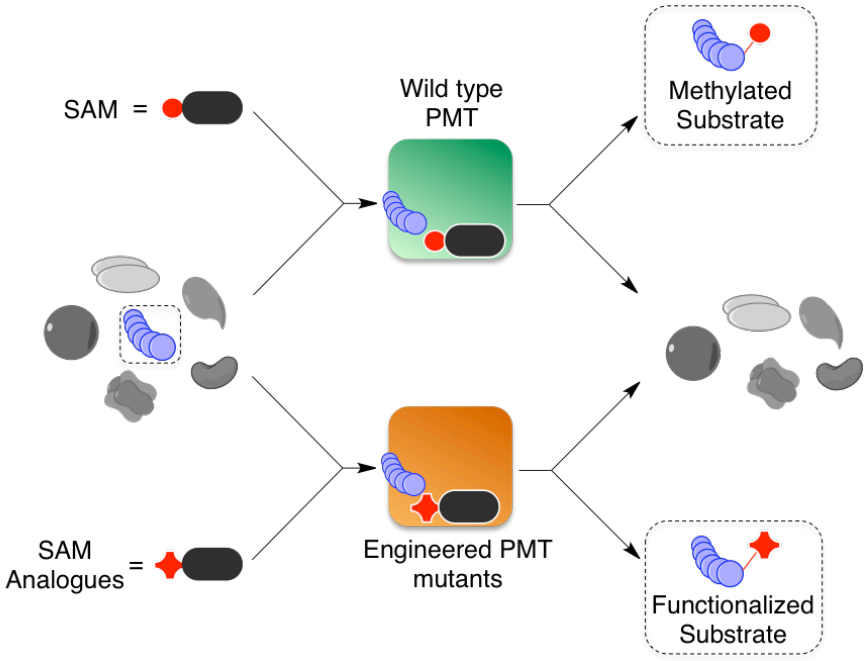

Figure 2.1: Schematic Description of Bioorthogonal Profiling of Protein Methylation (BPPM) Technology. In the context of this design, designated PMTs can be engineered to selectively utilize 'click'-able SAM analogues to functionalize their targets for subsequent study.

Bioorthogonal Profiling of Protein Methyltransferases (BPPM)

Given limitations inherent in many traditional biochemical techniques to determine PMT substrates, our group proposed a novel chemical biology-based approach for the elucidation of substrates for specific PMTs, termed BPPM. The rationale for BPPM technology has its foundation in the 'bump and hole' strategy popularized by the Shokat group to study kinase activity,[8, 9] in which a mutation in the active site of an enzyme allows for the accommodation of a specific non-natural substrate or cofactor (Figure 2.1). Based on this principle, the aim of BPPM was to first rationally engineer the G9a and GLP1 enzymes, through crystal structure-guided site-directed mutagenesis, in order to allow them to utilize non-natural SAM analogues. Ideally, these analogues would contain chemical handles attached to the carbon that is enzymatically transferred to the target protein. In fact, a library of these analogues had been previously synthesized

and characterized by our lab and others, and is often used for screening procedures (Figure 2.3).[6, 7, 10-12] Following reintroduction of the engineered enzyme back into a biological system, this would allow for the subsequent visualization or identification of enzyme-specific methylation targets through bioorthogonal chemistry, proteomics, and traditional biochemical methods.

The G9a and GLP1 PKMTs

The G9a and GLP1 (G9a-like protein 1) enzymes were identified in 2001 and 2002, respectively, and were amongst the first histone H3K9 di/tri-methyltransferases to be reported.[13, 14] The overall domain structures of these enzymes are quite similar, with both containing glutamate/aspartate rich and cysteine rich regions near their N-termini, followed by several tandem ankyrin repeat domains and the canonical catalytic SET domains near their C-termini (Figure 2.2b).[15] Furthermore, both enzymes have been shown to form multimeric complexes *in vivo* with one another, other methyltransferases (SETDB1 and SUV39H1), and additional protein factors such as the Wiz (widely-interspaced zinc finger containing) protein.[15, 16]

To date, several non-histone targets have been reported for these enzymes, which serve to highlight their biological importance. For example, these enzymes are known to methylate the ACINUS (apoptotic chromatin condensation inducer in the nucleus) protein, which has been shown to be essential for apoptotic chromatin condensation,[17] as well as Reptin, which is a RuvB-like DNA helicase thought to be part of the NuA4 histone acetyltransferase complex.[18] It has also been recently demonstrated that G9a and GLP1 di-methylate the tumor suppressor protein p53 at lysine 373, which serves to inhibit its

function and could potentially contribute to carcinogenesis in some cell types.[19] Furthermore, these enzymes have been shown to methylate DNA cytosine methyltransferase 3A, as well as myogenic regulatory factor MyoD to regulate skeletal muscle differentiation.[20, 21] All told, the function of these enzymes has currently been implicated in chromatin remodeling, silencing of proviral and tumor suppressor genes, regulating skeletal muscle and neuronal differentiation, and establishing *de novo* DNA methylation.[15, 21] Furthermore, these enzymes' relevance to human disease has also been implicated in developmental disorders, cancer development and progression, and addiction (Figure 2.2a). However, a deeper understanding of their biological functions requires a more comprehensive appreciation for the spectrum of substrates that they can potentially modify. With this in mind, we set about examining current crystal structure data in order to inform our BPPM engineering strategy.

G9a and GLP1 both contain canonical SET domain structures sharing a high degree of homology.[15, 22] The catalytic channel is composed of several conserved phenylalanine and tyrosine residues including: Y1124, Y1142, F1144, F1195, F1209, Y1211, and F1215 in GLP1; and Y1067, Y1085, R1109, F1152, Y1154, and F1158 in G9a (Figure 2.2c).[2] Furthermore, the F1209 and F1152 residues in GLP1 and G9a, respectively, have previously been shown to serve as regulators of enzyme processivity.[23] Also known as the 'switch' position, this conserved residue is often a tyrosine in lysine mono-methyltransferases and phenylalanine in di/tri-methyltransferases. With this information in hand, a number of potential candidate residues in or around the cofactor-binding pocket were selected for enzyme engineering including: Y1124, Y1142, F1144, Y1211, F1215, and W1216 in GLP1; and Y1067, Y1085, F1087, F1138, F1152, Y1154,

F1158, and W1159 in G9a. Following identification of suitable mutant/analogue pairs, implementation in cellular systems and subsequent target identification were performed.

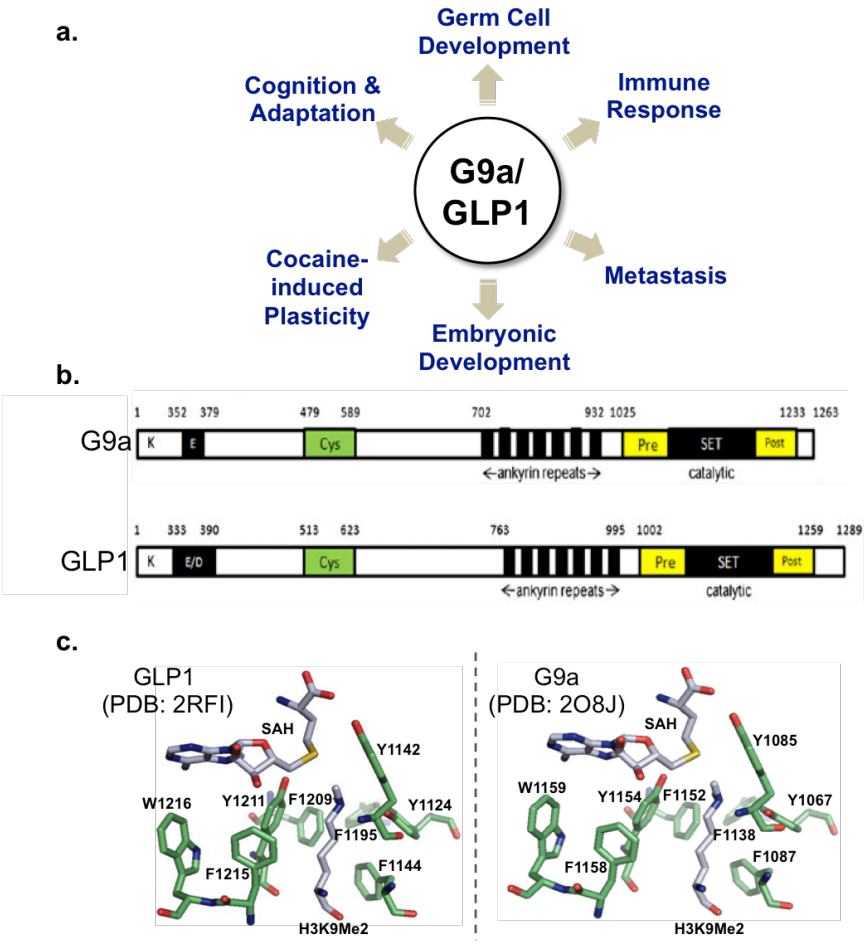

Figure 2.2: Overview of the G9a and GLP1 PKMTs. (a) Biological processes thought to be influenced by the activity of the G9a and GLP1 PKMTs. (b) Domain organization of the G9a and GLP1 PKMTs. K, potential automethylation sites; E, glutamate-rich region; E/D, glutamate/aspartate-rich region; Cys, cysteine-rich region; Pre, pre-SET domain; SET, SET domain; Post, post-SET domain.[15] (c) Crystallographic data highlighting key residues located in the SAM-binding pocket and hydrophobic catalytic channel. SAH, S-adenosyl-L-methionine.

2.1 MATERIALS AND METHODS

General Material and Methods

Chemical synthesis of cofactor analogues is detailed in chapter 6, or has been reported previously.[6, 7, 11] Polyacrylamide gels (12%/18% Tris HCl) and pre-stained ladders were purchased from Bio-Rad Laboratories. Cell culture media was purchased

from Gibco or Fisher Scientific. Streptavidin Sepharose™ was purchased from GE Healthcare. Recombinant human histones were purchased from New England Biolabs. EDTA-free protease inhibitor was purchased from Roche Applied Science. CuAAC labeling reagents and azido-conjugated teramethylrhodamine were purchased from Aldrich and Invitrogen, respectively. Azido-azo-biotin for pull-down experiments was synthesized and purified by Gil Blum, as described previously.[24, 25] Click-iT biotin-DIBO alkyne was purchased from Invitrogen. Histone H3 peptide (aa1-21; ARTKQTARKSTGGKAPRKQLAGGK) was synthesized by the Proteomics Resource Center at Rockefeller University. MALDI-MS spectra were collected on a Voyager-DE STR (Applied Biosystems, Framingham, MA, USA) MALDI-TOF mass spectrometer. In order to analyze peptide samples, 1μL of reaction mixture was added to 1 μL of saturated α-cyano-hydroxycinnamic acid (Protease Biosciences) on a MALDI plate and allowed to air dry. Spectra were then gathered using delayed extraction in positive ion mode. Desorption was achieved using a 337 nm nitrogen laser with a 3ns pulse width.

Protein Expression and Purification

N-terminal His_6-tagged methyltransferase SET domains of human GLP1(aa 951-1235) and G9a (aa 913-1193) were obtained as a generous gift from Dr. Jingrong Min at the University of Toronto.[26] Mutants for these enzymes were generated using QuickChange (Stratagene) site-directed mutagenesis kits according to manufacturer's instruction and confirmed via DNA sequencing. Mutant and native enzymes were then expressed and purified in *E. coli* Arctic Express (DE3) strain (Novagen) using a pET28a-LIC kanamycin^R vector. Single colonies were selected and grown at 37 ^oC in 5 mL Difco

LB culture medium containing 50 μg/mL kanamycin overnight. These starter cultures were then added to 1 L culture medium and allowed to grow at 30 ^{o}C to and OD_{600} of approximately 0.6-0.7. Expression was then induced through the addition of 0.6 mM IPTG and 25 μM $ZnSO_4$ and the cultures were allowed to shake at 10 ^{o}C for 24 hours. All mutant and native enzymes were purified according to the following protocol: harvested cells were suspended in 50 mM Tris HCl (pH = 8.0) containing 50 mM NaCl, 5 mM β-mercaptoethanol, 10% glycerol, 25 mM imidazole, and Roche protease inhibitor cocktail. Cells were then lysed using a French Press Cell Disruptor (Thermo) and centrifuged at 13,000 g for 45-60 mins at 4 ^{o}C. The supernatants were then subjected to gravity-flow purification over Ni-NTA agarose resin (Qiagen) according to manufacturer's instruction. All column-bound extracts were washed with six column volumes of washing buffer containing 50 mM Tris-HCl (pH = 8.0), 50 mM NaCl, 5 mM β-mercaptoethanol, and 25 mM imidazole. Proteins were then eluted with buffer containing 50 mM Tris HCl (pH = 8.0), 50 mM NaCl, 5 mM β-mercaptoethanol, and 400 mM imidazole, and further purified by size-exclusion chromatography (Superdex-75, GE Healthcare) using buffer containing 25 mM Tris HCl (pH = 8.0), 200 mM NaCl, and 15% glycerol. Finally, purified proteins were concentrated using Amicon Ultra-10K centrifugal filter devices, and protein concentration was determined via Bradford assay (BioRad) with BSA as a standard. All enzymes were stored at -80 ^{o}C and thawed on ice prior to use.

***In vitro* Methyltransferase Assay with Recombinant Enzymes**

Enzymatic reactions (20 μL) were setup containing 1 μM enzyme, 10 μM histone H3 peptide, and 100 μM cofactor or cofactor analogue in 50 mM Tris HCl (pH = 8.0)

buffer at 25 ^{o}C. Samples were then subject to MALDI-MS analysis as described above. For reactions containing full length histone as substrate, 1 μM GLP1 Y1211A or G9a Y1154A mutant was incubated with 20 μM recombinant histone H3 and 100 μM cofactor for 2 hours at 25 ^{o}C in buffer (40 μL) containing 50 mM Tris HCl (pH = 8.0) and 1 mM TCEP prior to trypsin digestion and LC/MS-MS analysis.

Cloning and Mutagenesis of Full-Length Human G9a and GLP1

For expression in eukaryotic cells, pCDNA3-FLAG vector encoding full-length human G9a were obtained as a generous gift from Dr. Jing Huang at the National Cancer Institute (NCI). Incorporation of full-length human GLP1 into the pCDNA3-FLAG vector was achieved by first installing a KPNI restriction site in its pFLAG-CMV2 vector using the QuickChange (Stratagene) site-directed mutagenesis kit according to manufacturer's instruction. Subsequent cloning was performed using KPNI and ECORI.HF restriction enzymes and confirmed by DNA sequencing. Y1211A and Y1154A mutants were generated on these mammalian vectors as described above.

Steady-State Kinetic Measurements

Confirmation of relative ionization efficiencies for independently synthesized R-modified histone H3 peptides was reported previously.[27] Reactions (10 μL) were initialized by addition of 1 μM recombinant enzyme into buffer (50 mM Tris HCl pH = 8.0) containing 25 μM histone H3 peptide (aa 1-21) and various concentrations of cofactor. MALDI matrix solution (1 μL) was then spotted and allowed to dry on a MALDI plate prior to addition of samples. At each time interval, 1 μL of sample was

applied to the MALDI plate on top of the previously spotted matrix solution. An additional 1.5 μL acetonitrile containing 0.1% TFA was added to each sample spot to ensure complete quenching of the reactions. The resultant sample spots were then air dried at room temperature and quantified by MALDI-TOF mass spectrometry as described above. Data was analyzed by first calculating the %Modification*min^{-1} for time-dependent experiments based on integrated peak areas observable in the MS. These data were then converted to Rate (min^{-1}) by multiplying by a factor of 0.25 (conversion of %Modification to μM of modified peptide) and then dividing the concentration of the enzymes. These rates were plotted against cofactor concentration, with k_{cat} and K_M calculated according to the standard Michaelis-Mentin formula.

Fluorescent Labeling of G9a/GLP1 Substrates

HEK293T cells transfected with GLP1 Y1211A, G9a Y1154A, or empty vector control were lysed via sonication (Misonix Ultrasonic Liquid Processor with a single 15 minute pulse at 65% amplitude). For samples containing recombinant G9a Y1154A or GLP1 Y1211A (2 μM), mock treated HEK293T cell lysates were used. Crude lysates were then centrifuged at 15,000 g for 45 minutes at 4 ^{o}C and the supernatant collected. Total protein concentrations in the supernatant were then calculated via Bradford assay as described above. Lysate (40 μg total protein) in 20 μL was incubated with 50 μM Hey-SAM or 250 μM Ab-SAM for 1-2 hours. Upon completion of the reaction, samples were passed through a detergent removal spin column and eluted with buffer containing 50 mM Tris HCl (pH = 8.0), 10% glycerol, 2 mM TCEP, and Roche protease inhibitor cocktail.

Samples treated with Hey-SAM were subjected to CuAAC according to the following procedure. CuAAC reaction was conducted using 100 μM Azido Rhodamine. 100 μM TBTA ligand, 1 mM $CuSO_4$ and 2.5 mM TCEP as final concentrations. Following a 1 hour reaction time, samples were precipitated with 600 μL methanol, 200 μL chloroform, and 400 μL water, then washed with 600 μL volumes of methanol 3 times. Protein pellets were allowed to air dry before being dissolved in protein loading buffer and subjected to SDS-PAGE.

Samples (whole cell lysates, modified histone proteins or peptides) treated with Ab-SAM were subjected to strain-promoted azide-alkyne cycloaddition (SPAAC) according to the following procedure. Modified samples were directly treated with 100 μM Click-It TAMRA-DIBO alkyne (no. C10410, Invitrogen) and shaken gently for 1 hour at room temperature in the absence of light. Following the reaction, protein samples were precipitated with 600 μL methanol, 200 μL chloroform, and 400 μL water, then washed with additional volumes of methanol 3 times. The resulting pellet was allowed to air dry for 15 minutes at room temperature, before being dissolved in protein loading buffer and resolved by SDS-PAGE.

After separation by SDS-PAGE, gels were washed with 10% acetic acid, 40% methanol, 50% water solution prior to visualized of fluorescently labeled proteins. Gels were imaged using an Amersham Biosciences Typhoon 9400 fluorescence imager (excitation = 532 nm, 580 nm filter, and 30 nm band-pass). Gels were lastly stained with Coomassie Blue to confirm protein loading.

Autoradiography Assay for GLP1 and G9a Substrates

Reactions (20 μL) were carried out at 25 ^{o}C overnight in buffer containing 50 mM Tris HCl (pH = 8.0) with 2.25 μM [methyl-3H]-SAM and 2 μM recombinant G9a or GLP1 in the presence of various substrates. Following the reaction, samples were resolved by SDS-PAGE and analyzed by autoradiography. Non-histone human substrates were obtained either from Origene Technologies (ACLY, PRMT5, IDH1), Abnova (TARS, PKIM1/2, Nucleolin, HAT1, EEF1A1, and HNRPK), or were gifts from Dr. Martin Walsh (POLR2A) and Dr. Hening Lin (PARP1).

Protein Crystallization and X-ray Structure Determination

Crystallographic experiments were performed by our collaborator, Dr. Jinrong Min. In brief, purified GLP1 Y1211A enzyme (10 mg/mL) was complexed with SAH and H3K9 N^{ε}-allyl peptide at 1:5:5 molar ratio of enzyme:SAH:peptide and crystallized using hanging drop vapor diffusion method at 20 ^{o}C by mixing 1 μL of the protein solution with 1 μL of the reservoir solution containing 20% PEG 4000, 10% isopropanol and 0.1 M HEPES (pH = 7.5). X-ray diffraction data were collected at 100K at the beamline23ID of Advanced Photon Sources (APS), Argonne National Laboratory. Data were processed using the HKL-2000 suite. The structure was solved by molecular replacement using MOLREP, using the crystal structure of GLP1 (PDB code 2IGQ) as the search model. ARPw/ARP was used for automatic model building and REFMAC was used for structure refinement. Graphics program COOT was used for model building and visualization. Crystal diffraction data and refinement statistics are given in Table 2.1.

Table 2.1: Crystallographic Data and Refinement Statistics.

	Y1211A+ H3K9(allyl)
PDB Code	4H4H
Data collection	
Space group	$P2_12_12_1$
Cell dimensions	
a, *b*, *c* (Å)	83.50, 83.80, 95.05
α, β, γ (°)	90, 90, 90
Resolution (Å) (highest resolution shell)	50.00-1.90 (1.95-1.90)
R_{merge}	7.2 (56.1)
$I/\sigma I$	31.6 (2.2)
Completeness(%)	98.6 (83.0)
Redundancy	7.9 (5.2)
Refinement	
Resolution (Å)	50.00-1.90
No. reflections	50,279
R_{work}/ R_{free}	0.179/0.224
No. atoms	
Protein	4,334
Cofactor	52
Water	518
Peptide	118
B-factors (Å^2)	30.4
Protein	18.9
Cofactor	24.9
Peptide	27.7
Water	27.0
RMSD	
Bond lengths (Å)	0.008
Bond angles (°)	1.145
Ramachandran plot % residues	
Favored	98.0
Additional allowed	2.0
Generously allowed	None
Disallowed	None

Proteomics Analysis of G9a/GLP1 Labeled Substrates in HEK293T Cells

HEK293T cell lysates of 10 mg from mock-transfected, GLP1 Y1211A-, and G9a Y1154A-transfeted cells were incubated with 50 μM Hey-SAM in a total 5 mL volume for 2 hours at ambient temperature (22 ^{o}C). Methanol of 25 mL was then added into each sample and kept at -80 ^{o}C overnight. The resultant samples were centrifuged for 30 min at 4,000 rpm. Supernatant was then removed and protein pellets were washed with 15 mL cold methanol. The pellets were air-dried for 25 min and re-dissolved with 4.5 mL SDS buffer containing 50 mM TEA (pH = 7.4), 150 mM NaCl, 4% SDS and 1×Roche protease inhibitor. Into the samples was added 0.5 mL click cocktail (100 μL of 5 mM azido-azo-biotin in DMSO, 100 μL of 100 mM TCEP, 250 μL of 2 mM of TBTA in DMSO, and 100 μL of 50 mM of $CuSO_4$). The click reaction was performed for 1.5 hrs and the samples were mixed with 25 mL methanol and kept at -80 ^{o}C overnight. The samples were resuspended in 1 mL SDS buffer (50 mM TEA pH = 7.4, 150 mM NaCl, 4% SDS, 1×Roche protease inhibitor and 10 mM EDTA), followed by the addition of 2 mL of the dilution buffer (50 mM TEA (pH = 7.4), 150 mM NaCl, 1% Brij97, and 1×Roche protease inhibitor). Streptavidin bead of 100 μL in the dilution buffer was mixed with the protein samples and rotated end-over-end at ambient temperature (22 °C) for 1 h. The resultant mixture was further diluted with 10 mL PBS buffer supplemented with 0.2% SDS and centrifuged at 2,000 rpm for 2 min. The streptavidin beads were washed with the buffer containing 10 mL PBS and 250 mM ammonium bicarbonate buffer (ABC) and then transferred into 1.5 mL micro centrifuge tubes. The resultant streptavidin beads were treated with the freshly-prepared reduction buffer (500 μL of 8 M urea, 25 μL of 200 mM TCEP, and 25 μL of 400 mM iodoacetamide) for 40 min in dark,

followed by the washing with 250 mM ABC buffer. The bead-immoblized proteins were treated twice with 250 μL of the elusion buffer (25 mM $Na_2S_2O_4$, 1% SDS and 250 mM ABC) for 30 minutes. Eluted samples were analyzed by LC-MS/MS as described below.

For Ab-SAM treated lysates, 10 mg total protein of mock-, Y1211A-, and Y1154A- transfected HEK293T cell lysates was used. These samples were incubated with/without 200 μM of Ab-SAM for 2 hours at room temperature. Lysates were then precipitated, washed, resuspended and treated with 200 μM of Click-iT biotin DIBO alkyne (cat. no. C10412, Invitrogen) and gently shaken for 1 hour at room temperature. 5 mL methanol was added to each sample and kept at -80 °C overnight. Precipitated proteins were centrifuged for 30 min at 4000 rpm at 4 °C and washed twice with 5 mL of cold methanol. Protein residues were dried for 20 min and resuspended with 400 μL of dilution buffer (50 mM triethylamine at pH 7.4, 150 mM NaCl, Roche protease inhibitor cocktail, 0.5% SDS) with brief sonication. Protein concentration was determined by Bradford assay. Twenty-five microliters of streptavidin bead in dilution buffer was added to the remaining protein and rotated end-over-end at room temperature for 1 hour. Samples were diluted with 10 mL of PBS buffer supplemented with 0.2% SDS and centrifuged for 2 min at 2000 rpm. Beads were successively washed with 10 mL of PBS and 250 mM ABC buffer and transferred to 1.5 mL micro centrifuge tubes. 40 μL of 1× sample buffer (Bio-RAD) was added and heated at 100 °C for 10 min. Prior to heating the streptavidin bound proteins with loading buffer, beads were treated with freshly made reduction buffer (500 μL of 8 M urea, 25 μL of 200 mM TCEP, and 25 μL of 400 mM iodoacetamide) for 40 min in dark and washed thoroughly with ABC buffer. The eluted proteins were separated on SDS-PAGE. Each lane on the 1D SDS PAGE was cut into

seven pieces, which were subjected to in-gel digestion. The gel bands ware reduced with 25 mM of DTT, and then alkylated with 55 mM iodoacetamide. The in-gel digestion was implemented with the trypsin (Promega, Fitchburg, WI) in 50 mM ABC at 37 °C overnight. The peptides were extracted with 0.1% formic acid in 50% acetonitrile at 37 °C for 30 min. Lastly, the peptide extraction was concentrated by speedvac.

For LC−MS/MS analysis, the digestion product was separated by a 65 min gradient elution at a flow rate 0.250 μL/min with the EASY-nLCII integrated nano-HPLC system (Proxeon, Denmark), which is directly interfaced with the Thermo LTQ-Orbitrap mass spectrometer. The analytical column was a homemade fused silica capillary column (75 μm ID, 150 mm length; Upchurch, Oak Harbor, WA) packed with C-18 resin (300 A, 5 μm, Varian, Lexington, MA). Mobile phase A consisted of 0.1% formic acid, and mobile phase B consisted of 100% acetonitrile and 0.1% formic acid. The LTQ-Orbitrap mass spectrometer was operated in the data-dependent acquisition mode using the Xcalibur 2.0.7 software, and there is a single full-scan mass spectrum in the Orbitrap (400−1800 m/z, 30 000 resolution) followed by 20 data-dependent MS/MS scans in the ion trap at 35% normalized collision energy.

The Thermo Proteome Discoverer 1.2.0 software was used to search the MS/MS data against in ipi.HUMAN.v3.82 database. The searching parameters included peptide mass tolerance of 10 ppm, ms/ ms tolerance of 0.8 Da, and two missed cleavages allowed. The fixed modification of carbamidomethylation on cysteine and variable modifications of oxidation on methionine, deamidated on asparagine and glutamine, and Hey-SAM/Ab-SAM modified Lys were also used in the database searching. The decoy database search was added with the criteria of FDR at 0.01. The criteria used for filtering peptide were the

following: 2, 2.75, and 3 for singly charged, doubly charged, and triply or higher charged ions, respectively.

Tandem Mass Tagging (TMT) for Quantitative MS Analysis of Proteome-wide Substrates of G9a/GLP1

For quantitative comparison of BPPM-revealed target proteins, samples were prepared as described above. Briefly, Hey-SAM incubated HEK293T cell lysates (either mock-, Y1211A-, or Y1154A-transfected) were precipitated using methanol. Precipitated proteins were redissolved in SDS buffer and subjected to 'click' chemistry with azido-azo-biotin. The ligated proteins were further precipitated using methanol and subsequently enriched with streptavidin beads prior to elution with 25 mM $Na_2S_2O_4$ as detailed in the preceding section. Eluted proteins were first resolved by SDS PAGE. The gel bands of corresponding molecular weights were excised, reduced with 10 mM of DTT and alkylated with 55 mM iodoacetamide. In gel digestion was then carried out with the sequence grade modified trypsin (Promega, Fitchburg, WI) in 50 mM ABC at 37 ^{o}C overnight. The peptides were extracted twice with 1% trifluoroacetic acid in 50% acetonitrile aqueous solution for 30 min. The extracts were then centrifuged in a Speedvac to reduce the volume. Peptides from different samples were labeled with TMT reagents (Thermo, Pierce Biotechnology, Rockford, IL) according to the manufacture's instruction. Briefly, the TMT label reagents were dissolved by anhydrous acetonitrile, carefully added to each digestion products (126, 128 and 131 mass tagging were used for control vector-, GLP1- and G9a-transfetcted samples, respectively). The reaction

mixtures were incubated for 1 hour at ambient temperature (22 ^{o}C) and then quenched by hydroxylamine. The TMT-labeled peptides were desalted using the stage tips.

For the subsequent LC-MS/MS analysis, the TMT-labeled peptides were separated by a 65 min gradient elution at a flow rate 0.250 μL/min with the EASY-nLCIITM integrated nano-HPLC system (Proxeon, Denmark), which is directly interfaced with the Thermo LTQ-Orbitrap mass spectrometer. The analytical column was a home-made fused silica capillary column (75 μm ID, 150 mm length; Upchurch, Oak Harbor, WA) packed with C-18 resin (300 A, 5 μm, Varian, Lexington, MA). Mobile phase A consisted of 0.1% formic acid, and mobile phase B consisted of 100% acetonitrile and 0.1% formic acid. The LTQ-Orbitrap mass spectrometer was operated in the data-dependent acquisition mode using the Xcalibur 2.0.7 software and there is a single full-scan mass spectrum in the Orbitrap QE (400-1800 m/z, 30,000 resolution) followed by 10 MS/MS scans in the quadrupole collision cell using the higher energy collision dissociation (HCD). The MS/MS spectra from each LC-MS/MS run were searched against the selected database using an in-house Mascot or Proteome Discovery (Version 1.3) searching algorithm.

2.3 RESULTS AND DISCUSSION

Qualitative Determination of Enzyme/Cofactor Pairs for BPPM

Initial examination of cofactor/mutant enzyme compatibility was carried out via MALDI-MS screening. These efforts primarily focused on β-sp^2-hybridized SAM analogues, as it had previously been established that β-sp^3- and β-sp^1-hybridized analogues were either unreactive or unstable, respectively.[10, 11, 28] Additionally, a library

of mutant G9a and GLP1 enzymes containing smaller aliphatic residues in their cofactor binding sites was generated and tested. Interestingly, the majority of these mutant enzymes demonstrated no observable activity towards any of the SAM analogues examined (Figure 2.3). In fact, mutation of several tyrosine or phenylalanine residues in G9a (Y1067, Y1085, F1087, F1138, F1158, and W1159) and GLP1 (Y1124, Y1142, F1144, F1195, F1215, and W1216) also resulted in a significant loss of activity towards endogenous SAM (Figure 2.3). Given these two observations, it is likely that mutation of these residues results in disruption of the catalytic channel or cofactor-binding pocket.

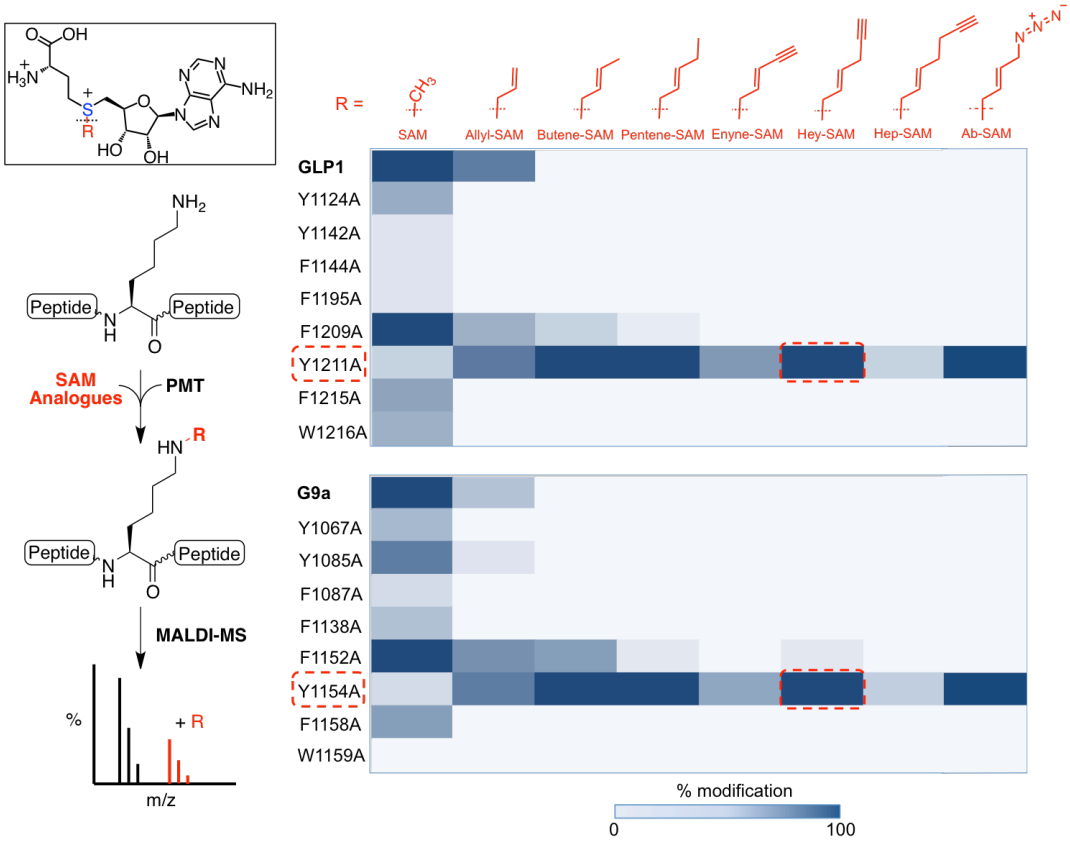

Figure 2.3: Qualitative Assessment of SAM Analogue Compatibility with Engineered G9a or GLP1. Extent of modification of H3K9 peptide by SAM or SAM analogues by wild-type or engineered G9a and GLP1 as examined by MALDI-MS analysis. Data is represented in heat-map format as % modification of peptide substrate.

In contrast, a structurally conserved mutant for both GLP1 (F1209A) and G9a (F1152A) was identified that maintained enzyme activity towards SAM or several of the SAM analogues tested. Compared to wild-type enzymes, these mutants demonstrate slightly increased activity towards the bulkier butene-SAM and pentene-SAM (Figure 2.3). However, no compatibility for these mutants was observed towards our 'click'-able alkyne- or azide-containing SAM analogues. Fortunately, mutation of a conserved residue for both G9a (Y1154A) and GLP1 (Y1211A) were identified that demonstrate excellent compatibility towards a wide variety of SAM analogues tested (Figure 2.3). Importantly, these mutant enzymes demonstrated good activity primarily towards the alkyne-containing Hey-SAM and the azide-containing Ab-SAM cofactor analogues, which are not compatible with wild-type enzymes. Furthermore, these mutants displayed very low activity toward SAM, which is ideal for BPPM as it limits competition between endogenous SAM and our non-natural SAM analogues.

Kinetic Analysis of Enzyme/Cofactor Pairs

In order to further explore the structure-activity relationship between our engineered enzymes and cofactor analogues, we performed steady-state kinetics analysis for the determination of apparent k_{cat} and K_M values with the Y1211A and Y1154A mutants using MALDI-MS detection. It had been previously demonstrated that the relative ionization efficiencies for the R-modified peptides examined were roughly equivalent to that of methylated or unmodified peptides.[27] These studies were essential for accurate measurement of kinetic parameters, as a difference in ionization efficiency would result in an artificial increase or decrease in the observable rate.

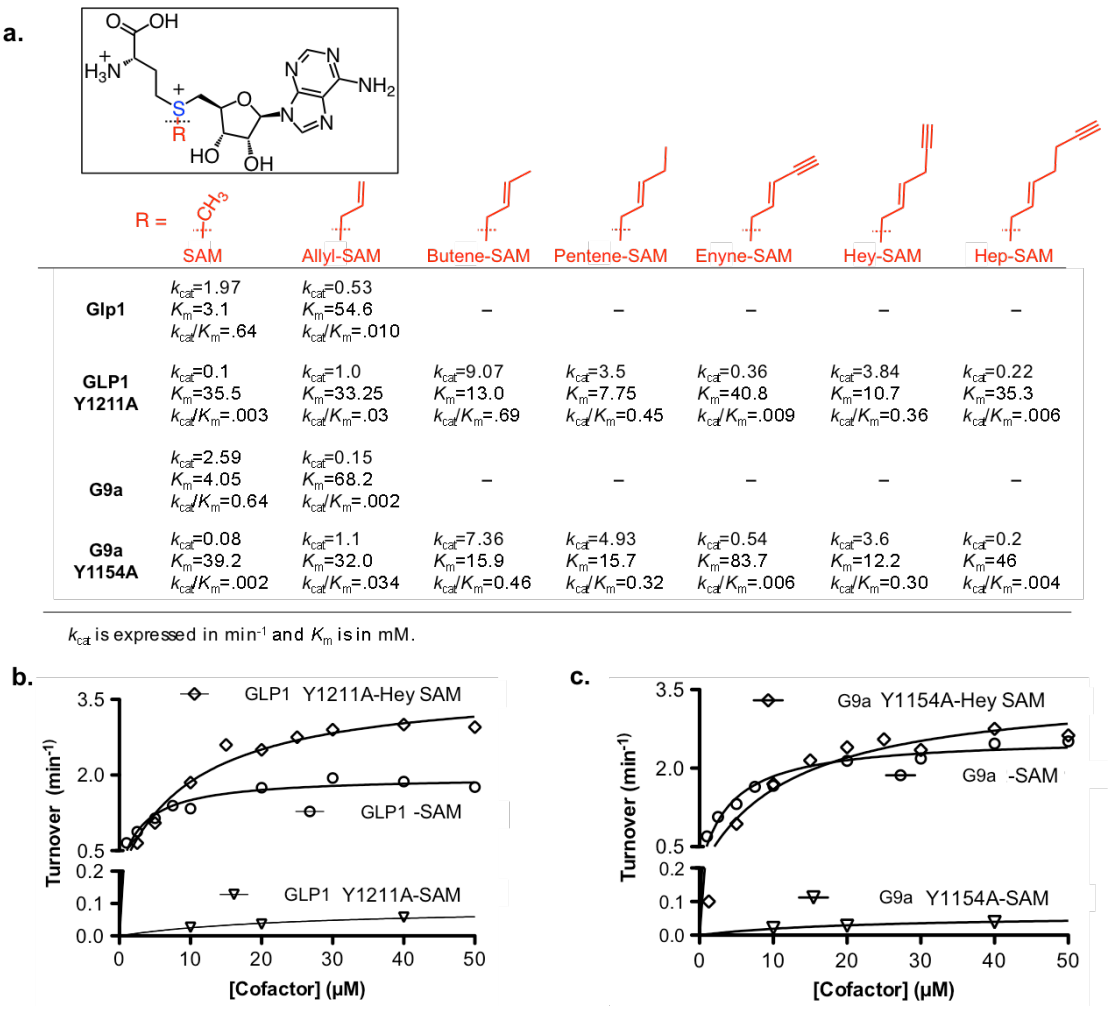

Figure 2.4: Steady-state kinetic analysis of wild-type G9a/GLP1 and the Y1154A/Y1211A mutants with SAM analogues. (a) Apparent K_M and k_{cat} were determined using 25 μM H3K9 (aa 1-21) peptide and varied cofactor concentrations. (b) Rate comparison between wild-type GLP1 with SAM vrs. GLP1 Y1211A with SAM or Hey-SAM. (c) Rate comparison between wild-type G9a with SAM vrs. G9a Y1154A with SAM or Hey-SAM.

With this foundation established, reaction rates for wild-type GLP1, GLP1 Y1211A, wild-type G9a, and G9a Y1154A enzymes in the presence of a panel of cofactors were determined and fitted to the Michaelis-Menten formula prior to extraction of kinetics values (Figure 2.4a). Interestingly, catalytic efficiencies (k_{cat}/K_M) correlated nicely with our previous qualitative assessment of cofactor compatibility (Figure 2.3).

Both mutants displayed very low catalytic efficiency towards native SAM, which was important for their application in cell lysates where native SAM could potentially compete with our cofactor analogues. Furthermore, the G9a Y1154A and GLP1 Y1211A mutants displayed highest compatibility towards butane-SAM, pentene-SAM, and Hey-SAM analogues, with k_{cat}/K_M values comparable to those of wild-type enzymes towards SAM (Figure 2.4a, b). Given that Hey-SAM was the only of these three analogues to contain a viable chemical handle, it was selected as the primary candidate for BPPM. Here, the kinetics of the azide-containing Ab-SAM analogue was not examined. However, due to the fact that Ab-SAM is roughly equivalent in size to the Hep-SAM analogue (Figure 2.4a), which was shown to be relatively inactive in comparison to Hey-SAM, it was predicted that Hey-SAM would be an optimal candidate for BPPM analysis. Despite this, the Ab-SAM cofactor was also used for comparison during labeling full-length proteins and proteomic analysis of cell lysates (see below).

Structural Basis for GLP1 Y1211A Compatibility Toward SAM Analogues

In order to examine the structural basis for the recognition of bulkier SAM analogues by the GLP1 Y1211A and G9a Y1154A mutants, the crystal structure of the Y1211A mutant in ternary complex with an H3K9 ε-amino-allyl-lysine-modified peptide and SAH was determined through collaboration with the laboratory of Dr. Jinrong Min (PDB: 4H4H). As was predicted, the allyl-modified peptide appeared to nicely occupy a cavity created by the Y1211A mutation (Figure 2.5a). This preexisting cavity appears to be composed of the hydrophobic side chains of the H1170, F1209, F1215, and W1216 residues, as well as the backbone peptides bonds of I1168 and N1169. Given that the

allyl moiety is pointed towards this preexisting hydrophobic cavity and resembles many of the SAM analogues previously shown to be enzyme compatible, it is expected that other SAM analogues make use of the space created by the Y1211A/Y1154A mutation for substrate labeling as well.

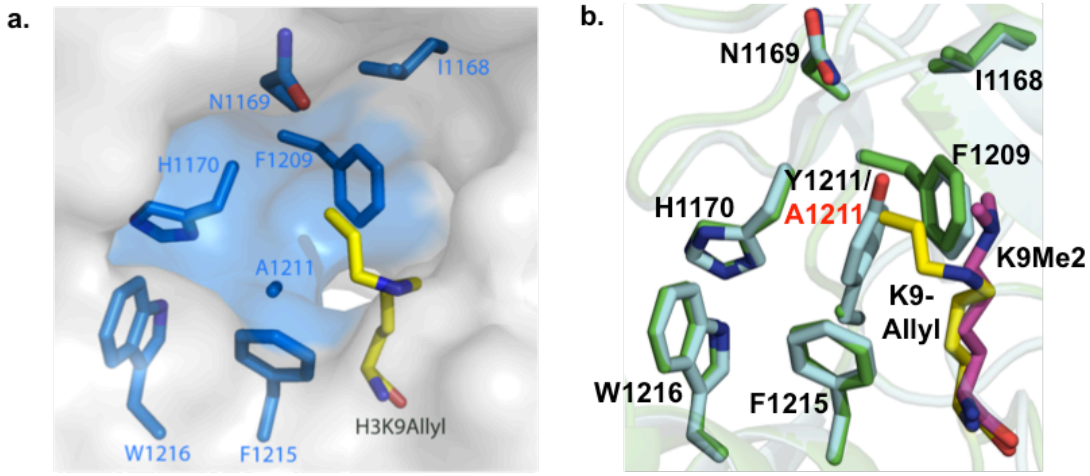

Figure 2.5: Structural Basis for GLP1 Y1211A Mutant Recognition of SAM Analogues. (a) Allylated histone H3K9 peptide is accommodated by the hydrophobic cavity generated by mutation of Y1211 (PDB 4H4H). (b) Superimposed structures of wild-type GLP1 (Teal; PDB 2RFI) and the Y1211A mutant with allylated peptide (Green; PDB 4H4H). Both wild-type and mutant GLP1 shared a very high degree of structural homology.

Close examination of the overlaid structures of wild-type GLP1 and the Y1211A mutant further reveals that the terminal β-sp^2-hybridized allyl carbon rests in close proximity to the Y1211 side-chain (Figure 2.5b). This suggests that the Y1211 residue in the wild-type enzyme acts to block the bulkier β-sp^2-hybridized SAM analogues and prevent their interaction with the active site. In contrast, replacing the Y1211 residue with the smaller alanine mutant not only avoids such steric clash, but also allows access to and additional interactions with the extended hydrophobic pocket. Given that the Y1211/Y1154 residues are generally conserved residues in the hydrophobic channels of

most SET domain-containing PKMTS,[2] we suspect that corresponding residues in other enzymes will likely be important target residues for enzyme engineering efforts as well.

Labeling of Full-Length Histone with SAM Analogues

In order to further characterize the activities of the GLP1 Y1211A and G9a Y1154A mutants with functionalized SAM analogues, we next attempted to label known protein substrates for these enzymes. For these purposes, both full-length histone H3 and reconstituted histone octamers were used to confirm engineered enzyme activity and specificity. As seen in Figure 2.6c, labeled H3 was observable by fluorescence imaging in samples treated with G9a Y1154A and Hey-SAM, followed by conjugation to a fluorescent probe. In addition, only labeled histone H3 was observed upon treatment with the Ab-SAM cofactor analogue, even within the context of a reconstituted histone octamer (Figure 2.6a, b). Importantly, no labeling could be observed in any no-enzyme or no-cofactor controls, or on non-substrate histone components. Lastly, LC-MS/MS analysis of G9a/GLP1-modified tryptic histone H3 confirmed transfer of Hey-SAM's or Ab-SAM's R-groups to lysine 9 of histone H3 (Figure 2.7). Together, these data suggest that both enzyme processivity and specificity are maintained for the mutant enzymes and cofactors tested.

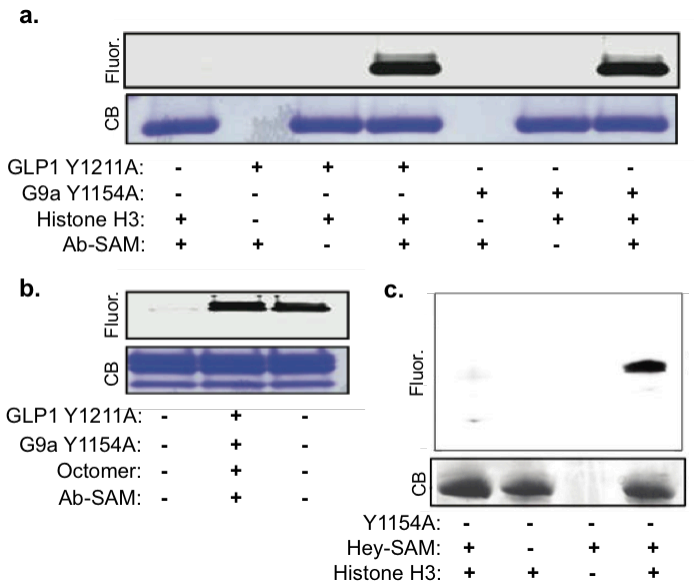

Figure 2.6: In-Gel Fluorescence Analysis of Ab-SAM or Hey-SAM Modified Full-Length Histone H3. (a) Modification of recombinant H3 by G9a Y1154A and GLP1 Y1211A by Ab-SAM. (b) In a reconstituted octomer consisting of histones H2A, H2B, H3, H4, only histone H3 appeared to be modified with Ab-SAM by G9a/GLP1 mutants. (c) Hey-SAM demonstrated similar activity towards engineered enzyme for the labeling of full-length Histone H3. No labeling was observed in no-enzyme or no-cofactor controls.

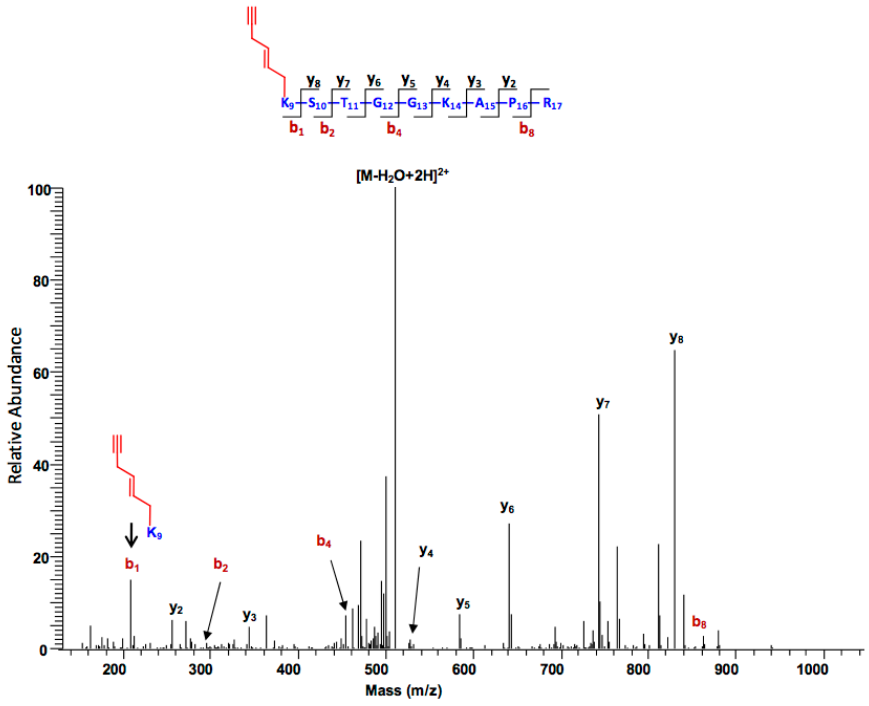

Figure 2.7: MS/MS Spectrum of Hey-SAM Modified Tryptic Histone H3 Peptide. Full-length H3 was reacted with Hey-SAM and G9a Y1154A enzyme prior to trypsinization and LC-MS/MS.

Labeling of G9a/GLP1 Substrates in HEK293T Cell Lysates

Successful identification of active mutant-cofactor pairs, as was described above, allowed for further application of this technology to more complicated biochemical mixtures. For this purpose, HEK293T cells were transfected with empty vector, wild-type or G9a Y1154A/GLP1 Y1211A enzymes (Figure 2.8a) prior to lysis and treatment with our cofactor analogues. Subsequent conjugation with fluorescently labeled chemical probes allowed for visualization of engineered enzyme targets in cell lysate. As shown in Figure 2.8b, significant labeling could be observed in G9a Y1154A and GLP1 Y1211A transfected cell lysates treated with Ab-SAM, but not in cells transfected with wild-type G9a/GLP1 or those treated with empty vector. Furthermore, treatment of cells with Hey-SAM resulted in similar labeling. Indeed, G9a Y1154A- and GLP1 Y1211A-transfected cells treated with Hey-SAM demonstrated a very similar fluorescent pattern to that of Ab-SAM. In contrast, very little labeling could be observed in mock-transfected HEK293T cells (Figure 2.8b). Together, the observed labeling patterns suggest that the Ab-SAM and Hey-SAM cofactors act with transfected G9a and GLP1 mutants to label substrates in cell lysate.

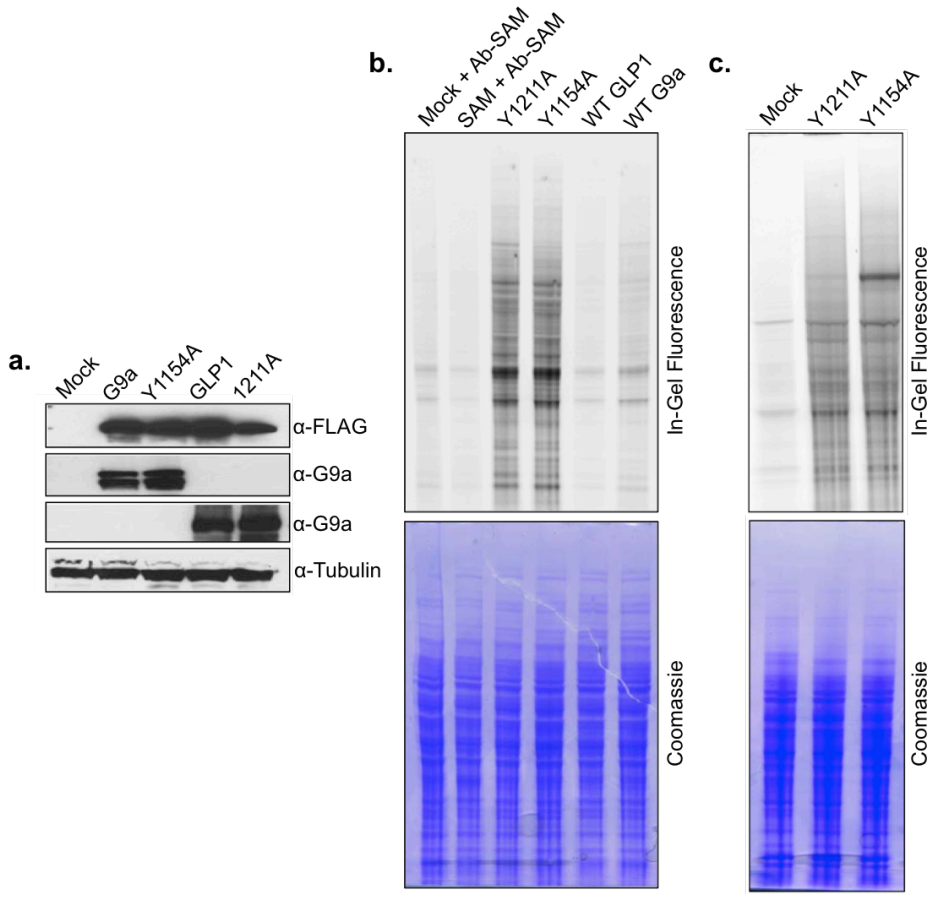

Figure 2.8: Labeling of G9a/GLP1 Substrates in HEK293T Cell Lysate. (a) Western blot demonstrating transfection and expression of G9a, GLP1 and mutant proteins. Tubulin was used as a loading control. (b) Cell lysates treated with Ab-SAM followed by conjugation to a fluorescent TAMRA-DIBO probe. Top panel, increased labeling in mutant-transfected, but not mock-treated or Ab-SAM + SAM treated, HEK293T cells by in-gel fluorescence. Bottom panel, coomassie staining of SDS-PAGE resolved lysate. (c) Cell lysates treated with Hey-SAM followed by conjugation to a fluorescent TAMRA-azide probe. Top panel, increased labeling in mutant-transfected, but not mock-treated, HEK293T cells by in-gel fluorescence. Bottom panel, coomassie staining of SDS-PAGE resolved lysate.

Proteomics Analysis of G9a/GLP1 Substrates in HEK293T Cell Lysates

Given the apparent success of BPPM-based fluorescent labeling of PKMT targets in cell lysates, we next sought to couple substrate labeling with proteomics-based identification of G9a/GLP1 candidate substrates. Initial experiments examined labeling of enzyme substrates in HEK293T cell lysates using both Ab-SAM and Hey-SAM for comparison (Figure 2.9a). These experiments were performed using empty vector or

wild-type enzymes as controls and was achieved through the use of affinity-based biotin-DIBO or azido-azo-biotin probes for Ab-SAM and Hey-SAM modified proteomes, respectively.

Subsequent proteomic analysis of Ab-SAM treated samples identified a combined total of 128 potential substrates for both the G9a and GLP1 enzymes, of which 18 were shared (Figure 2.9a). Despite the relatively low number of putative substrates, several previously verified targets of the GLP1/G9a PKMTs were observed in the mutant-transfected data sets, including histone H3, histone H1.4, Wiz, CDYL, and G9a/GLP1 (automethylation) suggesting the experiment was behaving correctly. Given our previous quantitative assessment of mutant/cofactor compatibility (Figure 2.4), however, we suspected that the relatively small size of the data sets derived using the Ab-SAM cofactor was likely the result of low catalytic efficiency towards the Y1211A and Y1154A mutants. As discussed in the above subsection, Ab-SAM closely resembles the Hep-SAM analogue in terms of R-group size, which displayed significantly lower catalytic efficiency in comparison to the 'click'-able Hey-SAM analogue. Therefore, because Hey-SAM had k_{cat}/K_M values towards our engineered enzymes that were very comparable to those of wild-type enzymes with SAM, it was decided to perform further study with this mutant/cofactor pair in order to improve the efficiency of our BPPM approach. Indeed, pull-down and proteomic analysis of HEK293T lysate using the Hey-SAM analogue resulted in a much larger data set for both G9a and GLP1 after comparison to empty-vector controls. By this approach, data sets for GLP1 and G9a contained 1,324 and 1,648 potential targets, respectively, with roughly 36% (799

proteins) overlap (Figure 2.9a). This roughly six-fold increase in target identification was consistent with the increased compatibility of Hey-SAM towards our engineered enzymes.

Following our initial qualitative proteomic studies, additional studies incorporated a common quantitative proteomic approach using an isobaric tandem mass tagging (TMT) strategy. Here, tryptic peptides derived from pulled-down PKMT substrates in Hey-SAM treated experimental and control samples were reacted with isobaric reagents containing different reporter *m/z* values, mixed, and analyzed LC-MS/MS. Reporter ions distinct to the isobaric TMT reagents used provided quantitative abundance measurements for the identified protein sequences, which resulted in a total of 1,145 potential PMT substrates with >1.5 fold enrichment by TMT analysis (Figure 2.9b). Further cross-analysis between TMT-labeled and non-TMT-labeled proteomic data sets allowed for the identification of 774 overlaid targets (Figure 2.9c), which were designated as 'high-confidence' substrates for the G9a and GLP1 PKMTs. Included in this list high confidence substrates was, again, the previously identified substrates discussed above, as well as several others including: DNMT1, p53, and HDAC1 (Figure 2.9d). Such consistency implies the robustness of the BPPM approach to label, enrich and identify the substrates of designated enzymes in complex biochemical settings. Of these high confidence substrates, several commercially available proteins were validated as genuine substrates for the G9a and GLP1 PKMTs as is described in the following subsection.

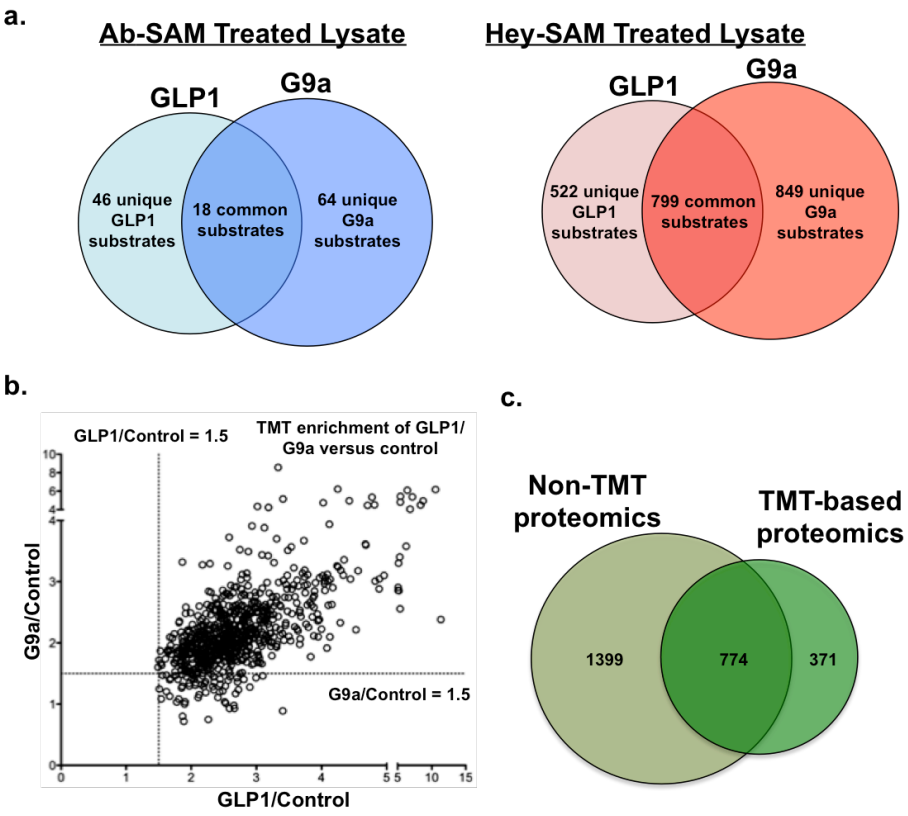

d.

Substrate	G9a/GLP1 Transfected	Control
Histone H1.4	Yes	No
Histone H3	Yes	No
GLP1	Yes	No
G9a	Yes	No
Wiz protein	Yes	No
CDYL protein	Yes	No
DNMT1	Yes	No
p53	Yes	No
HDAC1	Yes	No

Figure 2.9: Proteomic Analysis of BPPM-Derived Putative Substrates for the G9a and GLP1 PKMTs. (a) Non-quantitative proteomic analysis of GLP1 and G9a substrates in HEK293T cells using either Ab-SAM or Hey-SAM. As predicted by kinetics analysis of mutant/cofactor compatibility, Hey-SAM treated samples resulted in the identification of a significantly larger number of putative substrates. (b) Correlation analysis of high confidence GLP1/G9a targets. Abundance ratios for TMT-analyzed samples were plotted against unique target ID. (c) Comparison of data sets between quantitative TMT-proteomic data sets and non-TMT data sets. (d) Previously identified GLP1/G9a proteins that were also identified in our mutant/cofactor sample sets but not controls.

Validation of Novel Substrates for the G9a/GLP1 PKMTs

To validate high-confidence proteomic targets as *bona fide* substrates of the GLP1 and G9a PKMTs, a representative panel of commercially available substrates was selected from our proteomics lists. This included proteins such as nucleolin, EEF1A1, POLR2A, HAT1, PARP1, PKIM1, HNPRK, TARS, ACLY, PRMT5 and IDH1. For these experiments, wild-type recombinant G9a and GLP1 were incubated with the putative substrates in the presence of radioactive ^{3}H-SAM. Subsequent autoradiographic analysis confirmed methylation by either GLP1 or G9a for 11 of the non-histone substrates examined (Figure 2.10). Interestingly, some of the methylated substrates appeared to be differentially methylated by both G9a and GLP1, suggesting these enzymes may exhibit different substrate preferences despite their high degree of enzyme homology. The ready validation of these proteins as substrates for G9a and GLP1 thus demonstrates the merit of BPPM technology to identify novel substrates of PKMTs in complex biochemical mixtures.

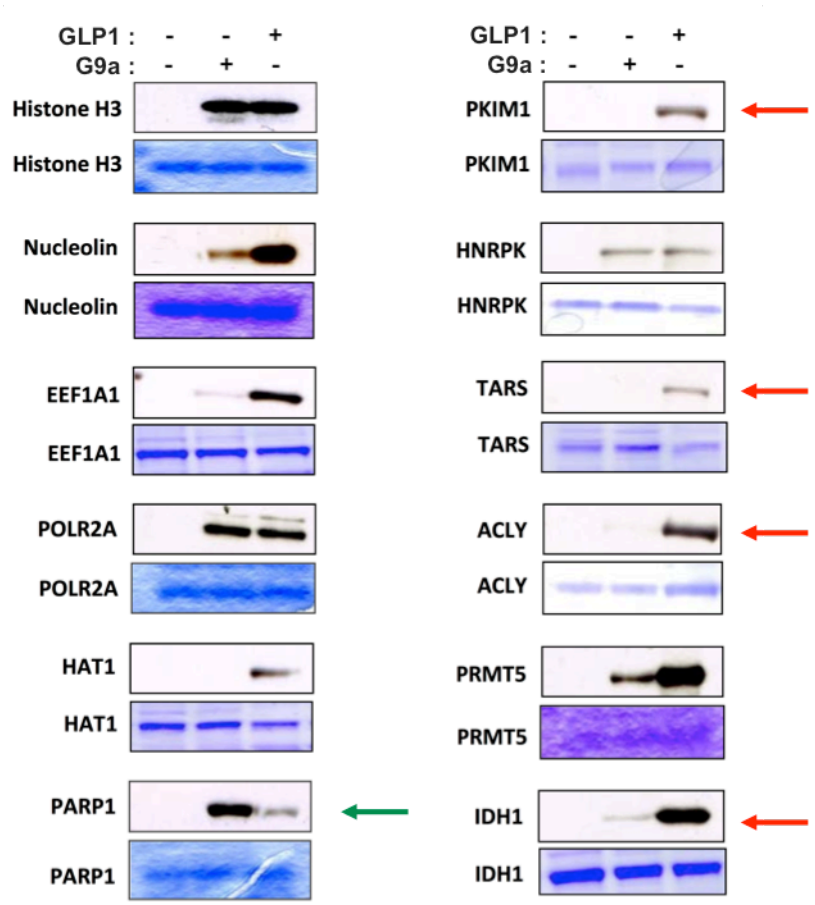

Figure 2.10: Validation of *in vitro* methylation activities of G9a/GLP1 via autoradiography assay. Wild-type G9a/GLP1 were used to examine a panel of commercially available non-histone substrates identified by BPPM: TARS, threonyl-tRNA synthetase; ACLY, ATP citrate synthase/lyase; IDH1, soluble isocitrate dehydrogenase 1 (NADP+); PRMT5, protein arginine N-methyltransferase 5; EEF1A1, eukaryotic translation elongation factor 1 alpha 1; POLR2A, DNA-directed RNA polymerase II subunit RPB1 (C-terminal domain); HAT1, histone acetyltransferase 1; PARP1, poly-[ADP-ribose] polymerase 1; PKIM1/2, pyruvate kinase isozymes M1/M2; HNRPK, heterogeneous nuclear ribonucleoprotein K. Green arrows highlight substrates preferentially methylated by G9a, whereas red arrows highlight substrates preferentially methylated by GLP1.

2.4 CONCLUSIONS

Based on the research presented herein, we have been able to demonstrate the viability of BPPM technology to dissect the substrate profiles of the closely related G9a and GLP1 PKMTs. This was achieved through the establishment of several key pieces of information: (i) the identification efficient mutant/cofactor analogue pairs, (ii) use of these mutant enzymes for substrate labeling of full length proteins in complex

biochemical milieu, and (iii) proteomics analysis of bioorthogonally labeled substrates in cell lysate for validation as enzyme substrates.

Establishment of mutant/cofactor pairs was initially achieved through the screening of recombinant enzyme and cofactor analogue libraries. After identification of promising pairs, catalytic efficiency was then confirmed through steady-state kinetic analysis. By this approach, the GLP1 Y1211A and G9a Y1154A mutants were established as having comparable catalytic efficiency to wild-type enzyme when using the 'click'-able Hey-SAM analogue. As such, this enzyme/cofactor pair was primarily used for subsequent application of BPPM, although the azide-containing Ab-SAM also demonstrated some merit as well. After showing that full-length protein substrates could be modified selectively, full-length engineered enzymes were expressed in HEK293T cells. Subsequent lysis and supplementation with cofactor analogues allowed for labeling of G9a and GLP1 substrates in a complex biochemical setting. Finally, through proteomics analysis, putative targets labeled by our approach were isolated and identified. Through this approach, a total of 11 novel substrates for the G9a and GLP1 enzymes were validated, along with a large number of putative targets that remain to be examined.

All told, these experiments may serve as a roadmap for future application of BPPM to various other enzymes. As discussed above, many SET-domain containing PKMTs share key structural features in their catalytic domain. By focusing engineering efforts on these conserved residues in other enzymes, application of BPPM for the identification of their substrates may be greatly facilitated. Indeed, ongoing work by other members of our lab has been successful for the application of BPPM to the SET7/9, SET8, and SETDB1 enzymes. Furthermore, our initial application in HEK293T cells

also serves as a demonstration of the potential application of BPPM in a more disease relevant context. Future work will likely be focused on determining the biological effects associated with the methylation of the identified substrates, as well as application of BPPM in cancer cell-lines or disease models, in order to better understand the pathological effects associated with aberrant methyltransferase function.

2.5 REFERENCES

1. Taverna, S. D.; Li, H.; Ruthenburg, A. J.; Allis, C. D.; Patel, D. J., How chromatin-binding modules interpret histone modifications: lessons from professional pocket pickers. *Nat. Struct. Mol. Biol.* **2007,** *14*, 1025-1040.
2. Dillon, S. C.; Zhang, X.; Trievel, R. C.; Cheng, X., The SET-domain protein superfamily: protein lysine methyltransferases. *Genome biology* **2005,** *6*, 227.
3. Schapira, M., Structural Chemistry of Human SET Domain Protein Methyltransferases. *Current chemical genomics* **2011,** *5*, 85-94.
4. Chiu, V. K.; Silletti, J.; Dinsell, V.; Wiener, H.; Loukeris, K.; Ou, G.; Philips, M. R.; Pillinger, M. H., Carboxyl methylation of Ras regulates membrane targeting and effector engagement. *J Biol Chem* **2004,** *279*, 7346-52.
5. Strahl, B. D.; Allis, C. D., The language of covalent histone modifications. *Nature* **2000,** *403*, 41-5.
6. Islam, K.; Bothwell, I.; Chen, Y.; Sengelaub, C.; Wang, R.; Deng, H.; Luo, M., Bioorthogonal profiling of protein methylation using azido derivative of S-adenosyl-L-methionine. *J Am Chem Soc* **2012,** *134*, 5909-15.
7. Islam, K.; Chen, Y.; Wu, H.; Bothwell, I. R.; Blum, G. J.; Zeng, H.; Dong, A.; Zheng, W.; Min, J.; Deng, H.; Luo, M., Defining efficient enzyme-cofactor pairs for bioorthogonal profiling of protein methylation. *Proc Natl Acad Sci U S A* **2013,** *110*, 16778-83.
8. Bishop, A.; Buzko, O.; Heyeck-Dumas, S.; Jung, I.; Kraybill, B.; Liu, Y.; Shah, K.; Ulrich, S.; Witucki, L.; Yang, F.; Zhang, C.; Shokat, K. M., Unnatural ligands for engineered proteins: new tools for chemical genetics. *Annual review of biophysics and biomolecular structure* **2000,** *29*, 577-606.
9. Bishop, A. C.; Ubersax, J. A.; Petsch, D. T.; Matheos, D. P.; Gray, N. S.; Blethrow, J.; Shimizu, E.; Tsien, J. Z.; Schultz, P. G.; Rose, M. D.; Wood, J. L.; Morgan, D. O.; Shokat, K. M., A chemical switch for inhibitor-sensitive alleles of any protein kinase. *Nature* **2000,** *407*, 395-401.
10. Dalhoff, C.; Lukinavicius, G.; Klimasauskas, S.; Weinhold, E., Direct transfer of extended groups from synthetic cofactors by DNA methyltransferases. *Nat. Chem. Biol.* **2006,** *2*, 31-32.

11. Islam, K.; Zheng, W.; Yu, H.; Deng, H.; Luo, M., Expanding cofactor repertoire of protein lysine methyltransferase for substrate labeling. *Acs Chem Biol* **2011,** *6*, 679-84.
12. Wang, R.; Zheng, W.; Yu, H.; Deng, H.; Luo, M., Labeling substrates of protein arginine methyltransferase with engineered enzymes and matched S-adenosyl-L-methionine analogues. *J Am Chem Soc* **2011,** *133*, 7648-51.
13. Tachibana, M.; Sugimoto, K.; Fukushima, T.; Shinkai, Y., SET domain-containing protein, G9a, is a novel lysine-preferring mammalian histone methyltransferase with hyperactivity and specific selectivity to lysines 9 and 27 of histone H3. *J. Biol. Chem.* **2001,** *276*, 25309-25317.
14. Ogawa, H.; Ishiguro, K.; Gaubatz, S.; Livingston, D. M.; Nakatani, Y., A complex with chromatin modifiers that occupies E2F-and Myc-responsive genes in G(0) cells. *Science* **2002,** *296*, 1132-1136.
15. Shinkai, Y.; Tachibana, M., H3K9 methyltransferase G9a and the related molecule GLP. *Genes Dev* **2011,** *25*, 781-8.
16. Fritsch, L.; Robin, P.; Mathieu, J. R.; Souidi, M.; Hinaux, H.; Rougeulle, C.; Harel-Bellan, A.; Ameyar-Zazoua, M.; Ait-Si-Ali, S., A subset of the histone H3 lysine 9 methyltransferases Suv39h1, G9a, GLP, and SETDB1 participate in a multimeric complex. *Mol Cell* **2010,** *37*, 46-56.
17. Rathert, P.; Dhayalan, A.; Murakami, M.; Zhang, X.; Tamas, R.; Jurkowska, R.; Komatsu, Y.; Shinkai, Y.; Cheng, X. D.; Jeltsch, A., Protein lysine methyltransferase G9a acts on non-histone targets. *Nat. Chem. Biol.* **2008,** *4*, 344-346.
18. Lee, J. S.; Kim, Y.; Kim, I. S.; Kim, B.; Choi, H. J.; Lee, J. M.; Shin, H. J.; Kim, J. H.; Kim, J. Y.; Seo, S. B.; Lee, H.; Binda, O.; Gozani, O.; Semenza, G. L.; Kim, M.; Kim, K. I.; Hwang, D.; Baek, S. H., Negative regulation of hypoxic responses via induced Reptin methylation. *Mol Cell* **2010,** *39*, 71-85.
19. Huang, J.; Dorsey, J.; Chuikov, S.; Perez-Burgos, L.; Zhang, X.; Jenuwein, T.; Reinberg, D.; Berger, S. L., G9a and Glp methylate lysine 373 in the tumor suppressor p53. *J Biol Chem* **2010,** *285*, 9636-41.
20. Chang, Y.; Sun, L.; Kokura, K.; Horton, J. R.; Fukuda, M.; Espejo, A.; Izumi, V.; Koomen, J. M.; Bedford, M. T.; Zhang, X.; Shinkai, Y.; Fang, J.; Cheng, X., MPP8 mediates the interactions between DNA methyltransferase Dnmt3a and H3K9 methyltransferase GLP/G9a. *Nature communications* **2011,** *2*, 533.
21. Ling, B. M.; Bharathy, N.; Chung, T. K.; Kok, W. K.; Li, S.; Tan, Y. H.; Rao, V. K.; Gopinadhan, S.; Sartorelli, V.; Walsh, M. J.; Taneja, R., Lysine methyltransferase G9a methylates the transcription factor MyoD and regulates skeletal muscle differentiation. *Proc Natl Acad Sci U S A* **2012,** *109*, 841-6.
22. Wu, H.; Min, J.; Lunin, V. V.; Antoshenko, T.; Dombrovski, L.; Zeng, H.; Allali-Hassani, A.; Campagna-Slater, V.; Vedadi, M.; Arrowsmith, C. H.; Plotnikov, A. N.; Schapira, M., Structural biology of human H3K9 methyltransferases. *PLoS One* **2010,** *5*, e8570.
23. Collins, R. E.; Tachibana, M.; Tamaru, H.; Smith, K. M.; Jia, D.; Zhang, X.; Selker, E. U.; Shinkai, Y.; Cheng, X. D., In vitro and in vivo analyses of a Phe/Tyr

switch controlling product specificity of histone lysine methyltransferases. *J. Biol. Chem.* **2005,** *280*, 5563-5570.
24. Blum, G.; Bothwell, I. R.; Islam, K.; Luo, M., Profiling protein methylation with cofactor analog containing terminal alkyne functionality. *Current protocols in chemical biology* **2013,** *5*, 67-88.
25. Yang, Y. Y. G., M.; Raghavan, A. S.; Charron, G.; Hang, H. C., Comparative Analysis of Cleavable Azobenzene-Based Affinity Tags for Bioorthogonal Chemical Proteomics. *Chemistry & Biology* **2010**, 1212-1222.
26. Wu, H.; Min, J. R.; Lunin, V. V.; Antoshenko, T.; Dombrovski, L.; Zeng, H.; Allali-Hassani, A.; Campagna-Slater, V.; Vedadi, M.; Arrowsmith, C. H.; Plotnikov, A. N.; Schapira, M., Structural Biology of Human H3K9 Methyltransferases. *Plos One* **2010,** *5*, e8570.
27. Chakraborty, D.; Islam, K.; Luo, M. K., Facile synthesis and altered ionization efficiency of diverse N-epsilon-alkyllysine-containing peptides. *Chem Commun* **2012,** *48*, 1514-1516.
28. Peters, W.; Willnow, S.; Duisken, M.; Kleine, H.; Macherey, T.; Duncan, K. E.; Litchfield, D. W.; Luscher, B.; Weinhold, E., Enzymatic site-specific functionalization of protein methyltransferase substrates with alkynes for click labeling. *Angew Chem Int Ed Engl* **2010,** *49*, 5170-3.

CHAPTER 3: DEVELOPMENT OF A SELENIUM-BASED CHEMICAL REPORTER FOR WILD-TYPE PROTEIN METHYLTRANSFERASES

3.1 INTRODUCTION

As with many other posttranslational modifications (PTMs), methylation has been shown to be an important means of modulating protein function, activity, and localization.[1-5] These modifications are catalyzed by SAM-dependent protein methyltransferases (PMTs), which transfer the methyl group of SAM to various amino acid side-chains, including glutamate/aspartate, cysteine, lysine, arginine, and histidine.[3-5] As discussed in Chapter 1, numerous biological processes are thought to be influenced by protein methylation, including: epigenetic regulation through histone modification and modulation of chromatin structure, bacterial chemotaxis through the methylation of methyl-accepting chemotaxis proteins, and evasion of host immune responses by pathogenic bacteria. Furthermore, other classes of SAM-dependent methyltransferases are also essential for their roles in nucleic acid methylation and natural product biosynthesis (Chapter 4). Due to the broad spectrum of substrates and the potential impact of SAM-dependent methyltransferases, significant efforts have been made to develop tools for the elucidation of their substrates and associated biological effects.[6-8]

A powerful approach for the study of PTMs, such as methylation, in biological systems has been through the use of chemical reporters containing bioorthogonal chemical handles.[9] Following incorporation into target molecules, these chemical handles can subsequently be coupled to different chemical probes through bioorthogonal 'click' chemistry in order to analyze PTMs. This approach has already been reported for the

examination of protein glycosylation, acetylation, malonylation, transglutamination, lipidation, poly(ADP-ribosyl)ation, and AMPylation.[10-18] Given the importance of posttranslational methylation, these examples have inspired our group and others to develop similar approaches for the study of protein methyltransferases.[19, 20] Indeed, we have previously reported the use of bulky SAM analogues containing sulfonium-β-sp^2-hybridized alkyne/azide clickable functionalities for the identification of specific PMT substrates, termed bioorthogonal profiling of protein methylation (BPPM).[7, 21] As discussed in chapters 1 and 2, however, application of these analogues generally requires the engineering of specific enzymes to achieve efficient substrate labeling due to a general incompatibility with wild-type enzymes.

In light of this limitation, we sought to develop a chemical reporter compatible towards wild-type methyltransferases, which would have several potential advantages. First, such a cofactor could demonstrate broad-spectrum compatibility across the various classes of methyltransferase, including protein, nucleic acid, and natural product methyltransferases, making it a potentially useful tool for the study of many biological processes. Secondly, application of a wild-type PMT-compatible SAM mimic would be complimentary towards technologies like BPPM for the identification of potential PMT substrates, through cross-referencing of proteomic data sets to build confidence in potential targets. Furthermore, implementation of BPPM has thus far only been applied to a small group of enzymes, and it is not yet known if all PMTs can be easily engineered and introduced back into cellular systems. A wild-type compatible SAM mimic would preclude this issue by eliminating the necessity for enzyme engineering.

The optimal candidate for a wild-type PMT compatible SAM mimic was originally predicted to be propargyl-SAM ("ProSAM"; Figures 3.1 and 3.10), which had been previously reported in the literature.[8, 22, 23] This compound was expected to be of particular value as a reporter for wild-type methyltransferases, as it contains the smallest transferable chemical handle suitable for CuAAC chemistry, and thus should be more compatible with the active sites of these enzymes. While attempting to develop this compound for use, however, our attention was caught by several discrepancies concerning ProSAM in the literature. This compound had been previously reported as a SAM mimic for both small-molecule methyltransferases (NovO and CouO) and the lysine methyltransferase SETDB1.[22, 23] However, the same compound had also been reported to be unstable at physiological pH.[8, 20] Intrigued by these findings, we explored the nature of this instability and eventually circumvented it by developing a structurally similar, but significantly more stable propargylic Se-adenosyl-L-selenomethionine (ProSeAM, Figures 3.2 and 3.10).[24] We further demonstrated that ProSeAM is a suitable cofactor mimic for multiple wild-type PMTs through its ability to label and identify PMT substrates in various biochemical contexts (Figures 3.4, 3.5, 3.8 and 3.9).

3.2 MATERIALS AND METHODS

General Materials and Methods

Chemical synthesis of cofactor analogues is detailed in chapter 6, or has been reported previously.[20, 22] All chemical reagents were purchased from Aldrich Chemical or Acros Organics and used without further purification. Optima grade acetonitrile was obtained from Fisher Scientific and degassed under vacuum prior to HPLC analysis.

Analytic HPLC was carried out on a Waters 600 Controller HPLC/2998 diode array detector using XBridge^{TM} reversed-phase C18 5 μm 4.6×150 mm column with UV detection at 260 nm and with the linear gradient of acetonitrile to 10% in 15 min and then to 70% in 5 min in 0.1% aqueous trifluoroacetic acid (flow rate of 1 mL/min). The column was equilibrated with the 0.1% aqueous trifluoroacetic acid solution prior to each injection. CuAAC labeling reagents and azido-conjugated teramethylrhodamine were purchased from Aldrich and Invitrogen, respectively. Proton nuclear magnetic resonance spectra (^{1}H NMR) were recorded on Bruker Ultrashield^{TM} Plus 500 or 600 MHz instruments at 24 ^{o}C. Chemical shifts of ^{1}H NMR spectra are reported as δ in units of parts per million (ppm) relative to tetramethylsilane (δ 0.0) or residual deuterium oxide-d_2 (δ 4.80, singlet).

Histone H3 (aa1-21) peptide (ARTKQTARKSTGGKAPRKQLAGGK), histone H4(aa10- 30)-biotin peptide (LGKGGAKRHRKVLRDNIQGITGGK-[Biotin]) and RGG-Biotin peptide (GGRGGFGGRGGFGGRGGFGGGK-[Biotin]) were obtained from the Proteomics Resource Center of the Rockefeller University and purified by HPLC. Recombinant full-length human histone H3.1 was obtained from New England Biolabs. Prior to use, the full-length histone solution was subject to Amersham Biosciences PD-10 desalting columns and eluted with 50 mM Tris HCl (pH = 8.0) containing 1 mM TCEP for buffer exchange.

Analysis of Stability of ProSAM and ProSAM by Analytical HPLC and LCMS

ProSeAM and ProSAM in 0.1% aqueous TFA (pH ~ 2.0) are stable for at least 8 h at ambient temperature (conditions of synthesis and HPLC; chapter 6) and for more than

three months at -80 °C (storage conditions). To characterize the stability of these compounds, stock solutions of either ProSAM or ProSeAM were prepared in 50 mM Tris HCl (pH = 8.0). Aliquots were removed and analyzed by analytic HLPC or LCMS at various time intervals. Half-life calculations were calculated based on integrated peak areas (measured at 260 nm for the adenine moiety) for the various species observed by HPLC. Rapid decomposition of ProSAM was featured by the loss of the expected m/z of 423.38 and the accumulation of a new hydrated species with the m/z of 441.58 (423.38 + 18). The HPLC profile, ^{1}H NMR and ESI-MS of the decomposition product match those of KetoSAM, which was synthesized by an independent method (Chapter 6).[25]

For the analysis of ProSeAM in the presence of thiol-containing reducing agents, stock solutions (200 μL) containing 200 μM ProSeAM, 100 μM Tris HCl (pH = 8.0), and increasing concentrations of β-mercaptoethanol (0, 1, and 5 mM) were incubated at ambient temperature (22 ^{o}C). Aliquots (65 μL) were removed at 0, 35, and 70 minutes and monitored by analytical reversed-phase HPLC with UV detection at 260 nm. The % ProSeAM remaining was calculated relative to the amount present at t = 0 min.

Protein Expression and Purification

The expression and purification of recombinant protein lysine methyltransferases and protein arginine methyltransferases was described previously or in Chapter 2.[20, 26-28] The GLP1 F1209Y mutant was generated using QuickChange (Stratagene) site-directed mutagenesis kits according to manufacturer's instruction and confirmed via DNA sequencing. PRMT1 and PRMT3 were generously provided by Dr. Rui Wang and Han Guo, respectively. Lysine mono-methyltransferases, SET8 and SET7/9, were expressed

and purified as described previously and were provided by Dr. Gil Blum and Dr. Jamie McBean, respectively. For the bacterial cysteine methyltransferase NleE, the His×6-SUMO-NleE plasmid was obtained from Dr. Feng Shao (National Institute of Biological Science; Beijing, China) and expressed in BL-21 (DE) cells according to manufacturer's instruction with the exception that 10 μM $ZnSO_4$ was included in the growth medium and 0.2 mM IPTG was used for induction at OD_{600} = 0.70 and 22 ^{o}C overnight. His×6-SUMO-NleE was purified with Ni-NTA agarose resin (Qiagen), followed by overnight dialysis against 50 mM Tris HCl (pH = 7.5), 150 mM NaCl, 10% glycerol. Protein concentrations were determined via Bradford assay kit (Bio-Rad) with BSA as standards. All enzymes were stored at -80 °C and thawed on ice prior to use.

MALDI-MS Screening for ProSeAM Compatibility with Wild-Type PMTs

In general, all reactions (50 μL) were carried out for 2 hours at ambient temperature (22 °C). Both biotinylated peptides and nonbiotynylated peptides were used as substrates. Nonbiotinylated peptide products were purified over Sep-Pak (Waters) C18 cartridges according to manufacturer's protocol, whereas biotinylated peptides were enriched by Streptavidin-Sepharose (GE Healthcare) beads after enzymatic reaction. These samples were then subjected to MALDI mass spectroscopy as described previously. Assay conditions for individual enzymes are described below. For G9a and GLP1, reactions contained 2 μM enzyme, 25 μM histone H3 (aa 1-21) peptide and 100 μM SAM, ProSAM or ProSeAM in 50 mM Tris HCl (pH = 8.0). The reactions of SUV39H2 contained 2 μM enzyme, 25 μM histone H3 (aa 1-21) peptide and 100 μM cofactors in 50 mM Tris HCl (pH = 8.0), 1 mM tris(2-carboxyethyl)phosphine hydrochloride (TCEP)

and 2.5 mM $MgCl_2$. The reaction of SET8 contained 5 μM enzyme, 25 μM histone H4 (aa 10-30) peptide and 100 μM cofactors in 50 mM HEPES (pH = 8.0), 0.005% Tween 20 and 0.0005% BSA. The reaction of SET7/9 contained 1 μM enzyme, 25 μM histone H3 (aa 1-21) peptide and 100 μM cofactor in 50 mM HEPES (pH = 8.0), 0.005% Tween 20 and 0.0005% BSA. The reaction of PRMT1 contained 2 μM enzyme, 100 μM RGG-biotin peptide and 100 μM cofactors in 50 mM Tris-HCl (pH = 8.0). The reaction of PRMT3 contained 1 μM enzyme, 100 μM RGG-biotin peptide and 100 μM cofactors in 200 mM HEPES (pH = 8.0).

Kinetics Analysis of ProSeAM as a SAM surrogate Cofactor for GLP1

Steady-state kinetics was performed to compare ProSeAM and SAM as cofactors of GLP1. For the analysis of GLP1 and SAM, a 10 μL reaction mixture containing 0.5 μM recombinant GLP1 and 25 μM Histone H3 (aa 1-21) in 50 mM Tris HCl (pH = 8.0) was incubated at ambient temperature (22 ^{o}C) with increasing concentrations of SAM (0.5, 1, 2.5, 5, 7.5, 10, 20, 30, 40, or 50 μM). For analysis of GLP1 and ProSeAM, a 10 μL reaction mixture containing 1 μM recombinant GLP1 and 25 μM Histone H3 (aa 1-21) in 50 mM Tris HCl (pH = 8.0) was incubated at ambient temperature (22 ^{o}C) with increasing concentrations of ProSeAM (1, 5, 10, 20, 30, 40, 50, 100, 150, or 200 μM). At 5, 10, 15, 20, and 25 minute time-points, 1 μL aliquots were removed and the reaction quenched by spotting on the top of a MALDI plate pre-arranged with 1.5 μL (10 μg/μL) α-cyano-4-hydroxycinnamic acid (CHCA) matrix dissolved in 1:1 H_2O:acetonitrile (0.1% TFA). An additional 1.5 μL of acetonitrile (0.1% TFA) was added to each spot and

allowed to dry prior to MALDI-MS analysis as described previously. MALDI-MS data was analyzed based on %modification of peptide and fit to the Michaelis-Menten equation to obtain k_{cat} and K_m values.

Cell Culture Materials and Procedures

All cell lines were purchased from American Type Culture Collection (ATCC; with the exception of HEK293T and Jurkat cell lines, which were from the laboratory of Dr. Stephen Nimer at Memorial Sloan Kettering Cancer Center). These cell lines were cultured according to ATCC protocols (Table 3.1). Prior to collection, the cells were treated with 25 μM adenosine-2', 3'-dialdehyde for 24-48 hrs. Upon harvesting, the cells were washed with PBS three times and pelleted by centrifugation at 1,000 g for 10 min at 4 ^{o}C.

Table 3.1: List of Cell Lines and Corresponding Culture Media Used.

Cell Line	Type	Culture Media
A549	Alveolar Adenocarcinoma	F12K with 10% FBS
HEK293T	Embryonic Kidney	DMEM with 10% FBS
HT-29	Colorectal Adenocarcinoma	McCoy's 5A with 10% FBS
H1299	Non-Small Cell Lung Carcinoma	RPMI 1640 with 10% FBS
Jurkat	T-Cell Leukemia	RPMI 1640 with 10% FBS
MCF-7	Breast Adenocarcinoma	1:1 F12K:DMEM with 10% FBS
MDA-MB-231	Breast Adenocarcinoma	1:1 F12K:DMEM with 10% FBS
RKO	Colon Carcinoma	MEM with 10% FBS
U937	Histiocytic Lymphoma	RPMI 1640 with 10% FBS

Labeling of Full-Length Proteins with ProSeAM

For the G9a/GLP1-catalyzed labeling of full-length histone H3.1 with ProSeAM, 2 μM G9a or GLP1 was incubated with 25 μM recombinant human histone H3.1 (New England BioLabs) and 50 μM ProSeAM for 1 hour at 25 °C in 50 mM Tris-HCl (pH = 8.0). For NleE- catalyzed labeling of GST-TAB2-NZF with ProSeAM, 3 μM His×6-SUMO-NleE was incubated with 50 μM GST-TAB2-NZF and 100 μM ProSeAM for 30 min in the buffer containing 50 mM Tris HCl (pH = 7.5), 150 mM NaCl, 5 mM DTT and 0.1% NP-40. Alternatively, 3 μM His×6-SUMO-NleE was preincubated with 500 μM SAH for 15 min prior to addition of ProSeAM. Upon the completion of the reaction, the crude samples were precipitated with 1:2:3 $CHCl_3$/H_2O/methanol (1.2 mL) and washed with 1 mL methanol 3 times. Samples were then subjected to CuAAC as described below.

Labeling Cell Lysates with ProSeAM

Whole cell lysates were prepared fresh from HEK293T cells suspended in buffer containing 50 mM Tris HCl (pH = 8.0), 50 mM KCl, 10% glycerol, 1 mM TCEP, 0.005% Tween 20 and 1× Roche protease inhibitor cocktail and incubated on ice for 20 min. The suspended cells were then lysed via sonication (Misonix Ultrasonic Liquid Processor with a single 15 min pulse at 65% amplitude) and centrifuged at 15,000g for 30 min. The supernatants were isolated and their protein concentrations measured via Bradford assay (Bio-Rad) with BSA as standards.

For each 50 μL labeling reaction, 100 μg of total lysate protein was incubated with the indicated concentrations of ProSeAM or ProSAM. Here 0.1 μM 5'-

methylthioadenosine/SAH nucleosidase (MTAN) was also added into the samples to degrade SAH and thus release the potential inhibition of SAH in lysates or from the byproduct of methylation reaction. MTAN treatment was omitted when the samples were treated with SAH to inhibit endogenous methyltransferases. SAH treated samples were preincubated for 15 min with 500 μM SAH, 2 μM adenosine-2',3'-dialdehyde (an irreversible inhibitor of SAH hydrolase to block SAH degradation) and 2 μM methylthio-DADMe-ImmA (an inhibitor of S-methyl-5'-thioadenosine phosphorylase to block SAH degradation, a generous gift from the Schramm lab at Albert Einstein College of Medicine). After 2 hour treatment of ProSeAM or ProSAM, the samples were precipitated and washed with 1:2:3 $CHCl_3$/H_2O/methanol and subjected to CuAAC chemistry as described below.

Conjugation of Labeled Substrates to Fluorescent Probe via CuAAC

After treating full-length histone H3.1 (20 μL reaction mixture of 25 μM histone H3.1) or whole cell lysates (100 μg total protein) with ProSeAM or ProSAM as described above, samples were precipitated with a mixture containing 600 μL of methanol, 200 μL of chloroform and 400 μL of water, and centrifuged at 15,000g for 10 min. The aqueous phase was discarded and the pellets in the interface were washed three times with 1 mL methanol, followed by centrifugation at 15,000g. The supernatants were decanted and the protein pellets air-dried for 1 hour. The samples were then dissolved in 20 μL of solution containing 50 mM TEA (pH = 7.4), 150 mM NaCl and 4% SDS. This mixture was subjected to CuAAC chemistry by adding 100 μM azido-rhodamine, 2 mM TCEP, 1 mM $CuSO_4$ and 100 μM Tris[(1- benzyl-1H-1,2,3-triazol-4-yl)methyl]amine (TBTA) for

1 hour at ambient temperature (22 °C) and in the absence of light. After the CuAAC reaction, samples were precipitated with 1.2 mL of 1:2:3 $CHCl_3$/ H_2O/methanol mixture as described above. The aqueous phase was discarded and the protein precipitate washed three times with 1 mL methanol. The dried samples were dissolved in protein loading buffer and heated for 10 min at 100 ^oC, followed by SDS-PAGE separation. The fluorescent bands were visualized by in-gel fluorescence using an Amersham Biosciences Typhoon 9400 fluorescent scanner (excitation at 532 nm, 580 nm filter and 30 nm band-pass). After the in-gel fluorescence, Coomassie Blue staining was carried out as loading control.

Affinity Pull-Down of ProSeAM-Labeled Proteins from HEK293T Cell Lysates

ProSeAM (final concentration = 25 μM) was added to a total of 10 mg total protein from HEK293T cell lysate (prepared as described above) in 5 mL 50 mM Tris HCl (pH = 8.0), 50 mM KCl, 10% glycerol, 1 mM TCEP, 0.005% Tween20, and Roche protease inhibitor cocktail. Non-inhibitor-treated sample buffer was also supplemented with 100 nM MTAN in order to release any potential inhibition from SAH present in cell lysates. By contrast, inhibitor treated samples contained 0.5 mM SAH or sinefungin, 2 μM adenosine-2'-3'dialdehyde, and 2μM methylthio-DADMe-ImmA.

After a 1 hour reaction time, the samples were precipitated with 1:2:3 $CHCl_3$/H_2O/methanol (42.5 mL), centrifuged at 3,000 g for 45 minutes and the resultant pellets were washed twice with 50 mL of methanol. The protein pellets were then suspended in (4.45 mL) 50 mM TEA (pH = 7.4), 150 mM NaCl, 4% (w/v) SDS buffer, into which was added 550 μL of CuAAC reaction cocktail containing 100 μL of 5 mM

azido-azo-biotin[29] (100 μM final concentration), 100 μL of 50 mM TCEP (1 mM final concentration), 250 μL of TBTA (100 μM final concentration), and 100 μL of 50 mM $CuSO_4$ (1 mM final concentration). After a 1.5 h incubation period at ambient temperature (22 ^oC), the proteins were precipitated again by addition of 45 mL of methanol at -80 ^oC, centrifuged at 3,000 g and washed twice with 45 mL of methanol. Protein was dried for 15 minutes and then suspended in 1 mL of 50 mM TEA (pH = 7.4), 150 mM NaCl, 10 mM EDTA, 4% (w/v) SDS buffer, and diluted through addition of 2 mL of 50 mM TEA (pH = 7.4), 150 mM NaCl, and 1% (w/v) Brij97. Into these mixtures was added 100 μL of Streptavidin-Sepharose beads (GE Healthcare) prewashed 3 times with PBS. The samples were incubated for 1 hour with agitation, centrifuged at 3,000 g and 4 ^oC for 2 minutes, and then washed three times with 10 mL of PBS containing 0.2% SDS, followed by two additional washes with 10 mL of 250 mM ammonium bicarbonate. After removing supernatant and adding 500 μL of 8 M Urea, 25 μL of 200 mM TCEP, and 25 μL of 400 mM iodoacetamide, the protein samples were then incubated for 40 min in the absence of light. Samples were then washed twice with 10 mL of 250 mM ammonium bicarbonate. The bead-immobilized proteins were then liberated by two consecutive 30-min incubations with 250 μL of 1% SDS, 250 mM ammonium bicarbonate, and 25 mM sodium dithionite. The released proteins were then collected and concentrated using Amicon Ultra 3K centrifugal filter units (Millipore), lyophilized and stored at -80 ^oC prior to proteomics analysis.

Proteomics Analysis

Pull-down samples were separated by SDS-PAGE, extracted, and trypsinized as described previously.[21] The digestion product was then analyzed by LC-MS/MS via separation on a 60 min gradient elution at a flow rate of 0.30 μL/min with the UltiMate 3,000 RSLCnano System (Thermo Scientific), which was directly interfaced with the Thermo Q Exactive bench top mass spectrometer. The analytical column was a homemade fused silica capillary column (75 μm i.d., 150 mm length; Upchurch, Oak Harbor, WA) packed with C-18 resin (300 Å, 5 μm; Varian, Lexington, MA). Mobile phase A consisted of 0.1%formic acid, and mobile phase B consisted of 100% acetonitrile and 0.1% formic acid. The LTQ-Orbitrap mass spectrophotometer was operated in the data-dependent Acquisition mode using Xcalibur 2.2.0 software with a single full-scan mass spectrum in the Orbitrap followed by 8 MS/MS scans in the quadrupole collision cell using higher energy collision dissociation (HCD).

The MS/MS data was analyzed using Thermo Proteome discoverer 1.2.0 software against the ipi.HUMAN.v3.82 database with the following search parameters: 10 ppm peptide mass tolerance, 0.8 Da ms/ms tolerance, and two missed cleavages allowed. In addition, modification of carbamidomethylation on cysteine, oxidation of methionine, deamidated asparagine and glutamine, and $C_{11}H_{12}N_4O$ (ProSeAM + cleaved azido-azo-biotin linker) or $C_{22}H_{24}N_8O_2$ (2× ProSeAM + cleaved azido-azo-biotin linker) were also used to search the database. A decoy database search was added with the criteria of FDR at 0.01. Peptide filtering criteria were the following: 2, 2.75, and 3 for singly charged, doubly charged, and triply or higher charged ions, respectively.

3.3 RESULTS AND DISCUSSION

ProSAM vrs. ProSeAM Stability

It had been previously shown that ProSAM underwent rapid degradation at pH ranges commonly used for enzymatic reactions (pH = 7-9).[20, 26, 30] Through careful time-dependent HPLC and LCMS analysis, we discovered that ProSAM has an extremely short half-life of 1-2 minutes at pH 8.0. Furthermore, the major byproduct associated with ProSAM instability was characterized by its +18 molecular ion peak, which we surmised was the result of hydration (+H_2O) of the alkyne moiety via a putative allene intermediate to yield a ketone containing SAM analogue (KetoSAM; Figures 3.1 and 3.10). The formation of this byproduct was later confirmed upon spectral comparison of HPLC-purified degradation products with independently synthesized KetoSAM (Chapter 6).[25]

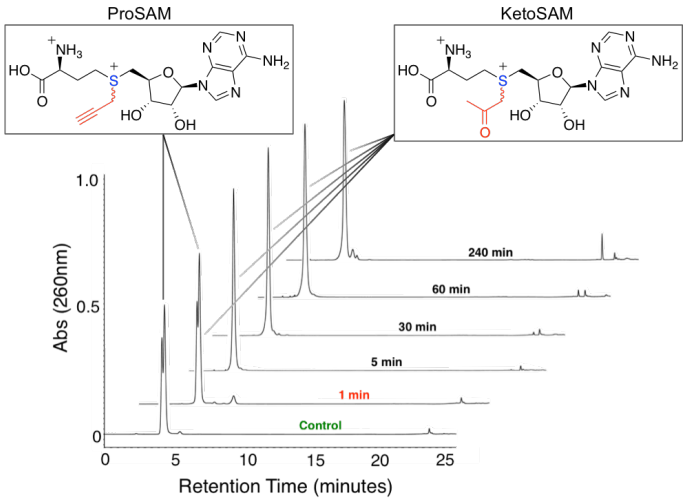

Figure 3.1: Analysis of ProSAM Stability. The ProSAM analogue demonstrated extreme instability at physiologically relevant pH ranges. In Tris HCl (pH = 8) buffer, ProSAM is converted to KetoSAM with an estimated half-life of approximately 1-2 minutes.

The stability of ProSeAM was also examined under identical conditions. Interestingly, no significant conversion (<5%) of the alkyne moiety to the corresponding

ketone could be observed over the course of the experiment. Rather, ProSeAM decomposed primarily to Se-propargyl-5'-selenoadenosine via intramolecular lactonization, which is an established decomposition pathway for SAM or SeAM (discussed previously in chapter 1; Figures 3.2a and 3.10). Overall, the half-life of ProSeAM was approximately 60-fold longer than that of ProSAM (~60 minutes vrs. < 2 minutes in Tris HCl pH = 8.0), and conveniently falls within the time range required for most methyltransferase-catalyzed reactions. Furthermore, the stability of ProSeAM was also analyzed in the presence of thiol-containing reducing agents. Despite the expected high electrophilicity of the carbons adjacent to the selenonium moiety, ProSeAM was found to be stable in the presence of 5 mM β-mercaptoethanol (<10% decrease in overall half-life; Figure 3.2b).

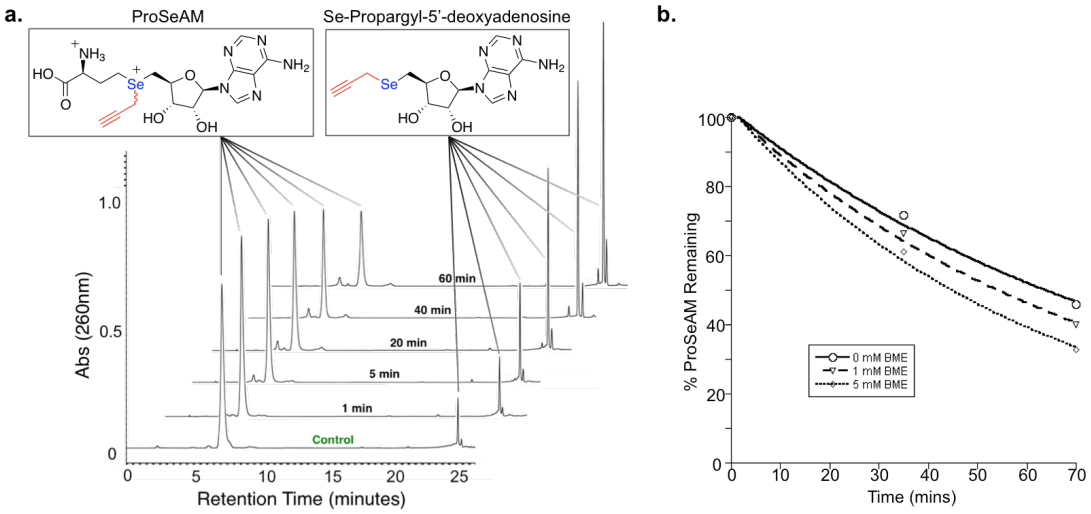

Figure 3.2: Analysis of ProSeAM Stability. In contrast to ProSAM, the propargyl moiety of the selenium-based ProSeAM analogue does not rapidly degrade to the corresponding ketone in Tris HCl (pH = 8) buffer. (a) The primary decomposition pathway for ProSeAM was through intramolecular lactonization of the α-aminobutyrate moiety to form Se-propargyl-5'-deoxyadenosine rather than loss of the propargylic chemical handle. The overall half-life of ProSeAM was found to be roughly 60 fold greater than that of ProSAM. (b) Furthermore, ProSeAM was found to be compatible towards the thiol-containing reducing agent β-mercaptoethanol, with only a <10% decrease in overall stability.

ProSeAM Compatibility of ProSeAM with Wild-Type Methyltransferases

The improved stability of ProSeAM enabled us to examine its compatibility towards wild-type protein lysine/arginine methyltransferases (PKMTs/PRMTs). MALDI-TOF mass spectrometry was applied to monitor the abilities of a panel of PKMTs/PRMTs (GLP1, SET7/9, SET8, G9a, SUV39H2, PRMT1 and PRMT3) to modify known peptide substrates in the presence of ProSeAM (Figure 3.3a, b). Parallel reactions containing SAM or reactions in which enzymes were omitted were also carried out as positive and negative controls, respectively. Of the initial panel of PMTs examined, ProSeAM was shown to be compatible toward three PKMTs (GLP1, G9a, and SUV39H2) for efficient modification of N-terminal histone H3 peptide. Interestingly, ProSeAM could be processed twice by the GLP1 and SUV39H2 enzymes to generate the dipropargylated peptide product, which is consistent with the processive activity of these enzymes (both are H3K9 di/tri-methyltransferases).[31-33] No modification was observed in either the no-enzyme/no-cofactor controls, or in samples treated with the unstable ProSAM analogue. Furthermore, no modified peptide products resulting from nucleophilic attack at C5' of ProSeAM's ribose or the γ-carbon of its α-aminobutyrate moiety were observed. Together, these observations suggest that ProSeAM indeed acts as a cofactor surrogate, rather than a nonspecific alkylation reagent.

To evaluate catalytic efficiency with ProSeAM, we performed steady-state kinetics analysis using the GLP1 PKMT. Initial rates for GLP1-catalyzed modification were determined for ProSeAM and plotted against cofactor concentration using the Michaelis-Menten equation, yielding an apparent k_{cat} of 0.375 min^{-1} and a K_M of 45.4 μM. Compared to GLP1 with SAM (k_{cat} of 1.97 min^{-1}; K_M of 3.1 μM), these kinetic

parameters differed by only 5-15 fold and are sufficient for labeling of cell lysates, as is demonstrated later in this chapter.

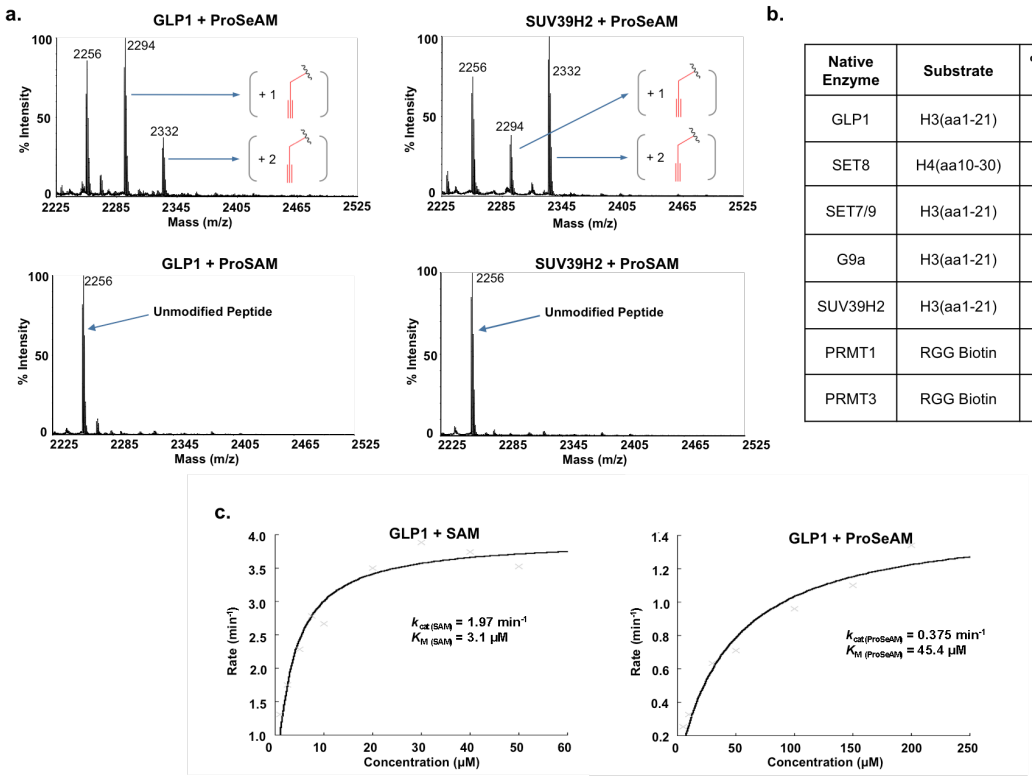

Native Enzyme	Substrate	% Modification by MALDI
GLP1	H3(aa1-21)	61%
SET8	H4(aa10-30)	N.D.
SET7/9	H3(aa1-21)	N.D.
G9a	H3(aa1-21)	39%
SUV39H2	H3(aa1-21)	65%
PRMT1	RGG Biotin	N.D.
PRMT3	RGG Biotin	N.D.

Figure 3.3: Compatibility of ProSeAM with Wild-Type PMTs. (a) MALDI-MS analysis of ProSeAM compatibility towards GLP1 and SUV39H2 revealed the addition of multiple propargyl groups to histone H3 peptide substrate. No modification could be observed when the unstable sulfur-based ProSAM was used. (b) List of wild-type arginine and lysine methyltransferases examined. Of the enzymes tested, only lysine di/tri-methyltransferases appeared to be compatible. N.D., not detected (c) Steady state kinetics analysis of ProSeAM compatibility towards wild-type GLP1 (1 μM) in comparison to SAM. $K_{M\ (ProSeAM)}$ and $k_{cat\ (ProSeAM)}$ were calculated to be 45.4 μM and 0.375 min^{-1}, respectively.

Rationale for ProSeAM's Preference Towards Lysine Di/Tri-Methyltransferases

Of the three PKMTs shown to be compatible with ProSeAM in our initial screen, all were di/tri-methyltransferases (both mono-methyltransferases tested appeared to be incompatible). Given this observation, we set out to examine the possible reason for this selectivity. To explore this further, we first generated the F1209Y mutation of GLP1, which had previously been shown to act as a di/tri-to-mono-methyltransferase "switch"

mutation for SET domain containing PKMTs. In lysine mono-methyltransferases, such as SET8 or SET7/9, this residue is a tyrosine, whereas in di/tri-methyltransferases, this residue is typically a phenylalanine.[34] As predicted, this mutation altered the processivity of GLP1, converting it to a predominantly lysine mono-methyltransferase (Figure 3.4). Interestingly, no modification of the peptide substrate could be observed with the GLP1 F1209Y mutant in the presence of ProSeAM. This loss-of-function experiment thus suggests that the di/tri-PKMTs may utilize a pre-existing vacancy in their active sites to accommodate the propargyl group of ProSeAM.

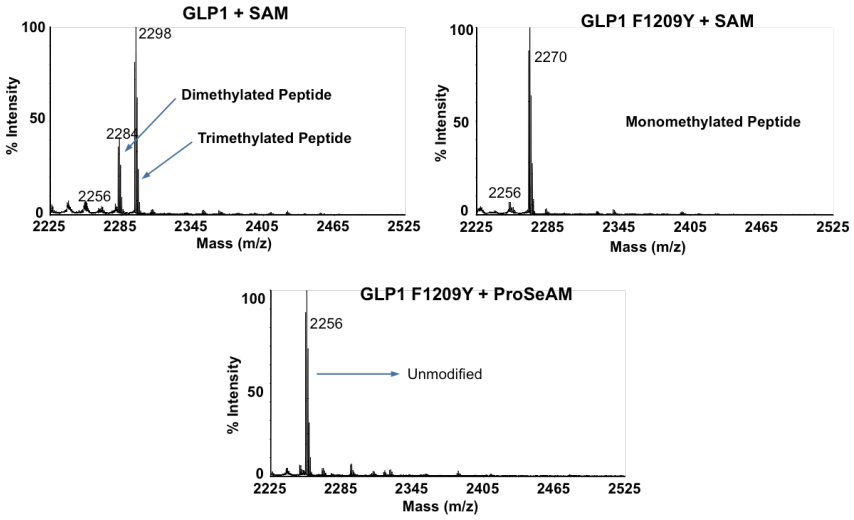

Figure 3.4: Basis for ProSeAM Compatibility Towards Lysine Di/Tri-Methyltransferases. Mutation of phenylalanine 1209 to tyrosine converts GLP1 from a di/tri-methyltransferases to a mono-methyltransferase. As a result, GLP1 is no longer compatible towards the ProSeAM analogue.

Enzymatic Labeling of Full-Length Protein Substrates with ProSeAM

Compatibility of ProSeAM with wild-type enzymes was further examined via in-gel fluorescence with full-length recombinant histone H3.1 as a substrate. As seen in Figure 3.5a, multiple labeled bands of H3.1 were observable by fluorescence imaging. No labeling was observed in no-enzyme or no-cofactor controls. Furthermore, the striation pattern (0.7 kDa increase per modification after conjugation to the fluorescent

probe) correlates well with the degree of alkylation observed by MALDI-MS. In addition, ProSeAM demonstrated compatibility towards the NleE cysteine methyltransferase for the labeling of its TAB2-NZF substrate.[3] No significant labeling could be observed in no-enzyme/no-cofactor controls or in samples treated with the PMT inhibitor, SAH (Figure 3.5b). Lastly, LC-MS/MS analysis of GLP1-modified tryptic histone H3.1 peptides confirmed transfer of ProSeAM's propargyl group to lysine 9. No transfer of the propargyl group to other residues on H3 could be detected by this method. Together, these data suggest that ProSeAM can be efficiently utilized for the labeling of full-length protein substrates. In addition, these data indicate that both enzyme processivity and specificity are maintained when utilizing the ProSeAM cofactor mimic.

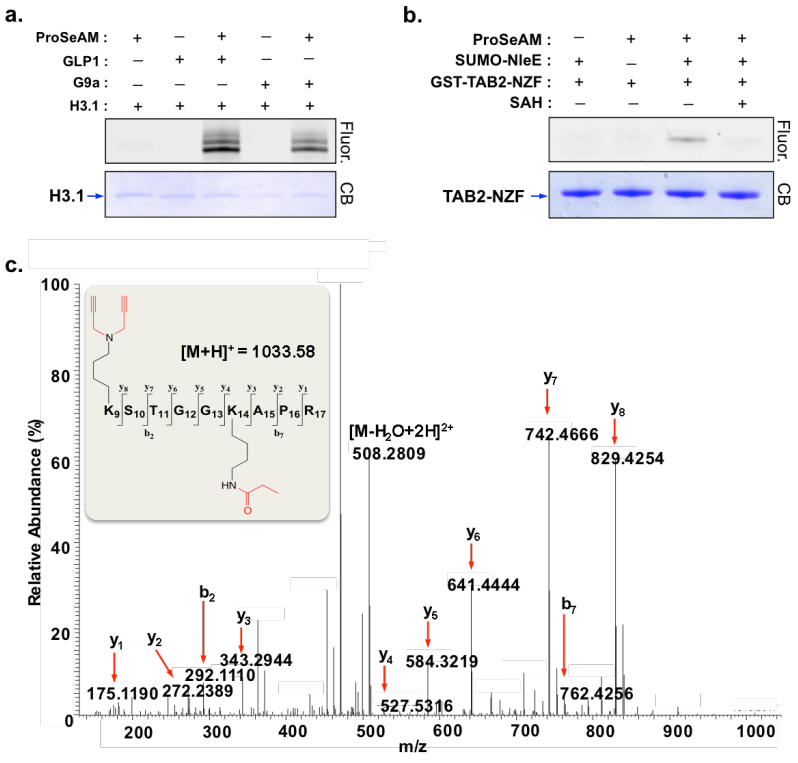

Figure 3.5: Labeling of Full-Length Protein Substrates using ProSeAM *in vitro*. (a) In-gel fluorescence validation of G9a and GLP1 activity on recombinant histone H3.1 using ProSeAM as a cofactor. The striation pattern is the result of the addition of multiple fluorescent probes to the substrate. (b) In-gel fluorescence validation of NleE cysteine PMT activity on the TAB2-NZF substrate. (c) LC-MS/MS analysis of tryptic histone H3.1 treated with GLP1 and ProSeAM revealed di-propargylated lysine 9.

Endogenous Labeling of Proteins in HEK293T Cell Lysate using ProSeAM

To demonstrate the utility of ProSeAM in more complex biochemical systems, HEK293T cell lysates were labeled with ProSeAM. For this purpose, HEK293T cells were treated with adenosine-2',3'-dialdehyde, a SAH hydrolase inhibitor that was reported previously to generate hypomethylated proteomes through the accumulation of the PMT product inhibitor, SAH.[35] These lysates were then treated with ProSeAM, conjugated to an azido-rhodamine dye, and visualized by in-gel fluorescence. Labeled proteins were clearly observable in the treated samples, even at low ProSeAM concentrations (Figure 3.6). In contrast, samples treated with the unstable ProSAM cofactor showed barely detectable labeling, even at 1 mM cofactor concentration. Furthermore, labeling with ProSeAM was proportional to cofactor concentration and could be suppressed by treatment with SAH or heat-inactivation (100 ^{o}C for 10 minutes). Indeed, much of the labeling of substrates that were inhibited by SAH treatment also appeared to be inhibited by heat-inactivation. These data are consistent with labeling by endogenous methyltransferases already present in the lysate using ProSeAM as a cofactor mimic.

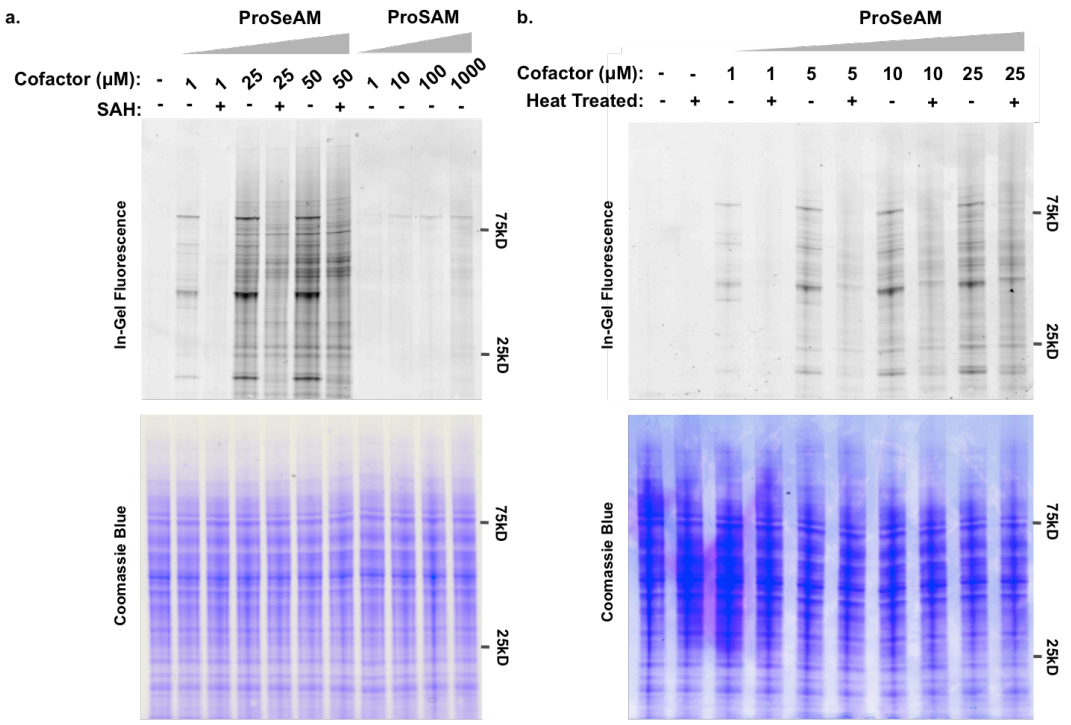

Figure 3.6: Labeling of HEK293T Cell Lysates by Endogenous PMTs with ProSeAM. (a) HEK293T cell lysates were treated with ProSeAM or ProSAM in the presence or absence of SAH inhibition. (b) HEK293T cell lysates were heated to 100 ^{o}C for 10 minutes prior to treatment with increasing concentrations of ProSeAM. Following each labeling reaction, propargylated proteins were conjugated to fluorescent probes and resolved by SDS-PAGE prior to fluorescent visualization. The inhibitor and heat-sensitive labeling of proteins in lysate suggests that labeling is an enzyme-dependent process.

Proteomic Analysis of Labeled Substrates in HEK293T Cell Lysate

Encouraged by ProSeAM's activity *in vitro* and apparent ability to label protein substrates in cell lysate, we sought to expand its application further through the proteomic analysis of labeled substrates in HEK293T cell lysates. For experimental comparison, HEK293T lysates were labeled in the presence of absence of the SAH and sinefungin pan-specific PMT inhibitors.[36] Propargylated proteins were then conjugated to a cleavable azido-azo-biotin affinity probe via CuAAC and enriched over streptavidin beads. Bound proteins were then liberated through treatment with sodium dithionite, separated by SDS-PAGE, subjected to trypsin digestion and analyzed by LC/MS-MS (Figure 3.7).

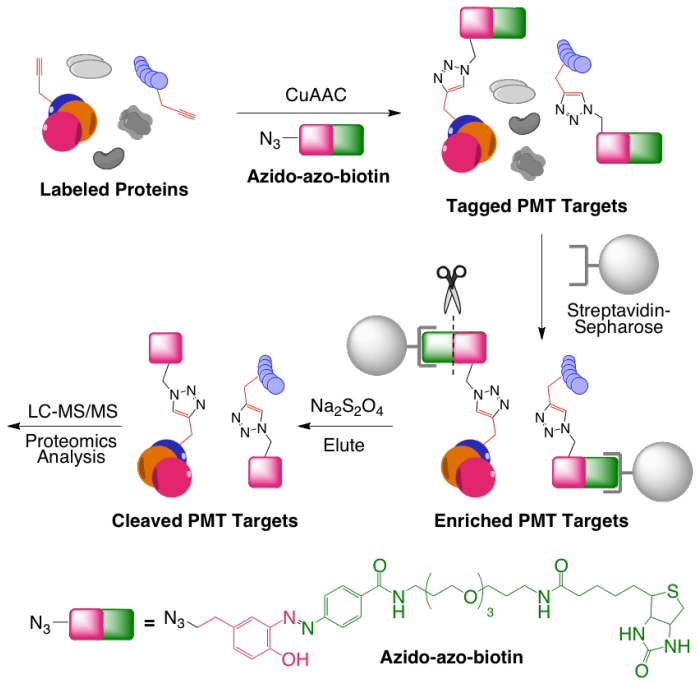

Figure 3.7: Representation of the Affinity-Based Pull-Down Procedure for ProSeAM Labeled Proteins in Cell Lysates. Wild-type methyltransferases present in cell lysate are treated with ProSeAM to label endogenous substrates. These propargylated substrates are then conjugated to a cleavable biotin probe (azido-azo-biotin) and isolated through affinity-based enrichment over streptavidin beads. Enriched protein substrates are then eluted by cleavage of the biotin probe through treatment with the sodium dithionite reducing agent, trypsinized, and analyzed by LC-MS/MS proteomics.

Data sets were analyzed through comparison and overlap between no-inhibitor and inhibitor-treated samples (Figure 3.8a). Analysis revealed a total of approximately 300 potential targets by comparison of no-inhibitor to SAH-treated data sets. In addition, roughly 450 potential targets were identified by comparison of no-inhibitor to sinefungin-treated data sets. Interestingly, comparison of these potential targets between the two data sets treated with different inhibitors indicated that the SAH inhibitor treated samples shared approximately 80% identity toward the putative targets identified in the sinefungin treated data set (Figure 3.8a). This may suggest that two different pan-specific PMT inhibitors prevent the labeling of many of the same protein substrates, as might be expected. In addition, approximately 30% of the proteins identified in the SAH-treated

data sets had also previously been reported as PMT substrates through other methods.[37-41] Several examples of such targets are provided in figure 3.8b. Lastly, of the 11 novel substrates validated for the G9a and GLP1 enzymes through application of BPPM technology (Chapter 2), 10 were also observed in our ProSeAM-treated data sets. Complete lists of identified proteins in our proteomics analysis are provided in the Appendix section.

a.

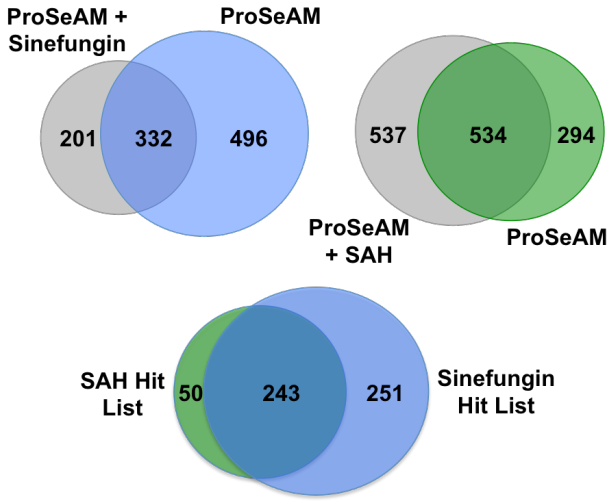

b.

Accession #	Description	Score
IPI00215884.4	Serine/arginine-rich splicing factor 1	6.0
IPI00217465.5	Histone H1.2	6.2
IPI00018534.4	Histone H2B type 1-L	7.9
IPI00395674.1	Small nuclear ribonucleoprotein-associated proteins B and B'	13.3
IPI00020194.1	TATA-binding protein-associated factor 2N	16.2
IPI00216493.1	Heterogeneous nuclear ribonucleoprotein H3	16.4
IPI00455457.4	Histone H3	18.2
IPI00798375.2	Probable ATP-dependent RNA helicase DDX5	20.2
IPI00220919.1	DNMT1	38.3
IPI00418313.3	Interleukin enhancer-binding factor 3	48.4

Figure 3.8: Proteomics Analysis of ProSeAM Labeled Proteins in HEK293T Lysates. (a) Comparison of inhibitor-treated proteomic data sets. Data sets from ProSeAM-treated samples were first compared to sinefungin- or SAH-treated data sets. Identities that did not overlap with inhibitor-treated samples were taken as putative PMT substrates and defined as either SAH or sinefungin "Hit Lists". Furthermore, comparison between SAH and sinefungin hit lists indicated a high degree of identity overlap (~80%). (b) A short list of previously reported PMT targets that were detected in HEK293T lysate treated with ProSeAM, but not in lysate treated with inhibitor.

ProSeAM Labeling in Lysate Across Cancer Cell Lines

To further highlight ProSeAM's potential utility as a chemical reporter for protein methylation, we compared fluorescent labeling patterns across eight common cancer cell lines (Figure 3.9). Examination of these labeling patterns revealed that, although many labeled proteins are shared across all cell lines and could be suppressed by inhibitor treatment, a subset of labeling events appeared to be cell-type specific. For exampled, protein *c* appeared to be strongly labeled in MCF7, HT-29, RKO, A549, and H1299 cells, but not in MDA-MB-231, Jurkat, or U937 cells (Figure 3.9). Similar patterns could also be observed for other labeled proteins, such as *a*, *b*, *c*, *d*, and *f*. Interestingly, labeling patterns also showed variation between cell lines derived from the same tissue type (protein *e* is labeled in RKO, but not in HT-29 colon cancer cell lines). As cancer is thought to be a complex, biochemically heterogeneous disease and has been linked to aberrant protein methylation, these data suggest ProSeAM may be a useful tool for determining PMT substrates in complex systems without the need for genetic manipulation.

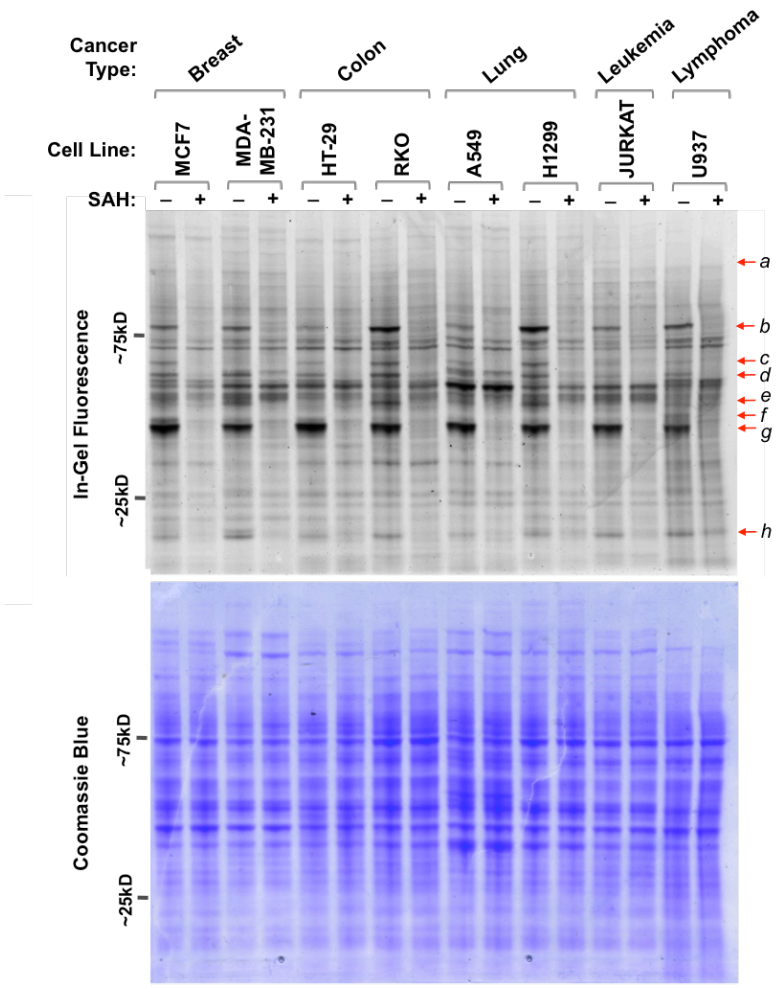

Figure 3.9: In-gel Fluorescence Analysis of ProSeAM Labeling Across Cancer Cell Lines. Protein labeling with ProSeAM as a chemical reporter of endogenous methyltransferases in cancer cell lysates. Cells were treated with adenosine-2', 3'-dialdehyde during growth to generate hypomethylated proteomes for more efficient labeling. Cell lysates were then treated with ProSeAM in the presence or absence of the SAH inhibitor prior to conjugation to a fluorescent chemical probe and in-gel visualization.

3.4 CONCLUSIONS

Motivated by limitations inherent in current technologies for the study of biological transmethylation reactions, we set out to develop a chemical reporter for wild-type protein methyltransferases. Based on experimental data and literature reports, we determined that the initial candidate for this purpose, ProSAM, was unstable at biochemically relevant pH ranges (Figure 3.1). Furthermore, we have demonstrated this

this compound undergoes rapid hydration of its propargylic chemical handle, likely a result of the relative acidity of protons adjacent to the sulfonium moiety, to form the KetoSAM byproduct. This instability renders this cofactor impractical for the study of methylation for several potential reasons. First, the short half-life of ProSAM means it is unlikely to be efficiently utilized by methyltransferases, which typically require longer time periods for efficient substrate modification. Concomitantly, ProSAM's instability results in the rapid buildup of a potentially competitive species (KetoSAM), which has been shown to be a viable cofactor analogue for some methyltransferases. Lastly, intermediates formed during ProSAM's transformation may act as nonspecific alkylating reagents, potentially inactivating certain enzymes.

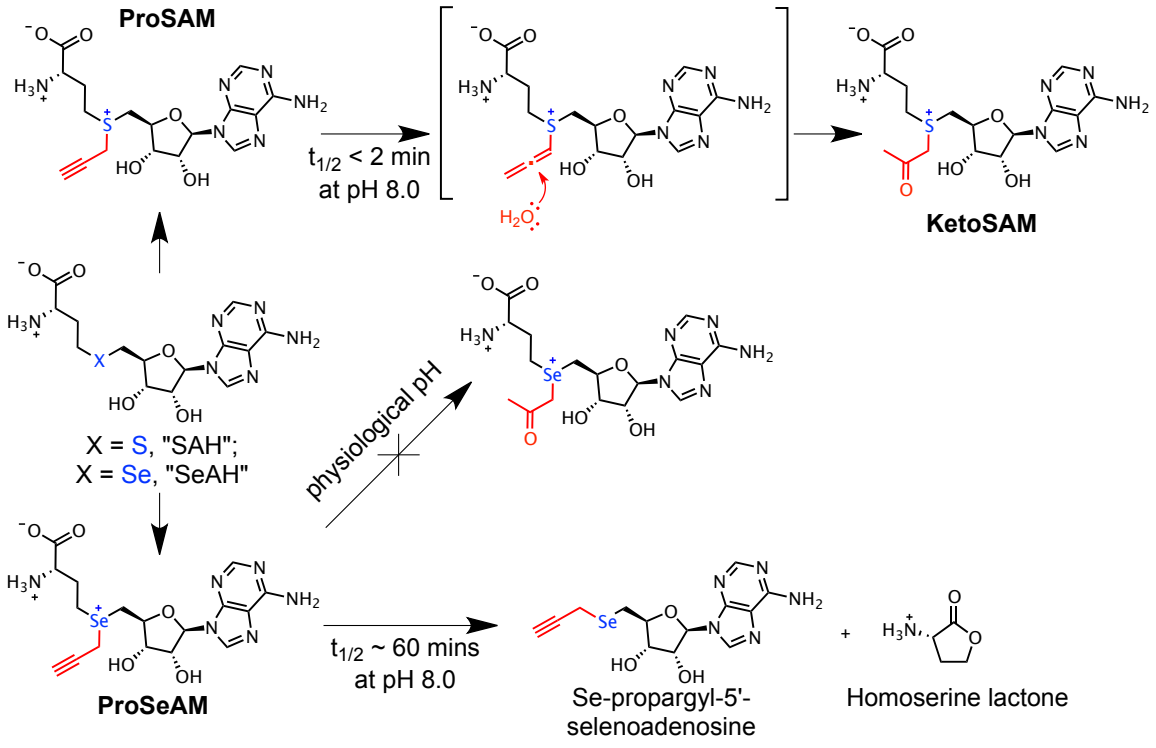

Figure 3.10: Stability of ProSAM and ProSeAM Cofactor Analogues. The sulfur-based cofactor mimic, ProSAM, is highly unstable at physiologically relevant pH values and degrades to KetoSAM. In contrast, the selenium-based ProSeAM is significantly more stable under the same conditions. SAH, S-adenosyl-L-methionine; SeAH, Se-adenosyl-L-selenomethionine.

In order to circumvent these limitations, we developed a selenium-based analogue, dubbed ProSeAM, with the hypothesis that the presence of a selenonium moiety would prevent degradation due to the decreased acidity of protons adjacent to the reactive center.[42] Indeed, this cofactor analogue displayed significantly increased stability of its propargyl chemical handle under identical conditions used to study ProSAM (Figure 3.2). Further experimentation confirmed ProSeAM to be a suitable cofactor (Figure 3.3 and 3.5) for a number of wild-type recombinant PKMTs (G9a, GLP1, and SUV39H2) and the NleE cysteine PMT, although it was not compatible with all of the PMTs tested under our conditions (SET7/9, SET8, PRMT1, and PRMT3). In contrast to our findings, Weinhold and colleagues have reported compatibility of ProSeAM towards wild-type SET7/9 and PRMT1.[43] However, the source of this discrepancy may be related to the different detection methods used for the two studies. In their report, the Weinhold group utilized antibody-coupled horseradish peroxidase visualization, which is expected to detect even extremely weak labeling. In our work, however, we used MALDI-MS and in-gel fluorescence, which, although less sensitive, are expected to better reflect the degree of ProSeAM's compatibility towards wild-type enzymes. Despite this, we cannot rule out other possibilities for the discrepancy, such as differences between the enzyme constructs and peptide substrates used for each study.

We have also gone on to demonstrate ProSeAM's utility for in-gel fluorescence and the proteomic identification of a significant number of potential PMT substrates. (Figure 3.6, 3.9, 3.11) The fact that the labeling of substrates could be inhibited in cell lysate, and that many previously identified PMT substrates appeared in our data sets

lends confidence to our approach. In addition, the complementarity of a wild-type PMTs reporter towards BPPM was also demonstrated through identification of 10 of the 11 novel GLP1/G9a substrates reported in Chapter 2.[7]

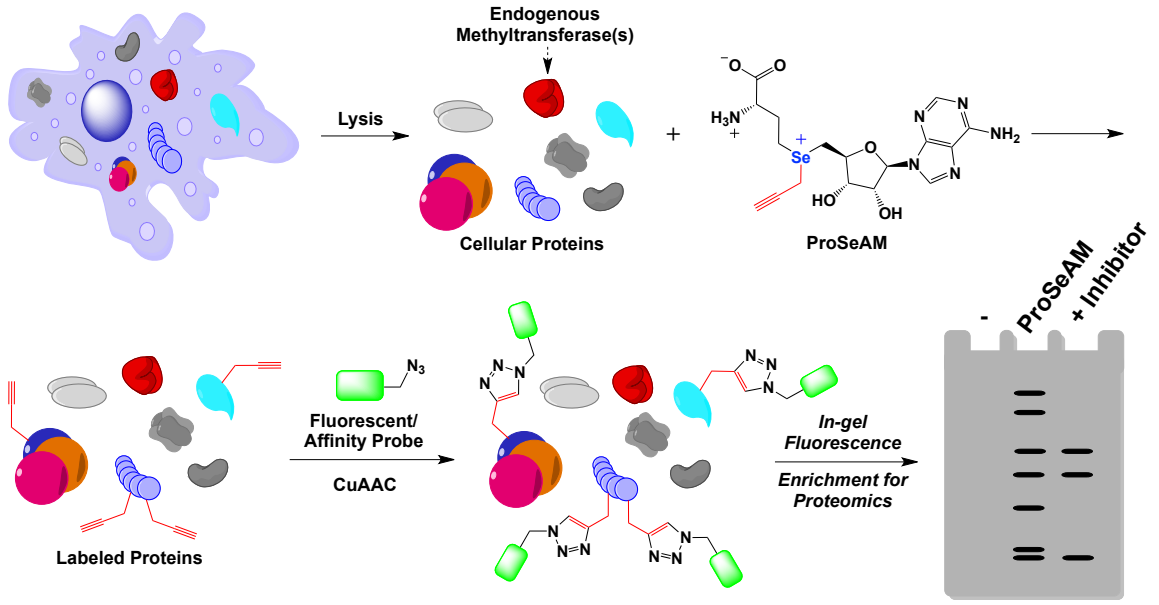

Figure 3.11: Application of ProSeAM as a Chemical Reporter for Protein Methylation. Endogenous methyltransferases can utilize ProSeAM to label cellular proteins. These modified proteins can be subsequently coupled to chemical probes for analysis through in-gel fluorescence or proteomics.

In summary, we have successfully overcome a major limitation in the development of a wild-type PMT-compatible SAM mimic through the development of the selenium-based ProSeAM analogue. In this chapter, we have demonstrated its utility for the study of PMTs and the identification of novel substrates in HEK293T cell lysate (Figure 3.11). Given that nucleic acid, small molecule, and other protein methyltransferases have been shown to act on SAM analogues that are structurally similar or even bulkier, we expect that additional wild-type enzymes will also demonstrate compatibility towards ProSeAM in the future. Research aimed at the exploration of ProSeAM's compatibility towards natural product methyltransferases will be presented in chapter 4.

3.5 REFERENCES

1. Chiu, V. K.; Silletti, J.; Dinsell, V.; Wiener, H.; Loukeris, K.; Ou, G.; Philips, M. R.; Pillinger, M. H., Carboxyl methylation of Ras regulates membrane targeting and effector engagement. *J Biol Chem* **2004,** *279*, 7346-52.
2. Shi, X. B.; Kachirskaia, L.; Yamaguchi, H.; West, L. E.; Wen, H.; Wang, E. W.; Dutta, S.; Appella, E.; Gozani, O., Modulation of p53 function by SET8-mediated methylation at lysine 382. *Mol. Cell* **2007,** *27*, 636-646.
3. Zhang, L.; Ding, X. J.; Cui, J.; Xu, H.; Chen, J.; Gong, Y. N.; Hu, L. Y.; Zhou, Y.; Ge, J. N.; Lu, Q. H.; Liu, L. P.; Chen, S.; Shao, F., Cysteine methylation disrupts ubiquitin-chain sensing in NF-kappa B activation. *Nature* **2012,** *481*, 204-+.
4. Van Der Werf P, K. D. J., Identification of a gamma-glutamyl methyl ester in bacterial membrane protein involved in chemotaxis. *J Biol Chem* **1977,** *252*, 2793-5.
5. Walsh, C. T.; Garneau-Tsodikova, S.; Gatto, G. J., Jr., Protein posttranslational modifications: the chemistry of proteome diversifications. *Angew Chem Int Ed Engl* **2005,** *44*, 7342-72.
6. Luo, M., Current chemical biology approaches to interrogate protein methyltransferases. *Acs Chem Biol* **2012,** *7*, 443-63.
7. Islam, K.; Chen, Y.; Wu, H.; Bothwell, I. R.; Blum, G. J.; Zeng, H.; Dong, A.; Zheng, W.; Min, J.; Deng, H.; Luo, M., Defining efficient enzyme-cofactor pairs for bioorthogonal profiling of protein methylation. *Proc Natl Acad Sci U S A* **2013,** *110*, 16778-83.
8. Peters, W.; Willnow, S.; Duisken, M.; Kleine, H.; Macherey, T.; Duncan, K. E.; Litchfield, D. W.; Luscher, B.; Weinhold, E., Enzymatic site-specific functionalization of protein methyltransferase substrates with alkynes for click labeling. *Angew Chem Int Ed Engl* **2010,** *49*, 5170-3.
9. Prescher, J. A.; Bertozzi, C. R., Chemistry in living systems. *Nat. Chem. Biol.* **2005,** *1*, 13-21.
10. Chang, P. V.; Chen, X.; Smyrniotis, C.; Xenakis, A.; Hu, T.; Bertozzi, C. R.; Wu, P., Metabolic labeling of sialic acids in living animals with alkynyl sugars. *Angew Chem Int Ed Engl* **2009,** *48*, 4030-3.
11. Yang, Y. Y.; Ascano, J. M.; Hang, H. C., Bioorthogonal chemical reporters for monitoring protein acetylation. *J Am Chem Soc* **2010,** *132*, 3640-1.
12. Martin, B. R.; Cravatt, B. F., Large-scale profiling of protein palmitoylation in mammalian cells. *Nat Methods* **2009,** *6*, 135-8.
13. Charron, G.; Zhang, M. M.; Yount, J. S.; Wilson, J.; Raghavan, A. S.; Shamir, E.; Hang, H. C., Robust fluorescent detection of protein fatty-acylation with chemical reporters. *J Am Chem Soc* **2009,** *131*, 4967-75.
14. Hang, H. C.; Wilson, J. P.; Charron, G., Bioorthogonal chemical reporters for analyzing protein lipidation and lipid trafficking. *Acc Chem Res* **2011,** *44*, 699-708.
15. Jiang, H.; Kim, J. H.; Frizzell, K. M.; Kraus, W. L.; Lin, H., Clickable NAD analogues for labeling substrate proteins of poly(ADP-ribose) polymerases. *J Am Chem Soc* **2010,** *132*, 9363-72.

16. Lewallen, D. M.; Steckler, C. J.; Knuckley, B.; Chalmers, M. J.; Thompson, P. R., Probing adenylation: using a fluorescently labelled ATP probe to directly label and immunoprecipitate VopS substrates. *Mol Biosyst* **2012,** *8*, 1701-6.
17. Grammel, M.; Luong, P.; Orth, K.; Hang, H. C., A chemical reporter for protein AMPylation. *J Am Chem Soc* **2011,** *133*, 17103-5.
18. Bao, X.; Zhao, Q.; Yang, T.; Fung, Y. M.; Li, X. D., A chemical probe for lysine malonylation. *Angew Chem Int Ed Engl* **2013,** *52*, 4883-6.
19. Dalhoff, C.; Lukinavicius, G.; Klimasauskas, S.; Weinhold, E., Direct transfer of extended groups from synthetic cofactors by DNA methyltransferases. *Nat. Chem. Biol.* **2006,** *2*, 31-32.
20. Islam, K.; Zheng, W.; Yu, H.; Deng, H.; Luo, M., Expanding cofactor repertoire of protein lysine methyltransferase for substrate labeling. *Acs Chem Biol* **2011,** *6*, 679-84.
21. Islam, K.; Bothwell, I.; Chen, Y.; Sengelaub, C.; Wang, R.; Deng, H.; Luo, M., Bioorthogonal profiling of protein methylation using azido derivative of S-adenosyl-L-methionine. *J Am Chem Soc* **2012,** *134*, 5909-15.
22. Binda, O.; Boyce, M.; Rush, J. S.; Palaniappan, K. K.; Bertozzi, C. R.; Gozani, O., A Chemical Method for Labeling Lysine Methyltransferase Substrates. *Chembiochem* **2010**.
23. Stecher, H.; Tengg, M.; Ueberbacher, B. J.; Remler, P.; Schwab, H.; Griengl, H.; Gruber-Khadjawi, M., Biocatalytic Friedel-Crafts alkylation using non-natural cofactors. *Angew Chem Int Ed Engl* **2009,** *48*, 9546-8.
24. Bothwell, I. R.; Islam, K.; Chen, Y.; Zheng, W.; Blum, G.; Deng, H.; Luo, M., Se-adenosyl-L-selenomethionine cofactor analogue as a reporter of protein methylation. *J Am Chem Soc* **2012,** *134*, 14905-12.
25. Lee, B. W.; Sun, H. G.; Zang, T.; Kim, B. J.; Alfaro, J. F.; Zhou, Z. S., Enzyme-catalyzed transfer of a ketone group from an S-adenosylmethionine analogue: a tool for the functional analysis of methyltransferases. *J Am Chem Soc* **2010,** *132*, 3642-3.
26. Wang, R.; Ibanez, G.; Islam, K.; Zheng, W.; Blum, G.; Sengelaub, C.; Luo, M., Formulating a fluorogenic assay to evaluate S-adenosyl-L-methionine analogues as protein methyltransferase cofactors. *Mol Biosyst* **2011,** *7*, 2970-81.
27. Wu, H.; Min, J.; Lunin, V. V.; Antoshenko, T.; Dombrovski, L.; Zeng, H.; Allali-Hassani, A.; Campagna-Slater, V.; Vedadi, M.; Arrowsmith, C. H.; Plotnikov, A. N.; Schapira, M., Structural biology of human H3K9 methyltransferases. *PLoS One* **2010,** *5*, e8570.
28. Tomkuviene M, C.-d. O. B., Cerniauskas I, Weinhold E, Klimasauskas S., Programmable sequence-specific click-labeling of RNA using archaeal box C/D RNP methyltransferases. *Nucleic Acids Res* **2012**, 1-9.
29. Yang, Y. Y. G., M.; Raghavan, A. S.; Charron, G.; Hang, H. C., Comparative Analysis of Cleavable Azobenzene-Based Affinity Tags for Bioorthogonal Chemical Proteomics. *Chemistry & Biology* **2010**, 1212-1222.

30. Patnaik, D.; Chin, H. G.; Esteve, P. O.; Benner, J.; Jacobsen, S. E.; Pradhan, S., Substrate specificity and kinetic mechanism of mammalian G9a histone H3 methyltransferase. *J. Biol. Chem.* **2004,** *279*, 53248-53258.
31. Rice, J. C.; Briggs, S. D.; Ueberheide, B.; Barber, C. M.; Shabanowitz, J.; Hunt, D. F.; Shinkai, Y.; Allis, C. D., Histone methyltransferases direct different degrees of methylation to define distinct chromatin domains. *Mol Cell* **2003,** *12*, 1591-8.
32. Tachibana, M.; Ueda, J.; Fukuda, M.; Takeda, N.; Ohta, T.; Iwanari, H.; Sakihama, T.; Kodama, T.; Hamakubo, T.; Shinkai, Y., Histone methyltransferases G9a and GLP form heteromeric complexes and are both crucial for methylation of euchromatin at H3-K9. *Genes Dev.* **2005,** *19*, 815-826.
33. Wu, H.; Min, J. R.; Lunin, V. V.; Antoshenko, T.; Dombrovski, L.; Zeng, H.; Allali-Hassani, A.; Campagna-Slater, V.; Vedadi, M.; Arrowsmith, C. H.; Plotnikov, A. N.; Schapira, M., Structural Biology of Human H3K9 Methyltransferases. *Plos One* **2010,** *5*, e8570.
34. Collins, R. E.; Tachibana, M.; Tamaru, H.; Smith, K. M.; Jia, D.; Zhang, X.; Selker, E. U.; Shinkai, Y.; Cheng, X. D., In vitro and in vivo analyses of a Phe/Tyr switch controlling product specificity of histone lysine methyltransferases. *J. Biol. Chem.* **2005,** *280*, 5563-5570.
35. Chen, D. H.; Wu, K. T.; Hung, C. J.; Hsieh, M.; Li, C., Effects of adenosine dialdehyde treatment on in vitro and in vivo stable protein methylation in HeLa cells. *J. Biochem.* **2004,** *136*, 371-376.
36. Borchardt, R. T.; Eiden, L. E.; Wu, B.; Rutledge, C. O., Sinefungin, a potent inhibitor or S-adenosylmethionine: protein O-methyltransferase. *Biochem Biophys Res Commun* **1979,** *89*, 919-24.
37. Ong, S. E.; Mittler, G.; Mann, M., Identifying and quantifying in vivo methylation sites by heavy methyl SILAC. *Nat Methods* **2004,** *1*, 119-26.
38. Beck, H. C.; Nielsen, E. C.; Matthiesen, R.; Jensen, L. H.; Sehested, M.; Finn, P.; Grauslund, M.; Hansen, A. M.; Jensen, O. N., Quantitative proteomic analysis of post-translational modifications of human histones. *Mol Cell Proteomics* **2006,** *5*, 1314-25.
39. Rathert, P.; Dhayalan, A.; Murakami, M.; Zhang, X.; Tamas, R.; Jurkowska, R.; Komatsu, Y.; Shinkai, Y.; Cheng, X. D.; Jeltsch, A., Protein lysine methyltransferase G9a acts on non-histone targets. *Nat. Chem. Biol.* **2008,** *4*, 344-346.
40. Yague, J.; Vazquez, J.; Lopez de Castro, J. A., A post-translational modification of nuclear proteins, N(G),N(G)-dimethyl-Arg, found in a natural HLA class I peptide ligand. *Protein science : a publication of the Protein Society* **2000,** *9*, 2210-7.
41. Weiss, T. H., S.; Zeissler, U.; Izzo, A.; Tropberger, P.; Zee, B. M.; Dundr, M.; Garcia, B. A.; Daujat, S.; Schneider, R., Histone H1 variant-specific lysine methylation by G9a/GMT1c and Glp1KMT1D. *Epigenetics & chromatin* **2010,** *3*, 1-13.

42. Iwig, D. F.; Booker, S. J., Insight into the polar reactivity of the onium chalcogen analogues of S-adenosyl-L-methionine. *Biochemistry* **2004,** *43*, 13496-509.
43. Willnow, S.; Martin, M.; Luscher, B.; Weinhold, E., A Selenium-Based Click AdoMet Analogue for Versatile Substrate Labeling with Wild-Type Protein Methyltransferases. *Chembiochem* **2012**.

CHAPTER 4: ProSeAM COMPATABILITY TOWARDS NATURAL PRODUCT METHYLTRANSFERASES

4.1 INTRODUCTION

As discussed in chapter 1, SAM-dependent methyltransferases are a diverse class of enzyme, with examples of target substrates spanning essentially every type of biomolecule, from small-molecules and natural products to nucleic acids and proteins.[1-4] Although tremendous efforts are being made towards determining the roles of DNA/protein methylation in the regulation epigenetic processes,[5] the biological activity and function of many nonprotein-methyltransferases unrelated to epigenetics remains a fertile area of study.[6] In light of the development of chemical biology tools for the study of protein methyltransferases,[7-12] it was of general interest to expand the application of these compounds to the study of natural product methyltransferases (NPMTs). These enzymes represent the most diverse class of methyltransferase across species and are involved in the biosynthesis of a vast array of metabolites and pharmaceutically relevant compounds, where the addition of a methyl group is often essential for altering the pharmacological properties of the natural product. The activity of NPMTs can be exemplified across every class of small-molecule, with activities ranging from the production of essential metabolites to the biosynthesis or more complex natural products.[13-15] In addition to independently expressed dedicated NPMTs, many methyltransferase domains can also be found within larger multifunctional complexes responsible for the formation of polyketides and nonribosomal peptides.[16]

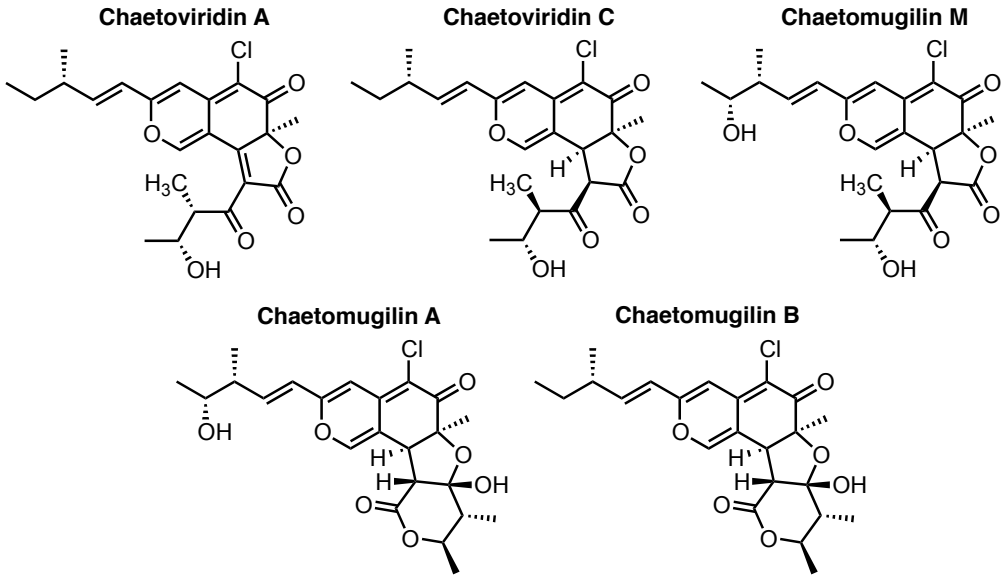

Figure 4.1: Structure of Chaetoviridin and Chaetomugilin Azaphilones.

Polyketide natural products, in particular, are a structurally diverse class of molecules that provide a rich source of pharmaceutically relevant compounds.[17] Interestingly, these molecules derive their complex structures through the utilization of very simple building blocks, such as malonyl-CoA, and repetitive cycles of β-keto reduction by polyketides synthases (PKS).[18, 19] Besides the enzyme domains responsible for the incorporation of the basic building blocks of polyketides, many PKS complexes also contain additional tailoring components, such as methyltransferase (MT) domains, responsible for the introduction of specific chemical motifs into the final product.[16] MT domains present in many PKSs catalyze the α-methylation of growing β-keto polyketide chains using SAM as a methyl source. Given the recent development of SAM analogues for use with wild-type human protein methyltransferases, it was of interest to explore their application towards the MT domains of PKS enzymes.

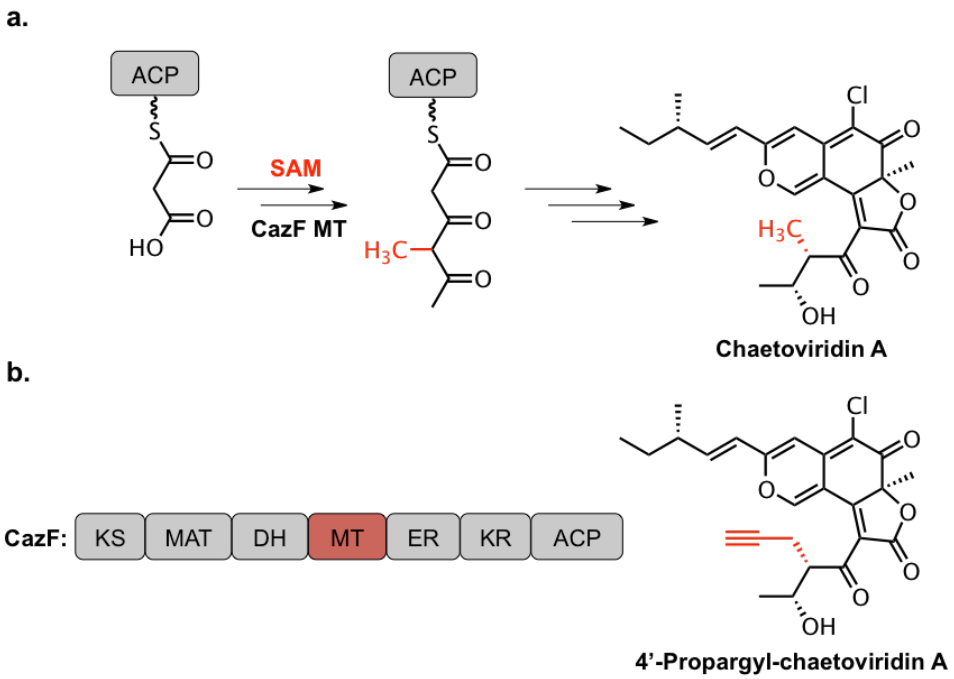

Figure 4.2: Biosynthesis of Chaetoviridin A. (a) The MT domain of CazF is responsible for the insertion of a methyl group early in the biosynthesis of chaetoviridin A. (b) Domain structure of CazF and the 4'-propargyl-chaetoviridin A analogue of interest for this study.

In order to explore the cofactor compatibility of PKS MT domains towards SAM analogues, we turned our attention to the modification of chaetoviridin A through collaboration with the laboratory of Dr. Yi Tang. In 2012, the Tang and Watanabe labs identified the *caz* gene cluster responsible for the biosynthesis of the chaetoviridin and chaetomugilin azaphilones (Figure 4.1).[20] Included in this cluster was the highly-reducing PKS, CazF, which contains an in-line MT domain. *In vitro* experiments using reconstituted CazF later confirmed that this MT domain is indeed active in the methylation of growing polyketide chains following the first chain-extending condensation step.[21] As such, CazF represented a good model system for exploring whether PKS MT domains are capable of accepting SAM analogues for the diversification of natural products (Figure 4.2). Furthermore, as no mutational

engineering efforts had been applied to this system previously, we utilized the ProSeAM and Keto-SAM analogues. These analogues were predicted to be prime candidates as they contain relatively small bioorthogonal chemical handles and had previously been shown to be compatible towards wild-type enzymes.[10-12, 22] If successful, it was predicted that the use of SAM analogues and/or protein engineering might provide a means of expanding the structural diversity of additional polyketide natural products, which might provide a means of altering their pharmacological properties or exploring their mechanism of action. As mentioned previously, this work was performed in collaboration with the laboratory of Dr. Yi Tang by Dr. Jaclyn Winter.[16]

4.2 MATERIALS AND METHODS

General Methods and Materials

All solvents and other chemicals used were of analytical grade. Azide-PEG_3-5(6)-carboxytetramethylrhodamine and click-chemistry protein reaction buffer kit was purchased from Click Chemistry Tools (Scottsdale, AZ). Acetoacetyl-*S*-*N*-acetyl cysteamine (acetoacetyl-SNAC) was a gift from Dr. Kangjian Qiao (UCLA). ProSeAM and Keto-SAM were prepared as described in chapter 6. All ^{1}H NMR spectra were obtained on a 500 MHz Bruker AV500 spectrometer with a 5 mm dual cryoprobe.

Synthesis of 3-[3-(trimethylsilyl)-2-propyn-1-yl]-2,4-pentanedione. To a flask containing 2,4-pentanedione (18.5 mL, 80.0 mmol, 5.0 equiv) in acetone (32 mL) was added 3-bromoprop-1-yn-1-yl-trimethylsilane (3.0 g, 16.0 mmol, 1.0 equiv). Potassium carbonate (11.0 g, 80.0 mmol, 5.0 equiv) was then added. The flask was topped with a

reflux condenser and the system placed under nitrogen. The reaction mixture was heated to reflux for 2 h. After cooling, the reaction was filtered and the filter cake was washed with acetone (3 x 20 mL). The filtrate was then concentrated under reduced pressure. The resultant oil was purified by flash chromatography (10:1 hexanes:EtOAc) to afford 3-[3-(trimethylsilyl)-2-propyn-1-yl]-2,4-pentanedione (3.3 g, quantitative yield) as a pale yellow oil in a 1:1 mixture of keto:enol tautomers. R_f 0.8 (6:1 hexanes:EtOAc); **^{1}H NMR (500 MHz, $CDCl_3$):** Enol tautomer: δ ppm 16.52 (s; 1H), 3.14 (s; 2H), 2.21 (s; 6H), 0.14 (s; 9H); Keto tautomer: δ ppm 3.84 (t; J = 7.65 Hz; 1H), 2.71 (d; J = 7.65 Hz; 2H), 2.40 (s; 6H), 0.13 (s; 9H). **^{13}C NMR (125 MHz, $CDCl_3$):** δ ppm 202.4, 190.9, 106.7, 103.8, 102.6, 87.6, 85.1, 66.7, 29.5, 23.2, 18.9, 18.8, 0.1, 0.01; **IR (film):** 2960, 2176, 1703, 1357, 1249 cm^{-1}. **HRMS-ESI:** (m/z) calculated for $C_{11}H_{17}O_2Si$: 209.1076. found: 209.0998.

Synthesis of 4-acetyl-3-oxo-7-(trimethylsilyl)-6-heptynoic acid methyl ester. To a flask containing a solution of 3-[3-(trimethylsilyl)-2-propyn-1-yl]-2,4-pentanedione (198.0 mg, 0.942 mmol, 1.0 equiv.) in THF (4.71 mL) at -78 ^oC was added a freshly made 1M solution of NaHMDS in THF (2.82 mL, 2.82 mmol, 3.0 equiv.). After stirring at -78 ^oC for 1 hour, dimethylcarbonate (95 mL, 1.03 mmol, 1.1 equiv.) was added. The resulting mixture was removed from the cooling bath and warmed until the internal temperature of the reaction reached -10 ^oC. The reaction was then quenched by the addition of 1 M HCl (10 mL). The reaction mixture was transferred to a separatory funnel containing EtOAc (20 mL). The layers were separated, and the aqueous layer was extracted with EtOAc (3 x 10 mL). The combined organic layers were washed with brine

(30 mL), dried over $MgSO_4$, and concentrated under reduced pressure. The resultant yellow oil was purified by flash chromatography (10:1 hexanes:EtOAc) to afford 4-acetyl-3-oxo-7-(trimethylsilyl)-6-heptynoic acid methyl ester (120.2 mg, 45% yield) as a clear oil. R_f 0.28 (6:1 hexanes:EtOAc); **^{1}H NMR (500 MHz, DMSO-*d6*):** δ ppm 4.21 (t; J = 7.25 Hz; 1H), 3.77 (d; J = 16.9 Hz; 1H), 3.70 (d; J = 16.9; 1H), 3.63 (s; 3H), 2.64 (dd; J_a = 7.25, J_b = 1.95; 2H), 2.21 (s; 3H), 0.10 (s; 9H); **^{13}C NMR (125 MHz, DMSO-*d6*):** δ ppm 202.5, 198.6, 166.9, 104.0, 86.6, 63.45, 52.0, 48.9, 30.0, 18.1, -0.11); **IR (film):** 2958, 2177, 1727, 1707, 1626, 1249 cm^{-1}; **HRMS-ESI:** (m/z) calculated for $C_{13}H_{21}O_4Si$, 269.1209. found 269.1201.

Synthesis of 4-hydroxy-6-methyl-5-[3-(trimethylsilyl)-2-propyn-1-yl]-2H-pyran-2-one. To a vial containing a solution of 4-acetyl-3-oxo-7-(trimethylsilyl)-6-heptynoic acid methyl ester (126.2 mg, 0.447 mmol, 1.0 equiv.) in benzene (844 mL) was added DBU (134 mL, 0.894 mmol, 2.0 equiv.) in one portion. The resulting solution was stirred at 60 ^oC for 3 h. After cooling, the reaction was quenched with saturated aqueous NH_4Cl (5 mL). The layers were separated and the aqueous layer was extracted with EtOAc (3 x 50 mL). The combined organic layers were washed with brine (50 mL), dried over $MgSO_4$, and concentrated under reduced pressure. The resultant solid was purified by flash chromatography (20:1 CH_2Cl_2:MeOH) to afford 4-hydroxy-6-methyl-5-[3-(trimethylsilyl)-2-propyn-1-yl]-2H-pyran-2-one (79.8 mg, 76% yield) as a white solid. Mp: 184–186 ^oC; R_f 0.5 (10:1 CH_2Cl_2:MeOH); **^{1}H NMR (500 MHz, $CDCl_3$)**: δ ppm 5.64 (s; 1H), 3.36 (s; 2H), 2.34 (s; 3H), 0.13 (s; 9H); **^{13}C NMR (125 MHz, $CDCl_3$):** δ ppm 171.2, 167.2, 161.6, 109.4, 102.2, 90.1, 85.5, 17.8, 14.9, 0.12; **IR (film):** 2958, 2176,

1727, 1645, 1608, 1560, 1248 cm^{-1}; **HRMS- ESI**: (m/z) $[M + H]^+$ calculated for $C_{12}H_{17}O_3Si$, 237.0947. found, 237.0955.

Synthesis of 4-hydroxy-6-methyl-5-(2-propyn-1-yl)-2H-pyran-2-one. To a vial containing a solution of 4-hydroxy-6-methyl-5-[3-(trimethylsilyl)-2-propyn-1-yl]-2H-pyran-2-one (16.6 mg, 0.058 mmol, 1.0 equiv) in THF (588 mL) was added a solution of TBAF (1.0M in THF, 88 mL, 0.088 mmol, 1.5 equiv). The reaction mixture was stirred at 23 ^oC for 14 hours and then transferred to a separatory funnel containing EtOAc (10 mL) and 1 M HCl (25 mL). The layers were separated and the resulting aqueous layer was extracted with EtOAc (3 x 20 mL). The combined organic layers were washed with brine (40 mL), dried over $MgSO_4$, and concentrated under reduced pressure to afford the crude product. The resultant solid was purified by flash chromatography (2:1 EtOAc:hexanes) to afford 4-hydroxy-6-methyl-5-(2-propyn-1-yl)-2H-pyran-2-one (9.2 mg, 97% yield) as a white solid. Mp: 209–210 oC; R_f 0.25 (100% EtOAc); **^{1}H NMR (500 MHz, acetone-*d6*):** δ ppm 10.70 (br s; 1H), 5.37 (s; 1H), 3.33 (d; J = 2.60, 2H), 2.42 (t; J = 2.60, 1H), 2.28 (s; 3H); **^{13}C NMR (125 MHz, acetone-*d6*):** δ ppm 169.5, 163.6, 161.6, 108.1, 90.0, 81.6, 69.8, 17.5, 13.9; **IR (film):** 2959, 2924, 1706, 1674, 1561, 1259 cm^{-1}; **HRMS-ESI:** (m/z) calculated for $C_9H_7O_3$, 163.0395; found, 163.0395.

CazF in vitro activity assays

CazF was expressed from *S. cerevisiae* BJ5464-NpgA[21] and purified by gravity-flow column chromatography as previously described.[20] The specificity of CazF's MT domain toward its natural SAM cofactor and unnatural analogs was analyzed by

incubating 5 μM CazF with 2 mM acetoacetyl-SNAC and 5 μM, 10 μM, 25 μM, 50 μM and 1 mM of SAM, ProSeAM, or Keto-SAM in 100 mM phosphate buffer pH = 7.4 in a total volume of 10 μL for one hour at room temperature. The reaction was quenched by adding 90 μL of MeOH and then centrifuged for ten minutes at room temperature. A 10 μL aliquot was analyzed on a Shimadzu 2010 EV LC-MS with a Phenomenex Luna 5μ 2.0 x 100 mM C18 column using a linear gradient of 5-95% MeCN/H_2O containing 0.1% formic acid over 30 minutes with a flow rate of 0.1 mL/min. The corresponding *m/*z peaks for methyl-acetoacetyl-SNAC and propargyl-acetoacetyl-SNAC were integrated and the amount of alkylated-SNAC product was quantified using a standard curve. Kinetic constants were calculated by fitting initial velocity data at various concentrations of SAM or ProSeAM to Michaelis-Menten parameters using nonlinear least squares curve fitting in GraphPad Prism.

To assess whether the KS domain of CazF would perform another round of elongation after the attachment of the propargyl group, 25 mM of protein was incubated at room temperature with 2 mM malonyl-CoA and 0.2 mM of SAM or ProSeAM in 100 mM phosphate buffer pH 7.4 in a total volume of 100 mL. After 1 hour, the reaction was treated with base to release the polyketide product by adding 20 mL 1M NaOH, incubated at 65 ^{o}C for 10 minutes, followed by addition of 40 μL 1N HCl. The reaction was then extracted two times with 200 mL of 99% ethyl acetate:1% acetic acid and the organic layer was dried using a Speedvac. The extract was resuspended in 20 μL MeOH and analyzed by LC-MS as mentioned above. The production of the propargyl-α-pyrone in the in vitro assay was confirmed using the synthetic standard 4-hydroxy-6-methyl-5-

(2-propyn-1-yl)-2H-pyran-2-one. The in vitro production of methyl-α-pyrone was previously confirmed.[20]

In vitro biosynthesis of 4'propargyl-chaetoviridin A using CazF and CazE

In a 100 μL reaction, 25 μM CazF; 25 μM CazE, which was expressed and purified as previously described;[20] 2 mM NADPH; 2 mM malonyl-CoA; and 2 mM cazisochromene were incubated with SAM or ProSeAM in 100 mM phosphate buffer pH 7.4 for one hour at room temperature. Due to the instability of SAM and ProSeAM at neutral conditions and at room temperature, 1 mM of SAM and ProSeAM were added at the start of the reaction and after 30 minutes. The final concentration of the cofactors was 2 mM. The reaction was extracted twice with 300 μL ethyl acetate containing 1% acetic acid. The organic layer was dried using a Speedvac and resuspended in 20 μL MeOH. The extract was analyzed by LC-MS using the same conditions as in the CazF *in vitro* activity assays. The in vitro biosynthesis of chaetoviridin A using SAM as the alkyl donor was confirmed previously.[20] The structure of 4'-propargyl-chaetoviridin A, which was formed using ProSeAM as the alkyl donor, was proposed based on its retention time, UV profile and observed *m/z* isotopic ratio.

Copper-catalyzed azide-alkyne cycloaddition reaction

The *in vitro* reaction for the enzymatic synthesis of 4'-propargyl-chaetoviridin A was repeated using the same conditions mentioned above. After incubating at room temperature for 1 hour, the reaction was extracted twice with 300 μL ethyl acetate containing 1% acetic acid and the organic layer was dried using a Speedvac. The crude

extract was then resuspended in 50 μL MeOH. Azide-PEG_3-carboxytetramethylrhodamine-modified product was dissolved in DMSO to a final concentration of 2.5 mM and the click labeling reaction was carried out using 2 μL of the 2.5 mM rhodamine-azide according to the manufacturer's instructions. After a four-hour incubation at room temperature, the reaction was extracted twice with 250 μL ethyl-acetate containing 1% acetic acid and the organic layer was dried using a Speedvac. The extract was resuspended in 20 μL MeOH and analyzed by LC-MS using the same conditions as mentioned previously in the CazF in vitro activity assay.

4.3 RESULTS AND DISCUSSION

Kinetics Analysis of CazF MT domain Towards SAM, Keto-SAM and ProSeAM

In order to examine the kinetics of the CazF MT domain towards our SAM analogues, recombinant CazF was incubated with Acetoacetyl-*S*-*N*-acetyl cysteamine (acetoacetyl-SNAC) and SAM, ProSeAM or Keto-SAM. The products were then analyzed by LC-MS and kinetic constants were calculated through fitting initial velocity at various concentrations of cofactor to the Michaelis-Menten equation. Interestingly, no product could be observed for reactions using Keto-SAM, suggesting that the MT domain of CazF was not able to accommodate this analogue (Figure 4.3a). In contrast, the steady-state kinetic parameters for methyl-acetoacetyl-SNAC and propargyl-acetoacetyl-SNAC were calculated as $k_{cat\ (SAM)}$ = 0.025 min^{-1} and $K_{M\ (SAM)}$ = 15.5 μM, and $k_{cat\ (ProSeAM)}$ = 0.036 min^{-1} and $K_{M\ (ProSeAM)}$ = 43.6 μM, respectively (Figure 4.3b, c). Although the K_M towards ProSeAM increased by 3-fold, the overall catalytic efficiency towards this cofactor was roughly half that of SAM's (k_{cat}/K_M = 8.25x10^{-4} $\mu M^{-1} \times min^{-1}$ for ProSeAM,

k_{cat}/K_M = 16.1x10^{-4} μM^{-1} × min^{-1} for SAM), which is quite adequate for further study. Furthermore, the slow turnover is likely the result of the acetoacetyl-SNAC substrate used instead of the endogenous acyl-carrier (ACP) protein-tethered substrate.

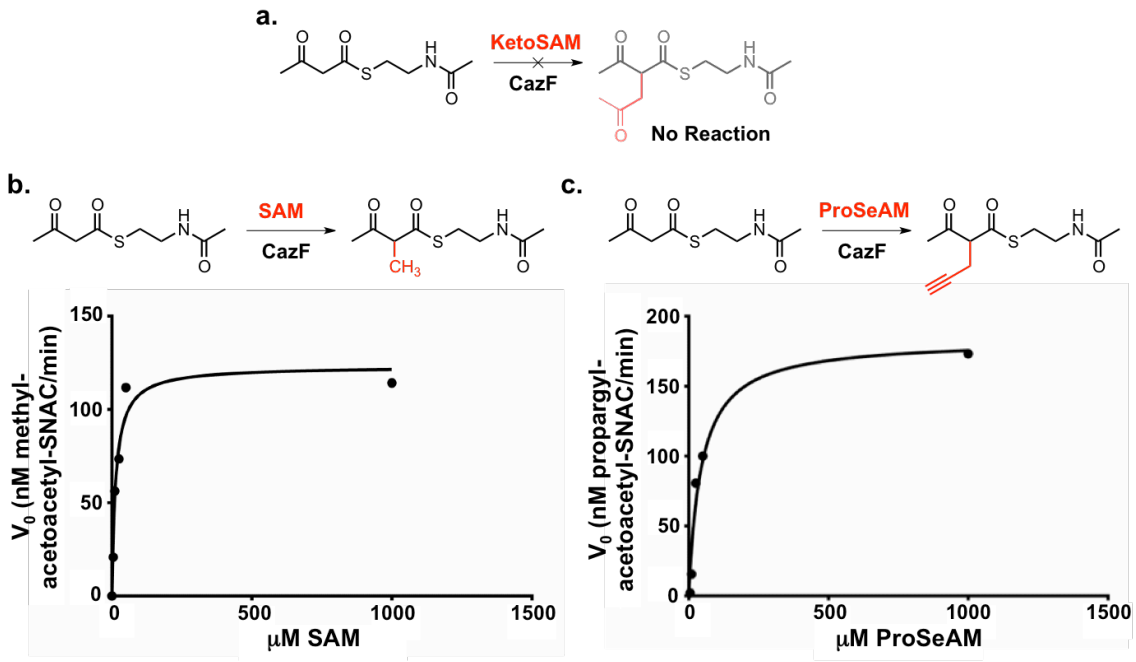

Figure 4.3: Steady-State Kinetics Analysis of Acetoacetyl-SNAC Alkylation by CazF and SAM Analogues. (a) CazF compatibility towards Keto-SAM was tested, although no modification could be detected. (b) Analysis of CazF activity towards SAM as a cofactor. Kinetic parameters were measured to be $k_{cat\ (SAM)}$ = 0.025 min^{-1} and $K_{M\ (SAM)}$ = 15.5 μM. (c) Analysis of CazF activity towards ProSeAM as a cofactor mimic. Kinetic parameters were measured to be $k_{cat\ (ProSeAM)}$ = 0.036 min^{-1} and $K_{M\ (ProSeAM)}$ = 43.6 μM.

Confirmation of Polyketide Chain Growth Following Propargyl Transfer

Following confirmation of CazF MT domain compatibility towards ProSeAM, the activity of the β-ketoacyl synthase (KS) domain towards the propargylated diketide intermediate was examined in order to establish if subsequent cycles of polyketide chain growth could still occur. Previous work had demonstrated that reconstituted CazF could produce 4-hydroxy-6-methyl-α-pyrone when incubated with malonyl-CoA, or the 4-hydroxy-5,6-dimethyl-α-pyrone when incubated with malonyl-CoA and SAM, followed

by treatment with base (Figure 4.4a).[20] To examine if the KS domain of CazF could accommodate the propargyl diketide, it was therefore incubated with malonyl-CoA and ProSeAM, followed by treatment with 1M NaOH. Indeed, LC-MS analysis of the organic extract following base hydrolysis revealed the formation of 4-hydroxy-5-propargyl-6-methyl-α-pyrone, which was confirmed by comparison to a synthetic standard (Figure 4.4b; materials and methods). However, a significantly higher amount of the 4-hydroxy-6-methyl-α-pyrone product was also observed in reactions containing ProSeAM, which suggests that the KS domain was able to outcompete the MT domain in catalyzing chain extension without alkylation. This is likely related to the slower rate of MT-alkylation with ProSeAM in comparison to SAM, as 4-hydroxy-5,6-dimethyl-α-pyrone was found to be the predominant product in reactions containing SAM as the cofactor (Figure 4.4b).

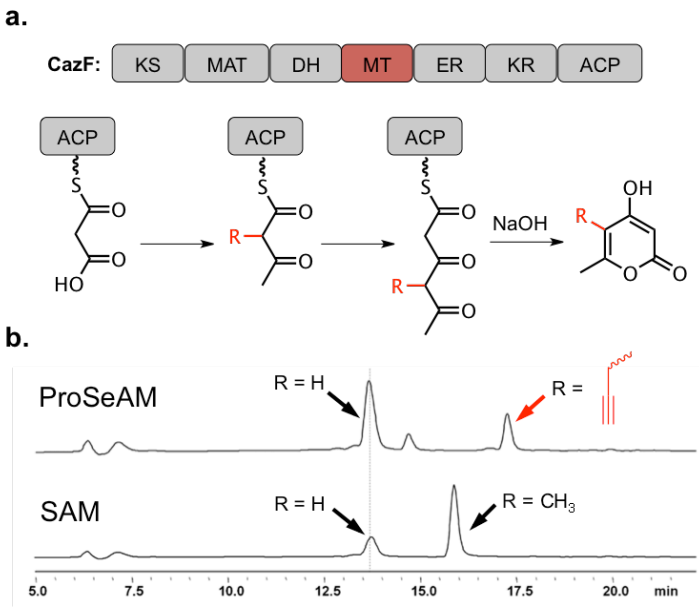

Figure 4.4: Propargyl Transfer does not Prevent Polyketide Chain Growth. (a) If, following transfer of the propargyl group of ProSeAM, the KS domain is capable of undergoing an additional round of chain-growth; the triketide product can be transformed to a α-pyrone through base hydrolysis. (b) HPLC analysis of base-hydolyzed reaction products of CazF-mediated polyketide chain growth.

In Vitro Enzymatic Synthesis of 4'-Propargyl-Chaetoviridin A

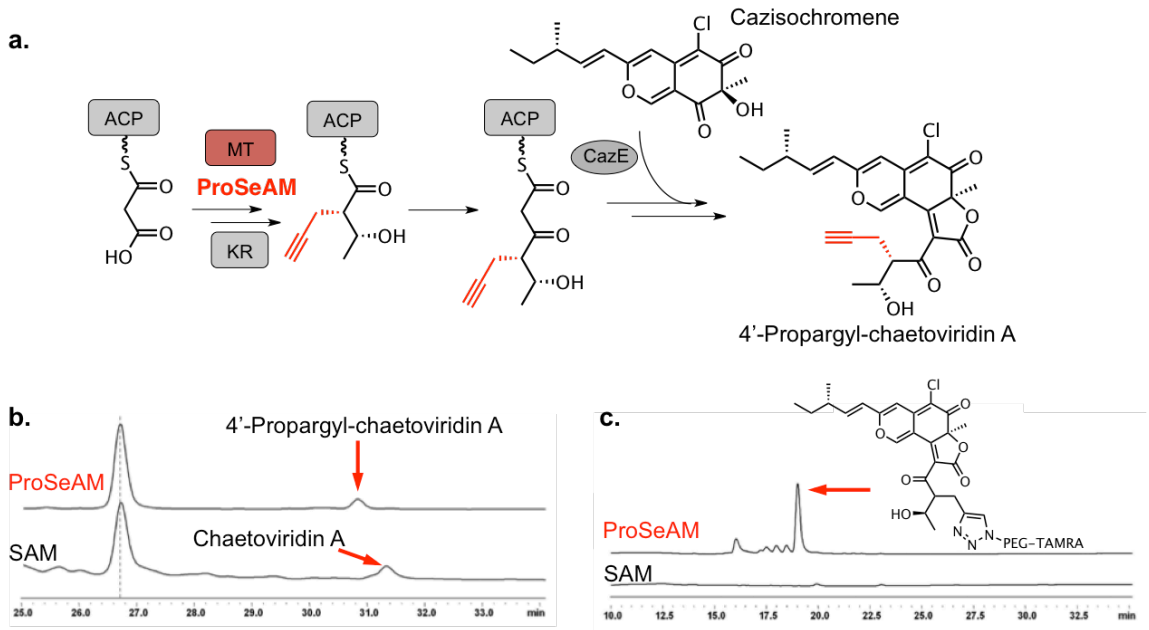

Figure 4.5: Analysis of Enzymatically Synthesized Chaetoviridin A and 4'-Propargyl-chaetoviridin A. (a) Reconstituted CazF reactions were treated with the CazE acyltransferase and cazisochromene to generate Chaetoviridin A or 4'-Propargyl-chaetoviridin A. Reactions contained malonyl-CoA, NADPH, cazisochromene, SAM/ProSeAM, CazF, and CazE. (b) HPLC analysis (360 nm) of chaetoviridins synthesized in the presence of ProSeAM or SAM as cofactors. Components were identified by MS. (c) HPLC analysis (550 nm) of the CuAAC-conjugated 4'-Propargyl-chaetoviridin A.

Previously, *in vitro* reconstitution of CazF supplied with NADPH, SAM and malonyl-CoA was able to produce the requisite triketide product prior to transacylation to cazisochromene by the CazE acyltransferase, yielding the chaetoviridin A product.[20] In order to further establish ProSeAM's compatibility towards the PKS domains of CazF and the CazE acyltransferase, the total enzymatic synthesis of 4'-propargyl-chaetoviridin A was performed (Figure 4.5a). For this experiment, equimolar CazF and CazE were incubated with malonyl-CoA, SAM/ProSeAM, NADPH, and cazisochromene. LC-MS analysis of the products of this reaction indeed revealed the formation of 4'-propargyl-chaetoviridin A based on *m/z* (Figure 4.5b). Further confirmation of the presence of the propargyl group in the final product was established through CuAAC conjugation to an

azide-PEG_3-5(6)-carboxytetramethylrhodamine. Formation of the conjugated product was confirmed by LCMS and exhibited a characteristic UV absorption λ_{max} at 550 nm, which is typical of the rhodamine dye (Figure 4.5c). Together, these data indicated that the propargyl group of ProSeAM could indeed be incorporated into the growing polyketide and propagated through to the final product.

4.4 CONCLUSIONS

In an attempt to explore the cofactor compatibility of PKS MT domains towards SAM analogues, we examined their activity towards the CazF HR-PKS MT domain for the modification of chaetoviridin A. *In vitro* experiments using reconstituted CazF confirmed that its MT domain was indeed active in the alkylation of growing polyketide chain with ProSeAM (Figure 4.3). Furthermore, additional cycles of chain growth were not inhibited by incorporation of the propargyl group of ProSeAM (Figure 4.4). Lastly, incorporation of the propargyl group could be carried through to the production of 4'-propargyl-chaetoviridin A through the transacylase activity of CazE towards cazisochromene (Figure 4.5). These data suggest that the use of SAM analogues may provide a strategy for the diversification of natural products. Although ProSeAM's compatibility towards other PKS systems has not yet been explored, independent corroboration by the laboratory of Dr. Jon Thorson has indicated that ProSeAM is compatible toward the RebM methyltransferase, which is involved in the biosynthesis of rebeccamycin.[23] Together, these independent reports provide a foundation for the potential use of SAM analogues for the modification of natural products, which may provide an alternative strategy for altering their pharmacological properties or exploring

their mechanism of action. Furthermore, these results serve to highlight the broad applicability of ProSeAM as a SAM mimic for wild-type methyltransferases.

4.5 REFERENCES

1. Cantoni, G. L., Biological methylation: selected aspects. *Annual review of biochemistry* **1975,** *44*, 435-51.
2. Schubert, H. L.; Blumenthal, R. M.; Cheng, X., Many paths to methyltransfer: a chronicle of convergence. *Trends Biochem Sci* **2003,** *28*, 329-35.
3. Law, J. H., Biosynthesis of Cyclopropane Rings. *Acc. Chem. Res.* **1971,** *4*, 199-203.
4. Siedlecki, P.; Zielenkiewicz, P., Mammalian DNA methyltransferases. *Acta Biochim Pol* **2006,** *53*, 245-56.
5. Strahl, B. D.; Allis, C. D., The language of covalent histone modifications. *Nature* **2000,** *403*, 41-5.
6. Huang, J.; Berger, S. L., The emerging field of dynamic lysine methylation of non-histone proteins. *Curr. Opin. Genetics Dev.* **2008,** *18*, 152-158.
7. Islam, K.; Zheng, W.; Yu, H.; Deng, H.; Luo, M., Expanding cofactor repertoire of protein lysine methyltransferase for substrate labeling. *Acs Chem Biol* **2011,** *6*, 679-84.
8. Islam, K.; Bothwell, I.; Chen, Y.; Sengelaub, C.; Wang, R.; Deng, H.; Luo, M., Bioorthogonal profiling of protein methylation using azido derivative of S-adenosyl-L-methionine. *J Am Chem Soc* **2012,** *134*, 5909-15.
9. Peters, W.; Willnow, S.; Duisken, M.; Kleine, H.; Macherey, T.; Duncan, K. E.; Litchfield, D. W.; Luscher, B.; Weinhold, E., Enzymatic site-specific functionalization of protein methyltransferase substrates with alkynes for click labeling. *Angew Chem Int Ed Engl* **2010,** *49*, 5170-3.
10. Lee, B. W.; Sun, H. G.; Zang, T.; Kim, B. J.; Alfaro, J. F.; Zhou, Z. S., Enzyme-catalyzed transfer of a ketone group from an S-adenosylmethionine analogue: a tool for the functional analysis of methyltransferases. *J Am Chem Soc* **2010,** *132*, 3642-3.
11. Bothwell, I. R.; Islam, K.; Chen, Y.; Zheng, W.; Blum, G.; Deng, H.; Luo, M., Se-adenosyl-L-selenomethionine cofactor analogue as a reporter of protein methylation. *J Am Chem Soc* **2012,** *134*, 14905-12.
12. Willnow, S.; Martin, M.; Luscher, B.; Weinhold, E., A Selenium-Based Click AdoMet Analogue for Versatile Substrate Labeling with Wild-Type Protein Methyltransferases. *Chembiochem* **2012**.
13. Liscombe, D. K.; Louie, G. V.; Noel, J. P., Architectures, mechanisms and molecular evolution of natural product methyltransferases. *Natural product reports* **2012,** *29*, 1238-50.
14. Zhang, Q.; van der Donk, W. A., Catalytic promiscuity of a bacterial alpha-N-methyltransferase. *FEBS letters* **2012,** *586*, 3391-7.

15. Ansari, M. Z.; Sharma, J.; Gokhale, R. S.; Mohanty, D., In silico analysis of methyltransferase domains involved in biosynthesis of secondary metabolites. *BMC bioinformatics* **2008,** *9*, 454.
16. Winter, J. M.; Chiou, G.; Bothwell, I. R.; Xu, W.; Garg, N. K.; Luo, M.; Tang, Y., Expanding the structural diversity of polyketides by exploring the cofactor tolerance of an inline methyltransferase domain. *Organic letters* **2013,** *15*, 3774-7.
17. O'Hagan, D., *The Polyketide Metabolites*. *Ellis Howard: Chichester* **1991**.
18. Fischbach, M. A.; Walsh, C. T., Assembly-line enzymology for polyketide and nonribosomal Peptide antibiotics: logic, machinery, and mechanisms. *Chemical reviews* **2006,** *106*, 3468-96.
19. Hertweck, C., The biosynthetic logic of polyketide diversity. *Angew Chem Int Ed Engl* **2009,** *48*, 4688-716.
20. Winter, J. M.; Sato, M.; Sugimoto, S.; Chiou, G.; Garg, N. K.; Tang, Y.; Watanabe, K., Identification and characterization of the chaetoviridin and chaetomugilin gene cluster in Chaetomium globosum reveal dual functions of an iterative highly-reducing polyketide synthase. *J Am Chem Soc* **2012,** *134*, 17900-3.
21. Lee, K. K.; Da Silva, N. A.; Kealey, J. T., Determination of the extent of phosphopantetheinylation of polyketide synthases expressed in Escherichia coli and Saccharomyces cerevisiae. *Anal Biochem* **2009,** *394*, 75-80.
22. Stecher, H.; Tengg, M.; Ueberbacher, B. J.; Remler, P.; Schwab, H.; Griengl, H.; Gruber-Khadjawi, M., Biocatalytic Friedel-Crafts alkylation using non-natural cofactors. *Angew Chem Int Ed Engl* **2009,** *48*, 9546-8.
23. Singh, S.; Zhang, J.; Huber, T. D.; Sunkara, M.; Hurley, K.; Goff, R. D.; Wang, G.; Zhang, W.; Liu, C.; Rohr, J.; Van Lanen, S. G.; Morris, A. J.; Thorson, J. S., Facile chemoenzymatic strategies for the synthesis and utilization of S-adenosyl-(L)-methionine analogues. *Angew Chem Int Ed Engl* **2014,** *53*, 3965-9.

CHAPTER 5: EXAMINATION OF SELENIUM-BASED SAM ANALOGUE COMPATIBILITY TOWARDS ENGINEERED PROTEIN METHYLTRANSFERASES

5.1 INTRODUCTION

S-Adenosyl-L-methionine (SAM) is a ubiquitous metabolite utilized in a variety of biochemical processes, ranging from the biosynthesis of small molecules to the methylation of macromolecules such as nucleic acids and proteins.[1] Methylation of DNA, RNA, and protein has garnered particular attention in recent years due to implicated influence over epigenetic and other essential biological phenomena.[2-7] Because of this, efforts have been made toward the development of SAM analogues as tools for the study of targets and functions of various methyltransferases.[8-14] These analogues have generally contained specific chemical groups, such as ketones, azides, and terminal alkynes, which are compatible with bioorthogonal chemistry and permit the conjugation of a fluorescent or affinity-based probe to the labeled substrate for target characterization.

Amongst the previously reported SAM analogues, a selenium-based Se-adenosyl-L-selenomethionine (SeAM; Chapter 3) analogue, ProSeAM, has demonstrated potential as a chemical reporter of wild-type methyltransferases.[12, 13] This SAM mimic is featured by its selenonium moiety, which is equivalent to the sulfonium of other SAM analogues. In the case of ProSeAM, replacement of the sulfonium group with a selenonium was shown to be essential for the suppression of undesired degradation of the propargylic chemical handle to a ketone byproduct, as is discussed in chapters 3. This turned out to be critical for the application of ProSeAM as a chemical reporter for various

methyltransferases, as the sulfur-based version of this compound was later shown to have an extremely short half-life (<2 minutes) at physiologically relevant pH.[15-17]

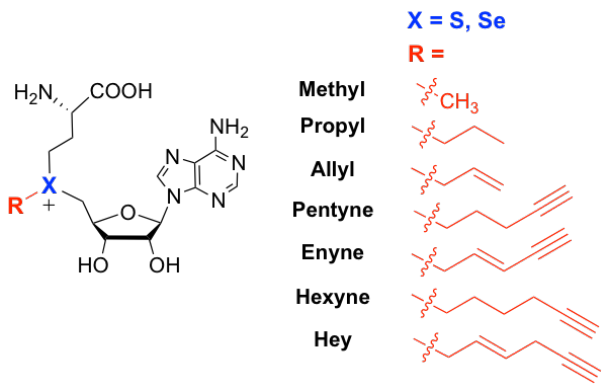

Figure 5.1: Panel of Selenium- and Sulfur-Based Analogues used in this Study. Selenium and sulfur versions of SAM analogues containing the R-groups listed above were synthesized and purified as described in chapter 6. Following spectral characterization, these analogues were tested for their compatibility towards wild-type and engineered PMTs in order to assess the effect of selenium substitution.

Given the apparent success associated with the development of ProSeAM, we next focused our efforts to expand the cofactor repertoire of chemical reporters for SAM-dependent methyltransferases using a similar approach. As such, we examined the effect of substituting selenium into SAM analogues that had otherwise been observed to be unreactive towards engineered methyltransferases. Previous reports had shown that bulky S-alkyl SAM analogues lacking sulfonium-β-sp^1/sp^2-hybridized carbons in their R-groups are typically inert as cofactor surrogates.[8, 11, 18] The proposed rationale for this inactivity stems from the notion that conjugative stabilization by β-sp^1- or β-sp^2-carbons in active SAM analogues facilitates the enzyme-catalyzed S_N2 transition state.[19] However, because Se-alkyl SeAM analogues are expected to have weaker carbon-chalcogen bonds than their sulfur-based counterparts,[20] it was hypothesized that selenium substitution in otherwise unreactive β-sp^3-hybridized SAM analogues would result in their activation. If

this hypothesis were to prove true, we predicted that it would enable access to a much wider variety of β-sp^3-hybridized analogues for the study of methyltransferases. Additionally, we predicted that selenium substitution may improve the activity of certain β-sp^1/sp^2-hybridized SAM analogues that otherwise have previously only demonstrated modest compatibility towards certain enzymes, such as the Enyne-SAM analogue (chapter 2).

In order to test this hypothesis, our efforts utilized the GLP1 Y1211A and G9a 1154A PKMT mutants described previously (as well as several protein arginine methyltransferase [PRMT] mutants reported by other members of the Luo laboratory to accommodate bulky SAM analogues)[21, 22] in combination with a panel of chemically synthesized selenium-based SAM analogues (Figure 5.1). Furthermore, to facilitate the development of cofactor libraries of SeAM analogues, we also optimized and scaled up the synthesis of their chemical precursor, Se-adenosyl-L-methionine, which is described in Chapter 6. Through comparison of SeAM analogues with their equivalent sulfur-based counterparts, we herein demonstrate that selenium substitution can enhance the compatibility of some cofactors towards specific methyltransferases, favoring otherwise less reactive SAM analogues.[23]

5.2 MATERIALS AND METHODS

General Methods and Materials

Chemical synthesis of cofactor analogues is detailed in chapter 6, or has been reported previously.[18, 23] Chemical reagents were purchased from Aldrich Chemical or Acros Organics and used without additional purification. Histone H3 (aa 1-21)

(ARTKQTARKSTGGKAPRKQLAGGK) and RGG-biotin (GGRGGFGGRGGFGGRG-GFGGGK-[Biotin]) peptides were obtained from the Proteomics Resource Center of the Rockefeller University and purified by HPLC. MALDI-MS analysis was performed on a Voyager-DE STR (Applied Biosystems, Framingham, MA, USA) MALDI-TOF mass spectrometer as described previously. In order to analyze peptide samples, 1 μL of reaction mixture was added to 1 μL of a saturated α-cyano-hyrdoxycinnamic acid (Protease Biosciences) on a MALDI plate and allowed to dry at ambient temperature (22 ^{o}C). Mass spectra were gathered using delayed extraction in a positive ion mode. Desorption was obtained using a 337-nm nitrogen laser with a 3 ns pulse width.

Protein Expression and Purification

All enzymes were expressed and purified according to previously described procedures (chapters 2 and 3).[18, 21, 22] Wild-type PRMT3 and PRMT3 M233G were generous gifts from Han Guo. Wild-type PRMT1 and PRMT1 Y39FM48G were provided as gifts from Dr. Rui Wang.

MALDI-MS Analysis of Methyltransferase-Catalyzed Reactions

For the assays of wild-type G9a, G9a Y1154A, wild-type GLP1, and GLP1 Y1211A, 1 μM enzyme and 25 μM H3K9 (aa 1-21) peptide were used. For the assays of wild-type PRMT1 and PRMT1 Y39FM48G, 2 μM enzyme and 20 μM RGG-Biotin peptide were used. For the assays of wild-type PRMT3 and PRMT3 M233G, 1 μM enzyme and 25 μM RGG-biotin peptide were used. The concentration of cofactor analogue was 100 μM for all samples. All reactions (10 μL) were carried out in 50 mM

Tris HCl (pH = 8.0) for 2 hours at ambient temperature (22 ^{o}C). Reactions were quenched by the addition of 1 μL H_2O containing 10% TFA and processed with C18 ZipTip® (Millipore) pipette tips according to manufacturer's instructions prior to MALDI-MS analysis as described above. Degrees of transalkylation (roughly equivalent to *units of cofactor consumed*) per unit peptide for each analogue were quantified by MALDI-MS according to the following formula:

$$\frac{\text{Units Cofactor Consumed}}{\text{Unit Peptide}} = \frac{(I_{alk1}) + (I_{alk2} \times 2) + (I_{alk3} \times 3)\ldots}{(I_{alk0}) + (I_{alk1}) + (I_{alk2}) + (I_{alk3})\ldots}$$

where *I* represents peak intensities for unmodified (alk^0), mono-(alk^1), di-(alk^2), and trialkylated (alk^3) products peptides, etc. Relative transalkylation activities for sulfur and selenium analogues with equivalent R-groups were then compared and categorized for each examined enzyme. These data are summarized in Table 5.1.

5.3 RESULTS AND DISCUSSION

Compatibility of Cofactor Analogues Towards Wild-Type and Mutant PMTs

In order to examine chalcogen-alkyl SAM or SeAM analogues as potential cofactor surrogates for PMTs, we selected a panel of wild-type and engineered PMTs (wild-type and Y39FM48G PRMT1, wild-type and M233G PRMT3, wild-type and Y1154A G9a, wild-type and Y1211A GLP1), which have previously been shown to be active toward either native SAM or β-sp^1/sp^2-carbon-activated SAM analogues as cofactors.[11, 21, 22] Enzymatic reactions with known peptide substrates were analyzed by MALDI-MS in order to assess the relative degrees of transalkylation with the various cofactor analogues. These results were then evaluated based on the difference of the

efficiency of transalkylation between S-alkyl SAM analogues and their Se-alkyl SeAM counterparts (Table 5.1).

Table 5.1: Summary of relative efficiency of transalkylation with SAM analogues versus equivalent SeAM analogues. Degree of transalkylation was defined as the equivalents of alkylation (or cofactor consumption) per unit peptide substrate according to relative peak intensity of MALDI-MS spectra (materials and methods). For instance, if 50% peptide is converted into a mono-alkylated product, the degree of the transalkylation will be "0.5"; if all the peptide is converted into a di-alkylated product, the degree of the transalkylation will be "2.0". The relative efficiency between of SeAM and their equivalent SAM analogues as cofactors were categorized as "=" for 0~0.1 change of the degree of alkylation; "+" or "–" for increase or decrease of 0.1 ~ 0.5 degree of transalkylation, respectively; "+ +" or "– –" for increase or decrease of >0.5 degree of transalkylation, respectively; NR for no reaction observed for SeAM or SAM analogues. These values are shown in parentheses as (S- analogue, Se-analogue). WT G9a, WT GLP1, WT PRMT1 and WT PRMT3 stand as wild-type enzymes.

S vrs. Se	WT G9a	G9a Y1154A	WT GLP1	GLP1 Y1244A	WT PRMT1	PRMT1 Y39FM48G	WT PRMT3	PRMT3 M233G
Methyl	+ (2.36, 2.84)	+ + (0.15, 1.03)	+ (2.70, 2.96)	+ (0.06, 0.34)	– – (3.16, 2.50)	+ (0.00, 0.13)	– (3.37, 3.01)	= (0.00, 0.08)
Propyl	NR	NR	NR	NR	NR	NR	NR	NR
Allyl	= (0.35, 0.32)	+ (0.78, 0.91)	= (0.77, 0.82)	+ (0.46, 0.69)	– (0.13, 0.00)	= (0.07, 0.10)	= (0.04, 0.06)	= (0.00, 0.09)
Pentyne	NR	NR	NR	NR	NR	NR	NR	NR
Enyne	NR	+ + (0.23, 0.71)	NR	+ (0.06, 0.46)	NR	– (0.74, 0.24)	NR	= (0.34, 0.39)
Hexyne	NR	NR	NR	NR	NR	NR	NR	+ (0.00, 0.13)
Hey	NR	– (0.96, 0.85)	NR	+ (0.77, 0.91)	NR	– – (1.31, 0.32)	NR	– – (2.29, 0.62)

Although the bulky, β-sp^3-carbon-containing Hexyne-SAM analogue was completely inert as a cofactor of the examined PMTs, its equivalent SeAM analogue demonstrated activity toward the PRMT3 M233G mutant (Figure 5.2). Despite modest transalkylation efficiency, this reaction was enzyme-dependent, as no modification was detected in the presence of native enzyme or in a no-enzyme control. Similarly, the Enyne-SAM analogue was only modestly active toward G9a Y1154A and GLP1 Y1211A mutants, while the equivalent Enyne-SeAM was shown to be at least 4-fold more reactive

under the same conditions (0−20% for the former versus 50−80% conversion for the latter; Figure 5.3a). These observations argue that the weaker selenium-carbon bond in Se-alkyl SeAM analogues has a positive effect on accelerating transalkylation reactions for a subset of PMTs.

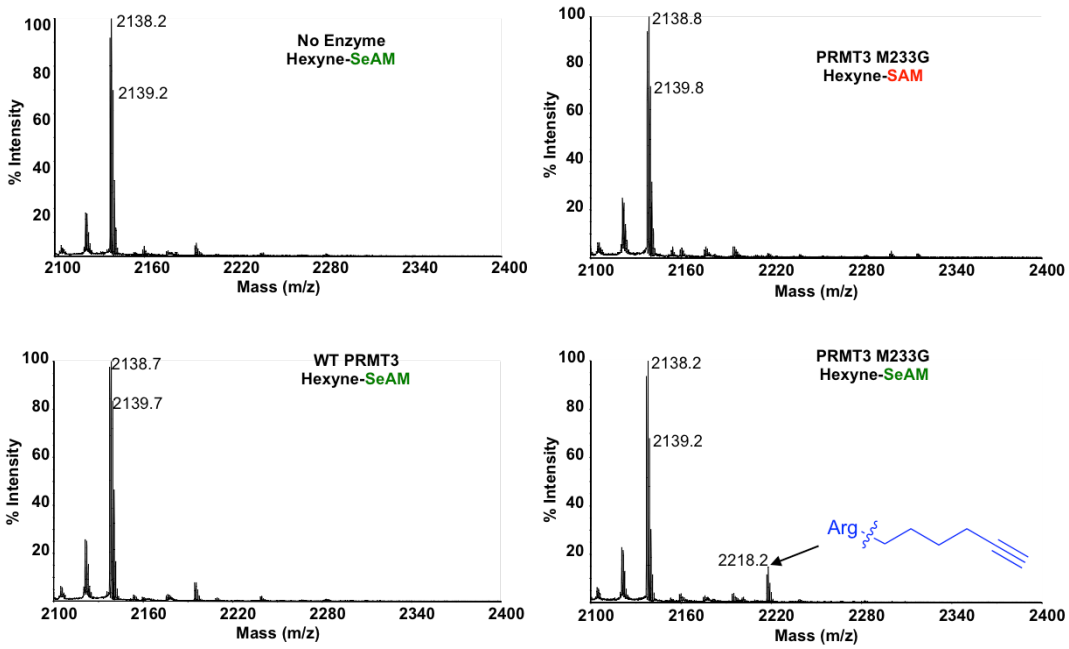

Figure 5.2: Examination of Enzyme Compatibility of Hexyne-SAM and -SeAM. MALDI-MS analysis revealed modest activity of the Hexyne-SeAM cofactor towards the PRMT3 M233G mutant. No modification of peptide substrate could be observed with the sulfur-based version of the compound or in WT or no-enzyme controls.

It was also noted that the effect of selenium substitution to facilitate PMT-catalyzed transalkylation was context-dependent. For instance, while the Enyne-SeAM analogue is more reactive than the Enyne-SAM analogue as a cofactor for G9a Y1154A and GLP1 Y1211A mutants, such an effect was not observed for the PRMT3 M233G mutant and was even reversed for the PRMT1 Y39FM48G mutant (Figure 5.3b; Table 5.1). Similarly, SeAM only showed higher reactivity than SAM as a cofactor for wild-type and G9a Y1154A, wild-type and GLP1 Y1211A, and the PRMT1 Y39FM48G

mutant, but not for wild-type PRMT1, wild-type and M233G PRMT3 (Figures 5.4a). In addition, the sulfonium-to-selenonium substitution in the Allyl-SAM analogue showed no effect on their cofactor reactivity for G9a Y1154A, GLP1 Y1211A, PRMT1 Y39FM48G, and PRMT3 M233G mutants (Figure 5.4b).

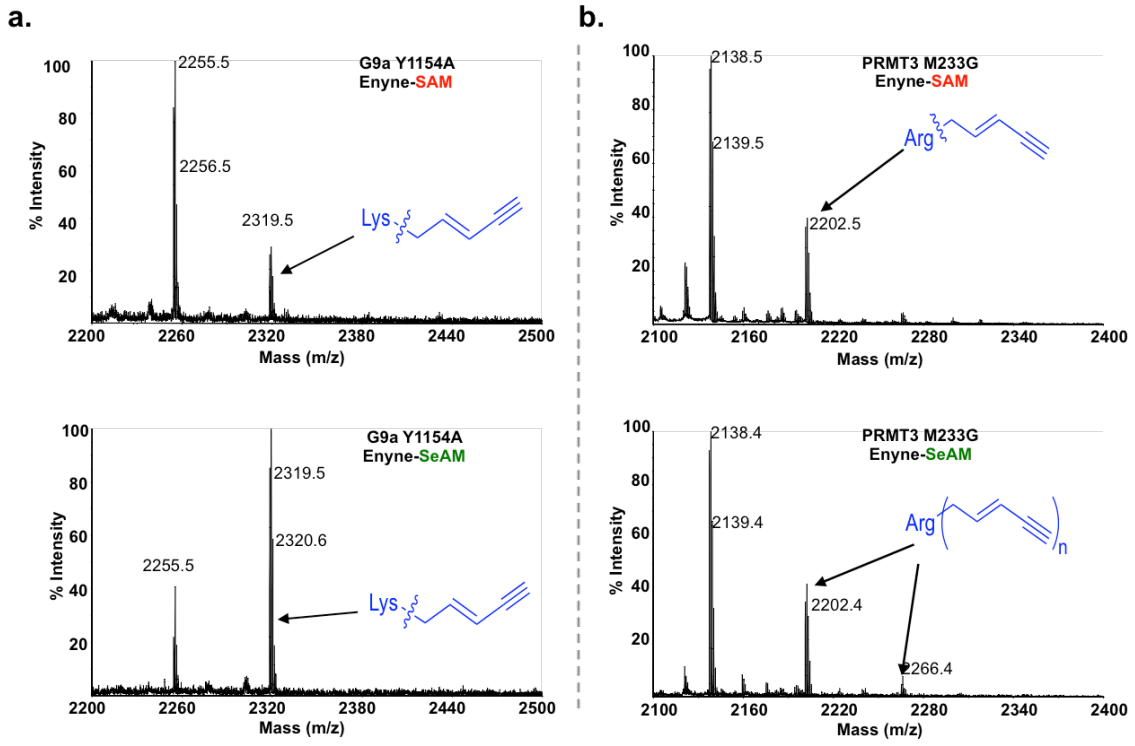

Figure 5.3: Comparison of Enyne-SAM and -SeAM Compatibility Towards G9a Y1154A and PRMT3 M233G Mutants. (a) In the case of the G9a Y1154A mutant, selenium-substitution appeared to activate the Enyne-SeAM cofactor towards enzyme-mediated transalkylation. Under identical conditions, treatment with Enyne-SeAM resulted in 4-fold increased modification of known peptide substrate in comparison to its sulfur-based counterpart. (b) The same effect was not observed for the PRMT3 M233G mutant, which displayed roughly equivalent activity between the Enyne-SAM and -SeAM.

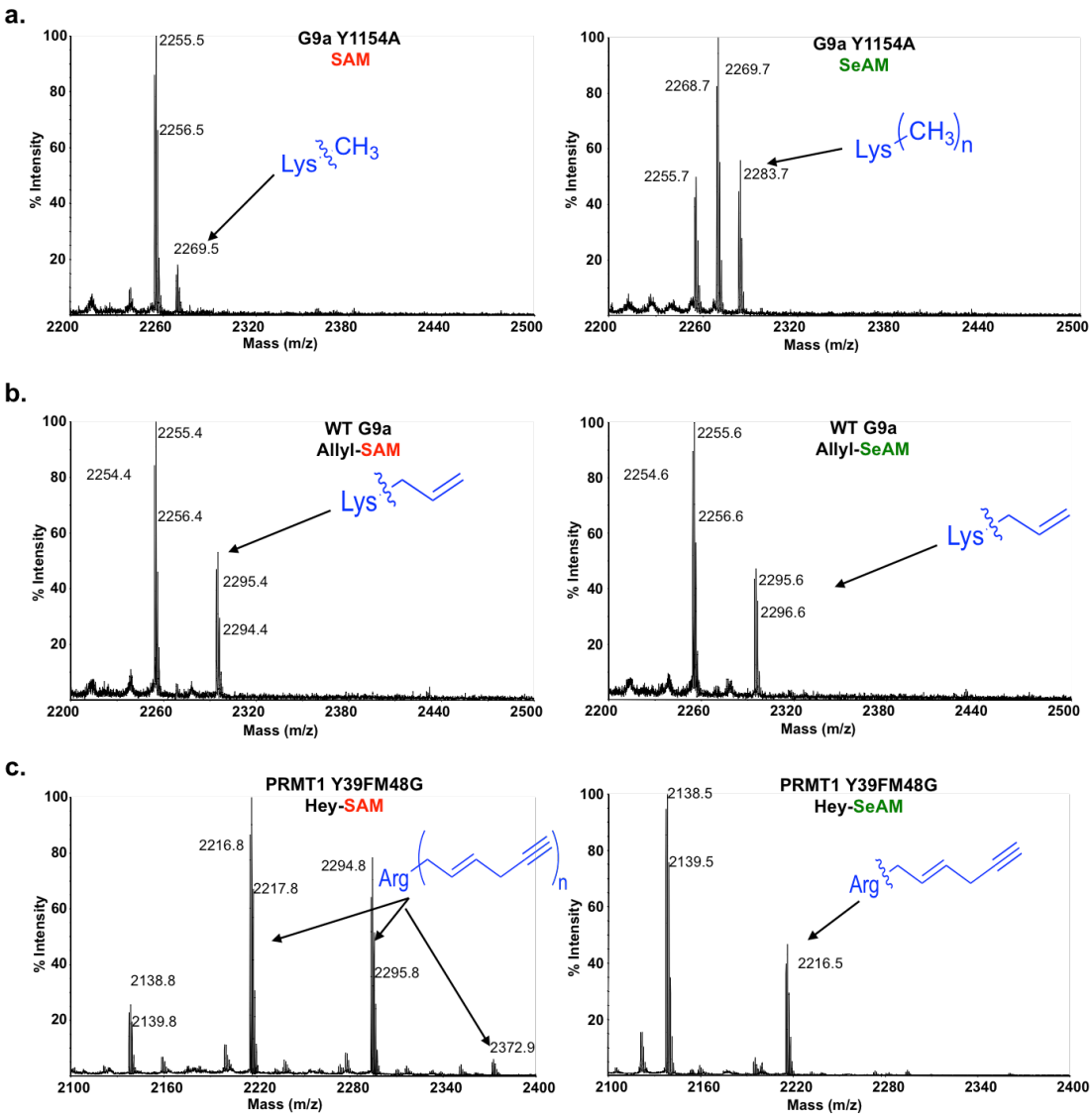

Figure 5.4: Cofactor Activation by Selenium-Substitution is Context Dependent. (a) SeAM demonstrated higher reactivity towards mutant PKMT G9a Y1154A than SAM. (b) In contrast, the Allyl-SeAM analogue demonstrated no difference in reactivity towards PKMTs including WT G9a. (c) Furthermore, the Hey-SeAM analogue demonstrated decreased reactivity towards PRMT1 Y29FM48G mutant.

Lastly, sulfonium-to-selenonium substitution in Hey-SAM also did not affect its cofactor activity toward G9a Y1154A and GLP1 Y1211A variants and even had a negative effect on PRMT1 Y39FM48G and PRMT3M233G variants (Figure 5.4c; Table 5.1). Furthermore, Propyl- and Pentyne-SAM and -SeAM analogues were inert toward all PMTs examined (Table 5.1). According to these data, we observed the general trend that

for less reactive SAM derivatives such as Hexyne- and Enyne-SAM analogues, which contain a β-sp^3-carbon and a rigid bulky alkyl chain, respectively, the replacement of sulfonium with selenonium can boost their reactivity as cofactors for certain PMTs. Admittedly, this observation needs to be further explored with more PMTs and SeAM analogues.

5.4 CONCLUSIONS

Through examination of a variety of Se-alkyl SeAM analogues and comparison to their equivalent S-alkyl SAM analogues, we observed context-dependent reactivity as cofactor surrogates for PMTs. In the case of protein lysine methyltransferases (PKMTs), selenium substitution was able to boost the reactivity of otherwise less reactive SAM analogues, such as Enyne-SAM. Although the β-unsaturated functionality remained essential for cofactor activity of S-alkyl SAM analogues, this functionality appeared to be dispensable for certain protein arginine methyltransferases (PRMTs) when Se-alkyl SAM analogues are used, as was observed for Hexyne-SeAM and PRMT3 M233G. These observations illustrate a complementary role for the weaker selenium-carbon bonds in facilitating the S_N2 transition state, and the potential application of Se-alkyl SeAM analogues as chemical reporters for other methyltransferases. Although the reported rates of the spontaneous cleavage of the chalcogen-carbon bonds can increase by 10-fold from SAM to SeAM,[24] the efficiency of the PMT-catalyzed transalkylation reactions increases by no more than 3-5 fold from S-alkyl SAM analogues to their equivalent Se-alkyl SeAM analogues. Such a discrepancy suggests that PMTs also leverage other mechanisms to

control the overall catalysis, a process that is currently being explored biochemically in our lab through the use of selenium-based and isotopically labeled SAM analogues.

5.5 REFERENCES

1. Cantoni, G. L., S-Adenosylmethionine; a new intermediate formed enzymatically from L-methionine and adenosinetriphosphate. *J Biol Chem* **1953,** *204*, 403-416.
2. Bernstein, B. E.; Meissner, A.; Lander, E. S., The mammalian epigenome. *Cell* **2007,** *128*, 669-81.
3. Chuikov, S.; Kurash, J. K.; Wilson, J. R.; Xiao, B.; Justin, N.; Ivanov, G. S.; McKinney, K.; Tempst, P.; Prives, C.; Gamblin, S. J.; Barlev, N. A.; Reinberg, D., Regulation of p53 activity through lysine methylation. *Nature* **2004,** *432*, 353-360.
4. Zhang, L.; Ding, X. J.; Cui, J.; Xu, H.; Chen, J.; Gong, Y. N.; Hu, L. Y.; Zhou, Y.; Ge, J. N.; Lu, Q. H.; Liu, L. P.; Chen, S.; Shao, F., Cysteine methylation disrupts ubiquitin-chain sensing in NF-kappa B activation. *Nature* **2012,** *481*, 204-+.
5. Van Der Werf P, K. D. J., Identification of a gamma-glutamyl methyl ester in bacterial membrane protein involved in chemotaxis. *J Biol Chem* **1977,** *252*, 2793-5.
6. Chiu, V. K.; Silletti, J.; Dinsell, V.; Wiener, H.; Loukeris, K.; Ou, G.; Philips, M. R.; Pillinger, M. H., Carboxyl methylation of Ras regulates membrane targeting and effector engagement. *J Biol Chem* **2004,** *279*, 7346-52.
7. Strahl, B. D.; Allis, C. D., The language of covalent histone modifications. *Nature* **2000,** *403*, 41-5.
8. Dalhoff, C.; Lukinavicius, G.; Klimasauskas, S.; Weinhold, E., Direct transfer of extended groups from synthetic cofactors by DNA methyltransferases. *Nat. Chem. Biol.* **2006,** *2*, 31-32.
9. Peters, W.; Willnow, S.; Duisken, M.; Kleine, H.; Macherey, T.; Duncan, K. E.; Litchfield, D. W.; Luscher, B.; Weinhold, E., Enzymatic site-specific functionalization of protein methyltransferase substrates with alkynes for click labeling. *Angew Chem Int Ed Engl* **2010,** *49*, 5170-3.
10. Lee, B. W.; Sun, H. G.; Zang, T.; Kim, B. J.; Alfaro, J. F.; Zhou, Z. S., Enzyme-catalyzed transfer of a ketone group from an S-adenosylmethionine analogue: a tool for the functional analysis of methyltransferases. *J Am Chem Soc* **2010,** *132*, 3642-3.
11. Islam, K.; Chen, Y.; Wu, H.; Bothwell, I. R.; Blum, G. J.; Zeng, H.; Dong, A.; Zheng, W.; Min, J.; Deng, H.; Luo, M., Defining efficient enzyme-cofactor pairs for bioorthogonal profiling of protein methylation. *Proc Natl Acad Sci U S A* **2013,** *110*, 16778-83.
12. Bothwell, I. R.; Islam, K.; Chen, Y.; Zheng, W.; Blum, G.; Deng, H.; Luo, M., Se-adenosyl-L-selenomethionine cofactor analogue as a reporter of protein methylation. *J Am Chem Soc* **2012,** *134*, 14905-12.

13. Willnow, S.; Martin, M.; Luscher, B.; Weinhold, E., A Selenium-Based Click AdoMet Analogue for Versatile Substrate Labeling with Wild-Type Protein Methyltransferases. *Chembiochem* **2012**.
14. Zhang, Y. X.; Pan, Y. B.; Yang, W.; Liu, W. J.; Zou, H. F.; Zhao, Z. B. K., Protein Arginine Allylation and Subsequent Fluorophore Targeting. *Chembiochem* **2013,** *14*, 1438-1443.
15. Winter, J. M.; Chiou, G.; Bothwell, I. R.; Xu, W.; Garg, N. K.; Luo, M.; Tang, Y., Expanding the structural diversity of polyketides by exploring the cofactor tolerance of an inline methyltransferase domain. *Organic letters* **2013,** *15*, 3774-7.
16. Singh, S.; Zhang, J.; Huber, T. D.; Sunkara, M.; Hurley, K.; Goff, R. D.; Wang, G.; Zhang, W.; Liu, C.; Rohr, J.; Van Lanen, S. G.; Morris, A. J.; Thorson, J. S., Facile chemoenzymatic strategies for the synthesis and utilization of S-adenosyl-(L)-methionine analogues. *Angew Chem Int Ed Engl* **2014,** *53*, 3965-9.
17. Tomkuviene M, C.-d. O. B., Cerniauskas I, Weinhold E, Klimasauskas S., Programmable sequence-specific click-labeling of RNA using archaeal box C/D RNP methyltransferases. *Nucleic Acids Res* **2012**, 1-9.
18. Islam, K.; Zheng, W.; Yu, H.; Deng, H.; Luo, M., Expanding cofactor repertoire of protein lysine methyltransferase for substrate labeling. *Acs Chem Biol* **2011,** *6*, 679-84.
19. Dalhoff, C.; Lukinavicius, G.; Klimasauskas, S.; Weinhold, E., Direct transfer of extended groups from synthetic cofactors by DNA methyltransferases. *Nat Chem Biol* **2006,** *2*, 31-2.
20. Iwig, D. F.; Booker, S. J., Insight into the polar reactivity of the onium chalcogen analogues of S-adenosyl-L-methionine. *Biochemistry* **2004,** *43*, 13496-509.
21. Wang, R.; Zheng, W.; Yu, H.; Deng, H.; Luo, M., Labeling substrates of protein arginine methyltransferase with engineered enzymes and matched S-adenosyl-L-methionine analogues. *J Am Chem Soc* **2011,** *133*, 7648-51.
22. Guo, H.; Wang, R.; Zheng, W.; Chen, Y.; Blum, G.; Deng, H.; Luo, M., Profiling Substrates of Protein Arginine N-Methyltransferase 3 with S-Adenosyl-l-methionine Analogues. *Acs Chem Biol* **2014,** *9*, 476-84.
23. Bothwell, I. R.; Luo, M., Large-scale, protection-free synthesis of Se-adenosyl-L-selenomethionine analogues and their application as cofactor surrogates of methyltransferases. *Organic letters* **2014,** *16*, 3056-9.
24. Klayman, D. L.; Griffin, T. S., Reaction of Selenium with Sodium-Borohydride in Protic Solvents - Facile Method for Introduction of Selenium into Organic-Molecules. *Journal of the American Chemical Society* **1973,** *95*, 197-200.

CHAPTER 6: SYNTHESIS AND CHARACTERIZATION OF CHEMICAL REAGENTS

6.1 INTRODUCTION

The foundation for much of the work presented in in this dissertation has rested heavily upon the chemical synthesis of SAM analogues and related compounds. Throughout the course of this research, significant progress was made both in the development of new SAM analogues for BPPM technology, as well as the improvement of existing methods for the synthesis of selenium-based cofactors.[1-4] Furthermore, collaborative research projects have prompted synthesis of a variety of other materials, including isotopically labeled SAH, cysteine, and L-selenomethionine analogues. Although not discussed in previous chapters due to these projects being in very preliminary stages, the synthesis of these materials will also be described in this chapter.

Given its importance in the research herein, synthetic information regarding the production of all materials presented throughout this dissertation has been consolidated into this chapter. For ease of reference, this chapter's methods and results section is arranged into subheadings according to topics presented previous chapters (i.e. synthesis of SAM analogues discussed in chapter 2 will be presented first, followed by selenium-based analogues and other synthetic materials). Complete spectra for compounds described are provided in the appendix section.

6.2 APPROACH

Development of SAM Analogues for BPPM

Although many of the SAM analogues presented in chapters 2 and 5 had been previously reported,[5, 6] several presented herein were synthesized and characterized for the first time.[1, 3, 4] These included the Pentene-SAM, Hep-SAM and azide-containing Ab-SAM cofactor analogues (Figure 6.1) used in the development and application of BPPM technology towards the G9a and GLP1 lysine methyltransferases. Conveniently, synthesis of Pentene- and Hep-SAM analogues made use of well-established conditions for the alkylation of S-adenosyl-L-methionine in acidic solvent with commercially available starting materials.[6] The preparation of Ab-SAM, however, first required the synthesis of (E)-1-azido-4-bromobut-2-ene, which was obtained through the treatment of (E)-1,4-dibromobut-2-ene with sodium azide in a mixture of THF and water (Figure 6.1).[3] Subsequent coupling to SAH and purification by HPLC then yielded the desired material for spectral characterization.

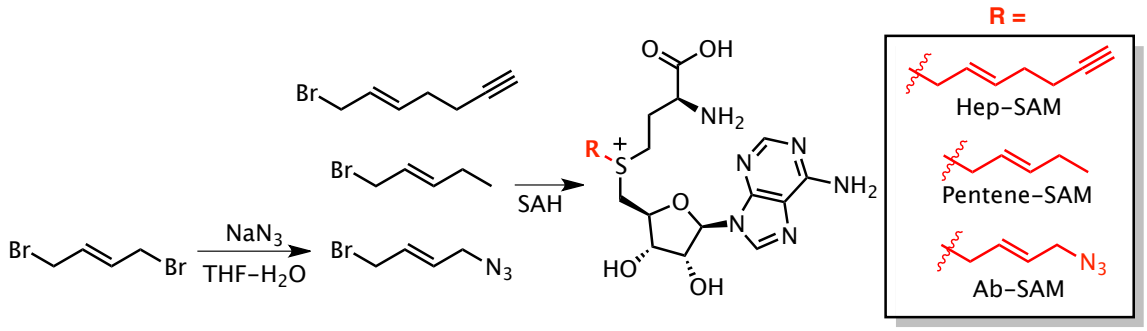

Figure 6.1: Synthesis of Previously Unreported SAM Analogues. Hep-SAM and Pentene-SAM were synthesized from commercially available materials. Ab-SAM was synthesized from SAH and (E)-1-azido-4-bromobut-2-ene, which was generated from (E)-1,4-dibromobutene.

Synthesis of Selenium-Based SAM Analogues

Although much of our preliminary research with ProSeAM relied upon a previously reported synthesis,[7] we found this protocol to be inefficient, time consuming,

and poorly suited for synthesis of libraries of SeAM analogues at larger scales. This proved to be a significant limitation, especially when examining larger panels of selenium-based analogues (chapter 5). Given this, we set out to develop a convenient protection-free strategy to access these materials easily and efficiently.[1]

SAM is generated *in vivo* by S-adenosylmethionine synthetase, which utilizes L-methionine and ATP as substrates (Figure 6.2).[8] Inspired by the biosynthesis of SAM, our synthetic strategy also relied upon comparable natural building blocks: L-methionine and adenosine, which can be converted into selenohomocystine and 5'-iodo-5'-deoxyadenosine, respectively. Subsequent conjugation of these materials would then result in the synthesis of Se-adenosyl-L-homocysteine (SeAH), which is the last converged precursor in the synthesis of the various Se-alkyl SeAM analogues examined in this work.

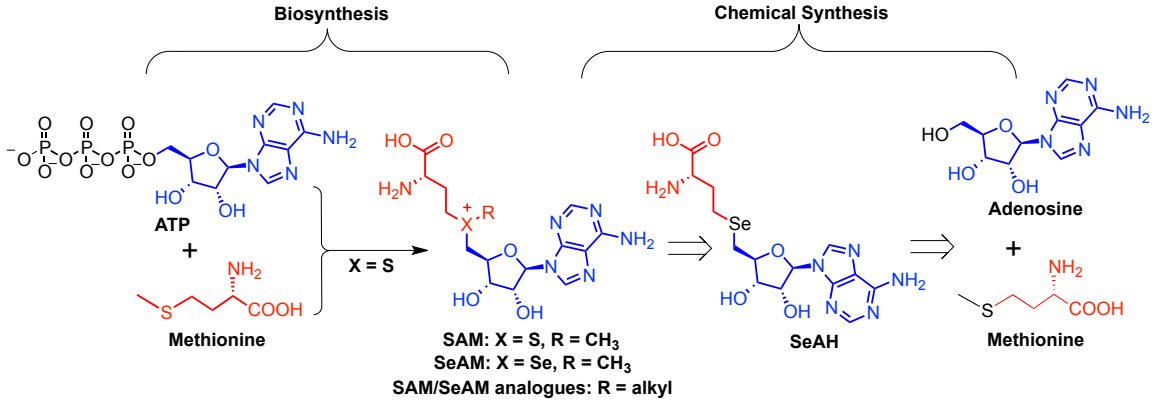

Figure 6.2: Biosynthesis of SAM and Retrosynthesis of SAM, SeAM and their Chalcogen-Alkyl Analogues.

In greater detail, L-methionine was first treated with iodomethane to generate S-methyl-L-methionine, which then underwent intramolecular displacement to form homoserine lactone.[9-11] Hydrolysis of this intermediate yielded α-amino-4-hydroxy-butanoic acid, which was easily precipitated from solution with a yield of 74%.[9, 11]

Treatment of α-amino-4-hydroxybutanoic acid with hydrogen bromide in acetic acid yielded α-amino-4-bromobutanoic acid with a yield of 62%.[10] This was then treated with Na_2Se_2, generated *in situ* from selenium powder and $NaBH_4$, to give the key building block selenohomocystine in 84% yield.[12] Selenohomocystine was readily purified by solid-phase extraction with acid-activated Dowex 50WX4 resin. The three-step synthesis is featured by its multigram scales, good yields from readily available materials, and facile purification (precipitation or solid-phase extraction; Figure 6.3).

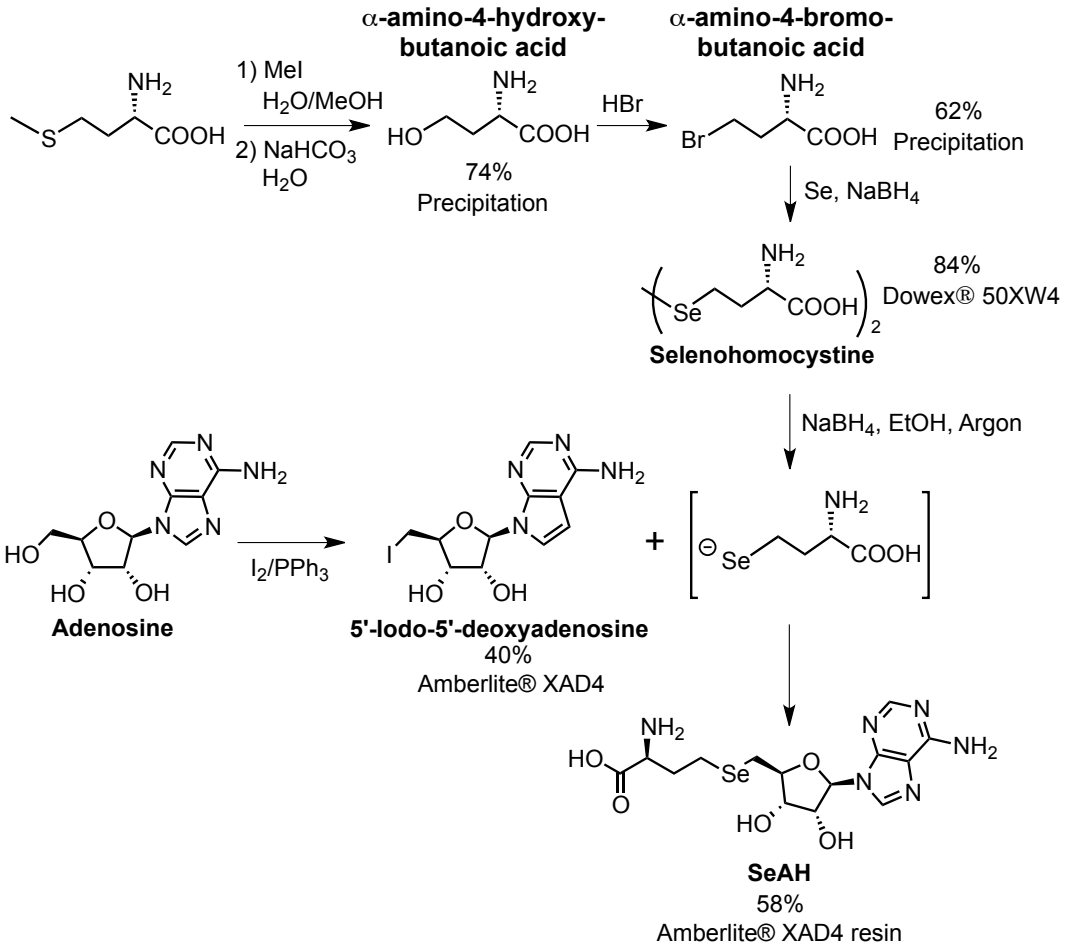

Figure 6.3: Chemical Synthesis of SeAH with Yields and Purification Methods Highlighted for Key Intermediates. MeI, iodomethane; PPh_3, triphenylphosphine.

Another key building block in the synthesis of SeAM analogues is 5'-iodo-5'-deoxyadenosine, which was readily prepared from adenosine via Appel reaction at gram-

scale (Figure 6.3).[13] SeAH, the last converged precursor in our synthesis of Se-alkyl SeAM analogues (Figure 6.2, 6.3), was generated through $NaBH_4$-mediated reduction of selenohomocystine to the selenide anion, followed by subsequent coupling with 5'-iodo-5'-deoxyadenosine with a yield of 58%. Here, a convenient solid-phase extraction protocol with Amberlite XAD4 resin was used to purify both 5'-iodo-5'-deoxyadenosine and SeAH.[14] Although previous syntheses used 5'-chloro-5'-deoxyadenosine[15] or 2',3'-O-isopropylidene-5'-O-p-toluenesulfonyladenosine[7] in similar coupling reactions, we found that 5'-iodo-5'-deoxyadenosine can be readily prepared and gave a more robust yield under these conditions. We further noted that the efficiency of the last coupling reaction would drop significantly if not performed under inert atmosphere, likely due to oxidation of the selenide anion and the resultant reformation of the diselenide. Collectively, this approach allowed access to SeAH through a protection-free, gram-scale synthesis with desired yields and convenient purification.

Although SeAH is readily subjected to alkylation to generate SeAM and Se-alkyl SeAM analogues, their weaker carbon-chalcogen bonds makes these compounds more susceptible to decomposition through intramolecular lactonization.[16] Thus, more care was taken during the purification and storage of these compounds than their sulfonium counterparts. We therefore freshly synthesized SeAM and a set of Se-alkyl SeAM analogues (Figure 6.4) in milligram scale and examined their reactivity as cofactor surrogates for native and engineered methyltransferases (chapter 5). For comparison, the equivalent sulfonium-based SAM analogues (Figure 6.4) were also prepared from S-adenosyl-L-homocysteine (SAH). Here, SeAH and SAH were treated with various alkyl halides in the presence of silver perchlorate (or mesolate for Enyne-SAM/Enyne-SeAM)

in a 1:1 acetic/formic acid mixture to give the desired products (Table 6.1).[5, 17, 18] These SAM and SeAM analogues contained either β-sp^2or β-sp^3 carbons for the purpose of comparing their roles on the transition-state stabilization of PMT-catalyzed S_N2 transalkylation reactions (Chapter 5).

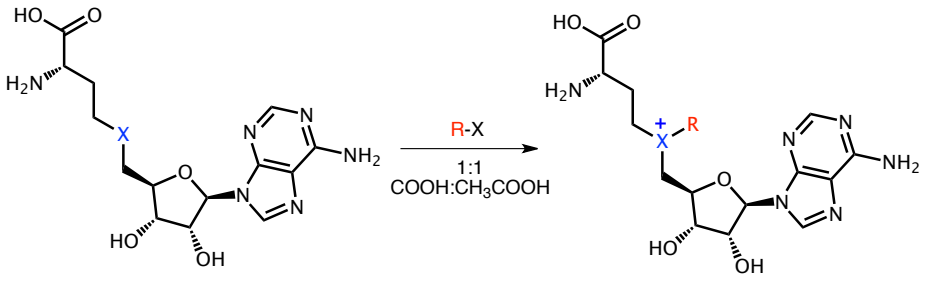

X = S	
R =	Name
	SAM
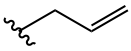	Allyl-SAM
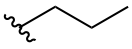	Propyl-SAM
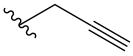	ProSAM
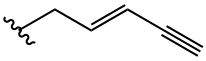	Enyne-SAM
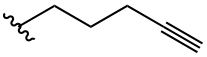	Pentyne-SAM
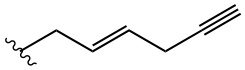	Hey-SAM
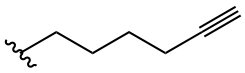	Hexyne-SAM

X = Se	
R =	Name
	SeAM
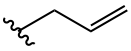	Allyl-SeAM
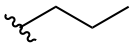	Propyl-SeAM
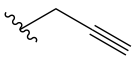	ProSeAM
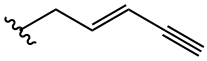	Enyne-SeAM
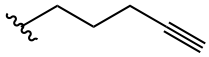	Pentyne-SeAM
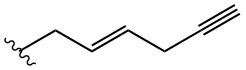	Hey-SeAM
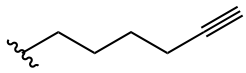	Hexyne-SeAM

Figure 6.4: Synthesis of a Panel of SAM and SeAM Analogues. SAM and SeAM analogues were synthesized and purified as described herein.

Synthesis of Isotopically Labeled Materials and Selenomethionine Analogues

In addition to SAM and SeAM analogues, several other compounds were synthesized for various purposes. These compounds included a selenium-based methionine analogue (ProSeMet; Figure 6.5a) for use in the *in vivo* biosynthesis of ProSeAM through the action of SAM synthetase, as well as a number of non-radioactive ^{34}S-labeled amino acids and SAM analogues. The latter were designed and synthesized as part of collaborative efforts with the laboratories of Drs. Steven Gross and Vern Schramm (as well as for a former member of the Luo lab: Dr. Joshua Linscott) for use in metabolomics and kinetic isotope effect experiments.

The synthesis of the selenium-based ProSeMet analogue was initiated from L-selenohomocystine, which had previously been prepared for use in the synthesis of SeAH (see above; Figure 6.5a).[1] This transformation was easily carried out in one step through $NaBH_4$-mediated reduction of L-selenohomocystine followed by alkylation of the selenide anion with propargyl bromide. Following purification by HPLC, this compound could be isolated in reasonable yield (48%) and high purity. Subsequent work by Dr. Rui Wang went on to demonstrate compatibility of this analogue toward wild-type and mutant SAM synthetase (unpublished data). In addition, application of ProSeMet for the *in situ* generation of ProSeAM and enzyme-coupled alkylation of rebeccamycin was independently corroborated by the lab of Dr. Jon Thorson.[19]

Incorporation of ^{34}S into labeled compounds was carried out according to previously reported methods.[20-22] The desired compounds synthesized included: ^{34}S-methionine, ^{34}S-cysteine and ^{34}S-SAH (Figure 6.5b, c). For the one pot synthesis of ^{34}S-methionine, elemental sulfur-34 was first treated with methyl lithium prior to addition of

α-amino-4-bromobutanoic acid in order to generate the desired material.[20] To generate ^{34}S-SAH, ^{34}S-methionine was subsequently subjected to Na/$NH_{4(l)}$ reduction conditions to generate ^{34}S-homocystine, which was then conjugated to 5′-iodo-5′-deoxyadenosine following $NaBH_4$ reduction.[21] Lastly, ^{34}S-cysteine was synthesized in a similar fashion to that of ^{34}S-methionine, in which elemental sulfur 34 was first treated with benzylmagnesium chloride prior to addition of α-amino-3-chloropropanoic acid.[22] The resultant ^{34}S-benzyl-cysteine was then subjected to Na/$NH_{4(l)}$ reduction conditions to afford ^{34}S-cysteine, which was purified by HPLC and characterized by ^{1}H NMR.

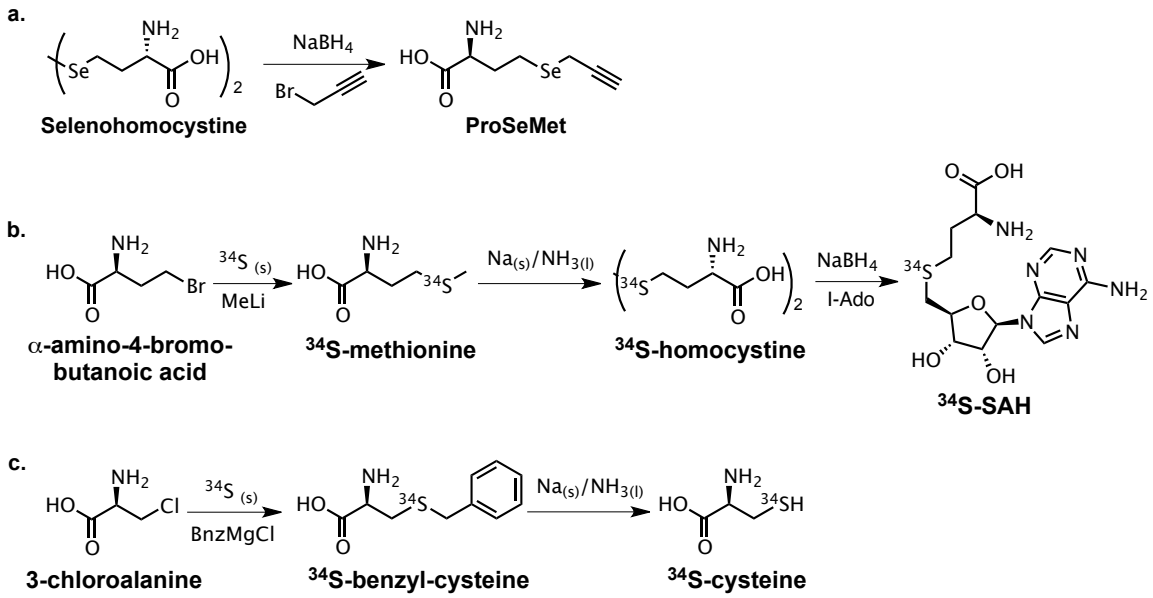

Figure 6.5: Synthesis of 34S and Selenium-Based Amino Acid Analogues. (a) Preparation of ProSeMet relies upon alkylation of selenohomocysteine following $NaBH_4$ reduction. (b) ^{34}S-Methionine is derived from elemental sulfur-34 treated with methyllithium (MeLi) and α-amino-4-bromo-butanoic acid. ^{34}S-Methionine may then be converted to ^{34}S-SAH following reductive cleavage by $Na_{(s)}/NH_{3(l)}$. I-Ado, 5'-iodo-5'-deoxyadenosine.

6.3 SYNTHETIC METHODS AND RESULTS

GENERAL MATERIALS AND METHODS

All chemical reagents were purchased from Aldrich Chemical or Acros Organics and used without additional purification unless noted otherwise. Optima grade

acetonitrile was obtained from Fisher Scientific and degassed under vacuum prior to HPLC purification. All reactions for the preparation of SAM and SeAM analogues were carried out in capped vials (4 mL) stirred with Teflon®-coated magnetic stir bars. Reaction solvents were removed by a Büchi rotary evaporator equipped with a dry ice-acetone condenser. Preparative HPLC purification of SAM and SeAM analogues was carried out using a Waters 6000 Controller HPLC/2998 diode array detector with an XBridge^{TM} Prep C18 5 μm OBD^{TM} 19x150 mm reverse phase column with UV detection at 260 nm. For preparative HPLC purification of SAM analogues, linear gradients of H_2O containing 0.1% TFA (solvent A) and acetonitrile containing 0.1% TFA (solvent B) were used at a flow rate of 10 mL/min (0–70% solvent B in 20 min, then 100% solvent A for 4 min). Preparative HLPC purification of ^{34}S-labeled amino acids and ProSeMet used linear gradients of H_2O containing 0.1% TFA (solvent A) and acetonitrile containing 0.1% TFA (solvent B) were used at a flow rate of 10 mL/min (0–70% solvent B in 11 min, then 100% solvent A for 4 min). Lyophilization and concentration of aqueous HPLC-purified samples was performed using a Flexi-Dry^{TM} mP Freeze-Dryer (FTS^{TM} Systems).

Nuclear magnetic resonance and mass spectral data were collected at MSKCC Analytical Core Facility. Nuclear magnetic resonance spectra were recorded on Bruker UltraShield^{TM} Plus 500 or 600 MHz instruments. NMR samples were performed in D_2O, except in the case of SeAH, SAM, and SeAM analogues, which were performed in D_2O containing 0.1% deuterated trifluoacetic acid to suppress their decomposition. High-resolution mass spectrometry (HRMS) was conducted using a Waters Acuity SQD LC-

MS with electrospray ionization (ESI). The concentrations of SAM analogues were determined by UV absorption with ε_{260} = 15400 L mol^{-1} cm^{-1}.

SYNTHESIS OF SAM ANALOGUES FOR BPPM

Synthesis of Pentene-SAM: Into a solution of *S*-adenosyl-L-homocysteine (15 mg, 0.039 mmol) in formic and acetic acids (1:1, 1 mL) was added (*E*)-1-bromopent-2-ene (288 mg, 1.95 mmol) and $AgClO_4$ (8 mg, 0.039 mmol) and stirred at ambient temperature (22 ^oC). After 4 hours, an additional batch of $AgClO_4$ and the bromide was added to drive the reaction to completion. The reaction was then quenched by distilled water containing 0.01% TFA (v/v). The aqueous phase was washed three times with diethyl ether (3×15 mL) and then passed through Nalgene 0.2 μM syringe filter. Pentene-SAM was then purified with preparative reversed-phase HPLC as described above. Diastereomeric mixture of the analogue was collected, concentrated and then lyophilized overnight. The resultant product (55% yield) was redissolved in water containing 0.01% TFA (v/v) and stored at -80 ^oC before use. **^{1}H-NMR (600 MHz, D_2O):** δ 8.35 (s, 1H), 8.34 (s, 0.5H), 8.33 (s, 0.5H), 6.08-6.03 (m, 1.5H), 5.94-5.89 (m, 0.5H), 5.37 (q, 0.5H, J = 7.56 Hz), 5.25 (q, 0.5H, J = 7.56 Hz), 4.55 (t, 0.5H, J = 6.18 Hz), 4.51 (t, 0.5H, J = 5.82 Hz), 4.43-4.40 (m, 1H), 4.0 (d, 1H, J = 7.56 Hz), 3.96 (d, 1H, J = 7.56 Hz), 3.85-3.80 (m, 1H), 3.77-3.65 (m, 2H), 3.44-3.38 (m, 1H), 3.36-3.28 (m, 1H), 2.02 (q, 1H, J = 7.02 Hz), 1.93 (q, 1H, J = 6.6 Hz), 0.86 (t, 1.5H, J = 7.44 Hz), 0.78 (t, 1.5H, J = 7.44 Hz). **^{13}C-NMR (150 MHz, D_2O):** δ 171.20, 171.14, 150.02, 148.70, 148.66, 147.94, 147.92,144.54, 144.48, 143.45, 143.41, 117.22, 115.28, 113.35, 112.11, 111.81, 90.02, 89.99, 78.61, 78.46, 73.0, 72.8, 72.6, 51.81, 51.76, 42.93, 42.23, 40.76, 40.40, 35.20,

34.93, 25.23, 25.15, 25.12, 25.03, 20.3, 11.96, 11.83. Total 38 peaks for two diastereomers. **ESI-MS (m/z):** 453.2$[M]^+$, 351.9 [5'-((*E*)-pent-2-enyl)thio-5'-deoxyadenosine+H]$^+$, 250.2 [5'-deoxyadenosine]$^+$, 135.8 [adenosine+H]$^+$. **HRMS:** Calculated for $C_{19}H_{29}N_6O_5S$: 453.1920; obtained: 453.1913.

Synthesis of Hep-SAM: Into a solution of *S*-adenosyl-*L*-homocystine (15 mg, 0.039 mmol) in formic and acetic acids (1:1, 1 mL) was added (*E*)-7-bromohept-5-en-1-yne (335 mg, 1.95 mmol) and $AgClO_4$ (8 mg, 0.039 mmol) and stirred at ambient temperature (22 ^oC). After 4 hours, an additional batch of $AgClO_4$ and (*E*)-7-bromohept-5-en-1-yne was added to drive the reactions to completion. The reaction was then quenched by distilled water containing 0.01% TFA (v/v). The aqueous phase was washed three times with diethyl ether (3×15 mL) and then passed through Nalgene 0.2 μM syringe filter. Hep-SAM was then purified with preparative reversed-phase HPLC as described above. Diastereomeric mixture of the SAM analogue was collected, concentrated and lyophilized overnight. The resultant product (40% yield) was re-dissolved in water containing 0.01% TFA (v/v) and stored at -80 ^oC before use. **^{1}H-NMR (600 MHz, D_2O):** δ 8.37 (s, 0.5H), 8.35 (s, 1H), 8.34 (s, 0.5H), 6.06 (dd, 1H, J = 3.18, 8.22 Hz), 6.04-6.0 (m, 0.5H), 5.85-5.81 (m, 0.5H), 5.49 (q, 0.5H, J = 7.56 Hz), 5.32 (q, 0.5H, J = 7.56 Hz), 4.58 (t, 0.5H, J = 6.54 Hz), 4.55 (t, 0.5H, J = 6.12 Hz), 4.44-4.41 (m, 1H), 4.03 (d, 1H, J = 7.62 Hz), 3.99 (d, 1H, J = 7.92 Hz), 3.81-3.64 (m, 3H), 3.46-3.39 (m, 1H), 3.35-3.30 (m, 1H), 2.25-2.21 (m, 5H), 2.12-2.09 (m, 2H). **^{13}C-NMR (150 MHz, D_2O):** δ 171.85, 171.75, 150.32, 150.24, 147.97, 147.95, 145.01, 144.84, 144.34, 144.26, 143.47, 143.38, 117.23, 115.29, 115.0, 114.67, 113.36, 90.08, 90.06, 84.93, 84.77, 78.69,

78.34, 72.99, 72.94, 72.66, 70.06, 70.04, 52.32, 52.29, 42.10, 41.34, 40.64, 40.24, 35.23, 35.02, 30.65, 30.59, 25.30, 25.12, 16.94, 16.76. Total 42 peaks for two diastereomers. **HRMS:** Calculated for $C_{21}H_{29}N_6O_5S$: 477.1920; obtained: 477.1903.

Synthesis of (E)-1-azido-4-bromobut-2-ene: (*E*)-1,4-dibromobut-2-ene (2 g, 9.34 mmol) was placed in a round-bottom flask and dissolved in THF (10 mL). Sodium azide (800 mg, 12.2 mmol) was dissolved in 1 mL water and added to the solution of (*E*)-1,4-dibromobut-2-ene. Reaction was stirred overnight at room temperature. Reaction was diluted with diethyl ether (100 mL) and successively washed with water (15 mL) and saturated NaCl solution (15 mL). The organic layer was dried over anhydrous Na_2SO_4 and evaporated under reduced pressure. Crude products were purified by silica gel column chromatography using petroleum ether-dichloromethane solvent system affording 800 mg of (*E*)- 1-azido-4-bromobut-2-ene (4.6 mmol, 49%) as a colorless liquid. **^{1}H-NMR (500 MHz, $CDCl_3$):** δ 6.03-5.97 (m, 1H), 5.85-5.79 (m, 1H), 3.97 (d, 2H, J=7.45 Hz), 3.81 (d, 2H, J=5.85 Hz). **^{13}C-NMR (125 MHz, $CDCl_3$):** 130.9, 128.1, 51.6, 30.9.

Synthesis of 4-azidobut-2-enyl-SAM (Ab-SAM): S-Adenosyl-L-homocysteine (12 mg, 0.031 mmol) was placed in a capped 4 mL glass vial and dissolved into a freshly prepared mixture of formic and acetic acids (1:1, 1 mL) and placed in an ice bath. To this acidic solution was added (E)-1-azido-4-bromobut-2-ene (269 mg, 1.55 mmol) and $AgClO_4$ (5.4 mg, 0.031 mmol). After the mixture was stirred for 5 min, the ice bath was removed, and the reaction was allowed to warm to ambient temperature (22 °C). After 5 hours, the addition of (E)-1-azido-4-bromobut-2-ene (269 mg, 1.55 mmol) and $AgClO_4$

(5.4 mg, 0.031 mmol) was repeated to drive the reaction to completion. The resultant reaction mixture was quenched by adding 20 mL of distilled water containing 0.01% TFA (v/v). The aqueous phase was washed three times with diethyl ether (3 × 15 mL) and passed through a Nalgene 0.2 μm syringe filter. Ab-SAM was purified with preparative reversed-phase HPLC as described above. Because the stereochemistry at sulfonium center could not be assigned unambiguously, a diastereomeric mixture of Ab-SAM was collected. The mixture was then concentrated by SpeedVac for 2 hours, followed by lyophilization overnight. The dried product was then redissolved in water containing 0.01% TFA (v/v) and stored at -80 °C before use. The compound was isolated in ~40% yield. **^{1}H NMR (600 MHz, D_2O):** δ 8.41 (s, 0.5H), 8.39 (s, 1H), 8.38 (s, 0.5H), 6.1 (t, 1H, J = 3.4 Hz), 6.09−6.06 (m, 0.5H), 5.96−5.91 (m, 0.5H), 5.79− 5.73 (m, 0.5H), 5.67−5.62 (m, 0.5H), 4.76 (q, 1H, J = 5.22 Hz), 4.6 (t, 0.5H, J = 6.54 Hz), 4.58 (t, 0.5H, J = 5.7 Hz), 4.5−4.47 (m, 1H), 4.15 (d, 1H, J = 7.56 Hz), 4.11 (d, 1H, J = 7.56 Hz), 3.88−3.8 (m, 5H), 3.56−3.38 (m, 2H), 2.3−2.28 (m, 2H). **^{13}C NMR (150 MHz, D_2O):** δ 171.59, 171.49, 163.06, 162.83, 150.15, 148, 144.78, 144.72, 143.5, 143.46, 138.23, 138.06, 119.37, 119.3, 117.92, 117.4, 117.28, 115.35, 90.1, 78.67, 78.41, 73.05 (2C), 72.88, 72.66, 52.11, 52.08, 51.2, 51.15, 42.03, 41.2, 40.81, 35.84, 35.55, 25.3, 25.16. **ESI-MS (m/z):** 480.1$[M]^+$, 379.09 [5'-(4-azidobut-2-en-1-ynyl)thio-5'-deoxyadenosine+H]$^+$, 250.2 [5′-deoxyadenosine]$^+$. **HRMS:** calculated for $C_{18}H_{26}N_9O_5S$, 480.1778; obtained, 480.1759.

SYNTHESIS OF SELENIUM-BASED SAM ANALOGUES

***Synthesis of* α-amino-4-hydroxybutanoic acid:** L-Methionine (15.0 g, 100 mmol) was suspended in a mixture of 140 mL distilled deionized H_2O and 200 mL methanol. Iodomethane (15 mL, 240 mmol) was then added and the resultant mixture was stirred vigorously for 48 hours at ambient temperature (22 ^oC). Bulk solvent was then removed by rotary evaporation to yield a white solid. The reaction product was dissolved in 100 mL H_2O. After adding sodium bicarbonate (8.4 g, 100 mmol), the solution was brought to 100 ^oC with reflux for 24 hours. After cooling the reaction mixture to ambient temperature (22 ^oC), the solvent was removed by rotary evaporation, affording the crude product as golden oil. This crude product was dissolved in 10 mL H_2O and 25 mL acetone. Ethanol (200 mL) was then slowly added while stirring the mixture, resulting in the precipitation of α-amino-4-hydroxybutanoic acid as a white solid. This product was then filtered and dried under high vacuum overnight to give 8.8 g product (74.0 mmol, 74 % yield). **^{1}H-NMR (600 MHz, D_2O):** δ ppm 1.87-2.06 (m; 2H; Hβ), 3.62- 3.69 (m; 2H; Hγ), 3.73 (dd; 1H; J_a = 7.56 Hz, J_b = 4.8 Hz; Hα). **^{13}C- NMR (150 MHz, D_2O):** δ ppm 174.38, 58.57, 53.31, 32.06.

***Synthesis of* α-amino-4-bromobutanoic acid hydrobromide:** In a 75 mL glass high-pressure reaction vessel, α-amino-4-hydroxybutanoic acid (5.1 g, 42.9 mmol) was suspended in 25 mL hydrobromic acid (33 wt.% in acetic acid). The reaction vessel was sealed and heated to 80 ^oC for 5 hours, and then allowed to cool down overnight to ambient temperature (22 ^oC). The reaction mixture was isolated by vacuum filtration and washed with 75 mL diethyl ether. The final product α-amino-4-bromobutanoic acid

hydrobromide was obtained by vacuum filtration and dried under high vacuum (7.1 g, 26.8 mmol, 62 % yield). **^{1}H-NMR (600 MHz, D_2O):** δ ppm 2.26-2.48 (m; 2H; Hβ), 3.47-3.56 (m; 2H; Hγ), 4.09 (t; 1H; J = 6.66 Hz; Hα). **^{13}C- NMR (150 MHz, D_2O):** δ ppm 173.06, 68.64, 49.83, 29.32.

Synthesis of selenohomocystine: In a 250 mL round bottom flask, 200-mesh selenium powder (3.6 g, 46.0 mmol) was suspended in 70 mL ethanol (200 proof). After adding sodium borohydride (1.74 g, 46.0 mmol), the mixture was heated to reflux at 80 ^{o}C for 2 hours (the solution became dark maroon in color). Into the reaction vessel was added α-amino-4-bromobutanoic acid hydrobromide (6.0 g, 23.0 mmol), resulting in a rapid formation of an opaque yellow mixture. The reaction was allowed to proceed under reflux at 80 ^{o}C overnight and then quenched with 10 mL 2 M HCl. After removing bulk solvent by rotary evaporation, the resulting residue was mixed with 25 mL 5% HCl. This aqueous solution was then washed three times with 75 mL diethyl ether and subjected to vacuum filtration to remove insoluble materials. A yellow solid was obtained after removal of aqueous solvent by rotary evaporation. This semi-crude product was then dissolved in 15 mL 1 M HCl and purified over Dowex® 50WX8 ion exchange resin according to manufacturer's specifications. In brief, activated resin (5.0 cm x 2.5 cm) was washed with 100 mL H_2O, followed by the loading of semi-crude product. The resin was then washed with an additional 100 mL H_2O to remove unbound impurities. Product was eluted from the resin using a 5% ammonium hydroxide solution. Fractions containing the desired product (bright yellow solution) were combined. After removing bulk solvent by rotary evaporation, the resulting yellow solid was placed under high vacuum overnight to

afford 3.4 g selenohomocystine 6 (9.5 mmol, 84% yield). **^{1}H-NMR (600 MHz, D_2O + 0.1% TFA-d):** δ ppm 2.21-2.34 (m; 2H; Hβ), 2.87-2.92 (m; 2H; Hγ), 3.98 (t; 1H; J = 6.30 Hz; Hα). **^{13}C- NMR (150 MHz, D_2O + 0.1% TFA-d):** δ ppm 172.25, 52.97, 31.39, 22.60. **HRMS:** Calculated for $C_8H_{17}N_2O_4Se_2$: 364.9519; obtained: 364.9518.

Synthesis of 5'-Iodo-5'-deoxyadenosine (I-Ado): Adenosine (10 g, 37.4 mmol) was suspended in 25 mL pyridine in a 100 mL round-bottom flask. Triphenylphosphine (15 g, 57.2 mmol) was added to the reaction vessel and stirred vigorously. Iodine (15 g, 59.1 mmol) was then slowly added to the mixture, which rapidly became brown in color. The vessel was protected from light and the reaction was allowed to proceed for 18 hours at ambient temperature (22 ^{o}C). Saturated sodium thiosulfate solution (3 mL) was then added to the reaction vessel and allowed to mix for 30 min in order to quench the reaction. Bulk solvent was removed by rotary evaporation. The residue was dissolved in 50 mL H_2O and washed with 75 mL chloroform three times. The aqueous phase was collected and the solvent was removed by rotary evaporation. The resulting off-white solid was stored at -20 ^{o}C as a crude product prior to further purification using Amberlite® XAD4 resin. In brief, the crude product was dissolved in 100 mL 0.5 M NaOH and loaded onto a 3 x 29 cm column of Amberlite XAD4 resin prewashed with 200 mL H_2O. The column was then washed with 200 mL 0.2 M ammonium acetate buffer (pH = 5.0) followed by 300 mL H_2O. The desired product was eluted from the resin with 350 mL methanol. After removing the solvent by rotary evaporation followed by high vacuum overnight, 5'-iodo-5'-deoxyadenosine 7 (5.7 g, 15.0 mmol) was obtained with a yield of 40%. **^{1}H-NMR (600 MHz, D2O):** δ ppm 3.46 (ddd; 2H; J_a = 27.54 Hz, J_b = 11.22 Hz, J_c = 4.98

Hz; H5'), 4.03 (dt; 1H; J_a = 4.98Hz, J_b = 4.92 Hz; H4'), 4.27 (dd; 1H; J_a = 5.10 Hz, J_b = 5.04 Hz; H3'), 4.77 (dd; 1H; J_a = 5.28 Hz, J_b = 5.28 Hz; H2'), 5.99 (d; 1H; J = 5.1 Hz; H1'), 8.13 (s; 1H; arom. H), 8.28 (s; 1H; arom. H). **^{13}C-NMR (150 MHz, D_2O):** δ ppm 155.63, 152.91, 148.96, 140.09, 118.72, 87.26, 82.93, 73.20, 73.11, 5.90. **HRMS:** Calculated for $C_{10}H_{13}N_5O_3I$: 378.0063; obtained: 378.0063.

Synthesis of Se-adenosylselenohomocysteine (SeAH): Selenohomocystine (1.4 g, 3.9 mmol) and sodium borohydride (1.47 g, 38.6 mmol) were suspended in 60 mL anhydrous ethanol in a 100 mL round-bottom flask. The mixture was stirred vigorously for 15 min under a steady flow of argon (the mixture became opaque white in color). 5'-Iodo-5'-deoxyadenosine (3.5 g, 9.3 mmol) was then added, the reaction vessel purged, and the reaction was allowed to proceed under argon overnight. After removal of bulk solvent by rotary evaporation, the residue was dissolved in 30 mL dilute HCl. The aqueous phase was washed three times with 50 mL diethyl ether, collected and dried by rotary evaporation to afford an off-white solid. This crude product was subject to further purification using Amberlite® XAD4 resin. In brief, the crude product was dissolved in 100 mL 0.5 M NaOH and then loaded onto a 3 x 29 cm column of Amberlite® XAD4 resin prewashed with 200 mL H_2O. The column was washed with 200 mL 0.2 M ammonium acetate buffer (pH = 5.0) followed by 300 mL H_2O. The desired product was eluted from the resin with 200 mL 1:1 H_2O:methanol. Fractions (25 mL each) were collected and analyzed by LCMS. Fractions containing the desired material were combined. Removal of solvent by rotary evaporation and the subsequent high vacuum overnight afforded *Se*-adenosylselenohomocysteine with 58% yield (1.94 g, 4.49 mmol).

^{1}H-NMR (600 MHz, D_2O + 0.1% TFA-d): δ ppm 2.05- 2.20 (m; 2H; Hβ), 2.60 (t; 2H; J = 7.86 Hz; Hγ), 2.95 (ddd; 2H; J_a = 28.86 Hz, J_b = 13.38 Hz, J_c = 5.22 Hz; H5'), 3.92 (t; 1H; J = 6.42 Hz; Hα), 4.26 (dt; 1H; J_a = 6.78 Hz, J_b = 5.1 Hz; H4'), 4.32 (dd; 1H; J_a = 5.07 Hz, J_b = 5.04 Hz; H3'), 4.77 (dd; 1H; J_a = 5.07 Hz, J_b = 5.04 Hz; H2'), 6.03 (d; 1H; J = 4.86 Hz; H1'), 8.33 (s; 1H; arom. H), 8.41 (s; 1H; arom. H). **^{13}C-NMR (150 MHz, D_2O + 0.1% TFA-d):** δ ppm 171.36, 149.18, 147.50, 143.73, 142.05, 118.11, 87.50, 83.30, 72.79, 72.07, 52.26, 30.01, 24.52, 17.90. **HRMS:** Calculated for $C_{14}H_{21}N_6O_5Se$: 433.0739; obtained: 433.0743.

Synthesis of ProSeAM: SeAH (15 mg, 34.8 μmol) was dissolved into a mixture of 1:1 formic acid and acetic acid (1 mL) and cooled on ice. Propargyl bromide (50 equiv, 80% v/v in toluene) was then slowly added. After addition $AgClO_4$ (5.4 mg, 34.8 μmol) in 0.5 mL of 1:1 formic and acetic acid mixture, the reaction was continued at ambient temperature (22 °C) for another 8 hours then quenched with 5 mL of distilled water containing 0.1% TFA (v/v). The aqueous phase was washed three times with diethyl ether, centrifuged to remove precipitate, and then passed through a Nalgene 0.2 μM syringe filter. ProSeAM was purified by preparative reversed-phase HPLC as described in the general methods. Collected fractions were then concentrated by lyophilization and redissolved in water containing 0.1% TFA. Stock solutions were stored at -80 ^{o}C before use. The overall yield for this reaction was 15%. **^{1}H NMR for ProSeAM (500 MHz, D_2O + 0.1% TFA-d):** δ = 2.34 (m, 2H), 3.15 (s, 1H), 3.52 (m, 2H), 3.86 (m, 1H), 3.9 (ddd, 2H; J_a =34.3 Hz, J_b = 12.8 Hz, J_c = 3.2 Hz), 4.14 (m, 2H), 4.49 (m, 1H), 4.56 (t, 1H, J = 6.13 Hz), 4.75 (m, 1H), 6.09 (d, 1H, J = 3.85 Hz), 8.37− 8.40 (m, 2H, arom.). **ESI-**

MS for ProSeAM (m/z): 471.11 $[M]^+$, 369.99 [5'-(propargyl)-selenoadenosine + $H]^+$, 249.91 [5′-deoxyadenosine]$^+$, 135.73 [adenine + $H]^+$. **HRMS:** 471.0871 calculated and 471.0880 observed for $C_{17}H_{24}N_6O_5Se$.

Synthesis and purification of SAM and SeAM analogues: A list of activated electrophiles used for the synthesis of SAM and SeAM analogues is presented in Table 6.1. These electrophiles were either purchased directly from Sigma-Aldrich and used without further purification or freshly prepared in house (Table 6.1).[1] Briefly, SAH (20 mg, 51,9 μmol) or SeAH (20 mg, 46.3 μmol) was dissolved in 500 μL 1:1 formic acid and acetic acid. Respective electrophiles (Table 6.1, 50 equivalents) and $AgClO_4$ (1 equivalent dissolved in 250 μL 1:1 formic:acetic acid) were then added to the reaction mixture. Reactions were allowed to proceed for 8 hours at ambient temperature (22 ^oC) and then quenched by addition of 3 mL distilled water containing 0.1% TFA. The aqueous phases were washed with diethyl ether (3x10 mL). Trace organic solvent in the crude sample was removed by rotary evaporation. After passing the sample through a Nalgene 0.22 μM syringe filter, the crude product was then purified by preparative reversed-phase HPLC as described in General Methods. Desired products were collected, lyophilized, dissolved in a small volume of 0.1% TFA and stored at -80 ^oC. Concentrations of SAM and SeAM analogues were determined by their UV absorption as described in the general methods. Their spectral characterization data are described below:

Table 6.1: Electrophiles used in the Preparation of SAM and SeAM Analogues

Name	Structure	Source
Iodomethane	CH_3I	Sigma-Aldrich
Iodopropane	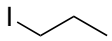	Sigma-Aldrich
Allyl bromide	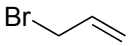	Sigma-Aldrich
Propargyl bromide	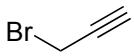	Sigma-Aldrich
5-Iodo-1-pentyne	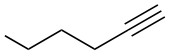	Sigma-Aldrich
(E)-Pent-2-en-4-yn-1-methanesulfonate	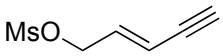	In-house
6-Iodo-1-hexyne	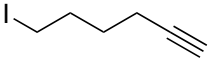	Sigma-Aldrich
(E)-6-bromohex-5-en-1-yne	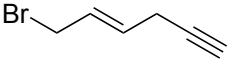	In-house

S-Adenosyl-L-methionine (SAM): Purification by HPLC (retention time = 6.0 min) afforded SAM as a mixture of sulfonium-*R,S*-epimers with a yield of 50%. **^{1}H-NMR (600 MHz, D_2O + 0.1% TFA-d):** δ ppm 2.29-2.41 (m, 2H, Hβ), 2.96/2.93 (s, 3H, 4:1 S-epimers, 1''), 3.42-3.68 (m; 2H; Hγ), 3.87-4.00 (m; 3H; H5', Hα), 4.50- 4.53 (m; 1H; H4'), 4.57 (dd; 1H; J_a = 5.88 Hz, J_b = 5.73 Hz; H3'), 4.79 (solvent overlap; H2'), 6.12 (d; 1H; J = 3.90 Hz; H1'), 8.40 (s; 1H; arom. H), 8.41 (s; 1H; arom. H). **^{13}C-NMR (150 MHz, D_2O + 0.1% TFA-d):** δ ppm 170.90, 149.96, 147.94, 144.41, 143.41, 119.32, 90.00, 78.42, 73.05, 72.60, 51.58, 44.22, 38.48, 24.81, 23.45. **HRMS:** Calculated for $C_{15}H_{23}N_6O_5S$: 399.1451; obtained: 399.1442.

Propyl-SAM: Purification by HPLC (retention time = 7.8 min) afforded Propyl-SAM as a mixture of sulfonium-*R,S*-epimers as reported previously.[6] **^{1}H-NMR (600 MHz, D_2O + 0.1% TFA-d):** δ ppm 0.84/0.87 (t; 3H; 1:1 epimers; J = 7.32 Hz; H3"), 1.64-1.74 (m; 2H; H2"), 2.23-2.32 (m; 2H; Hβ), 3.29.3.31 (t; 2H; 1:1 Se-epimers; H1"), 3.39-3.57 (m; 2H; Hγ), 3.83-3.86 (m; 2H; H5'), 3.88-3.90 (m; 1H; Hα), 4.43- 4.46 (m; 1H; H4'), 4.50-4.52 (m; 1H; H3'), 4.72-4.77 (m; 1H; solvent overlap; H2'), 6.07 (m; 1H; H1'), 8.35 (s; 2H; arom. H). **^{13}C-NMR (150 MHz, D_2O + 0.1% TFA- d):** δ ppm 171.00, 149.98, 147.95, 144.47, 143.39, 119.28, 89.99, 78.49, 73.01, 72.71, 51.67, 42.58, 41.84, 36.26, 25.08, 17.37, 11.79. **HRMS:** Calculated for $C_{17}H_{27}N_6O_5S$: 427.1764; obtained: 427.1758.

Allyl-SAM: Purification by HPLC yielded Allyl-SAM (retention time = 7.5 min) as a mixture of sulfonium-*R,S*-epimers as reported previously.[6] **^{1}H-NMR (600 MHz, D_2O + 0.1% TFA-d):** δ ppm 2.18-2.29 (m; 2H; Hβ), 3.31-3.48 (m; 2H; Hγ), 3.75- 3.79 (m; 2H; H5'), 3.81-3.88 (m; 1H; Hα), 4.00-4.04 (m; 2H; H1"), 4.39-4.43 (m; 1H; H4'), 4.47-4.50 (m; 1H; H3'), 4.69 (m; 1H; solvent overlap; H2'), 5.52 (d; 1H; J = 17 Hz; H3''), 5.57 (d; 1H; J = 10 Hz; H3''), 5.74 (ddt; 1H; J = 17 Hz, J = 10 Hz, J = 7.5 Hz; H2"), 6.02-6.03 (m; 1H, H1'), 8.30 (s; 2H; arom. H). **^{13}C-NMR (150 MHz, D_2O + 0.1% TFA-d):** δ ppm 170.90, 149.97, 147.93, 144.41, 143.46, 128.83, 122.31, 119.33, 90.03, 78.58, 73.03, 72.66, 51.53, 42.48, 40.88, 35.25, 25.04. **HRMS:** Calculated for $C_{17}H_{25}N_6O_5S$: 425.1607; obtained: 425.1592.

Pentyne-SAM: Purification by HPLC (retention time = 8.1 min) afforded Pentyne-SAM as sulfonium-*S*-epimer with a yield of 25%. **^{1}H-NMR (600 MHz, D_2O + 0.1% TFA-d):** δ ppm 1.76-1.87 (m; 2H; H3"), 2.08-2.18 (m; 4H; H5"; H2"), 2.21-2.34 (m; 2H; Hβ), 3.37 (t; 2H; 7.80 Hz; H1"), 3.39-3.51 (m; 2H; Hγ), 3.84-3.89 (m; 3H; H5'; Hα), 4.42-4.45 (m; 1H; H4'), 4.49-4.53 (m; 1H; H3'), 4.69-4.76 (m; 1H; solvent overlap; H2'), 6.03-6.04 (m; 1H; H1'), 8.34 (m; 2H; arom. H). **^{13}C-NMR (150 MHz, D_2O + 0.1% TFA-d):** δ ppm 170.96, 149.99, 147.93, 144.51, 143.54, 119.38, 90.10, 82.0, 78.86, 72.92, 72.60, 70.94, 51.63, 41.95, 39.98, 36.53, 25.03, 22.43, 16.35. **HRMS:** Calculated for $C_{19}H_{27}N_6O_5S$: 451.1764; obtained: 451.1743.

Enyne-SAM: Purification by HPLC (retention time = 8.1 min) afforded Enyne-SAM as a mixture of sulfonium-*R,S*-epimers with a yield of 30%. **^{1}H-NMR (600 MHz, D_2O + 0.1% TFA-d):** δ ppm 2.21-2.35 (m; 2H; Hβ), 3.35/3.4 (d; 1H; 40:60 epimers; J = 2.2 Hz; H5"), 3.37-3.54 (m; 2H; Hγ), 3.71-3.83 (m; 2H; H5'), 3.89- 3.97 (m; 1H; Hα), 4.07/4.12 (d; 2H; 40:60 epimers; J = 7.7 Hz; H1"), 4.38-4.44 (m; 1H; H4'), 4.53-5.62 (m; 1H; H3'), 4.67 (m; 1H; solvent overlap; H2'), 5.60/5.80 (dd; 1H; 40:60 epimers; J_a = 15.8 Hz, J_b = 1.6 Hz; H3"), 5.94/6.04 (dt; 1H; 40:60 epimers; J_a = 15.8 Hz, J_b = 7.8 Hz; H2"), 6.04 (d; 1H; J = 6.04 Hz; H1'), 8.32-8.34 (m; 2H; arom. H). **^{13}C-NMR (150 MHz, D_2O + 0.1% TFA-d):** δ ppm 169.81, 149.12, 147.05, 143.64, 142.99, 127.87, 120.36, 118.65, 89.68, 81.64, 78.18, 77.70, 72.21, 71.90, 50.49, 41.77, 40.35, 34.93, 24.20. **HRMS:** Calculated for $C_{19}H_{25}N_6O_5S$: 449.1607; obtained: 449.1598.

Hexyne-SAM: Purification by HPLC (retention time = 9.5 min) afforded Hexyne-SAM as a mixture of sulfonium-*R,S*-epimers with a yield of 35%. **^{1}H-NMR (600 MHz, D_2O + 0.1% TFA-d):** δ ppm 1.33-1.46 (m; 2H; H3"), 1.68-1.79 (m; 2H; H2"), 1.96/2.03 (dt; 2H; 40:60 epimers; J_a = 6.84 Hz, J_b = 2.5 Hz; H4"), 2.17/2.20 (t; 1H; 40:60 epimers; J = 2.5 Hz; H6"), 2.24-2.39 (m; 2H; Hβ), 3.31-3.38 (m; 2H H1"), 3.43-3.60 (m; 2H; Hγ), 3.84-3.87 (m; 2H; H5'), 3.94-4.00 (m; 1H; Hα), 4.43- 4.46 (m; 1H; H4'), 4.50-4.54 (m; 1H; H3'), 4.72-4.77 (dd; 1H; J_a = 5.46 Hz, J_b = 4.02 Hz; solvent overlap; H2'), 6.06 (d; 1H; J = 3.36 Hz; H1'), 8.36 (m; 2H; arom. H). **^{13}C-NMR (150 MHz, D_2O + 0.1% TFA-d):** δ ppm 170.44, 149.94, 147.92, 144.48, 143.47, 119.26, 90.00, 84.20, 78.24, 72.91, 72.61, 69.85, 51.22, 41.54, 40.49, 36.18, 25.94, 24.91, 22.56, 16.76. **HRMS:** Calculated for $C_{20}H_{29}N_6O_5S$: 465.1920; obtained: 465.1919.

Hey-SAM: Purification by HPLC (retention time = 9.5 min) afforded Hey-SAM as a mixture of sulfonium-*R,S*-epimers with a yield of 35%. ^{1}H-NMR (600 MHz, D_2O + 0.1% TFA-d): δ ppm 2.21-2.33 (m; 2H; Hβ), 2.40/2.44 (t; 1H; J = 2.58 Hz; 30:70 isomers; H6"), 2.89/2.97 (m; 2H; 30:70 isomers; H4"), 3.32-3.50 (m; 2H; Hγ), 3.69-3.91 (m; 3H; H5'; Hα), 4.04-4.08 (m; 2H; H1"), 4.43-4.46 (m; 1H; H4'), 4.51-4.53 (m; 1H; H3'), 4.72-4.74 (m; 1H; solvent overlap; H2'), 5.62/5.72 (dt; 1H; J_a = 15.3 Hz, J_b = 7.7 Hz; 30:70 isomers; H2"), 5.86/6.01 (dt; 1H; J_a = 15.3 Hz, J_b = 5.1 Hz; 30:70 isomers; H3"), 6.05-6.06 (m; 1H; H1'), 8.34-8.36 (m; 2H; arom. H). **^{13}C-NMR (150 MHz, D_2O + 0.1% TFA-d):** δ ppm 170.88, 149.98, 147.89, 144.50, 143.50, 139.15, 119.33 115.64, 90.08, 80.51, 78.59, 73.00, 72.62, 72.29, 51.60, 42.32, 41.07, 35.46, 25.06, 21.00. **HRMS:** Calculated for $C_{20}H_{27}N_6O_5S$: 463.1764; obtained: 463.1745.

Se-Adenosyl-L-methionine (SeAM): Purification by HPLC (retention time = 6.0 min) afforded SeAM as a mixture of sulfonium-*R,S*-epimers with a yield of 24%. **^{1}H-NMR (600 MHz, D_2O + 0.1% TFA-d):** δ ppm 2.22-2.31 (m; 2H; Hβ), 2.72/2.69 (s; 3H; 45:55 Se-epimers; H1''), 3.28-3.50 (m; 2H; Hγ), 3.74-3.90 (m; 3H; H5'; Hα), 4.41-4.45 (m; 1H; H4'), 4.48-4.49 (m; 1H; H3'), 4.72 (solvent overlap; H2'), 6.05 (d; 1H; J = 3.84 Hz; H1'), 8.34 (s; 2H; arom. H). **^{13}C-NMR (150 MHz, D_2O + 0.1% TFA-d):** δ ppm 171.00, 149.96, 147.93, 144.41, 143.38, 119.29, 89.85, 79.05, 73.24, 72.95, 52.17, 41.31, 35.44, 25.51, 19.44. **HRMS:** Calculated for $C_{15}H_{23}N_6O_5Se$: 447.0895; obtained: 447.0898.

Propyl-SeAM: Purification by HPLC (retention time = 7.8 min) afforded Propyl-SeAM as a mixture of sulfonium-*R,S*-epimers with a yield of 25%. **^{1}H-NMR (600 MHz, D_2O + 0.1% TFA-d):** δ ppm 0.79/0.85 (t; 3H; 55: 45 epimers; J = 7.32 Hz; H3"), 1.62-1.73 (m; 2H; H2"), 2.22-2.34 (m; 2H; Hβ), 3.24-3.47 (m; 4H; H1"; Hγ), 3.74- 3.81 (m; 2H; H5'), 3.84-3.94 (m; 1H; Hα), 4.41-4.44 (m; 1H; H4'), 4.47-4.49 (m; 1H; H3'), 4.72-4.77 (m; 1H; solvent overlap; H2'), 6.04-6.05 (m; 1H; H1'), 8.34- 8.35 (m; 2H; arom. H). **^{13}C-NMR (150 MHz, D_2O + 0.1% TFA-d):** δ ppm 170.68, 149.94, 147.92, 144.45, 143.43, 119.24, 89.86, 79.07, 73.34, 73.01, 52.01, 41.91, 39.98, 33.84, 25.78, 18.34, 12.73. **HRMS:** Calculated for $C_{17}H_{27}N_6O_5Se$: 475.1208; obtained: 475.1199.

Allyl-SeAM: Purification by HPLC (retention time = 7.5 min) afforded Allyl-SeAM as a mixture of sulfonium-*R,S*-epimers with a yield of 23%. **^{1}H-NMR (600 MHz,**

D_2O + 0.1% TFA-d): δ ppm 2.21-2.33 (m; 2H; Hβ), 3.23-3.37 (m; 2H; Hγ), 3.67- 3.76 (m; 2H; H5'), 3.81-3.89 (m; 1H; Hα), 3.96-4.0 (m; 2H; H1"), 4.40-4.43 (m; 1H; H4'), 4.47-4.51 (m; 1H; H3'), 4.73 (m; 1H; solvent overlap; H2'), 5.45 (d; 1H; J = 17 Hz; H3''), 5.49 (d; 1H; J = 10 Hz; H3''), 5.79 (ddt; 1H; J_a = 17 Hz, J_b = 10 Hz, J_c = 8 Hz; H2"), 6.04 (d; 1H, J = 3.66 Hz; H1'), 8.34 (s; 2H; arom. H). **^{13}C-NMR (150 MHz, D_2O + 0.1% TFA-d):** δ ppm 170.86, 149.95, 147.95, 144.44, 143.44, 127.63, 124.42, 119.26, 89.94, 79.04, 73.38, 72.97, 52.19, 41.17, 39.63, 33.42, 25.70. **HRMS:** Calculated for $C_{17}H_{25}N_6O_5Se$: 473.1052; obtained: 473.1068.

Pentyne-SeAM: Purification by HPLC (retention time = 8.2 min) afforded Pentyne-SeAM as a mixture of sulfonium-*R,S*-epimers with a yield of 12%. **^{1}H-NMR (600 MHz, D_2O + 0.1% TFA-d):** δ ppm 1.79-1.87 (m; 2H; 3"), 2.09-2.17 (m; 3H; H5"; H2"), 2.22-2.34 (m; 2H; Hβ), 3.33-3.52 (m; 4H; H1"; Hγ), 3.79-3.9 (m; 3H; H5'; Hα), 4.43-4.46 (m; 1H; H4'), 4.50-4.54 (m; 1H; H3'), 4.72-4.78 (m; 1H; H2'), 6.05- 6.06 (m; 1H; H1'), 8.37 (s; 2H; arom. H). **^{13}C-NMR (150 MHz, D_2O + 0.1% TFA- d):** δ ppm 170.65, 149.96, 147.91, 144.49, 143.59, 119.31, 90.00, 84.43, 78.88, 73.08, 72.89, 71.11, 51.96, 40.15, 39.03, 34.07, 25.74, 23.39, 17.14. **HRMS:** Calculated for $C_{19}H_{27}N_6O_5Se$: 499.1208; obtained: 499.1204.

Enyne-SeAM: Purification by HPLC (retention time = 8.2 min) afforded Enyne-SeAM as a mixture of sulfonium-*R,S*-epimers with a yield of 34%. **^{1}H-NMR (600 MHz, D_2O + 0.1% TFA-d):** δ ppm 2.26-2.32 (m; 2H; Hβ), 3.28-3.48 (m; 2H; Hγ), 3.36/3.40 (d; 1H; 30:70 epimers; J = 2.3 Hz; H5"), 3.73-3.87 (m; 3H; H5'; Hα), 4.02/4.06 (d; 2H;

30:70 epimers; J = 8.0 Hz; H1"), 4.40-4.44 (m; 1H; H4'), 4.52- 4.59 (m; 1H; H3'), 4.68-4.72 (m; 1H; solvent overlap; H2'), 5.64/5.79 (dd; 1H; 30:70 epimers; J_a = 1.9 Hz, J_b = 15.8 Hz; H3"), 5.99-6.14 (m; 1H; H2"), 6.05 (d; 1H; J = 3.6 Hz; H1'), 8.36-8.37 (m; 2H; arom. H.). **^{13}C-NMR (150 MHz, D_2O + 0.1% TFA-d):** δ ppm 170.65, 149.96, 147.86, 143.66, 142.84, 131.08, 119.83, 119.36, 90.10, 82.00, 78.90, 77.95, 72.89, 72.84, 51.92, 40.84, 39.89, 33.58, 24.71. **HRMS:** Calculated for $C_{15}H_{25}N_6O_5Se$: 497.1052; obtained: 497.1034.

Hexyne-SeAM: Purification by HPLC (retention time = 9.4 min) afforded Hexyne-SeAM as sulfonium-*S*-epimer with a yield of 16%. **^{1}H-NMR (600 MHz, D_2O + 0.1% TFA-d):** δ ppm 1.39 (p; 2H; J = 7.32 Hz; H3"), 1.77 (dp; 2H; J_a = 7.5 Hz, J_b = 3.18 Hz; H2"), 1.99 (dt; 2H; J_a = 6.96 Hz, J_b = 2.58 Hz; H4"), 2.25 (t; 1H; J = 2.58 Hz; H6"), 2.35-2.39 (m; 2H; Hβ), 3.34 (t; 2H; J = 8.0 Hz; H1"), 3.45-3.55 (m; 2H; Hγ), 3.80-3.89 (m; 2H; H5'), 3.98 (t; 1H; J = 6.84 Hz; Hα), 4.49-4.52 (m; 1H; H4'), 4.54-4.57 (m; 1H; H3'), 4.85 (dd; 1H; J_a = 5.46 Hz, J_b = 4.77 Hz; H2'), 6.12 (d; 1H; J = 4.02 Hz; H1'), 8.41-8.45 (2H, arom. H). **^{13}C-NMR (150 MHz, D_2O + 0.1% TFA-d):** δ ppm 171.03, 150.00, 147.99, 144.61, 143.44, 119.23, 89.59, 84.14, 79.23, 73.15, 73.08, 69.75, 52.17, 40.23, 39.01, 34.15, 26.78, 25.71, 23.8, 16.63. **HRMS:** Calculated for $C_{20}H_{29}N_6O_5Se$: 513.1365; obtained: 513.1356.

Hey-SeAM: Purification by HPLC (retention time = 9.4 min) yielded Hey-SAM as sulfonium-*S*-epimer with a yield of 23%. **^{1}H-NMR (600 MHz, D_2O + 0.1% TFA-d):** δ ppm 2.24-2.31 (m; 2H; Hβ), 2.43 (t; 1H; J = 2.64 Hz; H6"), 2.94-2.95 (m; 2H; H4"),

3.23-3.37 (m; 2H; Hγ), 3.65-3.76 (m; 2H; H5'), 3.83 (dd; 1H; J_a = 7.62 Hz, J_b = 5.46 Hz; Hα), 4.02 (d; 2H; J = 7.92 Hz; H1"), 4.40-4.43 (m; 1H; H4'), 4.50 (dd; 1H; J_a =6.06Hz, J_b =3.36Hz;H3'), 4.68 (dd;1H; J_a = 5.58Hz, J_b =3.48 Hz; solvent overlap; H2'), 5.76 (dt; 1H; J_a = 15.24 Hz, J_b = 8.04 Hz; H3"), 5.96 (dt; 1H; J_a = 15.24 Hz, J_b = 5.22 Hz; H2"), 6.04 (d; 1H; J = 3.66 Hz; H1'), 8.35 (s; 1H; arom. H), 8.36 (s; 1H, arom. H). **^{13}C-NMR (150 MHz, D_2O + 0.1% TFA-d):** δ ppm 171.00, 149.98, 147.90, 144.46, 143.47, 137.94, 119.32, 117.89, 90.02, 80.75, 78.98, 73.33, 72.92, 72.14, 52.22, 40.71, 39.46, 33.36, 25.76,20.92. **HRMS:** Calculated for $C_{20}H_{27}N_6O_5Se$: 511.1208; obtained: 511.1199.

SYNTHESIS OF ^{34}S-LABELED AND SELENOMETHIONINE ANALOGUES

***Synthesis of α-amino-4-(propargylselanyl)butanoic acid (ProSeMet*):** Selenohomocystine (300 mg, 0.83 mmol) and sodium borohydride (62.3 mg, 1.65 mmol) were suspended in 20 mL anhydrous ethanol. The mixture was stirred vigorously for 15 min under a steady flow of argon (the mixture became opaque white in color). Propargyl bromide solution (175 μL, 1.65 mmol) was then added and the reaction was allowed to proceed under argon overnight. After removal of bulk solvent by rotary evaporation, the residue was dissolved in dilute HCl. The aqueous phase was washed three times with diethyl ether, collected and dried by rotary evaporation to afford. Subsequent preparative HPLC purification of the desired compound was performed as described in general methods resulting in 174 mg of ProSeMet (48% yield). **^{1}H-NMR (500 MHz, D_2O):** δ ppm 2.22-2.30 (m; 2H;), 2.6 (s; 1H), 2.82 (t; 2H), 3.25 (s; 2H), 3.98 (t; 1H). **ESI-MS (*m/z*):** 221.76 $[M]^+$, 181.69 [selenohomocysteine]$^+$.

Synthesis of ^{34}S-methionine: Elemental sulfur-34 (50 mg, 1.56 mmol) was suspended in 7 mL dry THF under argon. To this suspension was added 9.25 mL methyllithium solution (1.6 M in diethyl ether) and the reaction allowed to proceed. After 10 minutes, α-amino-4-bromobutanoic acid hydrobromide (380 mg, 1.44 mmol) dissolved in 6 mL dry ethanol was slowly added to the reaction vessel. This addition was accompanied by the release of a significant amount of gas from the reaction solution. Following addition, the vessel was brought to reflex at 60 ^{o}C for 2 hours, after which time the reaction mixture had become opaque orange in color. After removal of bulk solvent by rotovap, the residue was dissolved in dilute HCl and washed three times with diethyl ether prior to purification by prep HPLC as described in the general methods. The calculated yield based on sulfur-34, was 89% (210 mg). **^{1}H-NMR (500 MHz, D_2O):** δ ppm 2.05 (s; 3H), 2.11-2.21 (m; 2H;), 2.61 (t; 2H), 4.05 (t; 1H). **ESI-MS (*m/z*):** 151.76 $[M]^+$, 134.71, 105.73.

Synthesis of ^{34}S-homocystine: ^{34}S-methionine (100 mg, 0.66 mmol) in a dry round bottom flask was placed in a -78 ^{o}C dry ice/acetone bath. $NH_{4(l)}$ (~10 mL) was condensed in the reaction vessel prior to addition of ~30 mg sodium metal (~2 equivalents). The solution immediately developed a deep blue color, which was maintained for 1 hour. The reaction was then quenched through the addition of a minimal NH_4Cl. The vessel was then brought to room temperature and left open to air to allow NH_4 to evaporate. Residual NH_4 was then removed on high vacuum and the residue dissolved in water containing 0.1% TFA. This crude material was then purified by

preparative HPLC (42 mg; 47% yield) and characterized by LCMS prior to use in the synthesis of ^{34}S-SAH. **ESI-MS (*m/z*):** 272.85 $[M]^+$, 137.69.

Synthesis of ^{34}S-adenosyl-L-methionine (^{34}S-SAH): ^{34}S-homocystine (42 mg, 0.15 mmol) sodium borohydride (29 mg, 0.75 mmol) were suspended in 10 mL anhydrous ethanol. The mixture was stirred vigorously for 30 min under a steady flow of argon. 5'-Iodo-5'-deoxyadenosine (174 mg, 0.46 mmol) was then added, the reaction vessel purged, and the reaction was allowed to proceed under argon overnight. After removal of bulk solvent by rotary evaporation, the residue was dissolved in dilute HCl. The aqueous phase was washed three times with diethyl ether prior to purification by preparative HPLC as described in the general methods. **^{1}H-NMR (600 MHz, D_2O + 0.1% TFA-d):** δ ppm 2.01- 2.15 (m; 2H; Hβ), 2.63 (t; 2H; J = 7.4 Hz; Hγ), 2.95 (m; 2H; H5'), 4.04 (t; 1H; J = 6.4 Hz; Hα), 4.22 (m; 1H; H4'), 4.32 (t; 1H; J = 5.16 Hz; H3'), 4.74 (m; 1H; H2'; solvent overlap), 6.02 (d; 1H; J = 4.8 Hz; H1'), 8.32 (s; 1H; arom. H), 8.40 (s; 1H; arom. H). **^{13}C-NMR (150 MHz, D_2O + 0.1% TFA-d):** δ ppm 171.57, 149.9, 148.26, 144.23, 142.84, 118.73, 88.40, 83.58, 72.99, 72.24, 51.54, 33.24, 29.52, 27.21. **ESI-MS (*m/z*):** 386.86 $[M]^+$, 251.78, 135.61.

Synthesis of ^{34}S-benzylcysteine: Elemental sulfur-34 (50 mg, 1.56 mmol) was placed in a dry conical flask flushed with argon. 1.5 mL benzylmagnesium chloride solution (1M) in diethyl ether was then added to the vessel and the reaction allowed to proceed overnight at room temperature. Following completion of the reaction, bulk solvent was first removed under a stream of nitrogen. The remaining white residue was

rinsed 3 times with hexanes and again dried under a stream of nitrogen. NaOH (1mL, 4M) was then added and the reaction vessel heated to 50 ^{o}C. β-chloro-L-alanine hydrochloride (250 mg, 1.5 mmol) dissolved in 10 drops H_2O was then slowly added to the reaction over the course of 5 minutes. The reaction was allowed to proceed at 50 oC for 1 hour prior to quenching with excess glacial acetic acid. The crude product mixture was then washed 3 times with hexanes, and the semicrude aqueous phase further purified by preparative HPLC as described in general methods and lyophilized to afford 96 mg (0.45 mmol) ^{34}S-benzylcysteine (30 % yield). **^{1}H-NMR (500 MHz, D_2O + 0.1% TFA-d):** δ ppm 2.82-2.97 (m; 2H), 3.69 (s; 2H), 3.99 (dd; Ja = 3.4 Hz, Jb = 7.7 Hz; 1H), 7.20-7.21 (m; 1H; aromatic H), 7.26-7.27 (m; 4H; aromatic H). **^{13}C-NMR (150 MHz, D_2O + 0.1% TFA-d):** δ ppm 170.34, 134.47, 128.94, 128.86, 127.56, 117.07, 51.90, 35.24, 30.35. **ESI-MS (*m/z*):** 213.71 $[M]^+$, 196.63, 131.77.

Synthesis of ^{34}S-cysteine: ^{34}S-benzylcysteine (96 mg, 0.45 mmol) in a dry round bottom flask was placed in a -78 ^{o}C dry ice/acetone bath. $NH_{4(l)}$ (~10 mL) was condensed in the reaction vessel prior to addition of 20 mg sodium metal (~2 equivalents). The solution immediately developed a deep blue color, which was maintained for 45 minutes. The reaction was then quenched through the addition of a minimal NH_4Cl. The vessel was then brought to room temperature and left open to air to allow NH_4 to evaporate. Residual NH_4 was then removed on high vacuum and the residue dissolved in water containing 0.1% TFA. This crude material was then purified by preparative HPLC and characterized (16 mg; 30% yield). **^{1}H-NMR (500 MHz, D_2O + 0.1% TFA-d):):** δ ppm

2.94-3.066 (m; 2H), 3.98 (m; 1H). **^{13}C-NMR (150 MHz, D_2O + 0.1% TFA-d):** δ ppm 171.71, 55.32, 24.38. **ESI-MS (*m/z*):** 121.75 $[M]^+$.

6.4 REFERENCES

1. Bothwell, I. R.; Luo, M., Large-scale, protection-free synthesis of Se-adenosyl-L-selenomethionine analogues and their application as cofactor surrogates of methyltransferases. *Organic letters* **2014,** *16*, 3056-9.
2. Bothwell, I. R.; Islam, K.; Chen, Y.; Zheng, W.; Blum, G.; Deng, H.; Luo, M., Se-adenosyl-L-selenomethionine cofactor analogue as a reporter of protein methylation. *J Am Chem Soc* **2012,** *134*, 14905-12.
3. Islam, K.; Bothwell, I.; Chen, Y.; Sengelaub, C.; Wang, R.; Deng, H.; Luo, M., Bioorthogonal profiling of protein methylation using azido derivative of S-adenosyl-L-methionine. *J Am Chem Soc* **2012,** *134*, 5909-15.
4. Islam, K.; Chen, Y.; Wu, H.; Bothwell, I. R.; Blum, G. J.; Zeng, H.; Dong, A.; Zheng, W.; Min, J.; Deng, H.; Luo, M., Defining efficient enzyme-cofactor pairs for bioorthogonal profiling of protein methylation. *Proc Natl Acad Sci U S A* **2013,** *110*, 16778-83.
5. Islam, K.; Zheng, W.; Yu, H.; Deng, H.; Luo, M., Expanding cofactor repertoire of protein lysine methyltransferase for substrate labeling. *Acs Chem Biol* **2011,** *6*, 679-84.
6. Dalhoff, C.; Lukinavicius, G.; Klimasauskas, S.; Weinhold, E., Direct transfer of extended groups from synthetic cofactors by DNA methyltransferases. *Nat. Chem. Biol.* **2006,** *2*, 31-32.
7. Skupin, J., Synthesis of Se-(5'-deoxyadenosine-5')-DL-selenomethionine *Roczniki Chemii* **1962,** *36*, 631-7.
8. Cantoni, G. L.; Durell, J., Activation of methionine for transmethylation. II. The methionine-activating enzyme; studies on the mechanism of the reaction. *J Biol Chem* **1957,** *225*, 1033-48.
9. Boyle, P. H.; Davis, A. P.; Dempsey, K. J.; Hosken, G. D., Synthesis of (S)-2-Amino-1,1-Diphenylbutan-4-Ol - Conversion of an Alpha-Amino-Acid into an Alpha-(Diphenylmethyl) Amine without Loss of Optical Purity. *Tetrahedron-Asymmetr* **1995,** *6*, 2819-2828.
10. Jamieson, A. G.; Boutard, N.; Beauregard, K.; Bodas, M. S.; Ong, H.; Quiniou, C.; Chemtob, S.; Lubell, W. D., Positional scanning for peptide secondary structure by systematic solid-phase synthesis of amino lactam peptides. *J Am Chem Soc* **2009,** *131*, 7917-27.
11. Koch, T.; Buchardt, O., Synthesis of L-(+)-Selenomethionine. *Synthesis-Stuttgart* **1993**, 1065-1067.
12. Klayman, D. L.; Griffin, T. S., Reaction of Selenium with Sodium-Borohydride in Protic Solvents - Facile Method for Introduction of Selenium into Organic-Molecules. *Journal of the American Chemical Society* **1973,** *95*, 197-200.

13. Perrone, P.; Daverio, F.; Valente, R.; Rajyaguru, S.; Martin, J. A.; Leveque, V.; Le Pogam, S.; Najera, I.; Klumpp, K.; Smith, D. B.; McGuigan, C., First example of phosphoramidate approach applied to a 4 '-substituted purine nucleoside (4 '-azidoadenosine): Conversion of an inactive nucleoside to a submicromolar compound versus hepatitis C virus. *Journal of medicinal chemistry* **2007,** *50*, 5463-5470.
14. Miles, R. W.; Nielsen, L. P. C.; Ewing, G. J.; Yin, D.; Borchardt, R. T.; Robins, M. J., Nucleic acid related compounds, part 117. S-homoadenosyl-L-cysteine and S-homoadenosyl-L-homocysteine. Synthesis and binding studies of non-hydrolyzed substrate analogues with S-adenosyl-L-homocysteine hydrolase. *J Org Chem* **2002,** *67*, 8258-8260.
15. Willnow, S.; Martin, M.; Luscher, B.; Weinhold, E., A Selenium-Based Click AdoMet Analogue for Versatile Substrate Labeling with Wild-Type Protein Methyltransferases. *Chembiochem* **2012**.
16. Iwig, D. F.; Booker, S. J., Insight into the polar reactivity of the onium chalcogen analogues of S-adenosyl-L-methionine. *Biochemistry* **2004,** *43*, 13496-509.
17. Peters, W.; Willnow, S.; Duisken, M.; Kleine, H.; Macherey, T.; Duncan, K. E.; Litchfield, D. W.; Luscher, B.; Weinhold, E., Enzymatic site-specific functionalization of protein methyltransferase substrates with alkynes for click labeling. *Angew Chem Int Ed Engl* **2010,** *49*, 5170-3.
18. Dalhoff, C.; Lukinavicius, G.; Klimasauakas, S.; Weinhold, E., Synthesis of S-adenosyl-L-methionine analogs and their use for sequence-specific transalkylation of DNA by methyltransferases. *Nat. Protocols* **2006,** *1*, 1879-1886.
19. Singh, S.; Zhang, J.; Huber, T. D.; Sunkara, M.; Hurley, K.; Goff, R. D.; Wang, G.; Zhang, W.; Liu, C.; Rohr, J.; Van Lanen, S. G.; Morris, A. J.; Thorson, J. S., Facile chemoenzymatic strategies for the synthesis and utilization of S-adenosyl-(L)-methionine analogues. *Angew Chem Int Ed Engl* **2014,** *53*, 3965-9.
20. Ogra, Y.; Kitaguchi, T.; Suzuki, N.; Suzuki, K. T., In vitro translation with [34S]-labeled methionine, selenomethionine, and telluromethionine. *Analytical and bioanalytical chemistry* **2008,** *390*, 45-51.
21. Stern, P. H.; Hoffman, R. M., The chemical synthesis of high specific-activity [35S]adenosylhomocysteine. *Anal Biochem* **1986,** *158*, 408-12.
22. Wood, J. L.; Van Middlesworth, L., Preparation of cystine from radioactive sulfur. *J Biol Chem* **1949,** *179*, 529-33.

APPENDIX

Table A1: Proteins identified from GLP1-Y1211A transfected HEK293T cells with AbSAM. These proteins were not pulled-down in the control-transfected HEK293T cell.

Serial	Accession number	Mol. Wt.	Score	Description
1	IPI:IPI00946054.2	138.2	243.08	Histone-lysine N-methyltransferase, H3 lysine-9 specific 5
2	IPI:IPI00023006.1	42.0	121.55	Actin, alpha cardiac muscle 1
3	IPI:IPI00011253.3	26.7	68.59	40S ribosomal protein S3
4	IPI:IPI00412492.4	211.9	52.46	Isoform 1 of Plexin-D1
5	IPI:IPI00414696.1	36.0	38.25	Isoform A2 of Heterogeneous nuclear ribonucleoproteins A2/B1
6	IPI:IPI00003918.6	47.7	38.18	60S ribosomal protein L4
7	IPI:IPI00217223.1	49.6	30.01	Multifunctional protein ADE2
8	IPI:IPI00940148.1	50.6	29.36	Rab GDP dissociation inhibitor beta
9	IPI:IPI00220301.5	25.0	29.20	Peroxiredoxin-6
10	IPI:IPI00783097.4	83.1	27.01	Glycyl-tRNA synthetase
11	IPI:IPI00893580.1	38.2	28.04	HLA-B associated transcript 1
12	IPI:IPI00216587.9	24.2	27.66	40S ribosomal protein S8
13	IPI:IPI00011937.1	30.5	26.98	Peroxiredoxin-4
14	IPI:IPI00640741.1	19.0	25.49	19 kDa protein
15	IPI:IPI00556485.2	27.4	23.80	RPLP0 protein
16	IPI:IPI00024279.4	242.2	23.03	HEAT repeat-containing protein 1
17	IPI:IPI00965459.1	30.1	22.92	30 kDa protein
18	IPI:IPI00334713.1	30.6	20.90	Isoform 3 of Heterogeneous nuclear ribonucleoprotein A/B
19	IPI:IPI00947227.3	66.6	20.38	plastin-3 isoform 2
20	IPI:IPI00332428.5	35.3	19.74	Protein MAK16 homolog
21	IPI:IPI00016801.1	61.4	19.18	Glutamate dehydrogenase 1, mitochondrial
22	IPI:IPI00295857.7	138.3	19.16	Isoform 1 of Coatomer subunit alpha
23	IPI:IPI00024524.4	27.9	18.13	RNA-binding protein PNO1
24	IPI:IPI00374151.1	25.8	17.93	thioredoxin-dependent peroxide reductase, mitochondrial isoform b
25	IPI:IPI00291006.2	35.5	17.54	Malate dehydrogenase, mitochondrial
26	IPI:IPI00884904.1	605.3	17.40	Isoform 3 of Protein AHNAK2
27	IPI:IPI00297779.7	57.5	17.29	T-complex protein 1 subunit beta
28	IPI:IPI00220621.1	82.0	17.18	Isoform PDE4B3 of cAMP-specific 3',5'-cyclic phosphodiesterase 4B
29	IPI:IPI00658013.1	28.4	16.87	nucleophosmin isoform 3
30	IPI:IPI00453476.2	28.8	16.47	29 kDa protein
31	IPI:IPI00217467.3	21.9	16.20	Histone H1.4
32	IPI:IPI00010796.1	57.1	16.02	Protein disulfide-isomerase
33	IPI:IPI00642716.6	225.7	15.42	myosin-7B
34	IPI:IPI00795527.1	20.8	15.28	21 kDa protein
35	IPI:IPI00216318.5	28.1	15.18	Isoform Long of 14-3-3 protein beta/alpha
36	IPI:IPI00909530.1	12.9	14.94	Histone H3
37	IPI:IPI00787460.3	134.4	14.65	Ovostatin homolog 1

38	IPI:IPI00022977.1	42.6	14.39	Creatine kinase B-type
39	IPI:IPI00028091.3	47.3	14.33	Actin-related protein 3
40	IPI:IPI00455599.4	49.1	14.15	Heat shock protein 90Bb
41	IPI:IPI00965269.1	55.3	13.72	cDNA, FLJ79275, highly similar to T-complex protein 1 subunit epsilon
42	IPI:IPI00031522.2	82.9	12.91	Trifunctional enzyme subunit alpha, mitochondrial
43	IPI:IPI00396321.1	34.9	12.68	Leucine-rich repeat-containing protein 59
44	IPI:IPI00005705.1	37.0	12.56	Isoform Gamma-1 of Serine/threonine-protein phosphatase PP1-gamma catalytic subunit
45	IPI:IPI00942832.2	437.8	12.38	Isoform 4 of Probable E3 ubiquitin-protein ligase C12orf51
46	IPI:IPI00305383.1	48.4	12.32	Cytochrome b-c1 complex subunit 2, mitochondrial
47	IPI:IPI00414101.4	177.4	12.04	Isoform 2 of DNA topoisomerase 2-alpha
48	IPI:IPI00411592.2	222.7	11.97	Isoform 2 of Chromodomain-helicase-DNA-binding protein 3
49	IPI:IPI00006196.3	236.4	11.86	Isoform 2 of Nuclear mitotic apparatus protein 1
50	IPI:IPI00241841.10	57.8	11.59	Keratin, type II cytoskeletal 79
51	IPI:IPI00413324.6	21.4	11.41	60S ribosomal protein L17
52	IPI:IPI00307749.2	32.8	11.34	NADH dehydrogenase [ubiquinone] iron-sulfur protein 7, mitochondrial
53	IPI:IPI00922697.2	43.3	11.27	Pyruvate dehydrogenase E1 component subunit alpha, somatic form, mitochondrial
54	IPI:IPI00030179.3	29.2	11.27	60S ribosomal protein L7
55	IPI:IPI00009368.4	35.6	11.16	Sideroflexin-1
56	IPI:IPI00910980.1	120.6	10.83	IARS protein
57	IPI:IPI00024719.1	49.5	10.76	Histone acetyltransferase type B catalytic subunit
58	IPI:IPI00552749.5	477.3	10.75	478 kDa protein
59	IPI:IPI00604431.1	117.8	10.35	Isoform 2 of Cullin-associated NEDD8-dissociated protein 1
60	IPI:IPI00910113.1	46.9	10.34	cDNA FLJ52902, highly similar to Rab GDP dissociation inhibitor alpha
61	IPI:IPI00168388.1	70.7	10.31	Isoform 1 of Signal recognition particle 68 kDa protein
62	IPI:IPI00178475.13	56.5	10.27	Chromodomain Y-like protein 2
63	IPI:IPI00025239.2	52.5	10.15	NADH dehydrogenase [ubiquinone] iron-sulfur protein 2, mitochondrial
64	IPI:IPI00021435.3	48.6	10.10	26S protease regulatory subunit 7

Table A2: Proteins identified from G9a-Y1154A transfected HEK293T cells by with AbSAM. These proteins were not pulled-down in the control-transfected HEK293T cell.

Serial	Accession number	Mol. Wt.	Score	Description
1	IPI:IPI00220795.4	128.9	223.37	Isoform 2 of Histone-lysine N-methyltransferase EHMT2
2	IPI:IPI00382470.3	98.1	106.16	Isoform 2 of Heat shock protein HSP 90-alpha
3	IPI:IPI00646779.2	50.1	81.85	TUBB6 protein
4	IPI:IPI00795257.3	31.5	74.07	Glyceraldehyde-3-phosphate dehydrogenase
5	IPI:IPI00011253.3	26.7	72.88	40S ribosomal protein S3
6	IPI:IPI00848226.1	35.1	69.91	Guanine nucleotide-binding protein subunit beta-2-like 1
7	IPI:IPI00644224.2	86.8	49.68	cDNA FLJ54020, highly similar to Heterogeneous nuclear ribonucleoprotein U
8	IPI:IPI00000816.1	29.2	44.92	Isoform 1 of 14-3-3 protein epsilon
9	IPI:IPI00003918.6	47.7	44.40	60S ribosomal protein L4
10	IPI:IPI00420014.2	244.4	39.54	Isoform 1 of U5 small nuclear ribonucleoprotein 200 kDa helicase
11	IPI:IPI00003865.1	70.9	34.67	Isoform 1 of Heat shock cognate 71 kDa protein
12	IPI:IPI00165486.11	31.4	33.83	31 kDa protein
13	IPI:IPI00939492.1	111.4	31.20	HLA-B associated transcript 8 BAT8 isoform a variant
14	IPI:IPI00030179.3	29.2	30.34	60S ribosomal protein L7
15	IPI:IPI00453476.2	28.8	29.82	29 kDa protein
16	IPI:IPI00025273.1	107.7	27.04	Isoform Long of Trifunctional purine biosynthetic protein adenosine-3
17	IPI:IPI00910980.1	120.6	23.55	IARS protein
18	IPI:IPI00643644.1	30.9	23.51	HCG1980662
19	IPI:IPI00396018.1	257.1	22.89	Isoform 3 of Acetyl-CoA carboxylase 1
20	IPI:IPI00302927.6	57.9	22.09	T-complex protein 1 subunit delta
21	IPI:IPI00216319.3	28.2	21.90	14-3-3 protein eta
22	IPI:IPI00397526.3	228.9	21.73	Isoform 1 of Myosin-10
23	IPI:IPI00797270.4	26.7	21.73	Isoform 1 of Triosephosphate isomerase
24	IPI:IPI00793177.1	24.2	21.61	24 kDa protein
25	IPI:IPI00783097.4	83.1	21.48	Glycyl-tRNA synthetase
26	IPI:IPI00909059.5	57.8	20.63	cDNA FLJ53910, highly similar to Keratin, type II cytoskeletal 6A
27	IPI:IPI00552419.3	75.0	20.34	propionyl-CoA carboxylase alpha chain, mitochondrial isoform c precursor
28	IPI:IPI00889541.2	80.2	20.20	Isoform 4 of Probable ATP-dependent RNA helicase DDX17
29	IPI:IPI00218342.10	101.5	19.07	C-1-tetrahydrofolate synthase, cytoplasmic
30	IPI:IPI00217223.1	49.6	18.82	Multifunctional protein ADE2
31	IPI:IPI00399170.1	123.0	18.34	Isoform 2 of Regulator of nonsense transcripts 1
32	IPI:IPI00216308.5	30.8	18.27	Voltage-dependent anion-selective channel protein 1
33	IPI:IPI00418813.2	25.1	18.11	Pseudogene candidate
34	IPI:IPI00295857.7	138.3	18.02	Isoform 1 of Coatomer subunit alpha
35	IPI:IPI00965964.2	129.1	17.59	cDNA FLJ58466, highly similar to Leucyl-tRNA synthetase, cytoplasmic
36	IPI:IPI00288940.6	867.9	17.40	Isoform 1 of Obscurin
37	IPI:IPI00376609.1	148.9	17.04	Isoform 2 of Nuclear pore complex protein Nup155
38	IPI:IPI00012772.8	28.0	17.01	60S ribosomal protein L8

39	IPI:IPI00741005.7	315.0	16.95	MAX gene-associated protein isoform 2
40	IPI:IPI00299214.7	25.5	15.66	Thymidine kinase, cytosolic
41	IPI:IPI00030578.2	45.9	16.51	Synaptic vesicle membrane protein VAT-1 homolog-like
42	IPI:IPI00007402.3	119.4	15.56	Importin-7
43	IPI:IPI01009017.1	50.9	16.55	cDNA FLJ50585, highly similar to T-complex protein 1 subunit beta
44	IPI:IPI00009329.2	394.2	16.38	Utrophin
45	IPI:IPI00016801.1	61.4	16.13	Glutamate dehydrogenase 1, mitochondrial
46	IPI:IPI00925578.1	518.2	15.09	Isoform 4 of Dynein heavy chain 14, axonemal
47	IPI:IPI00017334.1	29.8	14.75	Prohibitin
48	IPI:IPI00922165.1	24.6	14.55	Isoform 5 of Adenylate kinase 2, mitochondrial
49	IPI:IPI00909530.1	12.9	14.36	Histone H3
50	IPI:IPI00219994.2	107.7	14.36	Isoform 3 of Exportin-2
51	IPI:IPI00892976.1	99.5	14.33	Euchromatic histone-lysine N-methyltransferase 2
52	IPI:IPI00922694.1	69.9	14.23	cDNA FLJ51903, highly similar to Stress-70 protein, mitochondrial
53	IPI:IPI00979136.1	86.4	14.06	Ribonucleoside-diphosphate reductase
54	IPI:IPI00411592.2	222.7	13.94	Isoform 2 of Chromodomain-helicase-DNA-binding protein 3
55	IPI:IPI00332428.5	35.3	13.91	Protein MAK16 homolog
56	IPI:IPI00218408.1	46.0	13.87	Isoform Short of Trifunctional purine biosynthetic protein adenosine-3
57	IPI:IPI00185146.5	115.9	13.54	Importin-9
58	IPI:IPI00300371.5	135.5	13.17	Isoform 1 of Splicing factor 3B subunit 3
59	IPI:IPI00220301.5	25.0	13.17	Peroxiredoxin-6
60	IPI:IPI00791448.1	29.7	13.18	cDNA FLJ51469, highly similar to 60S acidic ribosomal protein P0
61	IPI:IPI00217563.4	88.4	12.98	Isoform Beta-1A of Integrin beta-1
62	IPI:IPI00640741.1	19.0	12.88	19 kDa protein
63	IPI:IPI00291006.2	35.5	12.46	Malate dehydrogenase, mitochondrial
64	IPI:IPI00936807.1	138.6	11.87	Isoform 4 of Myosin-VIIa
65	IPI:IPI00219525.10	53.1	11.77	6-phosphogluconate dehydrogenase, decarboxylating
66	IPI:IPI00910113.1	46.9	11.74	cDNA FLJ52902, highly similar to Rab GDP dissociation inhibitor alpha
67	IPI:IPI00413324.6	21.4	11.14	60S ribosomal protein L17
68	IPI:IPI00010796.1	57.1	10.95	Protein disulfide-isomerase
69	IPI:IPI00007074.5	59.1	10.87	Tyrosyl-tRNA synthetase, cytoplasmic
70	IPI:IPI00412579.6	24.8	10.80	60S ribosomal protein L10a
71	IPI:IPI00032304.2	70.2	10.79	Plastin-1
72	IPI:IPI00478689.5	180.6	10.71	Protein unc-13 homolog B
73	IPI:IPI00555744.6	23.8	10.71	Ribosomal protein L14 variant
74	IPI:IPI00293748.3	55.0	10.68	Isoform 1 of Multiple inositol polyphosphate phosphatase 1
75	IPI:IPI00797148.1	29.4	10.61	Isoform 2 of Heterogeneous nuclear ribonucleoprotein A1
76	IPI:IPI00291783.4	168.5	10.58	Gem-associated protein 5
77	IPI:IPI00941747.1	67.5	10.48	Calnexin
78	IPI:IPI00480077.3	92.7	10.43	Isoform 3 of Polyamine-modulated factor 1-binding protein 1
79	IPI:IPI00029079.5	76.7	10.24	GMP synthase [glutamine-hydrolyzing]
80	IPI:IPI00911026.1	31.4	10.20	cDNA FLJ57707, highly similar to Ketosamine-3-kinase
81	IPI:IPI00910327.1	75.0	10.09	cDNA FLJ54334, highly similar to Origin recognition complex subunit 3

Table A3: BPPM-revealed potential nonhistone targets for GLP1-Y1211A in HEK293T cells using HeySAM. These proteins are not present in the control.

Serial	Accession	Description	Score of EuHMT1
1	IPI00376215.2	Isoform 2 of DNA-dependent protein kinase catalytic subunit	208.3085556
2	IPI00793119.2	cDNA FLJ56274, highly similar to Transketolase	79.90027404
3	IPI00218319.3	Isoform 2 of Tropomyosin alpha-3 chain	70.50005794
4	IPI00007423.1	Isoform 1 of Acidic leucine-rich nuclear phosphoprotein 32 family member B	63.75586653
5	IPI00419373.1	Isoform 1 of Heterogeneous nuclear ribonucleoprotein A3	56.75522494
6	IPI00640006.1	rab GDP dissociation inhibitor beta isoform 2	53.96958017
7	IPI00965327.1	succinate dehydrogenase complex, subunit A, flavoprotein (Fp)	52.61379075
8	IPI00419880.6	40S ribosomal protein S3a	48.47704196
9	IPI00513955.1	cDNA FLJ55283, moderately similar to Protein mago nashi homolog	45.6518743
10	IPI00419258.4	High mobility group protein B1	43.15532923
11	IPI00219097.4	High mobility group protein B2	38.17082167
12	IPI00032158.3	Isoform 2 of N-alpha-acetyltransferase 15, NatA auxiliary subunit	37.94827914
13	IPI01015565.1	ubiquitin C	33.89626837
14	IPI00552715.1	T-complex protein 1 subunit gamma isoform c	33.83686447
15	IPI00375127.4	eukaryotic translation initiation factor 4H	33.41157961
16	IPI00552190.1	Proteasome (Prosome, macropain) 26S subunit, non-ATPase, 10	32.44333482
17	IPI00007797.3	Fatty acid-binding protein, epidermal	32.30974603
18	IPI00788942.1	Isoform 2 of RuvB-like 1	28.92567086
19	IPI00414696.1	Isoform A2 of Heterogeneous nuclear ribonucleoproteins A2/B1	28.35218573
20	IPI00018534.4	Histone H2B type 1-L	26.84758949
21	IPI00783118.2	5'-nucleotidase domain-containing protein 2 isoform 1	26.36745024
22	IPI00032140.4	Serpin H1	26.17618561
23	IPI00915869.3	malate dehydrogenase, cytoplasmic isoform 3	26.06665564
24	IPI01011970.1	phosphogluconate dehydrogenase	25.76162124
25	IPI01015355.1	aconitase 2, mitochondrial	25.55280709
26	IPI00984060.1	glutathione S-transferase Mu 2 isoform 2	25.12881255
27	IPI00980749.1	heat shock 70kDa protein 8	24.39236546
28	IPI00885057.1	Isoform 2 of Cysteine and histidine-rich domain-containing protein 1	24.32220984
29	IPI00909453.2	heat shock 27kDa protein 1	24.1226244
30	IPI01011083.1	cDNA FLJ55960, highly similar to Protein transport protein Sec23A	23.34211493
31	IPI00926815.1	ribosomal protein L37a	23.03368974
32	IPI00293305.4	Isoform Beta-1B of Integrin beta-1	22.0308578
33	IPI00793677.1	chromosome 21 open reading frame 33	21.87474656
34	IPI00815732.1	Isoform 2 of Multifunctional protein ADE2	21.49055624
35	IPI00027485.3	Eukaryotic translation initiation factor 4E	21.47505403
36	IPI00937278.2	26S proteasome non-ATPase regulatory subunit 8	21.38628244
37	IPI00945233.1	mitochondrial 2-oxoglutarate/malate carrier protein isoform 2	21.03095818
38	IPI00916818.1	Phosphoglycerate kinase	20.46259642
39	IPI00023086.3	39S ribosomal protein L15, mitochondrial	20.1815536
40	IPI00219065.2	Isoform 5 of Glycogen debranching enzyme	19.81091595
41	IPI00294159.3	Tricarboxylate transport protein, mitochondrial	19.68325853
42	IPI00984887.1	ribosomal protein S3	19.53965378
43	IPI00470674.5	NADH-cytochrome b5 reductase 1	19.51842237
44	IPI01011090.1	lactate dehydrogenase B	19.31844187
45	IPI00023530.7	Cyclin-dependent kinase 5	19.30037332
46	IPI00215884.4	Isoform ASF-1 of Serine/arginine-rich splicing factor 1	17.89297962

47	IPI00019927.2	26S proteasome non-ATPase regulatory subunit 7	17.84248114
48	IPI01015264.1	eukaryotic translation initiation factor 2B, subunit 1 alpha, 26kDa	17.81041503
49	IPI01013355.1	cDNA FLJ54349, highly similar to Vesicle-fusing ATPase	17.5288763
50	IPI00976247.1	peptidyl-prolyl cis-trans isomerase A-like, partial	17.42233348
51	IPI00386751.2	Isoform 2 of HD domain-containing protein 2	17.40248156
52	IPI00978313.2	cDNA FLJ53638, highly similar to Annexin A6	17.3944788
53	IPI00719549.2	RBM14-RBM4 protein isoform 1	17.1049633
54	IPI00217168.1	Isoform ZK of Plasma membrane calcium-transporting ATPase 4	16.99586105
55	IPI00015905.1	Exosome complex component RRP4	16.95224094
56	IPI00927114.1	ras homolog family member A	16.75960922
57	IPI00291922.2	Proteasome subunit alpha type-5	16.51718521
58	IPI00032955.1	Isoform 1 of RING finger protein 114	16.17715096
59	IPI00910270.1	PITH (C-terminal proteasome-interacting domain of thioredoxin-like) domain co	16.03422451
60	IPI00554742.3	Isoform 2 of Apoptosis inhibitor 5	15.79603648
61	IPI00411816.3	39S ribosomal protein L2, mitochondrial	15.5231719
62	IPI00011274.3	Isoform 1 of Heterogeneous nuclear ribonucleoprotein D-like	15.15570092
63	IPI00419802.4	Isoform 1 of 3-hydroxyisobutyryl-CoA hydrolase, mitochondrial	15.12682176
64	IPI00748145.2	Isoform 1 of Guanine nucleotide-binding protein G(i) subunit alpha-2	15.10663915
65	IPI00745568.2	Isoform 1 of TIP41-like protein	14.99305558
66	IPI00022314.1	Superoxide dismutase [Mn], mitochondrial	14.97399402
67	IPI00026519.1	Peptidyl-prolyl cis-trans isomerase F, mitochondrial	14.72927189
68	IPI00974011.1	inositol(myo)-1(or 4)-monophosphatase 1	14.70692635
69	IPI00473085.3	Isoform 3 of Dynamin-1-like protein	14.49450064
70	IPI00013184.1	N-alpha-acetyltransferase 10, NatA catalytic subunit	14.38066006
71	IPI00643459.1	mitochondrial ribosomal protein S16	14.00365901
72	IPI00830052.9	heat shock 70kDa protein 1-like	13.92066193
73	IPI01012108.1	ubiquitin-conjugating enzyme E2D 4 (putative)	13.79680896
74	IPI00793137.2	Uncharacterized protein	13.71066475
75	IPI00879451.2	cDNA FLJ61051, highly similar to HpaII tinys locus 9c protein	13.69041753
76	IPI00924536.1	eukaryotic translation initiation factor 4A2	13.61659217
77	IPI00032823.1	Exosome complex component CSL4	13.57395387
78	IPI00940872.2	Titin, isoform CRA_a	13.55056572
79	IPI00791634.5	prohibitin	13.17864013
80	IPI00917733.1	cDNA FLJ10185 fis, clone HEMBA1004509, highly similar to U4/U6.U5 tri-snRNP-ass	13.05751348
81	IPI00797969.1	guanine nucleotide binding protein (G protein), beta polypeptide 2	12.9626801
82	IPI01011952.1	cDNA FLJ59659, highly similar to Vinculin	12.95064139
83	IPI00789842.3	zinc phosphodiesterase ELAC protein 2 isoform 3	12.88316751
84	IPI01013371.1	cDNA FLJ58569, highly similar to Nucleosome assembly protein 1-like 1	12.66269946
85	IPI00385834.3	Isoform 2 of KH domain-containing, RNA-binding, signal transduction-associated	12.61974573
86	IPI00024662.1	Chromobox protein homolog 5	12.54557896
87	IPI00015869.2	Trichohyalin	12.49780846
88	IPI00925126.1	protein kinase, cAMP-dependent, regulatory, type II, alpha	12.47497773
89	IPI01011589.1	cDNA FLJ10484 fis, clone NT2RP2000161, highly similar to Exosome complex exonu	12.44991589
90	IPI01010049.1	ubiquitin specific peptidase 28	12.18280959
91	IPI00384122.5	cDNA FLJ55034, highly similar to Dihydrolipoyllysine-residue succinyltransferase	12.10097122
92	IPI00470503.2	Isoform 3 of Inorganic pyrophosphatase 2, mitochondrial	11.5182457
93	IPI00909437.1	Ribosomal protein L15	11.42085123
94	IPI00643324.1	Four and a half LIM domains 1	11.34323096

95	IPI01011965.1	Iron regulatory protein 1	11.27859068
96	IPI00892863.1	Isoform 2 of Collagen alpha-5(VI) chain	11.220891
97	IPI00978728.1	NADH dehydrogenase (ubiquinone) flavoprotein 1, 51kDa	11.14177203
98	IPI00059718.3	TRMT61A protein (Fragment)	11.04034781
99	IPI00946597.1	acylglycerol kinase	10.86086345
100	IPI01011463.1	cDNA FLJ40890 fis, clone UTERU2001024, highly similar to SPLICING FACTOR, ARGIN	10.85630155
101	IPI00186460.7	Isoform 1 of Collagen alpha-1(II) chain	10.79398465
102	IPI00793985.2	N(alpha)-acetyltransferase 50, NatE catalytic subunit	10.7655735
103	IPI00413214.3	importin subunit alpha-6	10.75346398
104	IPI00910176.1	cDNA FLJ57995, moderately similar to Ubiquitin-conjugating enzyme E2-25 kDa	10.74681306
105	IPI00976899.1	ribosomal protein L8	10.72774029
106	IPI00978608.1	cold shock domain containing E1, RNA-binding	10.65494323
107	IPI00915872.2	Trinucleotide repeat containing 6B (Fragment)	10.33702445
108	IPI00217519.3	Ras-related protein Ral-A	10.23424554
109	IPI00384061.2	Isoform 5 of Methyltransferase-like protein 13	10.20179272
110	IPI00983162.1	poly(A) binding protein, cytoplasmic 1	10.14514899
111	IPI00879783.1	metastasis associated 1 family, member 3	10.06823587
112	IPI01015038.1	T-complex protein 1 subunit delta	9.967740536
113	IPI00073779.1	Isoform 1 of 28S ribosomal protein S35, mitochondrial	9.904862165
114	IPI00005707.7	C-type mannose receptor 2	9.816804647
115	IPI00022316.3	28S ribosomal protein S18b, mitochondrial	9.807150364
116	IPI00016077.1	Protein NipSnap homolog 2	9.705330372
117	IPI00165393.1	Acidic leucine-rich nuclear phosphoprotein 32 family member E	9.69942975
118	IPI00910437.1	cDNA FLJ52417, highly similar to 3'(2'),5'-bisphosphate nucleotidase 1	9.686202049
119	IPI01009205.1	RAD23 homolog B (S. cerevisiae)	9.626133442
120	IPI00643915.1	Peptidyl-prolyl cis-trans isomerase	9.595445633
121	IPI00301518.6	Isoform 1 of Mps one binder kinase activator-like 1B	9.466370106
122	IPI01011967.1	cDNA FLJ54535, highly similar to Ribosomal protein S6 kinase alpha-1	9.457336903
123	IPI00910255.1	tRNA-yW synthesizing protein 3 homolog (S. cerevisiae)	9.457071781
124	IPI00798272.2	branched-chain-amino-acid aminotransferase, cytosolic isoform 2	9.186050892
125	IPI01015230.1	cDNA FLJ53354, highly similar to Puromycin-sensitive aminopeptidase	9.174034595
126	IPI01010261.1	cDNA FLJ30173 fis, clone BRACE2000969, highly similar to 6-phosphofructokinase,	9.135075808
127	IPI00922039.1	cDNA FLJ57628, highly similar to Homo sapiens membrane-associated ring finge	9.084560871
128	IPI00646978.4	lysophospholipase II	9.084253073
129	IPI00027096.2	39S ribosomal protein L19, mitochondrial	9.016253471
130	IPI00908791.2	L-lactate dehydrogenase	8.970396996
131	IPI01014610.1	tRNA methyltransferase 11-2 homolog (S. cerevisiae)	8.936521769
132	IPI00946498.1	stem-loop binding protein	8.920324326
133	IPI00643370.1	Tropomyosin 3	8.840212822
134	IPI00926959.1	asparagine synthetase (glutamine-hydrolyzing)	8.833948374
135	IPI00980330.1	RAP2A, member of RAS oncogene family	8.804337502
136	IPI00304082.8	Isochorismatase domain-containing protein 1	8.798935413
137	IPI00297089.4	A-kinase anchor protein 6	8.718411922
138	IPI00553138.4	Vesicle-associated membrane protein 2	8.685631752
139	IPI00643317.3	high mobility group box 3	8.609049082
140	IPI00399375.2	Isoform 2 of Thymocyte nuclear protein 1	8.576127291

141	IPI01011917.1	prohibitin 2	8.569286823
142	IPI00180128.4	Isoform 2 of Basic leucine zipper and W2 domain-containing protein 1	8.532663822
143	IPI00642864.2	Isoform 2 of FAD synthase	8.518769503
144	IPI01015433.1	Glutamate dehydrogenase	8.490028381
145	IPI01015600.1	CIP29 protein	8.445426226
146	IPI00893470.2	diffuse panbronchiolitis critical region 1	8.3966887
147	IPI00942050.2	Major histocompatibility complex, class I, C	8.314289093
148	IPI00383078.5	melanoma antigen family D, 1	8.299733639
149	IPI00016346.2	Proline synthetase co-transcribed homolog (Bacterial), isoform CRA_b	8.297941685
150	IPI00219421.3	Isoform 2 of Ephrin type-B receptor 2	8.289919376
151	IPI00914971.1	farnesyl pyrophosphate synthase isoform b	8.275914669
152	IPI00455457.4	Histone H3	8.2287395
153	IPI00647504.2	Isoform 2 of Protein FAM184A	8.141638517
154	IPI00000335.1	Histidine triad nucleotide-binding protein 2, mitochondrial	8.135605812
155	IPI00305887.1	Kinetochore protein Nuf2	8.077617884
156	IPI00940685.1	U5 small nuclear ribonucleoprotein 40 kDa protein	8.068724632
157	IPI00290184.4	tRNA (guanine-N(7)-)-methyltransferase	8.065582037
158	IPI00963822.1	septin 11	8.061227322
159	IPI00967259.1	glucosamine-6-phosphate deaminase 1	8.058110237
160	IPI00000940.1	Parathyroid hormone	8.038056374
161	IPI00784990.2	Ubiquitin C splice variant	8.036742687
162	IPI00012535.1	DnaJ homolog subfamily A member 1	8.005677223
163	IPI00219613.6	cDNA FLJ54537, highly similar to Homo sapiens pitrilysin metallopeptidase 1 (PI	8.003607035
164	IPI00012369.1	Mitotic spindle assembly checkpoint protein MAD2A	7.727428675
165	IPI00552360.2	Isoform 1 of Fumarylacetoacetate hydrolase domain-containing protein 1	7.611097336
166	IPI00012491.2	Heat-stable enterotoxin receptor	7.599328995
167	IPI00911081.2	glutaryl-CoA dehydrogenase	7.570792198
168	IPI00936634.1	Isoform 3 of SH2 domain-containing protein 2A	7.549822807
169	IPI00302176.5	Isoform 1 of H/ACA ribonucleoprotein complex subunit 1	7.544974566
170	IPI00400975.1	Conserved hypothetical protein	7.460657597
171	IPI00329352.4	Nodal modulator 1	7.442754984
172	IPI00935307.2	diaphanous homolog 1 (Drosophila)	7.417745352
173	IPI00514944.5	Uroporphyrinogen decarboxylase	7.410956621
174	IPI01014611.1	cDNA, FLJ79139, highly similar to Alkyldihydroxyacetonephosphate synthase, per	7.407764673
175	IPI01009451.1	MYC-associated zinc finger protein (purine-binding transcription factor)	7.374407053
176	IPI00908803.1	cDNA FLJ59584, highly similar to Mitochondrial-processing peptidase alpha subu	7.355117321
177	IPI01013039.1	proteasome (prosome, macropain) 26S subunit, non-ATPase, 9	7.351754189
178	IPI00302673.3	ATP synthase mitochondrial F1 complex assembly factor 1	7.347349405
179	IPI01008914.1	eukaryotic initiation factor 4A-I isoform 2	7.327119589
180	IPI00903226.1	cDNA FLJ46359 fis, clone TESTI4049786, highly similar to Hexokinase-1	7.286429644
181	IPI00749044.2	Similar to IQ motif and Sec7 domain 3	7.284358501
182	IPI01011924.1	ubiquitin specific peptidase 7 (herpes virus-associated)	7.239362478
183	IPI00219793.1	Isoform 2 of Suppressor of SWI4 1 homolog	7.234596014
184	IPI00001618.2	Ras-related protein Rab-39A	7.229089737
185	IPI00005573.3	Isoform 1 of 5'(3')-deoxyribonucleotidase, cytosolic type	7.172768831
186	IPI00940894.1	DNA polymerase	7.069058895
187	IPI00556204.1	Eukaryotic translation elongation factor 1 alpha 2 variant (Fragment)	7.016174316

188	IPI00552198.1	Phosphoprotein enriched in astrocytes 15	7.014993906
189	IPI00877618.1	mercaptopyruvate sulfurtransferase	7.01315403
190	IPI00177965.5	5'-nucleotidase domain-containing protein 1	7.002598286
191	IPI00019385.4	Translocon-associated protein subunit delta	6.980569601
192	IPI00646415.1	20 kDa protein	6.970712662
193	IPI00020771.3	microtubule-associated protein 7	6.955245972
194	IPI00043678.3	dedicator of cytokinesis 7	6.885029078
195	IPI00646459.1	Nuclear autoantigenic sperm protein	6.882386684
196	IPI00645630.2	enoyl-CoA hydratase domain-containing protein 1 isoform 3	6.879080772
197	IPI01009725.1	cDNA FLJ58302, highly similar to Importin-4	6.818561792
198	IPI00789806.2	Isoform 2 of Cytosol aminopeptidase	6.78508997
199	IPI00910150.1	cDNA FLJ60107, highly similar to DNA replication complex GINS protein PSF1	6.754507303
200	IPI00925176.1	trafficking protein, kinesin binding 1	6.746781588
201	IPI00743775.1	Isoform 2 of Coiled-coil domain-containing protein 47	6.72347331
202	IPI00010157.1	S-adenosylmethionine synthase isoform type-2	6.712624788
203	IPI00171844.3	COP9 signalosome complex subunit 4	6.679496765
204	IPI00549307.3	Isoform 3 of MOSC domain-containing protein 1, mitochondrial	6.634622574
205	IPI00157928.2	maleylacetoacetate isomerase isoform 2	6.594398022
206	IPI00894205.2	protein NipSnap homolog 1 isoform 2	6.587986231
207	IPI00922265.1	Isoform 1 of Membrane magnesium transporter 1	6.58423233
208	IPI00645291.1	Isoform 2 of Phosphoribosyltransferase domain-containing protein 1	6.583433151
209	IPI00296999.9	ATP synthase mitochondrial F1 complex assembly factor 2	6.480558157
210	IPI00292168.3	Histone chaperone ASF1A	6.463583946
211	IPI00291093.3	DNA-directed RNA polymerases I, II, and III subunit RPABC1	6.424916029
212	IPI00447177.1	Antigen MLAA-23	6.394483566
213	IPI00744932.1	Similar to Zinc finger, DHHC-type containing 1	6.381577492
214	IPI01013870.1	N(alpha)-acetyltransferase 40, NatD catalytic subunit, homolog (S. cerevisiae)	6.381153107
215	IPI00878669.2	chromobox homolog 1	6.380673409
216	IPI00007676.3	Estradiol 17-beta-dehydrogenase 12 (present in G9a with azido)	6.362389326
217	IPI00797738.1	Cytochrome c oxidase subunit 6B1	6.351295471
218	IPI00221222.7	Activated RNA polymerase II transcriptional coactivator p15	6.34903574
219	IPI00908651.1	cDNA FLJ57726, highly similar to Heterogeneous nuclear ribonucleoprotein H3	6.290336847
220	IPI00552365.7	EF-hand domain family, member D2	6.279866457
221	IPI00004454.3	Isoform 1 of Dolichol-phosphate mannosyltransferase subunit 3	6.272236586
222	IPI00936328.2	MARCKS-related protein-like, partial	6.246054411
223	IPI01013456.1	lactate dehydrogenase A	6.22026968
224	IPI00023748.3	Nascent polypeptide-associated complex subunit alpha	6.20839119
225	IPI00964587.1	DTW domain containing 2	6.206987619
226	IPI00013946.1	Synaptogyrin-2	6.194886208
227	IPI00514049.1	Cytidine monophosphate (UMP-CMP) kinase 1, cytosolic	6.14833951
228	IPI00797616.2	Isoform 3 of BRCA1-associated ATM activator 1	6.118052006
229	IPI00024524.4	RNA-binding protein PNO1	6.095901728
230	IPI01015706.1	tumor protein, translationally-controlled 1	6.084853888
231	IPI00916572.1	ribosomal protein L31	6.073718309
232	IPI00644020.1	Sterol O-acyltransferase 1	6.061112404
233	IPI00513717.3	Isoform 2 of Chromodomain-helicase-DNA-binding protein 6	6.06077528
234	IPI00031032.1	Musculin	6.05892539

235	IPI00917386.1	Sjogren syndrome antigen B (autoantigen La)	6.055042982
236	IPI00908843.1	cDNA FLJ53857, highly similar to Interferon-induced protein with tetratricopeptid	5.990872145
237	IPI00006408.4	Nitric oxide synthase-interacting protein	5.941011667
238	IPI00294486.1	Dual specificity protein phosphatase 9	5.81464982
239	IPI00063903.5	Up-regulated during skeletal muscle growth protein 5	5.796951056
240	IPI01011610.1	cDNA FLJ51181, highly similar to 7-dehydrocholesterol reductase	5.796531439
241	IPI00470515.7	chromosome 1 open reading frame 173	5.771541834
242	IPI01015586.1	glucosamine (N-acetyl)-6-sulfatase	5.769265652
243	IPI00889171.1	Isoform 2 of Junction-mediating and -regulatory protein	5.738581657
245	IPI00007019.1	Peptidyl-prolyl cis-trans isomerase-like 1	5.570055485
246	IPI00011898.3	Translation initiation factor eIF-2B subunit epsilon	5.532426834
247	IPI00008437.7	Probable ribosome biogenesis protein RLP24	5.482391119
248	IPI01011224.1	REX2, RNA exonuclease 2 homolog (S. cerevisiae)	5.463126659
249	IPI01015916.1	RNA-binding region (RNP1, RRM) containing 2, isoform CRA_b	5.447995663
250	IPI00643288.1	Pyrophosphatase (Inorganic) 1	5.435631037
251	IPI00980505.1	copper chaperone for superoxide dismutase	5.379751444
252	IPI00514094.3	serine/threonine kinase 32C	5.335237026
253	IPI00018691.1	Isoform 1 of 28S ribosomal protein S18a, mitochondrial	5.301540852
254	IPI00017972.3	Zinc finger protein 703	5.284733772
255	IPI01009339.1	paraspeckle component 1	5.243271112
256	IPI00008436.4	DNA polymerase epsilon subunit 4	5.213436604
257	IPI00513941.3	SAR1 homolog A (S. cerevisiae)	5.192499161
258	IPI01010811.1	ATP synthase, H+ transporting, mitochondrial Fo complex, subunit F2	5.147957802
259	IPI01014702.1	isovaleryl-CoA dehydrogenase	5.099872589
260	IPI00643597.2	Isoform 2 of Transmembrane channel-like protein 2	5.091242552
261	IPI00982452.1	sortilin-related receptor, L(DLR class) A repeats containing	5.085541248
262	IPI00909685.1	cDNA FLJ58965, highly similar to Nonspecific lipid-transfer protein	5.044857502
263	IPI00027729.1	Casein kinase I isoform epsilon	5.033119917
264	IPI00985162.1	nucleoporin 160kDa	4.960441113
265	IPI00926401.1	N-acylaminoacyl-peptide hydrolase	4.955853939
266	IPI00645702.1	CTP synthase 2	4.95538187
267	IPI00646381.1	mitochondrial ribosomal protein L24	4.934664011
268	IPI00746752.2	Isoform C of Bromodomain and WD repeat-containing protein 1	4.899923325
269	IPI01010215.1	lysine (K)-specific demethylase 2B	4.898071289
270	IPI00640671.3	Isoform 2 of Protein fantom	4.881556988
271	IPI00244111.10	Isoform 3 of Type II inositol-1,4,5-trisphosphate 5-phosphatase	4.875109196
272	IPI00967388.1	ribosomal protein S3A	4.861042738
273	IPI00977873.1	cDNA FLJ61146, highly similar to Cellular nucleic acid-binding protein	4.855553627
274	IPI00014301.3	Oxidase (Cytochrome c) assembly 1-like	4.830379963
275	IPI00644993.1	AMT protein	4.754335403
276	IPI00978059.1	chromosome 11 open reading frame 83	4.688630581
277	IPI00642016.1	crystallin, zeta (quinone reductase)	4.556134224
278	IPI00926007.2	FLJ00144 protein (Fragment)	4.520941734
279	IPI00220358.1	Isoform 2 of Cas scaffolding protein family member 4	4.520151138
280	IPI01013546.1	Hydroxymethylbilane synthase	4.499036312
281	IPI00218946.2	Potassium/sodium hyperpolarization-activated cyclic nucleotide-gated channel	4.445723534
282	IPI00902977.1	Isoform 6 of Oxidation resistance protein 1	4.443925381

283	IPI00180408.8	Myosin-15	4.442148209
284	IPI00026516.1	Succinyl-CoA:3-ketoacid-coenzyme A transferase 1, mitochondrial	4.442061901
285	IPI00983321.1	SOGA family member 3	4.439264774
286	IPI01009113.1	polymerase (RNA) II (DNA directed) polypeptide A, 220kDa	4.437465191
287	IPI00946286.1	collagen alpha-3(VI) chain isoform 4 precursor	4.436850071
288	IPI01015357.1	ATP-binding cassette, sub-family B (MDR/TAP), member 9	4.430781841
289	IPI00032900.1	BolA-like protein 1	4.410545349
290	IPI01010160.1	UPP1 protein	4.40027523
291	IPI00061987.4	uncharacterized LOC113230	4.396100521
292	IPI00976931.1	apoptosis-inducing factor, mitochondrion-associated, 1	4.378081322
293	IPI00797067.2	U2 snRNP-specific A' protein	4.372718811
294	IPI00976917.1	hypothetical protein LOC144481 isoform 1	4.371304512
295	IPI00646919.1	transmembrane protein 38B	4.367688656
296	IPI00795241.1	Isoform 2 of Enolase-phosphatase E1	4.339342117
297	IPI00291669.3	Ubiquitin-like domain-containing CTD phosphatase 1	4.331799507
298	IPI00964697.1	adrenoceptor alpha 2C	4.331721783
299	IPI00926562.1	wingless-type MMTV integration site family, member 10A	4.290638924
300	IPI00929228.1	Isoform 2 of Tudor domain-containing protein 3	4.273125172
301	IPI00333126.1	Leucine-rich repeat-containing protein 56	4.271798134
302	IPI00965978.1	Uncharacterized protein	4.250235081
303	IPI00978253.1	indoleamine 2,3-dioxygenase 1	4.244541645
304	IPI00942036.1	centrosomal protein 170B	4.241065502
305	IPI00793594.1	mediator complex subunit 24	4.21948576
306	IPI00300408.3	Copper homeostasis protein cutC homolog	4.212116718
307	IPI00909705.1	cDNA FLJ57896, highly similar to Arylsulfatase A	4.211012363
308	IPI00978643.1	transmembrane protein 41B isoform 2	4.194047928
309	IPI00186395.11	Putative methyltransferase-like protein LOC121952	4.174588203
310	IPI01011139.1	golgi transport 1B	4.172591209
311	IPI00894231.1	CAP-GLY domain containing linker protein family, member 4	4.172104359
312	IPI00169400.1	Isoform 1 of 28S ribosomal protein S5, mitochondrial	4.169184685
313	IPI00925074.1	BC1 (ubiquinol-cytochrome c reductase) synthesis-like	4.164148331
314	IPI00418599.2	Arachidonate 5-lipoxygenase variant (Fragment)	4.131789207
315	IPI00220716.2	Isoform 2 of Putative RNA-binding protein 15	4.124369621
316	IPI00973891.1	NudC domain containing 2	4.124117374
317	IPI00847423.1	Similar to Hematopoietic signal peptide-containing isoform 1	4.120315075
318	IPI01012850.1	cDNA FLJ58265, highly similar to Ubiquitin-protein ligase BRE1B	4.11916256
319	IPI00976464.1	Sjogren syndrome/scleroderma autoantigen 1	4.115839005
320	IPI00796662.2	cDNA FLJ57580, highly similar to Zinc finger protein 485	4.115236282
321	IPI00009111.1	Trophoblast glycoprotein	4.105669975
322	IPI00908950.1	Ribosomal protein L18	4.073968887
323	IPI01014744.1	microsomal glutathione S-transferase 1	4.063024998
324	IPI00942440.2	cDNA FLJ53389, highly similar to Homo sapiens RAB GTPase activating protein 1 (	4.048054695
325	IPI00017630.6	Nuclear fragile X mental retardation-interacting protein 1	4.046810627
326	IPI00103471.3	Selenoprotein M	4.043367386
327	IPI00024976.5	Mitochondrial import receptor subunit TOM22 homolog	4.042171001
328	IPI00917391.1	Uncharacterized protein	4.041543961
329	IPI00785127.1	Gm127 (Fragment)	4.038759232

330	IPI00454905.4	cDNA FLJ42124 fis, clone TESTI2009477, weakly similar to TRICHOHYALIN	4.021264553
331	IPI00879096.1	SWI/SNF related, matrix associated, actin dependent regulator of chromatin, sul	4.01543808
332	IPI00973955.1	voltage-dependent anion channel 3	3.995401144
333	IPI00171123.4	GATA zinc finger domain-containing protein 1	3.985080719
334	IPI00947213.1	phosphoribosyl pyrophosphate synthetase 2	3.976323605
335	IPI00555927.2	nudix (nucleoside diphosphate linked moiety X)-type motif 6	3.956722021
336	IPI00910237.1	proteasome subunit beta type-5 isoform 2	3.952091217
337	IPI00976591.1	chromosome 8 open reading frame 82	3.939365864
338	IPI00925558.1	CCR4-NOT transcription complex, subunit 10	3.932148218
339	IPI00909361.1	solute carrier family 35, member F6	3.895539284
340	IPI00910780.1	cDNA FLJ56706, highly similar to Bcl-2 homologous antagonist/killer	3.895368576
341	IPI00884448.1	Isoform 1 of Zinc finger protein 862	3.870273113
342	IPI00947310.1	single-stranded DNA binding protein 1, mitochondrial	3.845179558
343	IPI00945908.1	nitrilase family, member 2	3.827937365
344	IPI00925482.1	cleavage and polyadenylation specific factor 4, 30kDa	3.797110558
345	IPI00217949.12	Ubiquitin-conjugating enzyme E2 S	3.775313377
346	IPI00647050.1	RNA 3'-terminal phosphate cyclase	3.746369123
347	IPI00014539.2	Homeobox protein Hox-B9	3.746046543
348	IPI01015921.1	cDNA FLJ55361, highly similar to Nucleolar protein 11	3.741353989
349	IPI00922900.1	cDNA FLJ50656, highly similar to Surfeit locus protein 4	3.731828213
350	IPI00978191.1	catenin (cadherin-associated protein), alpha 1, 102kDa	3.726494074
351	IPI00926978.1	solute carrier family 25 (carnitine/acylcarnitine translocase), member 20	3.700134039
352	IPI00329742.2	Fumarylacetoacetate hydrolase domain-containing protein 2A	3.688626528
353	IPI00927280.1	Sin3A-associated protein, 18kDa	3.676407814
354	IPI00555624.2	RAB3GAP1 protein	3.675404549
355	IPI00449201.2	Isoform 2 of Ubiquitin-like-conjugating enzyme ATG3	3.65760088
356	IPI00922359.1	Protein-L-isoaspartate O-methyltransferase	3.632962704
357	IPI00305423.6	Charged multivesicular body protein 6	3.618782759
358	IPI00909111.1	cDNA FLJ59179, highly similar to 39S ribosomal protein L9, mitochondrial	3.615469456
359	IPI00908627.1	cDNA FLJ59271, highly similar to Component of gems 4	3.610473156
360	IPI00984850.1	Activation-induced cytidine deaminase	3.605342865
361	IPI00031022.2	Heat shock protein, 110 kDa	3.593075514
362	IPI00006092.1	Phosphomannomutase 2	3.558265448
363	IPI00640997.1	isopentenyl-diphosphate delta isomerase 1	3.542179108
364	IPI00893179.1	X-ray repair complementing defective repair in Chinese hamster cells 6	3.53842473
365	IPI00983931.1	non-SMC condensin II complex, subunit D3	3.53430891
366	IPI00909384.1	cDNA FLJ53505, highly similar to Chaperone-activity of bc1 complex-like, mitocho	3.516098738
367	IPI01012335.1	TatD DNase domain containing 1	3.515783548
368	IPI00009466.9	coiled-coil-helix-coiled-coil-helix domain-containing protein 2, mitochondrial-li	3.490503073
369	IPI00926034.1	coiled-coil domain containing 12	3.489398479
370	IPI00645836.1	esterase D	3.473929644
371	IPI00792109.1	coiled-coil domain containing 43	3.465866327
372	IPI00964365.1	Annexin A5	3.459147692
373	IPI00909718.1	cDNA FLJ59809, highly similar to Bone marrow stromal antigen 2	3.450926065
374	IPI00009659.3	Regulation of nuclear pre-mRNA domain-containing protein 1B	3.447496653
375	IPI00028376.1	Mitochondrial import inner membrane translocase subunit Tim8 A	3.438120604
376	IPI00908328.1	cDNA FLJ51585, moderately similar to Homo sapiens spindle pole body compone	3.432426691

377	IPI00478062.2	transducin-like enhancer of split 2 (E(sp1) homolog, Drosophila)	3.425706387
378	IPI00964581.3	cDNA FLJ53827, highly similar to Speckle-type POZ protein	3.420134544
379	IPI00967045.1	basic transcription factor 3	3.417832136
380	IPI00001632.4	Isoform 2 of Uncharacterized protein KIAA1522	3.405859947
381	IPI00396617.1	cDNA FLJ11699 fis, clone HEMBA1005047, highly similar to RAS-RELATED PROTEIN F	3.378495932
382	IPI00412272.2	SH3 domain-binding glutamic acid-rich-like protein 2	3.369605064
383	IPI00384116.3	Isoform 2 of Phosphoenolpyruvate carboxykinase [GTP], mitochondrial	3.349629402
384	IPI01011706.1	Superoxide dismutase 1 (Fragment)	3.342024565
385	IPI00871391.3	X-ray repair complementing defective repair in Chinese hamster cells 5 (double-	3.335588455
386	IPI00302674.3	coiled-coil domain containing 134	3.335077763
387	IPI00644866.1	cDNA FLJ12775 fis, clone NT2RP2001677	3.332522869
388	IPI00549413.2	Annexin A1	3.3319695
389	IPI00304163.5	cDNA FLJ57902, highly similar to Protein MYG1	3.321031094
390	IPI01018329.1	cDNA FLJ57316, highly similar to DNA mismatch repair protein Msh2	3.316637516
391	IPI00385751.6	cDNA FLJ52780, highly similar to Tissue alpha-L-fucosidase	3.296418428
392	IPI00965308.1	GTPase activating protein (SH3 domain) binding protein 2	3.28204298
393	IPI00161196.3	F-box/LRR-repeat protein 8	3.275252819
394	IPI00385021.1	ubiquinol-cytochrome c reductase complex chaperone	3.269675016
395	IPI01015633.1	ADP-ribosylation factor-like 6 interacting protein 1	3.264163017
396	IPI00903277.1	cDNA FLJ32474 fis, clone SKNMC2000593, highly similar to Tumor necrosis factor r	3.251574993
397	IPI00023939.1	Guanine nucleotide exchange factor MSS4	3.248258591
398	IPI00976381.1	casein kinase 1, alpha 1	3.242902279
399	IPI01011217.1	Full-length cDNA clone CS0DC001YO07 of Neuroblastoma of Homo sapiens	3.239886045
400	IPI00790053.1	RFT1 homolog (S. cerevisiae)	3.237701178
401	IPI00015806.3	Isoform 1 of General transcription factor 3C polypeptide 3	3.234821081
402	IPI01013001.1	G protein-coupled receptor 89C	3.234705448
403	IPI00925720.1	cleavage and polyadenylation specific factor 4, 30kDa	3.232334614
404	IPI00847495.2	cDNA FLJ55640, highly similar to Coiled-coil domain-containing protein 21	3.232254744
405	IPI00981963.1	FSHD region gene 1	3.232080936
406	IPI00892665.1	guanine nucleotide binding protein-like 1	3.211884499
407	IPI00903024.1	methylthioadenosine phosphorylase	3.206659317
408	IPI00852874.1	SEC13 homolog (S. cerevisiae)	3.198170185
409	IPI00640938.1	RNA binding protein, autoantigenic	3.198057652
410	IPI00027487.3	Creatine kinase M-type	3.193926573
411	IPI00879828.1	Isoform 2 of DIS3-like exonuclease 1	3.189982891
412	IPI00384120.1	Full-length cDNA 5-PRIME end of clone CS0DI052YD12 of Placenta of Homo sapier	3.184959173
413	IPI00332071.4	Isoform 1 of Tether containing UBX domain for GLUT4	3.180494785
414	IPI00940222.2	Isoform 3 of A-kinase anchor protein 12	3.180082798
415	IPI00917463.1	Isoform 3 of Ancient ubiquitous protein 1	3.17835784
416	IPI00217465.5	Histone H1.2	3.168960571
417	IPI00911013.1	cDNA FLJ57175, moderately similar to Pituitary tumor-transforming gene 1 protei	3.165185452
418	IPI00106491.3	mRNA turnover protein 4 homolog	3.163933516
419	IPI00925162.1	transferrin receptor (p90, CD71)	3.161654949
420	IPI00909338.2	lysosome membrane protein 2	3.15091753
421	IPI00155466.7	succinate-CoA ligase, GDP-forming, beta subunit	3.147031069
422	IPI01014601.1	aminopeptidase puromycin sensitive	3.144531012
423	IPI00878073.1	migration and invasion enhancer 1	3.144301653

424	IPI00413614.3	Isoform 2 of Symplekin	3.137643576
425	IPI00446667.1	cDNA FLJ41384 fis, clone BRCAN2014602, moderately similar to DIACYLGLYCEROL KI	3.132920265
426	IPI00183065.6	coiled-coil and C2 domain containing 1A	3.12879324
427	IPI00894209.1	Isoform 8 of Inhibitor of growth protein 4	3.127731085
428	IPI01018135.1	cDNA FLJ39696 fis, clone SMINT2011033, highly similar to Sorting and assembly m	3.12726903
429	IPI00012313.3	Golgi phosphoprotein 3-like	3.105096102
430	IPI00916612.1	gamma-glutamylcyclotransferase isoform 4	3.096665859
431	IPI00328390.2	Isoform 1 of Polycomb group RING finger protein 5	3.09583354
432	IPI00383290.1	leucyl-tRNA synthetase	3.094269037
433	IPI00332157.2	39S ribosomal protein L54, mitochondrial	3.093358755
434	IPI00966017.1	chromosome 5 open reading frame 24	3.079425335
435	IPI00922210.1	cDNA FLJ52564, moderately similar to Zinc finger protein 346	3.079051018
436	IPI01011569.1	cDNA, FLJ78951, highly similar to Creatine kinase, ubiquitous mitochondrial	3.063862324
437	IPI00019269.3	WD repeat-containing protein 61	3.061416388
438	IPI00983408.1	transforming growth factor, beta receptor III	3.056727171
439	IPI00927046.1	epithelial cell transforming sequence 2 oncogene	3.054199457
440	IPI00910126.1	cDNA FLJ59119, highly similar to Receptor expression-enhancing protein 6	3.046956062
441	IPI00935818.1	adenosylhomocysteinase isoform 2	3.045629501
442	IPI00797997.2	5-formyltetrahydrofolate cyclo-ligase isoform b	3.045045376
443	IPI00980553.1	cDNA FLJ50204, highly similar to 2,4-dienoyl-CoA reductase, mitochondrial	3.035377979
444	IPI00908957.1	cDNA FLJ61419, highly similar to RalA-binding protein 1	3.023126841
445	IPI00395401.3	Isoform 3 of Cdc42-interacting protein 4	3.016060829
446	IPI00216508.3	Isoform 2 of Sorting nexin-3	3.014677763
447	IPI00019487.3	Probable 7,8-dihydro-8-oxoguanine triphosphatase NUDT15	3.005639315
448	IPI00927053.2	26S protease regulatory subunit 7 2	3.003509283
449	IPI00168442.5	FAM75-like protein C9orf79	3.003401756
450	IPI00954159.1	Isoform 1 of Protein ELYS	2.998862505
451	IPI00970906.1	Isoform 1 of Transcription elongation factor A N-terminal and central domain-co	2.997951031
452	IPI00644228.1	cDNA FLJ52965, highly similar to Uridine-cytidine kinase 1	2.992982388
453	IPI00878538.1	signal transducer and activator of transcription 5A	2.991655588
454	IPI00001835.3	Zinc finger and BTB domain-containing protein 4	2.986486912
455	IPI00030296.6	Eukaryotic translation initiation factor 4A, isoform 2, isoform CRA_b	2.980415583
456	IPI00292393.5	Sodium channel protein type 4 subunit alpha	2.980061769
457	IPI01011145.1	OTU domain, ubiquitin aldehyde binding 1	2.975468874
458	IPI00983405.1	lin-7 homolog C (C. elegans)	2.975069761
459	IPI00910998.1	cDNA FLJ51306, highly similar to Homo sapiens citrate lyase beta like (CLYBL), tra	2.962366104
460	IPI00397801.4	Filaggrin-2	2.959728479
461	IPI00926172.1	WD repeat domain 12	2.95571661
462	IPI00298139.5	cDNA FLJ39639 fis, clone SMINT2003340	2.954498768
463	IPI00748303.3	zinc finger RNA binding protein	2.952274323
464	IPI00001830.1	Heterochromatin-specific nonhistone protein (Fragment)	2.950314045
465	IPI00908894.1	cDNA FLJ57473, highly similar to Ribonuclease P protein subunit p29	2.948116064
466	IPI01009115.1	N-acetylglucosamine kinase	2.947503805
467	IPI00556611.1	39S ribosomal protein L22, mitochondrial isoform b	2.935769081
468	IPI00449669.2	Isoform 2 of Translocon-associated protein subunit alpha	2.932744741
469	IPI00967585.1	guanine nucleotide binding protein (G protein), beta polypeptide 2-like 1	2.930656672
470	IPI00791495.2	HLA-B associated transcript 1	2.927881479

471	IPI00785036.8	nuclear GTPase, germinal center associated	2.927058935
472	IPI00216529.1	Isoform E of Plasma membrane calcium-transporting ATPase 1	2.924975872
473	IPI00219669.5	Carbonic anhydrase-related protein	2.921352863
474	IPI00480049.2	Isoform B of Inositol polyphosphate 5-phosphatase OCRL-1	2.917422295
475	IPI00641749.2	Isoform 1 of Janus kinase and microtubule-interacting protein 3	2.914739132
476	IPI00946474.1	NADH dehydrogenase (ubiquinone) 1 alpha subcomplex, 5, 13kDa	2.913308382
477	IPI00977662.1	Parkinson disease 7 domain containing 1	2.913131475
478	IPI00307665.4	Isoform 1 of Zinc finger protein 518A	2.90212512
479	IPI00975554.1	protein tyrosine phosphatase type IVA, member 2	2.90075922
480	IPI00977503.1	midline-1 isoform 5	2.899876595
481	IPI00981929.2	cDNA FLJ33978 fis, clone DFNES2004354, highly similar to Inhibitor of nuclear fact	2.894971848
482	IPI00022426.1	Protein AMBP	2.892508745
483	IPI00797343.2	coiled-coil domain containing 117	2.888273001
484	IPI00296219.4	Glutaminase liver isoform, mitochondrial	2.885802031
485	IPI00894139.1	golgi to ER traffic protein 4 homolog (S. cerevisiae)	2.883171082
486	IPI00910017.1	cDNA FLJ54153, weakly similar to Homo sapiens Mof4 family associated protein	2.88300252
487	IPI00220147.1	Isoform 3 of Pantothenate kinase 1	2.88271594
488	IPI00031650.3	Isoform 1 of Protein syndesmos	2.873019934
489	IPI00298409.3	Phosducin-like protein	2.870197058
490	IPI00910019.2	Major vault protein	2.869003296
491	IPI01009997.1	cDNA FLJ51981, highly similar to Histone deacetylase 1	2.865437031
492	IPI00985171.1	proteoglycan 4	2.86326766
493	IPI00028078.1	Isoform A of Potassium channel subfamily K member 10	2.862164259
494	IPI01013425.1	cDNA FLJ45045 fis, clone BRAWH3021580, highly similar to Restin	2.858755589
495	IPI00643380.2	chromosome 18 open reading frame 8	2.857409954
496	IPI00893403.1	exportin 1 (CRM1 homolog, yeast)	2.856910229
497	IPI00179408.3	Tetratricopeptide repeat protein 9C	2.856591225
498	IPI00005740.1	Neighbor of COX4	2.854933977
499	IPI00908538.1	arginine and glutamate rich 1	2.851033449
500	IPI00922399.1	cDNA FLJ57937, highly similar to DNA-directed RNA polymerase II 33 kDa polypep	2.848650932
501	IPI00384047.1	Isoform 1 of Trafficking protein particle complex subunit 6B	2.843178988
502	IPI00894369.1	neuroblastoma amplified sequence	2.830990076
503	IPI00927360.1	nuclear receptor subfamily 4, group A, member 2	2.830797911
504	IPI00432753.2	Isoform 1 of Torsin-2A	2.830038071
505	IPI00011865.2	Isoform 2 of Platelet-derived growth factor D	2.824905634
506	IPI00946064.1	geranylgeranyl diphosphate synthase 1	2.824784279
507	IPI01011129.1	cDNA FLJ38453 fis, clone FEBRA2019663, highly similar to Homo sapiens DEAD (As	2.811005831
508	IPI01012915.1	cDNA FLJ53462, highly similar to Transcription intermediary factor 1-alpha	2.80894351
509	IPI00651702.1	SATB2 protein	2.80437851
510	IPI00909427.1	cDNA FLJ59384, highly similar to Striatin-4	2.804109097
511	IPI00103004.4	Isoform 2 of Intracellular hyaluronan-binding protein 4	2.80377388
512	IPI00307805.5	Growth arrest and DNA damage-inducible protein GADD45 beta	2.800504923
513	IPI00219898.1	Isoform 2 of Nephrin	2.794588804
514	IPI00894394.1	Isoform 4 of Immunoglobulin-like and fibronectin type III domain-containing pr	2.789975643
515	IPI00013706.5	39S ribosomal protein L20, mitochondrial	2.773723125
516	IPI00290764.5	Isoform 2 of Chronic lymphocytic leukemia deletion region gene 6 protein	2.770787239
517	IPI00748058.1	Isoform 2 of SH3 and cysteine-rich domain-containing protein 3	2.77041173

518	IPI00396551.3	Isoform 2 of RAD51-associated protein 1	2.768308878
519	IPI00552983.6	Protein of unknown function DUF634 family protein	2.762229204
520	IPI00002535.2	Peptidyl-prolyl cis-trans isomerase FKBP2	2.761423111
521	IPI00554560.4	chromosome 16 open reading frame 88	2.757285118
522	IPI00646520.1	non-POU domain containing, octamer-binding	2.753503561
523	IPI00984596.1	leucine-rich repeats and IQ motif containing 1	2.752708912
524	IPI01011419.1	ATP9B protein	2.711783409
525	IPI00966190.2	SFRS protein kinase 1	2.696774483

Table A4: BPPM-revealed potential nonhistone targets of G9a Y1154A in HEK293T cells using Hey SAM. These proteins are not present in control samples.

Serial	Accession	Description	Score of EuHMT2
1	IPI00296337.2	Isoform 1 of DNA-dependent protein kinase catalytic subunit	683.7383871
2	IPI00220795.4	Isoform 2 of Histone-lysine N-methyltransferase EHMT2	466.1512184
3	IPI00302592.2	Isoform 2 of Filamin-A	207.2757595
4	IPI00909140.9	cDNA FLJ56903, highly similar to Tubulin beta-7 chain	134.9918664
5	IPI00024279.4	HEAT repeat-containing protein 1	120.841238
6	IPI00883857.2	Isoform Long of Heterogeneous nuclear ribonucleoprotein U	118.6945181
7	IPI00006482.1	Isoform Long of Sodium/potassium-transporting ATPase subunit alpha-1	108.9071741
8	IPI00414482.3	Isoform 1 of General transcription factor 3C polypeptide 1	108.9063585
9	IPI00893062.1	X-ray repair complementing defective repair in Chinese hamster cells 6	98.84765005
10	IPI00790636.1	HLA-B associated transcript 1	91.60756612
11	IPI01018179.1	Isoform 4 of Interleukin enhancer-binding factor 3	91.36282182
12	IPI00216049.1	Isoform 1 of Heterogeneous nuclear ribonucleoprotein K	88.98906755
13	IPI00293464.5	DNA damage-binding protein 1	81.18342185
14	IPI00402182.2	Isoform 2 of Heterogeneous nuclear ribonucleoprotein Q	74.11966062
15	IPI00026202.1	60S ribosomal protein L18a	70.69340944
16	IPI00010204.1	Serine/arginine-rich splicing factor 3	66.33425546
17	IPI00894141.2	DNA-directed RNA polymerase	65.24241805
18	IPI00030275.5	Heat shock protein 75 kDa, mitochondrial	59.69980907
19	IPI01015236.1	cDNA FLJ52378, highly similar to Tubulin beta-7 chain	58.46184039
20	IPI01014074.1	cDNA FLJ53296, highly similar to Serine/threonine-protein phosphatase 2A 65 kDa	58.19350886
21	IPI00745272.3	Isoform 2 of Glyoxalase domain-containing protein 4	57.74798656
22	IPI00646899.2	ribosomal protein L10	57.57459235
23	IPI00892976.1	Euchromatic histone-lysine N-methyltransferase 2	57.4455924
24	IPI00550451.1	Serine/threonine-protein phosphatase PP1-alpha catalytic subunit	56.66304755
25	IPI00301109.4	Isoform 1 of Inorganic pyrophosphatase 2, mitochondrial	54.79612994
26	IPI00026625.1	Isoform 1 of Nuclear pore complex protein Nup155	53.59179616
27	IPI00299608.3	Isoform 1 of 26S proteasome non-ATPase regulatory subunit 1	52.03631973
28	IPI00017617.1	Probable ATP-dependent RNA helicase DDX5	51.95726752
29	IPI00003348.3	Guanine nucleotide-binding protein G(I)/G(S)/G(T) subunit beta-2	50.74977994
30	IPI00939492.2	HLA-B associated transcript 8 BAT8 isoform a variant (Fragment)	50.66032219
31	IPI00003964.4	Isoform 2 of Probable ubiquitin carboxyl-terminal hydrolase FAF-X	50.29524088
32	IPI00291755.6	Isoform 1 of Nuclear pore membrane glycoprotein 210	49.22668934
33	IPI01015522.1	cDNA FLJ55253, highly similar to Actin, cytoplasmic 1	47.32136416
34	IPI00784332.4	Similar to Tubulin alpha-3C/D chain	47.26412559
35	IPI00064328.3	protein arginine N-methyltransferase 5 isoform b	46.35761309
36	IPI00647102.4	cDNA FLJ42590 fis, clone BRACE3009708, highly similar to Sodium/potassium-transp	45.72382426
37	IPI00604620.3	Nucleolin	45.58505511
38	IPI00216530.1	Isoform K of Plasma membrane calcium-transporting ATPase 1	45.45633245
39	IPI00940257.2	cDNA FLJ52362, highly similar to T-complex protein 1 subunit epsilon	45.03963923
40	IPI00793930.1	TUBA1B protein	44.1114819
41	IPI00642042.3	Putative uncharacterized protein DKFZp686J1372	43.91723847
42	IPI00965271.1	small subunit processome component 20 homolog	42.85621881
43	IPI00983023.1	phosphoglycerate mutase 1-like	42.1787138
44	IPI00964983.1	ribosomal protein S3A	41.65900421
45	IPI00796337.1	poly(rC)-binding protein 2 isoform a	41.27402925
46	IPI01013547.1	cystathionine-beta-synthase	40.56543255

47	IPI00472939.3	Signal peptidase complex subunit 2	40.41459775
48	IPI00171438.2	Thioredoxin domain-containing protein 5	39.3563168
49	IPI00456429.3	Ubiquitin-60S ribosomal protein L40	38.90302277
50	IPI00013891.1	Isoform Long of Transformer-2 protein homolog alpha	37.85644484
51	IPI00903323.1	cDNA FLJ38640 fis, clone HHDPC2003472, highly similar to CHLORIDE INTRACELLULAR	35.82258964
52	IPI00646721.1	Ubiquitin carboxyl-terminal hydrolase	35.46411991
53	IPI00787827.1	Isoform 2 of Presequence protease, mitochondrial	33.91579771
54	IPI00446235.2	Isoform 2 of NADH-cytochrome b5 reductase 3	33.31059861
55	IPI00166293.5	Histone H2B type 3-B	32.30172586
56	IPI00304417.7	Isocitrate dehydrogenase [NAD] subunit beta, mitochondrial precursor	32.26378059
57	IPI01014975.1	Talin 1	31.65581322
58	IPI01018004.1	3'(2'), 5'-bisphosphate nucleotidase 1	31.31366825
59	IPI00099986.5	Ketosamine-3-kinase	31.07059574
60	IPI00005719.1	Isoform 1 of Ras-related protein Rab-1A	30.42552304
61	IPI00306048.5	Isoform 1 of ATPase family AAA domain-containing protein 3B	30.22437739
62	IPI00220487.4	Isoform 1 of ATP synthase subunit d, mitochondrial	29.69207406
63	IPI00294701.1	CDK-activating kinase assembly factor MAT1	28.72710562
64	IPI00297492.2	Dolichyl-diphosphooligosaccharide--protein glycosyltransferase subunit STT3A	28.56105924
65	IPI00154473.5	Isoform 1 of Elongation factor G, mitochondrial	28.23124099
66	IPI00031627.4	DNA-directed RNA polymerase II subunit RPB1	27.87834454
67	IPI00908647.1	cDNA FLJ59942, highly similar to Prostaglandin E synthase 3	27.80573511
68	IPI00011307.4	Bifunctional methylenetetrahydrofolate dehydrogenase/cyclohydrolase, mitochon	27.65156341
69	IPI00008485.1	Cytoplasmic aconitate hydratase	27.61344528
70	IPI00328985.1	Isoform 1 of THO complex subunit 6 homolog	27.59589958
71	IPI00384456.4	Isoform GTBP-N of DNA mismatch repair protein Msh6	27.50466967
72	IPI00032304.2	Plastin-1	27.36275649
73	IPI00335130.5	mitochondrial ribosomal protein L37	27.21831703
74	IPI00018288.1	DNA-directed RNA polymerase II subunit RPB3	26.89926624
75	IPI01010848.1	Methionine aminopeptidase	26.41838145
76	IPI00946054.3	Isoform 3 of Histone-lysine N-methyltransferase EHMT1	25.92109776
77	IPI00472054.2	Isoform A of Constitutive coactivator of PPAR-gamma-like protein 1	25.78061318
78	IPI00924935.1	cDNA FLJ57106, highly similar to Transferrin receptor protein 1	24.9913497
79	IPI00168209.3	DTW domain-containing protein 2	24.76762366
80	IPI00032849.2	Nucleolar protein 16	24.5403409
81	IPI00983716.1	ubiquitin protein ligase E3 component n-recognin 5	24.53851151
82	IPI00418202.2	pyridoxal (pyridoxine, vitamin B6) kinase	24.44453502
83	IPI00305978.4	Aflatoxin B1 aldehyde reductase member 2	24.39702511
84	IPI00217975.4	Lamin-B1	24.35361624
85	IPI00010845.3	NADH dehydrogenase [ubiquinone] iron-sulfur protein 8, mitochondrial	24.22619653
86	IPI00926412.1	Transformation/transcription domain-associated protein variant	23.87043071
87	IPI00032872.3	28S ribosomal protein S16, mitochondrial	23.81681204
88	IPI00843975.1	Ezrin	23.72064447
89	IPI00915022.2	Isoform 1 of THO complex subunit 2	23.37501526
90	IPI00909083.1	eukaryotic peptide chain release factor GTP-binding subunit ERF3A isoform 2	23.2077117
91	IPI00927876.1	polymerase (RNA) II (DNA directed) polypeptide H	23.01699042
92	IPI00926706.1	actin related protein 2/3 complex, subunit 1A, 41kDa	22.53975105
93	IPI00975963.1	eukaryotic translation elongation factor 1 delta (guanine nucleotide exchange pro	22.28946233

94	IPI00975850.1	ribosomal protein L8	22.23127723
95	IPI00641040.1	esterase D	22.21193528
96	IPI00000792.1	Quinone oxidoreductase	22.15558577
97	IPI00009607.1	Ras-related protein Rap-2c	22.08097172
98	IPI00410017.1	Isoform 2 of Polyadenylate-binding protein 1	21.9293642
99	IPI00217992.1	Isoform 3 of Dystonin	21.92004824
100	IPI00339385.1	Isoform 2 of Retinol dehydrogenase 11	21.70267034
101	IPI00333985.2	Isoform 2 of Nodal modulator 2	21.68538427
102	IPI00465022.9	Isoform 2 of Structural maintenance of chromosomes flexible hinge domain-conta	21.6378448
103	IPI00037070.3	heat shock 70kDa protein 8	21.34835196
104	IPI00414860.6	60S ribosomal protein L37a	21.27662992
105	IPI01016026.1	cDNA FLJ53202, highly similar to Exportin-2	21.27041531
106	IPI00305258.4	Isoform 1 of MOSC domain-containing protein 1, mitochondrial	21.26810241
107	IPI01014700.1	cDNA FLJ51193, highly similar to DNA mismatch repair protein Msh2	21.0701077
108	IPI01010578.1	cytoplasmic FMR1 interacting protein 2	21.02910089
109	IPI00295992.4	Isoform 2 of ATPase family AAA domain-containing protein 3A	20.9871881
110	IPI00301204.2	Isoform 1 of Retinol dehydrogenase 13	20.79895854
111	IPI01013219.1	prohibitin 2	20.71885967
112	IPI00328815.4	Isoform 1 of Ubiquitin carboxyl-terminal hydrolase 48	20.68755722
113	IPI00056494.5	60S ribosomal protein L36a-like	19.84472513
114	IPI00182757.10	Isoform 1 of Protein KIAA1967	19.83158898
115	IPI00967041.1	Ubiquitin carrier protein	19.72968006
116	IPI00293260.5	Isoform 1 of DnaJ homolog subfamily C member 10	19.13160372
117	IPI01011635.1	CDC10 protein variant (Fragment)	19.08216
118	IPI00748807.2	Isoform 1 of Nuclear pore complex protein Nup160	19.02867842
119	IPI01014189.1	MYC binding protein 2	18.75863028
120	IPI00157908.4	Isoform 3 of Apoptosis-inducing factor 1, mitochondrial	18.59455872
121	IPI00844172.1	Myosin	18.58733106
122	IPI00295889.2	Signal recognition particle 19 kDa protein	18.56547809
123	IPI00980391.2	cDNA FLJ54047, highly similar to Alpha-1 catenin	18.41666961
124	IPI00014213.1	Probable leucyl-tRNA synthetase, mitochondrial	18.35570359
125	IPI00027699.2	Proteasome (Prosome, macropain) 26S subunit, non-ATPase, 10	18.28348708
126	IPI00885106.1	Similar to Transmembrane 9 superfamily member 4 precursor	18.13494015
127	IPI00420108.6	Dihydrolipoyllysine-residue succinyltransferase component of 2-oxoglutarate deh	18.09095812
128	IPI00514701.1	Isoform 2 of Mitotic checkpoint protein BUB3	17.8680315
129	IPI00903112.1	cDNA FLJ36533 fis, clone TRACH2004428, highly similar to Lactotransferrin (Fragmen	17.33468866
130	IPI00890827.1	Isoform 2 of Serine/threonine-protein phosphatase 6 catalytic subunit	17.32423234
131	IPI00215888.4	Signal recognition particle 72 kDa protein	17.1121819
132	IPI00619903.3	Isoform 2 of UDP-glucose:glycoprotein glucosyltransferase 1	16.92570233
133	IPI00902914.2	transmembrane 9 superfamily member 2	16.88384128
134	IPI00299254.4	Eukaryotic translation initiation factor 5B	16.79346323
135	IPI01012145.1	Hydroxymethylbilane synthase	16.78157663
136	IPI00908696.2	ADP-ribosylation-like factor 6 interacting protein 5	16.75019765
137	IPI00788781.1	fatty acid binding protein 5 (psoriasis-associated)	16.7113061
138	IPI01014596.1	ubiquitin C	16.70653343
139	IPI00019329.1	Dynein light chain 1, cytoplasmic	16.70442867
140	IPI00884904.1	Isoform 3 of Protein AHNAK2	16.68552947

141	IPI00295427.5	Isoform 1 of 39S ribosomal protein L39, mitochondrial	16.68056345
142	IPI00946099.1	sorcin	16.52582979
143	IPI00640401.1	ATPase, Na+/K+ transporting, alpha 2 (+) polypeptide	16.52371335
144	IPI00645329.1	Isoform 3 of Histone-binding protein RBBP4	16.43619323
145	IPI00020557.2	Prolow-density lipoprotein receptor-related protein 1	16.39069438
146	IPI00006252.3	Aminoacyl tRNA synthase complex-interacting multifunctional protein 1	16.3434124
147	IPI00658000.3	Isoform 1 of Insulin-like growth factor 2 mRNA-binding protein 3	16.23186374
148	IPI00024913.2	Isoform Long of ES1 protein homolog, mitochondrial	16.21972036
149	IPI00816106.3	Isoform 4 of Dedicator of cytokinesis protein 7	16.0455668
150	IPI00792218.1	proteasome subunit alpha type-4 isoform 2	16.04161143
151	IPI00647678.2	cDNA FLJ52703, highly similar to Asparaginyl-tRNA synthetase, cytoplasmic	15.62722707
152	IPI00554701.2	Cytochrome b-c1 complex subunit 9	15.61058617
153	IPI00305289.2	Kinesin-like protein KIF11	15.60377216
154	IPI00103732.1	Thymidylate synthetase, isoform CRA_a	15.59636855
155	IPI00642326.1	zinc finger, MYM-type 3	15.44959974
156	IPI00396203.7	Isoform 1 of Tubulin-specific chaperone D	15.43279815
157	IPI00645518.1	Isoform 1 of CDP-diacylglycerol--inositol 3-phosphatidyltransferase	15.31668091
158	IPI00024719.1	Isoform A of Histone acetyltransferase type B catalytic subunit	15.30857706
159	IPI00293735.2	Elongator complex protein 1	15.27497411
160	IPI00929313.1	coiled-coil domain containing 168	15.07390261
161	IPI01011651.1	nucleoporin 98kDa	15.02397823
162	IPI01012847.1	RAB35, member RAS oncogene family	14.94564271
163	IPI00398727.3	Isoform 2 of Acyl-protein thioesterase 1	14.82557869
164	IPI00981725.1	peptidylprolyl isomerase H (cyclophilin H)	14.69265079
165	IPI01013095.1	cDNA, FLJ79243, highly similar to Eukaryotic translation initiation factor 3 subunit 1	14.58456922
166	IPI00743813.3	Isoform 1 of Abnormal spindle-like microcephaly-associated protein	14.49706197
167	IPI00011619.4	Bifunctional 3'-phosphoadenosine 5'-phosphosulfate synthase 1	14.39087629
168	IPI00328361.7	Seryl-tRNA synthetase, mitochondrial	14.34127712
169	IPI00374272.3	chromosome 5 open reading frame 51	14.28932667
170	IPI00034159.1	V-type proton ATPase subunit d 1	14.14081883
171	IPI00032387.1	DNA replication complex GINS protein PSF1	14.1289773
172	IPI00216770.1	Isoform 2 of 26S protease regulatory subunit 6B	14.11542821
173	IPI00383500.3	Isoform 2 of Fermitin family homolog 2	14.09937
174	IPI00414384.1	Isoform 1 of Hydroxysteroid dehydrogenase-like protein 2	13.95179152
175	IPI00607577.2	superoxide dismutase [Mn], mitochondrial isoform B precursor	13.84640741
176	IPI00910755.1	cDNA FLJ51707, highly similar to Heat-shock protein 105 kDa	13.83009171
177	IPI00041325.1	H/ACA ribonucleoprotein complex subunit 2	13.82135797
178	IPI00177498.16	Isoform 3 of LIM and calponin homology domains-containing protein 1	13.80416584
179	IPI00552913.4	Isoform 2 of Syntaxin-7	13.76695967
180	IPI00028005.1	Nuclear pore complex protein Nup107	13.68241692
181	IPI00019407.1	Sterol-4-alpha-carboxylate 3-dehydrogenase, decarboxylating	13.59610152
182	IPI00852917.1	Copine I	13.57617283
183	IPI00300078.6	Periodic tryptophan protein 2 homolog	13.56396508
184	IPI00744711.2	Polyribonucleotide nucleotidyltransferase 1, mitochondrial	13.42098427
185	IPI00790334.1	Polymerase (DNA directed), epsilon, isoform CRA_a	13.40018821
186	IPI00166749.3	Mitochondrial-processing peptidase subunit alpha	13.38723707
187	IPI00952964.1	L-lactate dehydrogenase A chain isoform 4	13.30574989

188	IPI00966693.1	glutathione S-transferase, C-terminal domain containing	13.25156164
189	IPI00939526.1	Uncharacterized protein	13.2412262
190	IPI00965290.1	Isoform 3 of Cullin-4B	13.20198965
191	IPI00983406.1	branched-chain-amino-acid aminotransferase, cytosolic isoform 5	13.14481378
192	IPI00477424.4	DHX57 protein variant (Fragment)	13.1199398
193	IPI00790937.3	60S ribosomal export protein NMD3	13.08651328
194	IPI00979853.1	eukaryotic translation initiation factor 3, subunit M	13.01624179
195	IPI00798401.2	cDNA FLJ50992, highly similar to Coronin-1C	12.9656148
196	IPI00742682.2	Nucleoprotein TPR	12.95771432
197	IPI01015254.1	cDNA FLJ53681, highly similar to Glycogen (starch) synthase, muscle	12.92818904
198	IPI00910697.1	cDNA FLJ53703, highly similar to Histidyl-tRNA synthetase	12.88820577
199	IPI00658145.3	Isoform 1 of BRCA1-associated ATM activator 1	12.84551978
200	IPI00328911.3	E3 ubiquitin-protein ligase HECTD1	12.81816292
201	IPI00789281.2	Isoform 3 of Protein virilizer homolog	12.78548574
202	IPI01012511.1	cDNA FLJ50223, highly similar to Sterol O-acyltransferase 1	12.65474391
203	IPI00382699.2	Isoform 5 of Filamin-B	12.55565691
204	IPI00878236.3	fibrous sheath-interacting protein 2	12.4965713
205	IPI00944623.1	Isoform 3 of Golgin subfamily A member 3	12.46515846
206	IPI01011723.1	cDNA FLJ51704, highly similar to ADP-ribosylation factor-like protein 1	12.1291225
207	IPI01009186.1	cDNA FLJ58476, highly similar to Poly(rC)-binding protein 2	12.12248826
208	IPI00640096.2	cDNA FLJ57101, highly similar to SAC domain-containing protein 3	12.09884024
209	IPI00182180.2	OTU domain-containing protein 6B	11.93218946
210	IPI00871617.1	Isoform 1 of Lys-63-specific deubiquitinase BRCC36	11.8933475
211	IPI00893923.1	Isoform 2 of Golgi to ER traffic protein 4 homolog	11.80594444
212	IPI00003455.3	Isoform 4 of Nucleoporin NDC1	11.69121122
213	IPI00966935.1	methionyl aminopeptidase 1	11.54681015
214	IPI00976647.1	staufen, RNA binding protein, homolog 2 (Drosophila)	11.51790977
215	IPI00552886.1	Exosomal core protein CSL4	11.51610184
216	IPI00552920.2	Exosome complex component RRP43	11.48156738
217	IPI00218106.3	Isoform 2 of Transcription elongation factor A protein 1	11.38789392
218	IPI01011408.1	cDNA FLJ16235 fis, clone FEBRA2028516	11.30251765
219	IPI00646415.1	RAB14, member RAS oncogene family	11.29374671
220	IPI00743994.2	laminin subunit alpha-3 isoform 3	11.21005273
221	IPI00002335.1	huntingtin	11.17695832
222	IPI00797126.2	nascent polypeptide-associated complex subunit alpha isoform a	11.11984396
223	IPI00921912.2	rod cGMP-specific 3',5'-cyclic phosphodiesterase subunit beta isoform 3	10.99007988
224	IPI00297084.7	Dolichyl-diphosphooligosaccharide--protein glycosyltransferase 48 kDa subunit	10.89367771
225	IPI00294879.1	Ran GTPase-activating protein 1	10.86647868
226	IPI00917001.2	cDNA, FLJ79439, highly similar to NEDD8-activating enzyme E1 catalytic subunit	10.85314226
227	IPI00291175.7	Isoform 1 of Vinculin	10.82610989
228	IPI00171459.4	Inactive hydroxysteroid dehydrogenase-like protein 1	10.82172179
229	IPI00939530.1	cDNA FLJ34106 fis, clone FCBBF3008073, highly similar to SPLICING FACTOR, ARGININ	10.78457308
230	IPI00033907.1	Anaphase-promoting complex subunit 1	10.73571968
231	IPI00220665.6	Isoform 3 of Hexokinase-1	10.71835494
232	IPI00329719.1	Myosin-Id	10.68723392
233	IPI00910514.1	xaa-Pro dipeptidase isoform 2	10.65641642
234	IPI00014253.4	Ribosome biogenesis regulatory protein homolog	10.64323997

235	IPI00181135.4	Branched-chain-amino-acid aminotransferase	10.63430691
236	IPI00900328.3	transcription activator BRG1 isoform F	10.62978029
237	IPI00384745.4	guanine nucleotide binding protein-like 1	10.53790355
238	IPI00791573.1	Isoform 2 of Suppressor of G2 allele of SKP1 homolog	10.52630734
239	IPI00877948.1	Minichromosome maintenance complex component 5	10.50127697
240	IPI00394699.3	Uncharacterized protein	10.49009347
241	IPI00169168.1	Isoform 3 of F-box only protein 22	10.43747807
242	IPI00396218.2	SCY1-like protein 2	10.42661786
243	IPI00786874.1	Putative Golgi pH regulator C	10.37785602
244	IPI00908668.1	apoptosis inhibitor 5 isoform c	10.30549598
245	IPI00218922.5	Translocation protein SEC63 homolog	10.23215318
246	IPI00414980.2	Isoform 2 of Myosin-Ib	10.22754383
247	IPI00910169.1	cDNA FLJ54122, highly similar to Cytosol aminopeptidase	10.0674417
248	IPI00946283.1	transportin 3	10.05775833
249	IPI00968174.1	IQ motif containing GTPase activating protein 2	9.929574966
250	IPI00002557.1	Coatomer subunit gamma-2	9.908848047
251	IPI00843789.2	Glycine dehydrogenase [decarboxylating], mitochondrial	9.883997917
252	IPI00909961.1	cDNA FLJ50720, highly similar to Homo sapiens tropomyosin 3 (TPM3), transcript va	9.837865829
253	IPI00910728.1	cDNA FLJ57599, moderately similar to Eukaryotic translation initiation factor 3 subu	9.831304789
254	IPI00470922.2	Isoform 2 of N-alpha-acetyltransferase 50, NatE catalytic subunit	9.777771473
255	IPI00219526.6	Isoform 1 of Phosphoglucomutase-1	9.775624275
256	IPI00239415.4	Polytrophin	9.697652102
257	IPI00925016.1	N-acylaminoacyl-peptide hydrolase	9.694558859
258	IPI00215764.1	Isoform Short of Metastasis-associated protein MTA1	9.636773586
259	IPI00216999.2	Pumilio domain-containing protein C14orf21	9.629089594
260	IPI00074489.1	NDUFB10 protein	9.616615295
261	IPI00856038.2	cDNA FLJ53358, highly similar to Heterogeneous nuclear ribonucleoprotein R	9.535647154
262	IPI00646889.1	Uncharacterized protein	9.468101025
263	IPI00061245.4	28S ribosomal protein S10, mitochondrial	9.452897549
264	IPI00922035.1	cDNA FLJ52950	9.363273859
265	IPI00106847.3	Isoform GTBP-alt of DNA mismatch repair protein Msh6	9.361681223
266	IPI00000846.2	Isoform 1 of Chromodomain-helicase-DNA-binding protein 4	9.30049777
267	IPI00976265.2	dipeptidyl-peptidase 3	9.297903538
268	IPI00945912.1	cDNA FLJ59963, highly similar to Homo sapiens multiple substrate lipid kinase (MI	9.279073238
269	IPI00025710.1	chromosome 21 open reading frame 59	9.151694775
270	IPI00410069.4	zinc finger CCCH-type, antiviral 1	9.137892008
271	IPI00180681.6	coiled-coil domain-containing protein 41	9.098641634
272	IPI00647528.1	Exosome component 2, isoform CRA_b	9.083474636
273	IPI00920991.1	Similar to Cyclin k	8.956657887
274	IPI00294501.1	7-dehydrocholesterol reductase	8.902279615
275	IPI00022542.1	Rho-associated protein kinase 1	8.890659809
276	IPI00642838.3	Isoform 2 of Lysophospholipase-like protein 1	8.841372252
277	IPI00966031.1	Eukaryotic translation initiation factor 4E	8.82912755
278	IPI00922492.1	cDNA FLJ53090, moderately similar to RNA-binding motif, single-stranded-interacti	8.820865154
279	IPI01013010.1	eukaryotic translation initiation factor 2B, subunit 1 alpha, 26kDa	8.683921099
280	IPI00024317.1	Isoform Long of Glutaryl-CoA dehydrogenase, mitochondrial	8.629867792
281	IPI01015267.1	phosphoglucomutase 2	8.614906311

282	IPI00477355.3	KIF1-binding protein	8.612172127
283	IPI00065486.3	Isoform 2 of ATP-binding cassette sub-family B member 6, mitochondrial	8.608422995
284	IPI00910254.2	cDNA FLJ50983, highly similar to Homo sapiens lysocardiolipin acyltransferase (LY	8.607723951
285	IPI00470870.1	Putative uncharacterized protein DKFZp686J22257	8.564293146
286	IPI00184311.4	Ectonucleotide pyrophosphatase/phosphodiesterase family member 1	8.496405363
287	IPI00926796.1	procollagen-lysine, 2-oxoglutarate 5-dioxygenase 3	8.487639189
288	IPI00797314.1	COP9 constitutive photomorphogenic homolog subunit 3 (Arabidopsis)	8.480714321
289	IPI00017921.7	Isoform 2 of Protein bicaudal C homolog 1	8.418764591
290	IPI00853417.1	SCO2 cytochrome c oxidase assembly protein	8.412479877
291	IPI00005492.2	WD repeat-containing protein 5	8.403086901
292	IPI00947201.1	GLIS family zinc finger 3 transcript variant TS5	8.397313356
293	IPI00917299.1	gamma-glutamylcyclotransferase	8.375939608
294	IPI00878484.1	Ewing sarcoma breakpoint region 1	8.321173191
295	IPI00983652.2	cDNA FLJ61021, highly similar to Far upstream element-binding protein 1	8.286056519
296	IPI01009061.1	Truncated tumor suppressor protein P16	8.27630496
297	IPI00927188.1	Solute carrier family 4 sodium bicarbonate cotransporter member 7 type 2 variant	8.248812914
298	IPI00981773.1	cDNA FLJ53377, highly similar to Procollagen-lysine, 2-oxoglutarate 5-dioxygenase	8.229576111
299	IPI00018236.2	Ganglioside GM2 activator	8.210482597
300	IPI00903257.1	cDNA FLJ39170 fis, clone OCBBF2003028, highly similar to Rattus norvegicus basic le	8.172838449
301	IPI00024802.1	TATA-binding protein-associated factor 172	8.127103567
302	IPI00974096.1	family with sequence similarity 184, member A	8.075909615
303	IPI00398625.5	Hornerin	8.045919418
304	IPI00977865.1	non-specific lipid-transfer protein isoform 8 proprotein	8.02077508
305	IPI00008511.2	NADH dehydrogenase subunit 5	8.004798412
306	IPI00984992.1	non-SMC condensin II complex, subunit D3	7.977009058
307	IPI00216659.1	Isoform 2 of RNA-binding protein 8A	7.946021318
308	IPI00878524.1	ribosomal protein L3	7.911752939
309	IPI00853207.1	Protein phosphatase 2A activator, regulatory subunit 4	7.889402628
310	IPI00219833.2	Mitochondrial import inner membrane translocase subunit Tim17-B	7.879449368
311	IPI00983620.1	peptidyl-prolyl cis-trans isomerase A-like	7.864541054
312	IPI00098902.4	2-oxoglutarate dehydrogenase, mitochondrial	7.815811157
313	IPI00514769.3	Isoform 1 of Serine/threonine-protein phosphatase 6 regulatory ankyrin repeat su	7.812160254
314	IPI00946670.1	NADH dehydrogenase (ubiquinone) 1 alpha subcomplex, 5, 13kDa	7.799548864
315	IPI00885004.1	Isoform 2 of Xin actin-binding repeat-containing protein 2	7.798505783
316	IPI00980681.1	chloride channel, nucleotide-sensitive, 1A	7.791601181
317	IPI00977524.1	Isoform 1 of 39S ribosomal protein L22, mitochondrial	7.686861992
318	IPI00941385.2	Isoform 3 of Ubiquitin carboxyl-terminal hydrolase 10	7.675077915
319	IPI00908755.1	cDNA FLJ53392, highly similar to Ubiquitin-activating enzyme E1	7.640746355
320	IPI00974217.2	inositol(myo)-1(or 4)-monophosphatase 1	7.634245396
321	IPI00012837.1	Kinesin-1 heavy chain	7.632534742
322	IPI00968146.1	ribosomal protein S3A	7.612484217
323	IPI00657704.4	tumor protein p53 binding protein 1	7.589646816
324	IPI00914601.2	Ubiquitin carboxyl-terminal hydrolase	7.572229862
325	IPI00797590.4	NOP2 protein	7.556642294
326	IPI00878316.2	intraflagellar transport protein 27 homolog isoform 3	7.49800539
327	IPI00237446.7	Isoform 2 of Probable phospholipid-transporting ATPase IG	7.497519016
328	IPI00873472.1	Isoform 1 of Protein transport protein Sec24A	7.455308676

329	IPI00938044.2	3-hydroxyacyl-CoA dehydratase 3-like isoform 1	7.423033476
330	IPI00011522.3	cDNA, FLJ79450, highly similar to 3-ketoacyl-CoA thiolase, peroxisomal	7.394384146
331	IPI00853634.3	Isoform 6 of Trinucleotide repeat-containing gene 6A protein	7.388463974
332	IPI00747876.2	Isoform 4 of Protein CASC5	7.37757659
333	IPI01010425.1	angiopoietin-like 4	7.372381449
334	IPI00032137.2	Alpha-actinin-3	7.364738464
335	IPI00983323.1	Parkinson disease 7 domain containing 1	7.361906528
336	IPI00293242.1	Isoform 2 of General transcription factor II-I	7.329498291
337	IPI00385645.1	Isoform 2 of Fibroblast growth factor 17	7.319234848
338	IPI00854642.1	Isoform 1 of Sister chromatid cohesion protein PDS5 homolog A	7.312296152
339	IPI00477489.1	Isoform 1 of Ras-related protein Rab-4B	7.309978485
340	IPI00847558.1	Similar to Non-POU domain-containing octamer-binding protein	7.268417597
341	IPI00218465.10	Phospholipase A-2-activating protein	7.261775017
342	IPI00926241.1	Isoform 2 of TBC1 domain family member 4	7.246945143
343	IPI00917410.1	protein kinase, interferon-inducible double stranded RNA dependent activator	7.241206408
344	IPI00883900.2	cDNA FLJ61360, highly similar to Crumbs homolog 1	7.2365973
345	IPI01009317.1	cDNA FLJ50426, highly similar to Ubiquitin carboxyl-terminal hydrolase 7	7.222208738
346	IPI00168262.2	Procollagen galactosyltransferase 1	7.221436024
347	IPI00295502.6	Isoform 1 of Protein Wiz	7.207459211
348	IPI00555893.3	Isoform 3 of Vacuolar protein sorting-associated protein 54	7.203310013
349	IPI01015580.1	adaptor-related protein complex 2, beta 1 subunit	7.122530222
350	IPI00876931.1	Integrator complex subunit 1	7.115786314
351	IPI00103560.1	Isoform 1 of Dual specificity protein phosphatase CDC14B	7.115598679
352	IPI00910144.2	chromosome 22 open reading frame 28	7.101982832
353	IPI00908746.1	cDNA FLJ51535, highly similar to Phosphatidylethanolamine-binding protein 1	7.098308086
354	IPI00013949.1	Small glutamine-rich tetratricopeptide repeat-containing protein alpha	7.046792269
355	IPI01011241.1	eukaryotic translation initiation factor 3, subunit H	7.026051283
356	IPI00945735.1	RAB7A, member RAS oncogene family	7.024266958
357	IPI00984284.1	heterogeneous nuclear ribonucleoprotein H1 (H)	7.018344879
358	IPI00977201.1	FERM domain containing 8	6.955527067
359	IPI00301434.4	BolA-like protein 2	6.94065237
360	IPI00514321.1	Chromosome 20 open reading frame 72	6.917865992
361	IPI00867688.2	Similar to DEAH (Asp-Glu-Ala-His) box polypeptide 40	6.862523794
362	IPI00642443.3	General transcription factor IIIC, polypeptide 5, 63kDa	6.845027924
363	IPI01010581.1	cDNA FLJ51337, highly similar to Signal transducer and activator of transcription 4	6.833633184
364	IPI00644425.1	Ras homolog gene family, member C	6.826744556
365	IPI00747534.3	Pyrroline-5-carboxylate reductase	6.82123065
366	IPI00894206.2	tetratricopeptide repeat protein 27 isoform 2	6.798231125
367	IPI01014476.1	Aspartate aminotransferase	6.768373966
368	IPI00167806.3	Isoform 2 of RNA-binding protein Musashi homolog 2	6.729918718
369	IPI00894059.1	exportin 1 (CRM1 homolog, yeast)	6.72880125
370	IPI00444454.3	Isoform 2 of Putative helicase MOV-10	6.72008872
371	IPI00984387.1	cDNA FLJ53166, highly similar to Dihydropyrimidinase-related protein 2	6.719806194
372	IPI00607548.4	Isoform 5 of InaD-like protein	6.709991217
373	IPI00940377.1	glutathione S-transferase mu 2 (muscle)	6.697089434
374	IPI00642422.2	Isoform 2 of Probable histone-lysine N-methyltransferase ASH1L	6.681286812
375	IPI00977554.1	endoribonuclease Dicer isoform 2	6.647475004

376	IPI00903191.1	Eukaryotic translation initiation factor 3, subunit D	6.604324341
377	IPI00964248.1	transmembrane protein 165	6.596060276
378	IPI01010257.1	Similar to YLP motif containing 1	6.589266539
379	IPI00967340.1	LPS-responsive vesicle trafficking, beach and anchor containing	6.580407143
380	IPI00930380.1	Serine/threonine-protein phosphatase	6.571713686
381	IPI00937974.2	Delta-aminolevulinic acid dehydratase	6.566494703
382	IPI00007358.1	Zinc finger HIT domain-containing protein 1	6.555282831
383	IPI00217143.3	succinate dehydrogenase complex, subunit A, flavoprotein (Fp)	6.536279202
384	IPI00791794.1	Isoform 6 of Protein diaphanous homolog 3	6.527878284
385	IPI00909721.1	cDNA FLJ51562, highly similar to Prohibitin	6.50565052
386	IPI00556601.1	Solute carrier family 25 member 4 variant (Fragment)	6.498196125
387	IPI00387088.1	Isoform 4 of FAD synthase	6.477309942
388	IPI00978171.1	proteasome (prosome, macropain) 26S subunit, ATPase, 3	6.422775984
389	IPI00549343.3	Vesicle-associated membrane protein 3	6.397579193
390	IPI00947130.1	coiled-coil domain containing 14	6.365230799
391	IPI00787306.1	regulator of chromosome condensation isoform b	6.311150789
392	IPI00639828.1	Four and a half LIM domains 1	6.293713331
393	IPI00024129.1	Peptidyl-prolyl cis-trans isomerase C	6.268741608
394	IPI00984541.1	ectonucleotide pyrophosphatase/phosphodiesterase family member 7-like	6.262800455
395	IPI00658186.1	cDNA FLJ59463, highly similar to Geranylgeranyl pyrophosphate synthetase	6.249212265
396	IPI00789033.2	5'-nucleotidase, cytosolic III-like	6.247641563
397	IPI00412742.1	Isoform 2 of Calcium-binding mitochondrial carrier protein SCaMC-1	6.234661579
398	IPI00029744.1	Single-stranded DNA-binding protein, mitochondrial	6.233521223
399	IPI00556429.3	cDNA FLJ51423, highly similar to Serine/threonine-protein kinase PLK1	6.232278109
400	IPI00645206.2	Isoform 1 of Protocadherin-17	6.215114594
401	IPI00966157.1	SAR1 homolog B (S. cerevisiae)	6.206763029
402	IPI00176637.5	Eukaryotic translation initiation factor 2 subunit 2-like protein	6.189522028
403	IPI00788837.2	cDNA FLJ54752, highly similar to Poly(rC)-binding protein 2	6.184121609
404	IPI00641815.1	Isoform 2 of TIP41-like protein	6.180614471
405	IPI00297121.6	replication termination factor 2 domain containing 1	6.179140091
406	IPI01015730.1	DNA-directed RNA polymerase	6.136565924
407	IPI01013345.1	testis expressed 10	6.110919952
408	IPI00873716.1	Lamina-associated polypeptide 2, isoforms beta/gamma variant (Fragment)	6.102148771
409	IPI00657768.1	phosphoribosylglycinamide formyltransferase, phosphoribosylglycinamide synthe	6.102040291
410	IPI00027180.1	CAAX prenyl protease 1 homolog	6.094688416
411	IPI00916797.1	non-SMC condensin II complex, subunit G2	6.076131105
412	IPI00927458.1	ribosomal protein L32	6.071841955
413	IPI01011969.1	cDNA FLJ58372, highly similar to Nuclear pore complex protein Nup88	6.059197664
414	IPI00743576.1	Isoform 2 of V-type proton ATPase 116 kDa subunit a isoform 1	6.02908659
415	IPI00004506.3	BTB/POZ domain-containing protein KCTD5	5.988526583
416	IPI00741107.3	Isoform 3 of Melanoma inhibitory activity protein 3	5.979962349
417	IPI00642510.3	testis-expressed sequence 10 protein isoform 2	5.925148249
418	IPI00892532.1	glypican 1	5.92497921
419	IPI00647751.2	Isoform 2 of Calmodulin-regulated spectrin-associated protein 1	5.924484491
420	IPI00909684.1	cDNA FLJ57602, highly similar to Creatine kinase M-type	5.888777733
421	IPI00410091.3	chromosome 11 open reading frame 73	5.875143051
422	IPI00789008.1	Flotillin-2	5.873680592

423	IPI01013230.1	cDNA FLJ51319, highly similar to tRNA (adenine-N(1)-)-methyltransferase non-catal	5.834569693
424	IPI00964795.1	cDNA FLJ58215, highly similar to Homo sapiens leucine zipper transcription factor-	5.817508936
425	IPI00740909.1	Isoform 3 of Alstrom syndrome protein 1	5.813872099
426	IPI00056496.1	Ras-related protein Rab-24	5.811949492
427	IPI00790673.2	Isoform 3 of Cytoplasmic FMR1-interacting protein 1	5.76056695
428	IPI00007731.1	Isoform 1 of BAG family molecular chaperone regulator 5	5.752711296
429	IPI00045939.4	2-aminoethanethiol dioxygenase	5.743136883
430	IPI01011531.2	cDNA FLJ54191, highly similar to Annexin A7	5.737822056
431	IPI00909122.1	poly(A)-specific ribonuclease PARN isoform 2	5.656954288
432	IPI01010584.1	KIAA0586	5.6519382
433	IPI00645341.1	BCL6 corepressor	5.629693508
434	IPI00022430.1	Glyceraldehyde-3-phosphate dehydrogenase, testis-specific	5.616788387
435	IPI00011077.4	39S ribosomal protein L32, mitochondrial precursor	5.58299017
436	IPI00000156.3	Isoform Beta of DNA ligase 3	5.463475227
437	IPI00965501.2	cDNA FLJ54242, highly similar to Calnexin	5.423078299
438	IPI00654820.2	ATP synthase subunit a	5.402955532
439	IPI00929107.1	Seipin isoform 1	5.297815084
440	IPI00186139.8	Similar to Protein KRI1 homolog	5.294789791
441	IPI01010750.1	DNA ligase (Fragment)	5.294677258
442	IPI00872952.1	Ubiquinol-cytochrome c reductase hinge protein, isoform CRA_c	5.278233051
443	IPI00640947.2	Isoform 2 of tRNA-dihydrouridine synthase 3-like	5.276941299
444	IPI00514530.5	actin, alpha 1, skeletal muscle	5.267291546
445	IPI00550234.4	Isoform 1 of Actin-related protein 2/3 complex subunit 5	5.248762608
446	IPI00738216.3	KIAA0947	5.246402979
447	IPI00926196.2	cDNA FLJ56396, highly similar to Huntingtin-interacting protein 1	5.238226891
448	IPI00893074.1	Family with sequence similarity 118, member A	5.206407547
449	IPI00413144.6	Isoform 2 of Treslin	5.174490452
450	IPI00852843.1	Isoform 2 of N-alpha-acetyltransferase 25, NatB auxiliary subunit	5.157077789
451	IPI00477093.3	Isoform 3 of Integrator complex subunit 3	5.132245064
452	IPI00927271.1	transformer 2 beta homolog (Drosophila)	5.12930584
453	IPI00878795.1	RAN binding protein 1	5.125430346
454	IPI00980781.1	N-acetyltransferase 10 (GCN5-related)	5.037157536
455	IPI00982254.1	cDNA FLJ60573, highly similar to TNF receptor-associated factor 5	4.956015348
456	IPI01010224.1	zinc finger protein 844	4.917386532
457	IPI00647044.1	Microsomal glutathione S-transferase 3	4.916156292
458	IPI00953689.1	Alpha-2-HS-glycoprotein	4.895540237
459	IPI00019046.4	Isoform 1 of Pre-mRNA-splicing factor RBM22	4.87909627
460	IPI00982734.1	Conserved hypothetical protein	4.849043846
461	IPI00980903.1	phosphatidylinositol 4-kinase, catalytic, beta	4.841104031
462	IPI00172648.1	Isoform 5 of Ribosome-releasing factor 2, mitochondrial	4.790606499
463	IPI00456965.5	Isoform 1 of 2-methoxy-6-polyprenyl-1,4-benzoquinol methylase, mitochondrial	4.789173126
464	IPI00167818.3	SPANXA2 overlapping transcript 1 (non-protein coding)	4.770785332
465	IPI00792538.1	APEX nuclease (multifunctional DNA repair enzyme) 1	4.667920589
466	IPI00394874.3	Isoform 2 of Ectonucleoside triphosphate diphosphohydrolase 8	4.656054974
467	IPI00446850.1	chromosome 1 open reading frame 186	4.620590687
468	IPI00031047.2	IQ motif containing G	4.586830616
469	IPI00915457.1	Isoform 1 of POTE ankyrin domain family member C	4.578995228

470	IPI00922577.1	cDNA FLJ53768, highly similar to Hepatocyte growth factor-like protein	4.565380573
471	IPI00967531.1	peroxisomal biogenesis factor 10	4.541862965
472	IPI00791071.2	Isoform 2 of Protein PIEZO2	4.518009663
473	IPI00885017.1	cDNA, FLJ79527, moderately similar to Uroporphyrinogen decarboxylase	4.502159119
474	IPI00977526.1	family with sequence similarity 126, member B	4.491538048
475	IPI00941345.1	tenascin XB	4.478475571
476	IPI00385955.1	Brain my037 protein	4.467207432
477	IPI00878764.1	l(3)mbt-like 2 (Drosophila)	4.463213921
478	IPI00879449.1	sperm antigen with calponin homology and coiled-coil domains 1-like	4.461359024
479	IPI00470766.14	Isoform 1 of Olfactomedin-like protein 2B	4.452666759
480	IPI00945820.1	Uncharacterized protein	4.451300144
481	IPI00219478.3	Isoform 2 of Phosphoserine aminotransferase	4.419585705
482	IPI00985082.1	Receptor type protein tyrosine phosphatase gamma (Fragment)	4.407513142
483	IPI00220381.2	Isoform 2 of Transcription factor 20	4.401259422
484	IPI01012170.1	atlastin GTPase 3	4.385352135
485	IPI00293288.2	Isoform 1 of Glutamate receptor, ionotropic kainate 5	4.378353119
486	IPI00790281.2	cDNA FLJ51777, highly similar to Squamous cell carcinoma antigen recognized byT-	4.369580746
487	IPI01011431.1	cDNA FLJ60167, highly similar to Cytosolic acyl coenzyme A thioester hydrolase	4.365740776
488	IPI00909251.1	cDNA FLJ51165, highly similar to DNA damage-binding protein 1	4.331735611
489	IPI00008527.3	60S acidic ribosomal protein P1	4.300535679
490	IPI00171540.2	Chromosome transmission fidelity protein 8 homolog isoform 2	4.280999184
491	IPI00015580.3	Isoform 3 of Formin-binding protein 1-like	4.280753613
492	IPI00939219.1	Equilibrative nucleoside transporter 1	4.262634277
493	IPI00945125.1	superkiller viralicidic activity 2-like (S. cerevisiae)	4.259326458
494	IPI00978544.1	ATPase, H+ transporting, lysosomal 50/57kDa, V1 subunit H	4.258832932
495	IPI00292787.6	Actin-related protein 5	4.229960442
496	IPI00873684.1	Isoform 2 of Collagen alpha-1(IV) chain	4.200462341
497	IPI01010893.1	late endosomal/lysosomal adaptor, MAPK and MTOR activator 1	4.200406551
498	IPI00980323.2	cDNA FLJ51919, highly similar to Homo sapiens abhydrolase domain containing 8 (	4.197277546
499	IPI00171856.1	Deoxyhypusine hydroxylase	4.190542221
500	IPI00386885.1	cDNA FLJ14414 fis, clone HEMBA1004847, highly similar to SIGNAL RECOGNITION PAR	4.186115265
501	IPI00017533.2	Cytochrome c oxidase subunit 3	4.178531647
502	IPI01014582.1	lactate dehydrogenase A	4.168670654
503	IPI00745311.2	Killer cell immunoglobulin-like receptor 3DS1	4.165480137
504	IPI00945805.1	ribonuclease P/MRP 40kDa subunit	4.165179729
505	IPI00397498.1	Isoform 2 of Carbamoyl-phosphate synthase [ammonia], mitochondrial	4.142326355
506	IPI00006934.1	Hydroxyacid oxidase 1	4.140348434
507	IPI01009009.1	RBM14-RBM4 protein isoform 2	4.1335392
508	IPI00440719.2	N(alpha)-acetyltransferase 10, NatA catalytic subunit	4.089213848
509	IPI00976088.1	ribonucleotide reductase M1	4.08574295
510	IPI00411545.3	Isoform 3 of Thrombopoietin	4.053452492
511	IPI00477605.6	Isoform 1 of Acyl-coenzyme A synthetase ACSM5, mitochondrial	4.029726028
512	IPI00172656.6	FAS-associated factor 2	4.014418125
513	IPI00471914.6	Isoform 2 of FYVE, RhoGEF and PH domain-containing protein 6	3.978642225
514	IPI01010503.1	stress-induced-phosphoprotein 1	3.972180367
515	IPI00909754.1	cDNA FLJ61500, highly similar to NNP-1 protein	3.964648247
516	IPI00967973.1	Calnexin	3.95118475

517	IPI00549761.3	Chitobiosyldiphosphodolichol beta-mannosyltransferase	3.946815252
518	IPI00853224.1	StAR-related lipid transfer protein 7, mitochondrial	3.938904047
519	IPI00656111.1	Isoform E of Proteoglycan 4	3.934770823
520	IPI00167841.2	Isoform 2 of Activating transcription factor 7-interacting protein 2	3.929155827
521	IPI00924758.1	cDNA FLJ32188 fis, clone PLACE6002056, highly similar to Guanine nucleotide-bindi	3.922733784
522	IPI00016074.2	M-phase phosphoprotein 6	3.912299156
523	IPI00916247.2	exonuclease 3'-5' domain containing 2	3.891948462
524	IPI00914539.1	Isoform 2 of Ankyrin repeat and FYVE domain-containing protein 1	3.890255928
525	IPI00219090.1	Isoform 2 of Protein arginine N-methyltransferase 7	3.8867414
526	IPI00911085.1	cDNA FLJ53754, highly similar to Transmembrane emp24 domain-containing protei	3.886036158
527	IPI00893200.1	19 kDa protein	3.873499632
528	IPI00968217.1	NOP14 nucleolar protein	3.843609095
529	IPI00903259.2	cDNA FLJ54005, highly similar to Transcription elongation factor SPT5	3.842230082
530	IPI00981682.1	proline synthetase co-transcribed homolog (bacterial)	3.840254068
531	IPI00011201.1	NAD-dependent malic enzyme, mitochondrial	3.814752579
532	IPI00947372.2	structural maintenance of chromosomes 4	3.812386274
533	IPI00879643.1	mitochondrial fission process 1	3.807324171
534	IPI00980448.1	NADH dehydrogenase (ubiquinone) 1 beta subcomplex, 4, 15kDa	3.787592173
535	IPI00916763.1	heat shock 10kDa protein 1 (chaperonin 10)	3.747044325
536	IPI00745182.1	phospholipase C, gamma 1	3.731425047
537	IPI00185398.4	methionyl-tRNA synthetase	3.730978489
538	IPI01012564.1	cDNA FLJ52405, highly similar to Myosin Ic	3.730549574
539	IPI00966206.1	programmed cell death 6	3.729136467
540	IPI00031424.1	Isoform 2 of Phosphatidylinositol 4-kinase alpha	3.728237629
541	IPI00607610.1	Isoform 1 of Protein FAM36A	3.727309227
542	IPI00642862.1	Peptidyl-prolyl cis-trans isomerase-like 4	3.714351177
543	IPI01014635.1	solute carrier family 3 (activators of dibasic and neutral amino acid transport), me	3.713633299
544	IPI00007814.3	V-type proton ATPase subunit C 1	3.700995922
545	IPI00555788.2	Isoform 3 of Glycerophosphodiester phosphodiesterase domain-containing protei	3.698200703
546	IPI01015537.1	general transcription factor IIH, polypeptide 3, 34kDa	3.69206953
547	IPI00472003.1	Isoform 4 of BH3-interacting domain death agonist	3.677544594
548	IPI00981108.1	cDNA FLJ35898 fis, clone TESTI2009520, highly similar to Rattus norvegicus endopla	3.676934004
549	IPI00941876.2	Isoform 5 of PARP1-binding protein	3.670991421
550	IPI00329025.1	Protein jagunal homolog 1	3.655322552
551	IPI00964370.1	cDNA FLJ60877, highly similar to Zinc finger protein 346	3.633505821
552	IPI00980509.1	nucleosome assembly protein 1-like 4	3.629339695
553	IPI00977571.1	hypothetical protein LOC100508996	3.625877142
554	IPI00910915.1	cDNA FLJ54756, moderately similar to Homo sapiens nitric oxide synthase interacti	3.624631166
555	IPI00001141.4	Mitochondrial import inner membrane translocase subunit Tim22	3.610780239
556	IPI00005045.1	ATP-binding cassette sub-family F member 2	3.604427099
557	IPI00418277.3	Chondroitin sulfate synthase 3	3.575285912
558	IPI00645653.1	translocase of inner mitochondrial membrane 23 homolog B (yeast)	3.567307472
559	IPI00740019.3	Isoform 1 of Protein Daple	3.561594009
560	IPI00791914.2	BM-010 variant (Fragment)	3.551699877
561	IPI00975639.1	dynamin 3	3.546967268
562	IPI00291417.2	Isoform 1 of Dephospho-CoA kinase domain-containing protein	3.539319515
563	IPI00027705.2	Isoform 1 of DNA primase large subunit	3.534766436

564	IPI00382858.2	Isoform B of Trimethyllysine dioxygenase, mitochondrial	3.529125452
565	IPI00386667.2	Isoform 2 of Carboxypeptidase A6	3.528172255
566	IPI00844404.2	Isoform 2 of TRMT1-like protein	3.524603367
567	IPI00059242.3	Synapse-associated protein 1	3.520887136
568	IPI00145593.7	Nucleolar MIF4G domain-containing protein 1	3.505145788
569	IPI00010120.4	Isoform 1 of C-terminal-binding protein 2	3.504005671
570	IPI01012217.1	Full-length cDNA clone CS0DI035YL21 of Placenta of Homo sapiens	3.502397299
571	IPI00908319.1	cDNA FLJ51570, highly similar to Thioredoxin domain-containing protein 1	3.500628233
572	IPI00910984.1	cDNA FLJ57468	3.495084524
573	IPI00843886.1	apolipoprotein O	3.490085602
574	IPI00976697.1	family with sequence similarity 76, member A	3.488691807
575	IPI01012747.1	aldehyde dehydrogenase 5 family, member A1	3.485749245
576	IPI00942336.1	listerin E3 ubiquitin protein ligase 1	3.485023975
577	IPI00916551.1	malate dehydrogenase 1, NAD (soluble)	3.479502916
578	IPI00604702.1	Isoform 2 of Phosphopantothenoylcysteine decarboxylase	3.47889924
579	IPI00924999.1	IMP (inosine 5'-monophosphate) dehydrogenase 2	3.474856853
580	IPI00888266.3	n-acetylserotonin O-methyltransferase-like protein-like	3.474449635
581	IPI00829629.1	Isoform 3 of Proteasome activator complex subunit 4	3.460556269
582	IPI00297455.6	A-kinase anchor protein 8-like	3.456336975
583	IPI00982043.1	KIAA1967	3.451563597
584	IPI01010009.1	diablo, IAP-binding mitochondrial protein	3.451171875
585	IPI00964195.1	coproporphyrinogen oxidase	3.444897652
586	IPI00981208.1	cysteine and histidine-rich domain (CHORD) containing 1	3.443861723
587	IPI00965708.1	pleiotropic regulator 1	3.441361666
588	IPI00909062.2	CoA synthase	3.432289839
589	IPI00975884.1	solute carrier family 39 (zinc transporter), member 14	3.430989265
590	IPI00032995.1	LanC-like protein 2	3.424777269
591	IPI00257933.8	Protein BEX5	3.423010588
592	IPI00025344.1	NADH dehydrogenase [ubiquinone] iron-sulfur protein 6, mitochondrial	3.41641736
593	IPI00384224.4	Similar to dual specificity phosphatase 9	3.416248798
594	IPI00888802.1	coiled-coil domain containing 74A	3.416227818
595	IPI00985284.1	La ribonucleoprotein domain family, member 1	3.413938761
596	IPI00298353.4	Guanylate-binding protein 7	3.412475348
597	IPI00966636.1	matrin 3	3.411032677
598	IPI00419792.3	Similar to Dual specificity mitogen-activated protein kinase kinase 2	3.410777092
599	IPI00640296.1	Heterogeneous nuclear ribonucleoprotein K	3.410216331
600	IPI00954996.1	chromosome X open reading frame 56	3.409793377
601	IPI01014588.1	cDNA FLJ58155, highly similar to Cohesin subunit SA-2	3.409322023
602	IPI00647752.2	cDNA FLJ61735, highly similar to Zinc finger A20 domain-containing protein 1	3.407420635
603	IPI00217386.1	Isoform 2 of DNA-directed RNA polymerases I and III subunit RPAC1	3.404648304
604	IPI00007049.1	28S ribosomal protein S18c, mitochondrial	3.401761532
605	IPI01013137.1	cDNA FLJ58497, highly similar to Unc-13 homolog C	3.401104927
606	IPI01013452.1	proteasome (prosome, macropain) 26S subunit, non-ATPase, 9	3.400309563
607	IPI01014223.1	cDNA FLJ50851, highly similar to Tyrosine-protein phosphatase non-receptor type1	3.39807415
608	IPI01015742.1	serine/threonine kinase 38 like	3.397047043
609	IPI00878166.1	Isoform 2 of NHL repeat-containing protein 2	3.393936634
610	IPI00879999.1	Isoform 1 of ATP-dependent RNA helicase DDX54	3.385189056

611	IPI01009407.1	cDNA FLJ45137 fis, clone BRAWH3038827, highly similar to Homo sapiens leucine-zi	3.38276577
612	IPI00009771.6	Lamin-B2	3.380929232
613	IPI00306661.3	E3 ubiquitin-protein ligase KCMF1	3.376299381
614	IPI00909658.1	cDNA FLJ52759, highly similar to Plastin-2	3.375437975
615	IPI00902957.1	cDNA FLJ90012 fis, clone HEMBA1000462, highly similar to CCR4-NOT transcription co	3.371630907
616	IPI00867515.1	unc-51-like kinase 4 (C. elegans)	3.366783857
617	IPI00945024.1	staphylococcal nuclease and tudor domain containing 1	3.366449118
618	IPI00654793.2	NAD kinase domain containing 1	3.358320475
619	IPI00007979.4	NADH-ubiquinone oxidoreductase chain 2	3.349155188
620	IPI00916446.1	distal-less homeobox 1	3.343543053
621	IPI00375701.2	Isoform 2 of VIP peptides	3.336665392
622	IPI00395507.4	Isoform 2 of ELAV-like protein 4	3.335440874
623	IPI00943071.2	cDNA FLJ57184, highly similar to Bromodomain and WD repeat domain-containing	3.335140228
624	IPI01015469.1	2-oxoglutarate and iron-dependent oxygenase domain containing 1	3.333026171
625	IPI00645320.1	Isoform 3 of Beta-catenin-like protein 1	3.329285145
626	IPI00925850.2	cDNA FLJ54572, highly similar to Lysosomal alpha-mannosidase	3.327897787
627	IPI00902543.3	NOP2/Sun domain family, member 5	3.326188326
628	IPI00853433.1	ATPase, H+ transporting, lysosomal 31kDa, V1 subunit E1	3.324478149
629	IPI00215687.1	Isoform 3 of Glutaminase kidney isoform, mitochondrial	3.323078871
630	IPI00032406.1	DnaJ homolog subfamily A member 2	3.321737766
631	IPI00328938.4	Isoform 1 of E3 ubiquitin-protein ligase RNF138	3.315677643
632	IPI00307325.2	Zinc finger protein 161 homolog	3.315529585
633	IPI00000105.4	Major vault protein	3.314646006
634	IPI00856004.1	ras-related protein R-Ras2 isoform b	3.313657522
635	IPI00797490.2	cDNA FLJ53588, highly similar to Translocation-associated membrane protein 1	3.311407328
636	IPI00887254.2	Putative ferritin heavy polypeptide-like 19	3.30765748
637	IPI00930396.1	cDNA FLJ35812 fis, clone TESTI2006051, highly similar to Acyl-coenzyme A thioestera	3.304494143
638	IPI01018260.1	cDNA FLJ11747 fis, clone HEMBA1005530, highly similar to Anaphase-promoting com	3.300151587
639	IPI00376394.4	Sulfhydryl oxidase 2	3.298935175
640	IPI00019976.2	Coiled-coil domain-containing protein 85B	3.298585892
641	IPI00788816.1	Similar to Submaxillary gland androgen-regulated protein 3 homolog B precursor	3.295587301
642	IPI00915874.1	partner of NOB1 homolog (S. cerevisiae)	3.287039042
643	IPI00926620.1	cytochrome P450, family 51, subfamily A, polypeptide 1	3.286698818
644	IPI00646692.2	RAB31, member RAS oncogene family	3.285127401
645	IPI00640585.2	transmembrane protein 161A	3.283124447
646	IPI00909562.1	cDNA FLJ52462, moderately similar to Mus musculus proteasome (prosome, macro	3.279426575
647	IPI00402109.4	Isoform 2 of Phosphatidylinositol glycan anchor biosynthesis class U protein	3.278314352
648	IPI00795109.1	cDNA, FLJ79092, highly similar to GTP-binding nuclear protein Ran	3.278274775
649	IPI00470629.4	Isoform 1 of Calmodulin-lysine N-methyltransferase	3.274087906
650	IPI00152196.3	N-acylneuraminate-9-phosphatase	3.271921158
651	IPI00065521.5	Putative tRNA pseudouridine synthase Pus10	3.271898031
652	IPI00964345.1	casein alpha s1	3.271681547
653	IPI00927704.1	transmembrane protein 237	3.267240047
654	IPI00916096.1	Conserved hypothetical protein	3.264837265
655	IPI00922126.1	cDNA FLJ57759, moderately similar to Transgelin-2	3.261574507
656	IPI00847400.1	chromosome 19 open reading frame 47	3.252752066
657	IPI00855846.1	ABRA C-terminal like	3.250239372

658	IPI00759537.1	Isoform 2 of Mitochondrial Rho GTPase 2	3.247343302
659	IPI00909746.1	cDNA FLJ51502, highly similar to 60S ribosomal protein L18a	3.246116638
660	IPI01009730.1	Putative uncharacterized protein DKFZp547A1913	3.245847225
661	IPI00641449.2	Isoform 2 of Enhancer of mRNA-decapping protein 4	3.244997263
662	IPI00927183.1	Williams Beuren syndrome chromosome region 22	3.241432905
663	IPI01015062.1	cDNA FLJ45314 fis, clone BRHIP3005142, highly similar to Proteasome-associated pr	3.237799644
664	IPI00215905.1	Isoform IIC4 of Low affinity immunoglobulin gamma Fc region receptor II-c	3.235785246
665	IPI00031115.5	Golgin subfamily A member 1	3.234233856
666	IPI00965557.1	methyltransferase like 14	3.230890036
667	IPI00854630.2	proline rich 12	3.229253292
668	IPI00643530.1	cytochrome b5 reductase 1	3.228613853
669	IPI00792017.1	schlafen family member 12	3.222703695
670	IPI00217430.1	Isoform 2 of NLR family CARD domain-containing protein 4	3.215734959
671	IPI00478620.2	tripartite motif-containing protein 48	3.211925507
672	IPI00795573.1	NECAP endocytosis associated 1	3.210455894
673	IPI00514986.1	5'-nucleotidase domain containing 1	3.204140425
674	IPI01015523.1	coiled-coil serine-rich protein 2	3.202517986
675	IPI00556297.1	Arginine/serine-rich splicing factor 6 variant (Fragment)	3.202192783
676	IPI00917916.1	DIS3 mitotic control homolog (S. cerevisiae)-like 2	3.201835394
677	IPI00301163.1	Protein O-glucosyltransferase 1	3.19927907
678	IPI00173901.1	Isoform 2 of Histone-lysine N-methyltransferase, H3 lysine-36 and H4 lysine-20 spe	3.195893049
679	IPI01010263.1	ubiquitin protein ligase E3 component n-recognin 7 (putative)	3.194836617
680	IPI00984362.1	tissue specific transplantation antigen P35B	3.194470167
681	IPI00807384.2	cleavage and polyadenylation specific factor 3, 73kDa	3.189180136
682	IPI00976712.1	zinc finger, CCHC domain containing 11	3.18565011
683	IPI00100245.1	DNA-directed RNA polymerase III subunit RPC6	3.185195923
684	IPI00639912.2	nuclear autoantigenic sperm protein (histone-binding)	3.1851542
685	IPI00644568.1	budding uninhibited by benzimidazoles 3 homolog (yeast)	3.181827784
686	IPI00983570.1	HLA class I histocompatibility antigen, A-69 alpha chain-like isoform 17	3.178947449
687	IPI00220542.1	Isoform 2 of Serine protease HTRA2, mitochondrial	3.178910494
688	IPI00927837.1	zinc finger CCCH-type containing 15	3.177031517
689	IPI00552426.2	serine/threonine kinase 24	3.176285744
690	IPI01013073.1	mutS homolog 6 (E. coli)	3.175209284
691	IPI00160506.1	ADAM metallopeptidase with thrombospondin type 1 motif, 13	3.172572374
692	IPI00184433.2	Supported by Human ESTs AA017424.1 (NID:g1479799), H85906.1	3.16696763
693	IPI00642657.1	Isoform 3 of Choline transporter-like protein 1	3.166265965
694	IPI01010643.1	cDNA FLJ38844 fis, clone MESAN2003662, highly similar to Cullin-1	3.162334442
695	IPI00013296.3	40S ribosomal protein S18	3.146720648
696	IPI00916394.2	RAD54-like 2 (S. cerevisiae)	3.143470049
697	IPI00043262.1	SATB2 antisense RNA 1	3.139975071
698	IPI01014549.1	heme binding protein 1	3.139760256
699	IPI00514271.1	Phosphodiesterase 4B, cAMP-specific	3.136208773
700	IPI00178714.2	Isoform 2 of Serine/threonine-protein kinase PAK 4	3.135077715
701	IPI00939864.2	cDNA FLJ31273 fis, clone KIDNE2006299, weakly similar to BOB1 PROTEIN	3.133990526
702	IPI00976489.1	ribosomal protein S2	3.132829905
703	IPI00644349.4	cDNA FLJ60449, highly similar to Homo sapiens prion protein interacting protein (P	3.130381584
704	IPI00910594.2	DDB1 and CUL4 associated factor 7	3.127041578

705	IPI00759768.1	Isoform 2 of Elongation factor Tu GTP-binding domain-containing protein 1	3.126696348
706	IPI00556344.2	Isoform 2 of Lysophosphatidic acid phosphatase type 6	3.12577486
707	IPI00061282.2	Protein kinase, AMP-activated, alpha 1 catalytic subunit, isoform CRA_b	3.125466108
708	IPI00847729.2	thyroid hormone receptor interactor 13	3.121195316
709	IPI00795983.1	Coiled-coil alpha-helical rod protein 1	3.11758256
710	IPI00291525.1	Dimethyladenosine transferase 1, mitochondrial	3.115568638
711	IPI00413611.1	DNA topoisomerase 1	3.113761425
712	IPI00217005.7	Ankyrin repeat domain-containing protein 18A	3.111149788
713	IPI00909015.2	cDNA FLJ58500, highly similar to Cytoplasmic dynein 1 light intermediate chain 1	3.10572052
714	IPI00302309.6	tetratricopeptide repeat domain 17	3.10140872
715	IPI00947454.1	plastin 3	3.097033262
716	IPI00922127.1	cDNA FLJ54708, highly similar to 150 kDa oxygen-regulated protein	3.096722126
717	IPI00658002.1	Isoform 3 of Tyrosine-protein phosphatase non-receptor type 11	3.094691753
718	IPI00976000.1	integrator complex subunit 9	3.094225883
719	IPI00965867.1	importin 11	3.087956667
720	IPI01018192.1	cDNA FLJ30950 fis, clone HCASM1000061	3.086732626
721	IPI00450783.1	Isoform 2 of ER lumen protein retaining receptor 2	3.081044197
722	IPI00295394.2	Cytochrome c oxidase assembly protein COX11, mitochondrial	3.077878475
723	IPI00922333.1	cDNA FLJ50250, highly similar to Structural maintenance of chromosome 1-like 1 pr	3.076677799
724	IPI00333634.4	chromosome 20 open reading frame 194	3.076010942
725	IPI00921944.1	cDNA FLJ54863, highly similar to CTP synthase 1	3.073092699
726	IPI00945851.1	ribophorin I	3.064904928
727	IPI00910541.2	cDNA FLJ58838, highly similar to Homo sapiens radical S-adenosyl methionine and	3.061270952
728	IPI00218266.1	Isoform Long of Vasoactive intestinal polypeptide receptor 1	3.060194254
729	IPI00943678.1	anaphase-promoting complex subunit 1-like	3.059614897
730	IPI00795180.3	cDNA FLJ59673, highly similar to Homo sapiens growth and transformation-depend	3.055035353
731	IPI00329321.3	LYR motif-containing protein 7	3.053508282
732	IPI01013650.1	G protein-coupled receptor 126	3.051602125
733	IPI00977213.1	succinate dehydrogenase complex, subunit D, integral membrane protein	3.050844431
734	IPI00964658.1	septin 11	3.049089909
735	IPI00553172.1	caspase 3, apoptosis-related cysteine peptidase	3.046720266
736	IPI00414005.2	Isoform Short of Sodium/potassium-transporting ATPase subunit alpha-1	3.046513557
737	IPI00984321.2	excision repair cross-complementing rodent repair deficiency, complementation g	3.034834385
738	IPI00976594.1	cDNA FLJ55046, highly similar to Methionyl-tRNA synthetase	3.033221245
739	IPI00303335.3	Nebulin	3.027050972
740	IPI00910598.1	Isoform 2 of Nucleoside diphosphate kinase 6	3.023873806
741	IPI00045456.1	chromosome 10 open reading frame 113	3.021387339
742	IPI00983309.1	STT3, subunit of the oligosaccharyltransferase complex, homolog A (S. cerevisiae)	3.021257162
743	IPI00217240.1	WD repeat-containing protein 75	3.019135952
744	IPI00297626.4	Syntaxin-binding protein 3	3.017946482
745	IPI00217541.3	ATP-dependent RNA helicase DDX51	3.017280817
746	IPI00917443.2	dedicator of cytokinesis 5	3.015888929
747	IPI00855962.1	Isoform 2 of FK506-binding protein 15	3.014819384
748	IPI00983774.1	protein phosphatase 2, catalytic subunit, beta isozyme	3.01027441
749	IPI00184707.1	Isoform 2 of FERM domain-containing protein 6	3.009544134
750	IPI00002424.1	Pleckstrin homology domain-containing family F member 2	3.005003214
751	IPI00853068.2	Hemoglobin alpha-2	3.003887415

752	IPI00945467.1	phosphatidylinositol-specific phospholipase C, X domain containing 2	2.996738434
753	IPI01012689.1	Isoform E1S of G1/S-specific cyclin-E1	2.995843649
754	IPI00909081.2	protein tyrosine phosphatase type IVA 2 isoform 4	2.990827322
755	IPI00922246.1	cDNA FLJ58698, highly similar to cAMP-dependent protein kinase, alpha-catalytic s	2.987887621
756	IPI00965994.1	glucosamine-6-phosphate deaminase 1	2.97500205
757	IPI01010778.1	cDNA FLJ55806, highly similar to Golgi phosphoprotein 3	2.972642422
758	IPI00398129.6	Similar to 3-hydroxybutyrate dehydrogenase type 2	2.972138405
759	IPI00329369.8	ALS2 C-terminal-like protein isoform 3	2.967597723
760	IPI00963825.1	ATP synthase, H+ transporting, mitochondrial Fo complex, subunit C1 (subunit 9)	2.964182854
761	IPI00386679.1	ZNF607 protein	2.962964296
762	IPI00384478.3	family with sequence similarity 227, member B	2.959823608
763	IPI00386908.3	Isoform 2 of Alpha-parvin	2.959525824
764	IPI00785125.2	Putative uncharacterized protein FLJ00310	2.958783627
765	IPI01015780.1	cDNA FLJ57449, highly similar to Notchless homolog 1	2.957838058
766	IPI00792035.2	Isoform 3 of Glyoxalase domain-containing protein 4	2.955942154
767	IPI00909237.1	cDNA FLJ55703, highly similar to Solute carrier family 2, facilitated glucose transpo	2.955162048
768	IPI00966573.1	enolase-phosphatase 1	2.954790831
769	IPI01010550.1	cDNA FLJ55457, highly similar to ATP-dependent RNA helicase DHX8	2.953880548
770	IPI00830092.1	Isoform 2 of Twisted gastrulation protein homolog 1	2.953283787
771	IPI00952785.3	Ca++-dependent secretion activator 2	2.952512264
772	IPI00024464.1	PRO0843	2.951581955
773	IPI00926887.1	glioblastoma amplified sequence	2.949511766
774	IPI00300631.3	Scaffold attachment factor B1	2.948192596
775	IPI00927766.1	NCK interacting protein with SH3 domain	2.946702719
776	IPI00946316.1	karyopherin alpha 4 (importin alpha 3)	2.943986416
777	IPI00102918.1	Isoform 2 of ATR-interacting protein	2.94173336
778	IPI01009299.1	cDNA FLJ60635, highly similar to Angiotensin-converting enzyme, somatic isoform	2.940118551
779	IPI00795577.3	Isoform 7 of Mucin-4	2.939316511
780	IPI00982125.1	FCF1 protein	2.937950373
781	IPI00888999.1	Isoform 2 of PNMA-like protein 2	2.937551737
782	IPI00945513.1	TRAF3 interacting protein 3	2.932587147
783	IPI00980492.1	Conserved hypothetical protein	2.932492495
784	IPI00916535.1	prolyl 4-hydroxylase subunit alpha-1 isoform 3 precursor	2.931104183
785	IPI01010177.1	cDNA FLJ51879, highly similar to Prenylcysteine oxidase	2.928237677
786	IPI00941117.2	cDNA FLJ50310, highly similar to Zinc finger protein 198	2.926929235
787	IPI00984730.1	Similar to DnaJ (Hsp40) homolog, subfamily B, member 1	2.926818609
788	IPI00940357.2	RNA-directed DNA polymerase (reverse transcriptase) domain containing protein	2.926532984
789	IPI00893883.1	NME/NM23 nucleoside diphosphate kinase 4	2.924023867
790	IPI00917184.1	coiled-coil domain containing 150	2.923926115
791	IPI00879333.1	guanine nucleotide binding protein (G protein), beta polypeptide 1-like	2.922519684
792	IPI00902652.1	cDNA FLJ37148 fis, clone BRACE2025333, highly similar to Homo sapiens Na+/H+ exc	2.919394493
793	IPI01009695.1	Bromodomain adjacent to zinc finger domain, 1A isoform b variant	2.913550615
794	IPI00975761.1	processing of precursor 1, ribonuclease P/MRP subunit (S. cerevisiae)	2.907921314
795	IPI00984399.1	lamin-B1 isoform 2	2.905791283
796	IPI00979313.1	family with sequence similarity 118, member B	2.902616739
797	IPI00640929.1	Ribosomal protein S6	2.901382685
798	IPI00979873.1	ribosomal RNA-processing protein 7 homolog A-like, partial	2.89830637

799	IPI00028937.1	Ornithine decarboxylase antizyme 2	2.892297268
800	IPI00967823.1	ELMO/CED-12 domain containing 2	2.891439676
801	IPI00966960.1	acyl-CoA synthetase family member 2	2.886399746
802	IPI00291457.2	Serine/threonine-protein kinase 35	2.885710239
803	IPI00395967.2	TMEM97 protein	2.880130768
804	IPI00798339.4	Isoform 4 of E1A-binding protein p400	2.879770756
805	IPI00215907.2	serine/arginine-rich splicing factor 7	2.876781464
806	IPI00479058.2	40S ribosomal protein S15	2.875518322
807	IPI00792050.1	ribosomal protein L8	2.873644114
808	IPI00442921.1	CDNA FLJ26213 fis, clone ADG07906	2.872962952
809	IPI00514217.6	Succinate-CoA ligase, ADP-forming, beta subunit	2.869974375
810	IPI00552303.3	annexin A11	2.869552851
811	IPI00910936.1	cDNA FLJ61101, highly similar to Eukaryotic translation initiation factor 5	2.865088701
812	IPI00410547.1	uncharacterized LOC400940	2.860070944
813	IPI00917435.1	Isoform 4 of Thyroid adenoma-associated protein	2.85930419
814	IPI00967837.1	multimerin 1	2.855486393
815	IPI00019400.1	Thiopurine S-methyltransferase	2.852811098
816	IPI01013172.1	cDNA FLJ58642, highly similar to Homo sapiens elongation protein 3 homolog (ELP3	2.850491285
817	IPI00981200.1	SID1 transmembrane family, member 2	2.846666098
818	IPI00514742.3	Uncharacterized protein	2.842525959
819	IPI00514385.2	Isoleucyl-tRNA synthetase	2.841986895
820	IPI00917171.1	integrin-linked kinase-associated serine/threonine phosphatase	2.833169699
821	IPI01012107.1	defender against cell death 1	2.83266139
822	IPI00002225.6	LAG1 longevity assurance homolog 4	2.831745625
823	IPI00747361.3	aladin isoform 2	2.829845905
824	IPI00028083.1	Translation initiation factor eIF-2B subunit beta	2.825948238
825	IPI00385079.1	MSTP151	2.825237274
826	IPI00902967.1	cDNA FLJ44468 fis, clone UTERU2026025, moderately similar to SPLICING FACTOR, AR	2.824178696
827	IPI00072541.4	Isoform 3 of PCI domain-containing protein 2	2.824063301
828	IPI00383562.1	Isoform 4 of Fermitin family homolog 1	2.820923328
829	IPI00099463.2	Sphingosine-1-phosphate lyase 1	2.815997601
830	IPI00942583.1	Uncharacterized protein	2.814167023
831	IPI01009798.1	mitochondrial ribosomal protein S28	2.801440001
832	IPI00291643.4	SPRY domain-containing protein 4	2.797506809
833	IPI01011878.1	cDNA PSEC0228 fis, clone HEMBA1006099, weakly similar to COP-COATED VESICLE ME	2.790140152
834	IPI00329826.4	cDNA FLJ46853 fis, clone UTERU3009775, moderately similar to Rattus norvegicus PA	2.78877306
835	IPI00219484.1	Isoform 3 of U1 small nuclear ribonucleoprotein 70 kDa	2.782621145
836	IPI00908503.1	cDNA FLJ50605, moderately similar to Plastin-3	2.78034997
837	IPI00007234.1	Zinc finger protein 510	2.770253658
838	IPI00643715.1	DnaJ (Hsp40) homolog, subfamily C, member 14	2.766234398
839	IPI00383182.1	PP3895	2.7661376
840	IPI01010916.1	major histocompatibility complex, class II, DQ beta 1	2.765980482
841	IPI00936836.2	myomesin 3	2.750969172
842	IPI00964379.1	THO complex 3	2.744432688
843	IPI00001539.8	3-ketoacyl-CoA thiolase, mitochondrial	2.741857767
844	IPI00219866.2	Isoform 2 of Zinc finger Ran-binding domain-containing protein 2	2.718465805
845	IPI00218848.5	ATP synthase, H+ transporting, mitochondrial F0 complex, subunit E	2.712542772
846	IPI00382790.3	Isoform 2 of Sharpin	2.6983459
847	IPI00982409.1	RING finger protein C14orf164-like	2.66461277
848	IPI00028003.1	Cytochrome c oxidase subunit 7B, mitochondrial	2.619421244
849	IPI00945220.1	golgi integral membrane protein 4	2.604919434

Table A5: BPPM-revealed common nonhistone targets of GLP1 and G9a in HEK293T cells using HeySAM. The proteins are no found in control.

Serial	Accession	Description	Score of EuHMT1	score of EuHMt2
1	IPI00942420.2	Isoform 1 of Histone-lysine N-methyltransferase EHMT1	729.0146117	51.76659226
2	IPI00026781.3	Fatty acid synthase	391.2522674	759.7647235
3	IPI00304925.5	Heat shock 70 kDa protein 1A/1B	235.7833066	321.283962
4	IPI00220644.8	Isoform M1 of Pyruvate kinase isozymes M1/M2	166.911351	149.4408383
5	IPI00449049.5	Poly [ADP-ribose] polymerase 1	160.6497989	260.0815408
6	IPI00645078.1	Ubiquitin-like modifier-activating enzyme 1	148.5826547	212.3655384
7	IPI00420014.2	Isoform 1 of U5 small nuclear ribonucleoprotein 200 kDa helicase	121.9588175	366.528441
8	IPI00893035.1	carbamoyl-phosphate synthetase 2, aspartate transcarbamylase, an	121.9285016	238.1053216
9	IPI00645452.1	Tubulin, beta	118.182215	50.23914671
10	IPI00643041.3	GTP-binding nuclear protein Ran	116.9542315	70.04592967
11	IPI00019502.3	Isoform 1 of Myosin-9	115.9260545	237.2038248
12	IPI00000874.1	Peroxiredoxin-1	113.6827171	177.3387182
13	IPI00013452.11	Bifunctional aminoacyl-tRNA synthetase	106.737942	172.1725242
14	IPI00017726.1	Isoform 1 of 3-hydroxyacyl-CoA dehydrogenase type-2	104.8656714	61.59832907
15	IPI00018146.1	14-3-3 protein theta	103.0258706	77.91386127
16	IPI00219018.7	Glyceraldehyde-3-phosphate dehydrogenase	101.2805254	256.5314114
17	IPI00007928.4	Pre-mRNA-processing-splicing factor 8	100.3890626	291.0308721
18	IPI00021263.3	14-3-3 protein zeta/delta	99.24341798	64.90589786
19	IPI00456969.1	Cytoplasmic dynein 1 heavy chain 1	99.18983865	391.7522783
20	IPI00394838.3	cDNA FLJ56442, highly similar to ATP-citrate synthase	96.82186866	149.8845675
21	IPI00216587.9	40S ribosomal protein S8	94.91858125	49.05260539
22	IPI00218200.8	B-cell receptor-associated protein 31	94.08164167	40.01049781
23	IPI00383581.4	cDNA FLJ61290, highly similar to Neutral alpha-glucosidase AB	92.65108037	164.5848365
24	IPI00297779.7	T-complex protein 1 subunit beta	85.41790318	19.29311204
25	IPI00030179.3	60S ribosomal protein L7	84.80247474	51.23387122
26	IPI00967971.1	ubiquitin carboxyl-terminal esterase L1 (ubiquitin thiolesterase)	84.78158069	46.09521461
27	IPI00217223.1	Multifunctional protein ADE2	82.60718107	96.83288717
28	IPI00807545.1	Isoform 3 of Heterogeneous nuclear ribonucleoprotein K	82.27658319	65.32964873
29	IPI00008240.2	Methionyl-tRNA synthetase, cytoplasmic	80.92234015	117.8301554
30	IPI00793443.2	Isoform 1 of Importin-5	80.01624537	106.7574532
31	IPI00007188.6	ADP/ATP translocase 2	79.9827168	56.53837276
32	IPI00783097.4	Glycyl-tRNA synthetase	78.70939565	120.6101208
33	IPI00329801.12	Annexin A5	78.23380566	55.84255219
34	IPI00979136.1	Ribonucleoside-diphosphate reductase	77.46082282	108.3014402
35	IPI00329633.5	Threonyl-tRNA synthetase, cytoplasmic	77.27365184	120.9481163
36	IPI00025091.3	40S ribosomal protein S11	77.253052	71.76152396
37	IPI00889541.2	Isoform 4 of Probable ATP-dependent RNA helicase DDX17	76.96171999	94.11570525
38	IPI00412579.6	60S ribosomal protein L10a	74.75596213	47.42085719
39	IPI00294911.1	Succinate dehydrogenase [ubiquinone] iron-sulfur subunit, mitocho	74.74311042	42.59361458
40	IPI00220301.5	Peroxiredoxin-6	74.10010314	49.33346581
41	IPI00217030.10	40S ribosomal protein S4, X isoform	74.05303216	50.09114695
42	IPI01012026.1	chromodomain helicase DNA binding protein 4	74.04750729	151.010915
43	IPI00024175.3	Isoform 1 of Proteasome subunit alpha type-7	73.91543031	27.6172812
44	IPI00022774.3	Transitional endoplasmic reticulum ATPase	73.26129746	149.5695152
45	IPI00644224.2	cDNA FLJ54020, highly similar to Heterogeneous nuclear ribonucleop	72.63242865	145.3232844
46	IPI00978796.1	cofilin 1 (non-muscle)	71.99949503	85.76440644

47	IPI01014604.1	T-complex protein 1 subunit delta	69.65310025	78.14010024
48	IPI00140420.4	Staphylococcal nuclease domain-containing protein 1	69.51705146	89.10199308
49	IPI00029133.4	ATP synthase subunit b, mitochondrial	69.10584235	49.95107341
50	IPI00018465.1	T-complex protein 1 subunit eta	69.01046848	84.1580894
51	IPI00465365.4	Isoform A1-A of Heterogeneous nuclear ribonucleoprotein A1	66.49793029	212.3037598
52	IPI00291467.7	ADP/ATP translocase 3	65.61314964	51.63087511
53	IPI00012268.3	26S proteasome non-ATPase regulatory subunit 2	64.83733439	127.3789473
54	IPI00878075.1	RAN binding protein 1	64.83252692	38.07210541
55	IPI00917777.1	116 kDa U5 small nuclear ribonucleoprotein component isoform b	64.2363987	102.9461691
56	IPI00549248.4	Isoform 1 of Nucleophosmin	61.72652674	131.7312021
57	IPI00419585.9	Peptidyl-prolyl cis-trans isomerase A	61.64404869	70.94191241
58	IPI00867533.1	60S ribosomal protein L6	61.51985025	110.2808673
59	IPI00002966.2	Heat shock 70 kDa protein 4	61.04511046	85.93793941
60	IPI00027230.3	Endoplasmin	61.04120731	125.1475878
61	IPI00795292.1	Isoform 3 of Nucleoside diphosphate kinase B	60.4085772	53.31095743
62	IPI00215917.3	ADP-ribosylation factor 3	59.20805001	62.3566103
63	IPI00217966.9	Isoform 1 of L-lactate dehydrogenase A chain	58.67067504	178.4921441
64	IPI00029623.1	Proteasome subunit alpha type-6	57.18178296	28.82169819
65	IPI00020127.1	Replication protein A 70 kDa DNA-binding subunit	56.42424345	110.0033898
66	IPI00015018.1	Inorganic pyrophosphatase	56.11794639	170.3900266
67	IPI00027350.3	Peroxiredoxin-2	55.92931271	63.50261545
68	IPI00397526.3	Isoform 1 of Myosin-10	55.7543714	119.0089898
69	IPI00218988.4	Isoform 2 of Adenylate kinase 2, mitochondrial	55.4243381	44.54196548
70	IPI00465361.4	60S ribosomal protein L13	54.99939442	20.32618785
71	IPI00374151.1	thioredoxin-dependent peroxide reductase, mitochondrial isoform I	54.59023404	89.67426276
72	IPI00022891.3	ADP/ATP translocase 1	54.13334846	39.65227294
73	IPI00300371.5	Isoform 1 of Splicing factor 3B subunit 3	53.94768524	97.95910382
74	IPI00219306.1	Protein mago nashi homolog	53.76058745	40.29925013
75	IPI00783781.2	Nuclear pore complex protein Nup205	53.75590611	136.3286684
76	IPI00783378.3	Ubiquitin-conjugating enzyme E2 O	52.98222733	57.0727365
77	IPI00020075.4	Abhydrolase domain-containing protein 10, mitochondrial	52.12625527	25.16440916
78	IPI00941747.1	Calnexin	52.08898282	108.939739
79	IPI00895852.1	cellular nucleic acid-binding protein isoform 5	52.00794601	85.08035088
80	IPI00925853.1	cDNA FLJ60586, highly similar to NADH-ubiquinone oxidoreductase 7	51.66277575	3.832695961
81	IPI00013214.2	cDNA FLJ55599, highly similar to DNA replication licensing factor MCI	51.3785069	91.51911545
82	IPI00644127.2	Isoleucyl-tRNA synthetase, cytoplasmic	50.39426541	136.8429933
83	IPI00003886.3	Isoform 2 of Guanine nucleotide-binding protein-like 3	50.23450446	84.67073178
84	IPI00216308.5	Voltage-dependent anion-selective channel protein 1	49.92797661	30.21461153
85	IPI00216691.5	Profilin-1	49.36589336	39.42420149
86	IPI00642936.2	glutathione S-transferase omega-1 isoform 3	49.1392777	30.95730042
87	IPI00012048.1	Isoform 1 of Nucleoside diphosphate kinase A	48.40361905	43.98702502
88	IPI00170924.2	Histidine triad nucleotide-binding protein 3	48.3692143	64.2205677
89	IPI00739915.3	Putative tubulin beta chain-like protein ENSP00000290377	47.63914037	52.74071693
90	IPI00016832.1	Isoform Short of Proteasome subunit alpha type-1	47.40951896	19.06253815
91	IPI00848298.1	Isoform 2 of Apolipoprotein A-I-binding protein	47.40377808	20.14720654
92	IPI00015920.2	Isoform 1 of Mitochondrial dicarboxylate carrier	47.16355371	28.72216034
93	IPI00927606.1	Glutathione peroxidase 1	46.70900249	70.61924076

94	IPI00411680.11	Isoform 1 of Protein-L-isoaspartate(D-aspartate) O-methyltransferas	46.48782468	32.04926777
95	IPI00219217.3	L-lactate dehydrogenase B chain	46.39972949	175.9723818
96	IPI00555744.6	Ribosomal protein L14 variant	45.61308312	19.45099711
97	IPI00010896.3	Chloride intracellular channel protein 1	44.61412549	22.36223078
98	IPI00218606.7	40S ribosomal protein S23	44.01858759	41.93586826
99	IPI00789370.3	serine hydroxymethyltransferase, mitochondrial isoform 3	43.69448233	62.71231842
100	IPI00411592.2	Isoform 2 of Chromodomain-helicase-DNA-binding protein 3	42.26829982	54.09346461
101	IPI00221088.5	40S ribosomal protein S9	41.80261087	55.15500164
102	IPI00025329.1	60S ribosomal protein L19	41.73298621	33.53769732
103	IPI00289819.5	Cation-independent mannose-6-phosphate receptor	41.57298326	194.5548613
104	IPI00004968.1	Pre-mRNA-processing factor 19	41.54854751	23.14249349
105	IPI00216298.6	Thioredoxin	40.90045071	24.13620567
106	IPI00246975.8	Glutathione S-transferase Mu 3	40.52072382	16.22876978
107	IPI00219078.5	Isoform 1 of Sarcoplasmic/endoplasmic reticulum calcium ATPase 2	40.1899116	105.0190744
108	IPI01017942.1	cyclin-dependent kinase 1	40.14090967	20.30771685
109	IPI00965314.1	ATP-binding cassette, sub-family E (OABP), member 1	40.0531795	3.533854246
110	IPI00981739.1	tubulin folding cofactor A	39.8813827	26.229635
111	IPI00006980.1	chromosome 14 open reading frame 166	39.82267761	26.09525371
112	IPI00016342.1	Ras-related protein Rab-7a	39.55969405	56.70726061
113	IPI00221093.7	40S ribosomal protein S17	38.01497412	25.90276027
114	IPI00015833.1	Coiled-coil-helix-coiled-coil-helix domain-containing protein 3, mit	37.96621513	28.57314563
115	IPI00396321.1	Leucine-rich repeat-containing protein 59	37.65153241	95.53281498
116	IPI00215911.3	DNA-(apurinic or apyrimidinic site) lyase	37.33648491	152.2553763
117	IPI00953417.1	tubulin, beta class I	36.98217416	21.46094656
118	IPI00008998.3	3-hydroxyacyl-CoA dehydratase 3	36.8838954	73.19380951
119	IPI00002824.7	Cysteine and glycine-rich protein 2	36.07404995	55.03849053
120	IPI00515040.1	Isoform 2 of Alpha N-terminal protein methyltransferase 1A	35.88850784	27.32974958
121	IPI00025273.1	Isoform Long of Trifunctional purine biosynthetic protein adenosine	35.88418746	74.20943737
122	IPI00643368.1	Ras homolog gene family, member C	35.85121965	3.590638876
123	IPI00807491.2	Isoform 2 of General transcription factor 3C polypeptide 1	35.73834395	7.998302937
124	IPI00179330.6	Ubiquitin-40S ribosomal protein S27a	35.43276453	19.45930576
125	IPI00641437.1	HEAT repeat containing 1	35.142452	17.69447613
126	IPI00008530.1	60S acidic ribosomal protein P0	34.72628856	111.2969279
127	IPI00646304.4	Peptidyl-prolyl cis-trans isomerase B	34.28955984	48.38023973
128	IPI00220834.8	X-ray repair cross-complementing protein 5	33.88251209	107.6939523
129	IPI00910113.1	cDNA FLJ52902, highly similar to Rab GDP dissociation inhibitor alph	33.65728259	51.53565001
130	IPI00024911.1	Endoplasmic reticulum resident protein 29	33.55024695	7.204618931
131	IPI00295098.3	Signal recognition particle receptor subunit beta	33.44176197	25.10525703
132	IPI00413324.6	60S ribosomal protein L17	33.39969826	55.80420852
133	IPI00908896.2	heterogeneous nuclear ribonucleoprotein H1 (H)	33.32276654	30.50481462
134	IPI00156374.6	Isoform 1 of Importin-4	33.15105653	60.80217481
135	IPI00032903.3	Peptidyl-tRNA hydrolase 2, mitochondrial	33.08517528	37.90535879
136	IPI00012074.3	Isoform 1 of Heterogeneous nuclear ribonucleoprotein R	32.83499622	55.09549785
137	IPI00908754.1	cDNA FLJ50714, moderately similar to Ras-related protein Rap-1b	32.82168961	53.55689955
138	IPI00980410.1	mitochondrial carrier 2	32.69967675	34.56406307
139	IPI00375513.3	Isoform Soluble of Catechol O-methyltransferase	32.68832779	27.21326852
140	IPI00917575.2	cDNA FLJ51046, highly similar to 60 kDa heat shock protein, mitochor	32.64225578	28.52809048

141	IPI00001159.11	Translational activator GCN1	32.41869712	85.26480722
142	IPI00759663.1	Isoform Cytoplasmic+peroxisomal of Peroxiredoxin-5, mitochondrial	32.32378983	30.06219959
143	IPI00017672.4	cDNA FLJ25678 fis, clone TST04067, highly similar to PURINE NUCLEOS	32.2683475	15.28783107
144	IPI00005024.3	Isoform 1 of Myb-binding protein 1A	31.99996924	77.87896466
145	IPI00003870.1	Putative ATP-dependent Clp protease proteolytic subunit, mitochond	31.84814167	14.99601603
146	IPI00018931.6	Vacuolar protein sorting-associated protein 35	31.56291461	47.37325096
147	IPI00013180.2	Protein BUD31 homolog	31.43726826	39.22823119
148	IPI00219678.3	Eukaryotic translation initiation factor 2 subunit 1	31.36786199	38.0262506
149	IPI00073602.1	Exosome complex component MTR3	31.27500772	15.42575288
150	IPI00003815.3	Rho GDP-dissociation inhibitor 1	31.23469472	24.02476215
151	IPI00296913.1	ADP-sugar pyrophosphatase	30.79156375	17.39159036
152	IPI01014863.1	Acetyl-CoA acetyltransferase, cytosolic	30.49259949	22.96209049
153	IPI00893541.1	protein disulfide isomerase family A, member 3	30.36398935	31.07933569
154	IPI00297579.4	Chromobox protein homolog 3	30.30350041	33.87606478
155	IPI00292020.3	Spermidine synthase	30.29854989	14.65871668
156	IPI00031691.1	60S ribosomal protein L9	29.98712397	36.02842021
157	IPI00021347.1	Ubiquitin-conjugating enzyme E2 L3	29.80865288	21.37869477
158	IPI00028055.4	Transmembrane emp24 domain-containing protein 10	29.61652017	48.22544694
159	IPI00293331.3	Ribonucleases P/MRP protein subunit POP1	29.48490858	33.2104609
160	IPI00219153.4	60S ribosomal protein L22	29.35732174	18.14248013
161	IPI00413641.7	Aldose reductase	29.30551267	78.07148504
162	IPI00063242.6	Isoform 2 of Serine/threonine-protein phosphatase PGAM5, mitocho	29.15536594	2.969429731
163	IPI00007611.1	ATP synthase subunit O, mitochondrial	28.96623611	56.21613884
164	IPI00792330.2	ADP-ribosylation factor 4	28.81387091	39.91422415
165	IPI00647400.1	arginyl aminopeptidase (aminopeptidase B)	28.38294697	52.35423279
166	IPI00296370.2	leucine carboxyl methyltransferase 1	28.13103223	32.68146014
167	IPI00219622.3	Proteasome subunit alpha type-2	28.01113796	6.670053482
168	IPI00984405.1	DEAD (Asp-Glu-Ala-Asp) box helicase 5	27.97559333	9.441040039
169	IPI00182533.5	60S ribosomal protein L28	27.8903029	20.32191014
170	IPI00221091.9	40S ribosomal protein S15a	27.87808824	26.42860079
171	IPI00171199.5	Isoform 2 of Proteasome subunit alpha type-3	27.87724471	13.3510921
172	IPI00010414.4	PDZ and LIM domain protein 1	27.65128565	92.54963565
173	IPI00003217.3	Proteasome subunit beta type-7	27.62663984	14.19120789
174	IPI00411706.1	S-formylglutathione hydrolase	27.4816606	31.72799945
175	IPI00306280.4	Density-regulated protein	26.47071457	23.68208313
176	IPI00218693.8	Adenine phosphoribosyltransferase	26.11487603	40.49584842
177	IPI00169413.1	28S ribosomal protein S34, mitochondrial	25.91457605	19.98661828
178	IPI00607799.5	Isoform 1 of 3-hydroxybutyrate dehydrogenase type 2	25.69540119	15.34840512
179	IPI00878876.1	cDNA FLJ51872, highly similar to Small nuclear ribonucleoprotein Sm	25.57746196	15.92051387
180	IPI00456940.5	60S ribosomal protein L7-like 1	25.47294021	14.533535
181	IPI00030877.2	15 kDa selenoprotein isoform 1 precursor	25.47280741	22.05384469
182	IPI00218493.7	Hypoxanthine-guanine phosphoribosyltransferase	25.37085819	12.59149814
183	IPI00003386.3	E3 ubiquitin-protein ligase RBX1	25.28809643	20.6283741
184	IPI00438229.2	Isoform 1 of Transcription intermediary factor 1-beta	25.18329024	65.05789638
185	IPI00260318.3	cyclin-dependent kinase 2 isoform 2	25.16826892	10.64922738
186	IPI00946221.1	ribosomal protein L24	25.13393474	57.49180627
187	IPI00003588.1	Eukaryotic translation elongation factor 1 epsilon-1	25.08676624	28.65892458

188	IPI00926851.1	TRAM adaptor with GOLD domain isoform 2	25.0576334	12.12693405
189	IPI00895865.1	electron transfer flavoprotein subunit alpha, mitochondrial isoform	25.02187204	20.30047679
190	IPI00304612.9	60S ribosomal protein L13a	24.99991417	26.87083387
191	IPI00219155.5	60S ribosomal protein L27	24.93350792	12.54528141
192	IPI00300096.4	Ras-related protein Rab-35	24.8862865	18.3901031
193	IPI00940393.3	EEF1A1 protein	24.6656723	81.66274333
194	IPI00655650.2	40S ribosomal protein S26	24.61743641	23.73561382
195	IPI00025874.2	Dolichyl-diphosphooligosaccharide--protein glycosyltransferase sul	24.13459992	72.23646331
196	IPI00013917.3	40S ribosomal protein S12	24.00824642	11.29956412
197	IPI00007402.3	Importin-7	23.74324346	48.00437307
198	IPI00555749.1	Proteasome 26S ATPase subunit 5 variant (Fragment)	23.71801162	43.66379905
199	IPI01018104.1	cDNA FLJ52561, highly similar to Four and a half LIM domains protei	23.61455297	15.67550874
200	IPI01014503.1	Uncharacterized protein	23.49908495	25.88044834
201	IPI00007811.1	Cyclin-dependent kinase 4	23.48174167	15.09010434
202	IPI00873286.2	cDNA FLJ55750, highly similar to Eukaryotic translation initiation fac	23.45419812	11.49638867
203	IPI00303722.5	Protein FAM136A	23.30880928	36.111835
204	IPI00644674.1	Cytosolic Fe-S cluster assembly factor NUBP2	22.99330688	11.04510665
205	IPI00021828.1	Cystatin-B	22.94549203	24.37318659
206	IPI00006211.4	Isoform 1 of Vesicle-associated membrane protein-associated prote	22.8651557	14.96650648
207	IPI01013843.1	cDNA FLJ59776, highly similar to Prefoldin subunit 3	22.77480769	11.55967331
208	IPI00027270.1	60S ribosomal protein L26	22.55340433	23.58366847
209	IPI00011876.3	cDNA FLJ59758, highly similar to S-methyl-5-thioadenosine phospho	22.38703632	16.71141124
210	IPI00334907.3	Isoform 1 of Phosphatidylinositol transfer protein beta isoform	22.3500936	65.49831676
211	IPI01010050.1	cDNA, FLJ78818, highly similar to Voltage-dependent anion-selective	22.23621225	5.225667953
212	IPI00794911.3	Coatomer subunit gamma	22.19975686	17.72200608
213	IPI00215719.6	60S ribosomal protein L18	22.1474607	27.57744861
214	IPI00105598.3	Proteasome 26S non-ATPase subunit 11 variant (Fragment)	22.03928852	6.919309378
215	IPI00453473.6	Histone H4	21.98193645	11.90534139
216	IPI00643504.1	ring finger protein 2	21.96214581	7.100060463
217	IPI00456758.4	60S ribosomal protein L27a	21.87804031	19.38668346
218	IPI00746438.2	Isoform 2 of 60S ribosomal protein L11	21.80755496	29.98282504
219	IPI01011782.1	cDNA FLJ61430, highly similar to ATP-dependent RNA helicase DDX50	21.78792763	23.28930044
220	IPI00017297.1	Matrin-3	21.75937772	42.7282083
221	IPI00220667.3	Isoform 4 of Hexokinase-1	21.74832654	58.12198567
222	IPI01012526.1	glucosidase, alpha; neutral AB	21.72934151	9.832138062
223	IPI00026824.2	Heme oxygenase 2	21.72010708	72.25547433
224	IPI00221325.3	E3 SUMO-protein ligase RanBP2	21.49732208	30.0734508
225	IPI00908723.1	cDNA FLJ61039, highly similar to Stomatin-like protein 2	21.48810863	18.12077689
226	IPI00081836.3	Histone H2A type 1-H	21.4817996	25.64582062
227	IPI00167941.1	Midasin	21.46257401	114.3588099
228	IPI00429689.3	Serine/threonine-protein phosphatase 2A catalytic subunit beta iso	21.41615653	101.8603373
229	IPI00008380.1	Serine/threonine-protein phosphatase 2A catalytic subunit alpha is	21.40297103	101.5836127
230	IPI00294398.2	Isoform 1 of Hydroxyacyl-coenzyme A dehydrogenase, mitochondrial	21.36481214	6.69530654
231	IPI00006907.1	Probable fructose-2,6-bisphosphatase TIGAR	21.32082558	10.89680028
232	IPI00016458.3	Isoform 1 of L-2-hydroxyglutarate dehydrogenase, mitochondrial	21.23870134	15.10022569
233	IPI00029079.5	GMP synthase [glutamine-hydrolyzing]	21.20630789	37.17861724
234	IPI00028004.2	Proteasome subunit beta type-3	21.16501713	29.57798219

235	IPI00795892.1	profilin 2	21.044034	18.24080682
236	IPI00171611.7	Histone H3.2	20.88544345	28.79178953
237	IPI00645138.2	cDNA FLJ55652, highly similar to Nucleolar GTP-binding protein 1	20.81382537	48.12162352
238	IPI00295485.4	Heat shock 70 kDa protein 4L	20.73207259	50.60684347
239	IPI00022018.1	Dolichol-phosphate mannosyltransferase	20.72329092	19.41536641
240	IPI00009342.1	Ras GTPase-activating-like protein IQGAP1	20.70216203	43.39088202
241	IPI00220993.1	Isoform CNPI of 2',3'-cyclic-nucleotide 3'-phosphodiesterase	20.66739511	24.2182169
242	IPI00427330.3	Ribosome maturation protein SBDS	20.5949223	2.973943233
243	IPI00215790.6	60S ribosomal protein L38	20.52120352	11.53737783
244	IPI00549885.4	Isoform 2 of Pyruvate dehydrogenase E1 component subunit beta, m	20.50771928	63.37418199
245	IPI00010153.5	60S ribosomal protein L23	20.50240135	12.92345476
246	IPI01015295.1	cDNA FLJ30049 fis, clone ADRGL1000033, highly similar to 26S proteas	20.48267412	10.43838573
247	IPI00010271.3	Isoform A of Ras-related C3 botulinum toxin substrate 1	20.18120885	35.11968374
248	IPI00178440.3	Elongation factor 1-beta	19.93448758	11.65764499
249	IPI00445401.4	Isoform 2 of E3 ubiquitin-protein ligase HUWE1	19.93258858	129.8415353
250	IPI00016513.5	Ras-related protein Rab-10	19.7488091	37.5575211
251	IPI00219358.7	Isoform 1 of Mannose-6-phosphate isomerase	19.56478715	13.99072981
252	IPI00472633.7	Isoform 3 of Transformer-2 protein homolog beta	19.54099369	34.55797982
253	IPI00170692.4	Isoform 1 of Vesicle-associated membrane protein-associated prote	19.54041743	10.09439015
254	IPI00012795.3	Eukaryotic translation initiation factor 3 subunit I	19.50349522	62.16252136
255	IPI00019196.3	Ribonuclease P protein subunit p30	19.37051654	13.54499817
256	IPI00029631.1	Enhancer of rudimentary homolog	19.35223317	10.10195589
257	IPI00414168.1	E3 ubiquitin-protein ligase MARCH5	19.35148454	10.86114836
258	IPI00642046.1	ribosomal L1 domain containing 1	19.30265665	42.51666975
259	IPI00218728.4	Isoform 1 of Platelet-activating factor acetylhydrolase IB subunit alp	19.30063415	6.796374559
260	IPI00978910.1	Glia maturation factor beta	19.29461503	6.928934574
261	IPI00020599.1	Calreticulin	19.22097254	58.32678366
262	IPI00411937.4	Nucleolar protein 56	19.08992338	55.92416358
263	IPI00789582.2	cDNA FLJ51552, highly similar to Eukaryotic translation initiation fac	19.07729435	21.82286453
264	IPI00395887.4	Thioredoxin-related transmembrane protein 1	19.07211781	11.23121548
265	IPI00916060.1	DNA-directed RNA polymerase	19.04974222	38.15083671
266	IPI00644531.1	transgelin 2	18.88507462	29.70350599
267	IPI00003766.4	Protein ETHE1, mitochondrial	18.88325882	3.126749754
268	IPI01010461.1	hypoxia up-regulated 1	18.87546682	17.63665271
269	IPI00026970.4	FACT complex subunit SPT16	18.70021462	33.64892483
270	IPI01010797.1	cDNA, FLJ96158, highly similar to Homo sapiens calpain 2, (m/II) larg	18.66959786	30.85051012
271	IPI00219757.13	Glutathione S-transferase P	18.60493469	12.1351583
272	IPI00971018.1	Isoform 1 of TAR DNA-binding protein 43	18.56664896	19.22315741
273	IPI01012383.1	OTU domain, ubiquitin aldehyde binding 1	18.31986809	64.10212636
274	IPI00000821.2	39S ribosomal protein L16, mitochondrial	18.28165388	6.928866386
275	IPI00012750.3	40S ribosomal protein S25	18.24493194	7.302073002
276	IPI00025347.4	Ribosomal RNA small subunit methyltransferase NEP1	17.93830657	6.505105972
277	IPI01014133.1	cDNA FLJ32936 fis, clone TESTI2007533, highly similar to RuvB-like 2	17.87639046	30.22881627
278	IPI00910754.1	L-lactate dehydrogenase A chain isoform 2	17.84153605	9.799121618
279	IPI00017469.1	Sepiapterin reductase	17.78612185	8.42458725
280	IPI00032808.1	Ras-related protein Rab-3D	17.76695919	12.4209168
281	IPI00016786.1	Isoform 2 of Cell division control protein 42 homolog	17.71056509	50.16028833

282	IPI00031169.1	Ras-related protein Rab-2A	17.69229293	30.06599617
283	IPI00917181.1	Ribosomal protein L36a	17.68854117	26.74609089
284	IPI00003927.5	Peptidyl-prolyl cis-trans isomerase D	17.65873814	11.56363511
285	IPI00219077.4	Isoform 1 of Leukotriene A-4 hydrolase	17.58453393	26.63442516
286	IPI00556107.1	DNA-3-methyladenine glycosylase isoform c	17.57844281	34.92022943
287	IPI00029046.1	Malectin	17.57364154	13.42012191
288	IPI00219861.3	Isoform 1 of Low molecular weight phosphotyrosine protein phosph	17.48403931	13.03783321
289	IPI00794545.1	deoxyuridine 5'-triphosphate nucleotidohydrolase, mitochondrial is	17.41640306	20.93088627
290	IPI00185374.4	26S proteasome non-ATPase regulatory subunit 12	17.37279034	18.54274511
291	IPI00018783.1	Inosine triphosphate pyrophosphatase	17.35806489	23.23776221
292	IPI00023542.6	Transmembrane emp24 domain-containing protein 9	17.34732461	12.5365169
293	IPI00014053.3	Isoform 1 of Mitochondrial import receptor subunit TOM40 homolog	17.29182148	51.52494693
294	IPI00025084.3	Calpain small subunit 1	17.26847553	11.42881656
295	IPI00303954.3	cytochrome b5 type B precursor	17.2508781	32.84485555
296	IPI00868999.1	Similar to Acidic ribosomal phosphoprotein P0	17.19005585	6.193804741
297	IPI00942944.1	protein DEK isoform 2	17.0475266	18.61816978
298	IPI00005692.1	28S ribosomal protein S12, mitochondrial	16.97285175	8.977897167
299	IPI00013167.1	28S ribosomal protein S25, mitochondrial	16.91688275	26.91265559
300	IPI00023406.1	Cytochrome c-type heme lyase	16.86869431	6.956211329
301	IPI00396329.1	Ribosome production factor 2 homolog	16.69620633	50.31776333
302	IPI00023647.4	Isoform 1 of Ubiquitin-like modifier-activating enzyme 6	16.67186379	36.5750742
303	IPI00062866.4	Isoform 1 of Zinc finger CCCH-type antiviral protein 1-like	16.60305166	32.87110829
304	IPI00925601.1	5-aminoimidazole-4-carboxamide ribonucleotide formyltransferase	16.5197804	27.30317044
305	IPI00024821.1	26S proteasome non-ATPase regulatory subunit 14	16.49425149	46.22907114
306	IPI00410324.2	Isoform 1 of Protein LSM12 homolog	16.34122086	7.410131693
307	IPI00879638.2	cDNA FLJ58652, highly similar to Probable ATP-dependent RNA helica	16.28180313	8.521591902
308	IPI00005107.2	Niemann-Pick C1 protein	16.24896646	37.4597559
309	IPI00219365.3	Moesin	16.2058394	30.11094594
310	IPI01011282.1	23 kDa protein	16.15997243	13.28340149
311	IPI00168184.8	cDNA FLJ56053, highly similar to Serine/threonine-protein phosphat	16.04391837	5.994200945
312	IPI01011132.1	Isoform 1 of DNA topoisomerase 2-alpha	16.02649283	47.97874737
313	IPI00023064.1	NADH dehydrogenase [ubiquinone] 1 alpha subcomplex assembly f	16.00889349	19.44897747
314	IPI00916802.1	Sjogren syndrome antigen B (autoantigen La)	15.84578443	21.62210894
315	IPI00017283.2	Isoleucyl-tRNA synthetase, mitochondrial	15.54805946	79.32804489
316	IPI00021095.1	Protein Mis18-alpha	15.43418527	11.97754002
317	IPI00216057.6	Sorbitol dehydrogenase	15.38418078	16.8930974
318	IPI00640037.2	cDNA FLJ38496 fis, clone FELIV1000137, highly similar to 60S RIBOSOM	15.3722167	7.36440134
319	IPI00297241.4	Nucleolar pre-ribosomal-associated protein 1	15.26629472	64.38480663
320	IPI00383680.3	dolichyl-diphosphooligosaccharide--protein glycosyltransferase sub	15.2184515	21.20480132
321	IPI00060031.3	ADP-ribosylation factor-like protein 8A	15.20935559	36.73852849
322	IPI00398774.3	Isoform 2 of Mps one binder kinase activator-like 3	15.13529372	12.17595506
323	IPI00909577.1	cDNA FLJ52894, highly similar to Isocitrate dehydrogenase	15.11244202	20.18908143
324	IPI00185503.4	Isoform 2 of ATP-binding cassette sub-family D member 3	14.98766041	30.74609566
325	IPI00411765.3	Isoform 2 of 14-3-3 protein sigma	14.98706102	9.002167463
326	IPI00640703.3	Exportin-5	14.95011711	25.50934196
327	IPI00239077.5	Histidine triad nucleotide-binding protein 1	14.87256193	6.230341673
328	IPI00219575.5	Bleomycin hydrolase	14.86099052	4.411576271

329	IPI00924816.1	Myotrophin	14.80269027	25.96178555
330	IPI01013052.1	caspase 12 (gene/pseudogene)	14.80241656	20.2420795
331	IPI00910164.1	cDNA FLJ53381, highly similar to Monocarboxylate transporter 1	14.7109592	40.8945055
332	IPI00760588.2	Isoform 5 of Double-stranded RNA-specific adenosine deaminase	14.69395542	33.06698012
333	IPI00740142.2	u5 small nuclear ribonucleoprotein 200 kDa helicase-like, partial	14.67643595	13.38677335
334	IPI00304932.2	Ribosomal RNA-processing protein 8	14.64496183	28.81081104
335	IPI00029629.4	E3 ubiquitin/ISG15 ligase TRIM25	14.55224824	41.33140135
336	IPI00021785.2	Cytochrome c oxidase subunit 5B, mitochondrial	14.54167295	11.38466263
337	IPI00737530.1	actin-related protein 2/3 complex subunit 1B-like	14.47739291	17.5527246
338	IPI00218568.7	Pterin-4-alpha-carbinolamine dehydratase	14.44081759	15.21335578
339	IPI00479722.2	Proteasome activator complex subunit 1	14.4245286	8.93192625
340	IPI00646605.3	Isoform 3 of E3 ubiquitin-protein ligase UBR4	14.39617968	55.55451703
341	IPI00953109.2	Isoform 6 of Filamin-B	14.38293767	103.4262052
342	IPI00012315.2	Nucleoside diphosphate kinase 3	14.35925961	7.999052525
343	IPI01009435.1	THO complex subunit 2	14.33485222	37.97984362
344	IPI00853337.1	ADP-ribosylation factor 5	14.32359123	26.4231627
345	IPI00022597.1	NEDD8-conjugating enzyme Ubc12	14.31094575	18.13961244
346	IPI00984586.1	trypsin-3 isoform 4 preproprotein	14.28379822	2.935996056
347	IPI00246058.10	Programmed cell death 6-interacting protein	14.27806425	29.39755034
348	IPI00099996.2	Mitochondrial ribonuclease P protein 1	14.25307441	11.43853045
349	IPI00059764.4	Isoform 1 of Zinc finger protein 428	14.14135289	3.339945316
350	IPI00658013.1	nucleophosmin isoform 3	14.14046288	23.19569707
351	IPI00017381.1	Replication factor C subunit 4	14.09888244	13.64978266
352	IPI00017799.5	cDNA FLJ55158, highly similar to Thioredoxin, mitochondrial	14.06674433	3.320490599
353	IPI01015100.1	Membrane-associated progesterone receptor component 2	14.04842472	12.71248055
354	IPI00220648.5	Phosphomevalonate kinase	13.97088099	8.992396593
355	IPI00947020.2	Ras homolog enriched in brain	13.71872401	11.95468044
356	IPI00024157.1	Peptidyl-prolyl cis-trans isomerase FKBP3	13.6936903	3.0353055
357	IPI00604652.1	NEDD8-activating enzyme E1 regulatory subunit isoform c	13.66355371	18.91427255
358	IPI00329301.3	Isoform 1 of NADH dehydrogenase [ubiquinone] 1 alpha subcomple	13.64425278	16.18613505
359	IPI00893703.1	ribosomal protein S7	13.64069605	17.02438021
360	IPI00152695.2	WD repeat-containing protein 82	13.63987303	20.23001885
361	IPI00290543.5	Isoform 1 of Nuclear protein localization protein 4 homolog	13.63589573	27.5719955
362	IPI00909694.2	alpha-aminoadipic semialdehyde dehydrogenase isoform 3	13.55945539	6.823871851
363	IPI00940720.2	PARP1 protein (Fragment)	13.53916049	12.79487371
364	IPI00004165.1	Fos39347_1	13.52875137	3.22106123
365	IPI00550852.4	Isoform 1 of Dynactin subunit 4	13.52199078	29.76708961
366	IPI00017510.3	Cytochrome c oxidase subunit 2	13.47459793	16.73841619
367	IPI00927715.1	Ribosomal protein L15	13.45742917	15.7077837
368	IPI00927892.1	Mitochondrial-processing peptidase subunit beta	13.39058852	23.17147756
369	IPI00976817.1	poly-U binding splicing factor 60KDa	13.3136878	5.053713322
370	IPI00011694.1	Trypsin-1	13.29701853	25.8478961
371	IPI00916474.2	mannosyl-oligosaccharide glucosidase isoform 2	13.23869753	27.74307871
372	IPI00031647.2	Programmed cell death protein 2-like	13.20120621	12.38316584
373	IPI00443909.1	Isoform 1 of Protein canopy homolog 2	13.19260883	15.38165808
374	IPI01010565.1	cDNA FLJ51063, highly similar to Dihydrolipoyllysine-residue acetyltr	13.17704034	3.651170254
375	IPI01015427.1	cDNA FLJ58247, highly similar to 26S protease regulatory subunit 4	13.14909625	7.447316885

376	IPI00011916.1	Aminoacyl tRNA synthase complex-interacting multifunctional prote	13.07555175	26.68466663
377	IPI00007694.5	Isoform 1 of Protein phosphatase methylesterase 1	13.06180024	12.27838659
378	IPI00005161.3	Actin-related protein 2/3 complex subunit 2	13.05300403	13.93984199
379	IPI00793205.1	cDNA FLJ56571, highly similar to Splicing factor, arginine/serine-rich	13.04667401	2.993952513
380	IPI01013544.1	cDNA FLJ54328, highly similar to Heat shock 70 kDa protein 1	13.04402208	75.04023147
381	IPI00014577.1	Ras-related protein Rab-18	12.96826291	18.26451421
382	IPI00795257.3	Glyceraldehyde-3-phosphate dehydrogenase	12.95435119	42.29723239
383	IPI00917605.1	cytochrome c, somatic	12.88886666	11.01686788
384	IPI00216293.6	Thiosulfate sulfurtransferase	12.8551867	2.791210413
385	IPI00019326.1	Adrenodoxin, mitochondrial	12.77173233	8.928052902
386	IPI00009253.2	Alpha-soluble NSF attachment protein	12.71969557	2.872599125
387	IPI00018671.1	Dual specificity protein phosphatase 3	12.64930868	18.46640468
388	IPI00973816.1	proteasome (prosome, macropain) 26S subunit, non-ATPase, 13	12.64352679	27.08849835
389	IPI01013402.1	cDNA FLJ46429 fis, clone THYMU3014372, highly similar to DNA replic	12.61844373	40.9428072
390	IPI00643876.2	cDNA FLJ50466, highly similar to DNA (cytosine-5)-methyltransferase	12.58668089	15.16066217
391	IPI00025156.4	Isoform 1 of E3 ubiquitin-protein ligase CHIP	12.58575606	8.156795502
392	IPI00745893.2	small ubiquitin-related modifier 2 isoform b precursor	12.5713799	6.090990543
393	IPI00005050.1	28S ribosomal protein S14, mitochondrial	12.56365681	8.25626111
394	IPI00292135.1	Lamin-B receptor	12.54350257	22.18463612
395	IPI00645869.1	Isoform 2 of Protein LAS1 homolog	12.4950614	15.71039009
396	IPI00554521.2	Ferritin heavy chain	12.49393749	31.01583433
397	IPI00645898.3	X-prolyl aminopeptidase (Aminopeptidase P) 1, soluble	12.43623996	21.54259062
398	IPI00011997.4	chromosome 8 open reading frame 33	12.41482973	3.802040815
399	IPI00029266.1	Small nuclear ribonucleoprotein E	12.33372808	12.59852314
400	IPI00794746.1	Uncharacterized protein	12.33148813	6.071681738
401	IPI00945960.1	signal sequence receptor, gamma (translocon-associated protein ga	12.29565358	12.55513477
402	IPI00005705.1	Isoform Gamma-1 of Serine/threonine-protein phosphatase PP1-gar	12.20368648	62.51254654
403	IPI00966877.1	tRNA (cytosine-5-)-methyltransferase NSUN2 isoform 2	12.2026782	27.62003875
404	IPI00025340.3	Pyridoxal phosphate phosphatase	12.19011784	6.942385197
405	IPI01014044.1	Isoform 1 of NADH dehydrogenase [ubiquinone] 1 beta subcomplex	12.06624794	12.12593031
406	IPI00020510.1	CDGSH iron-sulfur domain-containing protein 1	12.0614717	8.634587288
407	IPI00965541.1	CCHC-type zinc finger, nucleic acid binding protein	11.95422387	13.28625417
408	IPI00480093.6	ERO1-like beta	11.92051363	6.071348906
409	IPI00927582.2	Isoform 5 of Serrate RNA effector molecule homolog	11.88848162	30.37669873
410	IPI00979721.1	Isoform 3 of Mini-chromosome maintenance complex-binding prote	11.88371491	12.42308044
411	IPI00218054.2	Selenoprotein H	11.86993909	5.228617668
412	IPI00788938.1	L-lactate dehydrogenase	11.76095319	35.13553357
413	IPI00028481.1	Ras-related protein Rab-8A	11.74769545	19.31895494
414	IPI00154590.6	MKI67 FHA domain-interacting nucleolar phosphoprotein	11.72099137	55.91034389
415	IPI00001655.1	chromosome 16 open reading frame 80	11.67676139	15.90857196
416	IPI00166483.2	transmembrane protein 256	11.63630533	6.518399239
417	IPI00798211.1	tubulin folding cofactor B	11.49359608	11.63812995
418	IPI00930694.1	insulin-like growth factor 2 mRNA-binding protein 1 isoform 2	11.47464442	9.614244461
419	IPI00028277.8	Isoform 1 of Alpha-ketoglutarate-dependent dioxygenase FTO	11.45226812	10.07923675
420	IPI00219512.2	Isoform 2 of Ubiquitin carboxyl-terminal hydrolase isozyme L5	11.39187741	20.55851364
421	IPI00298961.3	Exportin-1	11.3826592	52.11610389
422	IPI01013273.1	cDNA, FLJ79129, highly similar to T-complex protein 1 subunit zeta	11.35524893	7.006772041

423	IPI00793102.1	ribosomal protein L35a	11.35146785	12.99345636
424	IPI00016597.3	Ceroid-lipofuscinosis neuronal protein 6	11.30901694	7.689606667
425	IPI01015738.1	Alpha actinin 4 short isoform	11.29110169	6.77367425
426	IPI00759659.1	Isoform 2 of Golgi membrane protein 1	11.22557688	6.926651716
427	IPI00909691.1	cDNA FLJ50174, highly similar to Homo sapiens SNARE protein Ykt6 (Y	11.2249918	6.76971817
428	IPI00910422.2	cDNA FLJ52802, highly similar to Eukaryotic translation initiation fac	11.21058941	17.07328272
429	IPI01011335.1	cDNA FLJ60435, highly similar to Heterogeneous nuclear ribonucleop	11.08753657	17.91938734
430	IPI00217413.3	ATP-dependent RNA helicase DHX29	11.08337402	18.55859256
431	IPI00910455.1	cDNA FLJ60259, highly similar to Elongation factor Ts, mitochondrial	11.05444479	6.411585569
432	IPI00100460.2	Aspartyl-tRNA synthetase, mitochondrial	11.03229046	27.18651175
433	IPI00250297.3	L-aminoadipate-semialdehyde dehydrogenase-phosphopantethein	11.0196867	31.70700741
434	IPI00290416.3	Isoform 1 of Obg-like ATPase 1	11.0009377	15.52790523
435	IPI00414347.2	Isoform 2 of Ankyrin repeat and SOCS box protein 18	10.96737456	2.774348736
436	IPI00171665.1	Nucleoporin Nup37	10.9279871	10.40621829
437	IPI00984414.2	Elongation factor 1-alpha	10.92542124	18.99169207
438	IPI00908662.2	ribosomal protein L4	10.87329102	3.33714366
439	IPI00003949.1	Ubiquitin-conjugating enzyme E2 N	10.85238695	7.103901386
440	IPI00215920.8	ADP-ribosylation factor 6	10.78922439	8.970561504
441	IPI00002902.5	Polynucleotide 5'-hydroxyl-kinase NOL9	10.75507736	23.95106339
442	IPI00910298.1	cDNA FLJ56236, highly similar to Exportin-2	10.71265221	14.08889389
443	IPI01009326.1	cDNA FLJ53379, highly similar to T-complex protein 1 subunit theta	10.65254021	9.490504503
444	IPI00100656.3	Isoform 1 of Trans-2,3-enoyl-CoA reductase	10.63536382	10.27974463
445	IPI00178431.12	ATP-dependent DNA helicase Q1	10.52583528	25.62801909
446	IPI00011250.3	Ubiquitin carboxyl-terminal hydrolase isozyme L3	10.51327205	2.848175764
447	IPI00003968.1	NADH dehydrogenase [ubiquinone] 1 alpha subcomplex subunit 9, r	10.48416424	22.29064155
448	IPI00792023.2	Ariadne homolog 2 variant (Fragment)	10.43514371	8.87221384
449	IPI00788612.2	LIM and senescent cell antigen-like-containing domain protein 1	10.40838933	54.09051752
450	IPI01015006.1	cDNA FLJ14416 fis, clone HEMBA1005202, highly similar to SIGNAL REC	10.32061744	26.9031744
451	IPI00984941.1	lysophospholipase I	10.24244213	12.11687398
452	IPI01010794.1	THO complex subunit 4	10.18708611	7.619431019
453	IPI00167549.3	ADP-ribosylation factor-like 14 effector protein	10.16257095	2.859004498
454	IPI00299084.1	Transmembrane protein 33	10.13495803	16.83365798
455	IPI00980668.1	heterogeneous nuclear ribonucleoprotein H1 (H)	10.12468576	11.15116978
456	IPI00555878.1	Probable DNA dC->dU-editing enzyme APOBEC-3C	10.09930563	12.15285873
457	IPI00741996.9	KM-PA-2 protein	10.09748459	51.81624365
458	IPI00000006.1	GTPase HRas	10.09243774	15.75251102
459	IPI00744692.1	Transaldolase	10.09027243	24.16368175
460	IPI00015956.3	Exosome complex component RRP40	10.0793612	6.181510687
461	IPI00373882.2	replication factor C subunit 3 isoform 2	10.07904959	6.745334148
462	IPI00645646.1	17 kDa protein	9.952640533	15.1362884
463	IPI00793232.1	cDNA FLJ59109, highly similar to Pyridoxine-5'-phosphate oxidase	9.920525074	3.588242531
464	IPI00218857.1	Isoform 1 of Dual specificity mitogen-activated protein kinase kinas	9.890594721	3.283116579
465	IPI00294943.1	Protein ariadne-1 homolog	9.876232147	18.67661929
466	IPI00926585.1	eukaryotic translation elongation factor 1 beta 2	9.847770691	3.480661154
467	IPI00021266.1	60S ribosomal protein L23a	9.834607363	17.05376267
468	IPI00909181.1	GrpE protein homolog	9.780870676	6.555705309
469	IPI00020602.1	Casein kinase II subunit alpha'	9.737714052	5.432087421

470	IPI00927255.1	LanC lantibiotic synthetase component C-like 1 (bacterial)	9.692457914	16.40298176
471	IPI01012426.1	RAP1B, member of RAS oncogene family	9.666450977	2.987706423
472	IPI00759596.1	Isoform 4 of Heterogeneous nuclear ribonucleoproteins C1/C2	9.631971359	8.547278166
473	IPI00184525.2	Isoform 2 of Methylthioribose-1-phosphate isomerase	9.610852718	3.093814373
474	IPI00019912.3	Peroxisomal multifunctional enzyme type 2	9.566012144	22.61170793
475	IPI00847986.1	Isoform 2 of 40S ribosomal protein S24	9.536608696	15.47692728
476	IPI00939558.2	cDNA FLJ38696 fis, clone KIDNE2001931, highly similar to HETEROGEN	9.513035297	12.05787754
477	IPI00397904.6	Nuclear pore complex protein Nup93	9.509429932	32.65908766
478	IPI00006113.1	DNA-directed RNA polymerase II subunit RPB9	9.481889009	9.967593908
479	IPI00641665.1	interleukin enhancer binding factor 2, 45kDa	9.44649291	10.82668447
480	IPI00329600.3	Probable saccharopine dehydrogenase	9.4371171	9.199316978
481	IPI00100984.4	Isoform 1 of HEAT repeat-containing protein 3	9.334487915	10.81985712
482	IPI00967562.1	heterogeneous nuclear ribonucleoprotein D (AU-rich element RNA b	9.321878672	5.888921976
483	IPI00939491.1	Isoform 2 of Cysteinyl-tRNA synthetase, cytoplasmic	9.261469126	46.16977072
484	IPI00963816.1	phosphoribosylaminoimidazole carboxylase, phosphoribosylamino	9.248252392	7.062841654
485	IPI00012353.1	39S ribosomal protein L3, mitochondrial	9.221636057	23.34996629
486	IPI00215974.2	Queuine tRNA-ribosyltransferase	9.1964674	15.76839066
487	IPI00556157.1	Polypyrimidine tract-binding protein 1 isoform c variant (Fragment)	9.12130475	5.903226376
488	IPI00910419.1	cDNA FLJ52929, highly similar to Dolichyl-diphosphooligosaccharide	9.084523201	6.170256138
489	IPI00983417.1	CD59 molecule, complement regulatory protein	9.036623478	9.638309956
490	IPI00152912.1	Isoform B of Ectodysplasin-A receptor-associated adapter protein	9.005042553	4.228182316
491	IPI00893580.1	HLA-B associated transcript 1	8.983823538	17.40922332
492	IPI00921560.2	Isoform 2 of Polycomb group RING finger protein 1	8.963470936	3.294580221
493	IPI00155601.1	MACRO domain-containing protein 1	8.959338903	3.539744139
494	IPI01011575.1	cDNA FLJ60080, highly similar to 130 kDa leucine-rich protein (Fragm	8.913601875	12.86030412
495	IPI00924895.1	SNRPG protein	8.880480289	8.205285788
496	IPI00514956.1	Rab geranylgeranyltransferase, beta subunit	8.827101946	10.16696143
497	IPI00016746.1	Isoform 1 of Core-binding factor subunit beta	8.752801418	4.835932732
498	IPI00398131.4	Isoform 1 of Protein lin-28 homolog B	8.721138	40.98487496
499	IPI00382459.1	Isoform 3 of Cullin-3	8.651211977	7.626033545
500	IPI00642213.1	RNA binding protein, autoantigenic	8.526372194	18.50947499
501	IPI00184884.6	Non-structural maintenance of chromosomes element 1 homolog	8.472459793	3.866527081
502	IPI00037448.3	Glyoxylate reductase/hydroxypyruvate reductase	8.332123518	37.4287343
503	IPI00334282.2	Protein FAM3C	8.316915274	6.036994934
504	IPI00847896.1	Similar to Glutamate-rich WD repeat-containing protein 1	8.295090675	10.13525772
505	IPI00025086.4	Cytochrome c oxidase subunit 5A, mitochondrial	8.239332438	6.078767776
506	IPI00031106.1	Proteasome assembly chaperone 3	8.186425209	4.018624306
507	IPI00910980.1	IARS protein	8.16508317	13.75889993
508	IPI00927674.1	cDNA FLJ51867, highly similar to Ras-related protein Rab-5A	8.127687931	4.493696213
509	IPI00783302.1	Isoform 1 of Pentatricopeptide repeat-containing protein 3, mitocho	8.112862825	11.22996235
510	IPI00747810.3	fascin homolog 1, actin-bundling protein (Strongylocentrotus purpur	8.111647129	11.07534266
511	IPI00514399.1	ribosomal protein S27	8.091253519	18.15767574
512	IPI00007175.3	Isoform 1 of 60S ribosome subunit biogenesis protein NIP7 homolog	8.060260534	15.19271469
513	IPI00954146.2	cDNA FLJ31682 fis, clone NT2RI2005335, highly similar to MMS19-like	7.972952843	14.81135249
514	IPI00943181.1	proteasome (prosome, macropain) activator subunit 2 (PA28 beta)	7.944501638	6.811487913
515	IPI00336094.5	Isoform 2 of 3-hydroxyacyl-CoA dehydrogenase type-2	7.888287306	8.275798321
516	IPI00008438.1	40S ribosomal protein S10	7.886199474	11.52813387

517	IPI00014198.3	Exosome complex component RRP42	7.845750332	23.2186923
518	IPI00170972.2	UPF0553 protein C9orf64	7.828207016	19.82426786
519	IPI00965022.1	ring finger and CHY zinc finger domain containing 1, E3 ubiquitin pro	7.766227722	2.837225437
520	IPI00394982.1	DEAD (Asp-Glu-Ala-Asp) box polypeptide 52	7.727472305	24.68902898
521	IPI01011073.1	cDNA FLJ55446, highly similar to Superkiller viralicidic activity 2-like	7.663134575	18.66403675
522	IPI00011770.1	NADH dehydrogenase [ubiquinone] 1 alpha subcomplex subunit 4	7.633547544	11.51311016
523	IPI00784161.1	Isoform 1 of Transcription elongation factor SPT6	7.614886999	15.28077078
524	IPI00009471.1	WD repeat-containing protein 3	7.614540577	35.85176802
525	IPI00016372.1	Ras-related protein Rab-9A	7.587427855	7.753925085
526	IPI00412714.3	Isoform 4 of Plasminogen activator inhibitor 1 RNA-binding protein	7.568902731	13.90614605
527	IPI00908317.2	ring finger protein 114	7.559832811	2.772971153
528	IPI00973067.1	P450 (cytochrome) oxidoreductase	7.506262779	11.68334246
529	IPI00977430.1	cDNA, FLJ79286, highly similar to T-complex protein 1 subunit gamma	7.426075459	67.55640221
530	IPI00220919.1	Isoform 3 of DNA (cytosine-5)-methyltransferase 1	7.415436745	29.40709066
531	IPI00025178.3	Pre-mRNA-splicing factor SPF27	7.403060198	8.553205252
532	IPI00010218.1	Cytochrome P450 monooxygenase	7.382110596	8.127945662
533	IPI00413958.5	Isoform 2 of Filamin-C	7.362661839	6.055697441
534	IPI00646783.2	TRMT1-like protein isoform 2	7.26845789	11.58942533
535	IPI00979604.1	ribosomal protein S3	7.249117374	10.05483961
536	IPI00010418.6	Isoform 2 of Myosin-Ic	7.232308149	5.530830622
537	IPI00927400.1	leucine-rich repeats and calponin homology (CH) domain containing	7.231191158	10.10188627
538	IPI00642982.1	LONP1 protein	7.214317322	22.44947171
539	IPI00220114.1	Isoform 3 of Slit homolog 2 protein	7.173071146	7.331262827
540	IPI00910979.1	pyruvate kinase isozymes M1/M2 isoform e	7.110543251	16.17550302
541	IPI00967721.1	matrin 3	7.101774693	22.11561322
542	IPI00219840.4	Isoform 1 of AP-2 complex subunit sigma	7.097867489	2.949874163
543	IPI00967490.1	cDNA FLJ56719, highly similar to Probable dimethyladenosine transf	7.090898037	14.38364577
544	IPI01015385.1	Isocitrate dehydrogenase	7.07719636	15.28122592
545	IPI00909939.1	cDNA FLJ52195, highly similar to LIM and SH3 domain protein 1	7.049134731	18.06489325
546	IPI00145260.3	Putative transferase CAF17, mitochondrial	6.990388155	17.54720378
547	IPI00029264.4	Cytochrome c1, heme protein, mitochondrial	6.984880447	6.802279472
548	IPI00790752.1	NADH dehydrogenase (ubiquinone) 1 beta subcomplex, 9, 22kDa	6.95763278	4.443318844
549	IPI00008164.2	Prolyl endopeptidase	6.91545105	21.66241336
550	IPI00641719.1	Surfeit 4	6.90372467	10.94220948
551	IPI00178047.7	proline, glutamate and leucine rich protein 1	6.89819169	9.530154705
552	IPI00395777.6	CCR4-NOT transcription complex subunit 7 isoform 2	6.879837036	3.427024841
553	IPI00964815.1	hexosaminidase B (beta polypeptide)	6.878056526	3.192093849
554	IPI00419263.4	enoyl-CoA delta isomerase 2, mitochondrial isoform 1	6.834798098	12.46290755
555	IPI00514078.1	Isoform 5 of Pogo transposable element with ZNF domain	6.818772078	22.88752937
556	IPI00005154.1	FACT complex subunit SSRP1	6.817866087	22.53734565
557	IPI00979883.1	phosphatidylserine synthase 1	6.789215803	7.925734043
558	IPI00017704.3	Coactosin-like protein	6.788805962	3.505471468
559	IPI00915421.1	vitamin K-dependent gamma-carboxylase isoform 2	6.780940533	11.76735616
560	IPI00033770.5	Isoform 1 of Probable alpha-ketoglutarate-dependent dioxygenase	6.766112328	18.29696798
561	IPI00400922.5	Protein RRP5 homolog	6.764267206	92.87314916
562	IPI00976971.1	cDNA FLJ51637, highly similar to Metastasis-associated protein MTA	6.759697199	9.131706953
563	IPI00854687.2	Isoform 2 of Sister chromatid cohesion protein PDS5 homolog A	6.751713753	7.598765135

564	IPI00644653.1	cDNA FLJ56337, highly similar to High mobility group protein B1	6.738008976	33.20047784
565	IPI00969375.1	Hydroxyacyl-Coenzyme A dehydrogenase/3-ketoacyl-Coenzyme A thio	6.722335577	5.969776154
566	IPI01010659.1	ATP-binding cassette, sub-family C (CFTR/MRP), member 1	6.717027664	9.024774551
567	IPI00219504.1	Isoform 2 of Ubiquitin carboxyl-terminal hydrolase 15	6.623579979	6.502687693
568	IPI00061531.4	39S ribosomal protein L53, mitochondrial	6.616873503	4.070573807
569	IPI00879792.1	Cytochrome b5 reductase 3	6.559267282	2.853048086
570	IPI00871956.1	Similar to Ribosomal protein S2	6.558877945	5.107149363
571	IPI00061525.3	Glucosamine 6-phosphate N-acetyltransferase	6.554480791	15.9050281
572	IPI00922694.1	cDNA FLJ51903, highly similar to Stress-70 protein, mitochondrial	6.526292324	6.769001722
573	IPI00872800.3	cDNA FLJ13369 fis, clone PLACE1000610, weakly similar to MSN5 PROT	6.474249125	7.574740648
574	IPI00645201.1	Ribosomal protein S8	6.465322495	10.60897493
575	IPI00300299.6	Signal peptidase complex subunit 3	6.444749594	9.801193237
576	IPI00375145.1	Isoform Short of Ubiquitin carboxyl-terminal hydrolase 5	6.440598011	22.03447986
577	IPI00925437.1	proteasome (prosome, macropain) 26S subunit, non-ATPase, 2	6.434225321	3.400685072
578	IPI00328885.3	immunoglobulin-like and fibronectin type III domain-containing pro	6.432921171	9.719846487
579	IPI00746351.2	Isoform 1 of Exosome complex exonuclease RRP44	6.390559196	77.7708149
580	IPI00003327.1	ADP-ribosylation factor-like protein 3	6.376639128	15.37890005
581	IPI00908881.2	Glucose-6-phosphate isomerase	6.348568916	48.91212177
582	IPI00908776.2	actinin, alpha 4	6.348047733	11.78577113
583	IPI00964684.1	heat shock 70kDa protein 4-like	6.31890583	14.87951994
584	IPI00301364.3	Isoform 1 of S-phase kinase-associated protein 1	6.236357689	15.45435095
585	IPI00006970.2	Mitochondrial 28S ribosomal protein S2	6.224236012	5.738352776
586	IPI00984288.1	Conserved hypothetical protein	6.20807004	3.053001404
587	IPI00018364.2	Ras-related protein Rap-2b	6.203061819	15.88207364
588	IPI00940901.1	Isoform 2 of RRP12-like protein	6.19925189	26.62055063
589	IPI00854677.1	fused in sarcoma	6.19677496	16.18292904
590	IPI00152998.3	Leucine-rich repeat-containing protein 40	6.18484354	10.00075197
591	IPI00917086.1	cDNA FLJ53711, highly similar to TRF-proximal protein homolog	6.171779394	6.913748503
592	IPI00022832.1	Brain protein 44	6.114253283	5.5035429
593	IPI00293276.10	Macrophage migration inhibitory factor	6.095655203	5.905552149
594	IPI00032957.1	SUMO-conjugating enzyme UBC9	6.089789629	11.05720043
595	IPI00556640.1	PSAP protein	6.067298651	5.829153061
596	IPI00985413.1	e3 SUMO-protein ligase RanBP2-like	6.020735264	10.58321714
597	IPI00464999.2	HEAT repeat-containing protein 6	5.959110975	12.2603209
598	IPI00000181.2	mitochondrial ribosomal protein S24	5.954578161	8.018149137
599	IPI00604431.1	Isoform 2 of Cullin-associated NEDD8-dissociated protein 1	5.931916714	31.62165904
600	IPI00869040.2	Isoform 2 of Cytosolic Fe-S cluster assembly factor NUBP1	5.930080414	24.11399269
601	IPI00419531.2	Cleavage and polyadenylation specificity factor subunit 2	5.919741869	9.586447239
602	IPI00430472.2	Activating signal cointegrator 1 complex subunit 3	5.897911072	15.47793245
603	IPI00031615.3	Protein LLP homolog	5.780694723	3.592237473
604	IPI00292894.5	Pre-rRNA-processing protein TSR1 homolog	5.77294302	36.7349472
605	IPI00795212.1	Isoform 2 of Probable Xaa-Pro aminopeptidase 3	5.72518611	5.582162619
606	IPI00152240.3	Protein kish-A	5.718772411	2.775909185
607	IPI00877999.1	ribosomal protein L3	5.71636343	5.576543808
608	IPI00640892.1	Glyceronephosphate O-acyltransferase	5.714292765	5.636987925
609	IPI00982721.1	transcription elongation factor B (SIII), polypeptide 1 (15kDa, elongi	5.694688559	3.263932943
610	IPI00182289.6	40S ribosomal protein S29	5.664246559	2.92510581

611	IPI00301609.8	Serine/threonine-protein kinase Nek9	5.65256834	11.85293865
612	IPI00394987.3	Isoform 2 of F-box/LRR-repeat protein 12	5.642956734	8.256112576
613	IPI00974544.1	Isoform SV of 14-3-3 protein epsilon	5.52858901	5.959573984
614	IPI00943258.1	Uncharacterized protein	5.526394844	7.282265425
615	IPI00058192.1	Isoform 1 of GDP-fucose protein O-fucosyltransferase 1	5.434002638	26.76087356
616	IPI00743142.2	Isoform 1 of 6-phosphofructokinase, muscle type	5.428494692	22.03418517
617	IPI00472887.3	Isoform 2 of Cytoskeleton-associated protein 5	5.417030573	27.95958161
618	IPI00009597.1	Isoform SMN-delta7 of Survival motor neuron protein	5.387907982	35.93483925
619	IPI00059809.3	secretory carrier membrane protein 1	5.379752636	7.605496883
620	IPI00910384.1	family with sequence similarity 76, member A	5.370937824	4.471651554
621	IPI00917676.1	leucine-rich pentatricopeptide repeat containing	5.370515347	6.448785067
622	IPI00307259.12	DnaJ homolog subfamily C member 13	5.362244606	17.96756458
623	IPI00419919.6	Ribosomal protein L29	5.254568815	5.944256783
624	IPI00023728.1	Gamma-glutamyl hydrolase	5.247240782	13.57725263
625	IPI00021812.2	Neuroblast differentiation-associated protein AHNAK	5.227503061	8.485305548
626	IPI00795318.2	cDNA FLJ54365, highly similar to DNA replication licensing factor MCI	5.194228888	30.22742081
627	IPI00294495.5	Ubiquitin-fold modifier-conjugating enzyme 1	5.176022768	26.05916619
628	IPI00797850.2	Isoform 2 of Dual specificity mitogen-activated protein kinase kinas	5.119152308	3.745077372
629	IPI00300074.4	Phenylalanyl-tRNA synthetase beta chain	5.111426592	20.55725718
630	IPI00412741.1	Isoform 1 of Sideroflexin-4	5.057983398	7.226323843
631	IPI00917430.1	splicing factor 3b, subunit 1, 155kDa	5.043381691	8.899055958
632	IPI00744575.3	Isoform Short of Probable ubiquitin carboxyl-terminal hydrolase FAF	4.988269329	9.697586775
633	IPI00306383.2	Isoform 2 of Secretory carrier-associated membrane protein 3	4.843749523	10.43175745
634	IPI00747530.3	Isoform 3 of Tax1-binding protein 1	4.822367668	9.279594421
635	IPI00004839.1	Crk-like protein	4.729190826	7.640843868
636	IPI01012475.1	protein disulfide isomerase family A, member 3	4.72342968	3.185017109
637	IPI00020729.1	Insulin receptor substrate 4	4.552227974	8.339183807
638	IPI00644082.1	Isoform 3 of tRNA guanosine-2'-O-methyltransferase TRM11 homolo	4.451956272	4.14463377
639	IPI00977506.2	prohibitin	4.449507236	48.61954975
640	IPI00304409.3	Calcium-regulated heat stable protein 1	4.354152679	7.878768682
641	IPI00922290.1	cDNA FLJ53094, highly similar to Receptor expression-enhancing pro	4.316569328	3.844114304
642	IPI00439944.1	ARCN1 protein	4.308863163	6.997230768
643	IPI00022640.1	Neurogranin	4.29251194	3.468683958
644	IPI00013860.3	3-hydroxyisobutyrate dehydrogenase, mitochondrial	4.278584957	3.140899181
645	IPI00010463.5	GTP-binding protein 1	4.245082378	9.582326889
646	IPI00235412.7	dynamin 1-like	4.143373489	18.62033153
647	IPI00924593.1	cDNA FLJ52880, highly similar to Malate dehydrogenase, mitochondr	4.139891624	4.061082363
648	IPI00332511.5	Serine/threonine-protein phosphatase 2A 55 kDa regulatory subuni	4.128800392	10.31970835
649	IPI00894559.1	NDUFA10 protein	4.117241383	4.028757572
650	IPI00947406.1	chromosome 7 open reading frame 50	4.103247643	8.806075096
651	IPI00026328.3	Thioredoxin domain-containing protein 12	4.094028473	6.261412382
652	IPI00552646.1	chromosome X open reading frame 38	4.068939209	2.786943197
653	IPI00218050.2	Isoform 2 of DNA mismatch repair protein Mlh3	4.058671951	4.380568504
654	IPI00917166.1	dynactin 1	3.930629492	8.637899637
655	IPI00909432.1	Isoform 4 of Glutathione S-transferase kappa 1	3.926178217	3.271624804
656	IPI00925058.1	Ribosomal protein L15	3.923327684	3.402714968
657	IPI00293078.1	Probable ATP-dependent RNA helicase DDX27	3.905130386	10.28052139

658	IPI00032851.1	Coatomer subunit zeta-1	3.897438288	15.62135386
659	IPI00015891.1	Prefoldin subunit 4	3.881435871	3.21504283
660	IPI00749054.2	Isoform 3 of tRNA (uracil-5-)-methyltransferase homolog	3.856481314	8.432951927
661	IPI00847768.1	DEAD-box protein p72	3.846444368	3.573546648
662	IPI00217405.1	Isoform 1 of E3 ubiquitin-protein ligase UBR1	3.834622383	8.006597757
663	IPI00056357.3	UPF0556 protein C19orf10	3.834048986	5.605211735
664	IPI00106698.2	Protein pelota homolog	3.829904079	3.965002298
665	IPI00642454.1	Ribosomal protein L7a	3.825775385	2.914595127
666	IPI00026358.3	Gamma-aminobutyric acid receptor-associated protein-like 2	3.812661886	6.262497902
667	IPI00789134.5	Glyceraldehyde-3-phosphate dehydrogenase	3.793359756	20.75409532
668	IPI01015636.1	pogo transposable element with ZNF domain	3.788869143	3.18219471
669	IPI00005218.1	Molybdopterin synthase catalytic subunit	3.785743475	4.095580101
670	IPI00788157.1	Isoform 2 of 5'-3' exoribonuclease 2	3.778432369	31.18069959
671	IPI00930594.1	acyl-coenzyme A thioesterase 13 isoform 2	3.753232479	3.017426491
672	IPI00103599.1	BRI3-binding protein	3.745472908	7.51076436
673	IPI01010993.1	19 kDa protein	3.739369869	2.845736027
674	IPI00916188.1	Nucleolin	3.739291668	19.88579917
675	IPI00797533.2	mitochondrial ribosomal protein L46	3.728572607	2.894883871
676	IPI00965481.1	ribosomal protein S3A	3.728090525	3.205724955
677	IPI00219025.3	Glutaredoxin-1	3.71999979	3.495915413
678	IPI00456702.3	Isoform 2 of COMM domain-containing protein 4	3.700555325	3.986202955
679	IPI00647001.1	Acidic (Leucine-rich) nuclear phosphoprotein 32 family, member B	3.680024862	4.003193855
680	IPI00554617.2	cDNA FLJ57277, highly similar to Tripeptidyl-peptidase 1	3.667347193	7.41711092
681	IPI00031982.1	Isoform 1 of Nck-associated protein 1	3.667258739	22.90902853
682	IPI00893242.1	aminoacyl tRNA synthetase complex-interacting multifunctional pro	3.666265249	5.994104862
683	IPI00925990.1	DEAD (Asp-Glu-Ala-Asp) box helicase 56	3.663386106	3.793273449
684	IPI00026167.5	NHP2-like protein 1	3.65789938	16.38205147
685	IPI00299506.9	Isoform 2 of Glucosamine--fructose-6-phosphate aminotransferase	3.639338017	19.81249595
686	IPI00983028.1	proline synthetase co-transcribed homolog (bacterial)	3.639157534	2.893331528
687	IPI00003004.1	Mitochondrial glutamate carrier 1	3.633758783	3.708626747
688	IPI00794773.1	cDNA FLJ51912, highly similar to Fumarylacetoacetase	3.633337021	3.022817612
689	IPI00642816.2	Isoform 1 of Signal recognition particle 9 kDa protein	3.61745286	3.627454281
690	IPI00106642.4	Dihydropyrimidinase-like 2	3.612304211	4.149096012
691	IPI01018285.1	FAD-dependent oxidoreductase domain containing 1	3.607123137	2.839509249
692	IPI00032911.3	TATA box-binding protein-like protein 1	3.604743958	7.538852692
693	IPI00333763.7	Glutaredoxin-related protein 5, mitochondrial	3.548946619	4.103365421
694	IPI00743342.2	Four and a half LIM domains protein 2	3.543523312	8.178222895
695	IPI00009148.1	Diphosphoinositol polyphosphate phosphohydrolase 1	3.536843538	4.002020359
696	IPI00032827.1	Pre-mRNA branch site protein p14	3.524932384	8.709682941
697	IPI00306642.3	DDB1- and CUL4-associated factor 13	3.523300171	3.617166281
698	IPI00980440.1	aminopeptidase puromycin sensitive	3.513344288	3.441233397
699	IPI00926546.2	TIA1 cytotoxic granule-associated RNA binding protein	3.510085106	3.830174446
700	IPI01015488.1	estrogen-related receptor alpha	3.497158766	3.681059122
701	IPI00015609.1	DDB1- and CUL4-associated factor 16	3.492106438	3.067657709
702	IPI00658162.2	cDNA FLJ36570 fis, clone TRACH2011302, highly similar to SELENIDE,W	3.480367899	4.516431808
703	IPI00980890.2	cDNA FLJ58780, highly similar to Homo sapiens lysosomal-associate	3.47510457	6.85842371
704	IPI00642486.1	ubiquitin related modifier 1	3.474912643	3.344897985

705	IPI00917594.1	proteasome (prosome, macropain) 26S subunit, non-ATPase, 1	3.442355156	8.706087828
706	IPI00170596.1	Paired amphipathic helix protein Sin3a	3.438802481	5.449266911
707	IPI00927538.1	transducin (beta)-like 2	3.418755531	7.273132324
708	IPI00902463.1	cDNA FLJ46898 fis, clone UTERU3022168, highly similar to Protein FAM	3.396526098	21.77505827
709	IPI00783250.1	TRIP12 protein	3.389698505	9.825669765
710	IPI00412713.4	Sorting and assembly machinery component 50 homolog	3.37523222	7.850270987
711	IPI00909956.1	cDNA FLJ59103, highly similar to T-complex protein 1 subunit epsilon	3.369731665	4.03897047
712	IPI00797802.1	mitochondrial 2-oxoglutarate/malate carrier protein isoform 3	3.350028038	6.823238134
713	IPI00643263.1	Vps20-associated 1 homolog	3.347207785	11.76907969
714	IPI00384155.1	Full-length cDNA clone CS0DI002YH20 of Placenta of Homo sapiens	3.333331585	4.626288414
715	IPI00031526.3	chromosome 19 open reading frame 43	3.332810879	9.43253684
716	IPI00748354.1	Isoform 1 of Mitochondrial intermembrane space import and assem	3.330058098	12.85658073
717	IPI00642244.2	ER membrane protein complex subunit 1	3.329001665	6.481980085
718	IPI00816513.2	mutS homolog 2, colon cancer, nonpolyposis type 1 (E. coli)	3.318204403	3.714787483
719	IPI00646750.2	cytochrome c oxidase assembly factor 6 homolog (S. cerevisiae)	3.313561916	3.490073919
720	IPI00220373.5	Insulin-degrading enzyme	3.309896469	14.45638919
721	IPI00978986.1	nucleoporin 160kDa	3.309469938	31.80257511
722	IPI01009290.1	cDNA FLJ52916, highly similar to ribosomal RNA methyltransferase 1	3.304074526	2.816954136
723	IPI00396056.6	Isoform p18 of 7,8-dihydro-8-oxoguanine triphosphatase	3.296686649	3.553375483
724	IPI00646767.1	nuclear distribution C homolog (A. nidulans)	3.292669296	7.126162052
725	IPI01015765.1	cDNA FLJ57240, highly similar to Mitochondrial proteins import recep	3.291688919	14.81278539
726	IPI00927379.1	LUC7-like	3.282767773	3.292594433
727	IPI00013396.3	U1 small nuclear ribonucleoprotein C	3.261357307	7.142628908
728	IPI00169325.1	WD repeat-containing protein 36	3.25672245	25.42709994
729	IPI00384571.3	MRPL43 protein (Fragment)	3.250708818	3.587357759
730	IPI00978302.1	cofilin 1 (non-muscle)	3.245178699	9.820427179
731	IPI00218895.6	DNA-directed RNA polymerase II subunit RPB7	3.242640018	8.362938881
732	IPI00791782.2	Isoform 3 of Transmembrane protein 85	3.238839149	3.189184427
733	IPI00877664.1	HNRPC protein	3.229525328	6.038960695
734	IPI00218838.1	Isoform 2 of Glomulin	3.226986408	3.44948864
735	IPI00019380.1	Nuclear cap-binding protein subunit 1	3.226590872	38.25334501
736	IPI00294211.2	Pre-mRNA-splicing factor ATP-dependent RNA helicase PRP16	3.224330187	3.504382849
737	IPI00946754.1	Protease serine 1	3.217814922	9.725289345
738	IPI00640188.1	PRA1 domain family, member 2	3.215258598	3.194475889
739	IPI00006574.1	family with sequence similarity 49, member A	3.203294277	6.060539007
740	IPI00787239.1	Isoform 2 of Transmembrane protein 70, mitochondrial	3.190694809	3.062651634
741	IPI00927631.1	nuclear cap binding protein subunit 2, 20kDa	3.180920124	3.165471554
742	IPI00796478.1	Synaptogyrin 1	3.178820372	3.604151011
743	IPI00974419.1	minichromosome maintenance complex component 4	3.172092199	10.73406553
744	IPI00965753.1	neurolysin (metallopeptidase M3 family)	3.166867971	7.52709794
745	IPI01013815.1	cDNA FLJ54736, highly similar to Scaffold attachment factor B	3.160569906	6.301415205
746	IPI00908568.1	replication factor C subunit 5 isoform 3	3.156708956	10.77553797
747	IPI00552972.3	ribophorin II	3.154435635	3.805977583
748	IPI00105068.2	mannose-P-dolichol utilization defect 1	3.145113468	7.013731241
749	IPI00894025.1	ribosomal protein L10	3.142888308	3.099099159
750	IPI00966408.1	hydroxysteroid (17-beta) dehydrogenase 11	3.126099825	5.856959581
751	IPI00647467.1	Isoform 2 of Protein-tyrosine phosphatase mitochondrial 1	3.116794348	6.496219635

752	IPI00399195.1	Isoform 2 of Cirhin	3.110436678	3.85973525
753	IPI00983399.1	RAB15, member RAS oncogene family	3.108854532	3.227412224
754	IPI00030847.3	Transmembrane 9 superfamily member 3	3.108247519	6.353409529
755	IPI00908532.1	cDNA FLJ57633, highly similar to Lysosome-associated membrane gly	3.107279062	4.186969757
756	IPI00377084.1	ribonuclease P/MRP protein subunit POP5 isoform c	3.103389263	2.764899731
757	IPI00063130.2	Transmembrane protein 205	3.094141006	3.628275633
758	IPI00027704.5	DNA primase small subunit	3.088574886	10.48273039
759	IPI00940786.2	cDNA FLJ50873, highly similar to DNA replication licensing factor MCI	3.08483696	5.70458436
760	IPI00872761.2	fragile X mental retardation 1 protein isoform ISO12	3.077638626	3.697481632
761	IPI00916398.1	IMP4, U3 small nucleolar ribonucleoprotein, homolog (yeast)	3.07574439	10.13596678
762	IPI00152377.1	Dolichyl-diphosphooligosaccharide--protein glycosyltransferase sul	3.0711689	8.360854387
763	IPI00410157.4	Isoform 4 of CCR4-NOT transcription complex subunit 1	3.069497108	3.153642654
764	IPI00513841.1	Nicastrin	3.068019867	10.66344333
765	IPI00396331.4	Zinc finger protein 224	3.063132048	3.123922348
766	IPI00796102.1	actin related protein 2/3 complex, subunit 3, 21kDa	3.056749344	3.016141176
767	IPI01011483.1	Fanconi anemia, complementation group I	3.054372311	7.051631212
768	IPI00655681.1	succinate dehydrogenase cytochrome b560 subunit, mitochondrial is	3.052879572	3.373564482
769	IPI00006442.1	Coilin	3.052608252	8.148685455
770	IPI00007052.6	Mitochondrial fission 1 protein	3.050519466	3.074013233
771	IPI00166013.1	AAR2 splicing factor homolog (S. cerevisiae)	3.047001362	6.960672855
772	IPI00884370.1	DFNA5 protein family protein	3.045160055	2.985293627
773	IPI00879437.1	prolyl 4-hydroxylase, beta polypeptide	3.028154373	2.977276087
774	IPI00328089.16	Isoform 2 of Transcription factor HIVEP3	3.015028477	3.170693398
775	IPI00329332.1	Syntaxin-12	3.009957552	28.30562234
776	IPI00639819.1	TAR DNA binding protein	3.003374338	25.38175821
777	IPI00983093.1	poly(A) binding protein, cytoplasmic 1	2.986663818	2.845418215
778	IPI00982362.1	Uncharacterized protein	2.985399246	5.20803833
779	IPI00418523.1	Similar to Nucleolar complex protein 2 homolog	2.976199865	3.104102135
780	IPI00008753.1	Metallothionein-1X	2.968417406	2.829637289
781	IPI00001146.1	U6 snRNA-associated Sm-like protein LSm6	2.96451807	5.99358058
782	IPI00892695.1	brain and reproductive organ-expressed (TNFRSF1A modulator)	2.953055382	3.993766069
783	IPI00977024.1	ring finger protein 170	2.939703226	5.906941414
784	IPI00401264.5	Endoplasmic reticulum resident protein 44	2.93690753	6.655044317
785	IPI00024775.1	Ras-related protein Rab-7L1	2.936436415	5.391480207
786	IPI00304935.6	Protein SAAL1	2.925481319	2.954362869
787	IPI00797749.1	cDNA FLJ34514 fis, clone HLUNG2006599, highly similar to Syntaxin-4	2.903419971	3.420435667
788	IPI00916988.1	Isoform 2 of RNA pseudouridylate synthase domain-containing prot	2.897808552	8.946968317
789	IPI00221232.9	Guanine nucleotide-binding protein G(I)/G(S)/G(O) subunit gamma-	2.892389297	2.927713156
790	IPI00556364.1	Interleukin enhancer binding factor 3 isoform c variant (Fragment)	2.874989986	7.323945999
791	IPI00916648.1	WD repeat and FYVE domain containing 1	2.858377695	7.127812862
792	IPI00477181.2	ring finger protein 220	2.857547522	3.856014013
793	IPI00026119.6	Ubiquitin-activating enzyme E1	2.853475094	4.151154995
794	IPI00978325.1	cathepsin C	2.779670954	3.754447222
795	IPI00945551.1	cms1 ribosomal small subunit homolog (yeast)	2.775691748	7.515066147
796	IPI00643908.3	cDNA FLJ53700, highly similar to Hepatoma-derived growth factor	2.774966478	6.971341133
797	IPI00477012.1	Isoform 2 of Double-stranded RNA-specific editase 1	2.773857355	6.595125914
798	IPI00019488.1	U3 small nucleolar ribonucleoprotein protein IMP3	2.759111643	3.54423666
799	IPI00514669.1	SH3 domain binding glutamic acid-rich protein like 3	2.708771467	2.784610033

Table A6: TMT (tandem mass tagging) analysis of BPPM-revealed nonhistone targets of G9a and GLP1 in HEK293T cells with HeySAM.

Serial	Accession	Description	EuHMT1 /Control	EuHMT2/control	EuHMT2/EuHMT1
1	IPI00942420.2	Isoform 1 of Histone-lysine N-methyltransferase EHMT1	11.339	2.382	0.177
2	IPI00186290.6	Elongation factor 2	2.165	2.251	1.068
3	IPI00220795.4	Isoform 2 of Histone-lysine N-methyltransferase EHMT2	3.336	8.583	2.815
4	IPI00792677.1	cDNA FLJ60097, highly similar to Tubulin alpha-ubiquitous	3.235	2.486	0.974
5	IPI00218343.4	Tubulin alpha-1C chain	2.023	1.946	0.988
6	IPI00909140.9	cDNA FLJ56903, highly similar to Tubulin beta-7 chain	1.940	1.987	1.135
7	IPI00007752.1	Tubulin beta-2C chain	1.973	1.748	0.805
8	IPI00984352.1	protein arginine methyltransferase 1	2.422	2.021	0.829
9	IPI00031370.3	Tubulin beta-2B chain	1.870	1.780	0.964
10	IPI00396485.3	Elongation factor 1-alpha 1	2.624	2.212	0.906
11	IPI00021439.1	Actin, cytoplasmic 1	2.832	2.426	0.761
12	IPI00219018.7	Glyceraldehyde-3-phosphate dehydrogenase	2.653	2.468	0.964
13	IPI00414676.6	Heat shock protein HSP 90-beta	2.646	1.937	0.874
14	IPI00022977.1	Creatine kinase B-type	2.975	2.219	0.698
15	IPI00784295.2	Isoform 1 of Heat shock protein HSP 90-alpha	3.106	2.186	0.803
16	IPI00455383.4	Isoform 2 of Clathrin heavy chain 1	3.055	2.569	0.858
17	IPI00922693.1	cDNA FLJ53662, highly similar to Actin, alpha skeletal mus	3.362	2.119	0.630
18	IPI00304925.5	Heat shock 70 kDa protein 1A/1B	2.487	1.846	0.756
19	IPI00465248.5	Isoform alpha-enolase of Alpha-enolase	1.863	1.812	0.945
20	IPI00925572.1	asparagine synthetase [glutamine-hydrolyzing] isoform b	2.863	2.544	0.843
21	IPI00014424.1	Elongation factor 1-alpha 2	2.509	2.783	1.109
22	IPI00911039.1	cDNA FLJ54408, highly similar to Heat shock 70 kDa protein	2.594	1.448	0.558
23	IPI00807545.1	Isoform 3 of Heterogeneous nuclear ribonucleoprotein K	2.952	2.073	0.699
24	IPI00465439.5	Fructose-bisphosphate aldolase A	2.469	2.025	0.825
25	IPI00784154.1	60 kDa heat shock protein, mitochondrial	2.529	1.899	0.719
26	IPI00000874.1	Peroxiredoxin-1	2.765	2.032	0.763
27	IPI00658109.1	Isoform 1 of Creatine kinase U-type, mitochondrial	3.039	2.232	0.709
28	IPI00644224.2	cDNA FLJ54020, highly similar to Heterogeneous nuclear ri	2.624	1.702	0.683
29	IPI00219217.3	L-lactate dehydrogenase B chain	2.764	2.605	1.007
30	IPI00644079.4	cDNA FLJ44920 fis, clone BRAMY3011501, highly similar to H	2.731	1.798	0.658
31	IPI00026781.3	Fatty acid synthase	2.964	2.663	0.869
32	IPI00011200.5	D-3-phosphoglycerate dehydrogenase	2.619	1.963	0.741
33	IPI00219446.5	Phosphatidylethanolamine-binding protein 1	2.175	1.704	0.759
34	IPI00012011.6	Cofilin-1	3.308	2.653	0.824
35	IPI00784090.2	T-complex protein 1 subunit theta	2.631	2.103	0.802
36	IPI00003865.1	Isoform 1 of Heat shock cognate 71 kDa protein	2.102	1.703	0.773
37	IPI00011253.3	40S ribosomal protein S3	3.011	2.497	0.818
38	IPI01011191.1	cDNA FLJ59681, highly similar to Plastin-3	3.086	1.659	0.470
39	IPI00220327.4	Keratin, type II cytoskeletal 1	2.287	1.729	0.774
40	IPI00021290.5	ATP-citrate synthase	2.196	2.134	0.894
41	IPI00479186.7	Isoform M2 of Pyruvate kinase isozymes M1/M2	2.648	2.020	0.754
42	IPI00220740.1	Isoform 2 of Nucleophosmin	2.539	1.996	0.753
43	IPI00216691.5	Profilin-1	4.000	2.225	0.589
44	IPI00419585.9	Peptidyl-prolyl cis-trans isomerase A	2.683	1.953	0.661

45	IPI00418471.6	Vimentin	1.785	1.825	1.011
46	IPI00797270.4	Isoform 1 of Triosephosphate isomerase	2.634	1.881	0.729
47	IPI00291006.2	Malate dehydrogenase, mitochondrial	2.107	2.238	1.075
48	IPI01015565.1	ubiquitin C	3.479	2.517	0.582
49	IPI00643041.3	GTP-binding nuclear protein Ran	2.540	1.998	0.793
50	IPI00645078.1	Ubiquitin-like modifier-activating enzyme 1	2.139	2.097	0.918
51	IPI00909207.1	cDNA FLJ60461, highly similar to Peroxiredoxin-2	2.018	1.734	0.840
52	IPI01011912.1	Phosphoglycerate kinase	2.799	2.184	0.814
53	IPI00299524.2	Condensin complex subunit 1	3.358	2.968	0.859
54	IPI00795292.1	Isoform 3 of Nucleoside diphosphate kinase B	3.114	2.009	0.644
55	IPI00217966.9	Isoform 1 of L-lactate dehydrogenase A chain	2.646	2.818	1.050
56	IPI00855957.3	Isoform 2 of Far upstream element-binding protein 2	2.656	2.098	0.821
57	IPI00003362.3	78 kDa glucose-regulated protein	2.163	1.669	0.794
58	IPI00010796.1	Protein disulfide-isomerase	2.409	1.888	0.778
59	IPI00554786.5	Isoform 5 of Thioredoxin reductase 1, cytoplasmic	2.733	2.238	0.792
60	IPI00937615.2	Elongation factor 1-gamma	2.291	2.167	0.991
61	IPI00414696.1	Isoform A2 of Heterogeneous nuclear ribonucleoproteins	2.808	2.370	0.877
62	IPI00297779.7	T-complex protein 1 subunit beta	1.750	1.661	0.948
63	IPI00012048.1	Isoform 1 of Nucleoside diphosphate kinase A	2.553	1.936	0.802
64	IPI00793443.2	Isoform 1 of Importin-5	2.190	2.055	0.830
65	IPI00966238.2	cDNA FLJ51907, highly similar to Stress-70 protein, mitocho	2.193	1.918	0.863
66	IPI00019755.3	Glutathione S-transferase omega-1	2.420	2.095	0.818
67	IPI00013881.6	Heterogeneous nuclear ribonucleoprotein H	1.974	2.192	1.090
68	IPI00013452.11	Bifunctional aminoacyl-tRNA synthetase	2.831	2.270	0.795
69	IPI00604620.3	Nucleolin	2.230	1.946	0.881
70	IPI00024145.2	Isoform 2 of Voltage-dependent anion-selective channel	2.874	2.206	0.733
71	IPI00216298.6	Thioredoxin	3.674	2.068	0.536
72	IPI00001639.2	Importin subunit beta-1	2.224	1.761	0.821
73	IPI00008530.1	60S acidic ribosomal protein P0	2.829	2.782	0.962
74	IPI00016610.2	Poly(rC)-binding protein 1	3.121	2.617	0.862
75	IPI00554723.5	60S ribosomal protein L10	2.698	1.944	0.785
76	IPI00815732.1	Isoform 2 of Multifunctional protein ADE2	2.572	1.956	0.769
77	IPI00021304.1	Keratin, type II cytoskeletal 2 epidermal	2.336	3.532	1.906
78	IPI00411704.9	Isoform 1 of Eukaryotic translation initiation factor 5A-1	2.761	1.999	0.668
79	IPI00021263.3	14-3-3 protein zeta/delta	2.606	2.007	0.801
80	IPI00000816.1	Isoform 1 of 14-3-3 protein epsilon	2.601	1.814	0.760
81	IPI00449049.5	Poly [ADP-ribose] polymerase 1	2.248	1.965	0.893
82	IPI00303568.3	Prostaglandin E synthase 2	2.252	2.005	0.855
83	IPI00025273.1	Isoform Long of Trifunctional purine biosynthetic protein	2.376	2.243	0.935
84	IPI00027230.3	Endoplasmin	1.765	1.717	0.973
85	IPI00844578.1	ATP-dependent RNA helicase A	2.631	2.390	0.936
86	IPI01012004.1	cDNA PSEC0175 fis, clone OVARC1000169, highly similar to F	2.518	2.258	0.807
87	IPI00003881.5	Heterogeneous nuclear ribonucleoprotein F	2.285	2.199	0.900
88	IPI00413324.6	60S ribosomal protein L17	2.389	1.800	0.737
89	IPI00759596.1	Isoform 4 of Heterogeneous nuclear ribonucleoproteins C	2.809	2.386	0.685
90	IPI01014604.1	T-complex protein 1 subunit delta	2.465	1.999	0.819
91	IPI00027107.5	elongation factor Tu, mitochondrial precursor	2.899	1.277	0.435

92	IPI00011937.1	Peroxiredoxin-4	2.623	2.223	0.792
93	IPI00009865.4	Keratin, type I cytoskeletal 10	1.774	1.649	0.878
94	IPI00003918.6	60S ribosomal protein L4	2.463	2.400	0.971
95	IPI00010720.1	T-complex protein 1 subunit epsilon	2.437	2.078	0.835
96	IPI00900327.2	cDNA FLJ58339, highly similar to Poly(rC)-binding protein 2	2.898	2.771	0.909
97	IPI00027442.4	Alanyl-tRNA synthetase, cytoplasmic	1.977	1.806	0.924
98	IPI00848161.1	Isoform 1 of Spliceosome RNA helicase DDX39B	2.135	2.056	0.926
99	IPI00002966.2	Heat shock 70 kDa protein 4	2.014	2.007	0.935
100	IPI00646304.4	Peptidyl-prolyl cis-trans isomerase B	2.587	2.063	0.810
101	IPI00018146.1	14-3-3 protein theta	3.096	2.403	0.743
102	IPI00551024.5	Bifunctional ATP-dependent dihydroxyacetone kinase/FAD	2.701	1.988	0.714
103	IPI00438230.3	Isoform 2 of Transcription intermediary factor 1-beta	2.593	2.159	0.832
104	IPI00216492.1	Isoform 2 of Heterogeneous nuclear ribonucleoprotein H3	2.698	2.502	0.938
105	IPI00922367.1	non-POU domain-containing octamer-binding protein isof	2.443	2.058	0.789
106	IPI00018206.4	Aspartate aminotransferase, mitochondrial	2.269	1.801	0.826
107	IPI00022774.3	Transitional endoplasmic reticulum ATPase	1.894	1.957	0.947
108	IPI00952607.1	T-complex protein 1 subunit eta isoform d	2.592	2.064	0.803
109	IPI00024933.3	Isoform 1 of 60S ribosomal protein L12	3.286	2.632	0.784
110	IPI00005198.2	Interleukin enhancer-binding factor 2	2.264	1.786	0.848
111	IPI00465365.4	Isoform A1-A of Heterogeneous nuclear ribonucleoprotein	2.983	2.679	1.093
112	IPI00218606.7	40S ribosomal protein S23	3.860	2.426	0.633
113	IPI00179964.5	Isoform 1 of Polypyrimidine tract-binding protein 1	2.330	2.018	0.866
114	IPI00220684.1	Isoform 3 of Heterogeneous nuclear ribonucleoprotein D0	2.759	2.111	0.709
115	IPI00789370.3	serine hydroxymethyltransferase, mitochondrial isoform 3	1.993	2.084	1.076
116	IPI00009904.1	Protein disulfide-isomerase A4	2.055	1.763	0.871
117	IPI00003935.6	Histone H2B type 2-E	2.516	1.883	0.799
118	IPI00290566.1	T-complex protein 1 subunit alpha	2.716	2.105	0.737
119	IPI00909530.1	Histone H3	3.197	2.420	0.726
120	IPI00220642.7	14-3-3 protein gamma	2.460	2.071	0.771
121	IPI00413344.3	Cofilin-2	2.917	1.744	0.598
122	IPI00218342.10	C-1-tetrahydrofolate synthase, cytoplasmic	2.043	1.994	0.892
123	IPI00552590.1	T-complex protein 1 subunit zeta isoform b	2.699	1.851	0.731
124	IPI00374151.1	thioredoxin-dependent peroxide reductase, mitochondria	2.175	1.811	0.894
125	IPI00012007.6	Adenosylhomocysteinase	2.106	1.733	0.779
126	IPI00004534.5	Phosphoribosylformylglycinamidine synthase	3.384	2.866	0.958
127	IPI00941747.1	Calnexin	2.364	2.007	0.816
128	IPI00031804.1	Isoform 1 of Voltage-dependent anion-selective channel p	2.744	1.955	0.764
129	IPI00219160.3	60S ribosomal protein L34	4.626	2.366	0.741
130	IPI00218547.1	Isoform Short of Delta-1-pyrroline-5-carboxylate synthase	2.585	2.431	0.903
131	IPI00025091.3	40S ribosomal protein S11	3.019	2.648	0.816
132	IPI00383296.5	Isoform 2 of Heterogeneous nuclear ribonucleoprotein M	1.904	1.946	1.121
133	IPI00013917.3	40S ribosomal protein S12	3.238	2.003	0.602
134	IPI00008433.4	40S ribosomal protein S5	2.118	1.858	0.909
135	IPI00470498.1	Isoform 3 of Plasminogen activator inhibitor 1 RNA-bindin	2.108	1.729	0.731
136	IPI00549389.3	Conserved hypothetical protein	2.651	2.138	0.806
137	IPI00017334.1	Prohibitin	2.330	1.929	0.765
138	IPI00001734.3	Phosphoserine aminotransferase	3.067	2.378	0.777

139	IPI00298547.3	Protein DJ-1	1.960	1.566	0.778
140	IPI00746438.2	Isoform 2 of 60S ribosomal protein L11	2.442	1.992	0.816
141	IPI00299000.5	Proliferation-associated protein 2G4	1.805	1.927	1.096
142	IPI00218993.1	Isoform Beta of Heat shock protein 105 kDa	2.411	2.322	0.836
143	IPI00908543.1	cDNA FLJ56133, highly similar to Serine/threonine-protein	2.493	1.876	0.727
144	IPI00783097.4	Glycyl-tRNA synthetase	2.289	2.009	0.894
145	IPI00220766.5	Lactoylglutathione lyase	2.323	2.021	0.826
146	IPI01013559.1	cDNA FLJ58502, highly similar to Protein disulfide-isomera	1.772	1.750	0.977
147	IPI00013485.3	40S ribosomal protein S2	2.800	2.408	0.831
148	IPI00216319.3	14-3-3 protein eta	2.527	2.068	0.818
149	IPI00783271.1	Leucine-rich PPR motif-containing protein, mitochondrial	2.427	2.464	1.086
150	IPI00219330.2	Isoform 5 of Interleukin enhancer-binding factor 3	2.334	2.255	0.934
151	IPI00219616.7	Ribose-phosphate pyrophosphokinase 1	2.620	2.537	0.958
152	IPI00385834.3	Isoform 2 of KH domain-containing, RNA-binding, signal tr	3.117	2.534	0.847
153	IPI00917777.1	116 kDa U5 small nuclear ribonucleoprotein component is	1.919	1.816	0.959
154	IPI00744692.1	Transaldolase	2.543	2.313	0.896
155	IPI00178440.3	Elongation factor 1-beta	2.598	2.042	0.763
156	IPI00026202.1	60S ribosomal protein L18a	2.840	1.865	0.699
157	IPI00759832.1	Isoform Short of 14-3-3 protein beta/alpha	2.380	1.672	0.702
158	IPI00794545.1	deoxyuridine 5'-triphosphate nucleotidohydrolase, mitoch	2.982	2.176	0.735
159	IPI00215914.5	ADP-ribosylation factor 1	3.212	2.464	0.767
160	IPI00025491.1	Eukaryotic initiation factor 4A-I	1.982	2.041	1.041
161	IPI01012872.1	58 kDa protein	2.907	1.608	0.569
162	IPI00982539.1	Dha kinase/FMN cyclase splice variant	2.604	1.808	0.694
163	IPI00553169.5	filamin A, alpha	3.595	2.753	0.769
164	IPI00952778.2	Isoform 1 of Probable ATP-dependent RNA helicase DDX17	2.188	2.166	0.998
165	IPI00479306.1	Isoform 1 of Proteasome subunit beta type-5	2.075	1.847	0.890
166	IPI00335168.9	Isoform Non-muscle of Myosin light polypeptide 6	3.051	2.311	0.757
167	IPI00383539.5	Citrate synthase	2.626	2.139	0.840
168	IPI00015018.1	Inorganic pyrophosphatase	2.877	3.493	1.068
169	IPI00291467.7	ADP/ATP translocase 3	1.906	1.540	0.808
170	IPI00007188.6	ADP/ATP translocase 2	2.710	2.043	0.754
171	IPI00455457.4	Histone H3	3.622	2.653	0.670
172	IPI00867533.1	60S ribosomal protein L6	4.121	3.937	0.954
173	IPI00940237.1	ATP-dependent RNA helicase DDX39A	2.267	2.190	0.966
174	IPI00908881.2	Glucose-6-phosphate isomerase	1.526	1.871	0.995
175	IPI00019502.3	Isoform 1 of Myosin-9	3.147	2.392	0.799
176	IPI00303722.5	Protein FAM136A	2.845	2.172	0.760
177	IPI00853337.1	ADP-ribosylation factor 5	2.486	1.525	0.613
178	IPI00011454.1	Isoform 2 of Neutral alpha-glucosidase AB	1.920	1.740	0.923
179	IPI00642042.3	Putative uncharacterized protein DKFZp686J1372	2.689	2.093	0.735
180	IPI00413641.7	Aldose reductase	2.471	2.503	1.050
181	IPI00893035.1	carbamoyl-phosphate synthetase 2, aspartate transcarbar	3.780	2.951	0.803
182	IPI00909975.1	Ubiquitin carrier protein	3.120	2.066	0.677
183	IPI00979136.1	Ribonucleoside-diphosphate reductase	3.118	2.590	0.857
184	IPI00646055.2	cDNA FLJ58608, highly similar to Heat shock protein 75 kDa	2.115	1.816	0.968
185	IPI00307524.7	Arsenite methyltransferase	2.513	1.947	0.782

186	IPI00221092.8	40S ribosomal protein S16	2.986	1.775	0.548
187	IPI00553185.2	T-complex protein 1 subunit gamma	2.158	1.318	0.666
188	IPI00909336.1	cDNA FLJ59092	2.392	2.960	1.100
189	IPI00550689.3	tRNA-splicing ligase RtcB homolog	2.903	2.518	0.807
190	IPI00219306.1	Protein mago nashi homolog	3.163	2.403	0.724
191	IPI01012504.1	6-phosphogluconate dehydrogenase, decarboxylating	2.080	1.981	0.983
192	IPI00218988.4	Isoform 2 of Adenylate kinase 2, mitochondrial	2.317	1.885	0.808
193	IPI00925196.2	IMP dehydrogenase 2	2.465	2.711	1.194
194	IPI00008964.3	Ras-related protein Rab-1B	2.501	1.906	0.769
195	IPI00977640.1	sodium/potassium-transporting ATPase subunit alpha-1 i	3.750	2.818	0.748
196	IPI00878876.1	cDNA FLJ51872, highly similar to Small nuclear ribonucleop	4.885	2.883	0.658
197	IPI00012750.3	40S ribosomal protein S25	2.879	2.375	0.703
198	IPI00418262.5	Fructose-bisphosphate aldolase			0.701
199	IPI00943894.1	glycogen phosphorylase, liver form isoform 2	1.981	1.804	0.910
200	IPI00845388.1	destrin isoform b	3.043	2.164	0.711
201	IPI00550363.3	Transgelin-2	2.331	2.020	0.854
202	IPI00419880.6	40S ribosomal protein S3a	2.572	1.882	0.704
203	IPI00216613.1	Isoform Short of Splicing factor, proline- and glutamine-ri	2.088	1.825	0.874
204	IPI00045498.4	Isoform 3 of Heterogeneous nuclear ribonucleoprotein D-	2.142	2.281	1.053
205	IPI00219617.5	Isoform 1 of Ribose-phosphate pyrophosphokinase 2	3.052	3.192	1.046
206	IPI00944455.2	NCAPD2 protein (Fragment)	3.607	2.731	0.757
207	IPI01015230.1	cDNA FLJ53354, highly similar to Puromycin-sensitive amin	2.147	2.138	0.946
208	IPI00221093.7	40S ribosomal protein S17	3.664	2.495	0.679
209	IPI00009328.4	Eukaryotic initiation factor 4A-III	2.328	2.164	0.892
210	IPI00300371.5	Isoform 1 of Splicing factor 3B subunit 3	3.437	2.744	0.861
211	IPI00021828.1	Cystatin-B	3.225	1.946	0.556
212	IPI00003949.1	Ubiquitin-conjugating enzyme E2 N	3.313	1.931	0.777
213	IPI00182533.5	60S ribosomal protein L28	3.884	2.581	0.662
214	IPI00013214.2	cDNA FLJ55599, highly similar to DNA replication licensing	2.176	1.988	0.848
215	IPI00982482.2	isoleucyl-tRNA synthetase	3.378	2.595	0.872
216	IPI00022597.1	NEDD8-conjugating enzyme Ubc12	2.581	1.817	0.774
217	IPI00010153.5	60S ribosomal protein L23	3.639	2.198	0.614
218	IPI00220301.5	Peroxiredoxin-6	2.928	2.133	0.782
219	IPI00402182.2	Isoform 2 of Heterogeneous nuclear ribonucleoprotein Q	2.531	1.013	0.400
220	IPI00005719.1	Isoform 1 of Ras-related protein Rab-1A	1.923	1.450	0.754
221	IPI00981739.1	tubulin folding cofactor A	3.239	1.791	0.609
222	IPI00102128.1	Isoform 1 of Protein arginine N-methyltransferase 6	2.516	1.250	0.508
223	IPI00022239.7	Methionine aminopeptidase 1	2.676	2.228	0.813
224	IPI00217030.10	40S ribosomal protein S4, X isoform	2.486	1.903	0.772
225	IPI01013843.1	cDNA FLJ59776, highly similar to Prefoldin subunit 3	2.072	1.488	0.718
226	IPI00220834.8	X-ray repair cross-complementing protein 5	2.113	1.852	0.879
227	IPI00221088.5	40S ribosomal protein S9	2.907	2.537	0.976
228	IPI00008240.2	Methionyl-tRNA synthetase, cytoplasmic	1.964	2.173	0.995
229	IPI00740142.2	u5 small nuclear ribonucleoprotein 200 kDa helicase-like	3.199	2.812	0.858
230	IPI00021840.1	40S ribosomal protein S6	3.472	2.882	0.813
231	IPI00908512.2	cystathionine gamma-lyase isoform 3	2.494	2.115	0.808
232	IPI00798375.2	cDNA FLJ59357, highly similar to Probable ATP-dependent I	2.658	0.980	0.369

233	IPI00004860.2	Isoform Complexed of Arginyl-tRNA synthetase, cytoplasm	2.576	1.219	0.473
234	IPI00477179.1	Isoform 2 of Nucleolar RNA helicase 2	2.271	1.707	0.847
235	IPI00465044.2	Protein RCC2	2.981	2.172	0.727
236	IPI00856038.2	cDNA FLJ53358, highly similar to Heterogeneous nuclear ri	2.205	1.740	0.804
237	IPI00514399.1	ribosomal protein S27	1.900	1.000	0.559
238	IPI00940673.1	cDNA FLJ53217, highly similar to Transketolase	2.582	3.725	1.362
239	IPI00021187.4	Isoform 1 of RuvB-like 1	1.819	1.867	1.022
240	IPI00604431.1	Isoform 2 of Cullin-associated NEDD8-dissociated protein	2.267	2.225	0.949
241	IPI00007611.1	ATP synthase subunit O, mitochondrial	1.998	1.504	0.705
242	IPI00013894.1	Stress-induced-phosphoprotein 1	2.512	1.696	0.706
243	IPI00646689.1	Thioredoxin domain-containing protein 17	3.272	2.008	0.568
244	IPI00965913.1	albumin	2.578	1.305	0.508
245	IPI00219156.7	60S ribosomal protein L30	4.698	2.475	0.686
246	IPI00924816.1	Myotrophin	1.810	1.083	0.608
247	IPI00915869.3	malate dehydrogenase, cytoplasmic isoform 3	2.573	2.287	0.927
248	IPI00643915.1	Peptidyl-prolyl cis-trans isomerase	2.714	2.379	0.696
249	IPI00395887.4	Thioredoxin-related transmembrane protein 1	2.699	2.919	1.099
250	IPI00296370.2	leucine carboxyl methyltransferase 1	2.590	2.312	0.966
251	IPI00304612.9	60S ribosomal protein L13a	3.102	2.334	0.772
252	IPI00031517.1	DNA replication licensing factor MCM6	2.099	1.930	0.867
253	IPI00299904.3	Isoform 1 of DNA replication licensing factor MCM7	2.430	1.976	0.877
254	IPI00745335.7	Isoform Cytoplasmic of Phospholipid hydroperoxide glutat	2.756	2.100	0.748
255	IPI00908754.1	cDNA FLJ50714, moderately similar to Ras-related protein	1.763	1.468	0.807
256	IPI00967721.1	matrin 3	2.682	2.000	0.763
257	IPI00472176.1	Isoform 2 of tRNA (uracil-5-)-methyltransferase homolog A	2.569	2.333	0.875
258	IPI00008438.1	40S ribosomal protein S10	2.798	2.803	0.869
259	IPI00329633.5	Threonyl-tRNA synthetase, cytoplasmic	2.395	1.897	0.802
260	IPI00893541.1	protein disulfide isomerase family A, member 3	2.220	1.366	0.615
261	IPI00293655.3	ATP-dependent RNA helicase DDX1	2.810	2.056	0.758
262	IPI00550746.4	Nuclear migration protein nudC	2.717	1.852	0.658
263	IPI00301434.4	BolA-like protein 2	2.338	1.446	0.631
264	IPI00651660.1	60S ribosomal protein L3 isoform b	2.433	2.268	0.862
265	IPI00009032.1	Lupus La protein	1.876	1.758	0.898
266	IPI00456747.1	ATP synthase, H+ transporting, mitochondrial F0 complex,	1.850	1.564	0.759
267	IPI00030363.1	Acetyl-CoA acetyltransferase, mitochondrial	2.532	1.857	0.787
268	IPI00843996.1	cDNA FLJ52832, highly similar to Splicing factor, arginine/s	2.677	1.839	0.649
269	IPI00026824.2	Heme oxygenase 2	2.245	2.627	1.105
270	IPI00395674.1	Isoform SM-B of Small nuclear ribonucleoprotein-associat	2.976	2.256	0.716
271	IPI00010157.1	S-adenosylmethionine synthase isoform type-2	2.363	2.295	0.978
272	IPI00555749.1	Proteasome 26S ATPase subunit 5 variant (Fragment)	2.682	1.170	0.435
273	IPI00027834.3	Heterogeneous nuclear ribonucleoprotein L	2.854	1.555	0.545
274	IPI00020599.1	Calreticulin	2.525	1.775	0.697
275	IPI00977964.1	ribosomal protein L27a	3.685	2.431	0.638
276	IPI00019359.4	Keratin, type I cytoskeletal 9	2.577	1.511	0.652
277	IPI00795892.1	profilin 2	3.048	1.752	0.665
278	IPI00471928.6	ATP synthase subunit alpha	1.604	1.740	1.180
279	IPI00012493.1	40S ribosomal protein S20	3.104	1.922	0.824

280	IPI00220637.5	Seryl-tRNA synthetase, cytoplasmic	2.726	1.918	0.693
281	IPI00297579.4	Chromobox protein homolog 3	2.491	1.767	0.726
282	IPI00908647.1	cDNA FLJ59942, highly similar to Prostaglandin E synthase	2.397	1.828	0.751
283	IPI00910830.1	cDNA FLJ57715, highly similar to Voltage-dependent anion	3.417	3.018	0.883
284	IPI00021700.3	Proliferating cell nuclear antigen	2.613	3.443	1.242
285	IPI00305383.1	Cytochrome b-c1 complex subunit 2, mitochondrial	2.426	1.724	0.714
286	IPI00247583.5	60S ribosomal protein L21	2.955	2.268	0.785
287	IPI00219905.1	Isoform B of tRNA (cytosine(38)-C(5))-methyltransferase	2.473	1.993	0.806
288	IPI00009104.7	RuvB-like 2	1.944	1.952	0.971
289	IPI01009538.1	Putative uncharacterized protein DKFZp781B11202	1.822	2.116	1.069
290	IPI00019329.1	Dynein light chain 1, cytoplasmic	2.437	1.197	0.490
291	IPI00026268.3	Guanine nucleotide-binding protein G(I)/G(S)/G(T) subuni	2.580	2.206	0.960
292	IPI00642457.1	adenine phosphoribosyltransferase isoform b	1.561	1.470	0.926
293	IPI00000811.2	Proteasome subunit beta type-6	2.219	1.643	0.737
294	IPI00396321.1	Leucine-rich repeat-containing protein 59	2.733	2.549	1.010
295	IPI00470610.4	Pyrroline-5-carboxylate reductase 2	2.730	2.912	1.064
296	IPI00024993.4	Enoyl-CoA hydratase, mitochondrial	2.291	1.794	0.768
297	IPI00643876.2	cDNA FLJ50466, highly similar to DNA (cytosine-5)-methyltra	2.055	2.223	1.082
298	IPI00759663.1	Isoform Cytoplasmic+peroxisomal of Peroxiredoxin-5, mito	2.772	2.273	0.738
299	IPI00412579.6	60S ribosomal protein L10a	2.883	2.014	0.655
300	IPI00983652.2	cDNA FLJ61021, highly similar to Far upstream element-bir	2.515	1.037	0.412
301	IPI00299177.4	Isoform 1 of Cat eye syndrome critical region protein 5	2.661	2.257	0.907
302	IPI00792330.2	ADP-ribosylation factor 4	2.831	1.794	0.634
303	IPI00640006.1	rab GDP dissociation inhibitor beta isoform 2	2.195	1.889	0.898
304	IPI00003168.1	Phosphoribosyl pyrophosphate synthase-associated prote	2.765	3.034	1.025
305	IPI00794610.2	dnaJ homolog subfamily C member 7 isoform 2	3.180	2.308	0.787
306	IPI00760588.2	Isoform 5 of Double-stranded RNA-specific adenosine dea	2.359	2.056	0.954
307	IPI00655650.2	40S ribosomal protein S26	3.956	2.386	0.575
308	IPI00927101.1	Uncharacterized protein	2.348	2.029	0.762
309	IPI00016572.1	Small nuclear ribonucleoprotein G	2.693	1.639	0.603
310	IPI00298961.3	Exportin-1	2.290	2.011	0.807
311	IPI00179953.2	Isoform 1 of Nuclear autoantigenic sperm protein	4.306	2.624	0.660
312	IPI00026271.5	40S ribosomal protein S14	3.324	2.093	0.618
313	IPI00332511.5	Serine/threonine-protein phosphatase 2A 55 kDa regulato	2.089	2.177	0.998
314	IPI00219757.13	Glutathione S-transferase P	2.255	1.558	0.746
315	IPI00453473.6	Histone H4	3.666	1.977	0.580
316	IPI00644653.1	cDNA FLJ56337, highly similar to High mobility group prote	2.632	2.074	0.774
317	IPI00946221.1	ribosomal protein L24	3.166	2.986	0.959
318	IPI00430813.3	Isoform 2 of Cellular nucleic acid-binding protein	3.452	2.328	0.743
319	IPI01012383.1	OTU domain, ubiquitin aldehyde binding 1	2.543	2.404	1.055
320	IPI00927892.1	Mitochondrial-processing peptidase subunit beta	1.884	2.027	1.006
321	IPI00964409.3	heat shock 70kDa protein 4-like	1.898	1.798	0.896
322	IPI00023344.2	Isoform 1 of Symplekin	2.770	2.882	0.969
323	IPI00009901.1	Nuclear transport factor 2	1.866	1.086	0.528
324	IPI00029266.1	Small nuclear ribonucleoprotein E	5.050	2.859	0.671
325	IPI00964686.1	heterogeneous nuclear ribonucleoprotein A/B	2.133	2.047	0.923
326	IPI00016513.5	Ras-related protein Rab-10	2.019	1.484	0.735

327	IPI01014727.1	cDNA FLJ51983, highly similar to Phosphoglycerate mutase	2.442	2.157	0.830
328	IPI00299573.12	60S ribosomal protein L7a	3.146	2.365	0.761
329	IPI00926977.1	26S protease regulatory subunit 10B	2.729	2.219	0.763
330	IPI00792916.2	glucosidase 2 subunit beta isoform 2	3.032	3.188	1.019
331	IPI00027223.2	Isocitrate dehydrogenase [NADP] cytoplasmic	2.772	2.171	0.708
332	IPI00218829.9	Eukaryotic peptide chain release factor GTP-binding subu	2.355	2.137	0.924
333	IPI00336094.5	Isoform 2 of 3-hydroxyacyl-CoA dehydrogenase type-2	2.776	2.180	0.829
334	IPI00156374.6	Isoform 1 of Importin-4	3.711	3.138	0.955
335	IPI00081836.3	Histone H2A type 1-H	2.610	1.777	0.614
336	IPI00926258.1	proteasome (prosome, macropain) 26S subunit, non-ATPa	1.455	1.847	1.170
337	IPI00215780.5	40S ribosomal protein S19	3.179	1.974	0.706
338	IPI00290416.3	Isoform 1 of Obg-like ATPase 1	2.705	1.428	0.566
339	IPI00019927.2	26S proteasome non-ATPase regulatory subunit 7	2.663	2.910	1.093
340	IPI00984839.1	ATP-dependent RNA helicase DDX3X isoform 2	2.773	2.187	0.789
341	IPI01015454.1	PPM1G protein	2.933	2.651	0.882
342	IPI00644712.4	X-ray repair cross-complementing protein 6	1.530	1.665	1.054
343	IPI00031522.2	Trifunctional enzyme subunit alpha, mitochondrial	2.241	1.706	0.807
344	IPI00964635.1	annexin A5	2.091	1.914	0.908
345	IPI00479877.4	4-trimethylaminobutyraldehyde dehydrogenase	2.028	2.119	0.944
346	IPI00640037.2	cDNA FLJ38496 fis, clone FELIV1000137, highly similar to 60	2.537	2.810	1.121
347	IPI00030706.1	Activator of 90 kDa heat shock protein ATPase homolog 1	2.822	2.150	0.767
348	IPI00927606.1	Glutathione peroxidase 1	2.790	2.052	0.766
349	IPI00940851.1	ELAV-like protein 1	2.616	1.754	0.702
350	IPI00001159.11	Translational activator GCN1	3.908	2.981	0.757
351	IPI00170924.2	Histidine triad nucleotide-binding protein 3	1.997	1.849	0.977
352	IPI00029631.1	Enhancer of rudimentary homolog	2.223	1.190	0.535
353	IPI00382699.2	Isoform 5 of Filamin-B	3.789	3.114	0.822
354	IPI00010882.3	Isoform DFF45 of DNA fragmentation factor subunit alpha	2.698	2.386	0.856
355	IPI00300074.4	Phenylalanyl-tRNA synthetase beta chain	2.935	3.910	1.007
356	IPI00759824.2	Isoform 2 of Acidic leucine-rich nuclear phosphoprotein 3	2.556	2.023	0.840
357	IPI00032872.3	28S ribosomal protein S16, mitochondrial	3.591	2.262	0.645
358	IPI00910697.1	cDNA FLJ53703, highly similar to Histidyl-tRNA synthetase	1.774	1.922	1.084
359	IPI00293276.10	Macrophage migration inhibitory factor	2.049	1.409	0.788
360	IPI00012772.8	60S ribosomal protein L8	3.265	2.461	0.698
361	IPI00888475.2	Isoform 6 of Microtubule-associated protein 4	3.971	3.064	0.814
362	IPI01011421.1	Dihydrolipoyl dehydrogenase	2.756	2.171	0.763
363	IPI00005511.1	PHD finger-like domain-containing protein 5A	4.239	2.264	0.616
364	IPI00003588.1	Eukaryotic translation elongation factor 1 epsilon-1	2.903	2.165	0.801
365	IPI00910438.1	cDNA FLJ54574, highly similar to Staphylococcal nuclease d	2.253	2.024	0.894
366	IPI00291783.4	Gem-associated protein 5	3.627	3.024	0.839
367	IPI00026167.5	NHP2-like protein 1	2.445	1.411	0.607
368	IPI01009775.1	cDNA FLJ52574, highly similar to Septin-7	2.080	1.889	0.920
369	IPI00006865.4	Vesicle-trafficking protein SEC22b	2.504	1.632	0.660
370	IPI00216425.1	Isoform 2 of Testin	2.406	2.635	1.085
371	IPI00011913.1	Heterogeneous nuclear ribonucleoprotein A0	2.423	3.772	1.167
372	IPI00177817.4	Isoform 2 of Sarcoplasmic/endoplasmic reticulum calcium	3.494	2.739	0.799

373	IPI00219994.2	Isoform 3 of Exportin-2	2.087	2.078	0.893
374	IPI00376503.2	pyrroline-5-carboxylate reductase 1, mitochondrial isoform	2.419	1.740	0.719
375	IPI00335069.2	26S proteasome non-ATPase regulatory subunit 12 isoform	2.009	1.933	0.938
376	IPI00026519.1	Peptidyl-prolyl cis-trans isomerase F, mitochondrial	2.359	1.834	0.706
377	IPI00964515.1	guanine nucleotide binding protein (G protein), beta poly	2.204	1.897	0.878
378	IPI00218493.7	Hypoxanthine-guanine phosphoribosyltransferase	2.658	2.172	0.824
379	IPI00304417.7	Isocitrate dehydrogenase [NAD] subunit beta, mitochondr	2.485	1.925	0.786
380	IPI00945620.1	guanine monphosphate synthetase	2.460	2.106	0.944
381	IPI00456695.1	Isoform 2 of 26S proteasome non-ATPase regulatory subur	1.743	2.146	1.023
382	IPI00479934.1	non-specific lipid-transfer protein isoform 4 proprotein	3.317	1.981	0.611
383	IPI00011916.1	Aminoacyl tRNA synthase complex-interacting multifunctio	2.563	3.257	1.235
384	IPI00215911.3	DNA-(apurinic or apyrimidinic site) lyase	2.407	2.613	1.078
385	IPI00005024.3	Isoform 1 of Myb-binding protein 1A	4.018	3.097	0.797
386	IPI00877948.1	Minichromosome maintenance complex component 5	1.991	2.491	1.079
387	IPI00953696.1	glutathione reductase, mitochondrial isoform 4 precursor	1.697	1.817	1.064
388	IPI01012867.1	ubiquitin-conjugating enzyme E2 variant 2	2.900	2.056	0.709
389	IPI00867679.2	cDNA FLJ51729, highly similar to Proteasome subunit alpha	2.355	1.934	0.762
390	IPI00879160.1	RAN binding protein 1	2.349	1.866	0.735
391	IPI00291646.3	Methylenetetrahydrofolate dehydrogenase (NADP+ depen	2.101	1.845	0.820
392	IPI00306960.3	Asparaginyl-tRNA synthetase, cytoplasmic	2.708	1.922	0.698
393	IPI00922359.1	Protein-L-isoaspartate O-methyltransferase	2.136	1.790	0.743
394	IPI00012795.3	Eukaryotic translation initiation factor 3 subunit I	2.873	2.932	1.077
395	IPI00020127.1	Replication protein A 70 kDa DNA-binding subunit	2.588	0.928	0.421
396	IPI00644668.3	Four and a half LIM domains 1	3.269	2.602	0.797
397	IPI00025874.2	Dolichyl-diphosphooligosaccharide--protein glycosyltrans	3.456	2.953	1.200
398	IPI00645201.1	Ribosomal protein S8	3.017	2.595	0.804
399	IPI00218830.1	Isoform Short of Glycylpeptide N-tetradecanoyltransferase	2.927	2.990	0.837
400	IPI01014177.1	ST13 protein	2.168	2.041	0.934
401	IPI00023647.4	Isoform 1 of Ubiquitin-like modifier-activating enzyme 6	2.251	2.148	0.902
402	IPI00026833.4	Adenylosuccinate synthetase isozyme 2	2.565	2.145	1.243
403	IPI00306708.5	Lymphokine-activated killer T-cell-originated protein kina	3.457	2.599	0.826
404	IPI00607884.2	cDNA, FLJ79413, highly similar to Hematological and neuro	1.929	1.460	0.765
405	IPI00414384.1	Isoform 1 of Hydroxysteroid dehydrogenase-like protein 2	2.073	2.103	1.015
406	IPI00026328.3	Thioredoxin domain-containing protein 12	2.484	2.130	0.871
407	IPI00291175.7	Isoform 1 of Vinculin	2.028	1.556	0.818
408	IPI00549885.4	Isoform 2 of Pyruvate dehydrogenase E1 component subun	2.172	2.300	1.117
409	IPI00983098.1	lysophospholipase I	1.953	1.515	0.842
410	IPI00978288.1	proteasome subunit beta type-2 isoform 2	2.723	2.445	0.776
411	IPI00783982.1	Coatomer subunit gamma	2.143	2.359	1.145
412	IPI00062037.1	Dynein light chain 2, cytoplasmic	2.072	1.349	0.651
413	IPI00008552.6	Glutaredoxin-3	2.738	2.448	0.902
414	IPI00028055.4	Transmembrane emp24 domain-containing protein 10	2.436	1.852	0.801
415	IPI00917605.1	cytochrome c, somatic	3.302	2.253	0.632
416	IPI00788836.1	dihydrolipoamide S-acetyltransferase	2.669	2.481	0.899
417	IPI00003886.3	Isoform 2 of Guanine nucleotide-binding protein-like 3	2.995	1.429	0.410
418	IPI00939560.1	thioredoxin domain-containing protein 5 isoform 3	1.876	1.944	1.036
419	IPI00783378.3	Ubiquitin-conjugating enzyme E2 O	3.249	2.757	0.879
420	IPI00646415.1	RAB14, member RAS oncogene family	2.291	1.569	0.679

421	IPI01013402.1	cDNA FLJ46429 fis, clone THYMU3014372, highly similar to D	2.748	3.522	0.980
422	IPI00792135.2	ATP5H protein (Fragment)	2.015	1.670	0.823
423	IPI00397526.3	Isoform 1 of Myosin-10	1.916	1.825	0.953
424	IPI00963825.1	ATP synthase, H+ transporting, mitochondrial Fo complex,	2.567	2.802	0.735
425	IPI00001757.1	Isoform 1 of RNA-binding protein 8A	1.852	1.550	0.819
426	IPI00004839.1	Crk-like protein	3.577	3.226	0.874
427	IPI00026089.4	Splicing factor 3B subunit 1	3.141	2.627	0.814
428	IPI00006980.1	chromosome 14 open reading frame 166	2.526	1.296	0.550
429	IPI00554521.2	Ferritin heavy chain	1.796	1.404	0.788
430	IPI00786995.1	DNA-dependent protein kinase catalytic subunit-like	3.054	2.815	0.887
431	IPI00456969.1	Cytoplasmic dynein 1 heavy chain 1	3.743	2.938	0.818
432	IPI00946636.2	cDNA FLJ51804, highly similar to Vacuolar ATP synthase cat	2.456	2.394	0.955
433	IPI00302850.4	Small nuclear ribonucleoprotein Sm D1	2.722	1.543	0.577
434	IPI00645329.1	Isoform 3 of Histone-binding protein RBBP4	1.841	1.664	0.934
435	IPI00465361.4	60S ribosomal protein L13	2.926	2.482	0.736
436	IPI00977156.1	eukaryotic translation initiation factor 3, subunit E	2.152	1.995	0.975
437	IPI00218414.5	Carbonic anhydrase 2	3.112	2.365	0.760
438	IPI00291939.1	Structural maintenance of chromosomes protein 1A	3.833	2.920	0.790
439	IPI00514724.1	Ubiquitin-conjugating enzyme E2 variant 1	2.424	1.697	0.700
440	IPI00294911.1	Succinate dehydrogenase [ubiquinone] iron-sulfur subuni	2.630	2.067	0.795
441	IPI00031570.1	Cancer-related nucleoside-triphosphatase	2.373	1.870	0.786
442	IPI00982721.1	transcription elongation factor B (SIII), polypeptide 1 (15kI	3.939	2.470	0.627
443	IPI00294955.3	U6 snRNA-associated Sm-like protein LSm4	3.270	2.080	0.603
444	IPI01009339.1	paraspeckle component 1	2.809	1.405	0.500
445	IPI00017963.1	Small nuclear ribonucleoprotein Sm D2	3.255	1.929	0.589
446	IPI01014812.1	cDNA FLJ52595, highly similar to Medium-chain specific ac	2.609	2.024	0.737
447	IPI00642213.1	RNA binding protein, autoantigenic	2.319	2.608	1.074
448	IPI00221091.9	40S ribosomal protein S15a	4.289	2.330	0.565
449	IPI00063245.2	far upstream element (FUSE) binding protein 3	2.680	2.252	0.840
450	IPI00387130.1	Isoform 1 of Anamorsin	3.692	3.417	0.892
451	IPI00943173.1	Coronin-1C	3.450	2.288	0.723
452	IPI00220667.3	Isoform 4 of Hexokinase-1	1.491	1.603	0.919
453	IPI00105598.3	Proteasome 26S non-ATPase subunit 11 variant (Fragment)	1.822	2.353	1.232
454	IPI00103467.5	Aldehyde dehydrogenase X, mitochondrial	1.766	1.931	1.153
455	IPI00005613.3	Splicing factor U2AF 35 kDa subunit	2.546	2.539	0.988
456	IPI01015738.1	Alpha actinin 4 short isoform	1.959	1.818	0.928
457	IPI00031836.3	Developmentally-regulated GTP-binding protein 1	2.864	2.459	0.859
458	IPI00019640.1	Serine/threonine-protein kinase VRK1	2.123	2.207	1.040
459	IPI00979610.1	S-phase kinase-associated protein 1	3.144	2.327	0.726
460	IPI00927677.1	heterogeneous nuclear ribonucleoprotein A3	2.817	2.211	0.895
461	IPI00021435.3	26S protease regulatory subunit 7	1.684	1.884	1.093
462	IPI00219025.3	Glutaredoxin-1	1.888	0.717	0.380
463	IPI00218568.7	Pterin-4-alpha-carbinolamine dehydratase	1.621	1.205	0.743
464	IPI00014151.3	26S proteasome non-ATPase regulatory subunit 6	2.766	2.422	0.864
465	IPI00009922.3	SRA stem-loop-interacting RNA-binding protein, mitochon	2.769	1.678	0.597
466	IPI00297982.7	Eukaryotic translation initiation factor 2 subunit 3	1.987	1.966	0.985
467	IPI01010654.1	cDNA FLJ57899, highly similar to Mitotic checkpoint protein	2.735	2.133	0.776

468	IPI01009456.1	cDNA FLJ40884 fis, clone UTERU2000607, highly similar to A	1.505	1.721	1.143
469	IPI01015965.1	eukaryotic translation elongation factor 1 delta (guanine	2.301	2.462	1.070
470	IPI00925601.1	5-aminoimidazole-4-carboxamide ribonucleotide formyltr	3.186	2.035	0.683
471	IPI01012099.1	PRP6 pre-mRNA processing factor 6 homolog (S. cerevisiae	2.339	2.021	0.867
472	IPI00304409.3	Calcium-regulated heat stable protein 1	2.495	2.039	0.702
473	IPI00644813.1	Small nuclear ribonucleoprotein polypeptide C	2.109	1.495	0.677
474	IPI00745893.2	small ubiquitin-related modifier 2 isoform b precursor	4.159	2.626	0.631
475	IPI00295857.7	Isoform 1 of Coatomer subunit alpha	2.980	2.520	0.789
476	IPI00334907.3	Isoform 1 of Phosphatidylinositol transfer protein beta is	2.168	2.397	1.108
477	IPI00983658.1	adenosine kinase isoform d	2.747	1.499	0.542
478	IPI00008527.3	60S acidic ribosomal protein P1	5.131	3.303	0.644
479	IPI00942408.1	Isoform 1 of Cyclin-dependent kinase inhibitor 2A, isoform	4.106	2.614	0.637
480	IPI00909229.1	cDNA FLJ51308	1.955	1.410	0.623
481	IPI00921820.1	cDNA, FLJ78950, highly similar to Isocitrate dehydrogenase	2.266	1.847	0.815
482	IPI00945574.1	RAB7A, member RAS oncogene family	3.152	2.130	0.702
483	IPI00023234.3	SUMO-activating enzyme subunit 2	2.170	1.908	0.938
484	IPI00219153.4	60S ribosomal protein L22	2.934	1.647	0.530
485	IPI00815843.1	RPL14 protein (Fragment)	3.465	2.728	0.597
486	IPI00977658.1	Eukaryotic translation initiation factor 3 subunit H	3.359	2.620	0.767
487	IPI00029557.3	GrpE protein homolog 1, mitochondrial	2.130	1.665	0.797
488	IPI01009361.1	N(alpha)-acetyltransferase 15, NatA auxiliary subunit	1.890	2.033	1.050
489	IPI00012369.1	Mitotic spindle assembly checkpoint protein MAD2A	1.973	1.541	0.727
490	IPI00334627.3	Putative annexin A2-like protein	2.364	2.662	1.126
491	IPI00878484.1	Ewing sarcoma breakpoint region 1	2.594	2.068	1.092
492	IPI00977915.3	HYOU1 protein	3.330	2.779	0.812
493	IPI00170972.2	UPF0553 protein C9orf64	2.533	2.287	1.054
494	IPI00020451.4	Isoform 1 of Protein IMPACT	2.729	2.233	0.836
495	IPI00013847.4	Cytochrome b-c1 complex subunit 1, mitochondrial	2.240	1.852	0.827
496	IPI00965680.1	nucleoporin 155kDa	3.192	2.828	0.746
497	IPI00218372.1	Isoform 2 of Proteasome subunit alpha type-7	2.593	1.693	0.701
498	IPI01015591.1	cDNA FLJ55635, highly similar to pre-mRNA-splicing factorA	2.664	2.080	0.781
499	IPI00955815.2	pyruvate dehydrogenase E1 component subunit alpha, so	1.993	1.311	0.641
500	IPI00926495.1	ribosomal protein L35a	4.530	2.216	0.524
501	IPI00177008.1	Phosphoglycolate phosphatase	2.790	2.764	1.067
502	IPI00016736.1	Isoform 1 of 1-phosphatidylinositol-4,5-bisphosphate pho	4.052	2.856	0.603
503	IPI00789792.1	dynactin 2 (p50)	1.916	1.992	0.968
504	IPI00020602.1	Casein kinase II subunit alpha'	4.707	4.464	0.948
505	IPI01012417.1	NOP2/Sun RNA methyltransferase family, member 2	2.007	2.081	0.938
506	IPI00945855.1	profilin 2	4.255	2.485	0.584
507	IPI01014975.1	Talin 1	4.295	3.187	0.767
508	IPI00011698.4	histone deacetylase complex subunit SAP18	3.101	2.225	0.711
509	IPI00909657.1	cDNA FLJ50378, highly similar to Phenylalanyl-tRNA synthe	2.464	1.903	0.735
510	IPI00787559.1	thymidylate kinase isoform 2	2.353	2.289	0.895
511	IPI00299147.8	Small ubiquitin-related modifier 3	3.508	1.968	0.561
512	IPI00983602.1	mitochondrial carrier 2	4.026	4.743	1.093
513	IPI00789806.2	Isoform 2 of Cytosol aminopeptidase	2.420	2.435	1.044
514	IPI00514607.2	Isoform 2 of Histone-arginine methyltransferase CARM1	3.223	2.208	0.733

515	IPI00647813.1	Isoform 2 of Inosine-5'-monophosphate dehydrogenase 1	1.494	1.900	1.272
516	IPI00895865.1	electron transfer flavoprotein subunit alpha, mitochondri	2.323	1.938	0.934
517	IPI00982162.1	ras homolog family member C	2.886	2.151	0.648
518	IPI00215790.6	60S ribosomal protein L38	2.347	1.232	0.544
519	IPI00000643.1	BAG family molecular chaperone regulator 2	2.173	1.462	0.682
520	IPI01012205.1	cDNA FLJ53863, highly similar to Cystathionine beta-syntha	2.590	2.268	0.866
521	IPI00513775.1	Isoform 2 of 14 kDa phosphohistidine phosphatase	3.013	1.668	0.572
522	IPI00908582.1	cDNA FLJ50164, highly similar to Protein flightless-1 homol	3.886	2.917	0.736
523	IPI00428288.1	Isoform 4 of 39S ribosomal protein L43, mitochondrial	2.883	2.170	0.747
524	IPI00295386.7	Carbonyl reductase [NADPH] 1	2.657	1.919	0.722
525	IPI00022334.1	Ornithine aminotransferase, mitochondrial	2.702	0.991	0.413
526	IPI00022442.2	Acyl carrier protein, mitochondrial	2.275	1.668	0.768
527	IPI00973884.1	S-phase kinase-associated protein 1	2.482	2.757	1.111
528	IPI00759715.1	Isoform Cytoplasmic of Fumarate hydratase, mitochondria	2.456	2.400	1.000
529	IPI01012065.1	proteasome (prosome, macropain) subunit, alpha type, 1	2.530	2.068	0.831
530	IPI00003327.1	ADP-ribosylation factor-like protein 3	2.868	2.050	0.770
531	IPI00797249.1	L-xylulose reductase isoform 2	2.302	2.227	0.831
532	IPI01012026.1	chromodomain helicase DNA binding protein 4	3.096	2.470	0.830
533	IPI00012202.1	Methylosome protein 50	3.172	2.043	0.644
534	IPI01009016.1	Isoform 4 of Cellular tumor antigen p53	1.880	1.768	0.932
535	IPI00746004.2	40S ribosomal protein S27-like	2.465	1.973	0.800
536	IPI01014044.1	Isoform 1 of NADH dehydrogenase [ubiquinone] 1 beta su	2.259	1.868	0.752
537	IPI00873286.2	cDNA FLJ55750, highly similar to Eukaryotic translation init	2.191	1.650	0.841
538	IPI00171798.1	Metastasis-associated protein MTA2	2.589	2.486	0.956
539	IPI00016786.1	Isoform 2 of Cell division control protein 42 homolog	2.143	1.797	0.838
540	IPI00908889.1	cDNA FLJ54065, moderately similar to Mus musculus pitrily	1.954	1.726	0.912
541	IPI00925237.1	non-SMC condensin I complex, subunit H	2.001	2.088	0.960
542	IPI00980919.1	Serine/threonine-protein phosphatase	6.424	6.094	0.991
543	IPI00006052.3	Prefoldin subunit 2	3.667	2.536	0.622
544	IPI00794581.1	tropomodulin 2 (neuronal)	1.697	1.011	0.596
545	IPI00025039.1	rRNA 2'-O-methyltransferase fibrillarin	2.536	2.446	0.906
546	IPI00853093.3	Isoform 1 of Methyltransferase-like protein 2B	3.197	3.015	0.971
547	IPI00550234.4	Isoform 1 of Actin-related protein 2/3 complex subunit 5	2.465	1.953	0.674
548	IPI00010130.3	Glutamine synthetase	2.410	2.237	0.845
549	IPI00219077.4	Isoform 1 of Leukotriene A-4 hydrolase	2.484	1.213	0.447
550	IPI00384016.1	Full-length cDNA 5-PRIME end of clone CS0DJ009YL13 of T c	1.767	1.653	0.943
551	IPI00873948.3	DNA-directed RNA polymerase	3.095	2.516	0.773
552	IPI00184284.6	Isoform 2 of Vacuolar protein sorting-associated protein 2	2.456	2.214	0.901
553	IPI00419919.6	Ribosomal protein L29	2.336	2.074	0.848
554	IPI01018329.1	cDNA FLJ57316, highly similar to DNA mismatch repair prot	1.984	1.851	1.110
555	IPI00029534.1	Amidophosphoribosyltransferase	2.647	1.966	0.743
556	IPI00008454.1	DnaJ homolog subfamily B member 11	2.522	2.099	0.834
557	IPI00332371.9	Isoform 1 of 6-phosphofructokinase, liver type	1.713	2.082	1.216
558	IPI00216508.3	Isoform 2 of Sorting nexin-3	2.738	1.960	0.670
559	IPI00386755.2	ERO1-like protein alpha	2.784	1.933	0.709
560	IPI00743142.2	Isoform 1 of 6-phosphofructokinase, muscle type	2.405	1.901	0.790
561	IPI01010195.1	cDNA FLJ55629, highly similar to Transcription elongation f	3.271	3.311	0.997

562	IPI00021785.2	Cytochrome c oxidase subunit 5B, mitochondrial	2.684	1.725	0.609
563	IPI01014174.1	PRP19/PSO4 pre-mRNA processing factor 19 homolog (S. ce	2.372	2.729	0.945
564	IPI00977749.1	cysteine and histidine-rich domain (CHORD) containing 1	3.123	3.882	1.184
565	IPI00026546.1	Platelet-activating factor acetylhydrolase IB subunit beta	2.268	1.640	0.724
566	IPI00946039.1	tRNA methyltransferase 10 homolog C (S. cerevisiae)	2.603	2.502	0.922
567	IPI00005087.1	Tropomodulin-3	2.132	1.826	0.857
568	IPI00250297.3	L-aminoadipate-semialdehyde dehydrogenase-phosphop	4.238	3.259	0.987
569	IPI00910113.1	cDNA FLJ52902, highly similar to Rab GDP dissociation inhi	4.334	3.106	0.717
570	IPI00106495.1	Condensin complex subunit 3	2.017	2.265	1.013
571	IPI00007402.3	Importin-7	2.615	1.822	0.697
572	IPI00641924.2	28S ribosomal protein S9, mitochondrial	2.408	1.907	0.817
573	IPI00982694.1	serum amyloid A-like 1	3.281	2.116	0.627
574	IPI00644349.4	cDNA FLJ60449, highly similar to Homo sapiens prion prote	2.901	2.318	0.801
575	IPI00556021.3	DNA polymerase (Fragment)	3.485	3.511	1.007
576	IPI00028946.2	Isoform 3 of Reticulon-3	2.345	2.115	0.855
577	IPI00215719.6	60S ribosomal protein L18	10.555	6.181	0.577
578	IPI00219678.3	Eukaryotic translation initiation factor 2 subunit 1	2.674	2.529	1.043
579	IPI00013122.1	Hsp90 co-chaperone Cdc37	1.887	2.117	1.122
580	IPI00411937.4	Nucleolar protein 56	2.125	2.111	0.993
581	IPI01015342.1	cDNA, FLJ79540, highly similar to Serine-threonine kinase	3.143	2.997	0.985
582	IPI00433833.1	THOC3 protein	2.658	2.099	0.813
583	IPI00001589.1	Mitochondrial import inner membrane translocase subun	1.973	1.296	0.657
584	IPI00375145.1	Isoform Short of Ubiquitin carboxyl-terminal hydrolase 5	2.251	2.200	0.977
585	IPI00184821.1	Isoform 1 of Bifunctional coenzyme A synthase	3.020	1.866	0.681
586	IPI01010004.1	cDNA FLJ50858, highly similar to Homo sapiens abhydrolas	1.905	1.037	0.789
587	IPI00039626.3	Isoform D of Constitutive coactivator of PPAR-gamma-like	4.051	3.011	0.747
588	IPI00644724.1	HIV-1 Tat specific factor 1	2.112	1.905	0.905
589	IPI00937278.2	26S proteasome non-ATPase regulatory subunit 8	2.900	2.160	0.725
590	IPI00893431.2	cDNA FLJ53410, highly similar to Eukaryotic translation init	2.062	2.161	1.048
591	IPI00025019.3	Proteasome subunit beta type-1	2.227	1.719	0.755
592	IPI00335385.4	Scavenger mRNA-decapping enzyme DcpS	2.141	2.317	1.093
593	IPI00552546.1	Isoform 2 of Mini-chromosome maintenance complex-bin	2.857	3.062	1.096
594	IPI00023064.1	NADH dehydrogenase [ubiquinone] 1 alpha subcomplex a	2.233	1.979	0.765
595	IPI00556640.1	PSAP protein	2.281	2.291	1.005
596	IPI00019326.1	Adrenodoxin, mitochondrial	2.843	1.772	0.554
597	IPI01013095.1	cDNA, FLJ79243, highly similar to Eukaryotic translation ini	2.564	1.829	0.707
598	IPI00893219.2	LUC7-like	2.395	2.655	1.109
599	IPI00009464.1	Isoform 1 of Exosome component 10	2.320	1.863	0.829
600	IPI01015801.1	cDNA FLJ16138 fis, clone BRALZ2017531, highly similar to Gl	1.550	1.636	1.056
601	IPI00719622.1	40S ribosomal protein S28	2.497	1.144	0.458
602	IPI00012866.2	RAC-alpha serine/threonine-protein kinase	3.314	2.355	0.711
603	IPI00940656.2	ANP32A protein	2.559	2.043	0.798
604	IPI01014610.1	tRNA methyltransferase 11-2 homolog (S. cerevisiae)	2.243	1.697	0.720
605	IPI01011099.1	cDNA FLJ53046, highly similar to 26S proteasome non-ATPa	2.727	1.987	0.737
606	IPI00909299.1	cDNA FLJ51288, highly similar to Kinesin heavy chain	2.059	2.005	0.974
607	IPI00011770.1	NADH dehydrogenase [ubiquinone] 1 alpha subcomplex s	2.354	1.359	0.575
608	IPI01010794.1	cDNA FLJ61096, highly similar to THO complex subunit 2	2.589	2.183	1.121

609	IPI00553165.4	Protein (Peptidylprolyl cis/trans isomerase) NIMA-interact	2.601	1.513	0.537
610	IPI00019407.1	Sterol-4-alpha-carboxylate 3-dehydrogenase, decarboxylat	2.093	1.727	0.787
611	IPI00910487.1	cDNA FLJ52569, highly similar to Collagen-binding protein	2.138	1.930	0.980
612	IPI00967473.1	DEK oncogene	2.817	2.494	0.863
613	IPI01010979.1	zinc finger CCCH-type containing 15	3.031	2.044	0.768
614	IPI00550037.3	28S ribosomal protein S15, mitochondrial	2.172	1.506	0.693
615	IPI00639819.1	TAR DNA binding protein	2.500	2.116	0.805
616	IPI00983383.1	cDNA FLJ54904, highly similar to Homo sapiens dendritic c	2.542	1.920	0.755
617	IPI00220871.4	60S ribosomal protein L37	3.575	2.284	0.700
618	IPI00940152.1	ataxin-10 isoform 2	1.994	2.241	1.056
619	IPI00180128.4	Isoform 2 of Basic leucine zipper and W2 domain-containi	2.787	1.715	0.615
620	IPI00016676.1	Mitochondrial import receptor subunit TOM20 homolog	2.694	1.775	0.861
621	IPI00646917.1	Cleavage and polyadenylation specificity factor subunit 5	2.989	2.276	0.762
622	IPI01014783.1	cDNA FLJ58533, highly similar to Leucyl-tRNA synthetase, cy	2.830	1.974	0.691
623	IPI00037448.3	Glyoxylate reductase/hydroxypyruvate reductase	2.200	2.288	0.955
624	IPI00184525.2	Isoform 2 of Methylthioribose-1-phosphate isomerase	2.654	2.219	0.812
625	IPI00007074.5	Tyrosyl-tRNA synthetase, cytoplasmic	2.226	1.571	0.684
626	IPI01018318.1	cDNA FLJ54744, highly similar to Scaffold attachment facto	4.256	3.239	0.761
627	IPI01011782.1	cDNA FLJ61430, highly similar to ATP-dependent RNA helica	3.549	2.477	0.698
628	IPI00449201.2	Isoform 2 of Ubiquitin-like-conjugating enzyme ATG3	1.877	1.866	1.004
629	IPI00788781.1	fatty acid binding protein 5 (psoriasis-associated)	4.128	2.098	0.488
630	IPI00937239.2	40S ribosomal protein S21	1.875	1.002	0.546
631	IPI00940890.1	Isoform 3 of RNA-binding protein 4	2.917	2.405	0.824
632	IPI01015427.1	cDNA FLJ58247, highly similar to 26S protease regulatory su	2.919	1.830	0.627
633	IPI00032957.1	SUMO-conjugating enzyme UBC9	3.267	2.100	0.643
634	IPI00025086.4	Cytochrome c oxidase subunit 5A, mitochondrial	3.883	2.117	0.545
635	IPI00221325.3	E3 SUMO-protein ligase RanBP2	4.446	3.044	0.685
636	IPI00472003.1	Isoform 4 of BH3-interacting domain death agonist	3.018	4.338	0.843
637	IPI00167572.4	Protein FAM98B	2.057	2.368	1.184
638	IPI00937682.1	Opioid growth factor receptor	2.520	2.275	0.901
639	IPI00003927.5	Peptidyl-prolyl cis-trans isomerase D	2.491	2.630	1.056
640	IPI00968128.1	ribosomal protein L9	1.968	1.584	0.780
641	IPI00216770.1	Isoform 2 of 26S protease regulatory subunit 6B	1.890	1.884	0.997
642	IPI00925570.1	regulator of chromosome condensation 1	2.007	1.969	0.981
643	IPI01015278.1	cDNA FLJ58314, highly similar to Mitogen-activated protein	2.838	2.159	0.761
644	IPI00953925.1	Aryl hydrocarbon receptor interacting protein	3.696	3.745	1.013
645	IPI00966482.1	cDNA FLJ36919 fis, clone BRACE2003987, highly similar to C	2.641	2.597	0.984
646	IPI00979370.1	K-RAS protein (Fragment)	2.248	1.704	0.758
647	IPI00946099.1	sorcin	2.460	1.653	0.672
648	IPI00980330.1	RAP2A, member of RAS oncogene family	2.108	1.703	0.808
649	IPI00303207.3	ATP-binding cassette sub-family E member 1	2.586	1.565	0.555
650	IPI00289819.5	Cation-independent mannose-6-phosphate receptor	4.060	3.065	0.755
651	IPI00010896.3	Chloride intracellular channel protein 1	3.893	2.847	0.731
652	IPI00032900.1	BolA-like protein 1	1.672	1.397	0.835
653	IPI00306516.1	Mitochondrial import inner membrane translocase subun	2.452	2.514	1.026
654	IPI00792186.4	ATP-binding cassette, sub-family F (GCN20), member 1	2.301	1.794	0.780
655	IPI00909058.1	cDNA FLJ54246, highly similar to Homo sapiens BRCA2 and	2.050	2.164	1.107

656	IPI01011924.1	ubiquitin specific peptidase 7 (herpes virus-associated)	3.215	2.651	0.824
657	IPI00470922.2	Isoform 2 of N-alpha-acetyltransferase 50, NatE catalytic s	3.337	2.432	0.729
658	IPI00977975.1	chromosome 11 open reading frame 58	2.303	1.720	0.747
659	IPI00978083.1	Uncharacterized protein	2.164	1.699	0.785
660	IPI00014238.2	Isoform Cytoplasmic of Lysyl-tRNA synthetase	2.485	1.985	0.799
661	IPI01008912.1	NADH dehydrogenase (ubiquinone) Fe-S protein 8, 23kDa	2.285	1.636	0.716
662	IPI00982639.1	chromosome 11 open reading frame 31	2.657	1.695	0.638
663	IPI00967533.1	transmembrane protein 33	4.675	3.615	0.773
664	IPI00647084.2	programmed cell death protein 4 isoform 3	4.134	3.036	0.734
665	IPI01014222.1	damage-specific DNA binding protein 1, 127kDa	2.132	1.831	0.859
666	IPI00917463.1	Isoform 3 of Ancient ubiquitous protein 1	3.145	2.560	0.814
667	IPI00012197.1	dCTP pyrophosphatase 1	2.486	1.875	0.754
668	IPI00014230.1	Complement component 1 Q subcomponent-binding prote	2.123	1.198	0.564
669	IPI00410615.2	Isoform 3 of Low molecular weight phosphotyrosine prote	2.945	2.160	0.734
670	IPI00010414.4	PDZ and LIM domain protein 1	2.268	2.842	1.253
671	IPI00290142.5	CTP synthase 1	2.521	2.076	0.824
672	IPI00258833.1	sorting nexin-6 isoform a	2.005	1.829	0.913
673	IPI00646864.1	signal sequence receptor, delta	3.223	2.155	0.669
674	IPI00783302.1	Isoform 1 of Pentatricopeptide repeat-containing protein	2.715	1.697	0.625
675	IPI00017672.4	cDNA FLJ25678 fis, clone TST04067, highly similar to PURIN	2.141	1.724	0.805
676	IPI00010270.1	Ras-related C3 botulinum toxin substrate 2	1.842	1.709	0.928
677	IPI00218922.5	Translocation protein SEC63 homolog	1.813	2.331	1.286
678	IPI00984586.1	trypsin-3 isoform 4 preproprotein	1.541	1.084	0.704
679	IPI01012629.1	aspartyl aminopeptidase	2.393	2.180	0.911
680	IPI00642944.1	Poly(A) binding protein, cytoplasmic 4 (Inducible form), is	2.871	2.563	0.892
681	IPI00440719.2	N(alpha)-acetyltransferase 10, NatA catalytic subunit	2.611	2.049	0.785
682	IPI00973891.1	NudC domain containing 2	2.523	1.967	0.780
683	IPI00797679.1	Inosine triphosphatase (Nucleoside triphosphate pyroph	2.546	1.718	0.675
684	IPI00294495.5	Ubiquitin-fold modifier-conjugating enzyme 1	1.754	1.531	0.873
685	IPI00303105.3	Small ubiquitin-related modifier 1	3.897	2.277	0.584
686	IPI00028004.2	Proteasome subunit beta type-3	2.801	1.747	0.708
687	IPI00909879.1	cDNA FLJ50886, highly similar to Aconitate hydratase, mito	2.786	2.187	0.785
688	IPI00000606.5	Tetratricopeptide repeat protein 4	2.051	2.048	0.998
689	IPI00879792.1	Cytochrome b5 reductase 3	2.312	2.607	1.128
690	IPI00377080.1	COP9 signalosome complex subunit 8 isoform 2	2.156	1.576	0.731
691	IPI00556611.1	39S ribosomal protein L22, mitochondrial isoform b	2.767	1.976	0.714
692	IPI00448725.1	RAB4B protein	1.865	3.320	1.780
693	IPI00981273.2	cDNA FLJ14161 fis, clone NT2RM2001803, highly similar to I	3.562	3.791	1.064
694	IPI00001146.1	U6 snRNA-associated Sm-like protein LSm6	2.448	1.326	0.542
695	IPI00645836.1	esterase D	2.445	2.476	1.013
696	IPI00178047.7	proline, glutamate and leucine rich protein 1	2.174	3.276	1.507
697	IPI00925574.1	COP9 constitutive photomorphogenic homolog subunit 6 (A	3.088	3.438	1.113
698	IPI00073602.1	Exosome complex component MTR3	3.019	1.679	0.805
699	IPI00879002.1	Tubulin tyrosine ligase-like family, member 12	3.052	2.679	0.878
700	IPI00181728.1	Ribosome biogenesis protein BRX1 homolog	3.432	2.270	0.661
701	IPI00062866.4	Isoform 1 of Zinc finger CCCH-type antiviral protein 1-like	2.590	2.770	1.070
702	IPI00794082.2	cDNA FLJ57650, highly similar to Bleomycin hydrolase	2.534	2.463	0.972

703	IPI00291922.2	Proteasome subunit alpha type-5	2.973	2.087	0.702
704	IPI00015838.3	Cell growth-regulating nucleolar protein	2.101	2.243	1.067
705	IPI01014863.1	Acetyl-CoA acetyltransferase, cytosolic	4.044	2.972	0.735
706	IPI00162330.3	39S ribosomal protein L37, mitochondrial	2.667	2.284	0.856
707	IPI00022640.1	Neurogranin	3.763	2.308	0.613
708	IPI00976464.1	Sjogren syndrome/scleroderma autoantigen 1	2.177	1.595	0.733
709	IPI00014437.4	Sjoegren syndrome nuclear autoantigen 1	2.575	1.689	0.656
710	IPI00024821.1	26S proteasome non-ATPase regulatory subunit 14	2.690	2.618	0.973
711	IPI00646978.4	lysophospholipase II	2.039	1.463	0.718
712	IPI00925853.1	cDNA FLJ60586, highly similar to NADH-ubiquinone oxidore	5.404	4.810	1.117
713	IPI00235412.7	dynamin 1-like	2.466	1.987	0.806
714	IPI00030243.1	Isoform 1 of Proteasome activator complex subunit 3	3.658	1.704	0.466
715	IPI00966744.1	Ubiquitin carrier protein	2.630	1.922	0.731
716	IPI00299155.5	Proteasome subunit alpha type-4	2.387	1.962	0.822
717	IPI00794194.1	developmentally regulated GTP binding protein 2	2.134	1.856	0.870
718	IPI00016912.1	Tetratricopeptide repeat protein 1	6.247	6.968	1.115
719	IPI00784936.1	septin-9 isoform c	2.793	2.610	0.935
720	IPI00294398.2	Isoform 1 of Hydroxyacyl-coenzyme A dehydrogenase, mito	2.185	1.507	0.690
721	IPI00000873.3	Valyl-tRNA synthetase	2.085	2.211	1.060
722	IPI00032827.1	Pre-mRNA branch site protein p14	3.887	2.770	0.712
723	IPI00293434.2	Signal recognition particle 14 kDa protein	2.967	2.050	0.691
724	IPI00657698.2	cDNA FLJ59884, highly similar to Secernin-1	1.915	2.157	1.126
725	IPI00645380.1	Isoform 2 of E3 ubiquitin-protein ligase CHIP	2.305	2.593	1.125
726	IPI00643317.3	high mobility group box 3	2.203	1.336	0.606
727	IPI00448974.2	NUP107 protein	2.710	1.857	0.685
728	IPI00028414.3	Glia maturation factor gamma	2.044	1.554	0.760
729	IPI00060715.1	BTB/POZ domain-containing protein KCTD12	2.609	2.939	1.006
730	IPI00216057.6	Sorbitol dehydrogenase	2.541	2.083	0.820
731	IPI00939491.1	Isoform 2 of Cysteinyl-tRNA synthetase, cytoplasmic	2.690	2.003	0.786
732	IPI00290460.3	Eukaryotic translation initiation factor 3 subunit G	2.420	2.037	0.842
733	IPI00896410.1	Ribosomal protein L36a	5.359	2.556	0.477
734	IPI00936931.2	cDNA FLJ57553, highly similar to SPFH domain-containing p	2.319	2.025	0.873
735	IPI00412224.2	WD repeat-containing protein 11	1.928	2.150	1.115
736	IPI00554626.3	C-terminal-binding protein 1 isoform 2	1.644	1.853	1.127
737	IPI00922378.1	cDNA FLJ55038, highly similar to Nicotinamide phosphorib	1.455	1.441	0.990
738	IPI00639981.1	Phosphofructokinase, platelet	3.545	2.880	0.812
739	IPI01010750.1	DNA ligase (Fragment)	3.226	2.021	0.866
740	IPI00792207.3	aldehyde dehydrogenase, mitochondrial Isoform 2 precurs	2.414	2.194	0.909
741	IPI00030320.4	Probable ATP-dependent RNA helicase DDX6	1.995	1.821	0.913
742	IPI00009342.1	Ras GTPase-activating-like protein IQGAP1	2.655	2.012	0.758
743	IPI00026964.2	Cytochrome b-c1 complex subunit Rieske, mitochondrial	1.890	1.173	0.620
744	IPI01010035.1	cDNA FLJ52928, highly similar to COP9 signalosome comple	1.734	1.844	1.063
745	IPI00218200.8	B-cell receptor-associated protein 31	3.167	2.529	0.798
746	IPI01009610.1	cDNA FLJ57998, highly similar to Homo sapiens myo-inosit	1.925	2.807	1.458
747	IPI00642256.2	Isoform 2 of F-actin-capping protein subunit beta	2.434	1.922	0.789
748	IPI00399170.1	Isoform 2 of Regulator of nonsense transcripts 1	4.314	2.970	0.689
749	IPI00745613.2	Exosome complex component RRP41	2.900	2.337	0.806

750	IPI00027547.2	Dermcidin	1.686	0.837	0.496
751	IPI00429689.3	Serine/threonine-protein phosphatase 2A catalytic subun	3.300	2.694	0.817
752	IPI00018691.1	Isoform 1 of 28S ribosomal protein S18a, mitochondrial	2.826	2.264	0.801
753	IPI00967112.1	mitochondrial ribosomal protein S27	2.119	1.786	0.843
754	IPI00011726.1	Isoform 1 of RNA 3'-terminal phosphate cyclase	2.371	1.781	0.751
755	IPI00014458.1	Protein SCO2 homolog, mitochondrial	2.402	1.707	0.711
756	IPI00006113.1	DNA-directed RNA polymerase II subunit RPB9	2.582	1.927	0.746
757	IPI00031106.1	Proteasome assembly chaperone 3	6.824	4.055	0.594
758	IPI00383046.3	Carboxymethylenebutenolidase homolog	2.838	1.788	0.690
759	IPI00215777.1	Isoform B of Phosphate carrier protein, mitochondrial	3.545	2.478	0.699
760	IPI00946474.1	NADH dehydrogenase (ubiquinone) 1 alpha subcomplex, 5	3.101	1.462	0.924
761	IPI00030877.2	15 kDa selenoprotein isoform 1 precursor	2.540	1.853	0.729
762	IPI01012198.1	tRNA methyltransferase 11 homolog	2.098	2.159	1.029
763	IPI00921488.1	Isoform 4 of COP9 signalosome complex subunit 1	2.817	1.936	0.687
764	IPI00000335.1	Histidine triad nucleotide-binding protein 2, mitochondria	2.578	1.729	0.670
765	IPI00922583.1	phosphatidylinositol-4-phosphate 5-kinase type-1 alpha i	2.784	1.515	0.544
766	IPI01012747.1	aldehyde dehydrogenase 5 family, member A1	2.159	1.826	0.846
767	IPI00155054.3	cDNA FLJ50635, highly similar to ATP-dependent RNA helica	2.616	1.702	0.651
768	IPI00925071.1	nucleoporin 205kDa	3.645	3.072	0.843
769	IPI00375533.5	Isoform 2 of NEDD8-activating enzyme E1 catalytic subunit	2.371	1.816	0.766
770	IPI00793076.1	general transcription factor IIA, 2, 12kDa	2.122	1.153	0.543
771	IPI00219005.3	Peptidyl-prolyl cis-trans isomerase FKBP4	2.143	1.773	0.827
772	IPI00303318.2	Protein FAM49B	2.272	3.090	1.360
773	IPI00003217.3	Proteasome subunit beta type-7	3.059	1.995	0.652
774	IPI00026970.4	FACT complex subunit SPT16	4.823	3.009	0.624
775	IPI00926917.1	eukaryotic translation initiation factor 4 gamma, 1	3.165	2.438	0.770
776	IPI00377233.1	Isoform 2 of 39S ribosomal protein L11, mitochondrial	2.192	1.692	0.772
777	IPI01011967.1	cDNA FLJ54535, highly similar to Ribosomal protein S6 kina	2.600	1.925	0.740
778	IPI00430781.1	chromosome 8 open reading frame 82	2.416	1.799	0.745
779	IPI00220059.5	NADH dehydrogenase [ubiquinone] 1 beta subcomplex su	3.058	2.374	0.777
780	IPI00964692.1	exportin 5	2.475	2.114	0.854
781	IPI01013481.1	cDNA FLJ50601, highly similar to Glutathione synthetase	2.255	2.475	1.097
782	IPI00966735.1	28 kDa protein	2.747	2.290	0.834
783	IPI00966258.1	ubiquitin carboxyl-terminal esterase L1 (ubiquitin thioles	2.146	1.764	0.822
784	IPI00940901.1	Isoform 2 of RRP12-like protein	5.202	2.854	0.549
785	IPI00093057.6	Coproporphyrinogen-III oxidase, mitochondrial	2.577	2.605	1.011
786	IPI00031526.3	chromosome 19 open reading frame 43	1.864	1.295	0.695
787	IPI00908327.1	Isoform 2 of RING finger protein 114	2.511	2.192	0.873
788	IPI01013918.1	mannose-6-phosphate receptor (cation dependent)	2.134	1.635	0.766
789	IPI00397700.5	Isoform 2 of PHD finger protein 6	3.123	2.048	0.656
790	IPI00916535.1	prolyl 4-hydroxylase subunit alpha-1 isoform 3 precursor	2.800	2.054	0.734
791	IPI00909399.2	xaa-Pro dipeptidase isoform 3	2.437	2.567	1.053
792	IPI01011453.1	SUMO-activating enzyme subunit 1 isoform c	2.662	2.479	0.931
793	IPI00513841.1	Nicastrin	2.749	2.277	0.828
794	IPI00022648.2	Eukaryotic translation initiation factor 5	3.182	3.422	1.075
795	IPI00014263.1	Isoform Long of Eukaryotic translation initiation factor 4H	2.299	1.646	0.716
796	IPI00719256.2	SART3 protein	3.351	3.069	0.916

797	IPI00292020.3	Spermidine synthase	2.230	2.343	1.051
798	IPI00514522.1	chromosome 1 open reading frame 123	2.005	1.453	0.725
799	IPI00947116.1	dihydrofolate reductase-like 1	2.313	1.752	0.758
800	IPI00966243.1	cytochrome b5 type B (outer mitochondrial membrane)	2.299	1.775	0.772
801	IPI00894110.1	polyribonucleotide nucleotidyltransferase 1	2.189	1.886	0.861
802	IPI00514669.1	SH3 domain binding glutamic acid-rich protein like 3	1.780	1.033	0.581
803	IPI00003326.4	ADP-ribosylation factor-like protein 2	2.511	1.969	0.784
804	IPI00909691.1	cDNA FLJ50174, highly similar to Homo sapiens SNARE prot	3.220	2.524	0.784
805	IPI00980207.1	signal recognition particle 19 kDa protein isoform 3	3.782	2.620	0.693
806	IPI00940222.2	Isoform 3 of A-kinase anchor protein 12	4.888	3.044	0.623
807	IPI00182289.6	40S ribosomal protein S29	2.108	1.108	0.525
808	IPI00939707.1	clustered mitochondria (cluA/CLU1) homolog	2.519	2.489	0.988
809	IPI00005675.3	NF-kappa-B-repressing factor	1.993	2.072	1.040
810	IPI00396329.1	Ribosome production factor 2 homolog	2.990	2.136	0.714
811	IPI00299214.7	Thymidine kinase, cytosolic	4.849	4.582	0.945
812	IPI00023728.1	Gamma-glutamyl hydrolase	2.484	2.858	1.150
813	IPI00643709.1	Solute carrier family 16, member 1	3.415	2.668	0.781
814	IPI00917193.1	hexokinase 2	2.090	1.811	0.867
815	IPI00943181.1	proteasome (prosome, macropain) activator subunit 2 (PA	2.981	2.827	0.948
816	IPI00013180.2	Protein BUD31 homolog	2.944	2.154	0.732
817	IPI00892533.1	chromosome 7 open reading frame 50	2.682	1.828	0.681
818	IPI00005050.1	28S ribosomal protein S14, mitochondrial			0.343
819	IPI00978325.1	cathepsin C	2.305	1.492	0.647
820	IPI00452731.6	NADH dehydrogenase [ubiquinone] 1 alpha subcomplex s	3.039	1.675	0.551
821	IPI00641181.5	MARCKS-related protein	3.731	3.671	0.984
822	IPI00006754.1	DDB1- and CUL4-associated factor 7	2.423	1.968	0.812
823	IPI01015967.1	DnaJ (Hsp40) homolog, subfamily A, member 1	2.114	1.915	0.906
824	IPI00002824.7	Cysteine and glycine-rich protein 2	2.587	1.514	0.585
825	IPI00021266.1	60S ribosomal protein L23a	3.833	1.775	0.463
826	IPI00964725.1	succinate dehydrogenase complex, subunit A, flavoprotein	0.869		
827	IPI00967916.1	cytochrome c oxidase subunit VIIc	2.410	1.109	0.460
828	IPI00219351.3	Isoform 3 of 28S ribosomal protein S11, mitochondrial	3.212	2.152	0.670
829	IPI00604652.1	NEDD8-activating enzyme E1 regulatory subunit isoform c	2.773	1.721	0.621
830	IPI00514049.1	Cytidine monophosphate (UMP-CMP) kinase 1, cytosolic	3.965	2.380	0.600
831	IPI00016339.4	Ras-related protein Rab-5C	1.869	0.801	0.429
832	IPI00847896.1	Similar to Glutamate-rich WD repeat-containing protein 1	7.164	5.378	0.751
833	IPI00217563.4	Isoform Beta-1A of Integrin beta-1	3.743	3.076	0.822
834	IPI01009997.1	cDNA FLJ51981, highly similar to Histone deacetylase 1	2.711	1.364	0.503
835	IPI00032533.3	WD repeat-containing protein 18	2.950	2.088	0.708
836	IPI01018037.1	replication factor C subunit 5 isoform 4	2.413	2.617	1.084
837	IPI00023530.7	Cyclin-dependent kinase 5	2.616	2.035	0.778
838	IPI00844040.2	cDNA FLJ59759, highly similar to Protein SET	3.080	2.531	0.821
839	IPI00965548.1	thyroid hormone receptor interactor 13	1.950	2.213	1.135
840	IPI01015295.1	cDNA FLJ30049 fis, clone ADRGL1000033, highly similar to 2	2.738	2.641	0.965
841	IPI00745105.1	chromosome 16 open reading frame 13	2.094	1.559	0.745
842	IPI00964335.1	eukaryotic translation termination factor 1	3.823	4.749	1.242
843	IPI00641266.4	calpain-2 catalytic subunit isoform 2	2.380	2.177	0.915

844	IPI00902463.1	cDNA FLJ46898 fis, clone UTERU3022168, highly similar to Protein FAM62A			0.759
845	IPI00916207.1	3-hydroxyisobutyryl-CoA hydrolase	2.806	2.330	0.830
846	IPI00854677.1	fused in sarcoma	2.574	2.182	0.848
847	IPI00966135.1	histidine triad nucleotide binding protein 1	3.201	2.255	0.704
848	IPI00979071.1	tumor protein, translationally-controlled 1	2.653	1.824	0.687
849	IPI00797616.2	Isoform 3 of BRCA1-associated ATM activator 1	3.946	2.358	0.598
850	IPI00908614.1	cDNA FLJ51287, highly similar to WD repeat protein 39	2.637	1.951	0.740
851	IPI00798211.1	tubulin folding cofactor B	2.433	1.925	0.791
852	IPI00185146.5	Importin-9	2.664	0.929	0.349
853	IPI00008557.6	Insulin-like growth factor 2 mRNA-binding protein 1	2.263	0.748	0.330
854	IPI00980519.1	Conserved hypothetical protein	2.025	1.969	0.972
855	IPI00927827.1	replication factor C (activator 1) 4, 37kDa	2.698	2.152	0.798
856	IPI00917166.1	dynactin 1			0.397
857	IPI00980429.1	chloride channel, nucleotide-sensitive, 1A	2.701	2.561	0.948
858	IPI00791490.1	pyridoxal (pyridoxine, vitamin B6) kinase	4.426	4.951	1.119
859	IPI00641815.1	Isoform 2 of TIP41-like protein	3.098	2.525	0.815
860	IPI00005969.3	F-actin-capping protein subunit alpha-1	3.799	3.596	0.946
861	IPI00443657.2	cold inducible RNA binding protein	3.701	2.239	0.605
862	IPI00024911.1	Endoplasmic reticulum resident protein 29	2.356	1.632	0.693
863	IPI00964348.1	DTW domain containing 2	3.410	5.144	1.509
864	IPI00848298.1	Isoform 2 of Apolipoprotein A-I-binding protein	2.322	1.784	0.768
865	IPI00925058.1	Ribosomal protein L15	2.993	2.573	0.860
866	IPI00410714.5	Hemoglobin subunit alpha	2.568	1.389	0.541
867	IPI00917535.1	mitochondrial ribosomal protein L30	2.769	1.834	0.662
868	IPI01015489.1	cDNA FLJ60345, highly similar to Protein transport protein	2.280	1.720	0.755
869	IPI00174852.4	Mediator of RNA polymerase II transcription subunit 20	2.548	1.985	0.779
870	IPI00012315.2	Nucleoside diphosphate kinase 3	1.893	1.639	0.866
871	IPI01012187.1	cDNA, FLJ79426, highly similar to Serine/threonine-protein	3.187	4.229	1.327
872	IPI00747810.3	fascin homolog 1, actin-bundling protein (Strongylocentro	4.249	6.229	1.466
873	IPI00924813.1	Similar to Ribosomal protein L37a	3.527	2.034	0.577
874	IPI00025178.3	Pre-mRNA-splicing factor SPF27	3.303	1.948	0.590
875	IPI00030929.4	myosin regulatory light polypeptide 9 isoform b	2.667	1.790	0.671
876	IPI00029114.1	Peptidyl-tRNA hydrolase ICT1, mitochondrial	2.846	1.963	0.690
877	IPI00922290.1	cDNA FLJ53094, highly similar to Receptor expression-enha	3.823	2.661	0.696
878	IPI00018203.1	Isoform SRP55-2 of Serine/arginine-rich splicing factor 6	2.375	1.707	0.719
879	IPI00016532.4	chromosome 4 open reading frame 27			0.927
880	IPI00844002.1	LYST-interacting protein LIP5 (Fragment)	3.452	3.185	0.923
881	IPI00026496.3	Nucleoplasmin-3	2.001	1.537	0.768
882	IPI00419797.5	signal recognition particle 9kDa	1.806	0.879	0.487
883	IPI00029239.2	Isoform 2 of L-2-hydroxyglutarate dehydrogenase, mitocho	4.814	4.519	0.939
884	IPI00917449.1	gamma-glutamylcyclotransferase	2.296	1.721	0.750
885	IPI00910220.1	cDNA FLJ60230, highly similar to Arsenical pump-driving AT	3.281	2.688	0.819
886	IPI00981356.1	3-hydroxyacyl-CoA dehydratase 3-like isoform 3, partial	4.172	2.903	0.696
887	IPI00868858.1	Isoform 3 of MYC-induced nuclear antigen	2.429	2.772	1.141
888	IPI00925203.1	glutaminyl-tRNA synthetase			2.922
889	IPI00892788.1	high density lipoprotein binding protein	7.226	2.066	0.286
890	IPI01015780.1	cDNA FLJ57449, highly similar to Notchless homolog 1	1.859	2.084	1.121

891	IPI00909038.1	cDNA FLJ58068, highly similar to Seryl-tRNA synthetase, mi	1.866	2.015	1.080
892	IPI00219783.7	Ubiquitin-conjugating enzyme E2 G1	2.591	2.192	0.846
893	IPI00925737.1	phosphoserine phosphatase	2.759	2.181	0.791
894	IPI00100984.4	Isoform 1 of HEAT repeat-containing protein 3	2.466	2.494	1.011
895	IPI00004454.3	Isoform 1 of Dolichol-phosphate mannosyltransferase sul	2.544	2.135	0.839
896	IPI00915874.1	partner of NOB1 homolog (S. cerevisiae)	3.406	0.889	0.261
897	IPI00006379.1	Nucleolar protein 58	2.835	0.970	0.342
898	IPI00184854.1	FK506 binding protein 10, 65 kDa	2.422	2.057	0.849
899	IPI00101734.5	family with sequence similarity 105, member B	2.016	1.417	0.703
900	IPI00186338.1	barrier-to-autointegration factor-like	1.924	0.551	0.287
901	IPI00926139.1	mitochondrial ribosomal protein S25	4.682	3.599	0.769
902	IPI00409639.1	Isoform 4 of Methyltransferase-like protein 13	1.656	1.871	1.130
903	IPI00910420.1	Isoform 3 of Alpha-aminoadipic semialdehyde dehydroge	1.686	1.962	1.164
904	IPI00924740.1	programmed cell death 6 interacting protein	1.860	1.837	0.988
905	IPI00301051.3	Isoform 1 of NHL repeat-containing protein 2	3.799	2.256	0.594
906	IPI00335589.5	RNA methyltransferase-like protein 1	1.915	2.480	1.295
907	IPI00032849.2	Nucleolar protein 16	1.942	1.526	0.785
908	IPI00032903.3	Peptidyl-tRNA hydrolase 2, mitochondrial	3.312	3.700	1.117
909	IPI00552190.1	Proteasome (Prosome, macropain) 26S subunit, non-ATPas	2.192	1.287	0.587
910	IPI00940264.1	Galactokinase	2.557	3.010	1.177
911	IPI00218112.1	Isoform Short of Glutaryl-CoA dehydrogenase, mitochondri	2.354	1.449	0.616
912	IPI00983446.1	UV radiation resistance associated	4.931	1.856	0.376
913	IPI00061525.3	Glucosamine 6-phosphate N-acetyltransferase	2.142	1.885	0.880
914	IPI00017704.3	Coactosin-like protein	3.031	1.794	0.592
915	IPI00792829.1	cDNA FLJ57094, highly similar to Probable ATP-dependent l	2.587	2.343	0.906
916	IPI00926756.1	Isoform 4 of TBC1 domain family member 4	3.090	2.892	0.936
917	IPI00910540.1	cDNA FLJ51496, highly similar to Tyrosine-protein kinase C	1.915	2.219	1.159
918	IPI00922322.1	cDNA FLJ54129, highly similar to Nucleosome assembly pro	3.344	2.988	0.894
919	IPI00940293.5	cDNA FLJ56433, highly similar to Collagen alpha-2(IV) chai	2.944	1.794	0.609
920	IPI01011794.1	cDNA FLJ55643, highly similar to SEC23-interacting protein	1.859	1.320	0.710
921	IPI00965185.1	aminoacyl tRNA synthetase complex-interacting multifunc	2.288	3.295	1.440
922	IPI00395779.4	chromosome 20 open reading frame 27	2.534	1.686	0.666
923	IPI01015329.1	cDNA FLJ52203, highly similar to 3'(2'),5'-bisphosphate nuc	3.475	3.103	0.893
924	IPI00976190.1	splicing factor 3b, subunit 2, 145kDa	4.347	3.358	0.772
925	IPI00023542.6	Transmembrane emp24 domain-containing protein 9	1.739	1.681	0.967
926	IPI01014928.1	cDNA FLJ55328, highly similar to Homo sapiens BPY2 intera	3.894	2.818	0.724
927	IPI00845493.1	Brain type mu-glutathione S-transferase	4.100	3.005	0.733
928	IPI00219065.2	Isoform 5 of Glycogen debranching enzyme	3.575	2.946	0.824
929	IPI00979951.1	proteasome (prosome, macropain) 26S subunit, ATPase, 3	1.682	1.423	0.846
930	IPI00549993.3	Isoform 1 of Protein FAM188A	2.963	3.028	1.022
931	IPI00791680.1	cortactin	2.526	2.019	0.799
932	IPI01009790.1	cDNA, FLJ79293, highly similar to WD repeat protein 71	2.719	2.069	0.761
933	IPI00946316.1	karyopherin alpha 4 (importin alpha 3)	2.852	1.685	0.591
934	IPI01014354.1	cDNA FLJ54039, highly similar to Protein arginine N-methyltransferase 5			0.301
935	IPI00910350.1	cDNA FLJ52068, highly similar to Microtubule-associated p	2.320	1.855	0.799
936	IPI00384155.1	Full-length cDNA clone CS0DI002YH20 of Placenta of Homo	2.855	3.138	1.099
937	IPI00981694.1	ATX1 antioxidant protein 1 homolog (yeast)	2.160	1.436	0.665

938	IPI00946674.1	aldo-keto reductase family 7, member A2 (aflatoxin aldeh	8.035	7.719	0.961
939	IPI00001655.1	chromosome 16 open reading frame 80	2.139	1.582	0.740
940	IPI00654793.2	NAD kinase domain containing 1	6.247	3.579	0.573
941	IPI01015376.1	ATP synthase gamma chain	1.992	1.458	0.732
942	IPI00002214.1	Importin subunit alpha-2	3.253	2.384	0.733
943	IPI00908375.1	cDNA FLJ52821, highly similar to Protein transport protein S	3.052	1.676	0.549
944	IPI00978272.1	methylcrotonoyl-CoA carboxylase beta chain, mitochondria	3.035	1.741	0.574
945	IPI00945912.1	cDNA FLJ59963, highly similar to Homo sapiens multiple su	2.105	2.442	1.160
946	IPI00927809.1	DEAH (Asp-Glu-Ala-His) box polypeptide 30	3.310	2.757	0.833
947	IPI00927458.1	ribosomal protein L32	4.089	3.120	0.763
948	IPI00183603.3	Oligosaccharyltransferase complex subunit OSTC	8.362	4.496	0.538
949	IPI00894139.1	golgi to ER traffic protein 4 homolog (S. cerevisiae)	5.418	5.435	1.003
950	IPI00878039.2	coiled-coil domain containing 117	2.228	2.479	1.112
951	IPI00795057.1	mitochondrial ribosomal protein S28	2.925	2.252	0.770
952	IPI00641692.3	Ribonuclease P	3.031	1.810	0.597
953	IPI00642048.2	GDP-mannose 4,6-dehydratase	3.094	2.520	0.815
954	IPI00334282.2	Protein FAM3C			1.020
955	IPI01008950.1	Isoform 4 of UDP-N-acetylglucosamine--peptide N-acetylgl	2.168	1.951	0.900
956	IPI00885131.1	Isoform 3 of tRNA (adenine-N(1)-)-methyltransferase non-	2.616	1.633	0.624
957	IPI00903191.1	Eukaryotic translation initiation factor 3, subunit D	2.972	2.215	0.745
958	IPI00886797.1	Isoform 2 of 2',5'-phosphodiesterase 12	2.582	2.133	0.826
959	IPI01015636.1	pogo transposable element with ZNF domain	3.742	3.187	0.852
960	IPI00871780.1	RNA-binding protein 12B	3.431	3.040	0.886
961	IPI00908741.1	FAD-dependent oxidoreductase domain containing 1	1.919	2.585	1.347
962	IPI00893867.1	hydroxyacyl-CoA dehydrogenase/3-ketoacyl-CoA thiolase/e	1.488	1.894	1.273
963	IPI00940816.2	Isoform 3 of Rho guanine nucleotide exchange factor 2	2.306	1.978	0.858
964	IPI00007019.1	Peptidyl-prolyl cis-trans isomerase-like 1	2.867	1.869	0.652
965	IPI00945733.1	karyopherin alpha 1 (importin alpha 5)	4.379	5.617	1.283
966	IPI00399089.4	LDLR chaperone MESD	1.868	1.485	0.795
967	IPI01014449.1	chromobox homolog 1	2.312	1.698	0.734
968	IPI00292894.5	Pre-rRNA-processing protein TSR1 homolog	1.797	1.876	1.044
969	IPI00008436.4	DNA polymerase epsilon subunit 4	2.749	2.284	0.831
970	IPI00981292.1	cDNA FLJ53391, highly similar to ATP-binding cassette sub-	4.960	3.100	0.625
971	IPI00220835.7	Protein transport protein Sec61 subunit beta	5.362	3.242	0.605
972	IPI00061531.4	39S ribosomal protein L53, mitochondrial	3.948	2.101	0.532
973	IPI00297626.4	Syntaxin-binding protein 3	2.726	1.236	0.453
974	IPI01014726.1	cDNA, FLJ79305, highly similar to Calponin-1	2.413	1.579	0.654
975	IPI00024284.6	Basement membrane-specific heparan sulfate proteoglyc	2.833	2.348	0.829
976	IPI00329373.3	Protein QIL1	1.913	0.926	0.484
977	IPI00015833.1	Coiled-coil-helix-coiled-coil-helix domain-containing prot	2.578	1.907	0.740
978	IPI00874145.2	dyskeratosis congenita 1, dyskerin	2.384	1.598	0.670
979	IPI00788157.1	Isoform 2 of 5'-3' exoribonuclease 2	2.102	2.014	0.958
980	IPI00306290.5	Exportin-T	1.257	0.808	0.643
981	IPI00783001.1	Isoform 1 of Probable methyltransferase-like protein 15	2.824	2.151	0.762
982	IPI00477853.2	zinc finger protein 235	3.082	2.182	0.708
983	IPI00926599.1	glycerol-3-phosphate dehydrogenase 1-like	2.512	2.391	0.951
984	IPI00908410.1	cDNA FLJ56566, highly similar to Small glutamine-rich tetra	1.720	1.936	1.126

985	IPI00032881.2	28S ribosomal protein S23, mitochondrial	2.074	1.587	0.765
986	IPI00794240.1	mitochondrial ribosomal protein L39	2.990	2.768	0.926
987	IPI00966215.1	TROVE domain family, member 2	2.401	1.678	0.699
988	IPI00868803.2	Similar to Survival of motor neuron 2, centromeric isoform	2.784	3.119	1.120
989	IPI00985284.1	La ribonucleoprotein domain family, member 1	2.129	1.816	0.853
990	IPI01015748.1	cDNA FLJ54999, highly similar to Mitochondrial-processing	1.620	1.476	0.911
991	IPI00845477.1	Isoform 2 of Alpha-ketoglutarate-dependent dioxygenase	2.884	2.061	0.715
992	IPI00062882.4	Cytoplasmic tRNA 2-thiolation protein 1	2.931	2.506	0.855
993	IPI00941385.2	Isoform 3 of Ubiquitin carboxyl-terminal hydrolase 10	2.074	1.522	0.734
994	IPI01011431.1	cDNA FLJ60167, highly similar to Cytosolic acyl coenzyme A thioester hydrolase			0.666
995	IPI01009918.1	Protease serine 1	1.671	1.127	0.674
996	IPI00642982.1	LONP1 protein	3.097	2.134	0.689
997	IPI00647368.1	isocitrate dehydrogenase 3 (NAD+) gamma	2.886	2.075	0.719
998	IPI00446669.1	Isoform 2 of Multiple myeloma tumor-associated protein	2.754	3.241	1.177
999	IPI00398758.1	Isoform 2 of Enoyl-CoA delta isomerase 1, mitochondrial	2.832	2.088	0.737
1000	IPI01015385.1	Isocitrate dehydrogenase	8.725	4.943	0.566
1001	IPI00797738.1	Cytochrome c oxidase subunit 6B1	2.063	1.310	0.635
1002	IPI00946017.1	ubiquitin specific peptidase 9, X-linked	3.737	2.796	0.748
1003	IPI00030968.4	chromosome 9 open reading frame 142	2.547	1.776	0.697
1004	IPI01013430.1	Selenophosphate synthetase 1 +E9a variant	4.037	3.503	0.868
1005	IPI00107339.4	Isoform 1 of Guanine nucleotide-binding protein subunit	2.983	3.335	1.118
1006	IPI00967384.2	translocase of inner mitochondrial membrane 8 homolog	1.961	0.883	0.450
1007	IPI00644506.1	cDNA FLJ58756, highly similar to Nuclear pore complex pro	2.598	2.234	0.860
1008	IPI00328298.6	Isoform 2 of Structural maintenance of chromosomes prot	3.847	2.616	0.680
1009	IPI00514902.1	Ubiquitin protein ligase E3 component n-recognin 4	2.907	2.482	0.854
1010	IPI00018331.3	SNARE-associated protein Snapin	3.185	2.799	0.879
1011	IPI00975492.1	pyruvate dehydrogenase complex, component X	1.710	1.605	0.939
1012	IPI00880148.1	lectin, galactoside-binding, soluble, 1	2.954	1.842	0.624
1013	IPI00878100.2	GTP binding protein 1	2.220	1.955	0.881
1014	IPI00221089.5	40S ribosomal protein S13	2.269	2.011	0.886
1015	IPI00793395.1	cDNA FLJ37679 fis, clone BRHIP2012922, highly similar to Co	2.913	2.314	0.794
1016	IPI00291755.6	Isoform 1 of Nuclear pore membrane glycoprotein 210	3.019	2.519	0.834
1017	IPI00974419.1	minichromosome maintenance complex component 4	1.937	2.194	1.132
1018	IPI00025285.3	V-type proton ATPase subunit G 1	3.081	1.949	0.633
1019	IPI01011252.2	phosphatidylinositol transfer protein, alpha	2.155	3.220	1.494
1020	IPI00893025.1	mutS homolog 6 (E. coli)	4.563	3.178	0.696
1021	IPI00916549.1	budding uninhibited by benzimidazoles 1 homolog (yeast	1.859	1.930	1.038
1022	IPI00947340.1	FKBP8 isoform 1	2.999	1.948	0.650
1023	IPI00301609.8	Serine/threonine-protein kinase Nek9	2.673	2.473	0.925
1024	IPI00980165.2	Mesencephalic astrocyte-derived neurotrophic factor	1.674	1.749	1.045
1025	IPI00894420.1	dihydropyrimidinase-like 5	3.363	2.218	0.660
1026	IPI00915422.1	coatomer subunit delta isoform 2	2.156	1.560	0.724
1027	IPI00940506.2	cDNA FLJ58519, highly similar to Hermansky-Pudlak syndro	2.425	1.603	0.661
1028	IPI01011998.1	NADH dehydrogenase (ubiquinone) 1 alpha subcomplex, 8	2.381	1.972	0.828
1029	IPI00945124.1	Brain my045 protein	2.495	2.240	0.898
1030	IPI00300299.6	Signal peptidase complex subunit 3	2.157	1.833	0.850
1031	IPI00940755.2	density-regulated protein	2.503	1.962	0.784

1032	IPI00909010.1	cDNA FLJ59356, highly similar to N-acetylserotonin O-meth	2.876	2.446	0.851
1033	IPI00916807.1	MKI67 (FHA domain) interacting nucleolar phosphoprotein	2.286	2.563	1.121
1034	IPI00644418.3	endophilin-A2 isoform 3	2.160	1.980	0.917
1035	IPI00890793.1	iron-sulfur cluster scaffold homolog (E. coli)	2.828	1.839	0.650
1036	IPI00477468.1	RNA polymerase-associated protein CTR9 homolog	3.616	3.113	0.861
1037	IPI00984662.1	28S ribosomal protein S29, mitochondrial isoform 3	2.792	2.050	0.734
1038	IPI00015809.1	Probable tRNA threonylcarbamoyladenosine biosynthesis	2.388	2.535	1.062
1039	IPI00219411.3	Isoform 2 of RAC-gamma serine/threonine-protein kinase	2.772	1.837	0.663
1040	IPI00385642.1	WD repeat domain 57 (U5 snRNP specific), isoform CRA_b	2.357	2.232	0.947
1041	IPI00032851.1	Coatomer subunit zeta-1	1.899	1.618	0.852
1042	IPI00514469.1	N-acetylneuraminic acid synthase	2.521	2.133	0.846
1043	IPI00001539.8	3-ketoacyl-CoA thiolase, mitochondrial	2.258	1.561	0.691
1044	IPI00514444.1	Insulin-degrading enzyme	2.201	1.840	0.836
1045	IPI00017592.1	Isoform 1 of LETM1 and EF-hand domain-containing protei	2.241	1.815	0.810
1046	IPI00983309.1	STT3, subunit of the oligosaccharyltransferase complex, h	5.327	3.403	0.639
1047	IPI00145260.3	Putative transferase CAF17, mitochondrial	2.385	2.180	0.914
1048	IPI00374272.3	chromosome 5 open reading frame 51	2.387	2.624	1.100
1049	IPI00655644.4	inner membrane protein, mitochondrial	2.790	2.286	0.819
1050	IPI01011236.1	TUFT1	4.813	2.885	0.599
1051	IPI00643078.1	RAD23 homolog B	2.952	2.205	0.747
1052	IPI00025115.1	AP-3 complex subunit sigma-2	2.215	1.542	0.696
1053	IPI00220648.5	Phosphomevalonate kinase	4.776	5.338	1.118
1054	IPI00641843.3	cDNA, FLJ78963, highly similar to Ubiquitin carboxyl-termin	2.141	2.189	1.022
1055	IPI00830039.1	Isoform 2 of Splicing factor U2AF 65 kDa subunit	3.215	1.907	0.593
1056	IPI01012107.1	defender against cell death 1	2.112	1.590	0.753
1057	IPI00305668.7	28S ribosomal protein S6, mitochondrial	2.905	1.502	0.517
1058	IPI00643648.1	Phosphatidylserine decarboxylase	2.530	2.148	0.849
1059	IPI00028091.3	Actin-related protein 3	2.257	2.091	0.927
1060	IPI00427502.1	Isoform 2 of GH3 domain-containing protein	2.474	2.172	0.878
1061	IPI00029629.4	E3 ubiquitin/ISG15 ligase TRIM25	2.987	2.558	0.856
1062	IPI01010716.1	cDNA FLJ90324 fis, clone NT2RP2001817, highly similar to N	2.060	1.771	0.860
1063	IPI00396090.3	Isoform 3 of Diphosphoinositol polyphosphate phosphoh	2.252	1.608	0.714
1064	IPI00902580.1	cDNA FLJ11050 fis, clone PLACE1004564, highly similar to Cl	2.217	2.106	0.950
1065	IPI00022865.2	Cyclin-A2	2.254	2.302	1.021
1066	IPI00401804.3	Isoform 3 of Vesicle-associated membrane protein 7	2.024	1.739	0.859
1067	IPI00658162.2	cDNA FLJ36570 fis, clone TRACH2011302, highly similar to S	2.301	2.826	1.228
1068	IPI00974168.1	heat-responsive protein 12	3.834	2.102	0.548
1069	IPI00893645.1	septin 2	2.320	1.886	0.813
1070	IPI00005692.1	28S ribosomal protein S12, mitochondrial	4.084	1.917	0.469
1071	IPI00902652.1	cDNA FLJ37148 fis, clone BRACE2025333, highly similar to H	2.207	1.890	0.856
1072	IPI00977065.1	cold shock domain containing E1, RNA-binding	2.890	1.940	0.671
1073	IPI00398822.1	Isoform 2 of Zinc phosphodiesterase ELAC protein 2	1.850	2.177	1.177
1074	IPI00219090.1	Isoform 2 of Protein arginine N-methyltransferase 7	2.640	2.296	0.869
1075	IPI00219604.3	Isoform 1 of Dual specificity mitogen-activated protein kin	2.618	1.778	0.679
1076	IPI00411886.5	Nucleolar complex protein 2 homolog	2.064	1.977	0.958
1077	IPI00973882.1	ATPase, H+ transporting, lysosomal 50/57kDa, V1 subunit F	2.737	2.126	0.777
1078	IPI00025329.1	60S ribosomal protein L19	3.648	2.929	0.803

1079	IPI00041325.1	H/ACA ribonucleoprotein complex subunit 2	2.331	1.286	0.552
1080	IPI01013434.1	superoxide dismutase 2, mitochondrial	1.510	1.248	0.826
1081	IPI00176527.1	ATP synthase subunit epsilon-like protein, mitochondrial	2.254	1.263	0.560
1082	IPI00797314.1	COP9 constitutive photomorphogenic homolog subunit 3 (A	2.457	1.857	0.756
1083	IPI00943212.2	ATPase, H+ transporting, lysosomal 38kDa, V0 subunit d1	1.992	2.495	1.252
1084	IPI00556437.1	Dynamin 2 isoform 4 variant (Fragment)	3.066	2.248	0.733
1085	IPI00026219.4	Cleavage and polyadenylation specificity factor subunit 1	3.868	2.734	0.707
1086	IPI00219718.3	retinol-binding protein 1 isoform a	4.374	2.082	0.476
1087	IPI01012894.1	cell division cycle and apoptosis regulator 1	5.202	7.323	1.408
1088	IPI00847986.1	Isoform 2 of 40S ribosomal protein S24	2.579	2.005	0.777
1089	IPI00514217.6	Succinate-CoA ligase, ADP-forming, beta subunit	2.566	1.815	0.707
1090	IPI00926706.1	actin related protein 2/3 complex, subunit 1A, 41kDa	2.145	1.594	0.743
1091	IPI00549942.3	cDNA FLJ30306 fis, clone BRACE2003319	3.656	1.979	0.541
1092	IPI00979224.1	family with sequence similarity 203, member A	5.407	2.194	0.406
1093	IPI01009730.1	Putative uncharacterized protein DKFZp547A1913	3.538	3.570	1.009
1094	IPI00103263.3	Wings apart-like homolog	3.612	2.862	0.792
1095	IPI00742682.2	Nucleoprotein TPR	2.504	2.441	0.975
1096	IPI00003815.3	Rho GDP-dissociation inhibitor 1	2.717	2.175	0.800
1097	IPI01010344.1	PRP8 pre-mRNA processing factor 8 homolog (S. cerevisiae	5.064	2.906	0.574
1098	IPI00879774.1	Cysteine-rich with EGF-like domains 2	2.940	2.228	0.758
1099	IPI00005162.3	Actin-related protein 2/3 complex subunit 3	3.401	2.155	0.634
1100	IPI00984053.1	serine hydroxymethyltransferase 1 (soluble)	1.908	1.579	0.828
1101	IPI00658053.1	cathepsin D	3.031	1.859	0.613
1102	IPI00873515.2	Isoform 2 of Probable bifunctional methylenetetrahydrofo	2.020	2.302	1.139
1103	IPI00925248.1	Uncharacterized protein	2.724	2.571	0.944
1104	IPI00376117.1	Isoform 2 of Mitochondrial import receptor subunit TOM40	2.882	1.931	0.670
1105	IPI00916763.1	heat shock 10kDa protein 1 (chaperonin 10)	1.971	1.339	0.679
1106	IPI00423157.4	Isoform 11 of Serine/threonine-protein kinase Chk2	2.785	1.322	0.475
1107	IPI00216237.5	60S ribosomal protein L36	2.494	1.878	0.753
1108	IPI00784650.3	uncharacterized LOC100131551	5.900	3.021	0.512
1109	IPI00917636.1	acyl-CoA synthetase long-chain family member 3	2.455	2.460	1.002
1110	IPI00061282.2	Protein kinase, AMP-activated, alpha 1 catalytic subunit, is	3.425	2.043	0.596
1111	IPI00977736.1	calcyclin-binding protein isoform 2	2.736	2.001	0.732
1112	IPI00220919.1	Isoform 3 of DNA (cytosine-5)-methyltransferase 1	2.816	2.448	0.869
1113	IPI00014603.1	Ras-related protein Rab-9B	2.963	1.662	0.561
1114	IPI00418290.1	39S ribosomal protein L14, mitochondrial			1.284
1115	IPI00903276.1	cDNA FLJ36073 fis, clone TESTI2019697, highly similar to TH	2.725	1.973	0.724
1116	IPI00902466.1	cDNA FLJ11861 fis, clone HEMBA1006885, highly similar to P	2.473	1.926	0.779
1117	IPI00419898.1	uncharacterized LOC440157	2.161	1.533	0.709
1118	IPI00789985.1	Isoform 2 of Ran guanine nucleotide release factor	1.916	1.429	0.746
1119	IPI00975997.1	cancer/testis antigen family 45 member A5-like isoform 2,	2.885	2.298	0.796
1120	IPI00790648.2	transferrin	1.675	2.094	1.250
1121	IPI00978109.1	DIS3 mitotic control homolog (S. cerevisiae)	1.909	1.668	0.874
1122	IPI00017283.2	Isoleucyl-tRNA synthetase, mitochondrial	1.646	1.887	1.147
1123	IPI00939558.2	cDNA FLJ38696 fis, clone KIDNE2001931, highly similar to HI	2.542	1.978	0.778
1124	IPI00294742.7	Isoform 1 of La-related protein 7	2.653	2.077	0.783
1125	IPI00973715.2	dihydropyrimidinase	5.058	2.835	0.561

1126	IPI00909332.2	replication termination factor 2 domain containing 1	2.124	2.600	1.224
1127	IPI00301323.1	ATP-dependent RNA helicase DDX18	2.578	1.525	0.591
1128	IPI00788612.2	LIM and senescent cell antigen-like-containing domain pr	2.453	2.440	0.995
1129	IPI00247439.3	Isoform 2 of STE20-like serine/threonine-protein kinase	3.760	2.860	0.761
1130	IPI00219197.3	Isoform I of Ubiquitin-protein ligase E3A	2.008	2.234	1.112
1131	IPI00893703.1	ribosomal protein S7	2.254	2.147	0.953
1132	IPI00872684.2	cDNA FLJ54141, highly similar to Ezrin	2.026	1.668	0.823
1133	IPI00514858.1	Adenylyl cyclase-associated protein	2.345	2.532	1.080
1134	IPI00909477.1	cDNA FLJ54108, highly similar to Homo sapiens smooth mu	1.346	2.272	1.687
1135	IPI01009526.1	cDNA FLJ61034, highly similar to Mitochondrial dicarboxyla	2.514	1.811	0.720
1136	IPI00220716.2	Isoform 2 of Putative RNA-binding protein 15	2.848	2.472	0.868
1137	IPI00914006.2	cDNA FLJ56235, highly similar to Dynactin subunit 4	2.767	2.768	1.000
1138	IPI00219833.2	Mitochondrial import inner membrane translocase subun	2.900	2.237	0.771
1139	IPI00796237.1	DUSP3 protein	2.766	1.800	0.651
1140	IPI00443909.1	Isoform 1 of Protein canopy homolog 2	2.782	2.130	0.766
1141	IPI00910004.1	cDNA FLJ59139, highly similar to Vesicle-associated memb	3.625	2.229	0.615
1142	IPI01012992.1	Coiled-coil domain-containing protein 12	2.621	2.533	0.966
1143	IPI00020793.3	Isoform 2 of 60S ribosome subunit biogenesis protein NIP	1.861	1.630	0.876
1144	IPI00922847.1	cDNA FLJ50115, moderately similar to Membrane-associate	1.854	1.264	0.682
1145	IPI00479722.2	Proteasome activator complex subunit 1	3.502	2.108	0.602

Table A7. Positive proteins identified in HEK293T cell lysates treated with ProSeAM. Proteomic data sets from HEK293T lysate treated with ProSeAM or the lysates treated with ProSeAM and the pan-methyltransferase inhibitor, SAH, were cross-referenced to identify targets uniquely present in the non-inhibitor-treated sample. The listed proteins are present in HEK293T cell lysates treated with ProSeAM but not in the HEK293T cell lysates treated with ProSeAM and SAH, and arranged according to their accession number.

Accession	Description	Score	MW [kDa]
IPI00002824.7	Cysteine and glycine-rich protein 2	1.79	20.9
IPI00003783.1	Dual specificity mitogen-activated protein kinase kinase 2	3.48	44.4
IPI00003815.3	Rho GDP-dissociation inhibitor 1	5.78	23.2
IPI00003949.1	Ubiquitin-conjugating enzyme E2 N	6.87	17.1
IPI00005511.1	PHD finger-like domain-containing protein 5A	1.99	12.4
IPI00005719.1	Isoform 1 of Ras-related protein Rab-1A	2.21	22.7
IPI00007611.1	ATP synthase subunit O, mitochondrial	4.19	23.3
IPI00009342.1	Ras GTPase-activating-like protein IQGAP1	2.80	189.1
IPI00010105.1	Eukaryotic translation initiation factor 6	3.55	26.6
IPI00010153.5	60S ribosomal protein L23	2.16	14.9
IPI00011454.1	Isoform 2 of Neutral alpha-glucosidase AB	20.82	109.4
IPI00012340.1	Serine/arginine-rich splicing factor 9	3.68	25.5
IPI00012493.1	40S ribosomal protein S20	7.83	13.4
IPI00012866.2	RAC-alpha serine/threonine-protein kinase	7.39	55.7
IPI00013184.1	N-alpha-acetyltransferase 10, NatA catalytic subunit	1.92	26.4
IPI00013789.5	SET and MYND domain-containing protein 5	11.11	47.3
IPI00013885.1	Caspase-14	3.49	27.7
IPI00013933.2	Isoform DPI of Desmoplakin	1.87	331.6
IPI00013946.1	Synaptogyrin-2	3.52	24.8
IPI00014150.1	Isoform 2 of Pre-mRNA-splicing regulator WTAP	4.36	17.8
IPI00014424.1	Elongation factor 1-alpha 2	259.79	50.4
IPI00014808.1	Platelet-activating factor acetylhydrolase IB subunit gamma	4.39	25.7

IPI00015351.2	Isoform 1 of PITH domain-containing protein 1	6.26	24.2
IPI00015833.1	Coiled-coil-helix-coiled-coil-helix domain-containing protein 3, mitochondrial	6.04	26.1
IPI00016342.1	Ras-related protein Rab-7a	7.75	23.5
IPI00016786.1	Isoform 2 of Cell division control protein 42 homolog	1.61	21.2
IPI00018534.4	Histone H2B type 1-L	7.86	13.9
IPI00019385.4	Translocon-associated protein subunit delta	2.23	19.0
IPI00020194.1	Isoform Short of TATA-binding protein-associated factor 2N	16.16	61.5
IPI00021290.5	ATP-citrate synthase	57.88	120.8
IPI00021828.1	Cystatin-B	2.15	11.1
IPI00022149.1	Isoform 2 of Phosphatidylinositol-4-phosphate 5-kinase type-1 alpha	7.24	56.0
IPI00022334.1	Ornithine aminotransferase, mitochondrial	2.08	48.5
IPI00022430.1	Glyceraldehyde-3-phosphate dehydrogenase, testis-specific	23.12	44.5
IPI00022597.1	NEDD8-conjugating enzyme Ubc12	5.33	20.9
IPI00022648.2	Eukaryotic translation initiation factor 5	3.50	49.2
IPI00024266.3	Microsomal glutathione S-transferase 3	2.17	16.5
IPI00025039.1	rRNA 2'-O-methyltransferase fibrillarin	6.36	33.8
IPI00025512.2	Heat shock protein beta-1	1.92	22.8
IPI00026215.1	Flap endonuclease 1	4.57	42.6
IPI00027251.1	Serine/threonine-protein kinase 38	26.26	54.2
IPI00027497.5	Glucose-6-phosphate isomerase	18.84	63.1
IPI00027547.2	Dermcidin	9.51	11.3
IPI00028481.1	Ras-related protein Rab-8A	4.45	23.7
IPI00029643.3	Isoform 2 of Mitogen-activated protein kinase kinase kinase MLT	6.09	51.5
IPI00030182.1	Guanidinoacetate N-methyltransferase	13.20	26.3
IPI00031169.1	Ras-related protein Rab-2A	4.50	23.5
IPI00031526.3	Uncharacterized protein C19orf43	1.80	18.4
IPI00031820.3	Phenylalanyl-tRNA synthetase alpha chain	4.09	57.5
IPI00032158.3	Isoform 2 of N-alpha-acetyltransferase 15, NatA auxiliary subunit	9.44	101.1

IPI00032827.1	Pre-mRNA branch site protein p14	1.84	14.6
IPI00032995.1	LanC-like protein 2	7.01	50.8
IPI00045498.4	Isoform 3 of Heterogeneous nuclear ribonucleoprotein D-like	4.28	27.2
IPI00081836.3	Histone H2A type 1-H	3.46	13.9
IPI00101357.2	Protein RRNAD1	7.05	52.9
IPI00102128.1	Isoform 1 of Protein arginine N-methyltransferase 6	42.62	41.9
IPI00103467.5	Aldehyde dehydrogenase X, mitochondrial	6.24	57.2
IPI00104050.3	Thyroid hormone receptor-associated protein 3	1.75	108.6
IPI00140420.4	Staphylococcal nuclease domain-containing protein 1	15.68	101.9
IPI00166153.3	Cap-specific mRNA (nucleoside-2'-O-)-methyltransferase 1	30.38	95.3
IPI00180128.4	Isoform 2 of Basic leucine zipper and W2 domain-containing protein 1	2.00	40.5
IPI00184533.1	Ubiquitin carboxyl-terminal hydrolase 11	1.64	109.7
IPI00185146.5	Importin-9	2.32	115.9
IPI00215884.4	Isoform ASF-1 of Serine/arginine-rich splicing factor 1	6.07	27.7
IPI00216393.1	Isoform Non-brain of Clathrin light chain A	4.62	23.6
IPI00216493.1	Isoform 3 of Heterogeneous nuclear ribonucleoprotein H3	16.42	31.5
IPI00216770.1	Isoform 2 of 26S protease regulatory subunit 6B	1.74	43.5
IPI00217465.5	Histone H1.2	6.24	21.4
IPI00217661.4	ribonucleoprotein PTB-binding 1	1.92	79.5
IPI00217816.3	Isoform AGX1 of UDP-N-acetylhexosamine pyrophosphorylase	1.82	57.0
IPI00218070.1	Isoform GRB3-3 of Growth factor receptor-bound protein 2	3.92	20.5
IPI00218435.1	Isoform 2 of U4/U6 small nuclear ribonucleoprotein Prp4	2.14	58.3
IPI00218922.5	Translocation protein SEC63 homolog	8.51	87.9
IPI00219025.3	Glutaredoxin-1	6.62	11.8
IPI00219160.3	60S ribosomal protein L34	4.31	13.3
IPI00219617.5	Isoform 1 of Ribose-phosphate pyrophosphokinase 2	6.81	34.7
IPI00219669.5	Carbonic anhydrase-related protein	3.26	33.0

IPI00219762.4	Cellular apoptosis susceptibility protein variant 2	24.65	103.8
IPI00220336.1	Isoform 2 of Exosome component 10	4.49	98.0
IPI00220373.5	Insulin-degrading enzyme	3.92	117.9
IPI00220919.1	Isoform 3 of DNA (cytosine-5)-methyltransferase 1	38.28	144.4
IPI00221091.9	40S ribosomal protein S15a	9.51	14.8
IPI00221093.7	40S ribosomal protein S17	1.68	15.5
IPI00247583.5	60S ribosomal protein L21	6.26	18.6
IPI00249080.2	Isoform 2 of N-acetylserotonin O-methyltransferase-like protein	94.26	67.2
IPI00289800.7	Isoform Short of Glucose-6-phosphate 1-dehydrogenase	7.99	59.2
IPI00290341.1	Isoform 2 of Protein FAM86A	1.63	33.0
IPI00292135.1	Lamin-B receptor	3.59	70.7
IPI00292499.4	Heat shock 70 kDa protein 14	3.53	54.8
IPI00294696.4	Cyclin B1	5.73	44.1
IPI00296157.6	Isoform 1 of All-trans-retinol 13,14-reductase	22.53	66.8
IPI00296370.2	Uncharacterized protein	22.14	38.8
IPI00297265.1	Protein arginine N-methyltransferase 2	4.44	49.0
IPI00301434.4	BolA-like protein 2	5.47	16.9
IPI00302605.3	Zinc transporter 7	2.20	41.6
IPI00302850.4	Small nuclear ribonucleoprotein Sm D1	3.80	13.3
IPI00303397.5	Isoform 6 of C-Jun-amino-terminal kinase-interacting protein 4	1.81	95.8
IPI00304932.2	Ribosomal RNA-processing protein 8	20.95	50.7
IPI00306369.3	tRNA (cytosine(34)-C(5))-methyltransferase	99.19	86.4
IPI00333410.1	Isoform 1 of Ubiquitin-conjugating enzyme E2 Q1	3.61	46.1
IPI00334907.3	Isoform 1 of Phosphatidylinositol transfer protein beta isoform	1.73	31.5
IPI00335101.1	Ribosomal protein S6 kinase alpha-5	13.58	89.8
IPI00336094.5	Isoform 2 of 3-hydroxyacyl-CoA dehydrogenase type-2	5.36	26.0
IPI00375513.3	Isoform Soluble of Catechol O-methyltransferase	2.20	24.4
IPI00376228.2	Probable methyltransferase BCDIN3D	4.23	33.2

IPI00376503.2	pyrroline-5-carboxylate reductase 1, mitochondrial isoform 2	4.15	33.3
IPI00382458.1	Isoform 2 of Cullin-3	1.71	86.2
IPI00383680.3	dolichyl-diphosphooligosaccharide--protein glycosyltransferase subunit 2 isoform 2 precursor	2.57	67.7
IPI00384016.1	Full-length cDNA 5-PRIME end of clone CS0DJ009YL13 of T cells (Jurkat cell line) of Homo sapiens (Fragment)	6.63	29.6
IPI00386975.3	Isoform 1B of Desmocollin-1	2.93	93.8
IPI00397526.3	Isoform 1 of Myosin-10	12.37	228.9
IPI00397801.4	Filaggrin-2	9.75	247.9
IPI00410615.2	Isoform 3 of Low molecular weight phosphotyrosine protein phosphatase	5.50	14.3
IPI00411680.11	Isoform 1 of Protein-L-isoaspartate(D-aspartate) O-methyltransferase	42.01	24.6
IPI00412714.3	Isoform 4 of Plasminogen activator inhibitor 1 RNA-binding protein	30.69	42.4
IPI00412880.2	Isoform 1 of Histone-arginine methyltransferase CARM1	231.14	63.4
IPI00418313.3	interleukin enhancer-binding factor 3 isoform d	48.36	95.7
IPI00419258.4	High mobility group protein B1	10.97	24.9
IPI00427330.3	Ribosome maturation protein SBDS	5.45	28.7
IPI00429689.3	Serine/threonine-protein phosphatase 2A catalytic subunit beta isoform	7.00	35.6
IPI00432865.1	Putative 60S ribosomal protein L13a-like MGC87657	5.20	12.1
IPI00443485.2	Isoform 2 of CDK5 regulatory subunit-associated protein 1-like 1	8.88	54.6
IPI00449112.3	OGFR protein	6.34	54.1
IPI00455457.4	Histone H3	18.21	15.4
IPI00470629.4	Isoform 1 of Calmodulin-lysine N-methyltransferase	1.81	36.1
IPI00472106.4	Isoform D of Endothelin-converting enzyme 2	2.32	28.3
IPI00472176.1	Isoform 2 of tRNA (uracil-5-)-methyltransferase homolog A (Fragment)	1.85	61.9
IPI00477179.1	Isoform 2 of Nucleolar RNA helicase 2	6.43	79.6
IPI00477803.4	Putative uncharacterized protein DKFZp781L0540 (Fragment)	3.63	90.0
IPI00479209.2	cDNA FLJ54590, highly similar to KH domain-containing, RNA-binding, signaltransduction-associated protein 1	3.71	46.4

IPI00479595.3	Isoform 3 of Nuclear-interacting partner of ALK	3.92	47.7
IPI00514436.1	General transcription factor IIIC, polypeptide 5, 63kDa, isoform CRA_c	10.78	52.3
IPI00549467.3	Omega-amidase NIT2	2.11	30.6
IPI00553185.2	T-complex protein 1 subunit gamma	77.36	60.5
IPI00554737.3	Serine/threonine-protein phosphatase 2A 65 kDa regulatory subunit A alpha isoform	20.22	65.3
IPI00555749.1	Proteasome 26S ATPase subunit 5 variant (Fragment)	8.96	38.7
IPI00639819.1	TAR DNA binding protein	4.86	33.4
IPI00640462.1	Guanine nucleotide binding protein (G protein), beta polypeptide 1	1.83	12.3
IPI00641266.4	calpain-2 catalytic subunit isoform 2	1.84	71.4
IPI00642549.2	cDNA FLJ56531, highly similar to UV excision repair protein RAD23 homolog B	7.63	42.3
IPI00643634.2	Isoform 4 of Protein arginine N-methyltransferase 7	3.55	63.8
IPI00645053.1	Isoform 3 of E3 ubiquitin-protein ligase NEDD4-like	1.81	100.7
IPI00645836.1	Protein	6.09	25.5
IPI00651621.1	Isoform B of Histone acetyltransferase type B catalytic subunit	9.66	39.8
IPI00658162.2	cDNA FLJ36570 fis, clone TRACH2011302, highly similar to SELENIDE,WATER DIKINASE 2	5.55	41.3
IPI00719345.1	Isoform 3 of Serine/threonine-protein phosphatase 6 regulatory subunit 3	1.88	88.9
IPI00741576.1	Isoform 2 of tRNA guanosine-2'-O-methyltransferase TRM11 homolog	17.84	52.8
IPI00745893.2	small ubiquitin-related modifier 2 isoform b precursor	4.78	8.1
IPI00746062.1	Isoform 2 of Serine/threonine-protein phosphatase 4 regulatory subunit 2	1.84	40.2
IPI00746438.2	Isoform 2 of 60S ribosomal protein L11	3.75	20.1
IPI00759575.1	Isoform Cytoplasmic of Glutathione reductase, mitochondrial	6.86	51.7
IPI00759596.1	Isoform 4 of Heterogeneous nuclear ribonucleoproteins C1/C2	10.49	27.8
IPI00759663.1	Isoform Cytoplasmic+peroxisomal of Peroxiredoxin-5, mitochondrial	4.31	17.0
IPI00759723.1	Isoform Monomeric of Arginyl-tRNA synthetase, cytoplasmic	1.76	67.1
IPI00760722.1	serine/threonine-protein kinase MST4 isoform 2	1.73	37.7
IPI00783781.2	Nuclear pore complex protein Nup205	1.62	227.8

IPI00787559.1	thymidylate kinase isoform 2	1.62	21.1
IPI00789037.1	COUP transcription factor 2 isoform b	3.63	31.5
IPI00789428.1	Isoform 2 of Methylcrotonoyl-CoA carboxylase beta chain, mitochondrial	2.13	57.5
IPI00792135.2	ATP5H protein (Fragment)	1.75	11.5
IPI00792207.3	aldehyde dehydrogenase, mitochondrial Isoform 2 precursor	2.04	51.0
IPI00792482.1	Isoform 1 of 5'-AMP-activated protein kinase catalytic subunit alpha-1	2.05	64.0
IPI00793102.1	Uncharacterized protein	6.04	10.6
IPI00794545.1	deoxyuridine 5'-triphosphate nucleotidohydrolase, mitochondrial isoform 3	2.41	15.4
IPI00794951.1	peptide methionine sulfoxide reductase isoform b	2.72	21.7
IPI00798211.1	Uncharacterized protein	2.07	23.6
IPI00798375.2	cDNA FLJ59357, highly similar to Probable ATP-dependent RNA helicase DDX5	20.21	61.5
IPI00807524.1	BZW2 protein	3.79	21.5
IPI00807545.1	Isoform 3 of Heterogeneous nuclear ribonucleoprotein K	196.62	48.5
IPI00829824.1	PRKCSH protein (Fragment)	2.52	20.3
IPI00843984.2	Isoform 2 of Zinc finger protein 503	5.26	59.3
IPI00848298.1	Isoform 2 of Apolipoprotein A-I-binding protein	1.74	20.4
IPI00852631.1	Uncharacterized protein	1.64	21.6
IPI00853093.3	Isoform 1 of Methyltransferase-like protein 2B	1.68	43.4
IPI00853290.2	Uncharacterized protein	4.30	96.4
IPI00854834.2	echinoderm microtubule-associated protein-like 4 isoform b	4.37	102.4
IPI00871418.1	Uncharacterized protein	1.81	53.1
IPI00872684.2	cDNA FLJ54141, highly similar to Ezrin	3.78	65.5
IPI00872909.1	Isoform 2 of Putative ribosomal RNA methyltransferase NOP2	26.68	88.9
IPI00877935.2	Uncharacterized protein	1.95	21.7
IPI00878484.1	Protein	1.82	32.2
IPI00878876.1	cDNA FLJ51872, highly similar to Small nuclear ribonucleoprotein Sm D3	4.94	13.3
IPI00892653.2	cDNA FLJ61481, highly similar to PAS domain-containing serine/threonine-protein kinase	1.74	119.8

IPI00893179.1	X-ray repair complementing defective repair in Chinese hamster cells 6	4.23	64.0
IPI00900327.2	cDNA FLJ58339, highly similar to Poly(rC)-binding protein 2	7.47	33.9
IPI00903024.1	Uncharacterized protein	1.72	15.6
IPI00903259.2	cDNA FLJ54005, highly similar to Transcription elongation factor SPT5	1.95	96.9
IPI00908375.1	cDNA FLJ52821, highly similar to Protein transport protein Sec23A	3.49	45.0
IPI00908513.1	cDNA FLJ60039, highly similar to Proteasome subunit beta type 7	3.82	15.3
IPI00908582.1	cDNA FLJ50164, highly similar to Protein flightless-1 homolog	6.71	135.1
IPI00908824.1	Serine hydroxymethyltransferase	6.77	41.6
IPI00909251.1	cDNA FLJ51165, highly similar to DNA damage-binding protein 1	11.80	91.9
IPI00909525.1	cDNA FLJ51260, highly similar to DNA polymerase subunit delta 2	4.76	47.1
IPI00909694.2	alpha-aminoadipic semialdehyde dehydrogenase isoform 3	10.18	54.0
IPI00910140.2	tRNA wybutosine-synthesizing protein 3 homolog isoform 2	6.35	26.1
IPI00910614.1	heterogeneous nuclear ribonucleoprotein R isoform 4	6.21	59.6
IPI00910719.1	cDNA FLJ55705, highly similar to Threonyl-tRNA synthetase, cytoplasmic	6.45	70.3
IPI00910830.1	cDNA FLJ57715, highly similar to Voltage-dependent anion-selective channel protein 1	4.33	16.7
IPI00914573.1	cDNA FLJ50701	2.00	48.4
IPI00915960.1	Uncharacterized protein	1.78	252.0
IPI00916159.1	42 kDa protein	2.62	41.8
IPI00916572.1	Protein	2.06	12.8
IPI00916599.1	27 kDa protein	1.64	26.7
IPI00917605.1	Uncharacterized protein	12.40	11.3
IPI00921584.1	Uncharacterized protein	1.78	34.4
IPI00922165.1	Isoform 5 of Adenylate kinase 2, mitochondrial	6.27	24.6
IPI00922175.1	cDNA FLJ51678, highly similar to Ras-related protein Rab-18	1.89	22.4
IPI00922562.1	cDNA FLJ55085, highly similar to Glucosamine-6-phosphate isomerase	2.03	24.0

IPI00924801.1	9 kDa protein	1.81	9.3
IPI00924816.1	Myotrophin	8.84	12.9
IPI00924884.1	Protein	4.23	30.3
IPI00924895.1	SNRPG protein	4.47	7.1
IPI00925237.1	Uncharacterized protein	6.05	81.5
IPI00925511.1	cDNA FLJ54314, highly similar to Glutaminyl-tRNA synthetase	3.54	86.5
IPI00925539.1	57 kDa protein	1.81	56.7
IPI00926241.1	Isoform 2 of TBC1 domain family member 4	1.93	139.5
IPI00927374.1	cDNA FLJ52346, highly similar to Makorin-2	3.96	42.0
IPI00927648.1	cDNA FLJ57901, highly similar to Methyltransferase-like protein 6	13.09	28.2
IPI00927809.1	Uncharacterized protein	3.54	130.5
IPI00929464.1	signal recognition particle 54 kDa protein isoform 2	2.40	50.3
IPI00937239.2	40S ribosomal protein S21	3.84	8.8
IPI00939560.1	thioredoxin domain-containing protein 5 isoform 3	34.40	36.2
IPI00939707.1	Protein KIAA0664	1.70	146.6
IPI00940292.1	Isoform C of AP-1 complex subunit beta-1	7.88	103.5
IPI00940673.1	cDNA FLJ53217, highly similar to Transketolase	8.39	49.9
IPI00942236.1	cDNA FLJ59313, highly similar to Homo sapiens target of EGR1, member 1 (nuclear) (TOE1), mRNA	1.99	47.9
IPI00943071.2	cDNA FLJ57184, highly similar to Bromodomain and WD repeat domain-containing protein 2	1.80	84.6
IPI00943563.1	Isoform 2 of Filamin-B	9.36	275.5
IPI00943894.1	glycogen phosphorylase, liver form isoform 2	17.20	93.1
IPI00946257.1	Isoform 4 of Ubiquitin-associated protein 2-like	17.76	103.1
IPI00946476.1	Uncharacterized protein	1.95	24.2
IPI00947266.1	Uncharacterized protein	3.55	51.0
IPI00952872.2	Uncharacterized protein	3.43	14.7
IPI00955854.1	POU domain, class 4, transcription factor 3, isoform CRA_a	2.29	84.1
IPI00963822.1	Uncharacterized protein	10.62	43.1
IPI00964409.3	Uncharacterized protein	21.20	91.9

IPI00964648.1	30 kDa protein	12.47	29.7
IPI00964855.1	Uncharacterized protein	27.59	56.8
IPI00964903.2	26 kDa protein	3.99	26.4
IPI00965314.1	Uncharacterized protein	3.84	47.0
IPI00965782.1	Uncharacterized protein	1.61	19.0
IPI00967721.1	Uncharacterized protein	20.01	88.3
IPI00968146.1	Uncharacterized protein	6.28	22.6
IPI00969375.1	Hydroxyacyl-Coenzyme A dehydrogenase/3-ketoacyl-Coenzyme A thiolase/enoyl-Coenzyme A hydratase (Trifunctional protein), beta subunit, isoform CRA_b	3.61	40.4
IPI00974544.1	Isoform SV of 14-3-3 protein epsilon	33.78	26.5
IPI00975868.1	Annexin family protein	2.17	58.4
IPI00975903.1	cDNA FLJ55679, highly similar to Mus musculus cytoplasmic FMR1 interacting protein 2 (Cyfip2), mRNA	7.06	122.4
IPI00976162.1	Conserved hypothetical protein	2.08	9.9
IPI00977736.1	calcyclin-binding protein isoform 2	6.86	21.2
IPI00977844.1	17 kDa protein	3.67	16.7
IPI00978109.1	Uncharacterized protein	6.95	63.6
IPI00979915.1	Uncharacterized protein	9.06	15.3
IPI00980175.1	proteasome subunit beta type-2 isoform 3	3.56	9.6
IPI00980658.1	cDNA FLJ58444, highly similar to Vacuolar ATP synthase subunit H	2.59	52.7
IPI00980681.1	Uncharacterized protein	2.99	18.2
IPI00981395.1	cDNA FLJ53442, highly similar to Poly (ADP-ribose) polymerase 1	35.56	111.1
IPI00982610.1	Protein	2.01	95.7
IPI00983324.1	protein FAM115A-like	1.72	53.6
IPI00984067.1	Uncharacterized protein	2.02	7.3
IPI00984387.1	cDNA FLJ53166, highly similar to Dihydropyrimidinase-related protein 2	2.34	58.1
IPI00985068.1	Uncharacterized protein	5.40	21.7
IPI01009039.1	Isoform 5 of Cellular tumor antigen p53	5.83	33.5
IPI01009061.1	Truncated tumor suppressor protein P16	2.40	14.9

IPI01009435.1	THO complex subunit 2	1.78	169.5
IPI01010035.1	cDNA FLJ52928, highly similar to COP9 signalosome complex subunit 2	6.73	44.2
IPI01010050.1	cDNA, FLJ78818, highly similar to Voltage-dependent anion-selective channel protein 2	10.97	27.5
IPI01010316.1	cDNA, FLJ96168, Homo sapiens formin binding protein 3 (FNBP3), mRNA	1.94	95.0
IPI01010979.1	45 kDa protein	4.22	44.9
IPI01011132.1	Isoform 1 of DNA topoisomerase 2-alpha	3.88	174.3
IPI01011356.1	cDNA FLJ51818, highly similar to Phosphoglucomutase-1	6.36	58.7
IPI01011751.1	EIF-2B-delta-like protein	2.06	57.5
IPI01012026.1	215 kDa protein	6.15	215.2
IPI01012107.1	10 kDa protein	4.38	9.5
IPI01012250.1	13 kDa protein	5.01	13.3
IPI01012853.1	cDNA FLJ57898, highly similar to Adaptor-relatedprotein complex 1 mu-1 subunit	2.24	40.2
IPI01012872.1	58 kDa protein	119.11	58.3
IPI01013010.1	22 kDa protein	2.36	22.3
IPI01013230.1	cDNA FLJ51319, highly similar to tRNA (adenine-N(1)-)-methyltransferase non-catalytic subunit TRM6	2.70	36.4
IPI01013273.1	cDNA, FLJ79129, highly similar to T-complex protein 1 subunit zeta	40.78	54.8
IPI01013392.1	Uncharacterized protein	1.78	47.1
IPI01013927.1	51 kDa protein	1.86	50.9
IPI01013941.1	cDNA FLJ58196, highly similar to Zinc finger CCCH domain-containing protein 11A	3.48	82.7
IPI01014130.1	cDNA FLJ52538, highly similar to Dual specificity mitogen-activated proteinkinase kinase 4	6.51	42.5
IPI01014209.1	cDNA FLJ51843, highly similar to 14-3-3 protein gamma	13.95	25.6
IPI01014223.1	cDNA FLJ50851, highly similar to Tyrosine-protein phosphatase non-receptor type1	6.01	41.2
IPI01014382.1	cDNA FLJ55493, highly similar to Glutamate dehydrogenase 1, mitochondrial	2.05	56.6
IPI01014633.1	cDNA FLJ16322 fis, clone SPLEN2037678, highly similar to Protein D11Lgp1 homolog	3.35	50.9
IPI01014727.1	cDNA FLJ51983, highly similar to Phosphoglycerate mutase 1	9.63	27.1

IPI01015047.1	NUP153 variant protein (Fragment)	2.03	151.4
IPI01015228.1	86 kDa protein	2.16	85.6
IPI01015329.1	cDNA FLJ52203, highly similar to 3'(2'),5'-bisphosphate nucleotidase 1	1.74	27.5
IPI01015364.1	eukaryotic translation initiation factor 4 gamma 1 isoform 4	14.89	154.8
IPI01015380.1	cDNA FLJ33094 fis, clone TRACH2000703, highly similar to Mitochondrial-processing peptidase subunit beta, mitochondrial	5.15	37.9
IPI01015447.1	47 kDa protein	3.25	46.7
IPI01015928.1	106 kDa protein	5.57	106.1
IPI01015974.1	12 kDa protein	1.93	12.1
IPI01018104.1	cDNA FLJ52561, highly similar to Four and a half LIM domains protein 1	3.55	28.1

MALDI-MS Analysis of selenium-based SAM analogue compatibility towards engineered methyltransfterases:

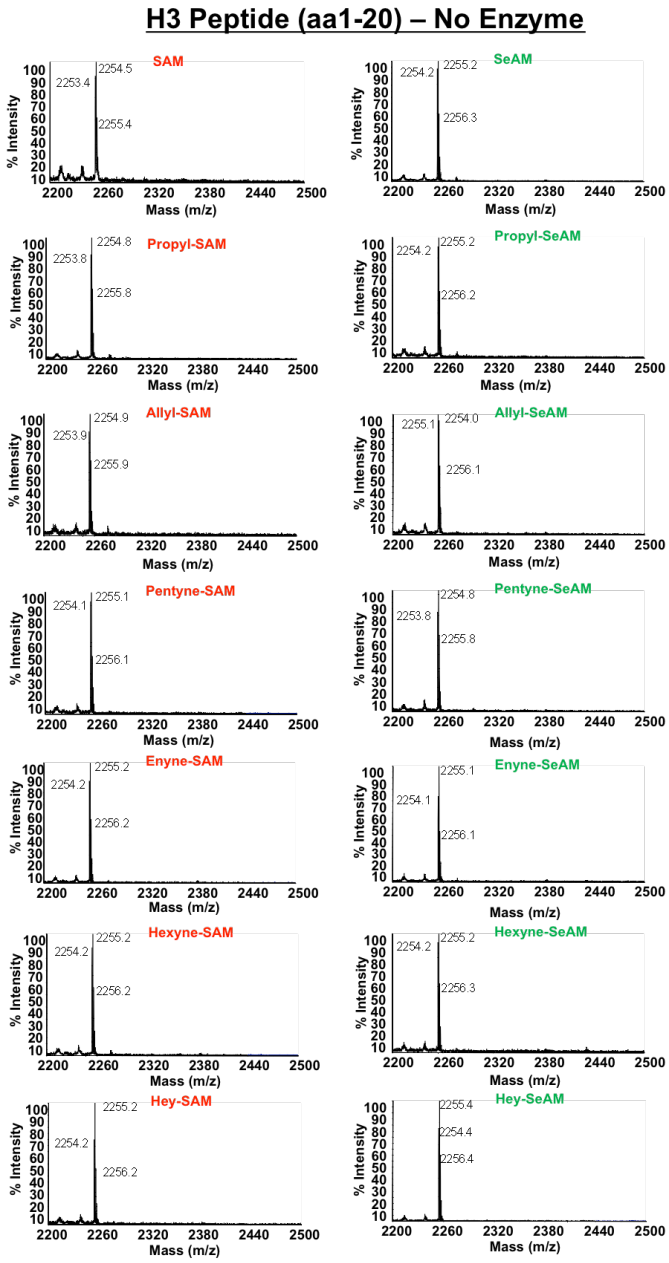

Figure A1. MALDI-MS spectra demonstrating a lack of modification of H3 peptide substrates by cofactor analogues in the absence of methyltransferase. Spectra in the left hand column are derived from reactions containing sulfur-based analogues (red labels); spectra in the right hand column are from the reactions containing selenium-based analogues (green labels).

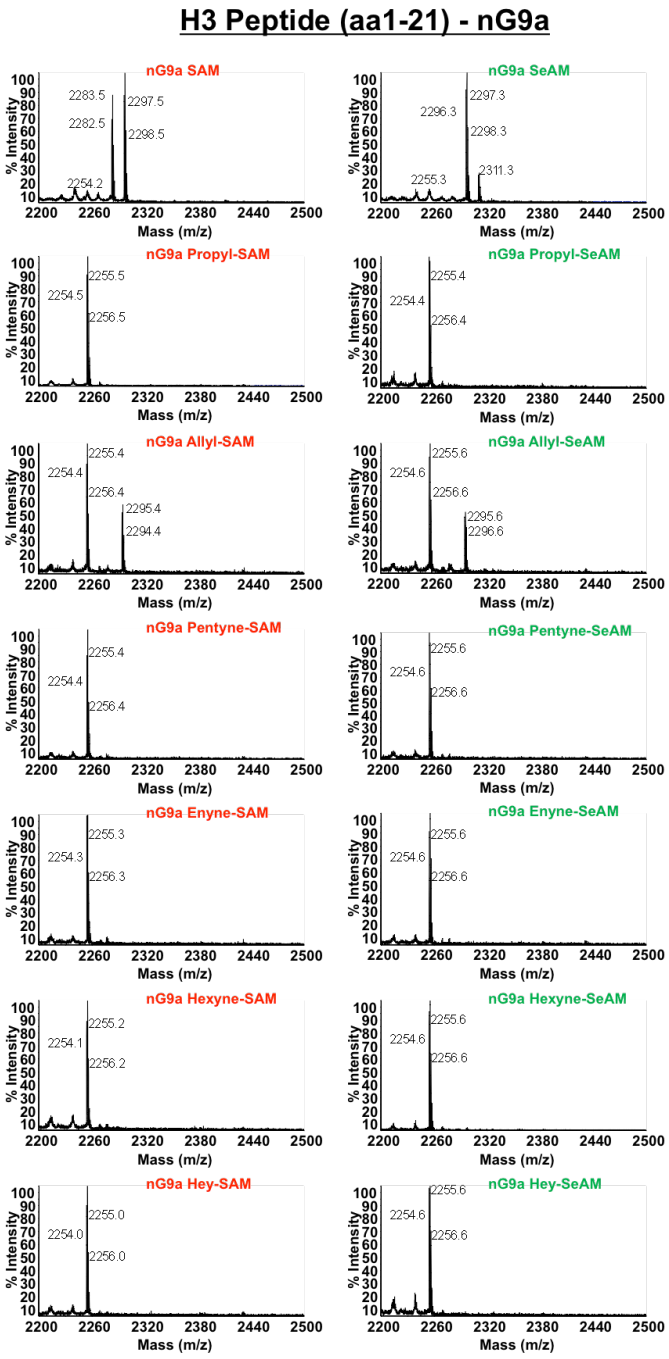

Figure A2. MALDI-MS spectra demonstrating sulfur and selenium-based cofactor analogue compatibility with native G9a. Spectra in the left hand column are derived from the reactions containing sulfur-based analogues (red labels); spectra in the right hand column are from the reactions containing selenium-based analogues (green labels).

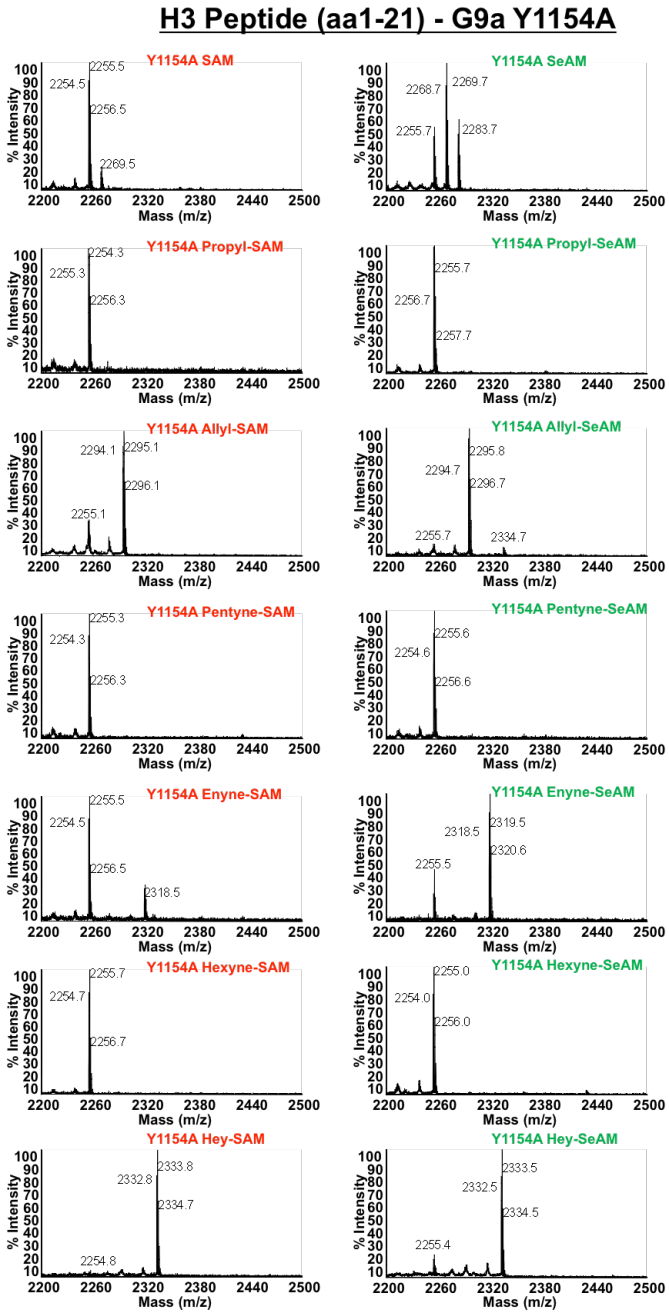

Figure A3. MALDI-MS spectra demonstrating sulfur and selenium-based cofactor analogue compatibility with the G9a Y1154A mutant. Spectra in the left hand column are derived from the reactions containing sulfur-based analogues (red labels), while spectra in the right hand column are from the reactions containing selenium-based analogues (green labels).

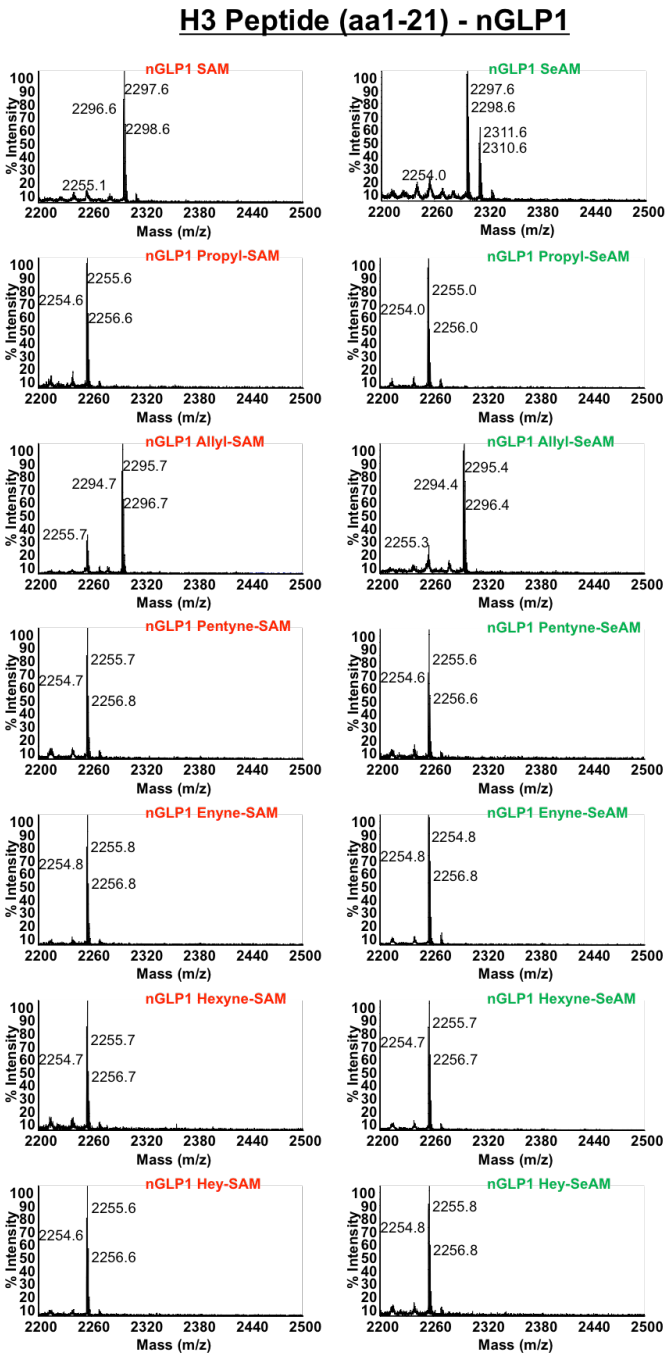

Figure A4. MALDI-MS spectra demonstrating sulfur and selenium-based cofactor analogue compatibility with native GLP1. Spectra in the left hand column are derived from the reactions containing sulfur-based analogues (red labels); spectra in the right hand column are from the reactions containing selenium-based analogues (green labels).

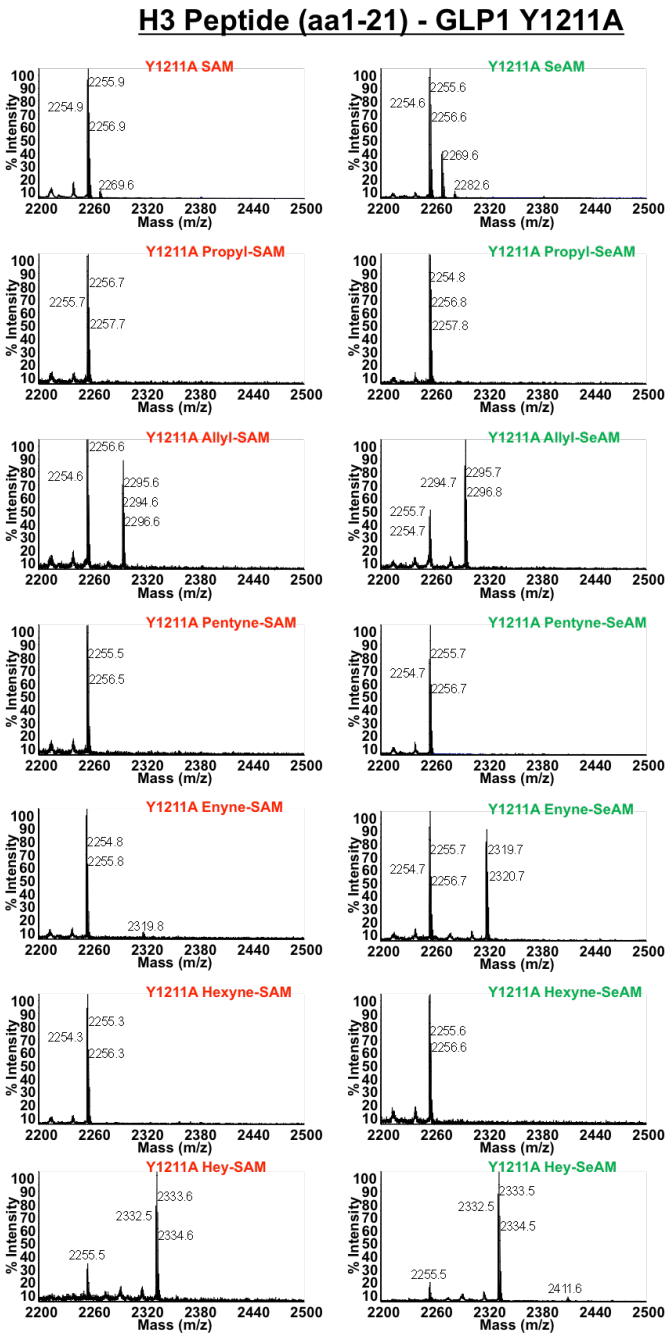

Figure A5. MALDI-MS spectra demonstrating sulfur and selenium-based cofactor analogue compatibility with the GLP1 Y1211A mutant. Spectra in the left hand column are derived from the reactions containing sulfur-based analogues (red labels); spectra in the right hand column are from the reactions containing selenium-based analogues (green labels).

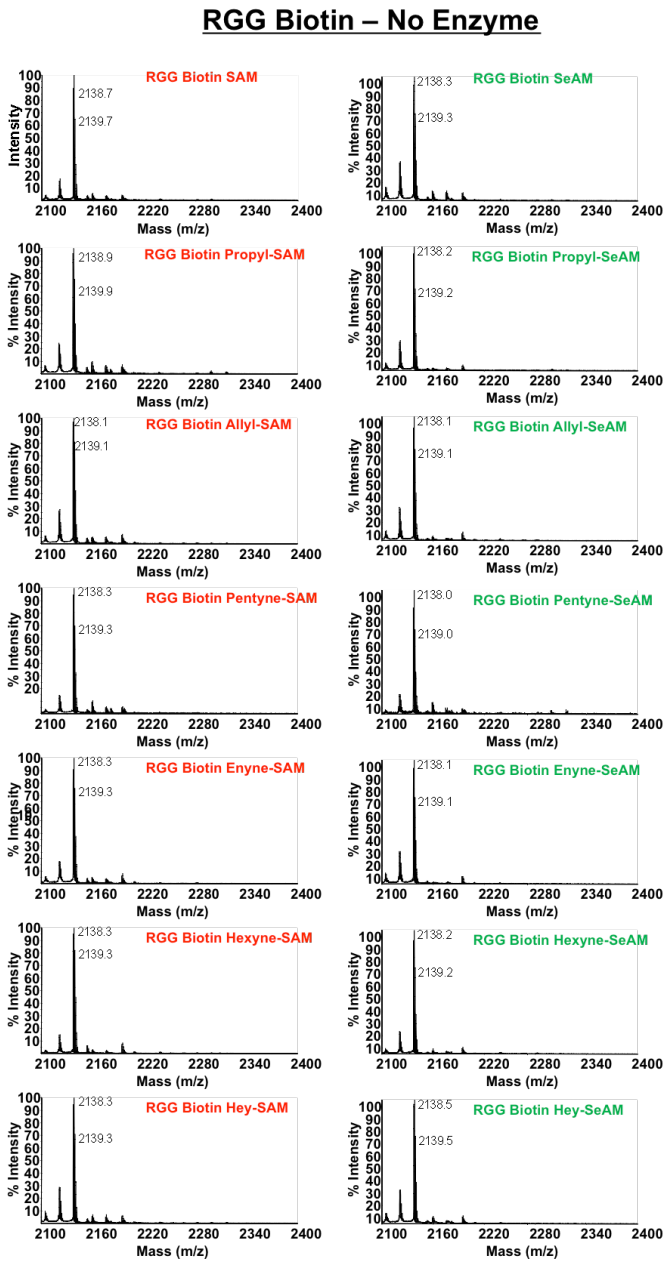

Figure A6. MALDI-MS spectra demonstrating a lack of modification of RGG-Biotin peptide substrates by cofactor analogues in the absence of methyltransferase. Spectra in the left hand column are derived from the reactions containing sulfur-based analogues (red labels); spectra in the right hand column are from the reactions containing selenium-based analogues (green labels).

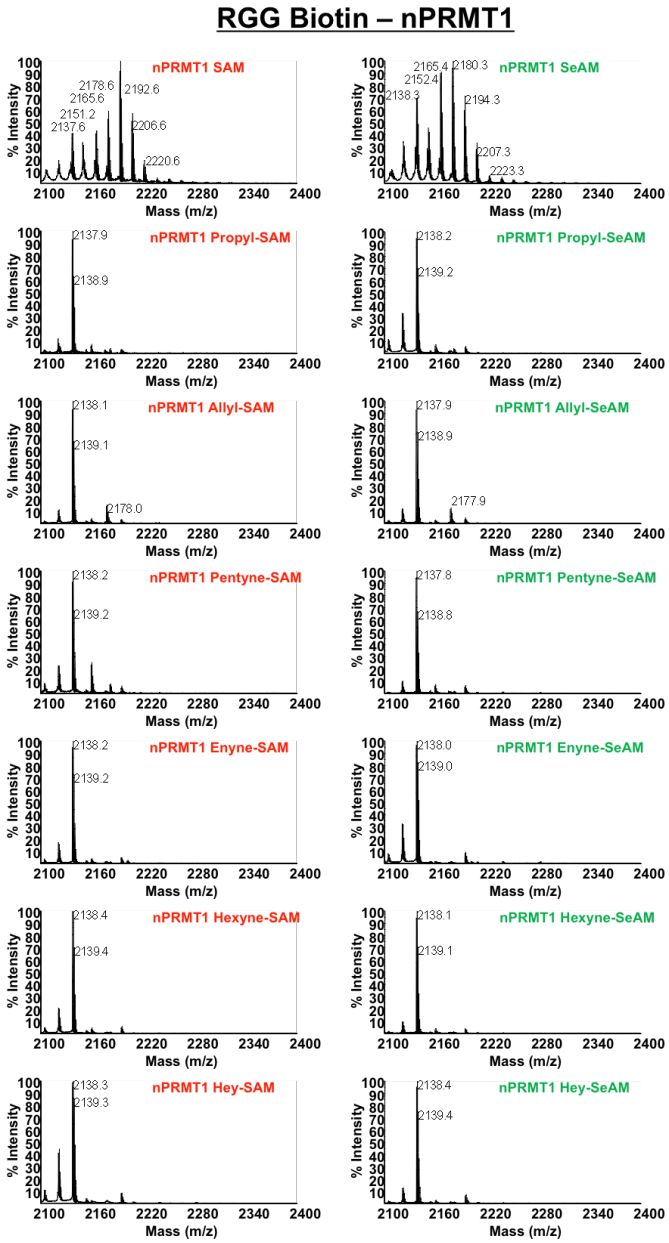

Figure A7. MALDI-MS spectra demonstrating sulfur and selenium-based cofactor analogue compatibility with native PRMT1. Spectra in the left hand column are derived from the reactions containing sulfur-based analogues (red labels); spectra in the right hand column are from the reactions containing selenium-based analogues (green labels).

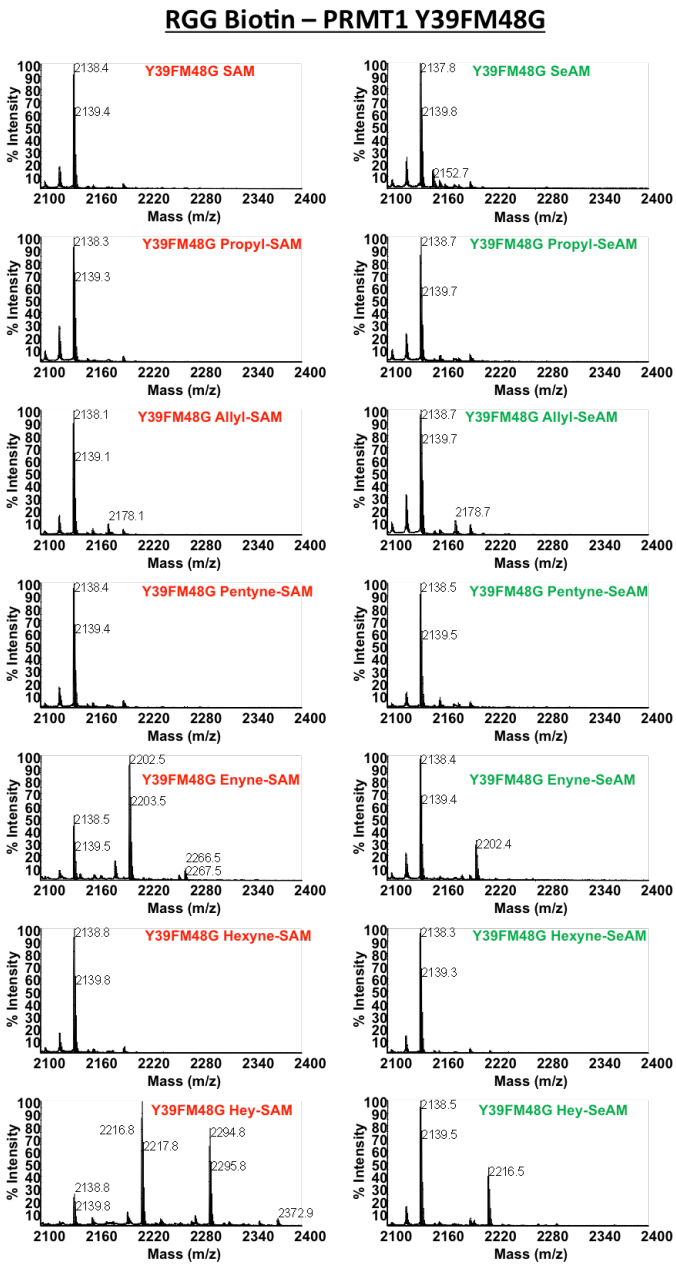

Figure A8. MALDI-MS spectra demonstrating sulfur and selenium-based cofactor analogue compatibility with the PRMT1 Y39FM48G mutant. Spectra in the left hand column are derived from the reactions containing sulfur-based analogues (red labels); spectra in the right hand column are from the reactions containing selenium-based analogues (green labels).

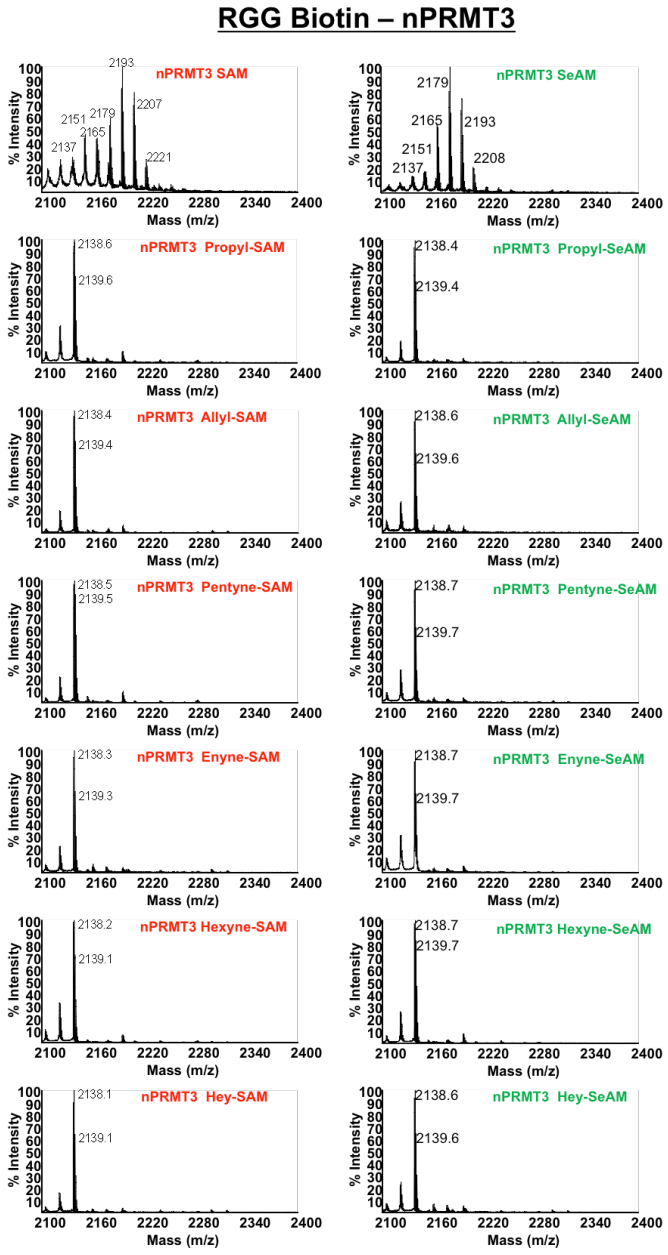

Figure A9. MALDI-MS spectra demonstrating sulfur and selenium-based cofactor analogue compatibility with native PRMT3. Spectra in the left hand column are derived from the reactions containing sulfur-based analogues (red labels), while spectra in the right hand column are from the reactions containing selenium-based analogues (green labels).

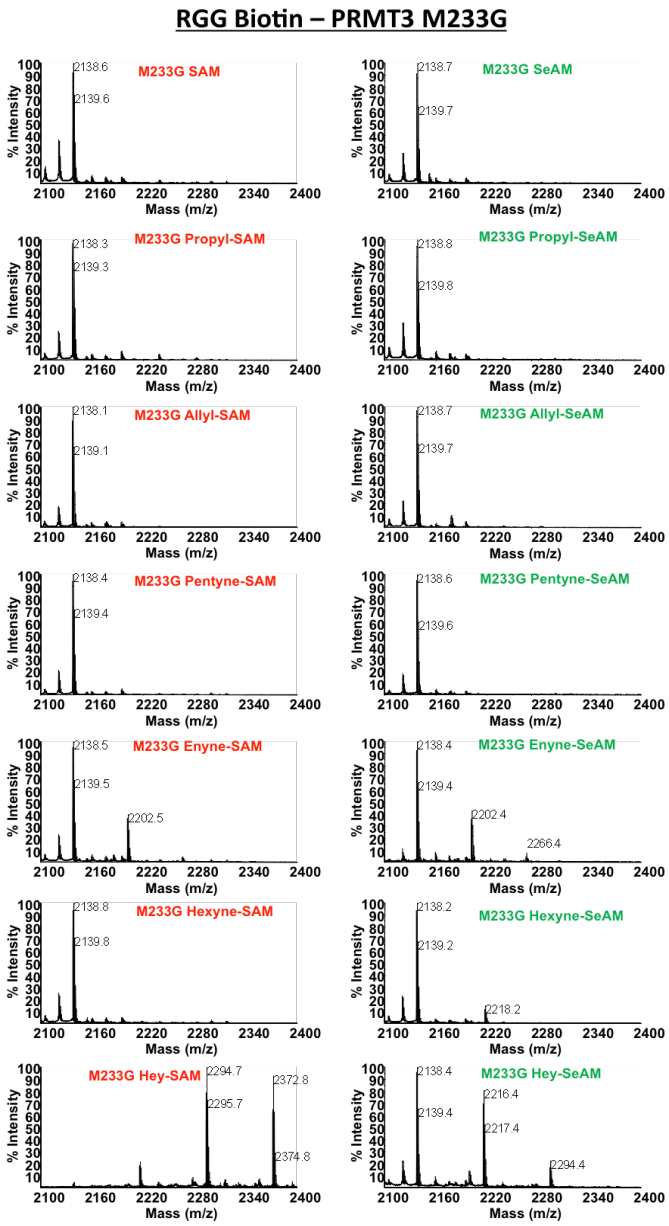

Figure A10. MALDI-MS spectra demonstrating sulfur and selenium-based cofactor analogue compatibility with the PRMT3 M233G mutant. Spectra in the left hand column are derived from the reactions containing sulfur-based analogues (red labels); spectra in the right hand column are from the reactions containing selenium-based analogues (green labels).

Spectral Data for Synthesized Compounds:

Selenohomocystine:

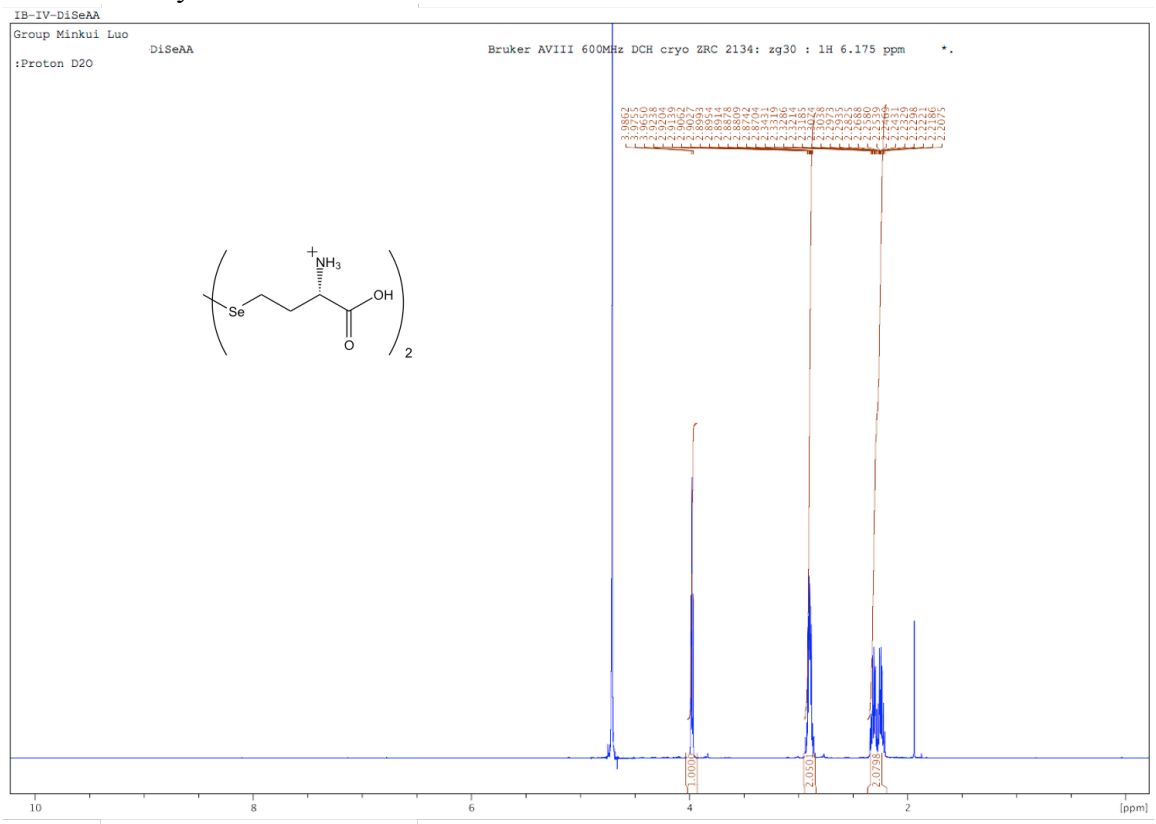

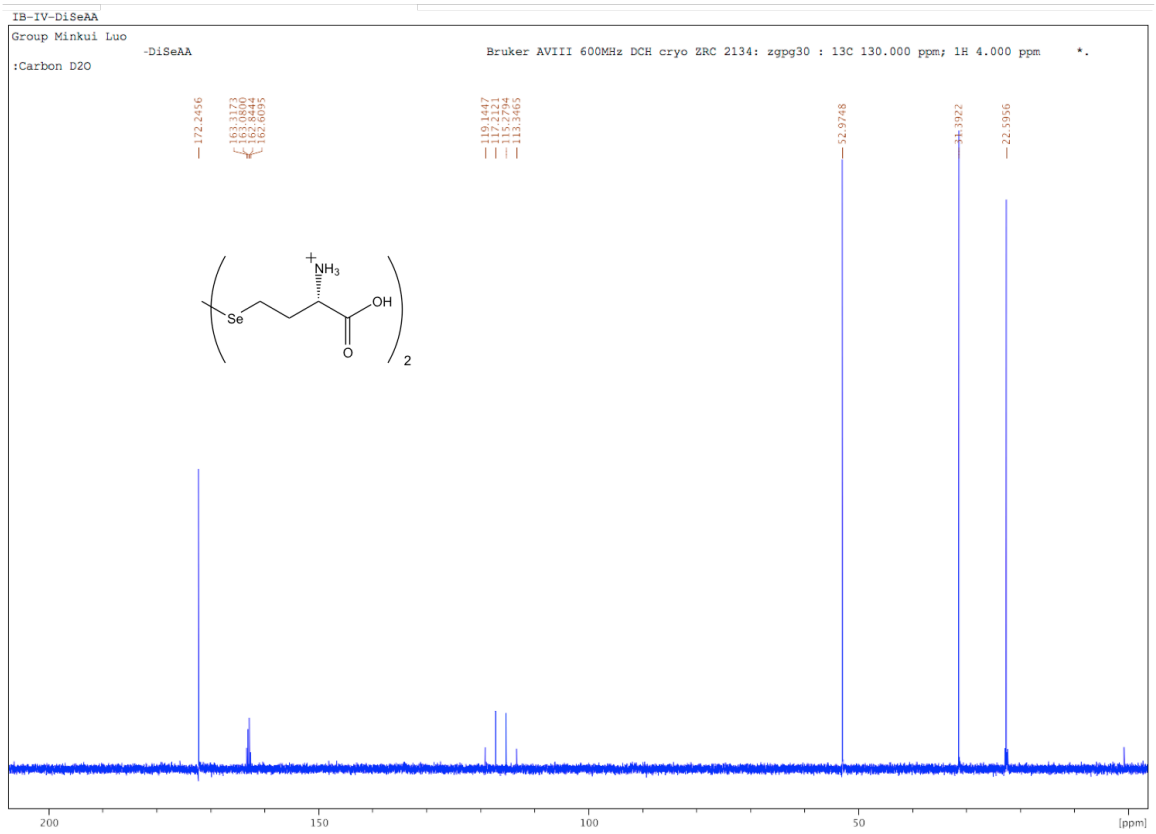

5’-Iodo-5’-deoxyadenosine:

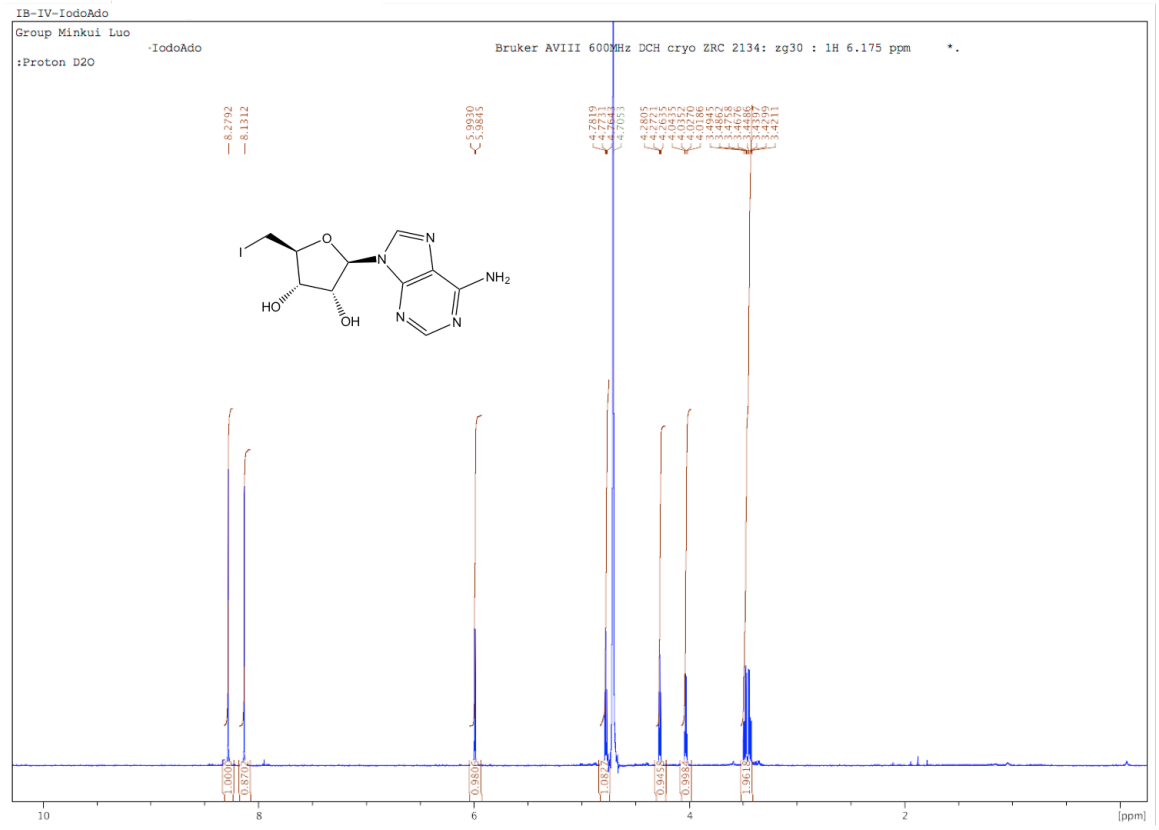

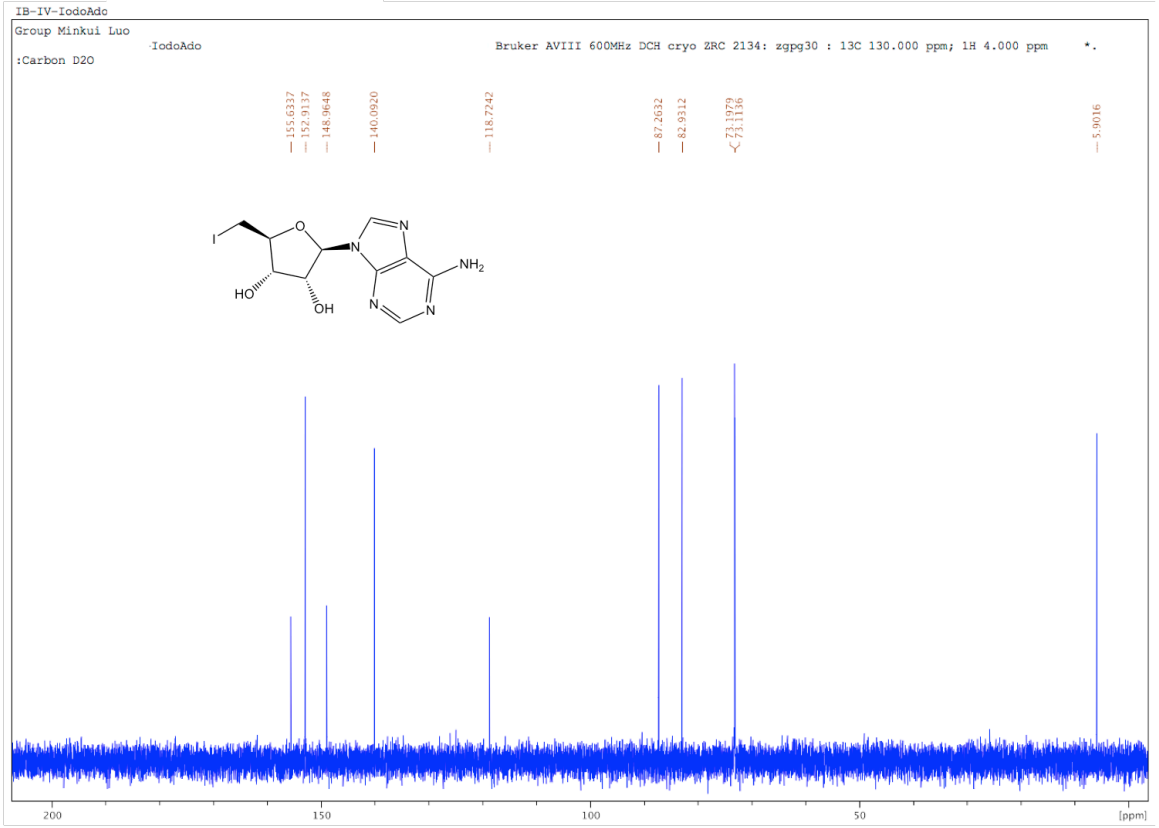

Se-Adenosylhomocysteine:

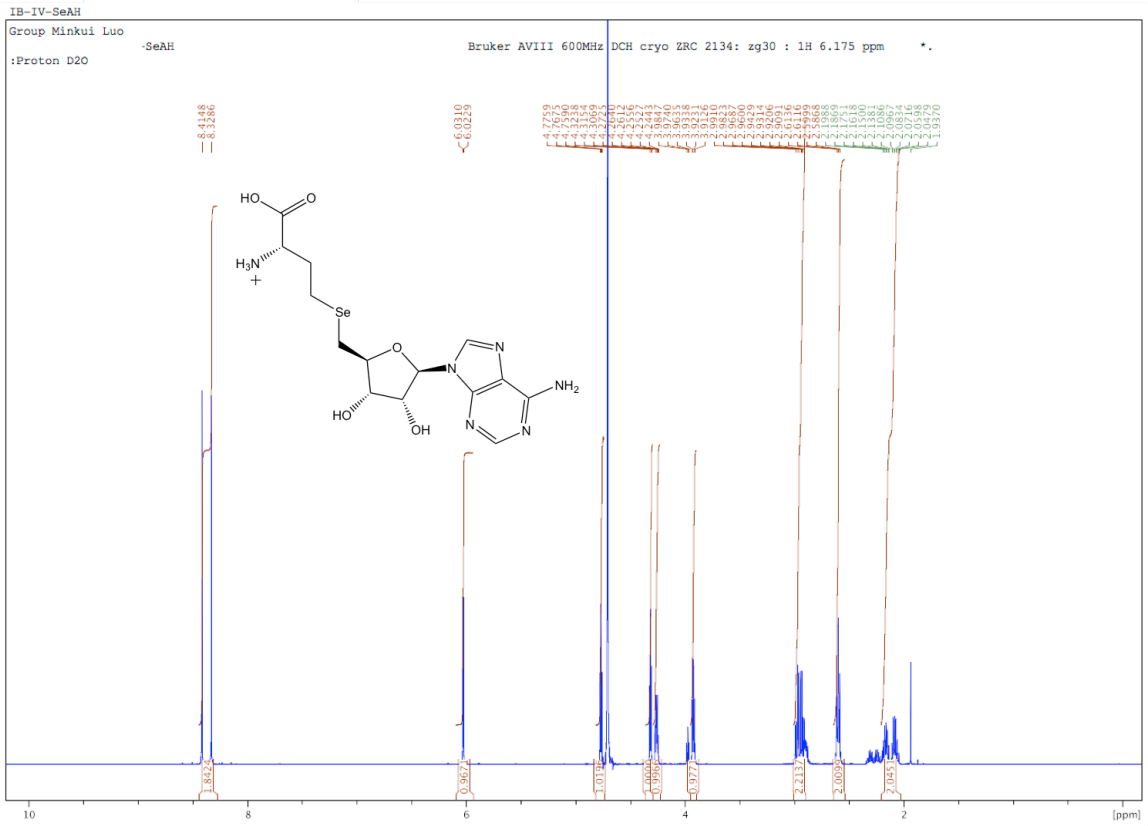

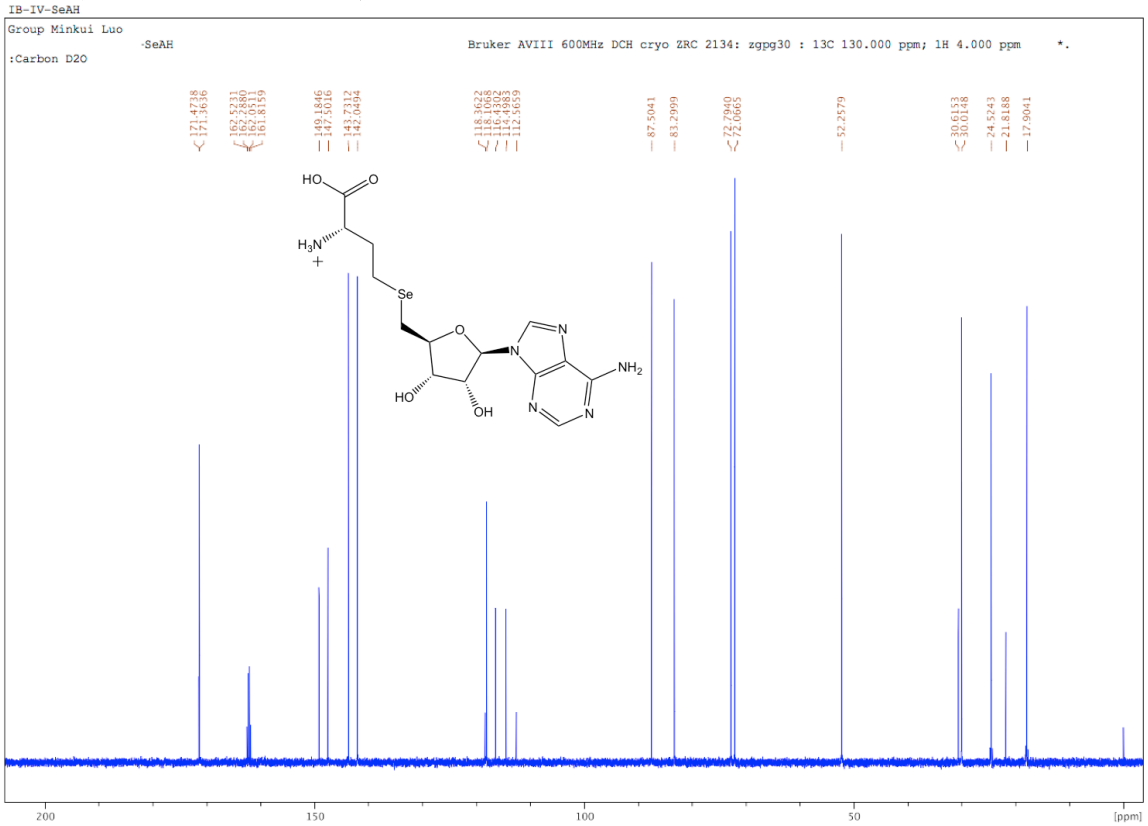

SAM:

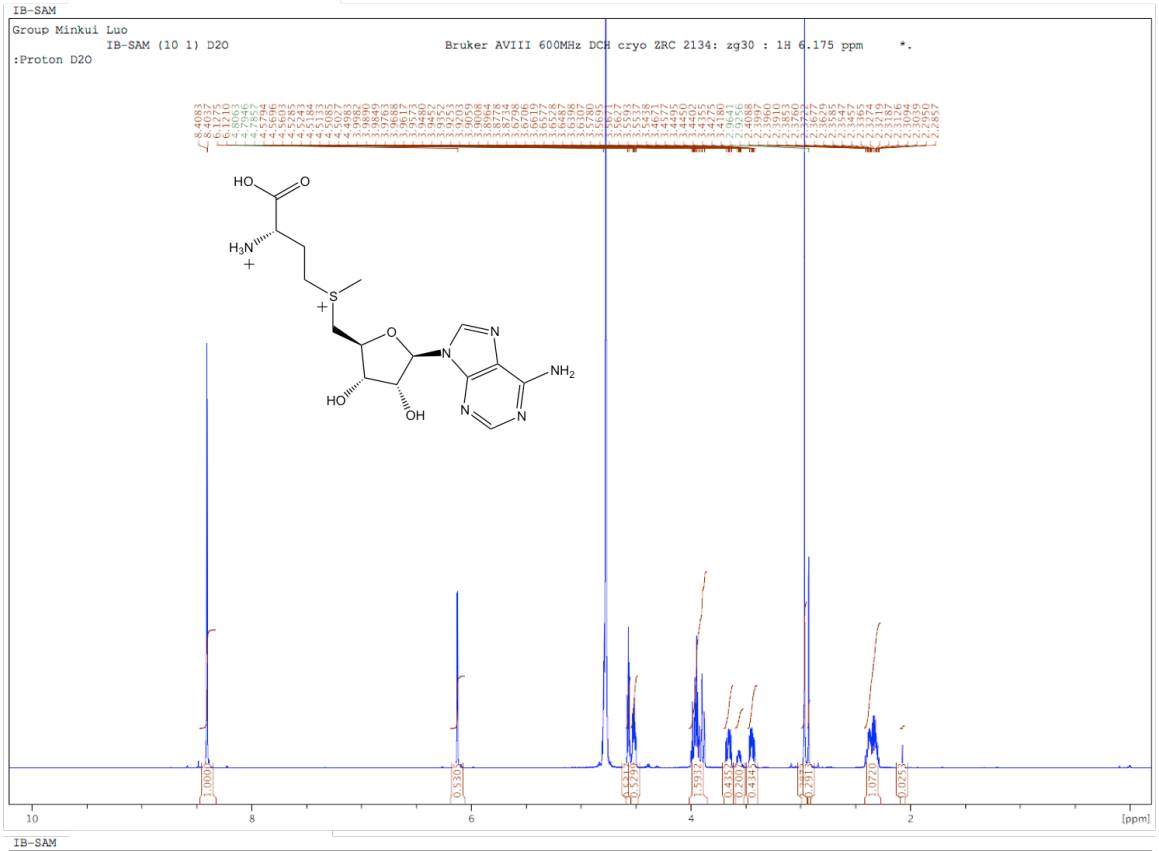
IB-SAM
Group Minkui Luo
IB-SAM (10 1) D2O
Bruker AVIII 600MHz DCH cryo ZRC 2134: zg30 : 1H 6.175 ppm
:Proton D2O
HO
O
H3N
S
O
N
N
NH2
HO
OH
N
N
10
8
6
4
2
[ppm]

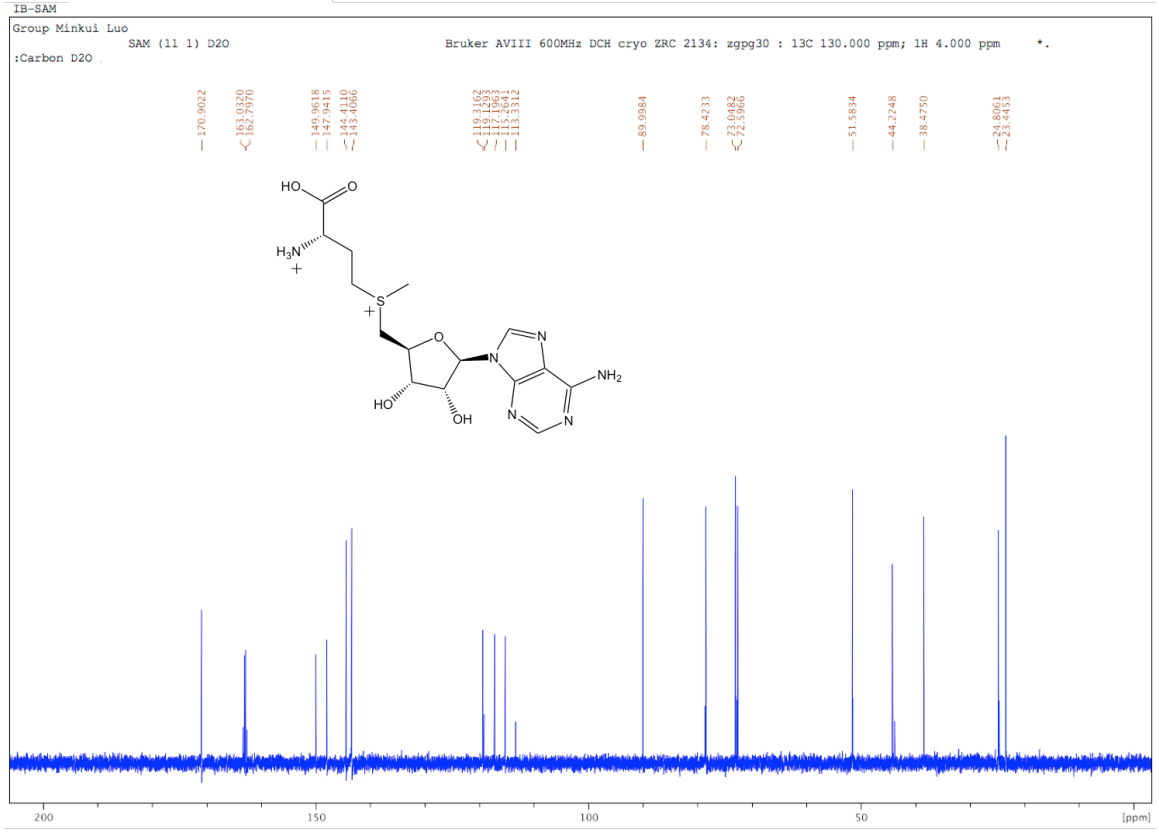
IB-SAM
Group Minkui Luo
SAM (11 1) D2O
Bruker AVIII 600MHz DCH cryo ZRC 2134: zgpg30 : 13C 130.000 ppm; 1H 4.000 ppm
:Carbon D2O
170.9022
163.0320
162.7970
149.9618
147.9415
144.4110
143.4066
120.2162
119.1293
117.1963
113.5441
113.3312
89.9984
78.4233
73.0482
72.5986
51.5834
44.2248
38.4750
24.8061
23.4453
HO
O
H3N
S
O
N
N
NH2
HO
OH
N
N
200
150
100
50
[ppm]

SeAM:

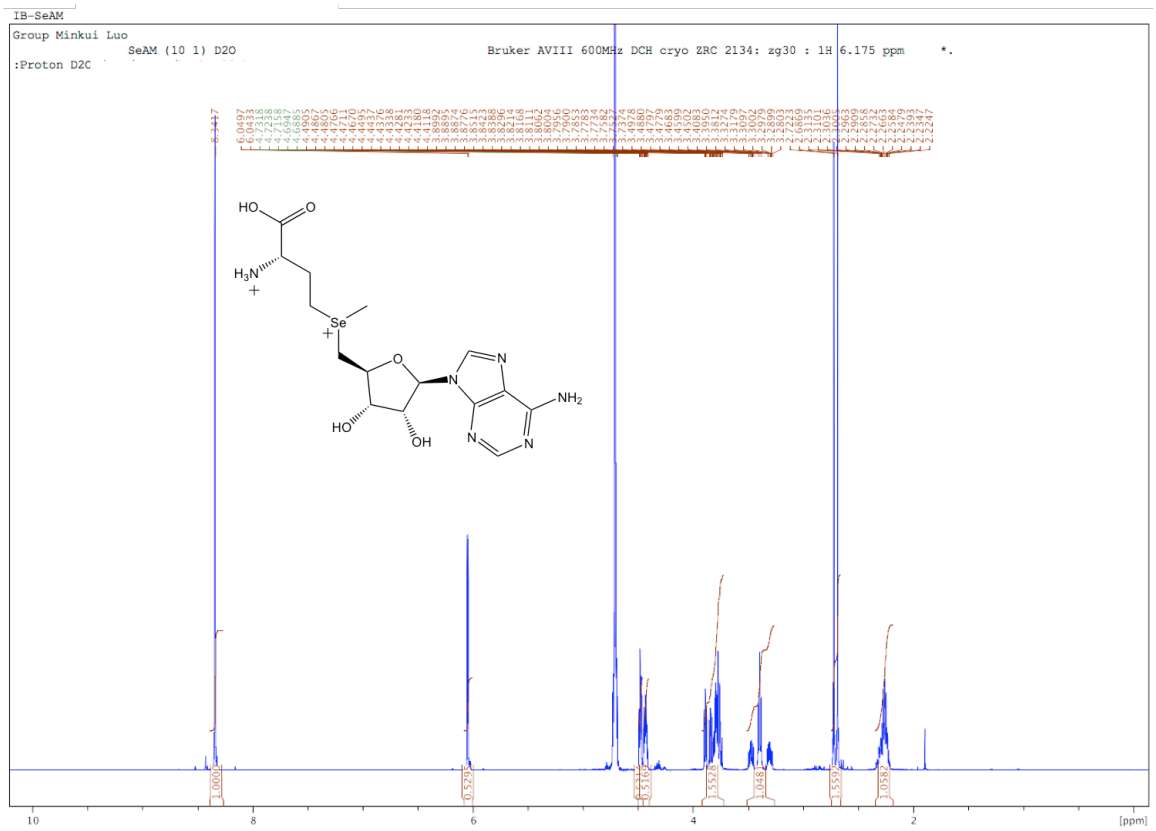
IB-SeAM
Group Minkui Luo
SeAM (10 1) D2O
Bruker AVIII 600MHz DCH cryo ZRC 2134: zg30 : 1H 6.175 ppm
:Proton D2C
[ppm]

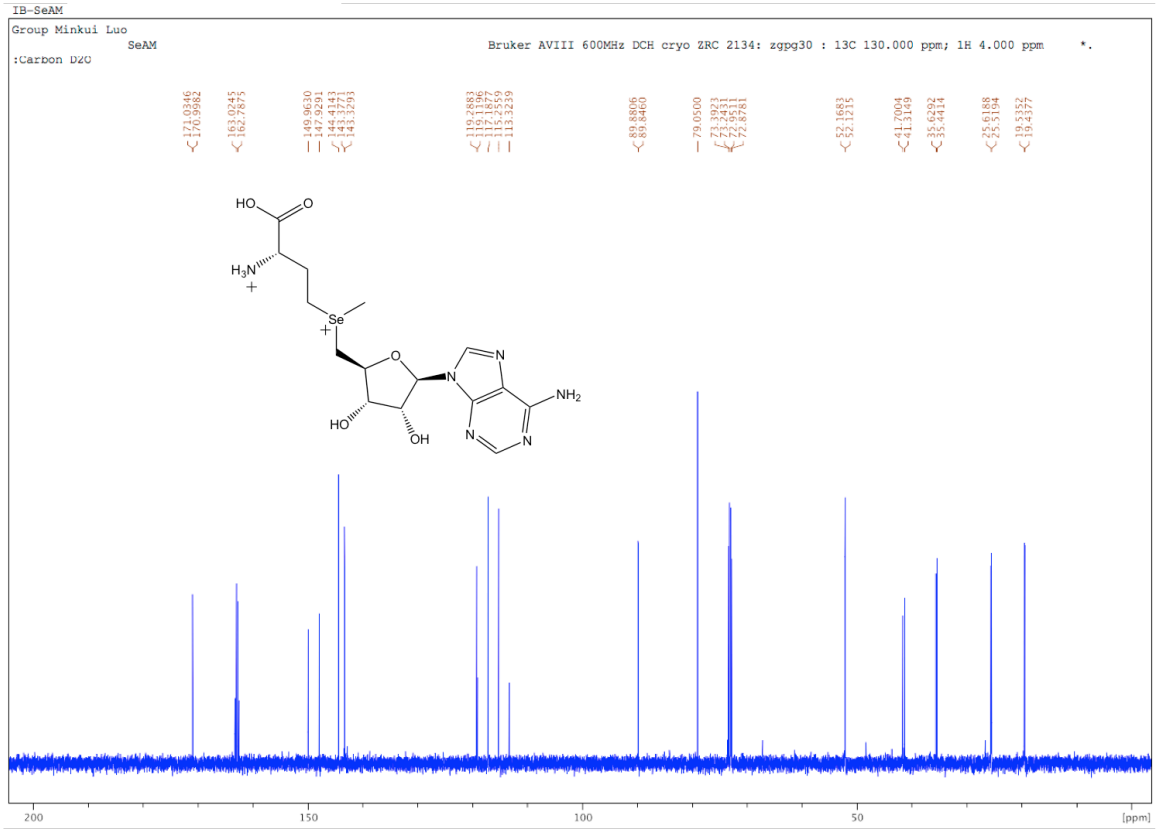
IB-SeAM
Group Minkui Luo
SeAM
Bruker AVIII 600MHz DCH cryo ZRC 2134: zgpg30 : 13C 130.000 ppm; 1H 4.000 ppm
:Carbon D2O
[ppm]

Propyl-SAM:

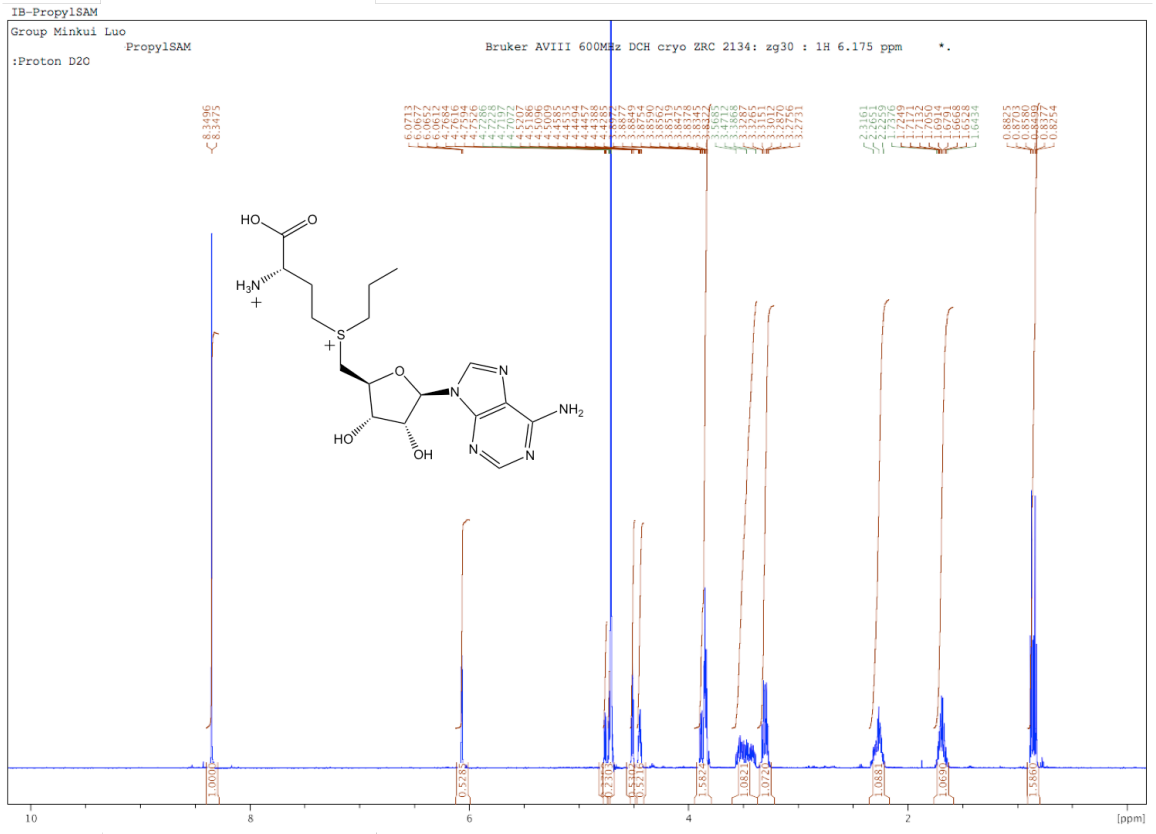
IB-PropylSAM
Group Minkui Luo
PropylSAM
:Proton D2O
Bruker AVIII 600MHz DCH cryo ZRC 2134: zg30 : 1H 6.175 ppm
[ppm]

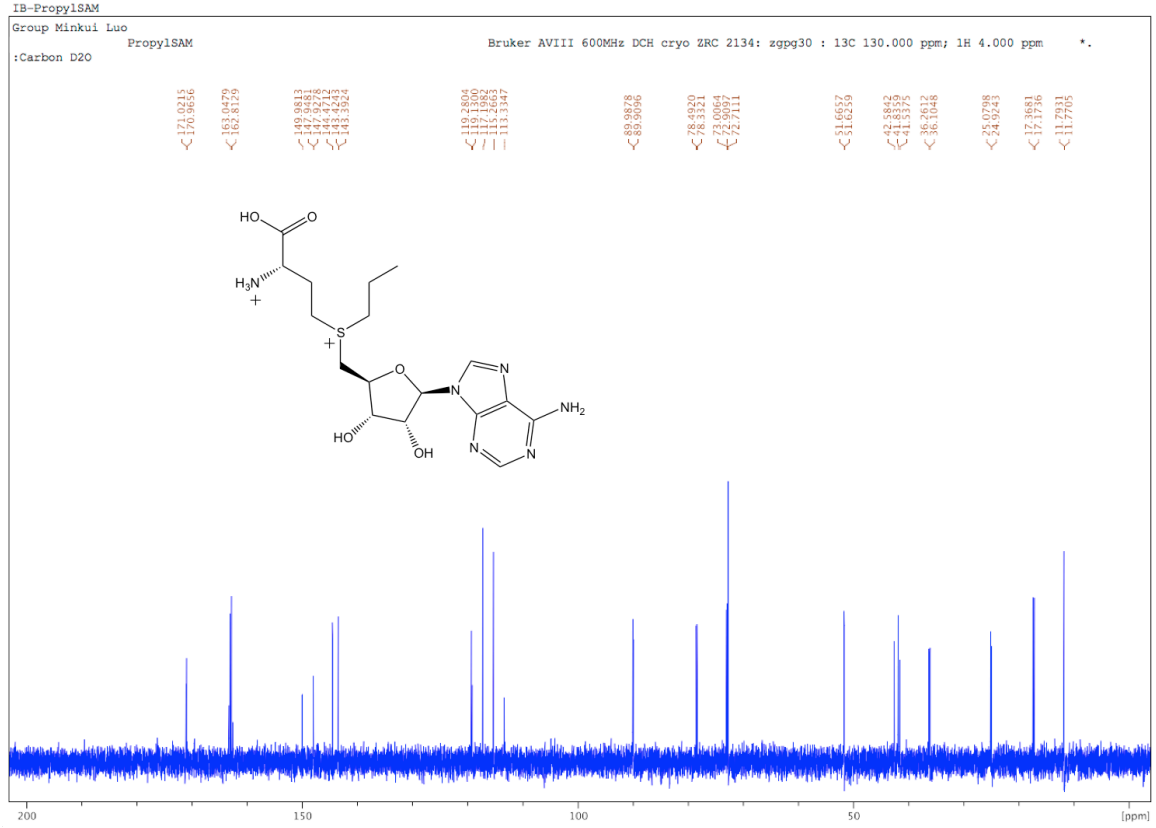
IB-PropylSAM
Group Minkui Luo
PropylSAM
:Carbon D2O
Bruker AVIII 600MHz DCH cryo ZRC 2134: zgpg30 : 13C 130.000 ppm; 1H 4.000 ppm
[ppm]

Propyl-SeAM:

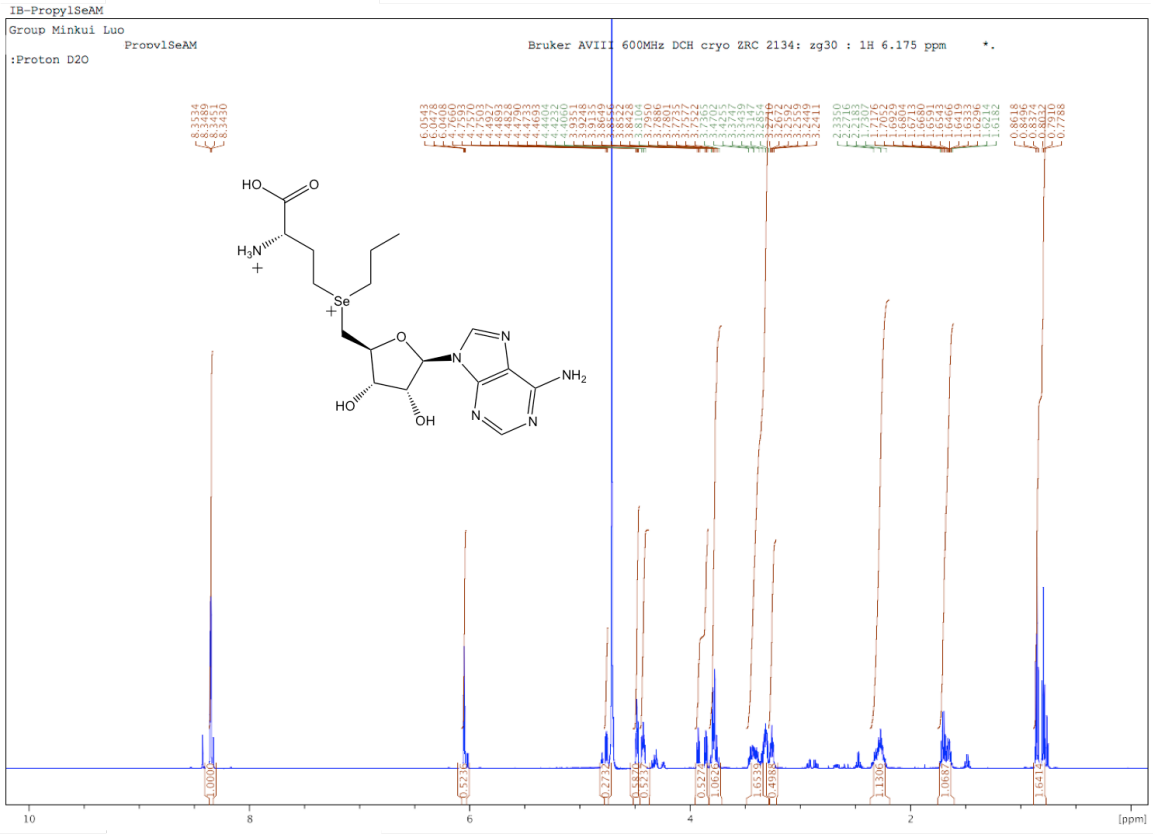
IB-PropylSeAM
Group Minkui Luo
ProovlSeAM
:Proton D2O
Bruker AVIII 600MHz DCH cryo ZRC 2134: zg30 : 1H 6.175 ppm
[ppm]

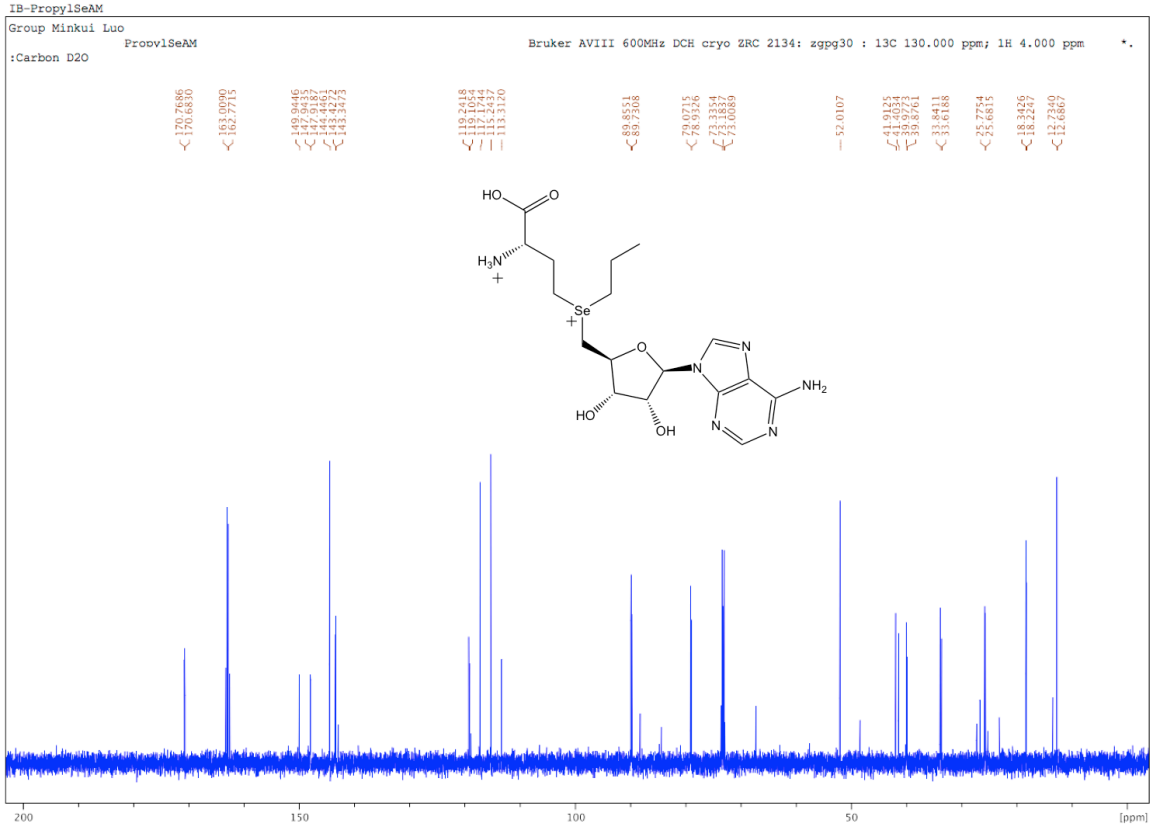
IB-PropylSeAM
Group Minkui Luo
ProovlSeAM
:Carbon D2O
Bruker AVIII 600MHz DCH cryo ZRC 2134: zgpg30 : 13C 130.000 ppm; 1H 4.000 ppm
[ppm]

Allyl-SAM:

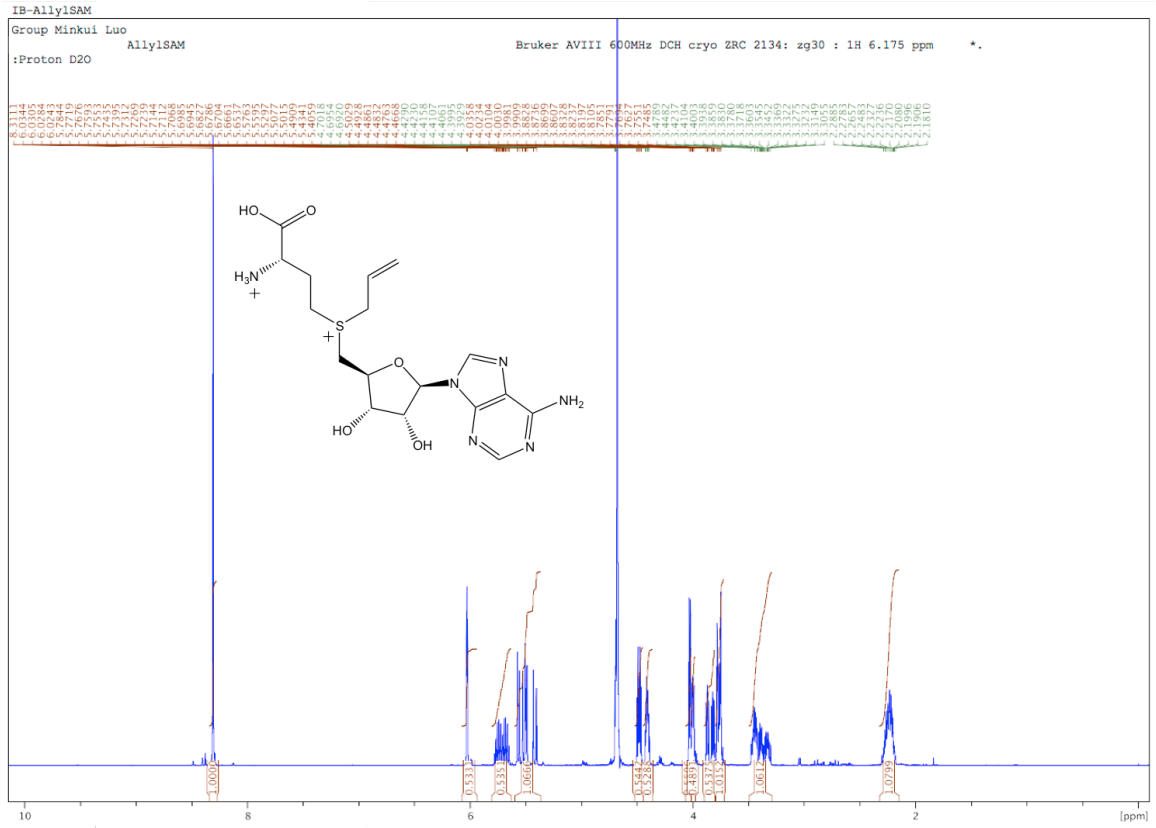
IB-AllylSAM
Group Minkui Luo
AllylSAM
Bruker AVIII 600MHz DCH cryo ZRC 2134: zg30 : 1H 6.175 ppm
:Proton D2O
HO
O
H3N
+
S
+
O
N
N
NH2
HO
OH
N
N
10
8
6
4
2
[ppm]

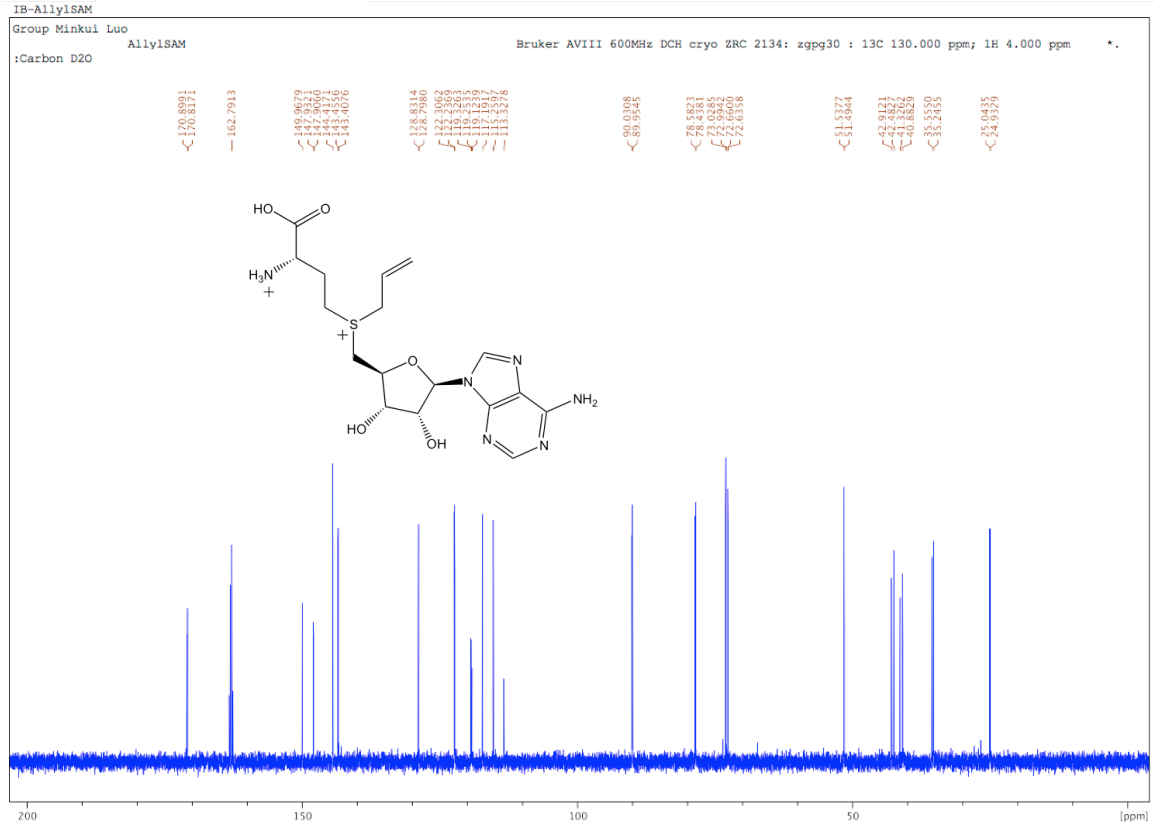
IB-AllylSAM
Group Minkui Luo
AllylSAM
Bruker AVIII 600MHz DCH cryo ZRC 2134: zgpg30 : 13C 130.000 ppm; 1H 4.000 ppm
:Carbon D2O
HO
O
H3N
+
S
+
O
N
N
NH2
HO
OH
N
N
200
150
100
50
[ppm]

Allyl-SeAM:

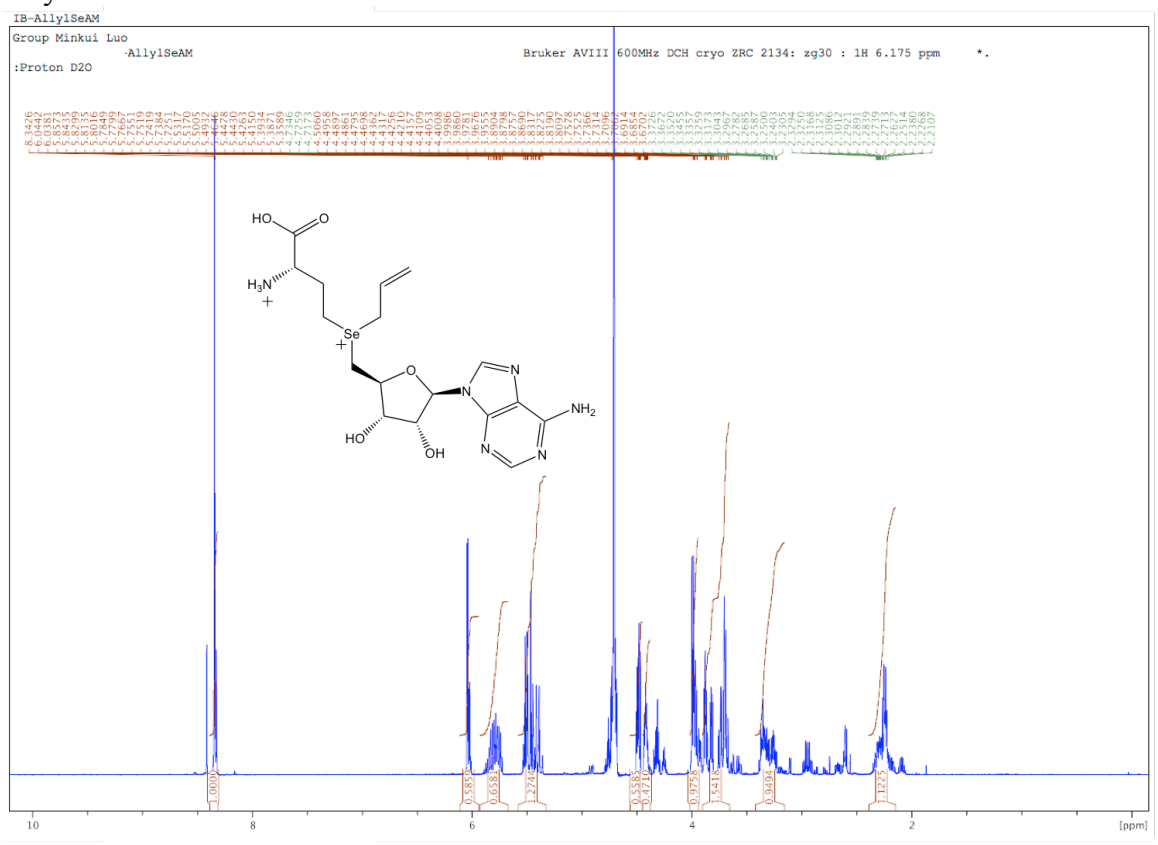
IB-AllylSeAM
Group Minkui Luo
AllylSeAM
:Proton D2O
Bruker AVIII 600MHz DCH cryo ZRC 2134: zg30 : 1H 6.175 ppm
[ppm]

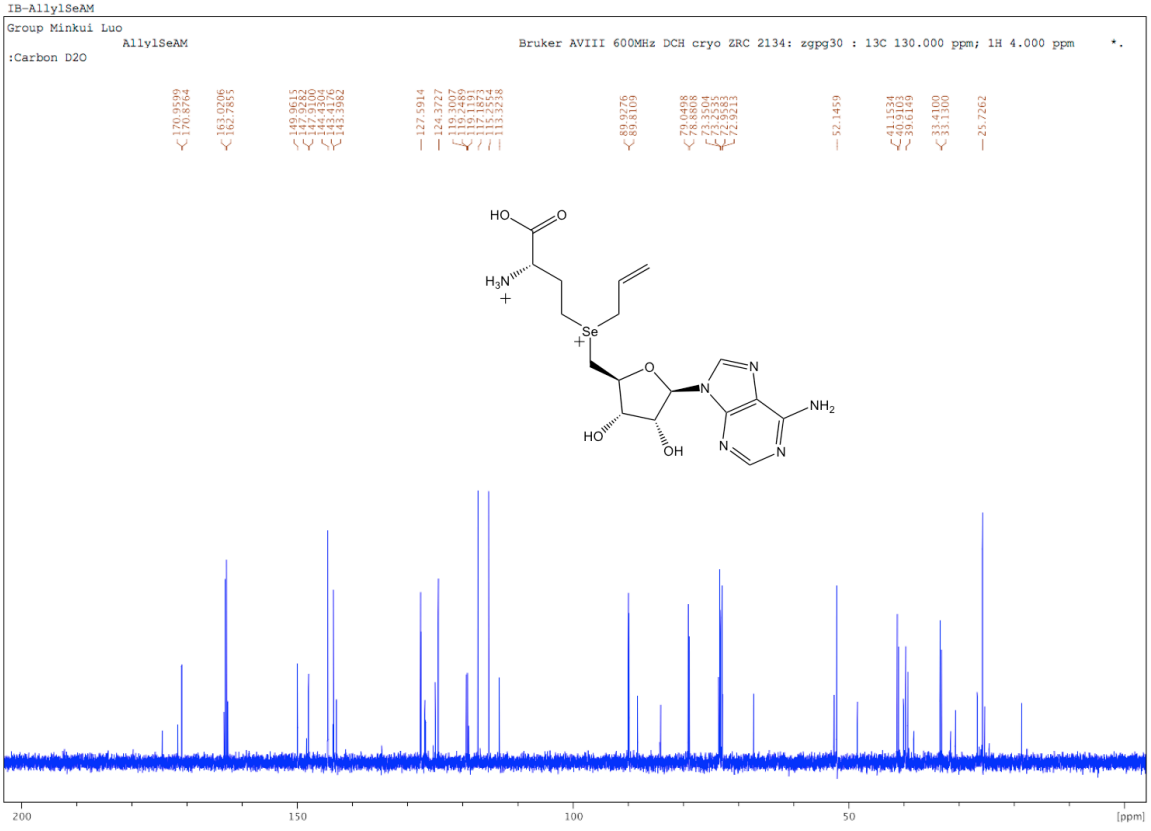
IB-AllylSeAM
Group Minkui Luo
AllylSeAM
:Carbon D2O
Bruker AVIII 600MHz DCH cryo ZRC 2134: zgpg30 : 13C 130.000 ppm; 1H 4.000 ppm
[ppm]

Pentyne-SAM:

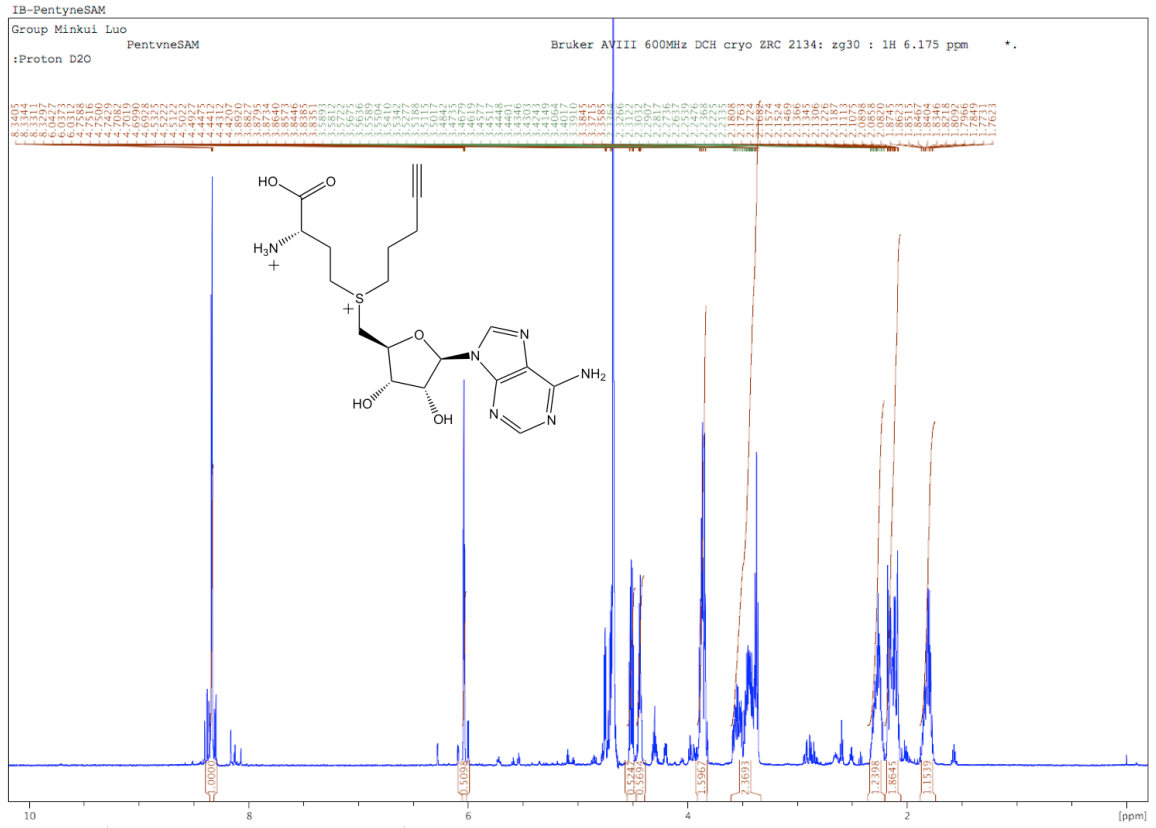
IB-PentyneSAM
Group Minkui Luo
PentvneSAM
Bruker AVIII 600MHz DCH cryo ZRC 2134: zg30 : 1H 6.175 ppm
:Proton D2O
HO
O
H3N
+
S
O
N
N
NH2
HO
OH
N
N
10
8
6
4
2
[ppm]

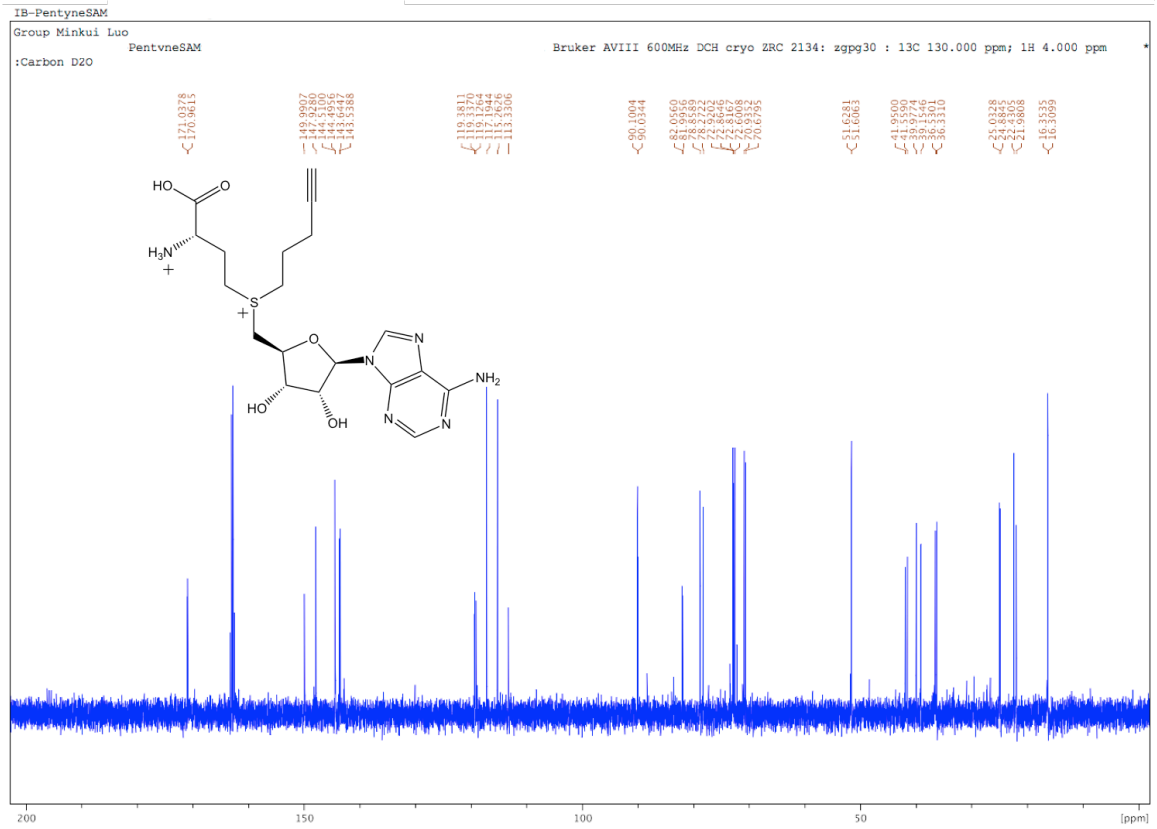
IB-PentyneSAM
Group Minkui Luo
PentvneSAM
Bruker AVIII 600MHz DCH cryo ZRC 2134: zgpg30 : 13C 130.000 ppm; 1H 4.000 ppm
:Carbon D2O
HO
O
H3N
+
S
O
N
N
NH2
HO
OH
N
N
200
150
100
50
[ppm]

Pentyne-SeAM:

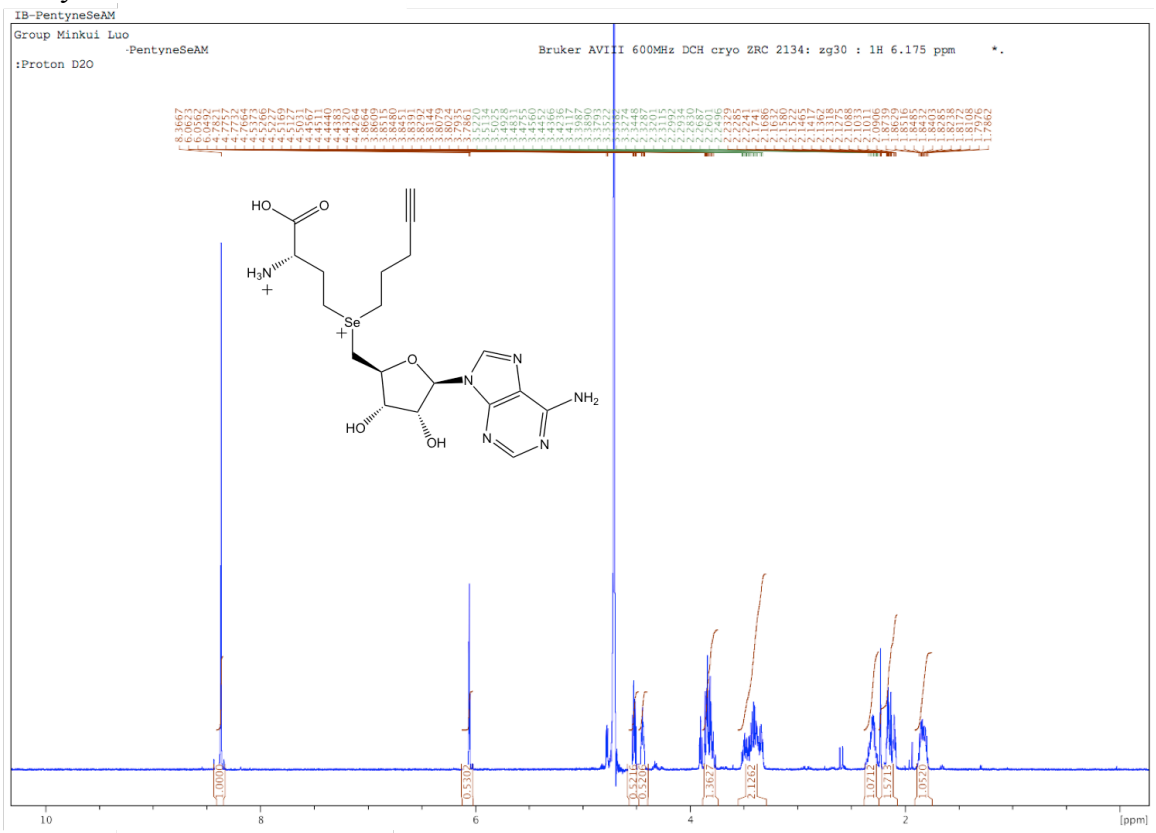

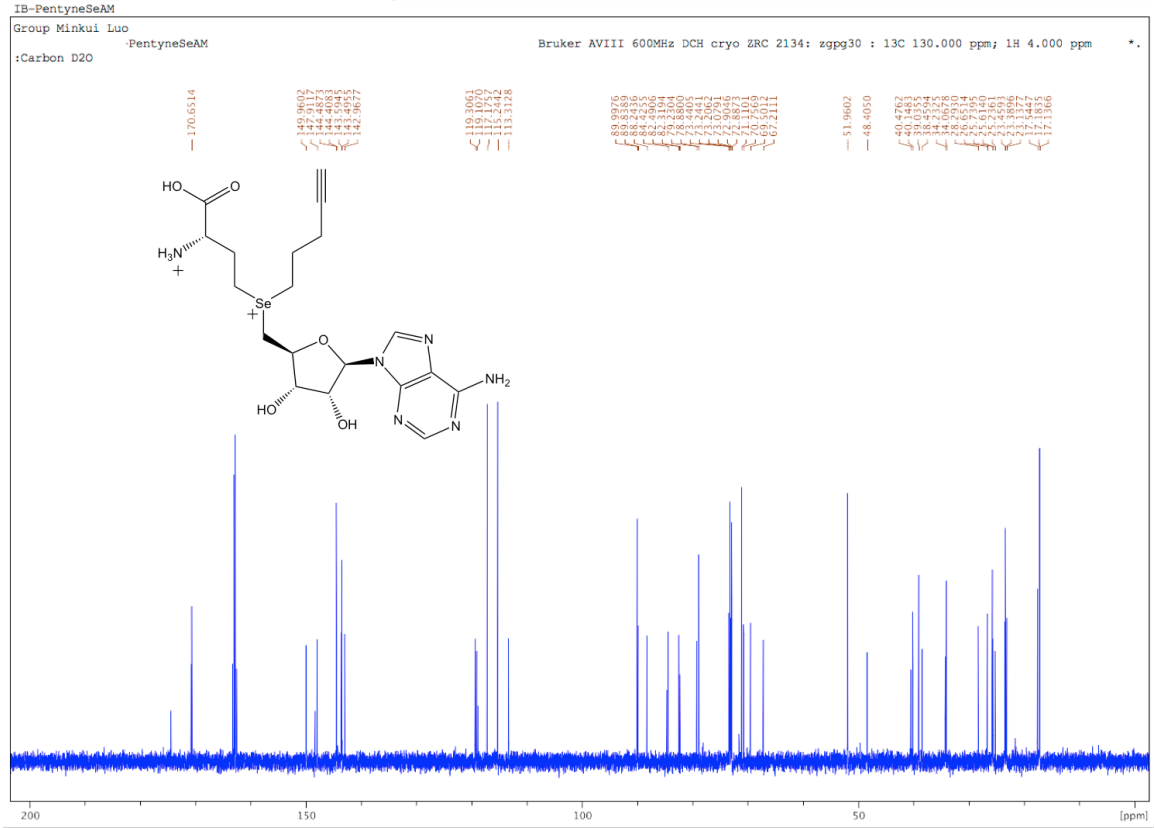

Enyne-SAM:

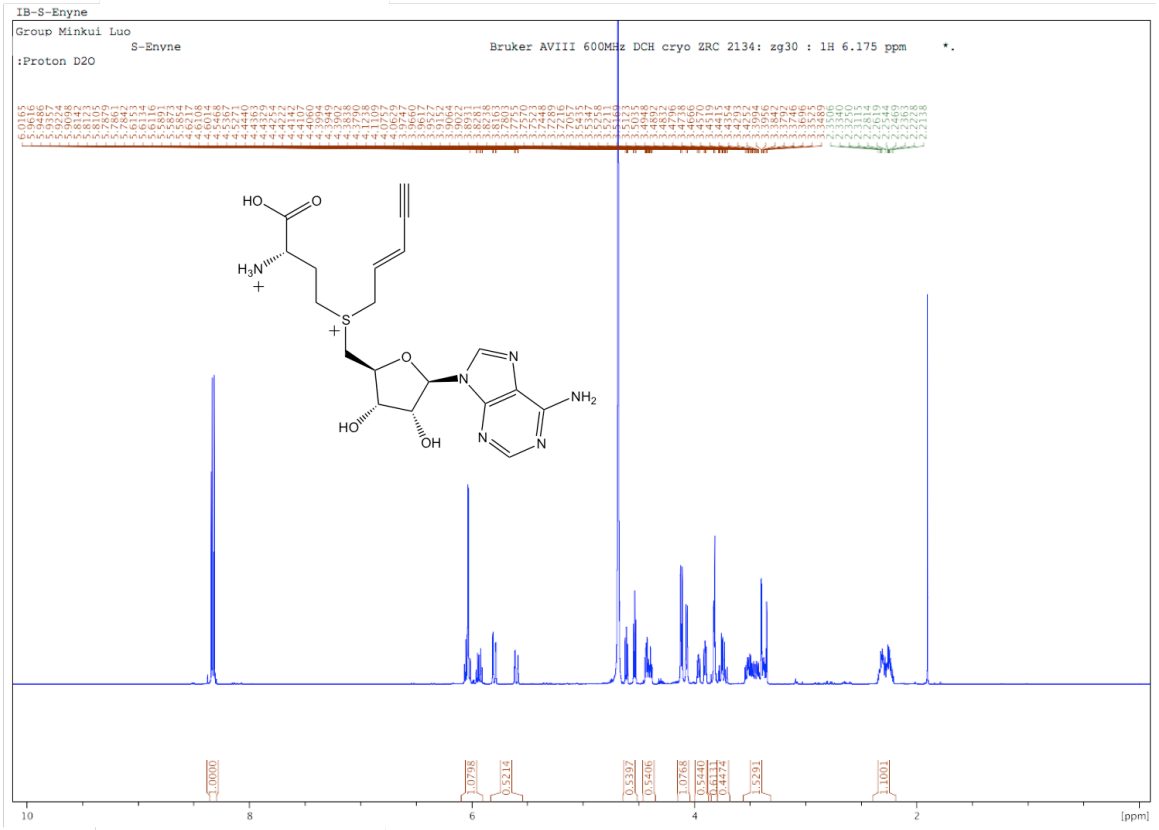
IB-S-Enyne
Group Minkui Luo
S-Envne
Bruker AVIII 600MHz DCH cryo ZRC 2134: zg30 : 1H 6.175 ppm
:Proton D2O
[ppm]

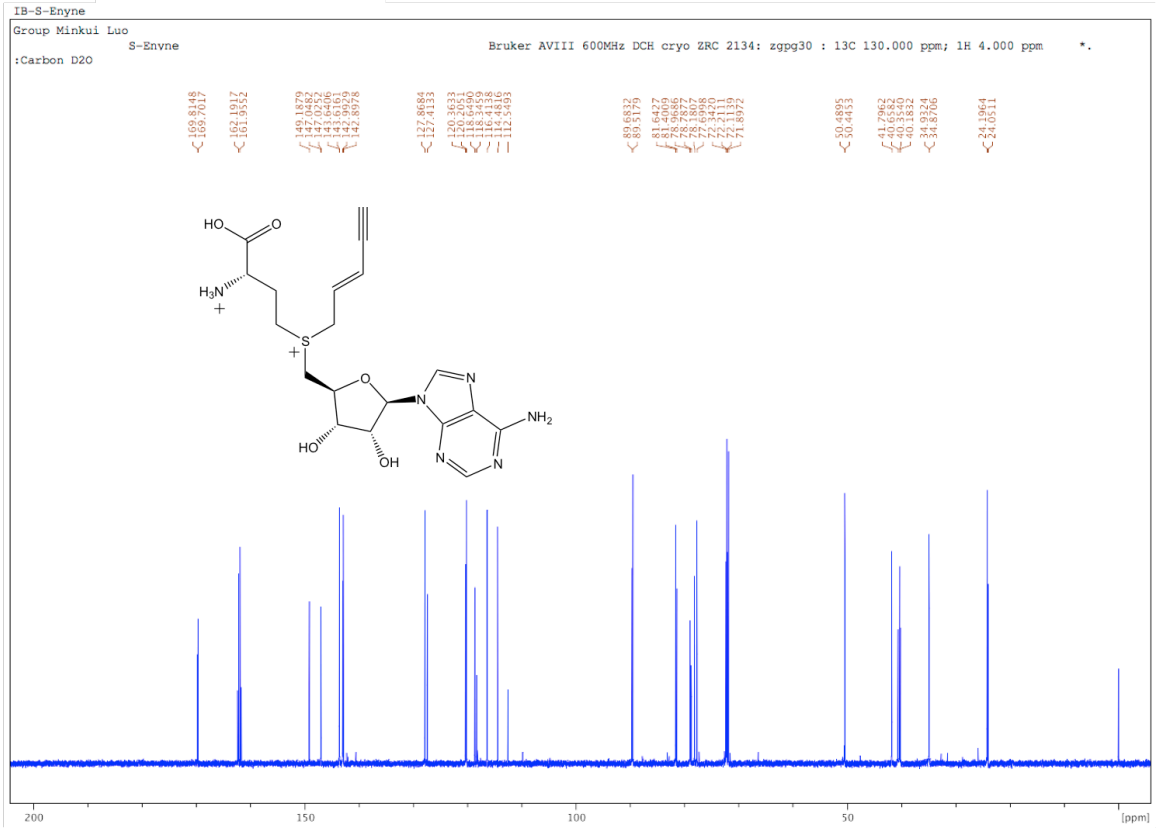
IB-S-Enyne
Group Minkui Luo
S-Envne
Bruker AVIII 600MHz DCH cryo ZRC 2134: zgpg30 : 13C 130.000 ppm; 1H 4.000 ppm
:Carbon D2O
[ppm]

Enyne-SeAM:

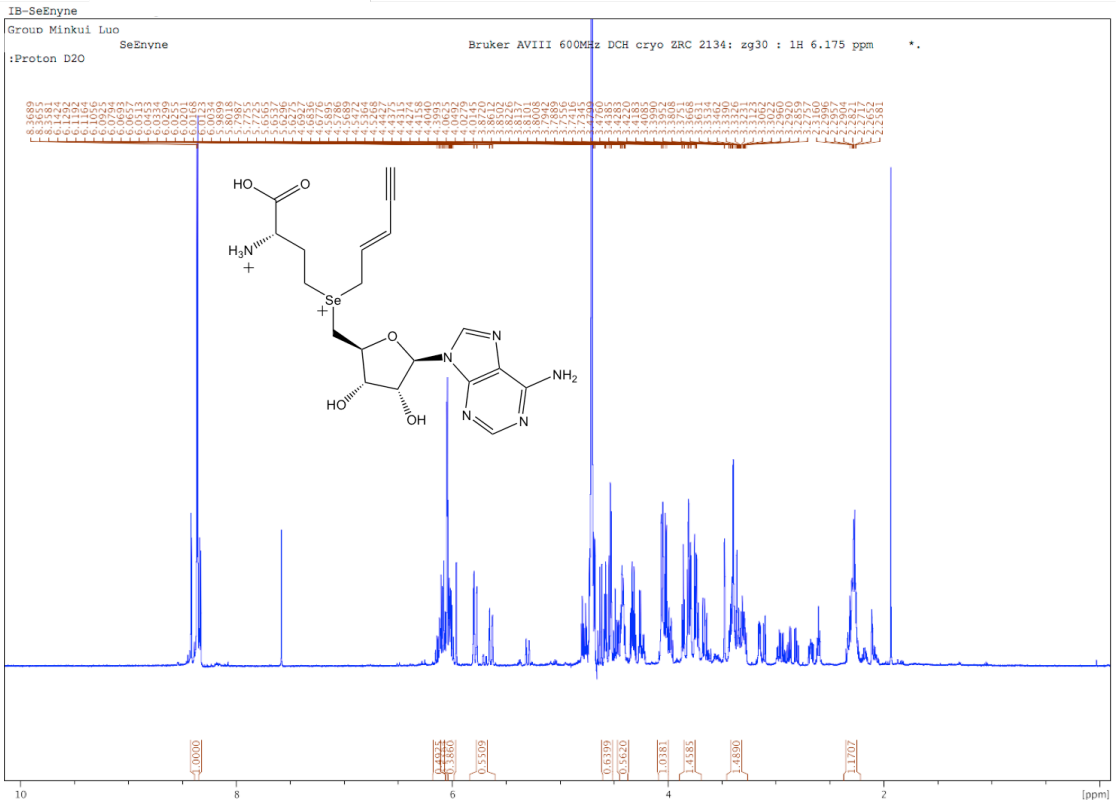
IB-SeEnyne
Group Minkui Luo
SeEnyne
Bruker AVIII 600MHz DCH cryo ZRC 2134: zg30 : 1H 6.175 ppm
:Proton D2O
[ppm]

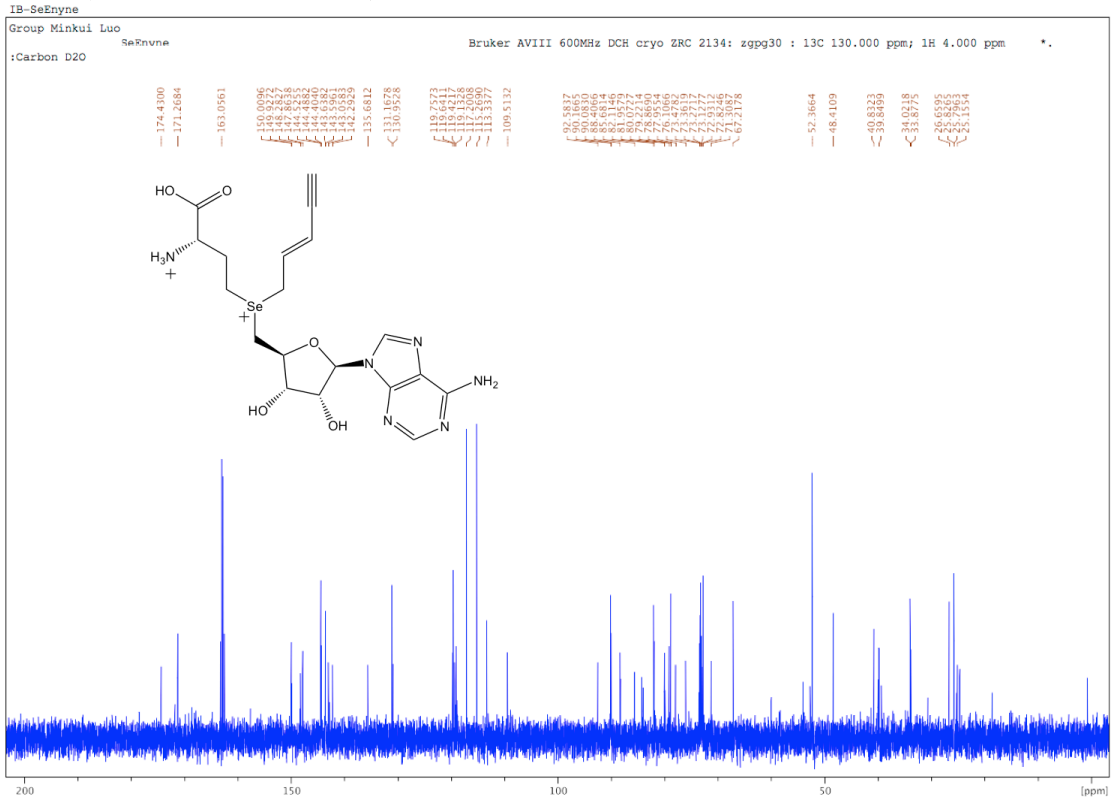
IB-SeEnyne
Group Minkui Luo
SeEnyne
Bruker AVIII 600MHz DCH cryo ZRC 2134: zgpg30 : 13C 130.000 ppm; 1H 4.000 ppm
:Carbon D2O
[ppm]

Hexyne-SAM:

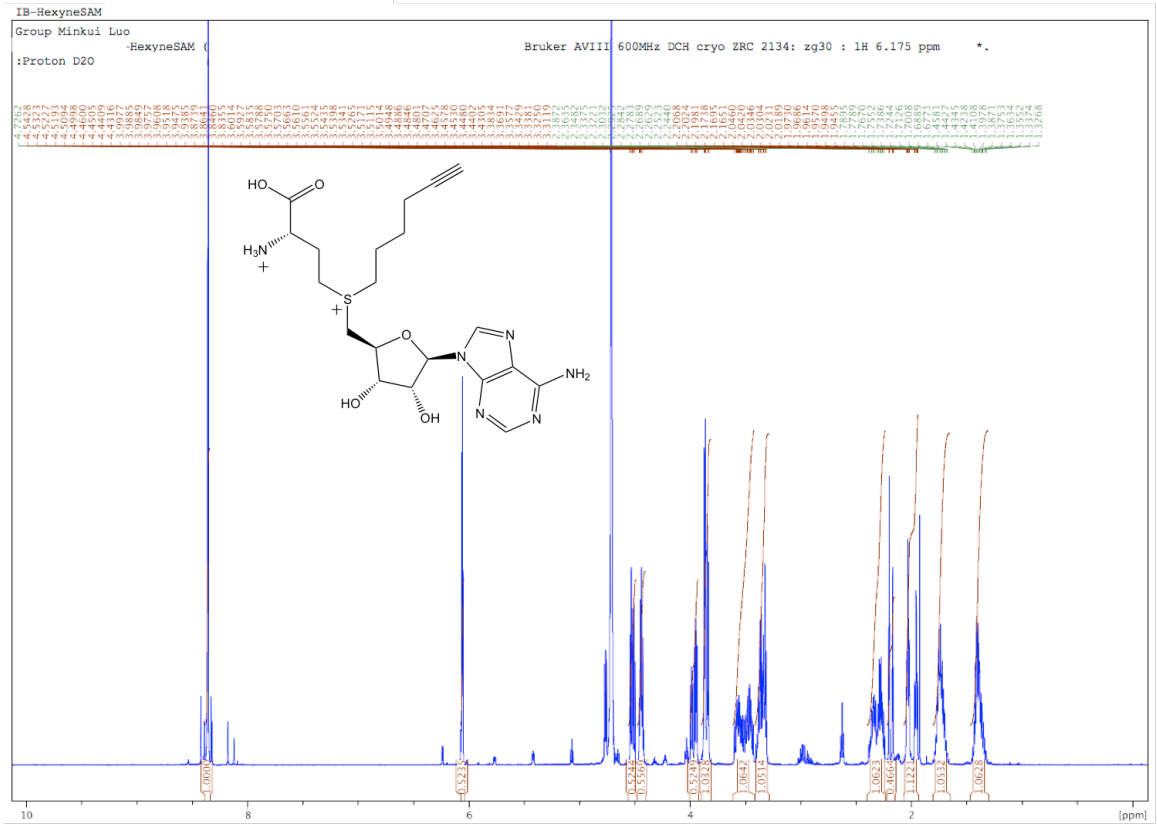
IB-HexyneSAM
Group Minkui Luo
HexyneSAM (
:Proton D2O
Bruker AVIII 600MHz DCH cryo ZRC 2134: zg30 : 1H 6.175 ppm
*.
HO
O
H3N
+
S
O
N
N
NH2
HO
OH
N
N
10
8
6
4
2
[ppm]

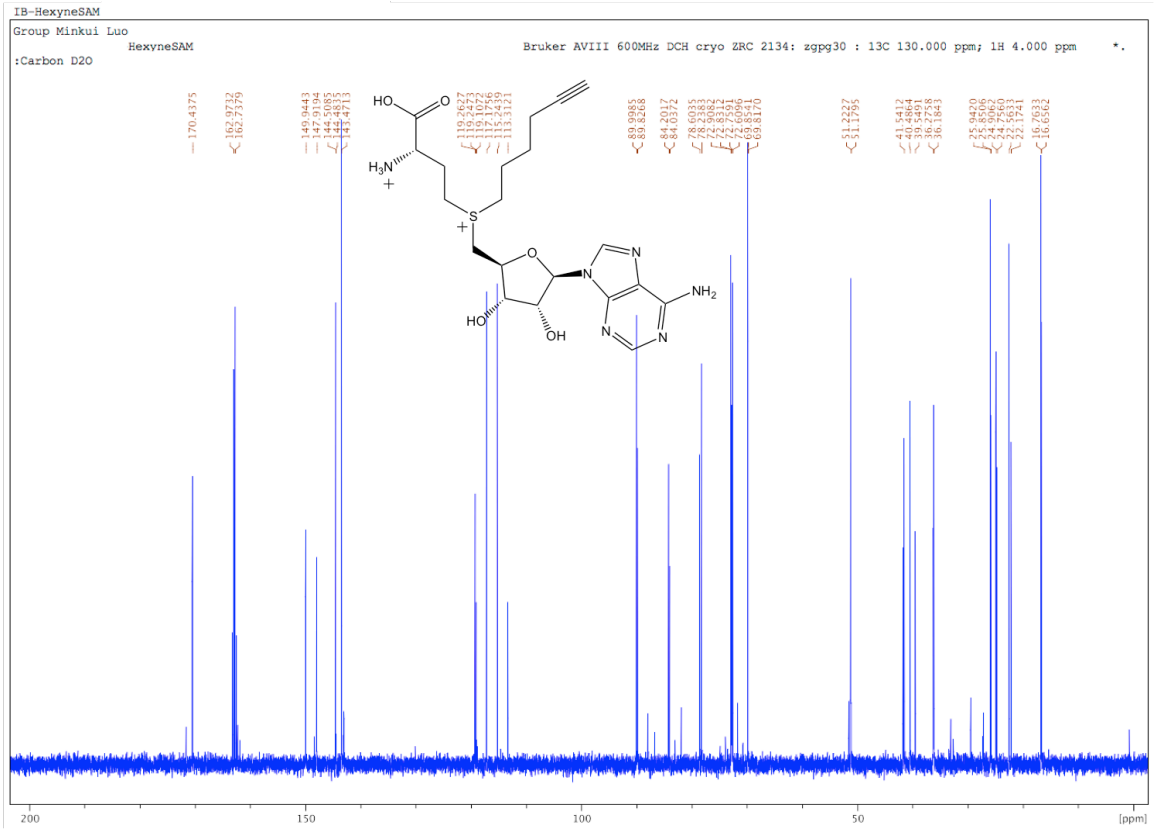
IB-HexyneSAM
Group Minkui Luo
HexyneSAM
:Carbon D2O
Bruker AVIII 600MHz DCH cryo ZRC 2134: zgpg30 : 13C 130.000 ppm; 1H 4.000 ppm
*.
HO
O
H3N
+
S
O
N
N
NH2
HO
OH
N
N
200
150
100
50
[ppm]

Hexyne-SeAM:

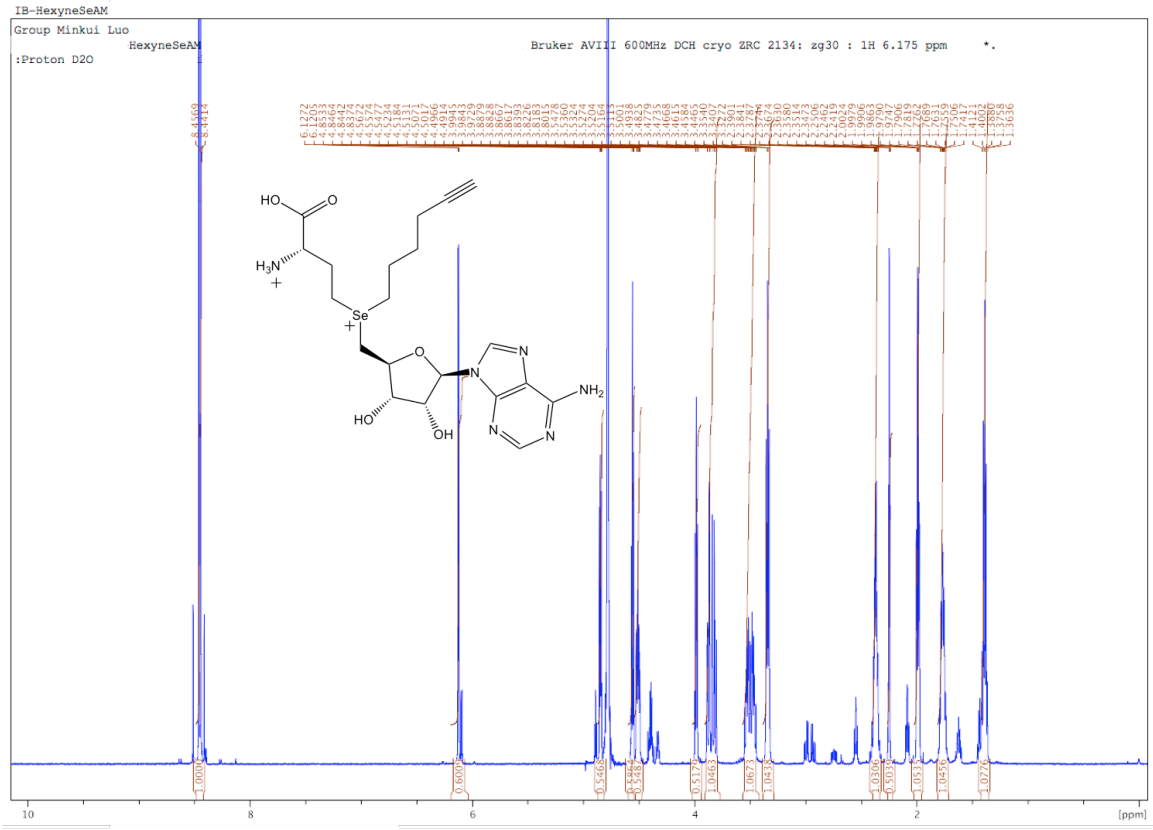
IB-HexyneSeAM
Group Minkui Luo
HexyneSeAM
:Proton D2O
Bruker AVIII 600MHz DCH cryo ZRC 2134: zg30 : 1H 6.175 ppm *.
[ppm]

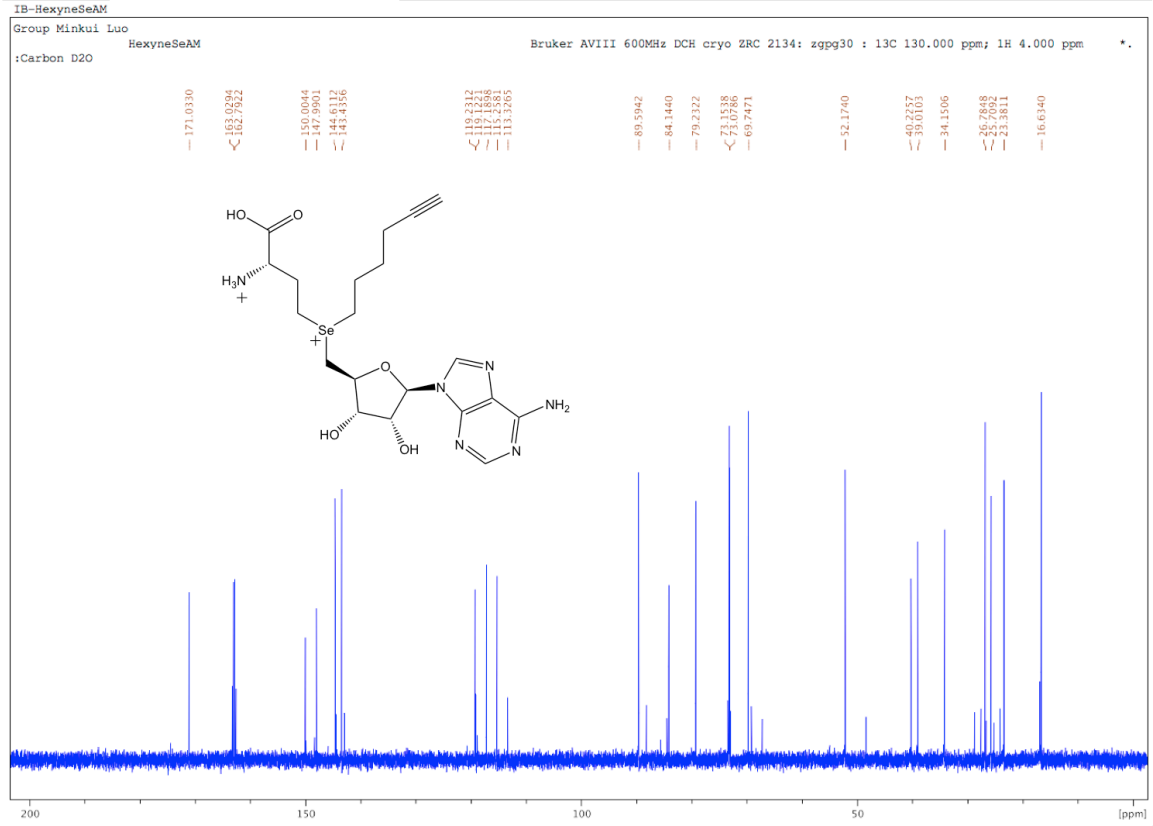
IB-HexyneSeAM
Group Minkui Luo
HexyneSeAM
:Carbon D2O
Bruker AVIII 600MHz DCH cryo ZRC 2134: zgpg30 : 13C 130.000 ppm; 1H 4.000 ppm *.
[ppm]

Hey-SAM:

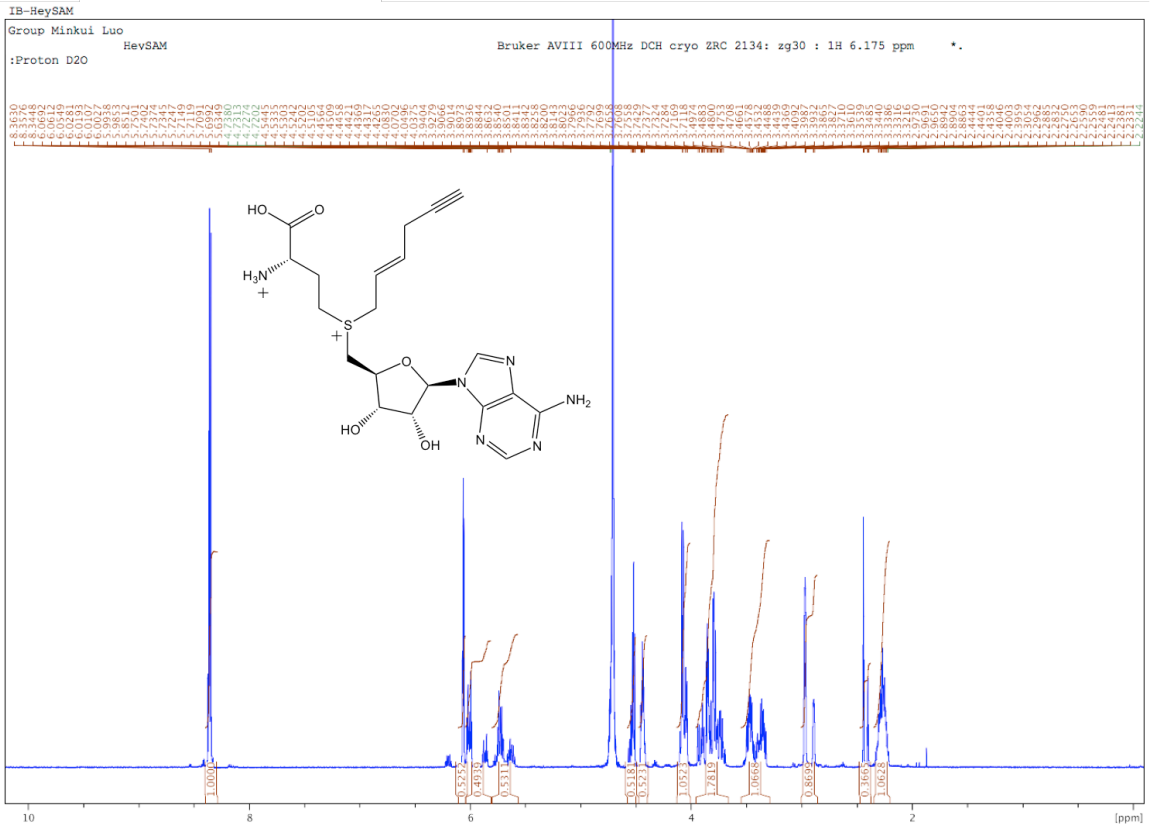
IB-HeySAM
Group Minkui Luo
HeySAM
Bruker AVIII 600MHz DCH cryo ZRC 2134: zg30 : 1H 6.175 ppm
:Proton D2O
[ppm]

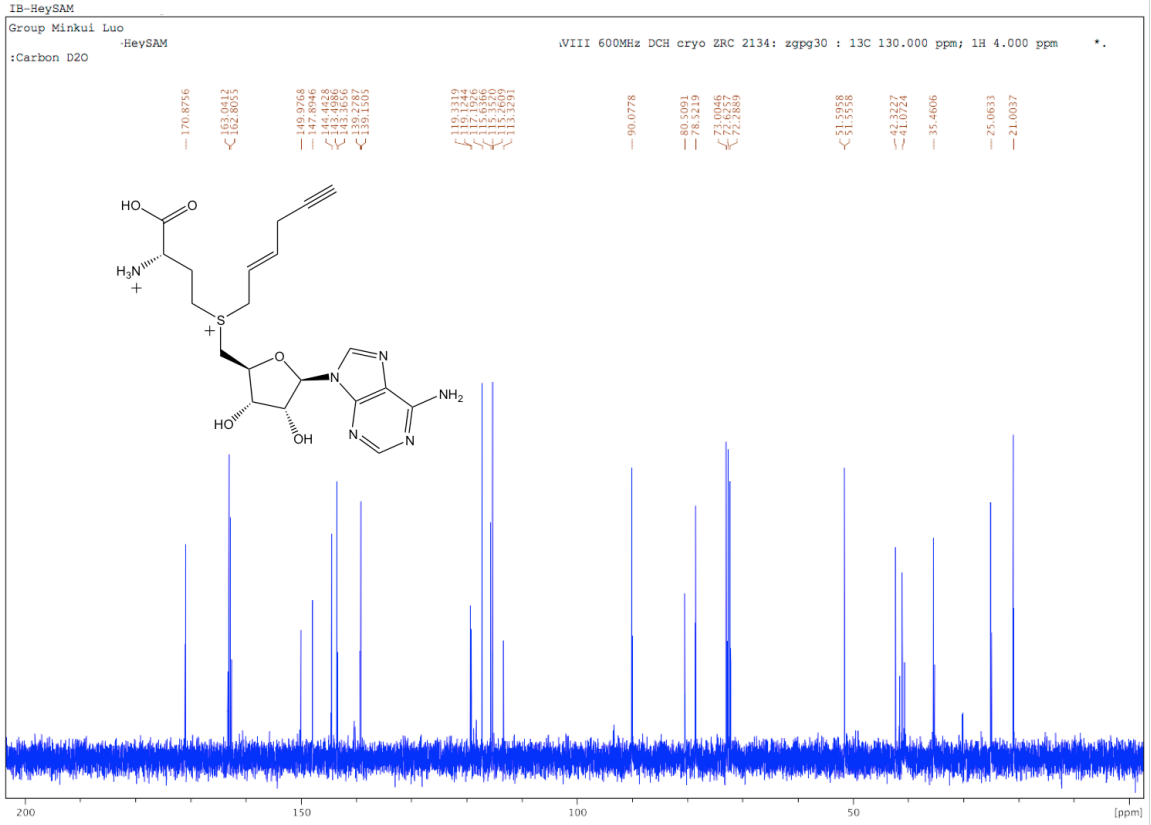
IB-HeySAM
Group Minkui Luo
HeySAM
AVIII 600MHz DCH cryo ZRC 2134: zgpg30 : 13C 130.000 ppm; 1H 4.000 ppm
:Carbon D2O
[ppm]

Hey-SeAM:

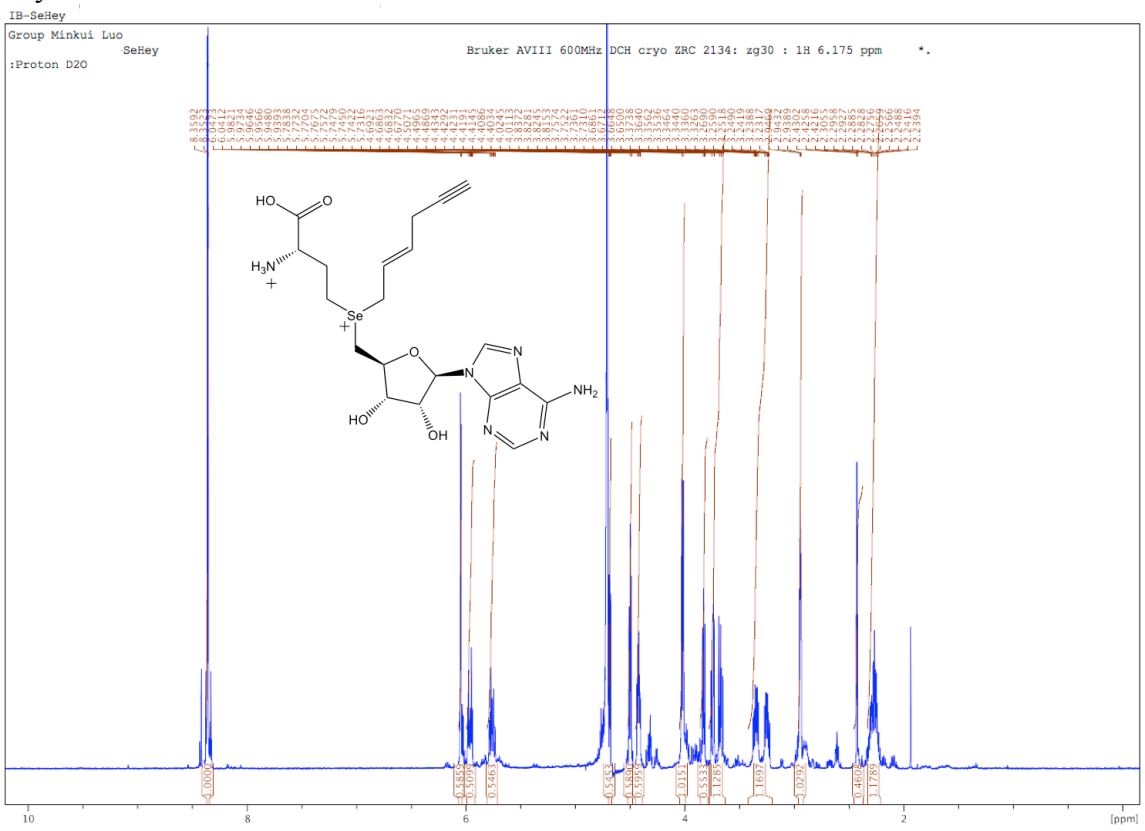
IB-SeHey
Group Minkui Luo
SeHey
:Proton D2O
Bruker AVIII 600MHz DCH cryo ZRC 2134: zg30 : 1H 6.175 ppm
[ppm]

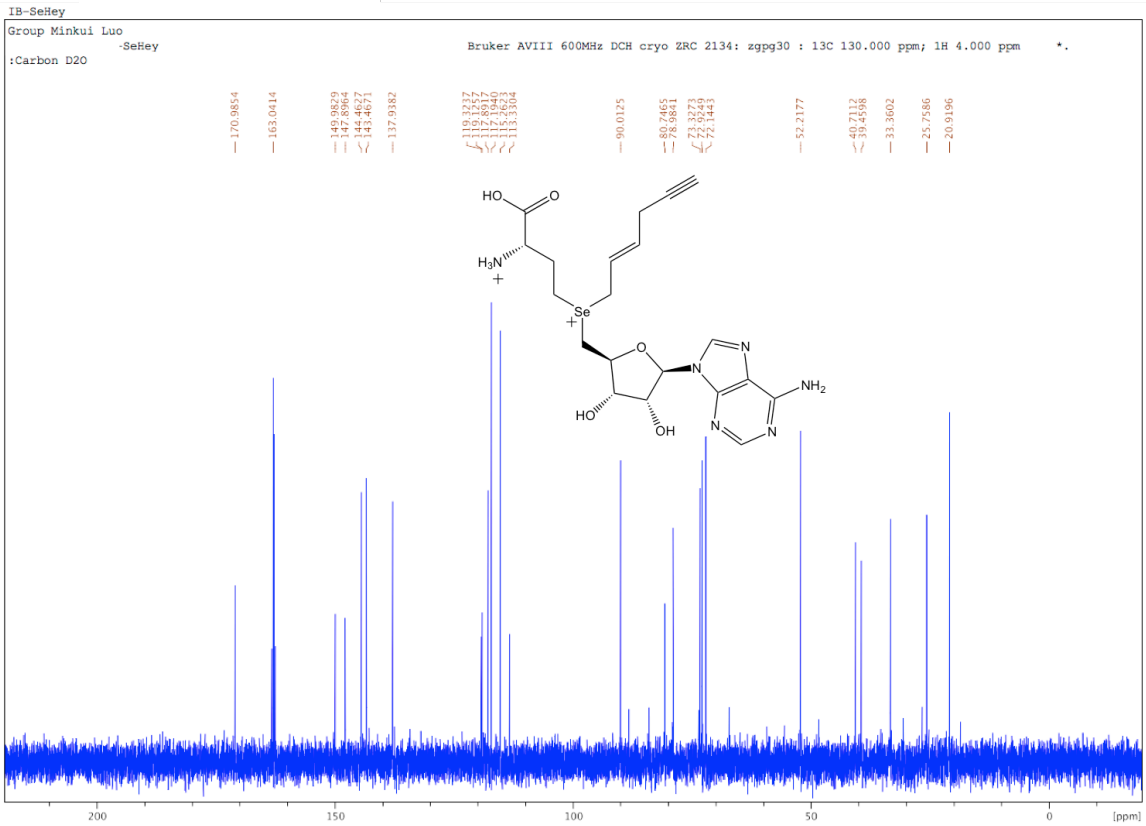
IB-SeHey
Group Minkui Luo
SeHey
:Carbon D2O
Bruker AVIII 600MHz DCH cryo ZRC 2134: zgpg30 : 13C 130.000 ppm; 1H 4.000 ppm
[ppm]